Investigation into the role of TRPV4 in asthma

Nadja Kobold

A thesis submitted for the Degree of Doctor of Philosophy in the Faculty of Medicine, Imperial College London

2022

Respiratory Pharmacology Group

National Heart and Lung Institute

Faculty of Medicine

Imperial College London

Statement of Originality

This thesis is a product of my own work except where appropriately referenced:

Experiments on isolated vagal nerve in Chapters 5 and 6 were performed by Dr Sara Bonvini. Characterisation and pharmacokinetic assessment of test compounds in Chapter 6 was performed by AstraZeneca (Research & Early Development, Respiratory & Immunology, BioPharmaceuticals R&D).

I was funded by Asthma UK Centre in Allergic Mechanisms of Asthma.

Copyright Declaration

The copyright of this thesis rests with the author. The thesis' contents are licensed under a Creative Commons Attribution-Non Commercial 4.0 International Licence (CC BY-NC). The material in this thesis may be copied or redistributed in any medium or format provided it is attributed to the author and not used for commercial purposes. When reusing or sharing the work, the licence terms of this work must be made clear.

Acknowledgements

I would like to thank my supervisors Prof Maria Belvisi and Dr Mark Birrell for the opportunity to pursue my PhD within the Respiratory Pharmacology group. Although challenging at times, this was an exceptional experience and I would like to thank you for all the guidance, support and scientific discussion during my PhD and beyond.

This PhD would not be possible without the rest of the Respiratory Pharmacology group. Thanks to all for guidance, support and creating an enjoyable and friendly environment. A very special thanks goes to Bilel Dekkak, Dr Pauline Flajolet, Dimitris Zervas, Dr Thomais Markou, Dr Sara Bonvini, Dr James Pinkerton and Dr Eric Dubuis for helping me realise all my "crazy" and never ending studies.

I am also grateful to Prof Robert Snelgrove, Dr Dhiren Patel and Imperial College Flow Cytometry facility for their extensive help with flow cytometry. I would like to Central Biomedical Services for providing invaluable support with management of colonies of genetically modified mice. My thanks also goes to Early Respiratory and Immunology department at AstraZeneca for providing PAR2 and TRPV4 inhibitors and PK support. I would also like to thank Dr David Jackson and Asthma UK Centre in Allergic Mechanisms of Asthma for all the support throughout my PhD. I am grateful to Asthma UK Centre in Allergic Mechanisms of Asthma for sponsoring my MRes and PhD studies and Imperial College for providing additional financial support and deadline extension due to COVID-19 pandemic.

Last but not least, I would like to thank my family and friends for being there for me and seeing me through the journey.

Abstract

TRPV4 has emerged as a novel therapeutic target in chronic respiratory disease. TRPV4-induced ATP release through Pannexin-1 channels and subsequent activation of P2X receptors has been implicated in chronic lung disease. We have recently demonstrated that TRPV4 deficiency or pharmacologic inhibition of TRPV4 abolished the development of allergic airway inflammation (AAI), airway hyper-responsiveness (AHR) or late asthmatic response (LAR) in rodent models of allergic airway disease (AAD). The aim of this thesis was to elucidate TRPV4 signalling cascade in AAD and identify key cells driving the cascade together with upstream and downstream targets.

Using a murine house dust mite (HDM) model of AAD, $CD4^+$ T cells and dendritic cells were identified as the initiators of immune responses to HDM and proposed as drivers of TRPV4 axis due to their *Trpv4* and *Panx-1* expression. Those cells expressed *P2rx1, P2rx4* and *P2rx7* which were dysregulated upon HDM challenge, suggesting their role downstream of TRPV4. P2X7 but not P2X4 or P2X1 deficiency ameliorated AAI upon HDM challenge, however none of the receptors modulated HDM-induced AHR. PAR2 was investigated as a potential mechanism of TRPV4 activation as HDM challenge was associated with dysregulated PAR2 ligand activity and immune cell *Par2* expression. While PAR2 deficiency ameliorated HDM-induced AAI, but not AHR, a PAR2 blocking antibody MEDI2344 offered no protection against HDM-induced AAD. Lastly, to confirm the preliminary observations, selective TRPV4 antagonists were tested in rodent models of AAD and were associated with a trend towards reduced AAI, but were inefficacious in AHR or LAR, respectively.

In conclusion, this thesis demonstrated a lack of role of TRPV4 in responses evoked by allergen challenge but rather implicated PAR2/TRPV4 signalling in allergen sensitisation. However, further work is needed to elucidate the role of TRPV4-ATP-P2X axis in other asthma phenotypes and associated symptoms such as cough.

Table of Contents

Investigation into the role of TRPV4 in asthma 1
Statement of Originality 2
Copyright Declaration 3
Acknowledgements 4
Abstract 5
Table of Contents 6
List of Tables 14
List of Figures 15
List of Abbreviations 19
1. Introduction 22
1.1. Asthma in general 23
1.1.1. Definition of asthma 23
1.1.2. Asthma heterogeneity 23
1.1.3. Atopic asthma pathophysiology 23
1.1.4. Treatment of asthma 26
1.2. Airway epithelium in asthma 30
1.3. Inflammatory cells in asthma 31
1.3.1. T cells 31
1.3.2. ILCs 33
1.3.3. Dendritic cells 35
1.3.4. Eosinophils 36
1.3.5. Mast cells 38
1.4. Inflammatory mediators in asthma 39
1.4.1. Th2 cytokines 39
1.4.1.1. IL-4 39
1.4.1.2. IL-13 40
1.4.1.3. IL-5 40
1.4.2. Chemokines 41
1.4.2.1. Eotaxin 41
1.4.2.2. MIP-1α (CCL3) 42
1.4.2.3. MCP-1 (CCL2) 42

1.4.2.4. CCL17 (TARC) and CCL22 ... 43
1.4.3. Epithelial derived cytokines ... 43
1.4.3.1. IL-25 ... 43
1.4.3.2. IL-33 ... 43
1.4.3.3. TSLP ... 44
1.4.4. Other proinflammatory cytokines ... 45
1.4.4.1. TNF-α ... 45
1.4.4.2. IL-1β and IL-18 ... 46
1.4.5. Extracellular ATP ... 47
1.5. Nerves in asthma ... 49
1.5.1. Neurophysiology of airway nerves ... 49
1.5.2. The role of nerves in asthma ... 51
1.6. TRP channels in asthma ... 52
1.6.1. Definition ... 52
1.6.2. TRPV1 ... 52
1.6.3. TRPA1 ... 53
1.6.4. TRPV4 ... 54
1.6.4.1. PAR2 – TRPV4 coupling ... 57
1.7. Animal models of AAD ... 58
1.7.1. Experimental animals ... 59
1.7.1.1. Mice ... 59
1.7.1.2. Rats ... 59
1.7.1.3. Guinea pigs ... 60
1.7.2. Approaches to modelling asthma in laboratory animals ... 60
1.7.2.1. Ovalbumin AAD models ... 60
1.7.2.2. HDM AAD models with systemic sensitisation ... 60
1.7.2.3. AAD models with mucosal sensitisation ... 61
1.8. Thesis plan ... 61
1.8.1. Hypothesis ... 64
1.8.2. Aims ... 64
2. Material and Methods ... 66
2.1. Animals ... 67
2.1.1. Ethics statement and animal housing conditions ... 67
2.1.2. Rats ... 67

2.1.3. Mice 67
2.1.4. Animal sacrifice 67
2.2. In vivo methodology 68
2.2.1. Assessment of airway responses by flow whole body plethysmography (FWBP) 68
2.2.1.1. The principles of FWBP 68
2.2.1.2. The use of Penh as lung function parameter 71
2.2.2. Murine HDM-induced model of AAD 72
2.2.2.1. HDM preparation 72
2.2.2.2. Study protocol 72
2.2.2.3. AHR assessment 73
2.2.3. Rat OVA-induced model of AAD 73
2.2.3.1. Study protocol 73
2.2.3.2. LAR assessment 74
2.2.4. NLRP3 inflammasome activation model 74
2.2.5. Pharmacokinetic (PK) studies 75
2.2.6. TRPV4 pharmacodynamic (PD) models 75
2.3. Sample collection and processing 76
2.3.1. Blood 76
2.3.2. Airway lumen cells 76
2.3.3. Lung tissue 77
2.3.3.1. Isolation of lung cells 77
2.3.3.2. Isolation of lung lobes for protein and gene expression assays 77
2.3.4. Mediastinal lymph nodes (MLN) 78
2.4. Gel based genotyping 78
2.4.1. Crude DNA extraction 78
2.4.1. Polymerase chain reaction 78
2.4.2. Gel electrophoresis 79
2.5. Flow cytometry 80
2.5.1. General extracellular staining protocol 80
2.5.2. General intracellular transcription factor staining protocol 80
2.5.3. Fluorescence activated cell sorting (FACS) 80
2.5.4. Compensation controls 81
2.5.5. Gating strategy 81

2.5.5.1. Gating strategy for identification of T cells, NK cells and B cells 81
2.5.5.2. Gating strategy for identification of ILCs 82
2.5.5.3. Gating strategy for isolation of ILC2s, CD4+ T cells and CD8+ T cells 84
2.5.5.4. Gating strategy for identification of myeloid cells 85
2.5.5.5. Gating strategy for identification and isolation of dendritic cells 87
2.5.6. List of antibodies 88
2.6. Assessment of soluble mediators in BAL 90
2.6.1. General enzyme-linked immunosorbent assay (ELISA) protocol 90
2.6.2. ProcartaPlex Immunoassay protocol 91
2.6.3. MSD assays 92
2.6.4. Tryptase-like activity assay 93
2.7. Assessment of plasma IgE levels 93
2.7.1. Total IgE ELISA 93
2.7.2. HDM specific IgE ELISA 94
2.8. Assessment of pSTAT5a,b 94
2.8.1. Sample preparation 94
2.8.2. Bradford assay 95
2.8.3. MSD assay 95
2.9. Assessment of gene expression 95
2.9.1. FACS isolated immune cell RNA isolation and reverse transcription (RT) 95
2.9.1.1. RNA isolation with RNeasy Plus Micro Kit 95
2.9.1.2. Reverse transcription 96
2.9.2. Lung tissue RNA isolation and RT 96
2.9.2.1. RNA isolation with RNeasy Plus Mini Kit 96
2.9.2.2. Reverse transcription 97
2.9.3. Quantitative real time polymerase chain reaction 97
2.9.3.1. Taqman® Gene Expression Assay principle 97
2.9.3.2. Taqman® Gene Expression Assay protocol 98
2.9.3.3. qRT-PCR data analysis 98
2.9.3.4. Taqman® Gene Expression Assay multiplex validation 98
2.9.3.5. List of Taqman® Gene Expression Assays 101
2.10. In vitro isolated vagus preparation 101
2.11. Statistical analysis 102
3. Identification of downstream targets in TRPV4 signalling pathway 103

3.1. Introduction 104
3.2. Hypothesis and aims 106
3.3. Methods 106
3.3.1. Murine HDM time course study 106
3.3.2. Isolation of key immune cell populations 107
3.3.3. Gene expression 107
3.4. Results 109
3.4.1. The development of early immune responses upon in the murine HDM model 109
3.4.1.1. HDM challenge induced Th2 immune responses 109
3.4.1.2. CD4+ T cells and ILC2s as drivers of type two immune responses 113
3.4.1.3. The role of dendritic cells in HDM-induced airway inflammation 117
3.4.2. TRPV4 signalling pathway in the key immune cells 118
3.5. Discussion 123
4. P2X receptors as downstream targets in TRPV4 signalling in HDM-induced model of allergic airway disease 138
4.1. Introduction 139
4.2. Hypothesis and aims 140
4.3. Methods 140
4.3.1. $P2X7^{-/-}$ in the HDM model 140
4.3.1.1. Validation of $P2X7^{-/-}$ mice 140
4.3.1.2. $P2X7^{-/-}$ HDM study 141
4.3.2. $P2X4^{-/-}$ in the HDM model 141
4.3.2.1. Validation of $P2X4^{-/-}$ mice 141
4.3.2.2. $P2X4^{-/-}$ HDM study 142
4.3.3. $P2X1^{-/-}$ in the HDM model 142
4.3.3.1. Genotyping of $P2X1^{-/-}$ mice 142
4.3.3.2. $P2X1^{-/-}$ HDM study 142
4.4. Results 143
4.4.1. The role of P2X7 in allergic airway disease 143
4.4.1.1. The validation of $P2X7^{-/-}$ mice 143
4.4.1.2. The role of P2X7 deficiency in the allergic airway inflammation 144
4.4.1.3. The effect of P2X7 deficiency on HDM-induced lung inflammation 145
4.4.1.4. The effect of P2X7 deficiency on cytokine and chemokine production 148
4.4.1.5. The role of P2X7 deficiency on IgE antibody production 149

4.4.1.6. The role of P2X7 deficiency in allergen-induced airway hyper-responsiveness 149
4.4.2. The role of P2X4 in allergic airway disease 150
4.4.2.1. Validation of P2X4$^{-/-}$ mice 150
4.4.2.2. The effect of P2X4$^{-/-}$ on HDM-induced airway inflammation 151
4.4.2.3. The effect of P2X4$^{-/-}$ on HDM-induced lung inflammation 152
4.4.2.4. The effect of P2X4$^{-/-}$ on type 2 cytokine and chemokine production 153
4.4.2.5. The effect of P2X4$^{-/-}$ on antibody production 155
4.4.2.6. The role of P2X4 in allergen-induced airway hyper-responsiveness 155
4.4.3. The role of P2X1 in allergic airway disease 156
4.4.3.1. Genotyping of P2X1$^{-/-}$ mice 156
4.4.3.2. The effect of P2X1$^{-/-}$ on HDM-induced airway inflammation 157
4.4.3.3. The effect of P2X1$^{-/-}$ on HDM-induced lung inflammation 158
4.4.3.4. The role of P2X1 in allergen-induced airway hyper-responsiveness 159
4.5. Discussion 160
5. PAR2 as a potential activator of TRPV4 signalling in HDM-induced model of allergic airway disease 171
5.1. Introduction 172
5.2. Hypothesis and aims 173
5.3. Methods 173
5.3.1. PAR2 signalling in the mouse HDM model 173
5.3.1.1. Tryptase-like activity of BAL 173
5.3.1.2. *Par2* expression 173
5.3.2. The role of PAR2 deficiency in the murine HDM model 174
5.3.2.1. Validation of PAR2$^{-/-}$ mice 174
5.3.2.1.1. Gel electrophoresis-based genotyping 174
5.3.2.1.2. Functional validation 174
5.3.2.2. PAR2$^{-/-}$ mice in the HDM study 175
5.3.3. Pharmacological inhibition of PAR2 during allergen challenge in the murine HDM model 175
5.4. Results 176
5.4.1. PAR2 signalling in the murine HDM model of AAD 176
5.4.2. The role of PAR2 deficiency in the murine HDM model 178
5.4.2.1. Validation of PAR2$^{-/-}$ mice 178
5.4.2.2. The effect of PAR2 deficiency on HDM-induced airway inflammation 179
5.4.2.3. The effect of PAR2 deficiency on HDM-induced lung inflammation 180

5.4.2.4. The effect of PAR2 deficiency on type 2 cytokine and chemokine production 181
5.4.2.5. The effect of PAR2 deficiency on antibody secretion 182
5.4.2.6. The effect of PAR2 deficiency on airway hyper-responsiveness 183
5.4.3. Pharmacological inhibition of PAR2 during the challenge phase 184
5.4.3.1. The effect of PAR2 blocking antibody on HDM-induced allergic airway inflammation 185
5.4.3.2. The effect of PAR2 blocking antibody on HDM-induced lung inflammation 186
5.4.3.3. The effect of PAR2 blocking antibody on HDM-induced AHR 187
5.5. Discussion 188
6. The effect of pharmacological inhibition of TRPV4 during allergen challenge in allergic airway disease models 198
6.1. Introduction 199
6.2. Hypothesis and aims 200
6.3. Methods 200
6.3.1. Validation of TRPV4 antagonists 200
6.3.1.1. Determination of IC_{50} in human, rat, guinea pig and mouse models 200
6.3.1.2. Characterisation of GSK2798745 in murine TRPV4 PD model 200
6.3.1.2.1. GSK2798745 dose response 200
6.3.1.2.2. GSK2798745 time course study 201
6.3.1.3. Characterisation of GSK2193874 in rat TRPV4 PD model 201
6.3.1.4. Characterisation of GSK2798745 in rat TRPV4 PD model 202
6.3.2. TRPV4 antagonists in murine HDM model 202
6.3.3. TRPV4 antagonists in rat OVA model 204
6.4. Results 206
6.4.1. Determination of IC_{50} in human, rat, guinea pig and mouse models 206
6.4.2. Characterisation of GSK2798745 in murine TRPV4 PD model 206
6.4.3. The effect of TRPV4 antagonists in murine HDM model of AAD 208
7.2.1.1. The effect of GSK279 on HDM-induced airway inflammation 209
7.2.1.2. The effect of GSK279 on HDM-induced lung inflammation 211
7.2.1.3. The effect of GSK279 on HDM-induced AHR 213
6.4.4. Characterisation of GSK2193874 in rat PD model 214
6.4.5. Characterisation of GSK2798745 in rat PD model 216
6.4.6. The effect of TRPV4 antagonists in rat OVA LAR model 218

6.4.6.1. The effect of GSK219 and GSK279 on OVA-induced LAR 218
6.4.6.2. The effect of GSK219 and GSK279 on OVA-induced airway inflammation 220
6.5. Discussion 222
7. Summary and future directions 231
7.1. Thesis summary 232
7.2. Thesis limitations 236
7.3. Future directions 238
7.3.1. Clarification of the role of TRPV4 in asthma pathogenesis 238
7.3.2. Elucidate the role of ATP and P2X receptors in asthma 240
7.3.3. Validating the role of PAR2 as an asthma target 242
7.3.4. Further characterisation of murine HDM-induced model of AAD 242
7.4. Concluding remarks 243
8. References 245

List of Tables

Table 1.1: Asthma treatment strategy for adults and adolescents older than 12 years old recommended by Global Initiative for Asthma 2021. 29

Table 2.*1*: Forward (FWD) and reverse (REV) primer sequences used in PCR for genotyping of $P2X1^{-/-}$, $P2X4^{-/-}$, $P2X7^{-/-}$ and $PAR2^{-/-}$ mice, respectively. 79

Table 2.2: Primary fluorophore conjugated anti-mouse antibodies used for identification and isolation of mouse immune cell populations..... 88

Table 2.3: List of Taqman® Gene Expression Assays..... 101

Table 3.1: Results of primer multiplex validation. 108

Table 5.1: Results of primer multiplex validation. 174

Table 6.1: Experimental groups in a study investigating TRPV4 antagonist GSK2798745 in the murine house dust mite (HDM) model. 204

Table 6.2: Experimental groups in a study investigating TRPV4 antagonists GSK2193874 and GSK2798745 in the rat Ovalbumin (OVA) model. 205

Table 6.3: pIC_{50} in human, rat, guinea pig (GP) and mouse determined by airway smooth muscle cell (ASMC) or Chinese hamster ovary cell (CHO) Fluorescence Imaging Plate Reader (FLIPR) assays or vagal nerve depolarisation technique (Vagus). 206

List of Figures

Figure 1.1: A summary of the development of type 2 inflammation in asthma. 26
Figure 1.2: $CD4^+$ T cell subsets. 33
Figure 1.3: Schematic representation of ATP signalling. 49
Figure 1.4: Sensory and parasympathetic innervation of the airways. 50
Figure 1.5: TRPV4 signalling in lung disease. 56
Figure 1.6: TRPV4 deficiency ($TRPV4^{-/-}$) abolished airway hyperresponsiveness (AHR) and eosinophilic airway inflammation in murine house dust mite (HDM) model of allergic airway disease. 63
Figure 1.7: Pannexin-1 deficiency ($Panx\text{-}1^{-/-}$) abolished airway hyperresponsiveness (AHR) and eosinophilic airway inflammation in murine house dust mite (HDM) model of allergic airway disease. 64
Figure 2.1: Principles of flow whole body plethysmography and a respiratory waveform. 70
Figure 2.2: Murine house dust mite (HDM)-induced allergic airway disease (AAD) model protocol. 73
Figure 2.3: Rat ovalbumin (OVA)-induced allergic airway disease model protocol. 74
Figure 2.4: A study protocol for NLRP3 inflammasome activation model. 75
Figure 2.5: A protocol for TRPV4 pharmacodynamic model. 76
Figure 2.6: Gating strategy for the identification of $CD4^+$ T cells, $CD8^+$ T cells, B cells and natural killer (NK) cells. 82
Figure 2.7: Gating strategy for the identification of innate lymphoid cell (ILC) populations. 83
Figure 2.8: Gating strategy for isolation of group 2 innate lymphoid cells (ILC2s), $CD4^+$ T cells and $CD8^+$ T cells. 84
Figure 2.9: Gating strategy for the identification of myeloid cells. 86
Figure 2.10: Gating strategy for the identification and isolation of lung dendritic cells (DCs). 87
Figure 2.11: Examples of Taqman® Gene Expression Assay multiplex validation. 100
Figure 3.1: Time course study design. 106
Figure 3.2: House dust mite (HDM) challenge evoked type 2 inflammation. 111
Figure 3.3: Type 1 and type 17 immune responses upon house dust mite (HDM) challenge. 112

Figure 3.4: House dust mite (HDM) challenge was associated with Th2 polarisation of $CD4^+$ T cells. 114
Figure 3.5: House dust mite (HDM) challenge was associated with dysregulation of alarmins, but triggered no changes in type 2 cytokine expression in ILC2s. 116
Figure 3.6: Dendritic cell (DC) dynamics upon house dust mite (HDM) challenge. 118
Figure 3.7: *Trpv4* and *Panx-1* expression in key immune cells. 120
Figure 3.8: P2XR expression in the HDM time course study. 122
Figure 3.9: Gene expression of P2X receptors on key immune cells. 123
Figure 4.1: Validation of P2X7 deficient ($P2X7^{-/-}$) mice. 144
Figure 4.2: The effect of P2X7 deficiency ($P2X7^{-/-}$) on house dust mite (HDM)-induced allergic airway inflammation 145
Figure 4.3: The effect of P2X7 deficiency ($P2X7^{-/-}$) on house dust mite (HDM)-induced lung inflammation. 147
Figure 4.4: The effect of P2X7 deficiency ($P2X7^{-/-}$) on cytokine and chemokine production. 148
Figure 4.5: The effect of P2X7 deficiency ($P2X7^{-/-}$) on IgE antibody production. 149
Figure 4.6: The effect of P2X7 deficiency ($P2X7^{-/-}$) on house dust mite (HDM) induced airway hyper-responsiveness. 150
Figure 4.7: Validation of P2X4 mice. 151
Figure 4.8: The effect of P2X4 deficiency ($P2X4^{-/-}$) on house dust mite (HDM)-induced allergic airway inflammation 152
Figure 4.9: The effect of P2X4 deficiency ($P2X4^{-/-}$) on house dust mite (HDM)-induced lung inflammation. 153
Figure 4.10: The effect of P2X4 deficiency ($P2X4^{-/-}$) on cytokine and chemokine production. 154
Figure 4.11: The effect of P2X4 deficiency ($P2X4^{-/-}$) on IgE antibody production. 155
Figure 4.12: The effect of P2X4 deficiency ($P2X4^{-/-}$) on house dust mite (HDM) induced airway hyper-responsiveness. 156
Figure 4.13: Representative genotyping gel of P2X1 mice. 157
Figure 4.14: The effect of P2X1 deficiency ($P2X1^{-/-}$) on house dust mite (HDM)-induced allergic airway inflammation 158

Figure 4.15: The effect of P2X1 deficiency (P2X1$^{-/-}$) on house dust mite (HDM)-induced lung inflammation. 159
Figure 4.16: The effect of P2X1 deficiency (P2X1$^{-/-}$) on house dust mite (HDM) induced airway hyper-responsiveness. 160
Figure 5.1: Pharmacological inhibition of PAR2 during allergen challenge in the mouse house dust mite (HDM) model – a study schematic. 176
Figure 5.2: PAR2 signalling in the house dust mite (HDM) time course study. 177
Figure 5.3: *Par2* expression in key immune cells in the house dust mite (HDM) model of allergic airway disease. 177
Figure 5.4: Validation of PAR2 deficient (PAR2$^{-/-}$) mice. 179
Figure 5.5: The effect of PAR2 deficiency (PAR2$^{-/-}$) on house dust mite (HDM)-induced allergic airway inflammation 180
Figure 5.6: The effect of PAR2 deficiency (PAR2$^{-/-}$) on HDM-induced lung inflammation 181
Figure 5.7: The effect of PAR2 deficiency (PAR2$^{-/-}$) on cytokine and chemokine production. 182
Figure 5.8: The effect of PAR2 deficiency (PAR2$^{-/-}$) on antibody production. 183
Figure 5.9: The effect of PAR2 deficiency on airway hyper-responsiveness. 184
Figure 5.10: The effect of PAR2 antibody on house dust mite (HDM)-induced airway inflammation. 185
Figure 5.11: The effect of PAR2 antibody on house dust mite (HDM)-induced lung inflammation. 187
Figure 5.12: The effect of PAR2 antibody on airway hyper-reactivity. 188
Figure 6.1: A schematic representation of the study investigating the effect of GSK2798747 on house dust mite (HDM)-induced allergic airway inflammation and airway hyper-responsiveness (AHR) in murine allergic airway disease model. 203
Figure 6.2: GSK2798745 dose response in murine TRPV4 pharmacodynamic (PD) model. . 207
Figure 6.3: The duration of GSK2798745 efficacy in murine TRPV4 pharmacodynamic (PD) model. 208
Figure 6.4: The efficacy of TRPV4 antagonist on allergic airway inflammation in the murine house dust mite (HDM) model. 210
Figure 6.5: The efficacy of TRPV4 antagonist on allergic lung inflammation in the murine house dust mite (HDM) model. 212

Figure 6.6: The efficacy of TRPV4 antagonist on airway hyper-responsiveness (AHR) in murine house dust mite (HDM) model. 214
Figure 6.7: GSK2193874 dose response in the rat TRPV4 pharmacodynamic (PD) model. . 216
Figure 6.8: GSK2798745 dose response in rat TRPV4 pharmacodynamic (PD) model. 217
Figure 6.9: The efficacy of TRPV4 antagonists on late asthmatic response (LAR) in rat Ovalbumin (OVA) model. 219
Figure 6.10: The efficacy of TRPV4 antagonists on allergic airway inflammation in rat Ovalbumin (OVA) model. 222

List of Abbreviations

5-HT	Serotonin
AA	Arachidonic acid
AAD	Allergic airway disease
AAI	Allergic airway inflammation
ACh	Acetylcholine
ADP	Adenosine diphosphate
AHR	Airway hyperresponsiveness
ALT	*Alternaria* sp.
Alum	Aluminium hydroxide
AM	Alveolar macrophages
AMP	Adenosine monophosphate
AP1	Alkaline protease 1
APC	Antigen presenting cell
ASM	Airway smooth muscle
Asp	*Aspergillus fumigatus*
ATP	Adenosine triphosphate
AUC	Area under curve
BAL	Bronchoalveolar lavage
BN	Brown-Norway
BSA	Bovine serum albumin
CCL	C-C motif chemokine ligand
CCR	C-C chemokine receptor
cDCs	Conventional DCs
CE	Cockroach extract
CHO	Chinese hamster ovary
COPD	Chronic obstructive pulmonary disease
CysLTs	Cysteinyl leukotrienes
DAMPs	Danger-associated molecular patterns
DC	Dendritic cell
EAR	Early asthmatic response
ECP	Eosinophil cationic protein
EDN	Eosinophil-derived neurotoxin
EGF	Epidermal growth factor
ELISA	Enzyme-linked immunosorbent assay
EPO	Eosinophil peroxidase
FACS	Fluorescence activated cell sorting
FCS	Fetal calf serum
FEV_1	Forced expiratory volume in first second
FLIPR	Fluorescence imaging plate reader
FMO	Fluorescence minus one
FSC	Forward scatter
FWBP	Flow whole body plethysmography
GINA	Global Initiative for Asthma
GM-CSF	Granulocyte-macrophage colony-stimulating factor
GP	Guinea pig
GPCR	G-protein coupled receptor
GSK101	GSK1016790a
GSK219	GSK2193874
GSK279	GSK2798745
GWAS	Genome-wide association studies
HDM	House dust mite
i.n.	Intranasal
i.p.	Intraperitoneal
i.t.	Intratracheal
IC_{50}	Half-maximal inhibitory concentration
ICS	Inhaled corticosteroid

Ig	Immunoglobulin
IL	Interleukin
IL-4Rα	IL-4 receptor α-subunit
ILC2s	Group 2 innate lymphoid cells
IFNγ	Interferon gamma
IP_3	Inositol triphosphate
IPF	Idiopathic pulmonary fibrosis
KH	Krebs-Henseleit
KO	Knockout
LABA	Long acting β2 adrenoreceptor agonists
LAMA	Long acting muscarinic receptor antagonists
LLOQ	Lower limit of quantification
LPS	Lipopolysaccharide
Lti	Lymphoid tissue-inducer
LTRA	Leukotrienes receptor antagonists
MBP	Major basic protein
MCP	Monocyte chemoattractant protein
MHC II	Major histocompatibility complex
MIP-1α	Macrophage inflammatory protein 1 alpha
MLNs	Mediastinal lymph nodes
moDCs	Monocyte-derived DCs
NK	Natural killer cells
NO	Nitric oxide
NOD	Nucleotide-binding olimerization domain
NLRs	NOD-like receptors
OCS	Oral corticosteroid
OVA	Ovalbumin
PAMPs	Pathogen-associated molecular patterns
Panx	Pannexin
PAR2	Protease activated receptor 2
PBF	PBS supplemented with 10 % FCS
PBS	Phosphate buffered saline
PCR	Polymerase chain reaction
PD	Pharmacodynamic
pDCs	Plasmacytoid DCs
PEF	Peak expiratory flow
Penh	Enhanced pause
PIF	Peak inspiratory flow
PK	Pharmacokinetic
PLC	Phospholipase C
PRRs	Pattern recognition receptors
qRT-PCR	Quantitative real time polymerase chain reaction
RANTES	Regulated upon Activation, Normal T Cell Expressed and Presumably Secreted chemokine
RORγt	Retinoid-related orphan receptor γt
SABA	Short acting β2 adrenoreceptor agonists
s.c.	Subcutaneous
SSC	Side scatter
STAT	Signal transducer and activator of transcription
TCR	T cell receptor
TDI	Toluene diisocyanate
Te	Expiration time
Tfh	T follicular helper cell

TGF-β	Transforming growth factor beta
Th	T helper cell
TLRs	Toll-like receptors
TNF-R	TNF receptors
TNF-α	Tumour necrosis factor alpha
Tr	Relaxation time
Treg	Regulatory T cells
TRP	Transient receptor potential
TSLP	Thymic stromal lymphopoietin
VCAM-I	Vascular cell adhesion molecule-I
VIP	Vasoactive intestinal peptide
WT	Wild type

1. Introduction

1.1. Asthma in general

1.1.1. Definition of asthma

Asthma is a chronic obstructive lung disease estimated to have affected more than 270 million people worldwide in 2017 (James et al. 2018). In the UK alone approximately 10 % of the population (1.1 million children and 4.3 million adults) are currently treated for asthma (Asthma UK 2021). Asthma is characterised by chronic airway inflammation, recurrent respiratory symptoms such as wheeze, shortness of breath, chest tightness or cough, and variable airflow obstruction which is often triggered by allergen or irritant exposure, viral infections, exercise or weather changes (Global Initiative for Asthma 2021). The severity of the disease varies considerably. The majority of asthmatic patients presents with a mild to moderate disease with symptoms and airflow limitation resolving spontaneously or in response to medication (Global Initiative for Asthma 2021). However, approximately 5 to 10 % of asthmatic patients have a severe form of the disease with poor disease control and refractory symptoms despite high-intensity therapy (Chung et al. 2014, Price et al. 2014). Severe asthma accounts for much of the asthma related morbidity and mortality, it significantly impacts patients' quality of life and is also associated with great socioeconomic burden (Nunes et al. 2017, Kuruvilla et al. 2019).

1.1.2. Asthma heterogeneity

Asthma was traditionally viewed as T helper (Th) 2 cell driven disorder. Currently, asthma is considered an umbrella diagnosis for a collection of distinct pathological processes (endotypes) leading to many different manifestations (phenotypes), which are all characterised by recurrent respiratory symptoms and variable airflow obstruction (Kuruvilla et al. 2019). Generally, asthma is divided into Th2 high (eosinophilic) endotype, encompassing atopic early-onset asthma, late-onset eosinophilic asthma and aspirin-exacerbated respiratory disease phenotypes, and non-Th2 (non-eosinophilic) endotype with phenotypes associated with obesity, smoking or old age (Kuruvilla et al. 2019). Atopic asthma is the most prevalent phenotype (Kuruvilla et al. 2019) and is thus the focus of this thesis.

1.1.3. Atopic asthma pathophysiology

In atopic asthma, individuals are sensitised to environmental aeroallergens originating from pets, pollen, fungi and house dust mites (HDM) (Kuruvilla et al. 2019). Antigen presenting cells

(APCs), such as dendritic cells (DCs) process the allergens and present them to T cells in local draining lymph nodes via major histocompatibility complex II (MHC II) (Lloyd and Snelgrove 2018). In atopic individuals this triggers polarisation of naïve Th cells into Th2 cells that secrete type 2 cytokines interleukin (IL)-4, IL-5 and IL-13 (Lloyd and Snelgrove 2018). A subset of T cells migrates to B cell zones and differentiate into T follicular helper (Tfh) cells which promote B cell responses and immunoglobulin (Ig) E class switching (Lloyd and Snelgrove 2018). Other Th2 cells egress from the lymph node and enter the tissue where they further produce type 2 cytokines (Lloyd and Snelgrove 2018). IgE immune complexes enter the circulation and bind to high-affinity FC receptors FcεR1 on mucosal mast cells and basophils (Lloyd and Snelgrove 2018) (Figure 1.1).

Subsequent allergen exposures in sensitised individuals can trigger episodes of bronchoconstriction, airway hyperresponsiveness (AHR) and chronic airway inflammation. Binding of allergens to allergen-specific IgE triggers degranulation of mast cells and basophils and release of cysteinyl leukotrienes (CysLTs) LTC_4, LTD_4, prostaglandin PGD_2 and histamine (Gauvreau et al. 2015). The release of these mediators is responsible for bronchoconstriction, mucus secretion and airway oedema (Gauvreau et al. 2015). This early asthmatic response (EAR) was characterised in clinical allergen provocation studies and is clinically recognised as a decline in lung function (forced expiratory volume in first second (FEV_1) decline greater than 20 % of baseline) within minutes of allergen exposure that subsides within a few hours (Gauvreau et al. 2015). In approximately 60 – 80 % of patients, bronchoconstriction recurs 3 to 4 hours after the exposure with a peak 6 to 12 hours after the exposure and is characterised by a decline in FEV_1 greater than 15 %, AHR and accompanying eosinophilic airway inflammation (Diamant et al. 2013, Gauvreau et al. 2015) (Figure 1.1).

In addition to the activation of mast cells, allergens trigger activation of Th2 cells and group 2 innate lymphoid cells (ILC2s) that are responsible for type 2 inflammation in the airways (Lloyd and Snelgrove 2018). Allergen exposure induces a release of prototypical cytokines IL-33, IL-25 and thymic stromal lymphopoietin (TSLP) from the airway epithelium (Lloyd and Snelgrove 2018). Subsequent activation of lung DCs promotes recruitment of circulating Th2 cells and activation of lung resident memory Th2 cells (Ito et al. 2005, Hondowicz et al. 2016, Bosnjak et al. 2019). In addition, epithelial derived cytokines activate ILC2s to produce type 2 cytokines, further stimulate DC - Th2 cell interaction or activate Th2 cells directly (Oliphant et

al. 2014, Halim et al. 2016, Halim et al. 2018). Activated Th2 cells are a source of type 2 cytokines as well as IL-2 which is crucial for ILC2 proliferation (Wilhelm et al. 2011, Mirchandani et al. 2014, Oliphant et al. 2014). IL-4, IL-5 and IL-13 are the main orchestrators of the hallmark pathophysiological changes observed in atopic asthma, including airway eosinophilia, excessive mucus production, airway remodelling and AHR (Lloyd and Snelgrove 2018) (Figure 1.1).

AHR is defined as the predisposition of the airways to narrow excessively in response to stimuli that would exert little effect in healthy individuals (Chapman and Irvin 2015). The presence of AHR increases a risk of lung function decline in asthmatic patients, while its severity is associated with an increased asthma severity, need for asthma therapy and risk of exacerbations (Chapman and Irvin 2015). The mechanisms behind AHR are complex and not yet fully understood. Airway structural changes (airway smooth muscle (ASM) thickening, increased collagen deposition), increased ASM contractility, airway inflammation and changes in the airway nervous system are all thought to contribute to the development of AHR (Chapman and Irvin 2015, Pincus et al. 2021).

Airway remodelling is another hallmark feature of asthma and encompasses changes in the airway structure that are often irreversible and can contribute to AHR and lead to a permanent loss of lung function (Holgate et al. 2015). These typically include epithelial damage, basal membrane thickening, ASM hypertrophy, neuronal proliferation, angiogenesis, goblet cell hyperplasia and excessive mucus production (Holgate et al. 2015, Pincus et al. 2021). Structural airway changes can be present even in mild disease and typically worsen with disease severity (Saglani and Lloyd 2015).

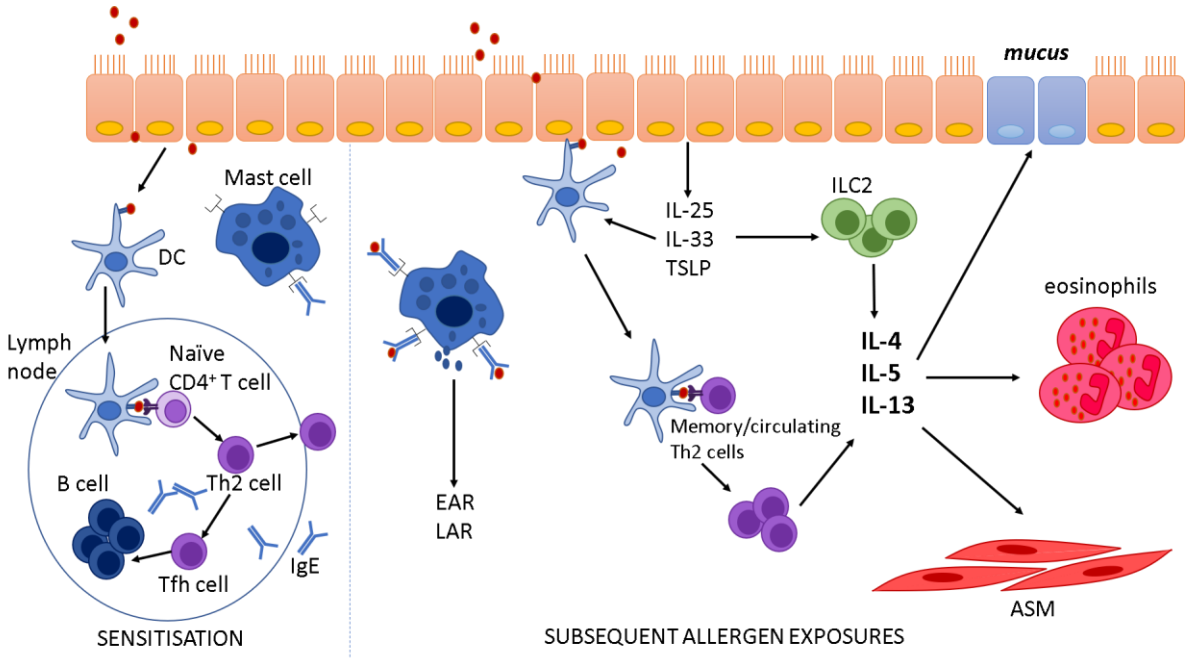


Figure 1.1: A summary of the development of type 2 inflammation in asthma.

During a first allergen encounter (sensitisation phase) allergens are taken up by dendritic cells (DCs) and in the regional lymph nodes presented to naïve CD4+ T cells which in turn polarise into type 2 T helper (Th2) cells. A subset to Th2 cells differentiates into follicular Th cells (Tfh) and stimulates IgE production by B cells. IgE enter the circulation and bind to Fc receptors on mast cells. The remaining Th2 cells egress from lymph nodes and enter the circulation and local tissue. Subsequent allergen exposures trigger degranulation of mast cells which is responsible for early and late asthmatic reaction (EAR and LAR, respectively). Airway epithelial cells release cytokines IL-25, IL-33 and TSLP which stimulate DCs to present allergens to Th2 cells. Activated Th2 cells start releasing type 2 cytokines IL-4, IL-5 and IL-13. Type 2 cytokines are also produced by group 2 innate immune cells (ILC2s) that are directly activated by epithelial derived cytokines. Type 2 cytokines are responsible for hallmark features of asthma, including increased mucus production, eosinophilia and AHR.

1.1.4. Treatment of asthma

The goal of asthma treatment is achieving good asthma control. Asthma control has two aspects, controlling the symptoms and minimising a future risk of adverse outcomes such as exacerbations, persistent airflow limitation, treatment side-effects and asthma-related death (Global Initiative for Asthma 2021).

Asthma medications are divided into three categories: reliever medications, controller medications, and add-on therapies (Global Initiative for Asthma 2021). Reliever medications are used as-needed to relieve breakthrough symptoms during asthma worsening or exacerbations (Global Initiative for Asthma 2021). β2 adrenoreceptor agonists are the main

bronchodilator medications to relieve smooth muscle spasm due to their effect on β2 adrenoreceptors on ASM (Williams and Rubin 2018). Short acting β2 adrenoreceptor agonists (SABA) are effective within minutes and are used for the treatment of acute symptoms. The duration of the effect is short (3 – 6 hours) and long acting β2 adrenoreceptor agonist (LABA) are used instead in chronic asthma management (Williams and Rubin 2018). However, the use of β agonists as monotherapy has been associated with worsened asthma control, partially due to poor adherence to controller therapies (Williams and Rubin 2018), thus the use of inhaled corticosteroid (ICS)- (LABA) combination as a reliever therapy has been advised instead since 2019 (Global Initiative for Asthma 2021).

Controller medications are used to reduce airway inflammation, control symptoms and reduce future risk of adverse outcomes and are the cornerstone of asthma management (Global Initiative for Asthma 2021). ICS (e.g. budesonide, beclomethasone) are the gold standard anti-inflammatory medications (Global Initiative for Asthma 2021). Briefly, they act on glucocorticoid receptor and translocate to the nucleus of various cells, broadly suppressing the expression of many proinflammatory cytokines and chemokines involved in asthma leading to suppression of eosinophilic airway inflammation (Barnes 2018). Steroids are the most effective treatment available for Th2 asthma and suppress airway inflammation in most patients with asthma (Barnes 2018).

Global Initiative for Asthma (GINA) recommends a stepwise approach to pharmacological treatment to achieve optimal treatment in asthma (Global Initiative for Asthma 2021) (summarised in Table 1.1). The preferred approach is using a combined ICS-LABA (ICS-formoterol preferred option) as a reliever and/or maintenance therapy (Global Initiative for Asthma 2021). If symptoms are mild and occurring less than 4 – 5 times a week (Steps 1 and 2), combined ICS-LABA therapy is recommended as needed for relief of symptoms (Global Initiative for Asthma 2021). When symptoms occur on most days or patients are waking due to asthma (Step 3) low dose ICS-LABA is recommended as maintenance and reliever therapy (Global Initiative for Asthma 2021). If symptoms occur daily, at night or are accompanied by low lung function (Step 4), medium dose ICS-LABA is recommended as maintenance and reliever therapy (Global Initiative for Asthma 2021). Patients are reviewed regularly to monitor symptom control and the response to treatment changes (Global Initiative for Asthma 2021). Treatment may be stepped down if asthma is well controlled or stepped up if

symptoms persist (Global Initiative for Asthma 2021). Some patients with severe asthma remain uncontrolled despite correct inhaler technique and good adherence with Step 4 treatment (Step 5) (Global Initiative for Asthma 2021). High ICS-LABA may be considered in these patients, but generally provides little additional benefit (Global Initiative for Asthma 2021). These patients may benefit from add-on bronchodilators such as long acting muscarinic receptor antagonists (LAMA, e.g. tiotropium) and leukotrienes receptor antagonists (LTRA, e.g. montelukast)(Global Initiative for Asthma 2021). Low dose oral corticosteroids (OCS) may be effective for some adult patients, however they are often associated with substantial side effects (Chung et al. 2014, Lefebvre et al. 2015, Barnes 2018, Global Initiative for Asthma 2021). A subgroup of patients with Th2 high endotype may additionally benefit from biologics targeting specific inflammatory mediators (Global Initiative for Asthma 2021). Currently available biologics for the treatment of severe asthma are anti-IgE (omalizumab), anti-IL-5 (mepolizumab, reslizumab), antil-IL-5R (benralizumab), anti-IL-4Rα (dupilumab) and anti-TSLP (tezepelumab) therapies (Global Initiative for Asthma 2021, US Food and Drug Administration 2021).

Despite the advances in asthma treatment, a subset of patients with poorly controlled asthma remains (González Barcala et al. 2010, Chung et al. 2014, Price et al. 2014, Beasley et al. 2020). In these patients corticosteroids are less effective at supressing airway inflammation and often high doses of ICS or even oral corticosteroids are required, resulting in adverse effects such as increased of fracture, cataracts, adrenal suppression and in children growth retardation (Chung et al. 2014, Lefebvre et al. 2015, Barnes 2018). In addition, severe asthma is associated with more symptoms and exacerbations as well as higher levels of anxiety and depression, further negatively impacting patients' quality of life (Shaw et al. 2015). Therefore, further understanding of molecular pathways driving airway asthma pathogenesis is needed.

Table 1.1: Asthma treatment strategy for adults and adolescents older than 12 years old recommended by Global Initiative for Asthma 2021.

Adapted from (Global Initiative for Asthma 2021). HDM – house dust mite. ICS – inhaled corticosteroid. LABA – long acting β2-adrenoreceptor agonist. LAMA – long acting muscarinic receptor. LTRA – leukotrienes receptor antagonists. OCS – oral corticosteroid. SABA – short acting β2-adrenoreceptor agonist. SLIT – sublingual immunotherapy.

<table>
<tr><td></td><td></td><td></td><td></td><td></td><td>STEP 5</td></tr>
<tr><td></td><td></td><td></td><td></td><td>STEP 4</td><td rowspan="3">Add-on LAMA
Phenotypic assessment and consider anti-IgE, anti-IL-5/5R, anti-IL-4
Consider high dose ICS-formoterol</td></tr>
<tr><td></td><td></td><td></td><td>STEP 3</td><td rowspan="3">Medium dose maintenance ICS-formoterol</td></tr>
<tr><td></td><td></td><td>STEP 2</td><td rowspan="3">Low maintenance dose ICS-formoterol</td></tr>
<tr><td rowspan="2">Preferred approach: Controller and preferred reliever</td><td>STEP 1</td><td rowspan="2">As-needed low dose ICS-formoterol</td></tr>
<tr><td rowspan="2">As-needed low dose ICS-formoterol</td></tr>
<tr><td colspan="5">As-needed low dose ICS-formoterol</td></tr>
<tr><td rowspan="2">Alternative approach:
Controller and alternative reliever (if preferred approach not possible or not preferred by a patient with no exacerbations on current therapy)</td><td>Low dose ICS whenever SABA taken</td><td>Low dose maintenance ICS</td><td>Medium dose maintenance ICS-LABA</td><td>Medium/high dose ICS-LABA</td><td>Add-on LAMA
Phenotypic assessment and consider anti-IgE, anti-IL-5/5R, anti-IL-4
Consider high dose ICS-formoterol</td></tr>
<tr><td colspan="5">As-needed SABA</td></tr>
<tr><td>Other controller options for either track</td><td></td><td>Add-on LTRA or HDM SLIT</td><td>Medium dose ICS
Add-on LTRA or HDM SLIT</td><td>Add LAMA or LTRA or HDM SLIT or high dose ICS</td><td>Add azithromycin (adults) or LTRA
Low dose OCS</td></tr>
</table>

1.2. Airway epithelium in asthma

The airway epithelium is the first barrier against allergens, microorganisms, fungi, viruses and environmental pollutants and is now considered an active player in asthma pathogenesis (Calvén et al. 2020). Genome-wide association studies (GWAS) have found several genes expressed by the airway epithelium that are related to epithelial barrier function (such as *PCDH1, CDHR3* and *ORMDL3*) and mucin production (*MUC5AC* and *CLCA1*) to be associated with asthma (Kamada et al. 2004, Moffatt et al. 2007, Koppelman et al. 2009, Bønnelykke et al. 2014, Shrine et al. 2019, Calvén et al. 2020). In asthma, airway epithelial function is impaired and disruption of tight junction and other adhesion molecules as well as a detachment of ciliated cells has been observed in asthmatic patients (Xiao et al. 2011, Calvén et al. 2020). The mechanism behind epithelial disfunction is not yet fully understood. Allergens such as HDM and *Alternaria* sp. (ALT) contain proteases that can cleave epithelial tight junction proteins or act on protease activated receptor 2 (PAR2) (Wan et al. 1999, Wan et al. 2000, Jacquet 2011, Snelgrove et al. 2014). Th2 cytokines IL-4 and IL-13 have an inhibitory effect on expression of adhesion proteins, further disrupting epithelial barrier (Calvén et al. 2020).

In addition to the barrier function, the airway epithelium can initiate and orchestrate immune responses to environmental stimuli, including allergens (Calvén et al. 2020). Airway epithelial cells express numerous pattern recognition receptors (PRRs) such as Toll-like receptors (TLRs) and nucleotide-binding olimerization domain (NOD)-like receptors (NLR), scavenger receptors as well as and PARs (D'Andrea et al. 1998, Schmidlin et al. 2002, Jairaman et al. 2016, Calvén et al. 2020). These receptors recognise pathogen-associated molecular patterns (PAMPs) and danger-associated molecular patterns (DAMPs) such as adenosine triphosphate (ATP) which trigger the release of inflammatory cytokines, chemokine and endogenous danger signals that alert both innate and adaptive immune cells and orchestrate their responses to environmental insults (Calvén et al. 2020). In asthma, airway epithelium has been recognised as a primary source of IL-25, IL-33 and TSLP which induce type 2 immune responses upon allergen exposure (Kouzaki et al. 2011, Kurokawa et al. 2011, Hardman et al. 2013, Kouzaki et al. 2013, Wang et al. 2018b, Hong et al. 2020). In addition, airway epithelium is also an important source of ATP, growth factors (e.g. granulocyte-macrophage colony-stimulating factor (GM-CSF)), chemokines (eotaxins, CCL17, CCL20 and MCP-1) as well as

proinflammatory cytokines such as IL-1β which promote allergic airway inflammation (Nathan et al. 2009, Osterlund et al. 2009, Kouzaki et al. 2011, Snelgrove et al. 2014, Calvén et al. 2020).

1.3. Inflammatory cells in asthma

1.3.1. T cells

T cells are central coordinators of the immune responses, characterised by the expression of T cell receptor (TCR) which is crucial for the initiation and specificity of the adaptive immune response (Regateiro et al. 2020). Based on the expression of glycoproteins CD4 or CD8 they are divided into $CD4^+$ T cells and $CD8^+$ T cells, respectively (Regateiro et al. 2020).

$CD4^+$ T cells numbers are increased in the airways of asthmatic patients in stable disease and after an allergen challenge, and have been traditionally considered responsible for airway inflammation in asthma (Metzger et al. 1987, Gerblich et al. 1991, Walker et al. 1991, Robinson et al. 1993a). Experimental animal models have confirmed their role in allergic airway disease (AAD) as depletion of $CD4^+$ T cells abolished allergic airway inflammation and AHR in rodents (Gavett et al. 1994, Foster et al. 2002, Joetham et al. 2005, Raemdonck et al. 2016).

$CD4^+$ T cells can be divided into Th cells, regulatory T cells (Treg) and Tfh cells (Figure 1.2), each subset playing a role in asthma pathogenesis (Regateiro et al. 2020). Depending on the cytokine milieu Th cells are polarised into Th1, Th2, Th9 or Th17 cells when presented with antigens (Figure 1.2). Th2 cells have been traditionally viewed as cells fundamental for the development of airway inflammation in asthma (Regateiro et al. 2020). Th2 cells are activated in asthmatic patients and produce high amounts of IL-4, IL-5 and IL-13 which stimulate eosinophils, mast cells, basophils as well as B cells (Metzger et al. 1987, Robinson et al. 1992, Bentley et al. 1993, Robinson et al. 1993a, Regateiro et al. 2020). Upon an initial allergen encounter, Th2 cells acquire a memory phenotype and are retained in the lungs and immediately respond to subsequent allergen exposures (Marathias et al. 1991, Walker et al. 1991, Robinson et al. 1993b, Mojtabavi et al. 2002, Hondowicz et al. 2016, Bosnjak et al. 2019). Th9 cells are responsible for IL-9 production which contributes to the development of allergic airway inflammation by enhancing Th2 cytokine production as well as eosinophil, basophil and mast cell differentiation (Shimbara et al. 2000, Regateiro et al. 2020). Interferon

gamma (IFNγ) producing Th1 and IL-17A producing Th17 cells have also be found in elevated numbers in asthmatic patients and are thought to be responsible for underlying neutrophilic inflammation, particularly in severe and refractory disease (Krug et al. 1996, Al-Ramli et al. 2009, Wisniewski et al. 2018).

In contrast to Th cells, the function of Tregs is to suppress or modulate the responses of other immune cells to prevent uncontrolled inflammation (Regateiro et al. 2020). Tregs secrete IL-10 or transforming growth factor beta (TGF-β) and can also downregulate the expression of CD80/CD86 on DCs and subsequently block the generation of allergen-specific Th2 cell responses (Martín-Orozco et al. 2017). In asthma, Treg suppressive functions are impaired as reduced Tregs numbers have been found in the lungs of asthmatic patients (Hartl et al. 2007, Lin et al. 2008). Tfh cells are needed for B cell responses and IgE class switching in regional lymph nodes after allergen exposure and depend on IL-4 produced by Th2 cells (Lloyd and Snelgrove 2018).

$CD8^+$ T cells have been initially proposed to balance the responses of $CD4^+$ T cells by producing interferon gamma (IFNγ) (Hinks et al. 2019). However, their role in asthma pathogenesis is not fully understood and conflicting evidence demonstrating both protective as well as pathogenic roles in the development of AAD and AHR have been demonstrated in preclinical studies (Hamelmann et al. 1996, Hansen et al. 1999, Huang et al. 1999, Isogai et al. 2004, Miyahara et al. 2004, Sawicka et al. 2004, Stock et al. 2004, Joetham et al. 2005, Koya et al. 2007, Koya et al. 2009, Takeda et al. 2009, Raemdonck et al. 2016). $CD8^+$ T cells have been found in increased numbers in the airways of asthmatic patients and have been associated with long term function decline and asthma related deaths (Walker et al. 1991, Coyle et al. 1995b, Lee et al. 2001, O'Sullivan et al. 2001, Sawicka et al. 2004, Cho et al. 2005, van Rensen et al. 2005, den Otter et al. 2016). Moreover, $CD8^+$ T cells have a capacity to undergo transcriptional programming from IFNγ producing Tc1 cells to IL-5 and IL-13 producing Tc2 cells which can acquire a memory phenotype and initiate allergen-induced type 2 immune responses (Sawicka et al. 2004, Hinks et al. 2019).

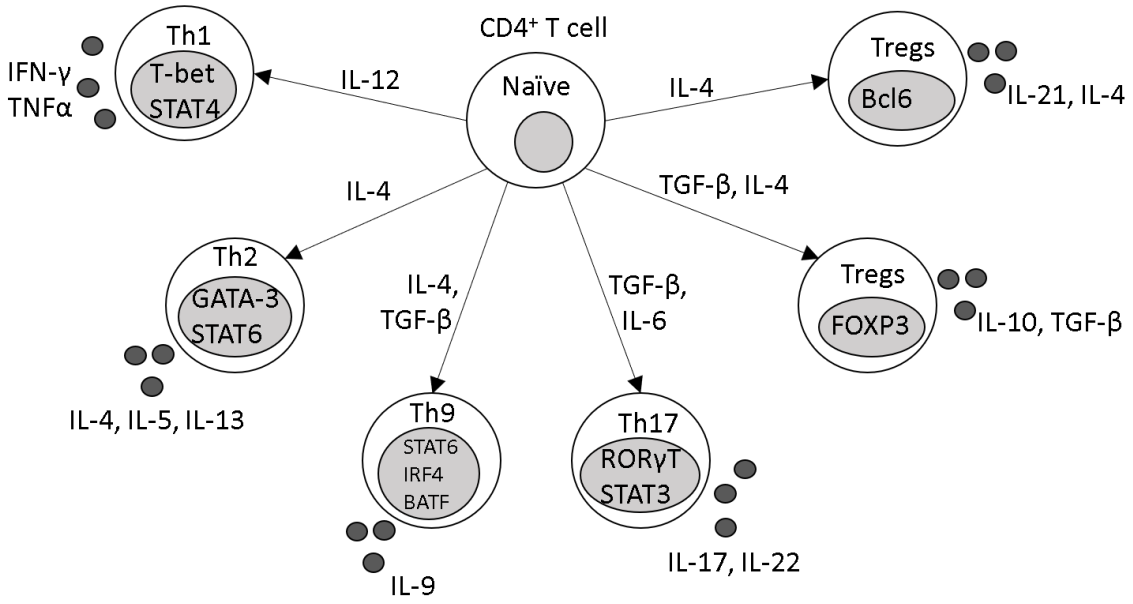


Figure 1.2: CD4⁺ T cell subsets.

Naïve T cells are differentiated into different subsets, depending on cytokine signals. Th1 cells are induced by IL-12 leading to expression of transcription factors (TF) T-bet and signal transducer and activator of transcription (STAT)4 and release of IFN-γ and TNFα. Th2 cells are induced by IL-4, express TFs GATA-3 and STAT6 and release IL-4, IL-5 and IL-13. Th9 cells require IL-4 and TGF-β for their generation, inducing TFs STAT6, IRF4 and BATF and production of IL-9. Th17 cells are induced by TGF-β and IL-6, leading to TFs expression RORγT and STAT3 and release of IL-17 and IL-22. Treg are under regulation of TGF-β and IL-4 and express TFs FOXP3 and release IL-10 and TGF-β. Summarised from (Regateiro et al. 2020).

1.3.2. ILCs

ILCs are a family of cells with lymphoid morphology characterised by a lack of adaptive antigen receptors (Vivier et al. 2018). They are primarily tissue resident cells and accumulate at mucosal surfaces of the lung and intestine, while they are extremely rare in peripheral blood (Vivier et al. 2018). ILCs are divided into 5 subpopulations ILC1, ILC2, ILC3, natural killer (NK) cells and lymphoid tissue-inducer (LTi) cells based on their development, transcriptional requirements and cytokine profiles (Huang et al. 2020). NK cells and ILC1s depend on the T-box transcription factor Tbet for their development and function and produce IFNγ as their main effector cytokine and play a protective role against viral and bacterial infections in mucosal tissues (Huang et al. 2020). In contrast to ILC1s which have not been yet implicated in asthma pathogenesis, natural killer (NK) cells have been shown to contribute to AAD in different manners, depending on the model used. For example NK cells have been shown to promote the development of AAD (Korsgren et al. 1999, Farhadi et al. 2014), prevent

allergen-induced allergic inflammatory responses (Bi et al. 2017, Ferrini et al. 2017, Simons et al. 2017), or are indispensable for the development of allergen-induced pathology (Haspeslagh et al. 2018), depending on the AAD model. LTi and ILC3s are dependent on retinoid-related orphan receptor γt (RORγt) and produce IL-17 and/or IL-22 (Huang et al. 2020). LTi are important during embryonic development, while ILC3s are important in bacterial and viral infections (Vivier et al. 2018, Huang et al. 2020). IL-17A^{+} ILC3s are increased in the bronchoalveolar lavage (BAL) of patients with severe asthma and were proposed to play a role in obesity-related asthma (Kim et al. 2014).

ILC2s are the most pertinent ILC subgroup in asthma pathophysiology and are considered to be the Th2 cell innate counterpart (Lloyd and Snelgrove 2018, Huang et al. 2020). ILC2 numbers are increased in the airways of asthmatic patients and appear to be the predominant source of IL-5 and IL-13 in severe disease (Christianson et al. 2015, Nagakumar et al. 2016, Smith et al. 2016, Nagakumar et al. 2019). ILC2s depend on the transcription factor Gata3 for their development and produce type 2 cytokines IL-4, IL-5 and IL-13 independently of the classical antigen-specific activation that is a hallmark of Th2 cells (Neill et al. 2010, Wilhelm et al. 2011, Klein Wolterink et al. 2012, Lloyd and Snelgrove 2018). Instead, they sense and respond to cytokines and stress signals such as IL-33, IL-25 and TSLP released from multiple cell types in the local environment upon allergen exposure, infection or injury (Lloyd and Snelgrove 2018). ILC2s engage in a complex cross-talk with DCs and Th2 cells to appropriately respond to the perceived environmental threat (Lloyd and Snelgrove 2018). For example, IL-13 produced by ILC2s promotes migration of activated lung DCs into the regional lymph nodes and subsequent Th2 priming (Halim et al. 2014). During antigen rechallenge ILC2-induced responses licence DCs to produce C-C motif chemokine ligand (CCL)17 and ensure Th2 recruitment and an establishment of an effector memory Th2 response at barrier sites (Halim et al. 2016). In addition, ILC2s pose an antigen presenting function and can directly activate Th2 cells and induce IL-2 and IL-4 production (Drake et al. 2014, Mirchandani et al. 2014, Oliphant et al. 2014). Th2-derived cytokines in turn promote ILC2 proliferation and are critical for their cytokine production (Neill et al. 2010, Wilhelm et al. 2011, Drake et al. 2014, Mirchandani et al. 2014, Oliphant et al. 2014). In addition to type 2 cytokines, ILC2s can also produce amphiregulin, the epidermal growth factor (EGF) family member, promoting wound repair after respiratory viral infection or intestinal inflammation (Monticelli et al.

2011, Monticelli et al. 2015). In asthmatic patients amphiregulin levels are increased (Enomoto et al. 2009, Kim et al. 2009, Hirota et al. 2012), however its contribution to wound repair or airway remodelling remains unclear.

1.3.3. Dendritic cells

DCs are specialised antigen presenting cells that play a central role in asthma pathogenesis (Vroman et al. 2017). DCs are not only critical for allergen sensitisation and Th2 priming but are also required for reactivation of memory Th2 cells and initiation of type 2 immune responses upon allergen challenge (Lambrecht et al. 1998, Lambrecht et al. 1999, Julia et al. 2002, van Rijt et al. 2005, Medoff et al. 2009, Plantinga et al. 2013).

Most of our current understanding about DC function in asthma is based on murine studies. Mouse lung DCs are a heterogenous population consisting of type one and type 2 conventional DCs (cDCs), cDC1s and cDC2s and a small population of plasmacytoid DCs (pDCs) under homeostatic conditions (Vroman et al. 2017, Morianos and Semitekolou 2020). Conventional DCs are located in the proximity of airway epithelium with dendrites extending into the airway lumen and are characterised by high expression of CD11c and are differentiated based on the expression of integrins CD103 (specific of cDC1s) and CD11b (specific for cDC2s). Plasmacytoid DCs are primarily based in lung parenchyma and express markers such as CD45R (B220) and PDCA1 (CD317) (Vroman et al. 2017, Morianos and Semitekolou 2020). Under pro-inflammatory conditions monocyte-derived DCs (moDCs) are recruited to the airways and lung parenchyma and are recognised based on the expression of integrins CD11c, CD11b and CD64 (van Rijt et al. 2005, Plantinga et al. 2013, Morianos and Semitekolou 2020).

cDC2s are specialised in antigen presentation to $CD4^+$ T cells and are the predominant DC population associated with allergen sensitisation and Th2 differentiation, although they are also required for the development of type 2 inflammation upon allergen challenge (del Rio et al. 2007, Raymond et al. 2009, Furuhashi et al. 2012, Plantinga et al. 2013, Morianos and Semitekolou 2020). Even though cDC1s are associated with anti-viral and anti-cancer immunity due to their superior antigen cross-presentation to $CD8^+$ T cells, they also are capable of allergen uptake and priming of type 2 immune responses (Sung et al. 2006, Medoff et al. 2009, Raymond et al. 2009, Nakano et al. 2012, Plantinga et al. 2013, Mishra et al. 2015,

Fear et al. 2016, Morianos and Semitekolou 2020). Monocyte-derived DCs are rapidly recruited to the lung upon allergen challenge (van Rijt et al. 2005, Plantinga et al. 2013, Wiesner et al. 2020). Although moDCs have the ability to uptake allergens, they are inferior to cDC2s in their capacity to induce Th2 proliferation and are instead a substantial source of cytokines, chemokines and co-stimulatory signals required for the recruitment and activation of memory Th2 cells during allergen challenge (Masten et al. 1997, Vissers et al. 2001, Huh et al. 2003, van Rijt et al. 2005, Medoff et al. 2009, Plantinga et al. 2013, Mishra et al. 2015). In contrast, pDCs have a limited capacity for allergen uptake and induce tolerance or restrain sensitisation to otherwise harmless protein antigens predominantly by induction of Treg responses (de Heer et al. 2004, Lewkowich et al. 2008, Kool et al. 2009, Lombardi et al. 2012, Plantinga et al. 2013, Morianos and Semitekolou 2020).

The role of human lung DCs in asthma is less defined. Human lung DCs are classified into two myeloid origin DCs BDCA1 (CD1c) expressing DC1s and BDCA3 (CD141) expressing DC2s resembling mouse cDC1s and cDC2s, respectively, and BDCA2 (CD123) expressing pDCs (Vroman et al. 2017, Morianos and Semitekolou 2020). In asthmatic patients, allergen challenge has been associated with recruitment of moDCs and expansion of lung conventional DC populations and enhanced Th2 responses (Moller et al. 1996, Hammad et al. 2001, Jahnsen et al. 2001, Huh et al. 2003, Dua et al. 2010, Dua et al. 2014).

1.3.4. Eosinophils

Eosinophils are granulocytes characterised by a segmented (usually bi-lobed) nucleus that stain with acidophilic dyes (McBrien and Menzies-Gow 2017). Eosinophils are a hallmark feature of Th2 high asthma and contribute to lung tissue damage, airway remodelling and AHR and amplify the ongoing airway inflammation (McBrien and Menzies-Gow 2017).

IL-5 is the major regulator of eosinophil recruitment and activation (McBrien and Menzies-Gow 2017). Although only a weak chemoattractant, IL-5 stimulates eosinophil release from bone marrow to bloodstream, enhances eosinophil chemotactic responsiveness and promotes their survival by inhibiting their apoptosis (McBrien and Menzies-Gow 2017). IL-3 and GM-CSF also promote eosinophil maturation, survival and function, while eotaxins, Regulated upon Activation, Normal T Cell Expressed and Presumably Secreted chemokine (RANTES), monocyte chemoattractant protein (MCP)-3 and MCP-4 bind to C-C chemokine

receptor (CCR)3 and strongly induce chemotaxis of eosinophils (McBrien and Menzies-Gow 2017, Matucci et al. 2019). Eotaxins in particular are responsible for guiding eosinophil migration to the specific sites (McBrien and Menzies-Gow 2017).

Eosinophil granules contain cytotoxic major basic protein (MBP), eosinophil cationic protein (ECP), eosinophil peroxidase (EPO) and eosinophil-derived neurotoxin (EDN) which cause tissue damage upon degranulation (McBrien and Menzies-Gow 2017). MBP, for example, is toxic for airway epithelial cells and is associated with epithelial damage in asthma related death cases (Ayars et al. 1985, Frigas and Gleich 1986). Eosinophils release growth factors and fibrogenic mediators such as TGF-β which promote collagen deposition and ASM proliferation and thus lead to remodelling (Ohno et al. 1996, Humbles et al. 2004, Pégorier et al. 2006).

Eosinophils have also been postulated to play a role in AHR. MBP and EPO have been demonstrated to trigger AHR in animal models of AAD and MBP can additionally trigger mast cell degranulation and subsequent release of histamine, a potent bronchoconstrictor (Gundel et al. 1991, Coyle et al. 1995a, Piliponsky et al. 2003, Ben-Zimra et al. 2013). Eosinophils can also release IL-13 and CysLTs which have been implicated in AHR (Schmid-Grendelmeier et al. 2002, Jacobsen et al. 2015, McBrien and Menzies-Gow 2017). However, eosinophil depletion in AAD models has been shown to be both protective and dispensable for the development of AHR (Humbles et al. 2004, Lee et al. 2004, Fattouh et al. 2011). Even so, patients with eosinophilic bronchitis do not exhibit AHR despite airway eosinophilia, suggesting eosinophilic inflammation alone is not sufficient to induce AHR (McBrien and Menzies-Gow 2017). Indeed, anti-IL-5 therapies have shown a reduction in blood and sputum eosinophilia, but had no effect on LAR or AHR in asthmatic patients (Leckie et al. 2000, Busse et al. 2019).

In addition, eosinophils can promote Th2 inflammation (McBrien and Menzies-Gow 2017). EDN can activate DCs which triggers T cell proliferation (De Yang et al. 2004). Eosinophils also express MHC II, CD80 and CD86 and can present allergens to T cells directly (Shi et al. 2000, Akuthota et al. 2010). They are also capable of releasing type 2 cytokines IL-4 and IL-13 as well as Th2 chemokines CCL17 and CCL22 (Schmid-Grendelmeier et al. 2002, Chen et al. 2004, Liu et al. 2007, Jacobsen et al. 2015).

Although the preclinical studies have not unanimously established the role of eosinophils in the pathogenesis of AAD (Humbles et al. 2004, Lee et al. 2004, Fattouh et al. 2011), the results

of clinical trials with anti-IL-5 treatments have demonstrated an improvement in FEV_1 and reduced risk of exacerbations in a subgroup of severe asthma patients with high eosinophil counts (Busse et al. 2019) as further discussed in section 1.4.1.3.

1.3.5. Mast cells

Mast cells are a small heterogenous long-lived tissue resident cell population that primarily act as sensors of the surrounding environment (Bradding and Arthur 2016). They are developed from a myeloid progenitor in the bone marrow and terminally differentiate in tissue (Bradding and Arthur 2016). In healthy people mast cells are commonly found in bronchial submucosa, however in asthmatic patients they additionally localise in airway epithelium and form characteristic bundles within ASM, which are thought to be responsible for variable airflow obstruction and AHR (Bradding et al. 1995, Brightling et al. 2002, Bradding and Arthur 2016).

Mast cells contain granules with histamine, CysLTs (LTC_4, LTD_4, LTE_4), prostaglandins (PGD_2) and proteases such as tryptase and chymase, that induce bronchoconstriction, mucus secretion and vascular leakage (Bradding and Arthur 2016). Mast cells are stereotypically activated by allergens cross-linking IgE-FcεRI complexes within minutes of allergen exposure and release histamine, LTC_4 and PGD_2 triggering EAR and contributing to LAR (Bradding and Arthur 2016). In addition, mast cells express numerous other receptors which mediate IgE-independent activation of mast cells by mediators such as IL-33, tumour necrosis factor alpha (TNF-α), proteases or complement (Hughes et al. 1995, Oskeritzian et al. 2005, Ho et al. 2007, Iikura et al. 2007, Bradding and Arthur 2016). There is evidence of ongoing mast cell degranulation and heightened activation state in asthma (Bradding and Arthur 2016). For example, BAL tryptase levels are increased in stable asthmatics compared to healthy controls and mast cells isolated from asthmatic patients express IL-4, IL-5, IL-6, IL-13, TNF-α, TSLP and amphiregulin, contributing to AHR, airway inflammation and airway remodelling (Wenzel et al. 1988, Broide et al. 1991, Bradding et al. 1994, Alvarez et al. 2000, Aubier et al. 2016, Bradding and Arthur 2016).

1.4. Inflammatory mediators in asthma

1.4.1. Th2 cytokines

1.4.1.1. IL-4

IL-4 is one of the main cytokines orchestrating type 2 immune responses (Marone et al. 2019). It signals through IL-4 receptor α-subunit (IL-4Rα) which can either form a type I receptor by pairing with the common γ chain or type II receptor by pairing with the IL-13 receptor α1-subunit (IL-13Rα1) (Moran and Pavord 2020). Type I receptors are expressed on hematopoietic cells, whilst type II receptors are found on stromal cells, including airway epithelial cells, smooth muscle cells and fibroblasts (Marone et al. 2019). IL-4 signalling has been associated with phosphorylation of transcription factor signal transducer and activator of transcription (STAT) 6 which initiates activation of genes critical for the development of Th2 inflammation (Marone et al. 2019). IL-4 signalling is fundamental for Th2 polarisation, production of other type 2 cytokines, B cell class switching and initiation of IgE synthesis, eotaxin synthesis and release by the airway epithelium and subsequent recruitment of eosinophils as well as airway remodelling (Marone et al. 2019, Moran and Pavord 2020).

Increased IL-4 levels have been detected in asthmatic patients and $CD4^+$ T cells are thought to be the main source of IL-4 (Robinson et al. 1993a, Bradding et al. 1994, Truyen et al. 2006). However, basophils, mast cells, NK cells and ILC2s have been recognised as alternative IL-4 sources (Moran and Pavord 2020). Murine studies have demonstrated a pivotal role of IL-4 in the development of allergic airway inflammation and AHR (Brusselle et al. 1994), however the results of clinical studies targeting IL-4 have been surprising. A selective anti-IL-4 monoclonal antibody (mAb) pascolizumab has failed to produce positive effects, possibly due to the overlap of IL-4 functions with IL-13 (Hart et al. 2002, Marone et al. 2019).

Indeed, dual IL-4/IL-13 inhibition via IL-4Rα appears more effective. Dupilumab, an anti-IL-4Rα mAb approved for treatment of treatment of severe type 2 asthma (Global Initiative for Asthma 2021), has significantly lowered asthma exacerbation rate, improved lung function and asthma control and demonstrated maintenance OCS sparing effects in patients with uncontrolled asthma in randomized controlled trials (Wenzel et al. 2016, Castro et al. 2018, Rabe et al. 2018, Xiong et al. 2019, Corren et al. 2020). Post hoc analysis of LIBERTY ASTHMA QUEST study (Castro et al. 2018) revealed beneficial effects of dupilumab on exacerbation

rate, lung function and asthma control also in patients with non-allergic asthma, demonstrating the importance of IL-4/IL-13 signalling in IgE-mediated and non-IgE-mediated type 2 inflammation (Corren et al. 2020).

1.4.1.2. IL-13

IL-13 is another type 2 cytokine that can be produced by variety of immune cells, including Th2 cells, $CD8^+$ T cells, ILC2s and mast cells (Marone et al. 2019). It binds to IL-13Rα1 which is a part of type II receptors together with IL-4Rα to induce downstream STAT6 signalling (Marone et al. 2019). Like IL-4, IL-13 promotes eosinophil recruitment by upregulating vascular cell adhesion molecule-I (VCAM-I) on endothelial cells as well as eotaxin release from the airway epithelium. In addition, IL-13 induces mucus production and goblet cell metaplasia, subepithelial fibrosis and AHR (Zhu et al. 1999, Marone et al. 2019).

IL-13 genetic polymorphisms have been associated with an increased risk of asthma and IL-13 was found upregulated in sputum, BAL and bronchial mucosa in asthmatic patients compared to non-asthmatic individuals (Huang et al. 1995, Berry et al. 2004, Truyen et al. 2006, Cui et al. 2012, Aarafi et al. 2020). In animal models neutralisation of IL-13 reduced eosinophilic airway inflammation, AHR and mucus production (Grunig et al. 1998, Mattes et al. 2001, Taube et al. 2002). Although a meta-analysis of first randomised controlled clinical trials with anti-IL-13 mAbs lebrikizumab and tralokinumab demonstrated beneficial effects of both treatments on lung function and exacerbation rates in patients with severe asthma (Li et al. 2019a), development of anti-IL-13 mAbs for treatment of asthma was discontinued due to inconsistent effects of tralokinumab on asthma exacerbation rate in STRATOS phase 3 clinical trials (Panettieri et al. 2018).

1.4.1.3. IL-5

IL-5 is secreted by multiple cells, including Th2 cells, mast cells, ILC2s and eosinophils (Robinson et al. 1992, Matucci et al. 2019). It acts on a heterodimeric receptor comprised of α, IL-5Rα, and β subunit which is identical to the β subunit of GM-CSF and IL-3 (McBrien and Menzies-Gow 2017). IL-5 is the most important factor influencing the differentiation, maturation and survival of eosinophils (McBrien and Menzies-Gow 2017). IL-5Rα is expressed on eosinophils as well as basophils (McBrien and Menzies-Gow 2017). In asthmatic patients increased IL-5 levels have been detected in BAL and bronchial mucosa in comparison to healthy individuals (Hamid et al. 1991, Walker et al. 1992, Robinson et al. 1993a). In murine

ovalbumin (OVA)-induced AAD model IL-5Rα deficiency has abrogated eosinophilic airway inflammation as well as AHR (Tanaka et al. 2000). The importance of IL-5 in asthma has been further demonstrated in clinical trials (Pavord et al. 2012, Bel et al. 2014, Ortega et al. 2014, Bleecker et al. 2016, FitzGerald et al. 2016, Nair et al. 2017, Harrison et al. 2020, Kavanagh et al. 2021). Mepolizumab, an anti-IL-5 mAb approved for treatment of uncontrolled severe eosinophilic asthma (Global Initiative for Asthma 2021), has demonstrated significant reduction in asthma exacerbations, maintenance OCS sparing effects and was associated with improved lung function and asthma control in randomised controlled trials in patients with severe eosinophilic asthma (Pavord et al. 2012, Bel et al. 2014, Ortega et al. 2014). REALITI-A, a global, prospective, observational cohort has confirmed the effectiveness of mepolizumab under real-world settings (Harrison et al. 2020). Benralizumab, an anti-IL-5R mAb approved for treatment of uncontrolled severe eosinophilic asthma (Global Initiative for Asthma 2021), has demonstrated significant reductions in exacerbation rates, improvements in lung function and asthma control as well as clinically relevant maintenance OCS sparing benefits in phase 3 randomised controlled trials in patients with uncontrolled severe eosinophilic asthma (Bleecker et al. 2016, FitzGerald et al. 2016, Nair et al. 2017). All clinical and maintenance OCS sparing benefits of benralizumab have been recently confirmed in real-world severe eosinophilic asthma cohort (Kavanagh et al. 2021).

1.4.2. Chemokines

Chemokines are chemotactic cytokines that orchestrate migration of immune cells to the site of inflammation (Castan et al. 2017). They are divided into four groups based on the arrangement of amino terminal cysteine residues: CC, CXC, C and CXC3C (Castan et al. 2017). They activate chemokine receptors (CCRs) expressed on immune cells that are coupled to G proteins (Castan et al. 2017).

1.4.2.1. Eotaxin

Eotaxins are a subfamily of CC chemokines that are potent eosinophil chemotactic proteins (Pease and Williams 2001). Three eotaxins exist in humans: eotaxin-1 (CCL11) and two functional analogues eotaxin-2 (CCL24) and eotaxin-3 (CCL26) (Pease and Williams 2001).

Eotaxins can be produced by lung fibroblasts, airway smooth muscle cells, alveolar macrophages, eosinophils and lymphocytes (Pease and Williams 2001). IL-4, IL-13 and TNF-α

can stimulate production of eotaxin in airway epithelial cells, airway smooth muscle cells and lung fibroblasts (Pease and Williams 2001). Eotaxins activate CCR3 receptor which is expressed on eosinophils, basophils, Th2 cells and monocytes and is considered one of the most promiscuous chemokine receptors (Pease and Williams 2001).

Increased expression of eotaxins has been observed in atopic and non-atopic asthmatics at the sites of allergic inflammation as well as the sputum (Ying et al. 1997, Ying et al. 1999, Coleman et al. 2012). Increased eotaxin levels are associated with sputum eosinophilia, reduced FEV_1 and increased asthma exacerbation rate (Coleman et al. 2012). In murine OVA models of AAD neutralisation of eotaxin has diminished the recruitment of Th2 cells upon allergen challenge and alleviated eosinophilic airway inflammation and AHR (Gonzalo et al. 1998, Lloyd et al. 2000).

1.4.2.2. MIP-1α (CCL3)

Macrophage inflammatory protein 1 alpha (MIP-1α) activates CCR1 and is expressed by most mature hematopoietic cells, including DCs, T cells, B cells, NK cells and neutrophils (Bhavsar et al. 2015). DCs have been identified as an important source of MIP-1α upon allergen challenge (Vissers et al. 2001, van Rijt et al. 2005, Plantinga et al. 2013). In asthmatic patients increased MIP-1α levels are measured in BAL (Lukacs et al. 1995b, Alam et al. 1996, Holgate et al. 1997) which potently stimulates chemotaxis of lymphocytes, eosinophils and monocytes, including dendritic cells (Lukacs et al. 1995b, Holgate et al. 1997, Maurer and Von Stebut 2004).

1.4.2.3. MCP-1 (CCL2)

MCP-1 is a key monocyte chemokine and a mediator of Th cell differentiation (Bianconi et al. 2018). It is produced by monocytes, dendritic cells, macrophages, endothelial, epithelial cells and smooth muscle cells and can be induced by proinflammatory cytokines such as IL-4 and TNF-α as well as growth factors (G-CSF and GM-CSF) (Vissers et al. 2001, van Rijt et al. 2005, Plantinga et al. 2013, Bianconi et al. 2018). It activates CCR2, expression of which is restricted to monocytes, T cells and vascular smooth muscle (Bianconi et al. 2018). In asthmatic patients MCP-1 levels are increased in BAL (Alam et al. 1996, Holgate et al. 1997) and neutralisation of MCP-1 in murine OVA-induced AAD model has alleviated the development of eosinophilic airway inflammation and AHR (Gonzalo et al. 1998).

1.4.2.4. CCL17 (TARC) and CCL22

CCL17 and CCL22 are potent lymphocyte chemokines (Castan et al. 2017). They activate CCR4 which is expressed predominantly by Th2 cells and promote allergic airway inflammation (Panina-Bordignon et al. 2001, Vijayanand et al. 2010, Castan et al. 2017). Activated DCs and airway epithelium have been identified as a source of CCL17 and CCL22 upon allergen exposure (Panina-Bordignon et al. 2001, Vissers et al. 2001, van Rijt et al. 2005, Vijayanand et al. 2010, Plantinga et al. 2013).

1.4.3. Epithelial derived cytokines

1.4.3.1. IL-25

IL-25 or IL-17E is a member of IL-17 cytokine family which in contrast to the other family members promotes Th2 rather than Th1/Th17 inflammation (Mitchell and O'Byrne 2017a). Numerous cells can be a source of IL-25, including airway epithelial cells, eosinophils, mast cells, basophils and Th2 cells (Kouzaki et al. 2013, Mitchell and O'Byrne 2017a). Airway epithelial cells constitutively express IL-25 which is stored in the cytoplasm to ensure rapid release upon exposure to allergens with intrinsic protease activity (Mitchell and O'Byrne 2017a). IL-25 acts on a heteromeric complex composed of IL-17RA and IL-17RB and induces expression of IL-4, IL-5 and IL-13 when administered intranasally to mice whilst suppressing Th1/Th17 responses (Barlow et al. 2013, Willis et al. 2015, Mitchell and O'Byrne 2017a). Even though asthma has been associated with upregulation of IL-25 (Cheng et al. 2014, Li et al. 2018b, Wang et al. 2018b), anti-IL17RA mAb brodalumab, directed against IL-25 receptor, has been ineffective in improving asthma control in poorly controlled asthmatics (Busse et al. 2013).

1.4.3.2. IL-33

IL-33 is a member of IL-1 cytokine family and is associated with type 2 immune responses as opposed to type 1 immune responses commonly associated with IL-1 family (Schmitz et al. 2005, Hong et al. 2020). In the lungs, airway epithelium is the main source of IL-33, but it can also be released from macrophages, DCs, mast cells and monocytes, albeit at lower levels (Kurokawa et al. 2011, Hardman et al. 2013, Hong et al. 2020). IL-33 is constitutively expressed and stored in the nuclei of airway epithelial cells where it exhibits anti-inflammatory properties (Hong et al. 2020). Upon activation IL-33 is readily released, though, and exerts proinflammatory activity by acting on ST2 receptors expressed on numerous immune cells,

including $CD4^+$ T cells, ILC2s, DCs and eosinophils (Mangan et al. 2007, Stolarski et al. 2010, Besnard et al. 2011b, Barlow et al. 2012, Bartemes et al. 2012, Endo et al. 2015). Proteases, including neutrophil elastase or cathepsin G, cleave IL-33 and produce a mature form with increased biological activity (Lefrançais et al. 2012). The function of IL-33 can be supressed by a decoy soluble ST2 receptor and its activity in extracellular environment can be rapidly terminated by oxidation or degradation by proteases (Ho et al. 2013, Cohen et al. 2015, Hong et al. 2020).

In the lungs, IL-33 has been shown to promote ILC2 recruitment and activation, triggering type 2 immune responses (Barlow et al. 2012, Bartemes et al. 2012). Disruption of IL-33 signalling in preclinical AAD models have exposed a crucial role of IL-33 in allergen sensitisation, development of allergic airway inflammation as well as AHR (Hayakawa et al. 2007, Besnard et al. 2011b, Tjota et al. 2013, Hiraishi et al. 2018). Indeed, IL-33 and ST2 have been recognised as major susceptibility loci in asthma in GWAS and increased expression of IL-33 has been observed in asthmatic patients (Préfontaine et al. 2010, Hamzaoui et al. 2013, Ho et al. 2013, Saglani et al. 2013, Guo et al. 2014, Savenije et al. 2014, Chauhan et al. 2015, Christianson et al. 2015, Kaur et al. 2015, Demenais et al. 2018, Li et al. 2018b, Wang et al. 2018a, Rabe et al. 2021). In a recent clinical trial, the anti-IL-33 mAb itepekimab has been associated with improvement in asthma control, reduced risk of exacerbations as well as improved lung function in moderate-to-severe asthma patients (Wechsler et al. 2021). Astegolimab, an anti-ST2 mAb, similarly reduced exacerbation rate in patients with severe inadequately controlled asthma (Kelsen et al. 2021), demonstrating the central role of IL-33 in asthma pathogenesis.

1.4.3.3. TSLP

TSLP is a part of IL-2 cytokine family and is expressed by airway epithelial cells as well as mast cells, DCs, ASM cells, and fibroblasts (Wang et al. 2018b, Matera et al. 2020). TSLP binds to the TSLP receptor (TSLPR) which forms a heterodimeric receptor together with IL-7Rα subunit (Matera et al. 2020). TSLPR is expressed on various immune cells, including DCs, T cells, ILC2s and mast cells (Matera et al. 2020). TSLP is crucial for the activation of moDCs and subsequent Th2 differentiation (Ito et al. 2005). In animal AAD models inhibition of TSLP signalling has ameliorated allergic airway inflammation, AHR and airway remodelling (Al-Shami et al. 2005, Shi et al. 2008, Chen et al. 2013, Hiraishi et al. 2018). In humans, genetic polymorphisms of

TSLP have been linked with asthma and increased TSLP expression in asthmatics correlates with airway obstruction and AHR (Ying et al. 2005, Cheng et al. 2014, Gluck et al. 2016, Li et al. 2018b, Wang et al. 2018b). Clinical trials have further implicated TSLP in asthma pathogenesis. Tezepelumab, an anti-TSLP mAb, reduced allergen-induced AHR and systemic inflammation markers in a proof-of-concept study (Gauvreau et al. 2014). Tezepelumab has further demonstrated significant reduction in asthma exacerbation rates, improved lung function and improved asthma control in severe asthmatics (Corren et al. 2017, Matera et al. 2020, Menzies-Gow et al. 2021). Tezepelumab has been approved by U.S. Food and Drug Administration as an add-on maintenance therapy in with severe asthma aged 12 years and older in December 2021 (US Food and Drug Administration 2021).

1.4.4. Other proinflammatory cytokines

1.4.4.1. TNF-α

TNF-α is a pleiotropic cytokine exerting proinflammatory effects in the context of asthma (Berry et al. 2007). It is generated by activated macrophages, lymphocytes, mast cells as well as stromal cells (Matera et al. 2010). It activates membrane glycoprotein TNF receptors 1 and 2 (TNF-R1 and TNF-R2, respectively) (Matera et al. 2010). TNF-R1 is ubiquitously expressed on most cells types, while TNF-R2 is primarily restricted to immune and endothelial cells (Matera et al. 2010).

In asthmatic patients TNF-α levels are increased in BAL fluid (Ying et al. 1991, Bradding et al. 1994, Baines et al. 2011) and TNF-α genetic polymorphisms have been associated with an increased risk of asthma, asthma severity and AHR (Kang et al. 2019, Zhu et al. 2020). TNF-α induces expression of eotaxin, MCP-1 and mucins and promotes eosinophil recruitment and degranulation as well as T cell activation (Scheurich et al. 1987, Slungaard et al. 1990, Lukacs et al. 1995a, Matera et al. 2010). TNF-α has also been implicated in the development of AHR by inducing hypersensitivity of vagal bronchopulmonary sensory nerves (Makwana et al. 2012, Lin et al. 2017). Despite compelling evidence implicating TNF-α in asthma pathogenesis, the effects of TNF-α inhibition in clinical trials have been variable and several studies failed to demonstrate clinical efficacy of TNF-α blockade (Berry et al. 2007, Morjaria et al. 2008, Wenzel et al. 2009, Holgate et al. 2011).

1.4.4.2. IL-1β and IL-18

IL-1β and IL-18 are IL-1 family members that have been implicated in asthma pathogenesis (Mutini et al. 1999, Wild et al. 2000, Nakae et al. 2003, Besnard et al. 2011a, Sawada et al. 2013, Bruchard et al. 2015). Their release and activation have been associated with inflammasome activation (Pinkerton et al. 2017). Inflammasomes are multimeric protein complexes formed with one or two NLR family members that regulate the activity of caspase-1 which cleaves IL-1 family members IL-1β and IL-18 into their biologically active forms (Guo et al. 2015). NLRP3 inflammasome is the most studied and best characterised member of NLR family in the context of lung disease (Pinkerton et al. 2017) and has been implicated in asthma pathogenesis (Mutini et al. 1999, Besnard et al. 2011a, Bruchard et al. 2015, Li et al. 2018a). The assembly and activation of NLRP3 inflammasome depends on an initial priming step (PAMP-mediated activation of PRRs) which induces expression of *NLRP3* and a secondary signal provided by DAMPs that triggers relocalisation and activation of NLRP3 and subsequent inflammasome assembly (Guo et al. 2015). Activation of TLR4 by lipopolysaccharide (LPS) followed by activation of purinergic P2X7 receptors by ATP is a well established example of NLRP3 priming and activation, respectively, triggering IL-1β and IL-18 release and is often exploited in vitro and in vivo (Griffiths et al. 1995, Perregaux et al. 2000, Mehta et al. 2001, Solle et al. 2001, Franchi et al. 2007, Myrtek et al. 2008, Eltom et al. 2011, Baxter et al. 2014, Englezou et al. 2015, Mishra et al. 2016, Di Virgilio et al. 2017).

IL-1β is a proinflammatory cytokine important for the initiation of acute inflammatory responses to infectious, noxious or cell-damage derived stimuli (Pinkerton et al. 2017). It is primarily produced by macrophages, but can be also expressed by neutrophils, lymphocytes, airway epithelial cells and fibroblasts (Pinkerton et al. 2017). IL-1β binds to IL-1R and triggers activation of nuclear factor kappa-light-chain-enhancer of activated B cells (NFκB) and subsequent recruitment and activation of innate immune cells as well as expression of proinflammatory cytokines such as TNF-α, IL-6 and IL-1β (Pinkerton et al. 2017). Increased levels of IL-β have been measured in BAL and sputum of asthmatic patients (Mattoli et al. 1991, Borish et al. 1992, Baines et al. 2011). Preclinical studies have implicated IL-1β in Th2 differentiation and demonstrated its key role for the development of type 2 airway inflammation and AHR in AAD (Mutini et al. 1999, Nakae et al. 2003, Besnard et al. 2011a, Bruchard et al. 2015).

IL-18 is constitutively expressed by mesenchymal cells, however it is primarily found in macrophages and DCs upon activation (Pinkerton et al. 2017). IL-18 genetic polymorphisms have been associated with asthma severity (Harada et al. 2009). In asthmatic patients increased IL-18 levels have been measured in serum in comparison to healthy individuals and IL-18 expression has been observed in airway epithelium and airway smooth muscle cells (Imaoka et al. 2011). However, reduced sputum IL-18 levels have been reported during asthma exacerbations or in severe asthma patients relative to healthy controls (Hossny et al. 2009, Rovina et al. 2015). Administration or overexpression of IL-18 in AAD models promotes production of IgE and Th2 cytokines and development of eosinophilic airway inflammation and AHR (Wild et al. 2000, Sawada et al. 2013).

1.4.5. Extracellular ATP

ATP has been long recognised for its fundamental role in cellular metabolism and energetics as an energy carrier within cells (Pelleg 2020). In addition, ATP can be released into extracellular space under physiological conditions to regulate airway mucus production and ciliary beat frequency, but it also serves as a ubiquitous danger signal when released from damaged or dying cells (Button et al. 2013, Droguett et al. 2017). ATP is released from cells in a controlled fashion via specific transmembrane channels (i.e. pannexin or connexin hemichannels) or vesicular exocytosis and it acts on P2 purinergic receptors in an autocrine and paracrine fashion (Dou et al. 2018, Pelleg 2020) (Figure 1.3). P2 receptors are divided into two families: ionotropic P2X family, consisting of seven ATP-gated ion channels, and metabotropic P2Y family consisting of eight G-protein coupled receptors (Dou et al. 2018, Pelleg 2020). ATP acts predominantly on P2X family members, but it can also activate several G-protein coupled P2Y receptors, P2Y1, P2Y2 and P2Y11 (Dreisig and Kornum 2016, Silva-Vilches et al. 2018, Pelleg 2020). P2Y11 is the only P2Y receptor exclusively activated by ATP, while other P2Y receptors more readily respond to various other purines such as adenosine diphosphate (ADP) and uridine nucleotides (Dreisig and Kornum 2016, Silva-Vilches et al. 2018). Due to potent proinflammatory actions, concentrations of extracellular ATP are maintained at low levels and ATP is rapidly broken down to adenosine diphosphate (ADP), adenosine monophosphate (AMP) and adenosine by the CD39 and CD73 families of ectoenzymes (Pelleg et al. 2016, Silva-Vilches et al. 2018)(Figure 1.3).

In chronic lung disease, including asthma, chronic obstructive pulmonary disease (COPD) and idiopathic pulmonary fibrosis (IPF), increased ATP levels have been reported in the airways and are thought to drive the underlying inflammation, airway remodelling and fibrosis as well as bronchoconstriction and cough (Pellegrino et al. 1996a, Basoglu et al. 2005, Idzko et al. 2007, Oguma et al. 2007, Lommatzsch et al. 2010, Mortaz et al. 2010, Riteau et al. 2010, Chavez et al. 2013, Baxter et al. 2014, Basoglu et al. 2015, Lazar et al. 2016, Müller et al. 2017). Regarding asthma, allergen exposure has been associated with increased ATP levels in asthmatic patients as well as in murine AAD models (Idzko et al. 2007, Vanderstocken et al. 2010, Chavez et al. 2013, Idzko et al. 2013). Inhibition of ATP signalling in AAD models has abrogated allergic airway inflammation, AHR and airway remodelling, and the purinergic receptors P2X4, P2X7 and P2Y2 have been implicated to mediate the pathogenic ATP actions in these models (Idzko et al. 2007, Muller et al. 2010, Kouzaki et al. 2011, Muller et al. 2011, Idzko et al. 2013, Ledderose et al. 2014, Amison et al. 2015, Li et al. 2015, Chen et al. 2016, Zech et al. 2016, Li et al. 2018a). Administration of exogenous ATP during allergen challenge aggravated allergen-induced allergic airway inflammation and AHR in murine models of AAD (Idzko et al. 2007, Chen et al. 2016). This has not been yet elucidated in man, however ATP-provoked bronchoconstriction is pronounced in asthmatic patients compared to healthy individuals (Pellegrino et al. 1996b). In addition, ATP is an important regulator of eosinophil, mast cell, T cell and DC function and is essential for Th2 priming and induction of type 2 immune responses upon allergen encounter (Muller et al. 2011, Burnstock and Boeynaems 2014, Zech et al. 2016, Silva-Vilches et al. 2018).

The mechanisms leading to increased ATP levels in asthma are not yet fully elucidated. As discussed in section 1.6, activation of transient receptor potential (TRP) channels such as TRPV4 has been linked to ATP release and both channels have been implicated in asthma pathogenesis (Belvisi and Birrell 2017).

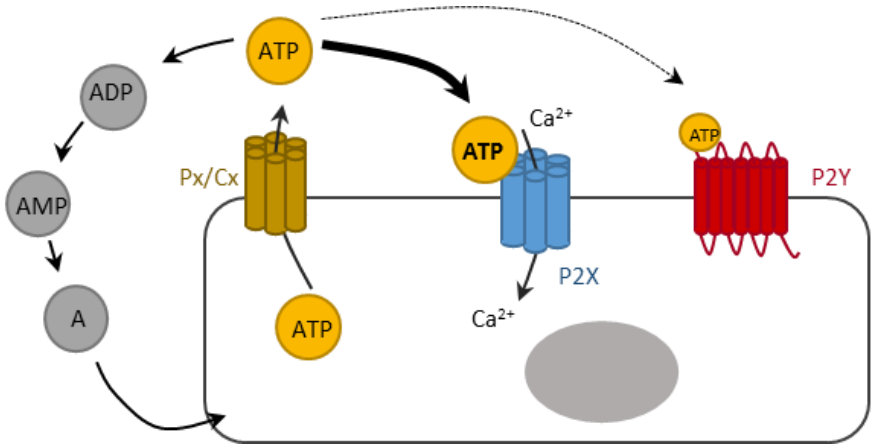


Figure 1.3: Schematic representation of ATP signalling.

ATP is released from Pannexin (Panx/Px) or Connexin (Cx) channels and mainly acts on P2X family of ion channels and to a smaller extent on P2Y family of G-protein coupled receptors. ATP action in extracellular space is short lived due to rapid breakdown to ADP, AMP and adenosine (A). Adenosine can be broken down to inosine by adenosine deaminase intracellularly or extracellularly.

1.5. Nerves in asthma

1.5.1. Neurophysiology of airway nerves

This section summarises airway innervation and is based on detailed reviews of airway nervous system cited here (Mazzone and Undem 2016, Kistemaker and Prakash 2019). The vagus nerve is the main nerve innervating the airways and supplies all parasympathetic efferent fibres and most of the sensory afferent fibres. The vagus divides into several branches with the superior laryngeal nerve innervating the larynx, recurrent laryngeal nerve innervating the trachea and main bronchi and smaller pulmonary branches innervating smaller airways and lung parenchyma. Around one percent of sensory innervation originates from the dorsal root ganglia and runs with spinal sympathetic nerves. Airway innervation regulates many aspects of airway function, including breathing, the Hering-Breuer reflex, airway smooth muscle tone, mucus secretion and cough. Although sympathetic nerves innervate the lungs, they do not significantly affect airway tone in humans.

Airway sensory neurons are pseudounipolar neurons with bodies located in the nodose and jugular ganglia. They are generally divided into mechanosensing myelinated A fibres (although there is a subgroup of Aδ nociceptors that can respond to chemical stimuli) and unmyelinated C fibres which are activated by chemical stimuli via a number of receptors and ion channels, such as TRP channels and purinergic receptors. Parasympathetic preganglionic

neurons originate in the brainstem and run along the vagus nerve to parasympathetic ganglia located in the proximity of the airways where they form synapses with post-ganglionic parasympathetic neurons. Post-ganglionic neurons innervate airway smooth muscle, submucosal glands and blood vessels. The cholinergic parasympathetic neurons release acetylcholine (ACh) which activates muscarinic receptors on ASM cells (typically M_3) and submucosal glands (typically M_1), triggering bronchoconstriction and mucus secretion, respectively. ACh release is normally limited by inhibitory M_2 muscarinic receptors on postganglionic parasympathetic nerves. Parasympathetic neurons release other mediators such as vasoactive intestinal peptide (VIP) and nitric oxide (NO) and trigger non-cholinergic vasodilatation and bronchorelaxation (Figure 1.4).

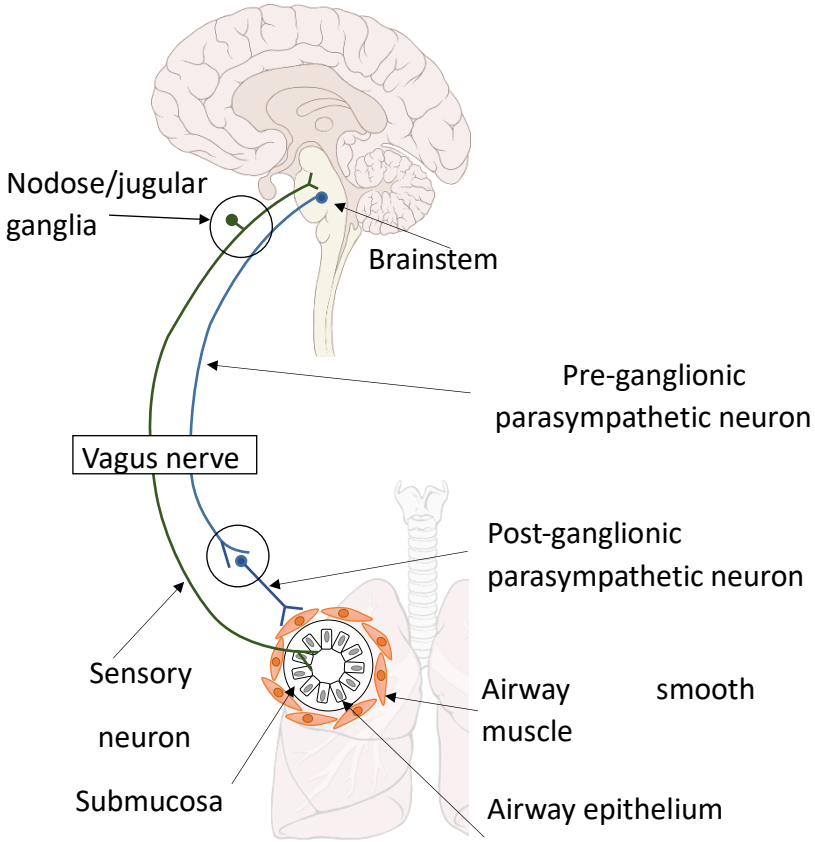


Figure 1.4: Sensory and parasympathetic innervation of the airways.

Airway sensory neurons with cell bodies located in the nodose and jugular ganglia innervate the airway mucosa and travel in vagus nerve to the brainstem. Pre-ganglionic parasympathetic neurons originate in brainstem and form synapses with post-ganglionic neurons in close proximity of the airways. Post-ganglionic neurons innervate airway smooth muscle cells and regulate airway tone.

1.5.2. The role of nerves in asthma

There is increasing evidence of a dysregulated airway nervous system which actively contributes to the development of AHR, airway inflammation and symptoms such as cough (Pincus et al. 2021). Epithelial nerve length and branching is increased in patients with persistent asthma and is associated with eosinophilic inflammation (Drake et al. 2018). Similar has been reported in IL-5 overexpressing mice, and IL-5 has also been shown to activate nociceptors, suggesting that the underlying eosinophilic airway inflammation leads to changes in airway innervation and AHR (Costello et al. 1999, Talbot et al. 2015, Drake et al. 2018, Lebold et al. 2020, Nie et al. 2020). In asthmatic patients, cholinergic tone is enhanced in comparison to healthy individuals (Molfino et al. 1993) which is thought to be a results of dysfunctional M_2 muscarinic receptors on postganglionic parasympathetic neurons, leading to the loss of the negative feedback control and significant increases in ACh release (Patel et al. 1995, Pincus et al. 2021). The loss of M_2 receptors appears to be dependent on eosinophils and eosinophil MBP has been shown to antagonise muscarinic M_2 receptors (Elbon et al. 1995, Evans et al. 1997). It is therefore not surprising that anticholinergics are effective bronchodilators in severe and moderate asthma (Kerstjens et al. 2012, Kerstjens et al. 2015, Brandt et al. 2016, Paggiaro et al. 2016, Virchow et al. 2019). In addition, preclinical studies have implicated the cholinergic nervous system in LAR as allergen-provoked delayed bronchoconstriction was prevented by tiotropium and the response was lost under ketamine/xylazine anaesthesia, which inhibited the central processing arc of the reflex, in rat and guinea pig (GP) LAR models (Raemdonck et al. 2012, Smit et al. 2014). Human cough studies have demonstrated an increase in spontaneous cough upon allergen provocation as well as an increased sensitivity to the TRPV1 agonist capsaicin in asthmatic patients, providing evidence of dysregulated airway sensory innervation in asthma (Satia et al. 2017, Satia et al. 2019).

In addition to AHR, the airway nervous system has been implicated in the development of allergic airway inflammation. Vagotomy or selective ablation of $TRPV1^+$, $TRPA1^+$ or Nav1. 8^+ sensory neurons has alleviated allergic airway inflammation and AHR in several AAD models (Trankner et al. 2014, Talbot et al. 2015, Dragunas et al. 2020). Sensory neurons were demonstrated to express VIP upon allergen challenge which promoted ILC2 proliferation and $CD4^+$ T cell cytokine production (Talbot et al. 2015). Cholinergic neurons were shown to

produce a neuropeptide neuromedin U which acts on the NMUR1 receptor on ILC2s and stimulate their proliferation and cytokine production during helminth infection as well as an allergen challenge (Cardoso et al. 2017, Wallrapp et al. 2017). Furthermore, IL-4 and IL-13 stimulate expression of eotaxin in parasympathetic nerves which further promoted eosinophil accumulation around airway nerves after allergen challenge (Fryer et al. 2006). On the other hand, the release of neurotrophin from airway epithelium, macrophages, T cells and mast cells is increased in asthmatic patients and neurotrophins have been shown to induce expression of TRPV1 in airway sensory neurons, potentially contributing to increased neuronal sensitivity (Lieu et al. 2012, Satia et al. 2020).

1.6. TRP channels in asthma

1.6.1. Definition

TRP ion channels were first discovered as phototransduction proteins in the *Drosophila melanogaster* (Montell and Rubin 1989). As of today 28 TRP channels have been identified in mammals and are categorised into seven subfamilies based on their sequence homology, namely: TRPC (canonical), TRPV (vanilloid), TRPM (melasatin), TRPP (polycystin), TRPML (mucolipin), TRPA (ankyrin) and TRPN (no mechanoreceptor potential C; not expressed in mammals) (Belvisi and Birrell 2017). TRP channels consist of intracellular C and N termini, six transmembrane spanning domains with a pore between domains 5 and 6 and variable amounts of ankyrin repeats (Belvisi and Birrell 2017). They are ubiquitously expressed throughout the body and respond to a plethora of intracellular and extracellular stimuli (De Logu et al. 2016). TRPA1, TRPV1 and TRPV4 are the most important TRP channels in the respiratory system due to their abundant expression and importance for airway function and lung homeostasis (De Logu et al. 2016, Belvisi and Birrell 2017).

1.6.2. TRPV1

TRPV1 is the most studies TRP channel and is directly activated by noxious temperatures (> 42 °C), acidic pH, capsaicin and lipid derivates, however bradykinin, PGE_2 or PAR2-activating proteases can cause G-protein coupled receptor (GPCR)-mediated activation of TRPV1 (Tominaga et al. 1998, Amadesi et al. 2004, Grace et al. 2012, Benítez-Angeles et al. 2020).

In the respiratory system TRPV1 is expressed on airway sensory neurons (Nassenstein et al. 2008, Lieu et al. 2012, Wortley et al. 2016) as well as non-neuronal structural and immune

cells, including airway epithelial cells, alveolar macrophages and $CD4^+$ T cells (Baxter et al. 2014, Bertin et al. 2014, Jia et al. 2014, McGarvey et al. 2014, Balestrini et al. 2021). TRPV1 expression is increased in airway epithelium in severe refractory asthma (McGarvey et al. 2014) and *TRPV1* genetic polymorphisms have been associated with asthma susceptibility (Wang et al. 2009, Cantero-Recasens et al. 2010). More specifically, a loss of function *TRPV1* variant has been associated with reduced wheezing and cough in asthmatic patients (Wang et al. 2009, Cantero-Recasens et al. 2010). In asthmatic patients increased capsaicin-evoked cough responses are observed compared to healthy individuals, suggestive of increased TRPV1-modulated airway sensory reflexes (Satia et al. 2017, Satia et al. 2019). The analysis of TRPV1 expression in AAD models has demonstrated increased TRPV1 expression in allergen exposed animals (Zhang et al. 2008, Lieu et al. 2012). Activation of TRPV1 on airway epithelial cells has been associated with TSLP release (Jia et al. 2014) and preclinical studies have further demonstrated a pathogenic role of TRPV1 in the development of allergic airway inflammation, LAR, AHR as well as airway remodelling (Delescluse et al. 2012, Mabalirajan et al. 2013, Rehman et al. 2013, Baker et al. 2016, Devos et al. 2016, Choi et al. 2018, Duan et al. 2020, Perner et al. 2020). However, the involvement of TRPV1 in AAD pathogenesis appears to be model dependent as TRPV1 has been found to be dispensable during allergen challenge in some studies (Caceres et al. 2009, Mori et al. 2011, Raemdonck et al. 2012).

1.6.3. TRPA1

TRPA1 can be found on airway sensory neurons (Nassenstein et al. 2008, Wortley et al. 2016) as well as non-neuronal cells including airway smooth muscle cells, airway epithelial cells, fibroblasts, $CD4^+$ and $CD8^+$ T cells (Mukhopadhyay et al. 2011, Nassini et al. 2012, Bertin et al. 2017, Sahoo et al. 2019). TRPA1 is activated by a range of natural products such as cinnamaldehyde, allyl isothiocyanate, allicin and cannabinol that are found in mustard, garlic, horseradish, cinnamon or cannabis, environmental irritants (such as acrolein in cigarette smoke, diesel exhaust particles, ozone and toluene diisocyanate (TDI)) as well as reactive and electrophilic by-products of oxidative stress (De Logu et al. 2016, Belvisi and Birrell 2017). Diesel exhaust particles have been demonstrated to induce mitochondrial reactive oxidative species production which activates TRPVA1 on sensory nerves which could be responsible for an asymptomatic drop in FEV_1 in asthmatic patients experienced when exposed to diesel traffic (McCreanor et al. 2007, Robinson et al. 2018). In addition to chemical ligands TRPA1

responds to mechanical stimuli and cold temperatures (< 17 °C) and can be sensitised in GPCR-mediated manner by PGE_2, bradykinin, or PAR2 ligands (Dai et al. 2007, Grace et al. 2012, Belvisi and Birrell 2017).

TRPA1 genetic polymorphisms have been associated with increased risk of childhood asthma (Gallo et al. 2017). Preclinical studies have implicated TRPA1 in the development of allergic airway inflammation, AHR and/or LAR (Caceres et al. 2009, Raemdonck et al. 2012, Reese et al. 2020), although a dispensable role of TRPA1 in the development of allergic airway inflammation or AHR has also been reported (Baker et al. 2017). In addition, $TRPA1^{-/-}$ has alleviated TDI-induced airway inflammation and AHR as well as hypochlorite induced AHR in OVA-induced model of AAD, suggesting the involvement of TRPA1 in mechanisms leading to non-allergic asthma (Hox et al. 2013, Devos et al. 2016, Yao et al. 2019)

1.6.4. TRPV4

TRPV4 is a polymodal non-selective cation channels that was originally discovered as an osmosensor responding to hypotonic solutions (Liedtke et al. 2000, Strotmann et al. 2000). It is also a thermosensor, constitutively active in the temperature range 24 – 42 °C with maximal activity at core body temperature and can also respond to shear stress and mechanical stretch (Güler et al. 2002, Watanabe et al. 2002b, Köhler et al. 2006, Loukin et al. 2010). In addition to physical stimuli, TRPV4 can be activated by a range of chemical stimuli, including arachidonic acid (AA) derivates, endocannabinoids and synthetic agonists 4α-phorbol-didecanoate (4αPDD) and GSK1016790A (Watanabe et al. 2002a, Watanabe et al. 2003, Thorneloe et al. 2008, Klausen et al. 2009). In addition, GPCR-activating inflammatory mediators such as histamine, 5-HT or PAR2 activating proteases can activate or sensitise TRPV4 in an indirect fashion via protein-kinase A and C and tyrosine-kinase mediated phosphorylation (Grant et al. 2007, Cenac et al. 2010, White et al. 2016) (Figure 1.5).

TRPV4 has been implicated in airway sensory reflexes, however its expression appears to be restricted to non-neuronal accessory cells (Bonvini et al. 2016). In addition, it is expressed in a wide range of lung structural and immune cells, including airway epithelial cells, airway smooth muscle cells, fibroblasts, T and B lymphocytes, DCs and alveolar macrophages (Fernández-Fernández et al. 2002, Jia et al. 2004, Andrade et al. 2005, Inada et al. 2006,

Hamanaka et al. 2010, Groot-Kormelink et al. 2012, Szollosi et al. 2013, Bertin et al. 2014, Rahaman et al. 2014, Majhi et al. 2015, Yu et al. 2017, Naert et al. 2019).

Activation of TRPV4 triggers ATP release through pannexin-1 (Panx-1) channels and downstream activation of P2X receptors (Seminario-Vidal et al. 2011, Baxter et al. 2014, Bonvini et al. 2016, Bonvini et al. 2020). Depending on the cell types and P2X receptors involved in the signalling cascade TRPV4 activation modulates various physiological and pathological processes. During homeostasis TRPV4 regulates airway calibre and ciliary beat frequency on airway epithelial cells (Lorenzo et al. 2008, Alenmyr et al. 2014). TRPV4 has been proposed to be protective against bacterial infections (Alenmyr et al. 2014, Scheraga et al. 2016, Alpizar et al. 2017, Scheraga et al. 2020), although not all reports are in agreement (Dalsgaard et al. 2016, Li et al. 2019b). On the other hand, an aberrant activation on neuronal accessory cells leads to activation of P2X2/P2X3 receptors on airway sensory neurons which triggers cough (Bonvini et al. 2016). TRPV4-induced ATP release from airway smooth muscle cells has been shown to activate P2X4 receptors on mast cells, promoting the release of CysLTs and subsequent bronchoconstriction (McAlexander et al. 2014, Bonvini et al. 2020). Smoke exposure has been linked to activation of TRPV4-ATP axis on alveolar macrophages (AMs) and airway epithelial cells resulting in P2X7 activation on AMs with subsequent NLRP3 inflammasome formation and IL-1β release, leading to neutrophilic airway inflammation (Baxter et al. 2014). TRPV4 signalling pathways relevant for lung disease are summarised in Figure 1.5.

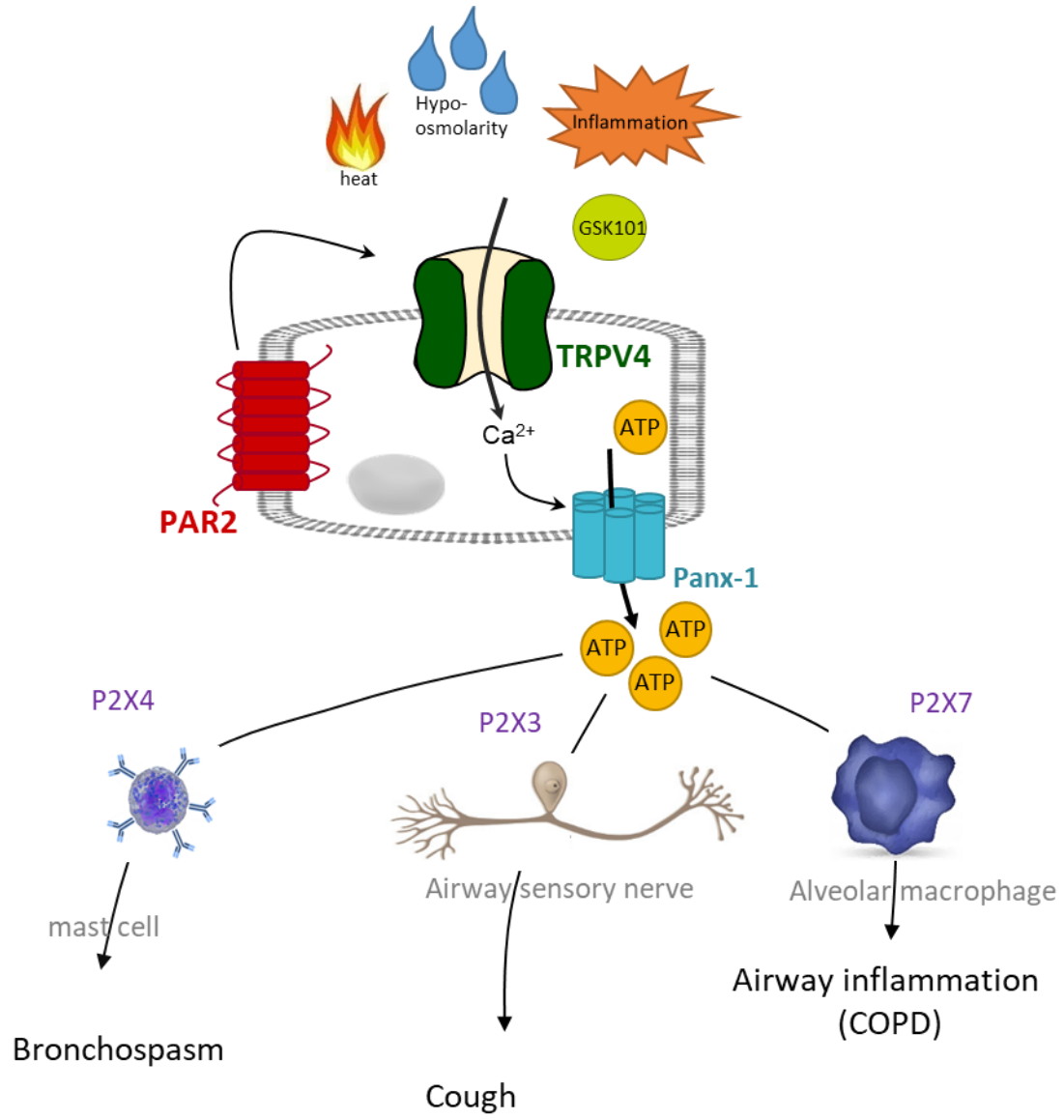


Figure 1.5: TRPV4 signalling in lung disease.

TRPV4 can be activated by a variety of environmental stimuli including hypo osmolar solutions and moderate temperatures, endogenous inflammatory mediators, synthetic agonists such as GSK1016790A (GSK101) and downstream of PAR2 signalling. Activation of TRPV4 causes influx of calcium ions into cells which triggers opening of Panx 1 channels and subsequent release of ATP into extracellular space. In the lungs this can activate various pathological processes, depending on cell types and P2X receptors activated by extracellular ATP. For example, activation of P2X4 on mast cells leads to bronchospasm, activation of P2X3 receptors on airway sensory nerves triggers cough and activation of P2X7 receptors on alveolar macrophages is responsible for development of airway inflammation in COPD models.

TRPV4 has been directly implicated in the pathogenesis of asthma, however the signalling pathways involved in those processes are not yet fully understood. TRPV4 genetic

polymorphisms have been associated with lung function parameters and were linked to the development of osmotic AHR in asthmatic patients (Obeidat et al. 2011, Naumov et al. 2016). Furthermore, TRPV4 genetic polymorphisms have also been associated with increased risk of sensitisation to fungal allergens and asthma incidence (Wiesner et al. 2020). In asthmatic patients increased expression of TRPV4 has been observed in the airway epithelium and this has been recapitulated in animal models of AAD (Wiesner et al. 2020) (Yu et al. 2017, Duan et al. 2020, Kim et al. 2020). Mechanistic studies have demonstrated that genetic disruption or pharmacological inhibition of TRPV4 ameliorated allergic airway inflammation, AHR, LAR and/or airway remodelling in AAD models (Birrell et al. 2016, Gombedza et al. 2017, Duan et al. 2020, Wiesner et al. 2020, Flajolet 2021), although a dispensable role of TRPV4 in the development of AAD has also been demonstrated (Palaniyandi et al. 2020). TRPV4 has also been implicated in non-allergic airway inflammation and AHR associated with TDI exposure (Yao et al. 2019).

1.6.4.1. PAR2 – TRPV4 coupling

PAR2 is a GPCR belonging to a unique PAR family consisting of PAR1, PAR2, PAR3 and PAR4. Instead of activation by endogenous ligands, proteases cleave the N-termini of PAR2 receptors and form a tethered ligand that causes receptor activation (Yau et al. 2016). In comparison to other PAR members, PAR2 displays insensitivity to thrombin but can be cleaved by proteases such as trypsin, tryptase, tissue factors, kallikreins, elastase and cathepsins (Yau et al. 2016). Trypsin and tryptase cleave N-terminus at the canonical site which exposes the tethered ligand and triggers PAR2 activation (Yau et al. 2016). Other proteases, including elastase or cathepsin S, cleave the PAR2 N-terminus at alternative sites and either inactivate the receptor or produce a different tethered ligand, activating an alternative, biased signalling (Hollenberg et al. 2014, Yau et al. 2016).

PAR2 activation has been coupled to activation or sensitisation of TRPV4 channels in mechanical hyperalgesia models as well as lung injury models (Grant et al. 2007, Poole et al. 2013, Zhao et al. 2014, Zhao et al. 2015, Rayees et al. 2019). The exact mechanism of TRPV4 activation remains unclear, however tyrosine phosphorylation by phospholipase Cβ or protein kinases A, C and D has been proposed (Grant et al. 2007, Poole et al. 2013, Zhao et al. 2014, Zhao et al. 2015). In addition, PAR2 has been shown to promote a generation of arachidonic acid metabolites that trigger opening of TRPV4 channels (Poole et al. 2013).

PAR2 is widely expressed in the respiratory system and can be found on airway epithelial cells, airway smooth muscle cells, fibroblasts and endothelial cells (Nystedt et al. 1996, D'Andrea et al. 1998, Akers et al. 2000, Ricciardolo et al. 2000, Schmidlin et al. 2001). It has also been found on leukocytes, including monocytes, eosinophils, neutrophils, dendritic cells, T cells, mast cells and macrophages and has been implicated in their migration, differentiation, cytokine production and other effector functions (Howells et al. 1997, Miike et al. 2001, Bolton et al. 2003, Colognato et al. 2003, Fields et al. 2003, Roche et al. 2003, Ebeling et al. 2005, Lim et al. 2006, Shichijo et al. 2006, Ebeling et al. 2007, Ramelli et al. 2010, Lewkowich et al. 2011, Francis et al. 2017, Feng et al. 2018, Garcia-Gonzalez et al. 2019). In the respiratory system PAR2 can exhibit proinflammatory and anti-inflammatory properties and appears to play an important role in the pathogenesis of asthma. PAR2 has been postulated to regulate airway tone and function in healthy airways, however the implications are confusing as PAR2 activation has been linked to bronchodilatation as well as bronchoconstriction (Cocks et al. 1999, Lan et al. 2000, Ricciardolo et al. 2000, Cicala et al. 2001, Schmidlin et al. 2001). In asthmatic patients PAR2 activating proteases such as tryptase are increased in BAL or sputum samples and PAR2 expression in upregulated in airway epithelium and airway smooth muscle (Wenzel et al. 1988, Broide et al. 1991, Sedgwick et al. 1991, Alvarez et al. 2000, Knight et al. 2001, Allard et al. 2014, Aubier et al. 2016). Allergens such as *Alternaria* have been shown to induce IL-33 release from airway epithelial cells which is dependent on PAR2 activation and ATP release (Snelgrove et al. 2014). A number of studies have demonstrated a fundamental role of PAR2 activation for the development of allergic airway inflammation and AHR and a role of PAR2 in sensitisation to airborne allergens in particular has been suggested (Schmidlin et al. 2002, Takizawa et al. 2005, Page et al. 2010, Arizmendi et al. 2011, Lewkowich et al. 2011, Davidson et al. 2013, de Boer et al. 2014, Yee et al. 2018). However, several studies have failed to confirm these observations and demonstrated PAR2 to be dispensable in AAD pathogenesis (Redes et al. 2019, Daines et al. 2020, Wiesner et al. 2020).

1.7. Animal models of AAD

Animal AAD models are commonly used to study the pathological mechanisms underlying disease and the effects of drugs (Zosky and Sly 2007). None of the existing models encompasses all features of asthma and each presents with its own limitations (Zosky and Sly

2007, Maltby et al. 2017). Rodents are most commonly used to model AAD, although other animals such as dog, sheep and horses can also be used (Aun et al. 2017).

1.7.1. Experimental animals

1.7.1.1. Mice

Mice are the most frequently used species due to the detailed understanding of their genetics, ability to manipulate their genome using transgenic technology as well as the availability of mouse specific tools to study allergic outcomes (Aun et al. 2017). In contrast to humans, mice do not spontaneously develop asthma, and the role and importance of eosinophils and mast cells varies considerably (Aun et al. 2017). For example, eosinophils recruited upon allergen exposure readily degranulate in humans, but not in mice and mouse mast cells release serotonin, which is not thought to be relevant for human disease (Zosky and Sly 2007, Aun et al. 2017). There are also considerable differences in lung anatomy including limited airway smooth muscle in mice and physiological responses to allergens (Zosky and Sly 2007, Bradding and Arthur 2016, Maltby et al. 2017). While EAR and LAR are commonly observed after allergen exposure in patients with atopic asthma, these responses are poorly defined in mice and AHR is the primary physiological outcome in murine AAD models (Zosky and Sly 2007). Studies into long-term airway remodelling are also limited due to the tolerance associated with repeated allergen exposure (Zosky and Sly 2007, Maltby et al. 2017). Even so, mouse studies have contributed significantly to our understating of the role of atopy and type 2 immune mechanisms in the pathogenesis of allergic asthma and remain the main means of generating new hypotheses (Zosky and Sly 2007, Foster et al. 2017). The BALB/c strain is often used due to the intrinsic predisposition to Th2 immune responses, although C57BL/6 and A/J strains have also been successfully used in experimental models of AAD (Aun et al. 2017).

1.7.1.2. Rats

Rats are also a popular species to model AAD, particularly for testing and establishing efficacy and toxicity of new drug therapies (Zosky and Sly 2007). Brown Norway (BN) rats are the strain of choice due to genetic predisposition to strong Th2 and IgE dependent responses (Foster et al. 2017). In comparison to mice, rats are more useful for studying airway physiology as BN rat have been shown to develop EAR and LAR after allergen exposure (Underwood et al. 2002, Zosky and Sly 2007, Raemdonck et al. 2012).

1.7.1.3. Guinea pigs

Guinea pigs, which possess similar airway physiological process and airway innervation to humans, have been one of the oldest species used to model allergic airway responses such as EAR and LAR (Zosky and Sly 2007, Aun et al. 2017). The main limitations to the use of GPs are high non-specific airway reactivity at baseline which often requires pre-medication to moderate the responses as well as a lack of specific probes and reagents for studying allergic outcomes (Zosky and Sly 2007, Sagar et al. 2015).

1.7.2. Approaches to modelling asthma in laboratory animals

1.7.2.1. Ovalbumin AAD models

OVA is derived from chicken egg white and is the most commonly used allergen to induce AAD (Sagar et al. 2015). In these models systemic sensitisation (via intraperitoneal (i.p.), subcutaneous (s.c.) or dermal routes) is required and is followed by a topical allergen challenge (aerosolised, intranasal (i.n.) or intratracheal (i.t.) administration) (Sagar et al. 2015). This triggers robust type 2 inflammation in the airways and can be accompanied by AHR, EAR, LAR or chronic remodelling, depending on a model and species used (Zosky and Sly 2007, Sagar et al. 2015). Depending on the length of the challenge phase, OVA models can be acute or chronic (Sagar et al. 2015).

There are several criticisms of OVA-induced models of AAD. Firstly, OVA is an artificial allergen which in not known to provide respiratory allergy in humans (Aun et al. 2017). An adjuvant (usually aluminium hydroxide (Alum)) is needed during sensitisation phase to induce Th2 polarisation in laboratory animals as OVA alone induces tolerance (Ebeling et al. 2007, Aun et al. 2017), further questioning the physiological relevance of OVA. In addition, unlike pathological processes, OVA-associated pathology reverses with the cessation of protein administration (Zosky and Sly 2007).

1.7.2.2. HDM AAD models with systemic sensitisation

To overcome some of the limitations of OVA, clinically relevant allergens have been increasingly used to induce AAD in experimental animals. HDM (*Dermatophagoides* sp.) is one of the most common allergens with 50 – 85 % of patients exhibiting allergy to HDM and possessing HDM-specific IgE (Sagar et al. 2015). In our laboratory a HDM model with systemic sensitisation phase without the need for an adjuvant has been developed (Raemdonck et al.

2016). In this model HDM challenge triggers strong eosinophilic airway inflammation and AHR which are dependent on $CD4^+$ T cells and $CD8^+$ T cells, but appear to be independent on IgE, B cell or mast cell responses (Raemdonck et al. 2016).

1.7.2.3. AAD models with mucosal sensitisation

Systemic sensitisation to allergens has been disputed in recent years as intermittent or continued exposure to aeroallergens is thought to be responsible for allergen sensitisation and the development of allergic airway inflammation in humans (Aun et al. 2017). Thus, models relying solely on local (i.n. or i.t.) administration of allergens have been developed and depending on the duration of the challenge, they can be acute or chronic (Aun et al. 2017). Clinically relevant allergens such as HDM, cockroach extract (CE), and fungal allergens (*Alternaria alternata*, *Aspergillus fumigatus* (Asp)) and ragweed extracts have been used in such models and their allergogenic properties of the allergens used seem to depend on their intrinsic protease activity (Page et al. 2010, Davidson et al. 2013, de Boer et al. 2014, Snelgrove et al. 2014, Sagar et al. 2015, Redes et al. 2019). Initial immune responses to allergens are associated with the development of neutrophilic airway inflammation while eosinophilic airway inflammation becomes predominant at the later time points (Patel et al. 2019). Airway inflammation in these models is driven by epithelial-ILC2 axis and only prolonged exposure to allergens is associated with allergen sensitisation and the development of adaptive immune responses (Alessandrini et al. 2020). However, in contrast to human disease, IgE responses in those models are weak and are often not measured, questioning the allergic component in these allergen-induced responses (Birrell et al. 2010).

1.8. Thesis plan

Despite the advances in asthma treatment, we are unable to achieve good disease control in a subset of patients (Chung et al. 2014, Kuruvilla et al. 2019). The biologics are medicines that target individual type 2 inflammatory mediators, however they are only efficacious in a defined subgroup of patients (Lambrecht et al. 2019). Thus, new approaches to controlling airway inflammation are needed. ATP has been recognised as an ubiquitous pro-inflammatory mediator controlling various physiological and pathophysiological processes (Pelleg 2020). Increased levels of ATP have been measured in asthmatic patients and there is a substantial body of preclinical literature demonstrating a crucial role of ATP in the development of allergen-induced pathology in AAD models (Idzko et al. 2007, Muller et al. 2011, Idzko et al.

2013, Chen et al. 2016, Zech et al. 2016, Li et al. 2020). However, the mechanisms behind increased airway ATP have not been yet elucidated. The TRPV4 channel is abundantly expressed in the respiratory system and its activation has been linked to ATP release and activation of P2X receptors (Belvisi and Birrell 2017). In the lungs, TRPV4 has been implicated in cough and bronchospasm, symptoms commonly experienced by asthmatic patients (McAlexander et al. 2014, Bonvini et al. 2016, Bonvini et al. 2020)(Figure 1.5). Our laboratory has demonstrated that inhibition of TRPV4 signalling in a rat OVA model alleviated LAR as well as airway eosinophilia (Birrell et al. 2016, Flajolet 2021). Furthermore, genetic ablation of TRPV4 in the murine HDM model prevented the development of IgE and abolished allergic airway inflammation and AHR (Birrell et al. 2016)(Figure 1.6). Similar outcomes were observed in Panx-$1^{-/-}$ mice, suggesting that these effects were mediated via ATP release (unpublished data, Figure 1.7). Although several other groups have demonstrated the pathogenic role of TRPV4 in the development of AAD in murine models in the recent years (Duan et al. 2020, Kim et al. 2020, Wiesner et al. 2020), TRPV4 signalling pathways in asthma have not been yet elucidated.

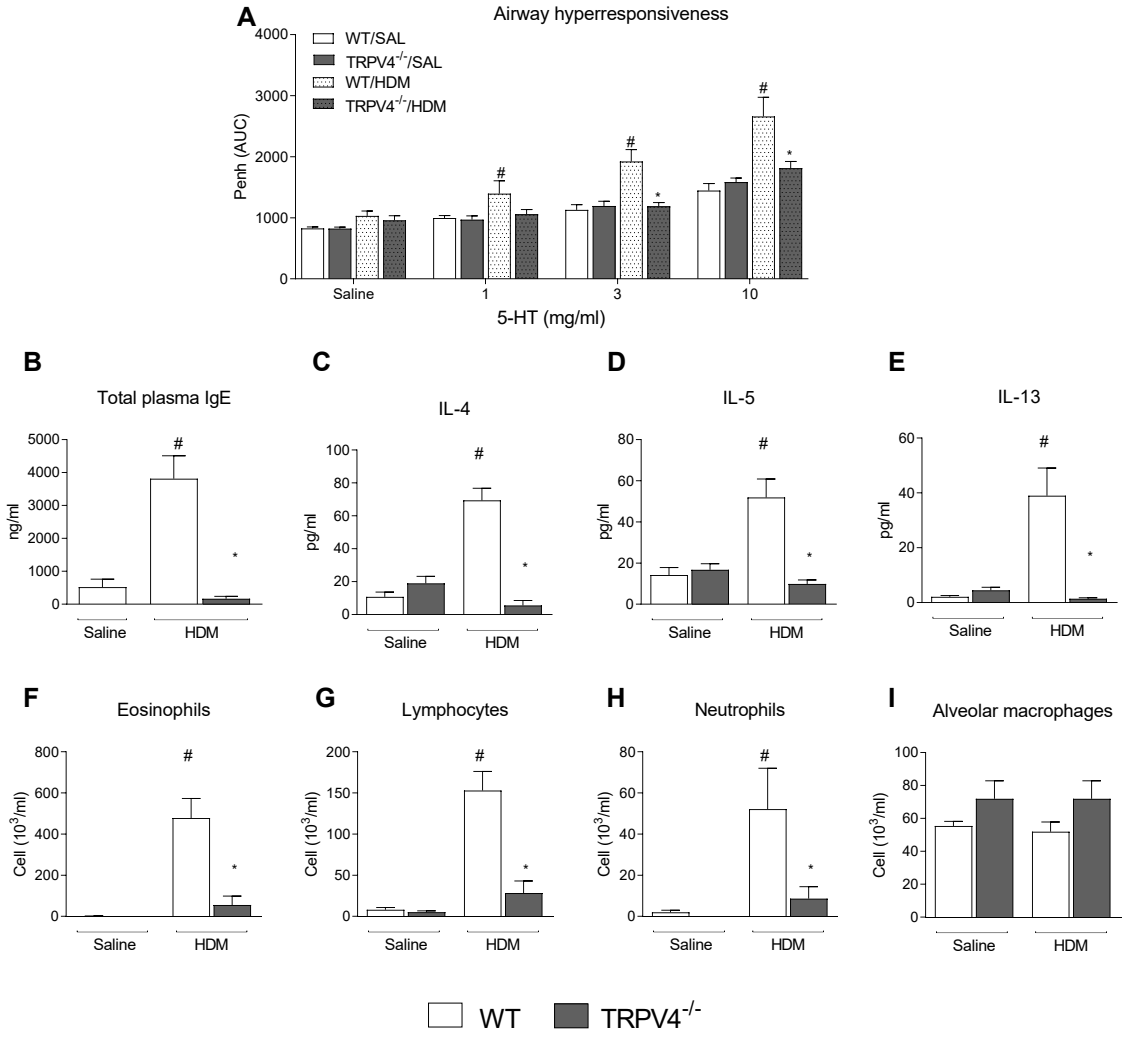


Figure 1.6: TRPV4 deficiency (TRPV4$^{-/-}$) abolished airway hyperresponsiveness (AHR) and eosinophilic airway inflammation in murine house dust mite (HDM) model of allergic airway disease.

Mice were systemically sensitised to HDM and then intranasally challenged with saline (SAL) or HDM on three consecutive days. Lung function, plasma IgE levels and airway inflammation were assessed 3 days after the last challenge. A) Enhanced pause (Penh) to increasing concentrations of serotonin (5-HT) was determined by whole body plethysmography. B) Total plasma IgE levels were determined by ELISA. C) IL-4, D) IL-5 and E) IL-13 were determined in bronchoalveolar lavage (BAL) by ELISA. F) Eosinophil, G) lymphocyte, H) neutrophil and I) alveolar macrophage numbers were determined in BAL by histological assessment. Data from a single experiment are presented as mean ± S.E.M., N=7-9. A) Two-way ANOVA was used to compare experimental groups. # denotes $p < 0.05$ comparing wild type (WT) SAL and WT HDM groups and * $p < 0.05$ comparing WT HDM and TRPV4$^{-/-}$ HDM groups. B-I) # denotes $p < 0.05$ comparing WT SAL group with WT HDM group using Mann-Whitney U test. * denotes $p < 0.05$ comparing WT HDM group with TRPV4$^{-/-}$ HDM group using Mann-Whitney U test. Presented at European Respiratory Society International Congress 2016 (Birrell et al. 2016).

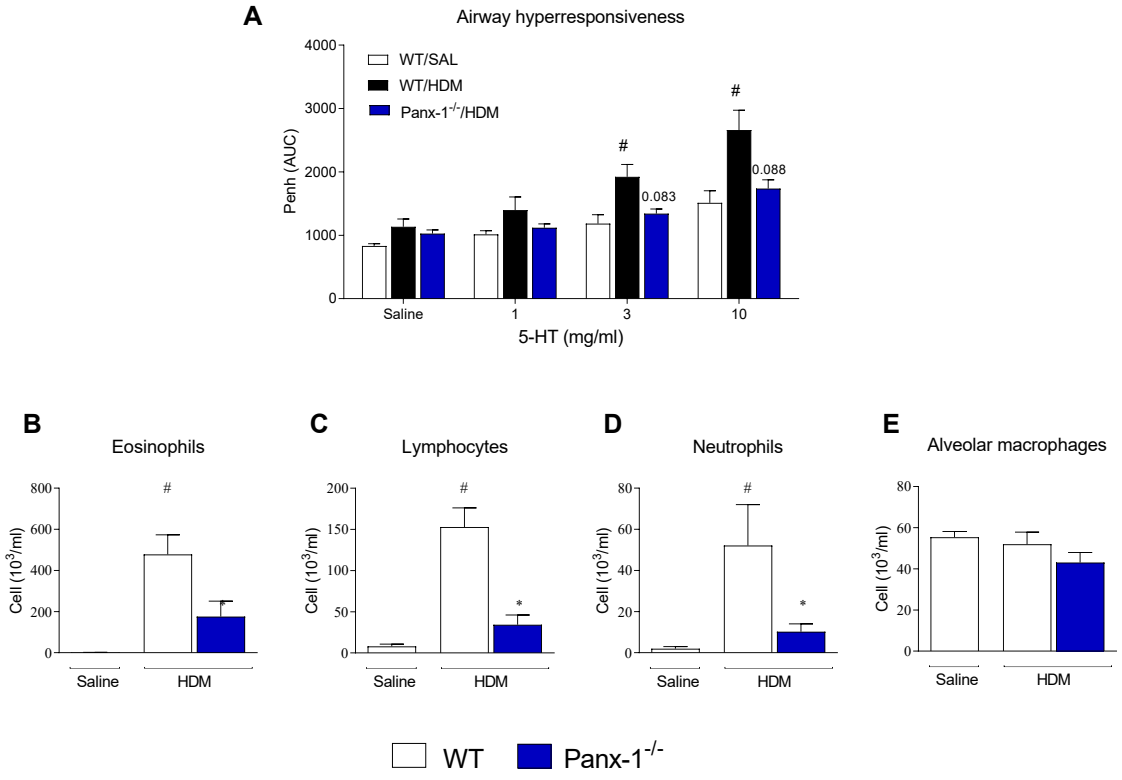


Figure 1.7: Pannexin-1 deficiency (Panx-1$^{-/-}$) abolished airway hyperresponsiveness (AHR) and eosinophilic airway inflammation in murine house dust mite (HDM) model of allergic airway disease.

Mice were systemically sensitised to HDM and then intranasally challenged with saline (SAL) or HDM on three consecutive days. Lung function and airway inflammation were assessed 3 days after the last challenge. A) Enhanced pause (Penh) to increasing concentrations of serotonin (5-HT) was determined by whole body plethysmography. B) Eosinophil, C) lymphocyte, D) neutrophil and E) alveolar macrophage numbers were determined in bronchoalveolar lavage (BAL) by histological assessment. Data from a single experiment are presented as mean ± S.E.M., N=7-9. A) Two-way ANOVA was used to compare experimental groups. # denotes $p < 0.05$ comparing wild type (WT) SAL and WT HDM groups and * $p < 0.05$ comparing WT HDM and Panx-1$^{-/-}$ HDM groups. B-E) # denotes $p < 0.05$ comparing WT SAL group with WT HDM group using Mann-Whitney U test. * denotes $p < 0.05$ comparing WT HDM group with TRPV4$^{-/-}$ HDM group using Mann-Whitney U test.

1.8.1. Hypothesis

TRPV4 is central to the development of allergic airway inflammation and AHR in asthma.

1.8.2. Aims

The overall aim of this thesis was to identify TRPV4 signalling pathways leading to allergic airway inflammation and AHR utilising experimental models of AAD disease.

The aim of Chapter 3 was to investigate whether immune cells key for the development of allergic airway inflammation could be responsible for the drivers of TRPV4 signalling in the murine HDM model of AAD and identify P2X receptors potentially involved in TRPV4 signalling pathway.

The aim of Chapter 4 was to investigate whether the identified candidate P2X receptors were part of the TRPV4 signalling axis responsible for the development of allergic airway inflammation and AHR utilising the murine HDM model.

The aim of Chapter 5 was to investigate PAR2 as a potential mechanism of TRPV4 activation in the murine HDM model.

Lastly, the aim of Chapter 6 was to investigate the efficacy of selective TRPV4 antagonists on the development of allergic airway inflammation, AHR and LAR during allergen challenge phase in the murine HDM and the rat OVA models of AAD.

2. Material and Methods

2.1. Animals

2.1.1. Ethics statement and animal housing conditions

All animal studies strictly conformed to the UK Home Office Guideline under the Animals act 1986. All studies were approved by Imperial College London Ethics Review Committee.

Mice and rats were housed in individually ventilated cages under specific-pathogen free conditions. Twelve hour light-dark cycle and ambient temperature of 21°C were maintained at all times. Autoclaved water and food were available ad libitum. All animals were allowed to acclimatise for seven days before commencing experimental work.

2.1.2. Rats

Male Brown Norway rats (200 – 250 g) were purchased from Charles River Laboratories (Germany).

2.1.3. Mice

Male and female 8 – 12 week old mice were used in the experiments presented in this thesis.

Wild type (WT) mice on C57BL/6J background were purchased from Envigo (UK). P2rx7^{tm1Gab} (P2RX7$^{-/-}$) mice (Solle et al. 2001) and B6.Cg-*F2rl1*^{tm1Mslb}/J (PAR2$^{-/-}$) mice (Schmidlin et al. 2002), both on C57BL/6J background, were purchased from The Jackson Laboratory (USA) and homozygous mutants were bred at Imperial College London. WT C57BL/6J mice were bred alongside P2X7$^{-/-}$ and PAR2$^{-/-}$ mice in separate cages and were used as controls. P2rx4$^{tm1b(EUCOMM)Wtsi}$ (P2X4$^{-/-}$) mice on C57BL/6NTac background were purchased from MRC Harwell Institute (UK) and heterozygous mutants were bred in house to generate P2X4$^{-/+}$ and P2X4$^{+/+}$ littermate controls. Genotyping was routinely carried out to determine the genotypes of newly born P2X4 mice. P2X1$^{-/-}$ mice on BALB/c background, originally developed by Evans, R. J. and colleagues (Mulryan et al. 2000) on C57BL/6 background, were a kind gift from Professor Praetorius, Aarhus University, Denmark. P2X1$^{+/-}$ were bred in house to generate P2X1$^{+/+}$, P2X1$^{+/-}$ and P2X1$^{-/-}$ littermate controls. Initially gel based genotyping was carried out to determine the genetic status of new born mouse. Subsequently, routine automated genotyping using real-time PCR was carried out by Transnetyx, Inc (USA).

2.1.4. Animal sacrifice

Mice and rats were culled with an overdose of an anaesthetic Pentobarbitone (200 mg/kg, intraperitoneal (i.p.) administration). Paw reflexes and heart beating were monitored to

assess the depth of the terminal anaesthesia. Death was confirmed by exsanguination from femoral artery or from other major vessels when cardiac puncture was performed to collect blood.

2.2. In vivo methodology

2.2.1. Assessment of airway responses by flow whole body plethysmography (FWBP)

2.2.1.1. The principles of FWBP

The principles of FWBP presented below are summarised from (Lomask 2006).

FWBP is based on the principle that in an enclosed chamber animal respiration provokes changes in box pressure. As the air is allowed to enter and exit the chamber, the changes in the chamber pressure create a flow that is detected by a pneumotachograph. Continuous monitoring of the box flow during respiration creates a respiratory waveform (Lomask 2006). When a breath is initiated, inspiration muscles expand and the chest relaxes, resulting in a negative pressure within the chest cavity which induces the air to enter the lungs. In the lungs the inhaled air expands due to the negative intrathoracic pressure as well as conditioning (an exchange of heat and moisture between the air and the body – typically, inhaled ambient air (23 °C, 50 % humidity) warms to body temperature (37 °C) and humidifies to 100 %). Increased lung volume increases the pressure in the chamber and triggers an outward chamber flow. When the maximal lung volume is reached at the end of inspiration, box pressure remains constant and the flow becomes zero. This is followed by a contraction of expiratory muscles which initiates the expiration. Due to the resistance of small airways, the air within the thorax is initially compressed before it can be exhaled. The thoracic displacement (reduction in lung volume) reduces the box pressure and induces the inward box flow (thoracic displacement flow). After a few milliseconds build-up of intrathoracic pressure enables exhalation of air through the nasal cavity. The exhaled air is cooled down and excess moisture deposited due to conditioning, further reducing the volume of the exhaled air. This contributes to the drop in chamber pressure and sustains the inward box flow. When the minimal lung volume is reached at the end of expiration, the box pressure remains constant and the flow falls to zero.

Pause and enhanced pause (Penh) operate on the respiratory waveform and are used to evaluate changes that occur during the transition from inspiration to expiration when the flow

is zero. Flow changes in the transition region are predominantly created by the compression (resistance) component enabling Pause and Penh to be used as indirect measures of airway resistance. Pause compares the transition region (early expiration, sensitive to resistance,) with a region that follow but does not include the transition region (late expiration). To achieve that, the expiratory waveform is divided into T_r (relaxation time) and T_e (expiration time) – T_r so that T_r encompasses 64 % of the total expiratory area. Pause is then calculated as $(T_e-T_r)/T_r$. Penh increases the sensitivity of Pause and is a product of Pause and the ratio between peak expiratory flow (PEF) and peak inspiratory flow (PIF) (Hamelmann et al. 1997a, Lomask 2006)(Figure 2.1).

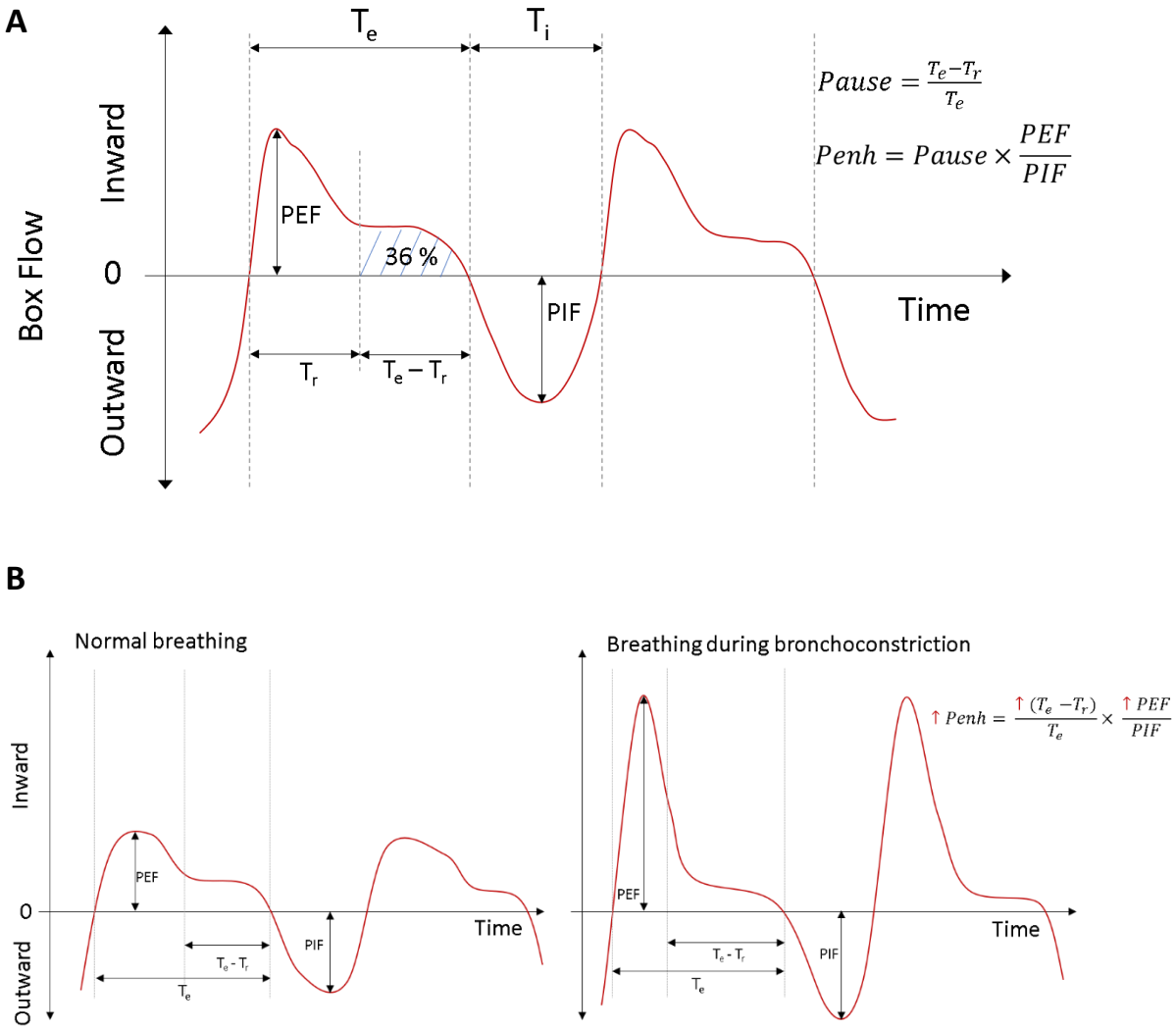


Figure 2.1: Principles of flow whole body plethysmography and a respiratory waveform.

A) Expiration is associated with reduced box pressure which triggers inward box flow. At the end of the expiration the pressure is not changing, resulting in the box flow to fall to zero. Inspiration is initiated which increases the pressure in the box, resulting in an outward flow. At the end of inspiration the box pressure is constant and the flow falls to zero. The respiratory waveform is divided into inspiratory time (T_i) and expiratory time (T_e). T_e is further divided into relaxation time (T_r) and $T_e - T_r$ in such a way that $T_e - T_r$ accounts for 36 % of the expiration flow. Pause and enhanced pause (Penh) are parameters operating on the respiratory waveform and can be used as indirect measures of airway resistance. B) Representation of respiratory waveform during normal breathing and bronchoconstriction. Bronchoconstriction creates a peak in early expiration, resulting in increased peak expiratory flow (PEF) and prolongation of $T_e - T_r$, resulting in increased enhanced pause (Penh). PIF: peak inspiratory flow.

2.2.1.2. The use of Penh as lung function parameter

Pause and Penh have been heavily criticised as a measure of airway resistance. The main concerns regarding the use of Penh as a measure of airway resistance are that Penh could be influenced by conditioning, changes in breathing pattern which do not involve change in airway resistance, air movement within the chamber due to animal movement as well as changes in resistance of upper airways (Bates and Irvin 2003, Bates et al. 2004, Lundblad et al. 2007). Penh is designed in such a way that changes are assessed during early expiration when the effect of conditioning is minimal (Lomask 2006). Conditioning drives the box flow predominantly during inspiration and less so during expiration, contributing little to Pause and Penh (Lomask 2006). Additionally, bronchoconstriction causes a delay between nasal and thoracic flow, which further increases the intrathoracic pressure (Lomask 2006). This creates a peak in the waveform in early expiration when no air expiration can be detected, eliminating conditioning as a reason for the observed peak (Lomask 2006) (Figure 2.1). Several groups have demonstrated a correlation between Penh and direct measurements of lung resistance in allergic airway disease models (Hamelmann et al. 1997a, Bergren 2001, Glaab et al. 2005, Verheijden et al. 2014). Hamelmann et al. have also shown that Penh was not affected by changes in respiratory rate alone as neither avertin nor increased CO_2 concentration affected Penh (Hamelmann et al. 1997a). Although animal movement may affect the respiratory waveform and subsequently Penh, Quindry et al. have obtained reproducible respiratory data when allowing experimental animals to acclimatise to FWBP chambers (Quindry et al. 2016). Rodents are obligatory nasal breathers and an increase in Penh has been shown to partially reflect an increase in nasal cavity resistance during methacholine challenge due to increased mucus production or mucosal swelling (Hamelmann et al. 1997a, Irvin and Bates 2003).

We acknowledge the limitations of FWBP as a lung function assessment technique and appreciate that it cannot be used to directly measure airway resistance. However, we and others have shown that it can be repeatedly used to evaluate airway responses in animal models of AAD (Hamelmann et al. 1997a, Underwood et al. 2002, Raemdonck et al. 2012, Verheijden et al. 2014, Raemdonck et al. 2016). To limit the effect of upper airway resistance due to mucus hypersecretion during AHR assessment in our murine AAD model, 5-HT rather than methacholine was used as a bronchoconstrictor (Raemdonck et al. 2016). More importantly, this is the only technique available to assess lung function in conscious,

unrestrained animals under physiological conditions as direct measurement of airway resistance and dynamic compliance such as forced oscillometry are only performed on anaesthetised animals (Bates and Irvin 2003, Verheijden et al. 2014). Allergen-provoked airway responses such as LAR are driven by nerve reflexes and our laboratory has previously established that OVA-induced LAR is lost in anaesthetised rats (Raemdonck et al. 2012), demonstrating that invasive lung function techniques are inappropriate for LAR assessment. Similarly, the mechanisms behind AHR are complex and not yet fully understood, and nervous system is thought to contribute to the regulation of airway tone and airway responsiveness (Pincus et al. 2021). TRPV4 has been implicated in airway nerve reflexes and responses such as cough and LAR (Birrell et al. 2016, Bonvini et al. 2016, Flajolet 2021), thus FWBP is better suited to study the role of TRPV4 in AHR as well. Moreover, FWBP had been previously used for the assessment of LAR and AHR in our rat and murine AAD models, respectively (Underwood et al. 2002, Raemdonck et al. 2012, Birrell et al. 2016, Raemdonck et al. 2016, Flajolet 2021), hence FWBP was chosen as a technique to evaluate allergen-associated airway responses in this thesis.

2.2.2. Murine HDM-induced model of AAD

An established model of AAD with distinct sensitisation and challenge phases (Raemdonck et al. 2016) was used in this thesis to study the role TRPV4 in allergic airway inflammation and AHR.

2.2.2.1. HDM preparation

Lyophilised HDM (Greer Laboratories, catalogue number XPB82D3A25, lot number 185637, Derp1 content 1019.3 µg/vial) was reconstituted with saline (Baymed, UK) to obtain 10 µg/ml Derp1 stock solution. Stock solution was aliquoted and stored at -80 °C. An aliquot was defrosted and further diluted in saline on the day of the experiment.

2.2.2.2. Study protocol

During sensitisation phase mice were administered 0.5 µg/kg Derp1 HDM extract prepared in saline by intraperitoneal injection on days 0 and 14. Mice were anaesthetised with isoflurane (Abbott Laboratories, UK) and administered HDM (1.25 µg/kg Derp1) or saline (intranasally (i.n.), 50 µl dosing volume) on days 24, 25 and 26. Assessment of airway inflammation and

AHR was performed on day 29 unless stated otherwise in individual result chapters (Figure 2.2).

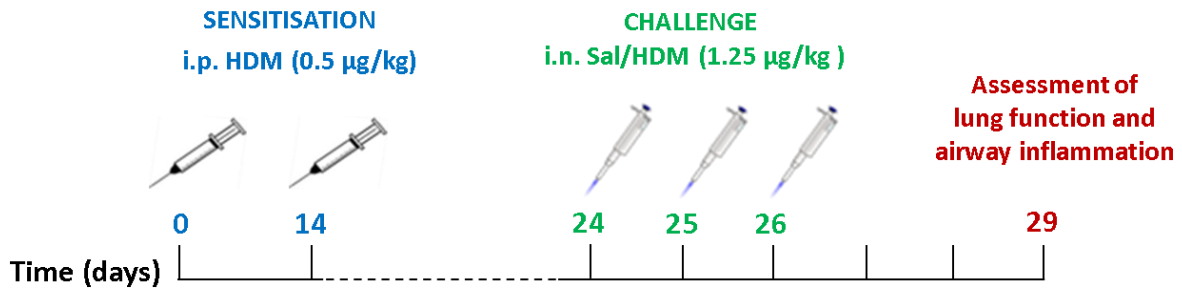


Figure 2.2: Murine house dust mite (HDM)-induced allergic airway disease (AAD) model protocol.
Mice were intraperitoneally (i.p.) sensitised to HDM on days 0 and 14. Mice were administered saline or HDM intranasally (i.n.) once daily on days 24, 25 and 26. Typically, airway inflammation and airway hyperresponsiveness were assessed on day 29.

2.2.2.3. AHR assessment

Conscious, unrestrained mice were placed into FWBP chambers connected to bias flow pumps (Buxco Electronics, UK) and allowed to acclimatise for 2 minutes. Mice were then challenged with saline followed by increasing concentrations of serotonin (5-HT, Sigma-Aldrich, UK) (1, 3 and 10 mg/ml made in saline) by nebulising 50 µl per chamber of each concentration. A response to each challenge was monitored for 15 minutes. Mice were being observed for the duration of the entire assessment. Penh was derived from the respiratory waveform by Buxco Finepointe Software (Buxco Electronics). Area under curve (AUC) was calculated for each challenge and used for statistical analysis.

2.2.3. Rat OVA-induced model of AAD

An established rat model of OVA-induced AAD (Underwood et al. 2002) was used to investigate the role of TRPV4 signalling in LAR.

2.2.3.1. Study protocol

Rats were sensitised with OVA (Sigma-Aldrich, 100 µg/rat) and Alum™ adjuvant (Thermo Fisher Scientific, UK, 20 mg aluminium hydroxide and 20 mg magnesium hydroxide per rat, diluted 1:1 in saline) by i.p. injection on days 0, 14 and 21. On day 28 rats were placed in Perspex chambers connected to bias flow pumps and challenged with either saline or OVA (1 % w/v in saline) for 30 min. Rats were placed in FWBP chambers one hour after the challenge

and LAR monitored for 5 hours. 24 hours after the challenge rats were sacrificed for the assessment of airway inflammation (Figure 2.3).

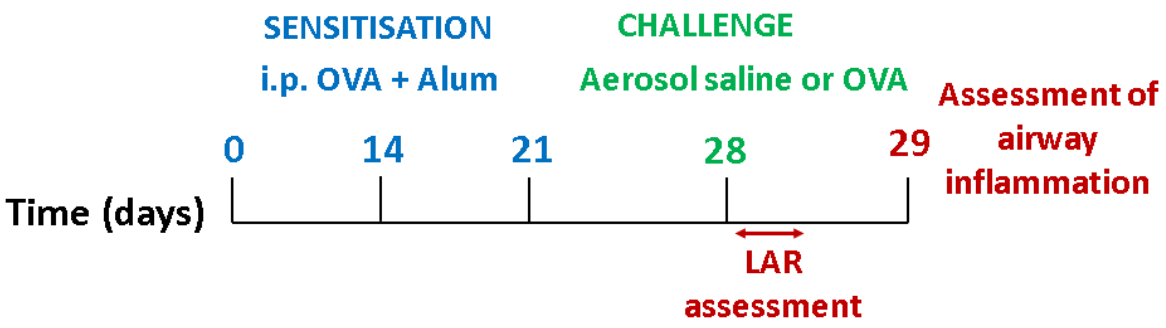


Figure 2.3: Rat ovalbumin (OVA)-induced allergic airway disease model protocol.

Rats were intraperitoneally (i.p.) administered OVA with aluminium hydroxide (Alum) on days 0, 14 and 21. On day 28 rats were challenged with aerosolised saline or OVA for 30 minutes. One hour later late asthmatic response (LAR) was monitored for 5 hours. On the next day (day 29), rats were sacrificed to evaluate airway inflammation.

2.2.3.2. LAR assessment

Conscious and unrestrained rats were placed in FWBP chambers one hour after OVA or saline challenge and their respiratory responses were recorded for 5 hours. Food and water were freely available during the assessment. Penh was derived from the respiratory waveform by Buxco Finepointe Software (Buxco Electronics). Average Penh was calculated every 10 min by the software over the duration of the recording. Average Penh over time was used to calculate AUC which was then used for further statistical analysis.

2.2.4. NLRP3 inflammasome activation model

NLRP3 inflammasome activation model was used for validation of $P2X7^{-/-}$ mice. WT and $P2X7^{-/-}$ mice were placed in Perspex chambers and were challenged with aerosolised saline or LPS (Sigma-Aldrich, 1 mg/ml in saline) for 30 minutes. Five hours after the start of the study mice were briefly anaesthetised with isoflurane and intranasally administered phosphate buffered saline (PBS) (Gibco, UK, 50 µl) or ATP (Sigma-Aldrich, 100 µg/mouse in PBS). Mice were sacrificed 90 minutes later with an overdose of Pentobarbitone (200 mg/kg, i.p.) for the assessment of inflammatory markers (Figure 2.4).

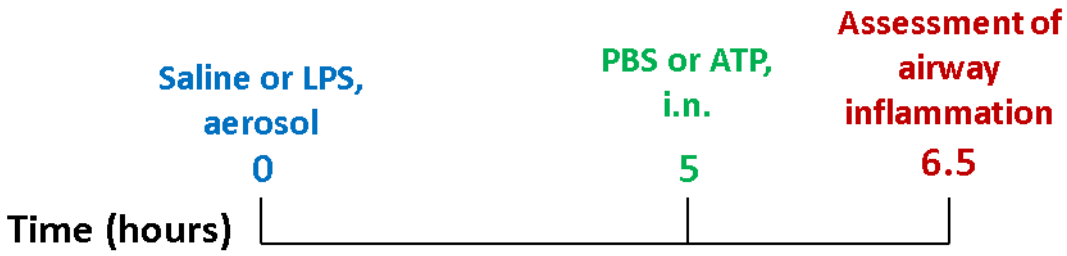


Figure 2.4: A study protocol for NLRP3 inflammasome activation model.

Mice were exposed to aerosolised saline or lipopolysaccharide (LPS) for 30 minutes. 5 hours after the start of the study mice were intranasally (i.n.) challenged with phosphate buffered saline (PBS) or adenosine triphosphate (ATP). Mice were sacrificed and airway inflammation assessed 1.5 hours after ATP/PBS challenge.

2.2.5. Pharmacokinetic (PK) studies

PK studies to determine PK profile or plasma concentration of TRPV4 antagonists GSK2798745 (GSK279) (Brooks et al. 2019) and GSK2193874 (GSK219) (Thorneloe et al. 2012, Cheung et al. 2017) in mice and rats, respectively were performed AstraZeneca (Research & Early Development, Respiratory & Immunology, BioPharmaceuticals R&D) using mass spectrometry.

2.2.6. TRPV4 pharmacodynamic (PD) models

Mice or rats, respectively, were paced in FWBP chambers and allowed to acclimatise for 5 minutes. Animals were initially monitored for 20 minutes to obtain a baseline recording and were then exposed to nebulised vehicle (1 % ethanol (Fisher Scientific, UK) + 1 % Tween 80 (Sigma-Aldrich) in saline) or a selective TRPV4 agonist GSK1016790A (GSK101, Sigma-Aldrich) (Thorneloe et al. 2008) for 10 minutes. Mice were monitored throughout the challenge for a total of 20 minutes (Figure 2.5). Penh was derived from the respiratory waveform and AUC calculated by Buxco Finepointe Software (Buxco Electronics). Baseline Penh AUC was subtracted from Challenge Penh AUC and used for statistical analysis.

10 µg/ml GSK101 was chosen for the rat studies based on the previous characterisation in our laboratory demonstrating 10 µg/ml to be a submaximal concentration provoking bronchospasm in rats (Flajolet 2021).

GSK101 concentration for murine studies was based on the extensive in-house characterisation of GSK101 responses in rat and GP in vitro and in vivo models (Bonvini et al.

2016, Flajolet 2021). 30 µg/ml GSK101 was the submaximal concentration triggering cough in GP cough model and was thus selected for the murine TRPV4 PD studies (Bonvini et al. 2016).

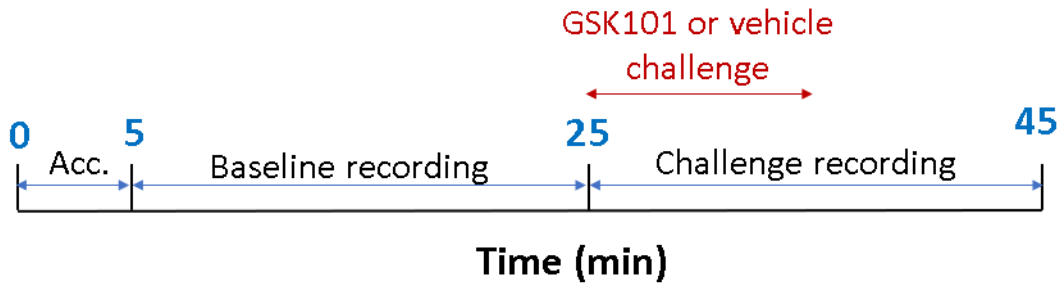


Figure 2.5: A protocol for TRPV4 pharmacodynamic model.

Experimental animals were placed into whole body plethysmography chambers and allowed to acclimatise (Acc.) for 5 minutes before determining 20-minute baseline. GSK1016790A (GSK101) or vehicle were then nebulised for 10 minutes and responses monitored for 20 minutes.

2.3. Sample collection and processing

2.3.1. Blood

Upon sacrifice, cardiac puncture using a heparinised syringe was performed to collect blood. Samples were kept on ice until centrifugation (10 minutes at 1200 g, 4°C). Plasma was collected and stored at -80 °C for further analyses.

2.3.2. Airway lumen cells

Trachea was exposed and a blunt-ended cannula inserted in caudal direction and secured with a suture thread. Mice were injected 300 µl of RPMI medium (RPMI 1640 Glutamax, Thermo Fisher Scientific) into the airways and recovered after 30 seconds using a 1 ml syringe (BD Biosciences, UK). The process was repeated 3 times and volume pooled. Rats were lavaged twice with 3 ml of RPMI. The medium was recovered after 30 seconds and volume pooled. The recovered BAL fluid was kept on ice until it was centrifuged at 800 x*g* for 10 minutes at 4 °C. The supernatant was collected and stored at -80°C.

The cell pellet was resuspended in RPMI medium. Total leukocyte numbers were determined by an automated cell counter Sysmex XP-300 (Sysmex Ltd, UK). BAL cells were mounted onto slides by spinning at 807 x*g* for 5 min at room temperature in a cytospin centrifuge (Shandon, Runcom, UK). Slides were stained with a Hematek modified Wright stain (Siemens

Heathineers, Germany) using a Hematek 2000 automated slide strainer (Ames Co., Elkhart, USA). Cytospins were used for differential counts as specified in individual results chapters. Differential cell counts were performed, counting 200 cells per slide under 40-times magnification on a light microscope by a blinded operator based of morphological criteria. Percentages of eosinophils, neutrophils, macrophages/monocytes and lymphocytes were determined and total numbers of each distinct cell type were determined based on total leukocyte numbers. As detailed in the individual results chapters, in some studies the remainder of BAL cells were kept on ice and stained for extracellular and intracellular markers for subsequent analysis by flow cytometry.

2.3.3. Lung tissue

2.3.3.1. Isolation of lung cells

The left lung lobe was isolated into R10F medium (RPMI 1640 Glutamax, supplemented with 10 % fetal calf serum (FCS; Gibco) and 1000 U/ml Penicillin-Streptomycin (Gibco)) and kept on ice (4°C) until it was finely chopped into 2 mm or smaller pieces using scissors. Samples were then incubated in 600 U/ml collagenase IV (Worthington Biochemicals, USA), 12 mg/ml Dispase II (Roche, UK) and 25 µg/ml DNase I (Roche) for 30 min at 37 °C in a shaking water bath. After incubation lungs were mashed through 70 µm cell strainers (Corning incorporated, USA) using a bat of a 2 ml syringe and centrifuged at 800 x*g* for 5 minutes at 4 °C. Supernatant was discarded and cells incubated for 3 minutes in 2 ml ammonium chloride based red blood cell lysing solution (155 mM NH_4Cl, 10 mM $KHCO_3$, 0.1 mM Na_2EDTA made in distilled water with pH adjusted to 7.2-7.4). The reaction was stopped by addition of 3 ml R10F medium. Cells were centrifuged again and after discarding the supernatant, resuspended in 500 µl PBF (PBS supplemented with 2 % FCS (Gibco), 2 mM EDTA (Promega, USA), and 0.05 % sodium azide (Sigma-Aldrich)) and filtered through 70 µm cell strainers. Total leukocyte numbers were determined by the automated cell counter Sysmex XP-300. 50,000 cells were used to prepare cytospins as described in section 2.3.2. The rest of the lung cell suspension was kept on ice until stained for extracellular and intracellular markers.

2.3.3.2. Isolation of lung lobes for protein and gene expression assays

The right lobes were isolated and flash frozen in liquid nitrogen and stored at -80 °C.

2.3.4. Mediastinal lymph nodes (MLN)

Tracheobronchial lymph node was identified in the proximity of the tracheal bifurcation. In healthy mice it was recognized as a 1 to 2 mm long ellipsoid pearly white structures, often surrounded with fat tissue (Kawashima et al. 1964, Van den Broeck et al. 2006). In mice with airway inflammation lymph nodes were enlarged, measuring around 3 to 5 mm, and were thus easier to identify.

MLNs were cleaned and teased apart in R10F medium and then incubated in R10F containing collagenase D (0.5 mg/ml, Roche) and DNAse I (0.25 µg/ml) at 37 °C for 30 minutes in a shaking water bath. Tissues were mashed through 70 µm strainers and centrifuged (400 g, 4 °C, 5 minutes). Supernatants were removed and cells resuspended in PBF.

2.4. Gel based genotyping

2.4.1. Crude DNA extraction

Extracta DNA prep for polymerase chain reaction (PCR) kit (Quanta Biosciences, USA) was used to extract DNA from ear punches or tail tips in accordance with the manufacturer's instructions. Briefly, tissues were incubated in 75 µl of extraction buffer at 95 °C for 30 min. After cooling to room temperature, 75 µl of stabilisation buffer was added. Absorbance at 260 nm and 280 nm was measured using a spectrophotometer PowerWave™ XS Microplate Reader (BioTek Instruments, UK) to determine DNA concentration and purity. DNA concentration was adjusted to 10 ng/µl with nuclease free water (Promega) before amplified in polymerase chain reaction (PCR).

2.4.1. Polymerase chain reaction

GoTaq Flexi DNA Polymerase kit (Promega) was used accordingly to manufacturer's instructions. A reaction mix containing 1x Green Go Taq Flexi Buffer, 0.4 mM dNTP, 2 mM $MgCl_2$, 0.04 U/µl GoTaq DNA polymerase, 0.4 pmol/µl primers (Table 2.) and 50 ng genomic DNA was prepared with nuclease free water in a total volume of 25µl. A single multiplex PCR was performed for genotyping of P2X4, P2X7 and PAR2 strains. Two singleplex PCRs (WT reaction with WT-FWD and WT-REV primers and knockout (KO) reaction with NEO-FWD and NEO-REV primers) were performed for genotyping of P2X1 mice. PCR was run using StepOnePlus™ Real-Time PCR System (Applied Biosystems, USA) under the following conditions: step 1 – 95 °C for 2 minutes, step 2 – 40 cycles of 95 °C for 30 sec, 60 °C for 30 sec

and 72 °C for 30 sec, step 3 – 75 °C for 10 min. Samples were then cooled to room temperature and loaded onto agarose gels.

2.4.2. Gel electrophoresis

2 % agarose (Sigma-Aldrich) gels were prepared in Tris/Borate/EDTA (TBE) buffer (89 mM Tris (Sigma-Aldrich), 89 mM Borate (Sigma-Aldrich), 2 mM EDTA) containing SafeView Nucleic Acid Stain (50 µl/l, NBS Biologicals, UK). 5 µl 1 kb DNA ladder (100 bp resolution, Hyperladder, Bioline, UK) and 20 µl samples were loaded to the gel. Gels were run for 1 hour at 100 mV and were visualised under UV light with Odyssey Fc (LI-COR Biosciences, Germany).

Table 2.*1*: Forward (FWD) and reverse (REV) primer sequences used in PCR for genotyping of P2X1$^{-/-}$, P2X4$^{-/-}$, P2X7$^{-/-}$ and PAR2$^{-/-}$ mice, respectively.

WT – wild type, NEO – mutant, bp – base pair.

Strain	Primer name	Primer sequence	Product size (bp)
P2X1	WT-FWD	TCACCCAATGACGTAGACCAGAAC	~300
	WT-REV	AACCCAGATCCCACCAACGAAC	
	NEO-FWD	CACCGATCGCCCTTCCCAACAGT	~500
	NEO-REV	TGCCGCTCATCCGCCACAT	
P2X4$^{-/-}$	WT-REV	AGCTCCAGGAGATGCACAGT	259
	NEO-REV	GAACTTCGGAATAGGAACTTCG	127
	FWD (common)	GGCTGGCTTAACCATTCTTT	
P2X7$^{-/-}$	WT-FWD	TCA CCA CCT CCA AGC TCT TC	246
	NEO-FWD	GCC AGA GGC CAC TTG TGT AG	200
	REV (common)	TAT ACT GCC CCT CGG TCT TG	
PAR2$^{-/-}$	WT-FWD	TCA AAG ACT GCT GGT GGT TG	345
	NEO-FWD	GCC AGA GGC CAC TTG TGT AG	196
	REV (common)	GGT CCA ACA GTA AGG CTG CT	

2.5. Flow cytometry

2.5.1. General extracellular staining protocol

Up to 2 million cells were loaded onto V-bottom 96-well plate (Thermo Fisher Scientific) and centrifuged at 800 g for 3 minutes. To identify live cells, cells were resuspended in 50 µl of LIVE/DEAD fixable near-IR (Invitrogen, UK) dead cell stain kit dye (1:1000 dilution in PBS) and incubated at 4 °C for 15 minutes. Cells were washed with 150 µl PBS and centrifuged to remove the supernatant. Next, cells were incubated in 30 µl anti-CD16/32 antibody (1:200 dilution in PBF, BD Bioscience) at 4 °C for 15 minutes to prevent any non-specific binding. After a wash with 180 µl of PBF (PBS supplemented with 10 % FCS), cells were incubated with a combination of fluorophore-labelled primary antibodies prepared in PBF at 4 °C for 30 minutes (30 µl/well). The antibodies used for extracellular staining are detailed in Table 2.2. Following the incubation, cells were washed 3 times with 200 µl PBF and fixed with 100 µl of 2 % formaldehyde (Sigma-Aldrich) in PBS for 15 minutes at room temperature. After a wash with PBF, cells were resuspended in 200µl PBF and stored at 4 °C until analysed with Fortessa (BD Bioscience, UK) flow cytometer.

2.5.2. General intracellular transcription factor staining protocol

Cells were stained for extracellular markers as described in the above section 2.5.1. After the incubation with extracellular antibodies, cells were washed 3 times with PBF and fixed with Fix/Perm buffer (Invitrogen, USA) and left overnight at 4 °C. Next day, cells were resuspended in permeabilization buffer (Invitrogen) and stained with fluorophore-labelled primary antibodies (50 µl/well) (Table 2.2) prepared in permeabilization buffer at 4°C for 30 minutes. After incubation, cells were washed twice with permeabilization buffer before the final wash with PBF. Cells were then resuspended in 200 µl PBF and stored at 4°C until the flow cytometric analysis on Fortessa flow cytometer.

2.5.3. Fluorescence activated cell sorting (FACS)

Mouse lungs were isolated and single cell suspension obtained as described in 2.3.3.1.1. Cells were plated onto 96 V-bottom plate at 2 million cells per well. Cells were incubated with anti-CD16/32 antibody to prevent non-specific binding, followed by incubation with fluorophore-labelled primary surface antibodies as specified in Table 2.2 at 4 °C for 30 minutes. Live-and-dead marker 4’,6-diamidino-2-phenylindole (DAPI) (Sigma-Aldrich) was

added to each sample prior to the sorting to allow for isolation of live cells. FACS was performed on Aria cell sorter (BD Bioscience) using BD FACSDiva™ Software (BD Biosciences, USA) by Flow Cytometry Facility at Imperial College London. Cell sorting was performed with > 95 % purity. Cells were sorted into PBS and immediately centrifuged at 160 g for 5 min at 4 °C. Cell pellets were resuspended in 350 µl RLT buffer (Qiagen, UK) containing 1 % β-mercaptoethanol (Sigma-Aldrich) for subsequent RNA extraction.

2.5.4. Compensation controls

VersaComp Antibody Capture Kit (Beckmam Coulter, USA) was used to prepare single fluorophore controls for each experiment to allow for the correction of fluorophores' spectral overlap. Briefly, a drop of negative and a drop of positive beads were combined in a 2 ml tube (StarLab, UK). 1 µl of a single antibody used in an experiment was added to the beads and briefly vortexed. Beads were incubated with antibodies for 20 minutes at room temperature in the dark. Beads were washed with 2 ml PBF and centrifuged at 6000 g for 3 minutes. For live-and-dead single colour control, two cell samples were prepared, one unstained and one stained with live-and-dead dye only. The supernatant was decanted and beads were resuspended in 1 ml PBF. Single colour controls were acquired on Fortessa flow cytometer or Aria cell sorter prior to analysing or sorting samples, respectively. Fluorescence compensation was performed BD FACSDiva™ Software.

2.5.5. Gating strategy

2.5.5.1. Gating strategy for identification of T cells, NK cells and B cells

A previously established strategy was used to identify T cells, NK cells and B cells (Patel et al. 2019) and is presented on Figure 2.6. Initially, clumped cells were excluded from the analysis by plotting the height (FSC-H) against the area (FSC-A) for forward scatter (FSC) (Figure 2.6A). Dead cells were excluded from the analysis based on the positive staining with a live-and-dead dye ((Figure 2.6B). A "lymphocyte gate" was defined next based on characteristic cell size (FSC-A) and cell granularity (side scatter SSC-A) and was used for the subsequent analysis of lymphocyte markers' expression ((Figure 2.6C). Cells positive for CD19 were recorded as B cells ((Figure 2.6D). Cells positive for CD3 and CD4 markers were recorded as $CD4^+$ T cells while cells positive for CD3 and CD8 markers were recorded as $CD8^+$ T cells ((Figure 2.6E). $CD3^-$ $CD19^-$ $NKp46^+$ cells were recorded as NK cells ((Figure 2.6F). Fluorescence minus one

(FMO; cells stained with all but one marker) controls were prepared the gating strategy. The analysis was performed by FlowJo™ version 10.6.2 (BD Biosciences).

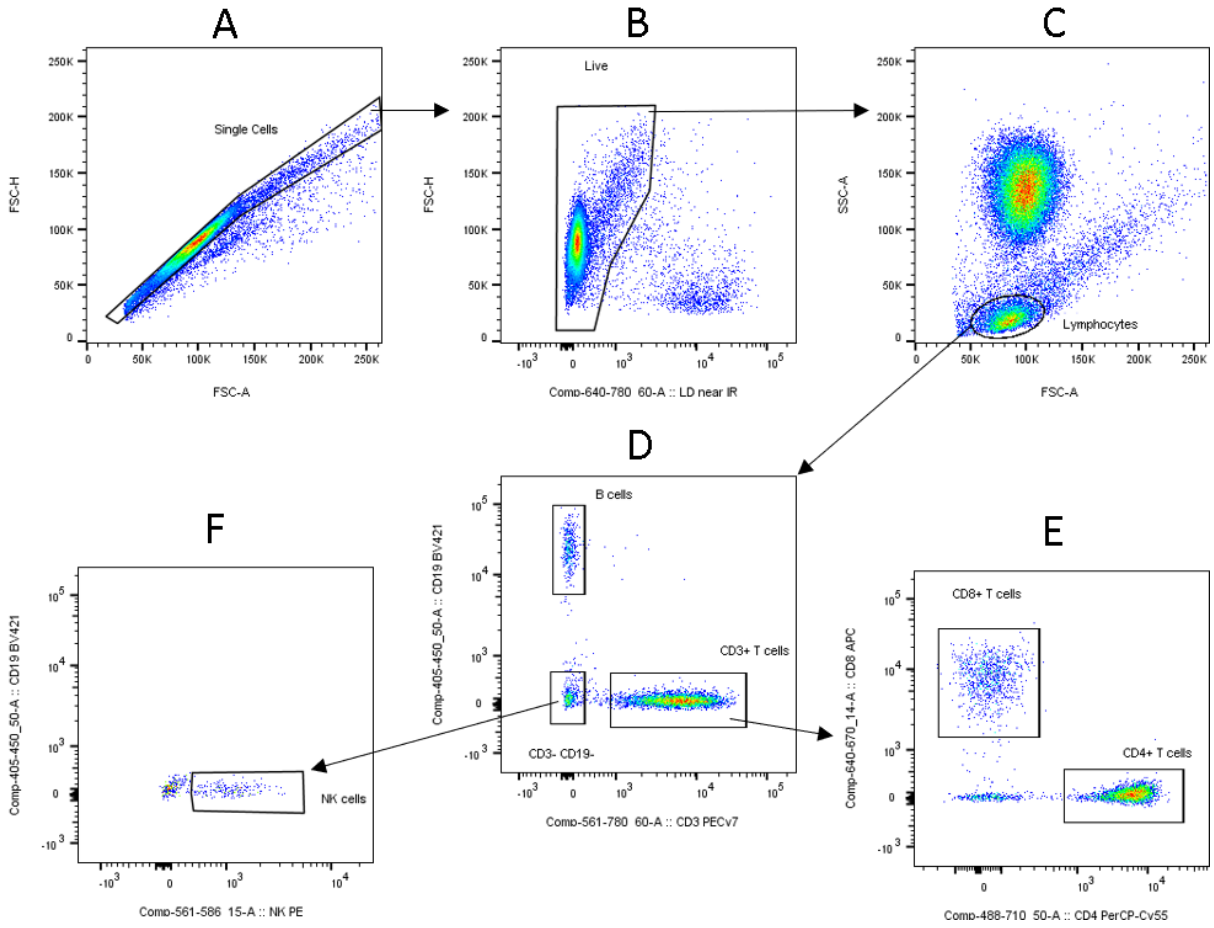


Figure 2.6: Gating strategy for the identification of CD4$^+$ T cells, CD8$^+$ T cells, B cells and natural killer (NK) cells. A) Single cell gate. B) Live cell gate. C) Lymphocyte gate. D) B cell, T cell and CD3$^-$ CD19$^-$ gate. E) CD4$^+$ and CD8$^+$ T cell gate. F) NK gate.

2.5.5.2. Gating strategy for identification of ILCs

A previously established and characterised strategy was used to identify ILCs subgroups (Dutton et al. 2017) and is presented in Figure 2.7. Clumped cells were excluded from the analysis based on the FSC-A/FSC-H profile (Figure 2.7A). Dead cells were excluded based on a positive staining with live-and-dead dye and haematopoietic cells were recognised based on the expression of CD45 marker (Figure 2.7B). A "lymphocyte gate" was determined for the subsequent analysis of extracellular and intracellular marker expression (Figure 2.7C). ILCs were recognised based on the lack of expression of lymphocyte, NK, myeloid lineage markers (see Table 2.2) and expression of CD127 (Figure 2.7D). Any contaminating T cells were excluded based on the expression of intracellular CD3 (Figure 2.7E) and ILCs subgroups were

identified based on the expression of transcription factors. Gata3 positive cells were recorded as ILC2s (Figure 2.7G), Tbet positive cells as ILC1s (Figure 2.7G) and RORγt positive cells as ILC3s (Figure 2.7F). The gating was determined by respective FMO controls. The analysis was performed by FlowJo™ version 10.6.2.

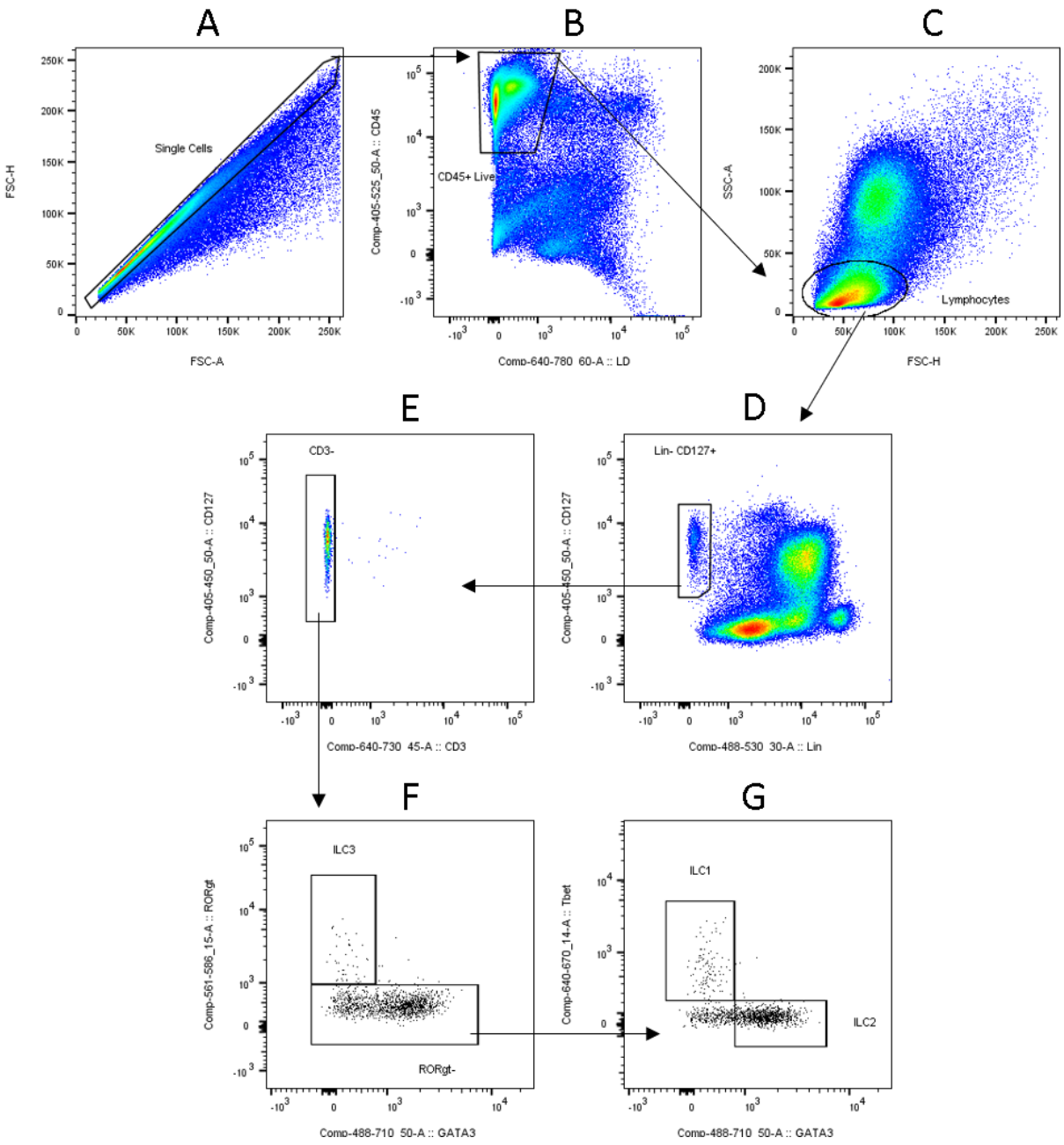


Figure 2.7: Gating strategy for the identification of innate lymphoid cell (ILC) populations.

A) Single cell gate. B) Live CD45^{+} gate. C) Lymphocyte gate. D) Lineage (Lin)$^{-}$ CD127^{+} gate. E) Intracellular CD3^{-} cells. F) RORγt^{+} cells were identified as ILC3s. G) RORγt^{-} cells positive for Tbet were recorded as ILC1s and GATA3^{+} cells as ILC2s.

2.5.5.3. Gating strategy for isolation of ILC2s, CD4+ T cells and CD8+ T cells

Lymphocytes were gated on based on their FSC-A/SSC-A profiles (Figure 2.8A). Single cells were included in the analysis based on the FSC-A/FSC-H profile(Figure 2.8B). Live cells (negative for live-and-dead dye) expressing CD45 marker were identified (Figure 2.8C). Next, CD127 was plotted against a combination of lymphocyte, NK and myeloid lineage markers (as detailed in Table 2.2) (Figure 2.8D). Lin^- cells expressing CD127 marker were checked for expression of KLRG1 and ICOS. Lin^- $CD127^+$ $KLRG1^+$ $ICOS^+$ cells were sorted as ILC2s (Figure 2.8E). Lin^+ cells were analysed for expression of CD4 and CD8 markers. Lin^+ $CD4^+$ cells were sorted as $CD4^+$ T cells and Lin^+ $CD8^+$ cells were sorted as $CD8^+$ T cells (Figure 2.8F). FMO controls were used to determine the respective gates. BD FACSDiva™ Software was used for the analysis and setting of the gates.

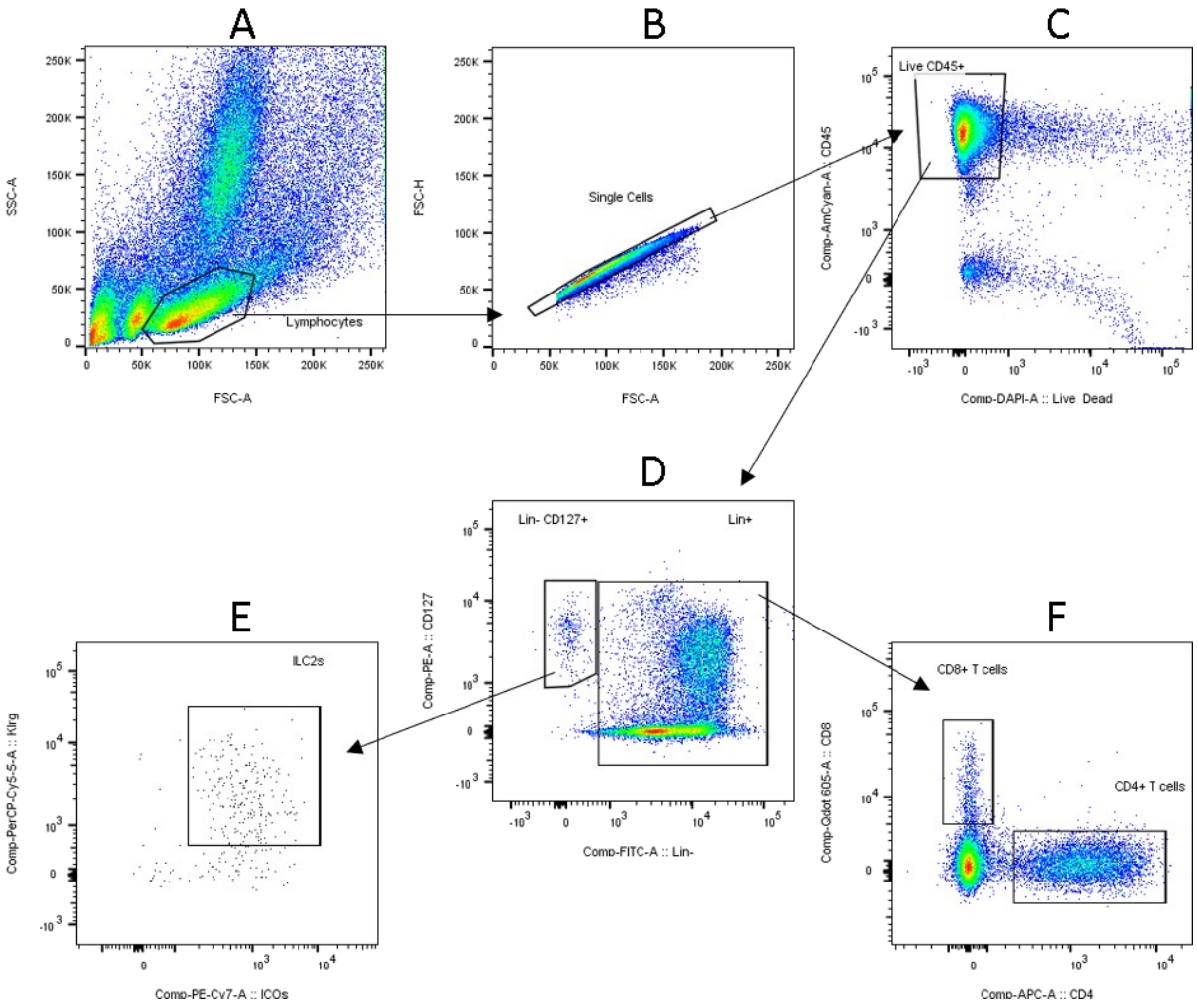


Figure 2.8: Gating strategy for isolation of group 2 innate lymphoid cells (ILC2s), $CD4^+$ T cells and $CD8^+$ T cells.

A) Lymphocyte gate. B) Single cell gate. C) Live $CD45^+$ cells. D) Lineage (Lin) was plotted versus CD127 expression to identify Lin^- $CD127^+$ cells and Lin^+ cells. E) Lin^- $CD127^+$ $ICOS^+$ $KLRG1^+$ cells were sorted as ILC2s. F) Lin^+ CD4 expressing cells were sorted as $CD4^+$ T cells and Lin^+ CD8 expressing cells as $DC8^+$ T cells.

2.5.5.4. Gating strategy for identification of myeloid cells

A previously established strategy was used to identify myeloid cells (Patel et al. 2019) and is depicted on Figure 2.9. Single cells were identified based on the FSC-A/FSC-H profile (Figure 2.9A). Dead cells were excluded from the analysis based on the positive staining with live-and-dead dye (Figure 2.9B). CD11c was plotted against CD11b and $CD11c^+$ and $CD11b^+$ $CD11c^-$ gates were drawn (Figure 2.9C). $CD11c^+$ positive cells were analysed for the expression of Siglec F and F4/80 and cells positive for both markers were recorded as alveolar macrophages (AMs) (Figure 2.9D). $CD11b^+$ $CD11c^-$ cells were also analysed for expression of Siglec-F and F4/80 and $CD11b^+$ $CD11c^-$ Siglec F^+ cells were recorded as eosinophils (Figure 2.9E). $CD11b^+$ $CD11c^-$ $Siglec\text{-}F^-$ cells were further analysed for expression of Ly6C and F4/80. $CD11b^+$ $CD11c^-$ $Siglec\text{-}F^-$ $F4/80^+$ cells expressing low levels of Ly6C were defined as $Ly6C^{low}$ monocytes while cells expressing high levels of Ly6C were defined as $Ly6C^{high}$ monocytes (Figure 2.9F). $CD11b^+$ $CD11c^-$ $Siglec\text{-}F^-$ $F4/80^-$ cells expressing intermediate levels of Ly6C ($Ly6c^{int}$) were analysed for expression of Ly6G. $CD11b^+$ $CD11c^-$ $Siglec\text{-}F^-$ $F4/80^-$ $Ly6C^{int}$ $Ly6G^+$ cells were recorded as neutrophils (Figure 2.9G). All myeloid cell populations were validated by characteristic FSC-A and SSC-A profiles (Figure 2.9H). All the gates were determined with the help of FMO controls. The analysis was performed by FlowJo™ version 10.6.2.

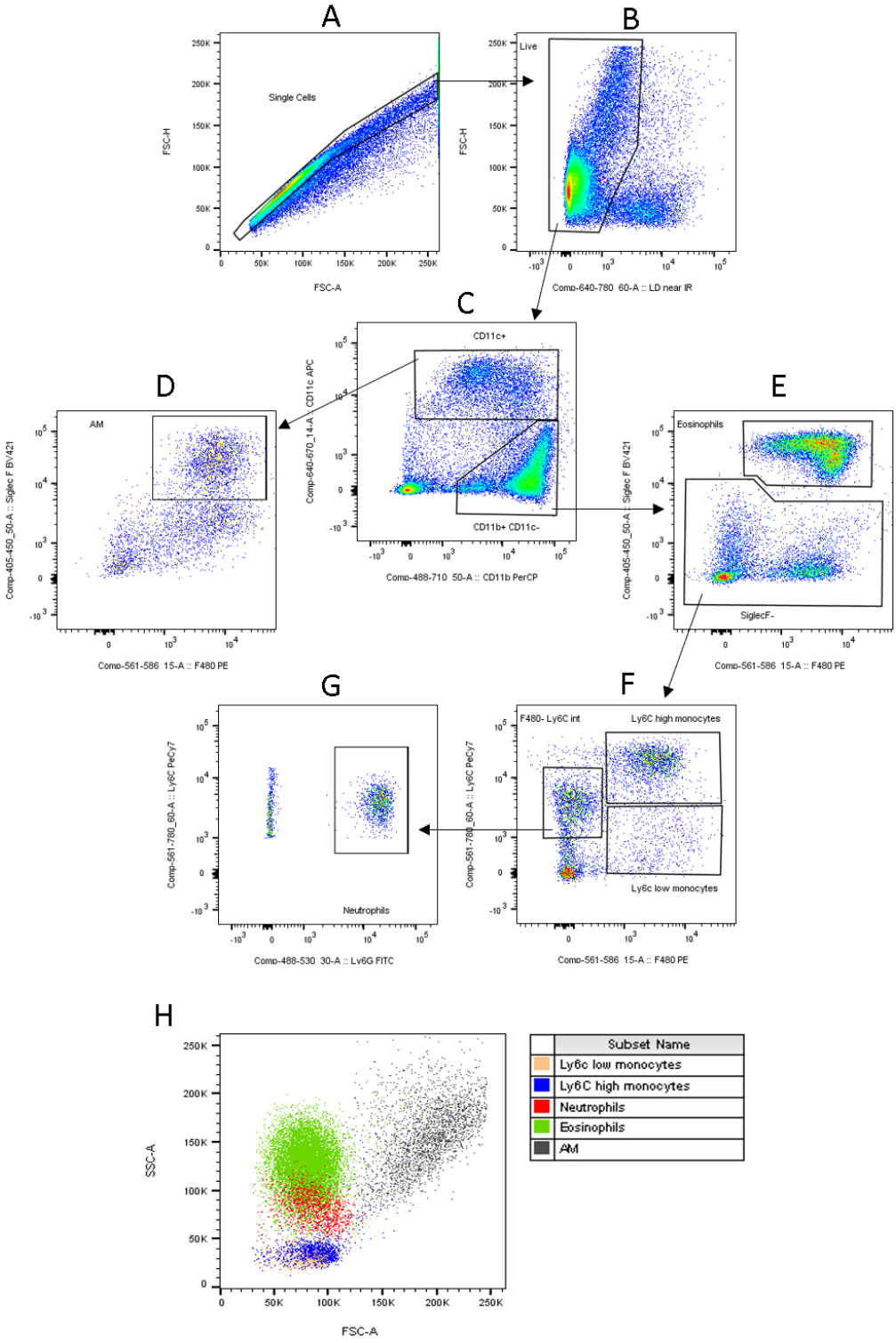


Figure 2.9: Gating strategy for the identification of myeloid cells.

A) Single cell gate. B) Live cell gate. C) CD11b vs CD11c plot for identification of $CD11c^{+}$ cells and $CD11c^{-}$ $CD11b^{+}$ cells. D) Alveolar macrophages (AM) were gated on $CD11c^{+}$ cells. E) $CD11c^{-}$ $CD11b^{+}$ cells were divided into Siglec-F^{+} eosinophils and Siglec-F^{-} cells. F) Siglec-F^{-} cells were$Ly6C^{high}$ monocytes, $Ly6C^{low}$ monocytes and $F4/80^{-}$ $Ly6C^{intermediate}$ cells. G) $F4/80^{-}$ $Ly6C^{intermediate}$ $Ly6G^{+}$ cells were recorded as neutrophils. H) Forward scatter (FSC) and side scatter (SSC) profiles of the identified populations.

2.5.5.5. Gating strategy for identification and isolation of dendritic cells

A previously established strategy was used to identify DCs (Patel et al. 2019) and is presented below (Figure 2.10).Single cells were identified based on the FSC-A/FSC-H profile (Figure 2.10A). Dead cells were excluded from the analysis based on the positive staining with live-and-dead dye (Figure 2.10B). Cells expressing highly expressing CD11c that were negative for lineage markers (CD3, CD19, CD90.2, NKp46, Siglec-F and Ly6G) (Figure 2.10C) were analysed for expression of MHC II and Lin^{-} $CD11c^{+}$ $MHC\ II^{+}$ cells were defined as DCs (Figure 2.10D). DCs expressing CD103 and lacking the expression of CD11b were defined as cDC1s. DCs expressing CD11b and lacking the expression of CD103 were further analysed for the expression of CD64 (Figure 2.10E). $CD11b^{+}$ $CD103^{-}$ $CD64^{-}$ cells were defined as cDC2s, while $CD11b^{+}$ $CD103^{-}$ $CD64^{+}$ cells were identified as moDCs (Figure 2.10F). The gates were determined with the help of FMO controls. The analysis was performed by FlowJo™ version 10.6.2.

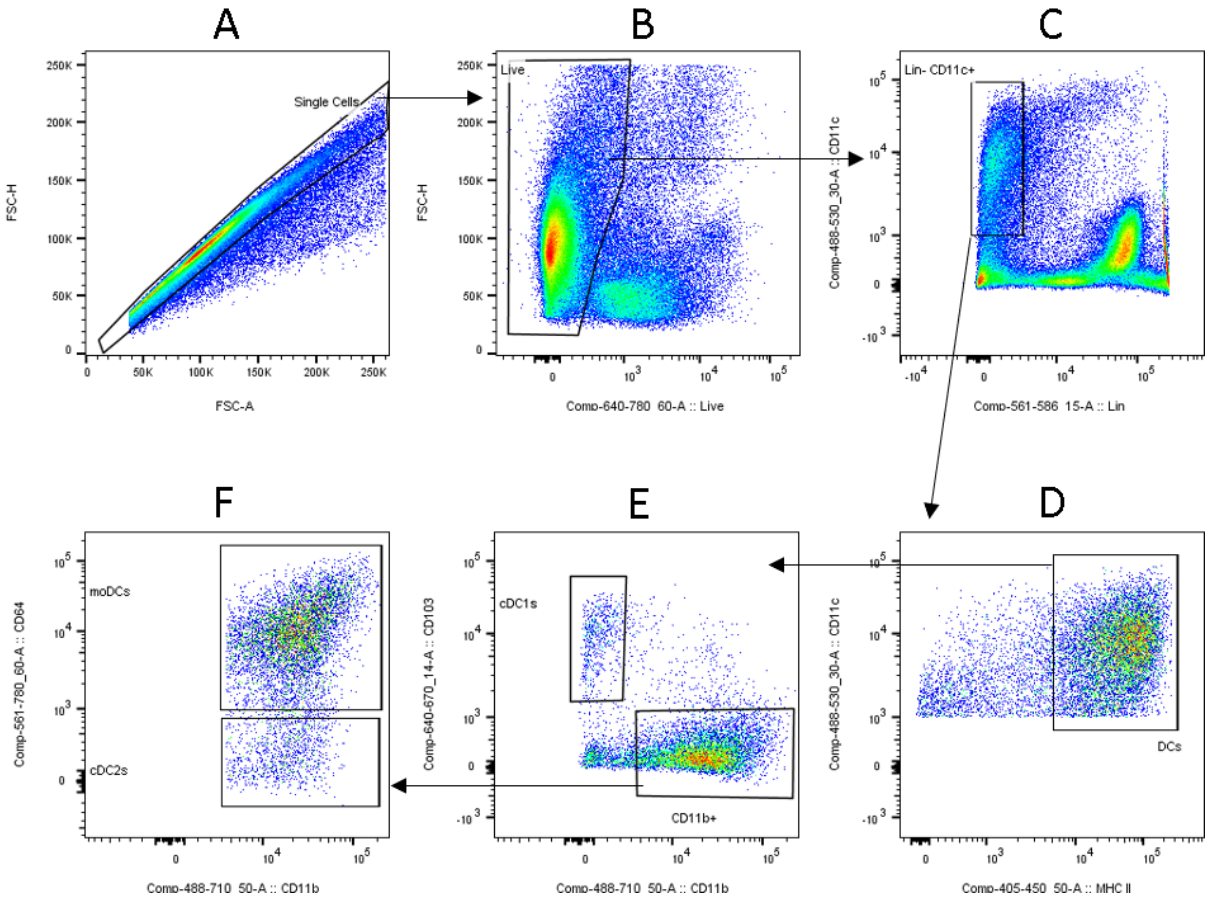


Figure 2.10: Gating strategy for the identification and isolation of lung dendritic cells (DCs).

A) Single cell gate. B) Live cell gate. C) Lineage (Lin) negative $CD11c^+$ gate D) Lin^- $CD11c^+$ MHC II^+ cells (DCs). E) $CD11b^+$ $CD103^-$ and $CD103^+$ $CD11b^-$ DCs (identified as group 1 classical DCs (DC1s)). F) $CD11b^+$ $CD103^-$ DCs were separated based on expression of CD64 into $CD64^-$ cDC2s and $CD64^+$ monocyte-derived DCs (moDCs).

2.5.6. List of antibodies

Table 2.2: Primary fluorophore conjugated anti-mouse antibodies used for identification and isolation of mouse immune cell populations.

Antibody	Clone	Conjugated Fluorophore	Dilution	Manufacturer
Extracellular markers for identification of ILCs				
Lineage markers				
B220	RA3-6B2	FITC	1:300	eBioscience
CD11b	M1/70	FITC	1:300	eBioscience
CD11c	N418	FITC	1:300	eBioscience
CD123	5B11	FITC	1:500	eBioscience
CD19	1D3	FITC	1:100	BD Pharmigen
CD3	145-12C11	FITC	1:100	BD Pharmigen
CD49b	DX5	FITC	1:200	Biolegend
CD5	53-7.3	FITC	1:100	Biolegend
CD8a	53-6.7	FITC	1:200	BD Pharmigen
F4/80	BM8	FITC	1:200	eBioscience
FcεRI	MAR-1	FITC	1:200	Biolegend
Gr1	RB6-8C5	FITC	1:2000	Biolegend
TCRβ	H57-597	FITC	1:100	BD Pharmigen
TCRγδ	GL3	FITC	1:100	BD Pharmigen
Ter119	TER-119	FITC	1:100	Biolegend
Other markers				
CD127	A7R34	BV421	1:100	Biolegend
CD45	30-F11	BV510	1:100	Biolegend
Intracellular markers for identification of ILCs				
CD3	17A2	AF700	1:100	eBioscience
GATA3	TWAJ	PerCP-eFluor710	1:50	eBioscience

RORγt	AFKJS-9	PE	1:50	eBioscience
Tbet	eBio4B10	eFluor660	1:50	eBioscience
Extracellular markers for identification of lymphocyte populations				
CD19	1D3	BV421	1:100	BD Pharmigen
CD3	M5-2C11	PE-Cy7	1:100	eBioscience
CD4	RM4-5	PerCP-Cy5.5	1:200	BD Pharmigen
CD8a	53-6.7	APC	1:200	BD Pharmigen
NKp46	29A1.4	PE	1:200	BD Pharmigen
Extracellular markers for sorting of ILC2s, CD4+ and CD8+ T cells				
B220	RA3-6B2	FITC	1:300	eBioscience
CD11b	M1/70	FITC	1:300	eBioscience
CD11c	N418	FITC	1:300	eBioscience
CD123	5B11	FITC	1:500	eBioscience
CD19	1D3	FITC	1:100	BD Pharmigen
CD3	145-12C11	FITC	1:100	BD Pharmigen
CD49b	DX5	FITC	1:200	Biolegend
CD5	53-7.3	FITC	1:100	Biolegend
CD8a	53-6.7	FITC	1:200	BD Pharmigen
F4/80	BM8	FITC	1:200	eBioscience
FcεRI	MAR-1	FITC	1:200	Biolegend
Gr1	RB6-8C5	FITC	1:200	Biolegend
TCRβ	H57-597	FITC	1:100	BD Pharmigen
TCRγδ	GL3	FITC	1:100	BD Pharmigen
Ter119	TER-119	FITC	1:100	Biolegend
CD127	A7R34	PE	1:100	Biolegend
CD4	RM4-5	APC	1:200	BD Pharmigen
CD45	30-F11	BV510	1:100	Biolegend
CD8a	53-6.7	BV605	1:200	Biolegend
ICOS	C398.4A	PE-Cy7	1:200	Biolegend
KLRG1	2F1	PerCP-Cy5.5	1:50	Invitrogen
Extracellular markers for identification of myeloid populations				

CD11b	M1/70	PerCP-Cy5.5	1:400	eBioscience
CD11c	HL3	APC	1:200	BD Pharmigen
F4/80	BM8	PE	1:50	eBioscience
Ly6C	AL-21	PE-Cy7	1:200	BD Pharmigen
Ly6G	1A8	FITC	1:100	BD Pharmigen
Siglec-F	E50-2440	BV421	1:100	BD Horizon
Extracellular markers for identification and sorting of dendritic cell populations				
CD11b	M1/70	PerCP-Cy5.5	1:400	eBioscience
CD11c	HL3	FITC	1:200	BD Pharmigen
CD103	2E7	APC	1:100	Invitrogen
CD19	1D3	PE	1:100	BD Pharmigen
CD3	145-2C11	PE	1:200	BD Pharmigen
CD64	X54-5/7.1	PE-Cy7	1:50	Biolegend
CD90.2	53-2.1	PE	1:100	BD Pharmigen
F4/80	BM8	PE-Dazzle	1:50	Biolegend
Ly6C	HK1.4	AF700	1:100	Biolegend
Ly6G	1A8	PE	1:200	BD Pharmigen
MHC-II	M5/114.15.2	BV421	1:100	Biolegend
MHC-II	M5/114.15.2	APC-Cy7	1:100	Biolegend
NKp46	29A1.4	PE	1:200	BD Pharmigen
Siglec-F	E50-2440	PE	1:200	BD Pharmigen

2.6. Assessment of soluble mediators in BAL

2.6.1. General enzyme-linked immunosorbent assay (ELISA) protocol

The concentration of IL-18 (mouse IL-18 ELISA kit, Invitrogen), CCL17 (mouse CCL17/TARC DuoSet ELISA, R&D Systems, USA) and CXCL11 (Mouse CXCL11/I-TAC DuoSet ELISA, R&D Systems), in BAL were measured by ELISA per manufacturers' specific instructions.

Briefly, high binding affinity 96-well plates (Thermo Fisher Scientific) were coated with 100 µl purified capture antibodies in PBS overnight at room temperature unless coated plates were provided with the assay (IL-18 ELISA kit). The next day plates were washed three times with

wash buffer (0.05 % Tween-20 (Sigma-Aldrich) in PBS) and blocked with 300 µl assay diluent (1% bovine serum albumin (BSA; Sigma-Aldrich) in PBS) for an hour. Plates were washed three times. 100 µl standards (7 serially diluted standards, run in duplicate), blanks (in duplicate) and samples were loaded onto the plate and incubated at room temperature for 2 hours. Plates were washed three times again and incubated in 100 µl biotinylated antibodies prepared assay diluent at room temperature for 2 hours. Plates were washed three times and 100 µl streptavidin-horseradish peroxidase (HRP; 1:200 dilution in 1% BSA PBS) added to the plate and incubated at room temperature for 30 minutes. After three washes, 100 µl TMB substrate (BD OptEIA^{TM}, USA) was added to each well and reaction was allowed to develop for up to half an hour in the dark. Once developed, the reaction was stopped by the addition of 0.19 N H_2SO_4. The absorbance was read immediately at 450 nm and at reference wavelength 620 nm using PowerWave XS Microplate Reader.

Reference wavelength absorbance and absorbance of blank samples were subtracted from the readings. Seven-point standard curve was generated and target concentration interpolated for each sample using Prism 9.0 (GraphPad Prism, LLC, USA).

2.6.2. ProcartaPlex Immunoassay protocol

ProcartaPlex immunoassays (Thermo Fisher Scientific) which are based on the principles of a sandwich ELISA and utilise magnetic microsphere technology were used to quantify inflammatory mediators in BAL supernatant as specified in the individual result chapters following manufacturer's instructions.

Simplex beads were sonicated for 10 sec in ultrasonic water bath and vortexed for another 30 sec. Simplex beads were then combined in wash buffer to obtain 1x multiplex bead solution and 50 µl of suspension was added to each well on a 96-well flat bottom plate. The plate was securely inserted into the hand-held magnet (Thermo Fisher Scientific) and beads were allowed 2 min to accumulate on the bottom of each well. The plate was then inverted to decant the liquid. To wash the beads, 150 µl of wash buffer was added and after 30 sec decanted for a total of 3 repeats. Next, the plate was removed from the magnet and 50 µl of standards, blanks (added in duplicates) and samples were added to the plate and incubated for 2 hours at room temperature on an orbital plate shaker at 500 rpm (StarLab). After the incubation the plate was washed three times as previously described. The detection

antibodies for each target were prepared together in detection antibody diluent and 50 µl was added to each well. The plate was incubated for 30 min at room temperature on the orbital plate shaker at 500 rpm. The plate was washed three times again and subsequently incubated with 50 µl of PE labelled streptavidin for 30 min at room temperature on the orbital plate shaker at 500 rpm. After three washes 120 µl of reading buffer was added to each plate and samples were analysed with Magpix® (Luminex Corporation, USA). A minimum of 50 beads per sample were acquired and median fluorescence intensity for each target was used to interpolate concentrations for all targets from the respective 7-point standard curve (7 serially diluted standards, run in duplicate). The analysis was performed by xPONENT® Software (Luminex Corporation).

2.6.3. MSD assays

MSD singleplex U-plex assays and multiplex V-plex cytokine assays (Meso Scale Diagnostics, LLC., USA), based on a sandwich ELISA that utilise electrochemiluminescence to quantify the target, were used to quantify inflammatory mediators in BAL supernatant. Inflammatory mediators quantified by MSD assays are detailed in individual results chapters. The assays were performed in accordance with manufacturer's instructions.

Prior to the start of the experiment, plates were washed three times with 150 µl wash buffer (0.01 % Tween-20 in PBS). Plates were coated with 50 µl of biotinylated capture antibody and incubated at room temperature for an hour on an orbital plate shaker at 500 rpm and washed three times. This step was omitted in V-plex assays supplied with precoated plates. 25 µl of Diluent 41 was added to each well, followed by addition of 25 µl standards (7 serially diluted standards, run in duplicate), blank (in duplicates) and samples. The plate and incubated shaking for 1 (U-plex assays) or 2 hours (V-plex assays) hours at room temperature. After three washes, 50 µl of detection antibody solution was added to each well and incubated shaking for 1 (U-plex assays) or 2 hours (V-plex assays) at room temperature. The plate was washed three times and 150 µl of Read Buffer was added to each well. The plate was immediately analysed with MESO QuickPlex SQ 120 (MesoScale Diagnostic, LLC). Target concentrations were interpolated from the standard curve by MSD Discovery Workbench software version 4.0.12 (Meso Scale Diagnostics, LLC.)

2.6.4. Tryptase-like activity assay

Mast Cell Degranulation Assay Kit (Merck Millipore, USA) based on spectrophotometric detection of the chromophore *p*-nitroaniline (*p*NA) nm after cleavage from the labelled substrate Tosyl-Gly-Pro-Lys-*p*NA (Schwartz et al. 1987), was used to determine tryptase-like activity in BAL accordingly to the manufacturer's protocol. Briefly, 180 µl of BAL supernatant was mixed with 20 µl substrate solution in a 96-well plate. Provided tryptase standards were used as a positive control. 7-point *p*NA standard curve (run in duplicates) was performed to quantify *p*NA concentration in BAL samples as a proxy for tryptase-like activity. RPMI medium was used instead of BAL samples as a negative control. The plate was incubated at 37 °C for 2.5 hours protected from light. Absorbance was measured at 405 nm and 602 nm with a PowerWave XS Microplate reader. Seven-point standard curve was generated and *p*NA concentration was interpolated for each sample with Prism 9.0.

2.7. Assessment of plasma IgE levels

2.7.1. Total IgE ELISA

The BD OptEIA™ Set for mouse IgE (BD Bioscience) was used as per manufacturer's instructions to determine the concentration of total IgE in plasma. Briefly, high binding affinity 96 well plates were coated with 100 µl IgE capture antibody (1:250 dilution) prepared in 0.1 M sodium carbonate (Sigma-Aldrich; pH=9.5)) and incubated overnight at 4 °C. Plates were washed at least 3 times and incubated in assay diluent (10 % FCS (Gibco) in PBS (Gibco)) for an hour at room temperature to prevent non-specific binding. 100 µl of standards (7 serially diluted standards, run in duplicate), samples (1:100 dilution in assay diluent) and controls were then added to the plate and incubated overnight at 4 °C. Guinea pig plasma was used as a negative control. After washing, a detection antibody (1:500 dilution) and an enzyme reagent (1:250 dilution) were prepared in assay diluent and 100 µl was added to each well. Following an hour incubation at room temperature, the plate was washed and incubated with 100 µl TMB substrate for 20 min in the dark. The reaction was then stopped with the addition of 50 µl of 0.19 N H_2SO_4. Absorbance was read immediately at 450 nm and reference wavelength 570 nm on PowerWave XS Microplate reader.

Reference wavelength absorbance and absorbance of blank samples were subtracted from the readings. Seven-point standard curve was generated and IgE concentration was interpolated for each sample Prism 9.0.

2.7.2. HDM specific IgE ELISA

A general ELISA protocol described in section 2.6.1. was adapted to detect HDM-specific IgE. High binding affinity 96 well plates were coated overnight at 4 °C with 100 µl of HDM (50 ng/µl of total protein) made up in 0.1 M $NaHCO_3$ (pH=9.6). The next day, the plate was washed and 50 µl of neat plasma samples were added to the plate and incubated overnight at room temperature. Guinea pig plasma was used as a negative control. The next day, the plate was washed and 100 µl of the detection Biotin rat anti-mouse IgE antibody (clone R35-118; BD Bioscience) diluted 1:250 in assay diluent was added to the plate. Following an hour incubation at room temperature, the plate was washed and 100 µl of HRP was added (1:200 dilution in assay diluent) for 30 min incubation at room temperature. Lastly, after a wash, 100 µl of the TMB substrate was added to the plate and reaction was allowed to develop in the dark at room temperature and stopped with 50 µl of 0.19 N H_2SO_4. Absorbance was read immediately at 450 nm and reference wavelength 570 nm on PowerWave XS Microplate reader. As no standard curve could be generated, data is presented as absorbance at 450 nm minus absorbance at 570 nm.

2.8. Assessment of pSTAT5a,b

MSD Phospho-STAT Panel Kit (MesoScale Diagnostic, LLC) was used to measure levels of phosphorylated STAT5a and 5b in lung whole cell lysate.

2.8.1. Sample preparation

Lungs frozen in liquid nitrogen were powdered using a mortar and a pestle. 20 – 30 mg of lung powder was resuspended in ice cold Complete Lysis Buffer (1X Tris lysis buffer containing 1X Protease Inhibitor Solution, 1X Phosphatase Inhibitor I and 1X Phosphatase Inhibitor II, Mesoscale Diagnostic). Samples were briefly vortexed and incubated on ice for 30 minutes. Samples were then centrifuged at 15 000 x*g* for 10 minutes at 4 °C and cell lysates transferred to a fresh tube. Protein concentration was determined using Bradford assay.

2.8.2. Bradford assay

10 µl of BSA (Sigma-Aldrich) standards (7 point standard curve, 1:2 serial dilution prepared in saline), samples (1:50 dilution in saline) or blanks were added to a 96-well plate. 190 µl of Bio-Rad Protein Assay Dye Reagent (Bio-Rad, UK) were added to the wells and gently mixed. The plate was incubated at room temperature for at least 5 minutes and the absorbance was measured at 595 nm with PowerWave XS Microplate reader. Protein concentration was interpolated from a standard curve using Prism 9.0. The concentration of all samples was adjusted to 0.4 µg/µl with the Complete Lysis Buffer.

2.8.3. MSD assay

The MSD assay was carried out accordingly to manufacturer's instructions. A 96-well precoated plate was blocked with Blocker A solution for one hour at room temperature on an orbital plate shaker at 500 rpm. The plate was washed three times with Tris Wash Buffer. 50 µl of samples (10 µg of protein/sample) and blanks were added to the plate and incubated on the orbital plate shaker at 500 rpm and room temperature for 1 hour. The plate was then washed 3 times and 25 µl of detection antibody solution was added to each well. Following one hour incubation at room temperature with shaking, the plate was washed three times and 150 µl of 1X Read Buffer T was added to the plate prior to the analysis on MESO QuickPlex SQ 120 (Meso Scale Diagnostics, LLC.). Target concentrations were interpolated from the standard curve by MSD Discovery Workbench software version 4.0.12 (Meso Scale Diagnostics, LLC.)

2.9. Assessment of gene expression

2.9.1. FACS isolated immune cell RNA isolation and reverse transcription (RT)

2.9.1.1. RNA isolation with RNeasy Plus Micro Kit

RNA was purified from isolated immune cells using RNeasy Plus Micro Kit (Qiagen, Germany) accordingly to manufacturer's protocol. Cell pellets were resuspended in 350 µl RLT buffer containing 1 % β-mercaptoethanol (Sigma-Aldrich) and cell lysate was transferred to QIAshredder (Qiagen) columns and centrifuged for 30 seconds at > 8000 x*g* to homogenise the lysate. The lysate was then transferred to a gDNA Eliminator spin column and centrifuged for 30 seconds at > 8000 x*g*. The flow-through was mixed with 350 µl 70 % ethanol, transferred to a RNeasy MinElute spin column and span for 15 sec at > 8000 x*g*. The

flow-through was discarded and the RNeasy MinElute spin column was washed with 700 µl RW1 buffer. After a 15 second spin at > 8000 x*g*, the flow-through was discarded and the column was washed with 500 µl RPE buffer and span again for 15 seconds at > 8000 x*g*. The flow-through was discarded and the column washed with 500 µl 80 % ethanol and centrifuged for 2 min at > 8000 g. The column was placed into a new 2 ml collection tube and centrifuged at full speed for 5 min to fully dry the membrane. The column was then transferred to a new 1.5 ml collection tube and 14 µl nuclease-free water was added to the centre of the spin column membrane and centrifuged for 1 min at full speed to elute the RNA. RNA concentration was determined using automated electrophoresis with TapeStation 2200 (Agilent, USA).

2.9.1.2. Reverse transcription

Due to low RNA concentration, all RNA was reverse transcribed to cDNA by SuperScript™ Vilo IV™ Master mix (ThermoFisher) following the manufacturer's protocol on StepOnePlus™ (Applied Biosystems, USA) thermal cycler. 4 µl SuperScript™ IV VILO™ Master Mix was mixed with 4 µl nuclease-free water and 12 µl RNA and gently mixed. After 10-minute incubation at 25 °C, samples were incubated at 50 °C for 10 minutes, followed by a 5-minute incubation at 85 °C. The concentration of cDNA was determined in a quantitative real-time PCR (qRT-PCR) amplifying *18S* along a 12-point cDNA standard curve ran in triplicates. All samples were then diluted to the same concentration using nuclease free water and stored at -80 °C until further use.

2.9.2. Lung tissue RNA isolation and RT

2.9.2.1. RNA isolation with RNeasy Plus Mini Kit

Lung tissue flash frozen in liquid nitrogen was powdered using a mortar and a pestle. 20 mg of powder was lysed in 350 µl 1% β-mercaptoethanol RLT buffer. Cell lysate was homogenised using QIAshredder columns. RNA was then purified using RNeasy Mini Plus Kit (Qiagen) accordingly to the manufacturer's instructions. Briefly, cell lysate was transferred to gDNA spin columns and after centrifugation at > 8000 g for 30 sec the flow-through was mixed with 350 µl 70 % ethanol and transferred to RNeasy spin column. After 15 sec centrifugation at > 8000 g the flow-through was discarded and the column washed with 700 µl Buffer RW1, followed by two washes with 500 µl Buffer RPE. After the final wash, the spin column was transferred to a fresh 2 ml collection tube and centrifuged for 1 minute at full speed to fully

dry the membrane. The RNeasy spin column was then transferred to 1.5 ml collection tube and 30 µl RNase-free water was added to the centre of the spin membrane. The column was spined at > 8000 g for 1 minute to elute the RNA.

2.9.2.2. Reverse transcription

RNA concentration and purity were determined by NanoDrop (Thermo Fisher Scientific). RNA was reverse transcribed to cDNA using TaqMan™ Reverse Transcription Reagents (Thermo Fisher Scientific) on StepOnePlus™ thermal cycler. A master mix for a 50 µl reaction was prepared by mixing 5 µl 10x RT buffer, 11 µl 25 mM $MgCl_2$, 10 µl 10 mM dNTP mix, 2.5 µl 50 µM Random hexamers, 1 µl 20 U/µl RNA inhibitor, 1.25 µl 50 U/µl Multiscribe™ reverse transcriptase. 1 µg of RNA was added and the volume was adjusted to 50 µl with nuclease-free water. Samples were incubated at 25 °C for 10 minutes, at 48 °C for 30 minutes and 95 °C for 2 minutes using StepOne™ thermocycler. All samples were diluted 1:4 in nuclease free water and stored at -80 °C until further use.

2.9.3. Quantitative real time polymerase chain reaction

Expression of target genes was quantified by qRT-PCR using Taqman® Gene Expression Assays (Thermo Fisher Scientific) relative to the housekeeping gene ribosomal *18S*.

2.9.3.1. Taqman® Gene Expression Assay principle

Taqman® Gene Expression Assays are based on 5' nuclease chemistry that uses a fluorogenic probe. A non-fluorescent quencher is also bound to the probe and inhibits emission of a fluorescent signal by the dye. A probe anneals to its specific target sequence along with unlabelled primers during annealing PCR phase. In the next phase *Taq* DNA polymerase synthesizes a new strand along a DNA template using the unlabelled primers. When a probe is reached, the *Taq* DNA polymerase 5' nuclease activity cleaves the probe and separates the dye from the quencher. The released dye molecule starts emitting fluorescent signals which are detected by real-time PCR systems. With each cycle more dye molecules are released, resulting in an increased fluorescence intensity. The use of probes with different dyes (FAM™ and VIC™, for example) allows for a combination of two Taqman Primer sets, resulting in the amplification of a target gene and a housekeeping control in the same, multiplex reaction, which reduces normalisation errors due to the inter-well variability and improves the precision of the assay.

2.9.3.2. Taqman® Gene Expression Assay protocol

20 µl reaction was prepared by mixing 10 µl 2x Taqman™ Universal Master Mix (Thermo Fisher Scientific), 1 µl 20x Taqman® Gene Expression Assay (Table 2.3) and 2.4 µl cDNA. The volume was adjusted to 20 µl with nuclease-free water. 1 µl 20x *18S* Taqman® Gene Expression Assay was added to the mix if target Taqman® Gene expression Assays were validated for multiplex reaction. Alternatively, a singleplex *18S* reaction was alongside singleplex target gene reaction. To control for contamination of the reagents, PCR mix without added cDNA was set up for each target gene reaction.

The qRT-PCR was run on StepOnePlus™ Real-Time PCR System under the following conditions: step 1 – 50 °C for 2 minutes, step 2 – 95 °C for 10 minutes, step 3 – 40 cycles of 95 °C for 15 sec and 60 °C for 1 min. Fluorescence intensity was measured after each cycle.

2.9.3.3. qRT-PCR data analysis

Fluorescence intensity, emitted by the reporter dye, was normalised to ROX passive reference and plotted against the corresponding PCR cycle number. A threshold was set in the middle of the linear phase of the amplification plot and the number of cycles needed for the signal to overshoot the threshold (threshold cycle, Ct) was calculated by StepOne™ Software version 2.3 (Applied Biosystems). The threshold was identical for all samples on the same plate, enabling comparison between the samples.

Target gene expression was normalised to the gene expression of the housekeeping gene *18S* by calculating ΔCt, a difference between Ct_{target} and Ct_{18S}. Relative gene expression was then calculated as $2^{-\Delta Ct}$ to account for the exponential doubling of cDNA with each cycle. The results were multiplied by 10^6 to allow for better discrimination between samples:

$$Relative\ gene\ expression = 2^{-\Delta Ct} \times 10^6, where\ \Delta Ct = Ct_{target} - Ct_{18S}.$$

2.9.3.4. Taqman® Gene Expression Assay multiplex validation

In a multiplex reaction, both amplification processes compete for the same reagents, such as *Taq* DNA polymerase and dNTPs, and can inhibit each other via primer, probe or amplicon interactions, resulting in the inhibition of one or both amplification processes. To ensure that the target gene expression and *18S* expression can be evaluated simultaneously in a multiplex reaction, all Taqman® Gene Expression Assays were validated for multiplexing with *18S* Taqman® Gene Expression Assay. RNA was isolated from a tissue with high target gene

expression and RT to cDNA as described in 2.9.2. A serial cDNA dilution was prepared and assayed in a multiplex reaction with a target gene and *18S* Taqman® Gene Expression Assays. Ct values for the target gene and *18S* were plotted against the corresponding cDNA concentrations. If the multiplex requirements were not met, the target gene and *18S* were assayed in singleplex reactions along one another. Primers were suitable for multiplexing if the following criteria were met:

1) The efficiency of each reaction was linear in whole cDNA range ($R^2 > 0.98$ in linear regression analysis).
2) Both reactions displayed high efficiency (90 – 105 % amplification), corresponding to a slope of linear regression around 3.3.
3) Both reactions displayed similar efficiencies, reflected by parallel linear regression curves, corresponding to a difference in linear regression slopes less than ± 0.1.

The examples of multiplex reactions that passed and did not pass the multiplex validation are presented on Figure 2.11.

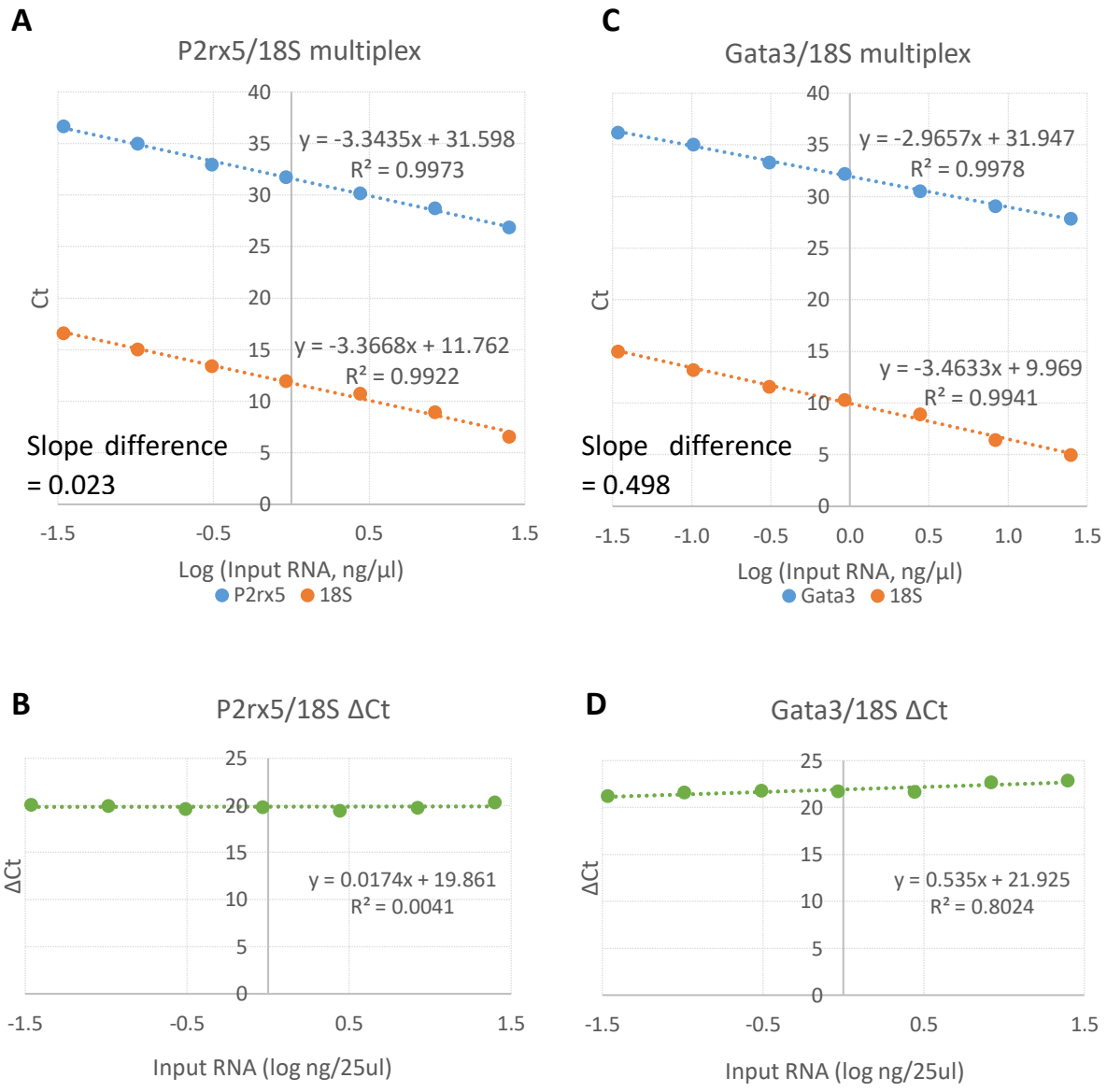


Figure 2.11: Examples of Taqman® Gene Expression Assay multiplex validation.

A, B) P2rx5 assay was multiplexed with 18S assay. A) Reaction efficiencies with linear regression demonstrated linear efficiency for both reactions ($R^2 > 0.98$), high efficiency of both reactions (slopes of linear regression ~ 3.3) and similar efficiencies of both reactions (slope difference < 0.1). B) ΔCt was maintained constant for all cDNA concentrations, validating the primers for multiplexing. C, D) Gata3 assay was multiplexed with 18S assay. C) The efficiency of both reactions was linear ($R^2 > 0.98$), however Gata3 assay demonstrated poor reaction efficiency (slope of linear regression < 3) and the reaction efficiencies were considerably different (slope difference > 0.1). D) ΔCt was not linear across cDNA concentration range, demonstrating that Gata3 and 18S assays were not suitable for multiplexing.

2.9.3.5. List of Taqman® Gene Expression Assays

Table 2.3: List of Taqman® Gene Expression Assays.

All assays were purchased from ThermoFisher Scientific, UK.

Gene	Assay ID
Eukaryotic 18S rRNA endogenous control	4310893E
Cd3e	Mm01179194_m1
Cd4	Mm00442754_m1
Cd8a	Mm01182107_g1
Gata3	Mm00484683_m1
Il13	Mm00434204_m1
Il-17a	Mm00439618_m1
Il-25	Mm00499822_m1
Il-33	Mm00505403_m1
Il-4	Mm00445259_m1
Il-5	Mm00439646_m1
Itagx	Mm00498701_m1

Gene	Assay ID
P2x1	Mm00435460_m1
P2x2	Mm00462952_m1
P2x3	Mm00523699_m1
P2x4	Mm00501787_m1
P2x5	Mm00473677_m1
P2x6	Mm00440591_m1
P2x7	Mm01199500_m1
Panx-1	Mm00450900_m1
Par2	Mm00433160_m1
St2	Mm00516117_m1
Trpv4	Mm00499025_m1
Tslp	Mm00498739_m1

2.10. In vitro isolated vagus preparation

In vitro isolated vagus preparation was used to assess sensory nerve activity and as a positive control to determine loss of receptor phenotype in response to various pharmacological stimuli in WT and $PAR2^{-/-}$ mice. All the experiments were performed by Dr Sara Bonvini.

Mice were sacrificed with an overdose of pentobarbitone (200 mg/kg, i.p.). Skin, muscles, connective tissue and the rib cage were removed to expose the vagal trunks running alongside the trachea from the base of the skull to the heart. Both vagal trunks were removed, cleaned of connective tissue and desheathed from the epineurium. The trunks were cut into 15 mm long segments and maintained in Krebs-Henseleit (KH) solution (118 mM NaCl, 5.9 mM KCl, 1.2 mM $MgCl_2$, 2.5 mM $CaCl_2$, 23.5 mM NaH_2PO_4, 5.6 mM glucose) at physiological pH (7.4) and 37 °C whilst supplied with 95 % O_2/ 5 % CO_2.

The dissected vagus nerve segments were mounted into a custom-made grease-gap recording chamber and the two ends were chemically and electrically isolated with petroleum jelly as previously described (Birrell et al. 2002). One end was maintained in KH solution throughout the experiment, while the other end was perfused with various stimuli/test solutions made up in KH. Each end was connected to an electrode (glass pipettes filled with Ag/AgCl pellets (Mere 2 Flexible reference electrodes, WPI, UK)), which were able to detect membrane depolarisation. Electrodes were connected to a DAM50 differential amplifier (WPI, UK) which measured, amplified (x 10 gain) and filtered (high cut-off 1 kHz, sample rate 5 Hz) the potential difference between the two electrodes and converted it into a digital signal. The signal was visualised and analysed by LabScribe 3 software (iWorx) and analysed using Clampfit Software (pClamp 10).

2.11. Statistical analysis

Statistical analysis was performed using Prism version 9.0 (GraphPad, USA) and is detailed in figure legends within the results chapters. In general, non-parametric tests were employed to assess the differences between study groups as no assumptions about normal distribution or and equal variance was required. Mann-Whitney test was used when comparing two groups and Kruskal-Wallis with post hoc Dunn's multiple comparison test when comparing three or more groups. Repeated measures ANOVA with Sidak's multiple comparison test was used to analyse AHR data in HDM studies. Parametric t-test was used to compare vagal nerve depolarisation between WT and PAR2$^{-/-}$ mice. Group sizes for initial exploratory studies were guided by in-house experience with the models used in this thesis. Group sizes for the follow up studies were chosen based on sample size calculation using the data from the pilot studies and technical feasibility.

3. Identification of downstream targets in TRPV4 signalling pathway

3.1. Introduction

TRPV4 is a non-selective cation channel that has been implicated in the pathogenesis of chronic respiratory disease, including asthma, COPD, chronic cough and IPF (Zhu et al. 2009, Baxter et al. 2014, Rahaman et al. 2014, Birrell et al. 2016, Bonvini et al. 2016, Naumov et al. 2016, Gombedza et al. 2017, Grace et al. 2017, Duan et al. 2020, Wiesner et al. 2020). TRPV4 is present in various tissues but is most abundantly expressed on airway epithelial cells, airway smooth muscle cells, fibroblasts and alveolar macrophages. TRPV4 can be activated by exposure to a variety of stimuli such as hypo-osmolar solutions, low pH, change in temperature, arachidonic acid metabolites as well as downstream of PAR2 activation (Liedtke et al. 2000, Suzuki et al. 2003, Watanabe et al. 2003, Jia et al. 2004, Grant et al. 2007, Fernandez-Fernandez et al. 2008, Lorenzo et al. 2008, Groot-Kormelink et al. 2012, Poole et al. 2013, Rahaman et al. 2014, Zhao et al. 2014, Zhao et al. 2015, Rayees et al. 2019). TRPV4 activation evokes an intracellular influx of calcium ions and subsequent opening of Panx-1 pores, leading to ATP release into the extracellular milieu (Seminario-Vidal et al. 2011, Dahl 2015, Rahman et al. 2018). Upon release, ATP then acts on purinergic receptors from predominantly P2X family in the vicinity of the release (Silva-Vilches et al. 2018).

In homeostatic conditions, TRPV4-induced ATP signalling in the airway epithelium regulates mucocilliary clearance (Lorenzo et al. 2008). However, aberrant activation of TRPV4 can contribute to respiratory disease and symptoms such as cough or bronchospasm. More specifically, activation of TRPV4 on sensory nerves has been demonstrated to trigger cough via P2X3 receptors, which have been implicated in chronic cough (Abdulqawi et al. 2015, Bonvini et al. 2016). ATP release from airway smooth muscle cells upon TRPV4 activation triggers P2X4 receptors activation on mast cells which then release leukotrienes and cause bronchoconstriction (McAlexander et al. 2014, Bonvini et al. 2020). In addition, TRPV4 activation has been linked to the development of airway inflammation. In a murine COPD model, for example, smoke exposure triggered TRPV4 activation on macrophages which resulted in ATP release (Baxter et al. 2014). Subsequent autocrine activation of P2X7 resulted in IL-1β release and neutrophilic airway inflammation (Baxter et al. 2014).

The importance of ATP signalling in asthma in the context of airway inflammation as well as lung function has been demonstrated by a substantial body of literature (Pellegrino et al. 1996b, Idzko et al. 2007, Muller et al. 2011, Chavez et al. 2013, Idzko et al. 2013, Amison et

al. 2015, Zhang et al. 2017, Pelleg et al. 2019). Bronchoprovocation studies have demonstrated the bronchoconstrictor properties of ATP in human and revealed increased sensitivity to ATP-induced bronchoconstriction in asthmatic patients (Pellegrino et al. 1996b, Basoglu et al. 2005, Basoglu et al. 2017). Allergen challenge studies have later showed that in comparison to saline challenge allergen challenge was associated with increased ATP levels in BAL of mild asthmatics (Idzko et al. 2007). This has been recapitulated in animal models of allergic airway disease which further demonstrated that elimination of ATP by exogenous ATPases ameliorated airway inflammation and AHR (Idzko et al. 2007, Chavez et al. 2013, Idzko et al. 2013, Amison et al. 2015, Zhang et al. 2017). Similar outcomes were observed when ATP signalling on P2X receptors was inhibited using non-selective P2 receptor antagonists as well as using selective inhibition of P2X4 or P2X7, respectively (Muller et al. 2011, Chen et al. 2016, Shi et al. 2016, Zech et al. 2016, Yin et al. 2017, Wang et al. 2018b).

The mechanism of ATP release is not yet fully understood, however our preliminary observations have suggested that TRPV4 may be involved in the process. Targeting TRPV4 by genetic disruption in mice ($TRPV4^{-/-}$ mice) or pharmacological inhibition in rat, our laboratory has demonstrated a detrimental role of TRPV4 in the pathogenesis of AAD (Birrell et al. 2016). In both models the inhibition of TRPV4 signalling abolished airway inflammation and allergen triggered changes in lung function (Birrell et al. 2016). Other groups have recently also demonstrated the involvement of TRPV4 in allergic airway inflammation, as well as airway remodelling (Gombedza et al. 2017, Duan et al. 2020, Wiesner et al. 2020). An amelioration of the disease was similarly observed in Panx-1 deficient mice (unpublished data), suggesting ATP was released downstream of TRPV4 activation. However, it remains unclear which cells are responsible for inducing aberrant TRPV4 activation in the context of asthma, or which P2X receptors are activated downstream.

Among T cells, DCs and ILC2s, the key players in type 2 immune responses in asthma (Vroman et al. 2017, Lloyd and Snelgrove 2018), T cells and DCs have been reported to express functional TRPV4 receptors (Bertin et al. 2014, Majhi et al. 2015, Naert et al. 2019) and ATP is important regulator of their functions (Schenk et al. 2008, Woehrle et al. 2010a, Silva-Vilches et al. 2018). We have previously demonstrated that $CD4^+$ and $CD8^+$ T cells were indispensable for the development of allergic airway inflammation and AHR in our murine model of AAD (Raemdonck et al. 2016). Yet, the role of DCs or ILC2s in the development of allergic airway

inflammation in our model remains uncertain as does the potential of T cells, ILC2s or DCs to drive pathogenic TRPV4 signalling in asthma.

3.2. Hypothesis and aims

We hypothesised that immune cells, key for the development of allergic airway inflammation, are the drivers of TRPV4 signalling in allergic airway disease via P2X receptors.

To address this hypothesis, we aimed to

- Identify immune cells central to the initiation of allergic airway inflammation,
- Investigate TRPV4 expression in the key immune cell populations, and
- Identify candidate P2X receptors involved in TRPV4 signalling pathway.

3.3. Methods

This section outlines and summarises the main methods used in this chapter. All the methodology and experimental protocols are presented in detail in Chapter Methods.

3.3.1. Murine HDM time course study

Female C57BL/6J mice were i.p. sensitised to house dust mite (HDM). Mice were then challenged with saline or HDM once daily on one (1) (day 24), two (2) (days 24 and 25) or three (3) consecutive days (days 24, 25 and 26). Mice were sacrificed 2 hours post-challenge as well as 24, 48 or 72 hours after the third and final challenge to collect bronchoalveolar lavage (BAL), lung and MLNs (Figure 3.1).

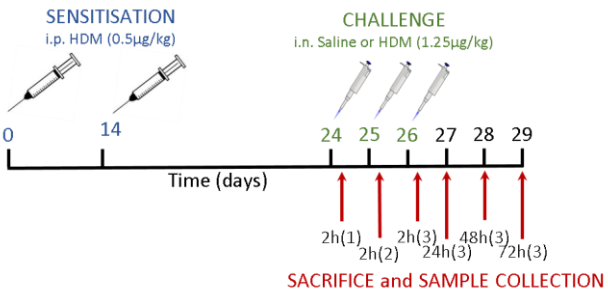


Figure 3.1: Time course study design.

Female C57BL/6 mice were sensitised to house dust mite (HDM; 0.5µg/kg) by intraperitoneal injection (i.p.) on days 0 and 14. Mice were administered saline or HDM (1.25µg/kg) intranasally (i.n.) on one, two or three consecutive days (days 24-26). Mice were sacrificed and samples collected for the assessment of inflammatory status 2 hours after each challenge as well as 24, 48 and 72 hours after the third challenge.

BAL cells were isolated and total leukocyte numbers determined by an automated cell counter (Sysmex XT-300) and leukocyte populations differentiated using flow cytometry (Fortessa). BAL supernatant was stored for subsequent analysis of inflammatory mediators. MSD V-plex kits were used to determine concentration of IL-1β, IL-2, IL-4, IL-5, IL-12, IL-17A, IL-22, IL-25, IL-33, IFNγ, CXCL1, CXCL10, CCL2 and MIP-1α. ProcartaPlex Simplex kits were used to determine concentration of IL-13, Eotaxin-1 and TSLP and R&D DuoSet ELISA was performed to measure concentrations of CCL17.

Lungs were enzymatically digested and then total leukocyte numbers determined by an automated cell counter (Sysmex XT-300). Flow cytometry was utilised to differentiate leukocyte populations (Fortessa). From a parallel set of animals, lungs were flash frozen in liquid nitrogen for subsequent protein and gene expression analyses. Nuclear proteins were extracted (Activ Motif) for determination of STAT5A,B levels (MSD U-plex assay). mRNA was isolated for the determination of *Il-4*, *Il-5, Il-13*, *Il-17*, *Il-25, Il-33*, *Tslp*, *P2rx1, P2rx2, P2rx3, P2rx4, P2rx5, P2rx6* and *P2rx7* expression.

MLNs were collected and enzymatically digested to obtain single cell suspension. Total leukocyte numbers were determined using an automated cell counter (Sysmex XT-300) while flow cytometry was used for differentiation of leukocyte populations (analysed on Fortessa).

3.3.2. Isolation of key immune cell populations

Female C57BL/6J mice were systemically sensitised to HDM and challenged once daily with saline or HDM intranasally on three consecutive days. Three days after the final challenge, mice were sacrificed and lungs collected. Lungs were enzymatically digested to obtain single cell suspension. Cells were then stained with fluorophore labelled primary antibodies to isolate $CD4^+$ T cells, $CD8^+$ T cells, ILC2s, moDCs, cDC1s and cDC2s using FACS. mRNA was isolated from sorted cells and used to determine the expression of *Cd3, Cd4, Cd8, Gata-3, St2, Il-4, Il-13, Il-5, Trpv4, Panx-1, P2rx1, P2rx2, P2rx3, P2rx4, P2rx5, P2rx6,* and *P2rx7*.

3.3.3. Gene expression

Expression of *Cd3, Cd4, Cd8, Gata-3, Il-4*, *Il-13*, *Il-5*, *Il-17, Il-25*, *Il-33*, *P2rx1, P2rx2, P2rx3, P2rx4, P2rx5, P2rx6, P2rx7, Panx-1, St2, Trpv4* and *Tslp* was determined by qRT-PCR with eukaryotic *18s* used as an internal control. All target primers were initially validated for use

in multiplex reactions with *18s* primers in tissues or cells with high target expression (Table 1). Linear regression (>0.98), slope of linear regression (around 3.3) and reaction efficiency (difference in slopes of linear regression between *18s* and target; <0.1) were evaluated and only targets meeting all the described criteria were assayed in multiplex reactions. All other targets were assayed in singleplex reactions beside *18s*.

Table 3.1: Results of primer multiplex validation.

Target	Primer	Linear regression	Slope of linear regression	Reaction efficiency	Suitability for multiplex	Sample used for validation
CD3	*18s*	>0.99	-3.309	0.009	YES	$CD4^+$ T cells
	Cd3	>0.99	-3.300			
CD4	*18s*	>0.99	-3.176	0.039	YES	$CD4^+$ T cells
	Cd4	>0.99	-3.215			
CD8	*18s*	>0.99	-3.504	0.124	NO	$CD8^+$ T cells
	Cd8	>0.99	-3.380			
GATA3	*18s*	>0.99	-3.274	0.034	YES	ILC2
	Gata-3	>0.99	-3.240			
IL-4	*18s*	>0.99	-3.920	0.660	NO	lung (HDM challenged)
	Il-4	>0.99	-3.259			
IL-5	*18s*	0.97	-3.831	0.768	NO	lung (HDM challenged)
	Il-5	0.98	-3.064			
IL-13	*18s*	>0.99	-3.720	0.306	NO	lung (HDM challenged)
	Il-13	>0.99	-3.414			
IL-17A	*18s*	>0.99	-3.052	0.223	NO	lung (HDM challenged)
	Il-17a	>0.99	-2.829			
IL-25	*18s*	>0.99	-3.460	0.010	YES	brain
	Il-25	>0.99	-3.450			
IL-33	*18s*	>0.99	-3.727	0.623	NO	lung (HDM challenged)
	Il-33	>0.99	-3.104			
P2X1	*18s*	0.99	-3.466	0.238	NO	thymus

	P2rx1	0.98	-3.228			
P2X2	*18s*	>0.99	-3.279	0.220	NO	testis
	P2rx2	>0.99	-3.059			
P2X3	*18s*	>0.99	-3.558	0.136	NO	testis
	P2rx3	>0.99	-3.422			
P2X4	*18s*	>0.99	-3.299	0.187	NO	spleen
	P2rx4	0.99	-3.486			
P2X5	*18s*	>0.99	-3.367	0.023	YES	heart
	P2rx5	>0.99	-3.344			
P2X6	*18s*	>0.99	-3.141	0.373	NO	lung
	P2rx6	>0.99	-3.514			
P2X7	*18s*	>0.99	-3.153	0.197	NO	spleen
	P2rx7	>0.99	-3.350			
Panx-1	*18s*	>0.99	-3.501	0.391	NO	thymus
	Panx-1	>0.99	-3.110			
ST2	*18s*	>0.99	-3.246	0.061	YES	ILC2
	St2	>0.99	-3.307			
TRPV4	*18s*	>0.99	-3.223	0.571	NO	kidney
	Trpv4	>0.99	-2.652			
TSLP	*18s*	>0.99	-3.463	0.497	NO	lung
	Tslp	>0.99	-2.966			
Multiplex requirements		>0.98	~-3.3	<0.1		

3.4. Results

3.4.1. The development of early immune responses upon in the murine HDM model

3.4.1.1. HDM challenge induced Th2 immune responses

A murine model of AAD, previously used to demonstrate the role of TRPV4 in the development of allergic airway inflammation and AHR (Birrell et al. 2016), was chosen to study the initiation

and the development of early immune responses upon an allergen challenge. Mice sensitised to HDM were exposed to saline or HDM once a day and airway inflammation was assessed 2 hours after a single, two or three consecutive challenges as well as 24, 48 and 72 hours after the third and final challenge (Figure 3.2). Compared to saline challenge, HDM exposure was associated with an increase in expression of type 2 cytokines *Il-4, Il-5* and *Il-13* in lung 2 hours post initial challenge as well as during the later time points (Figure 3.2A-C). In BAL, the concentrations of IL-4, IL-5 and IL-13 were elevated in HDM challenged mice compared to saline controls from the second time point (2h(2)) and throughout the study (Figure 3.2D-F). The initiation of type 2 immune responses in HDM challenged mice immediately resulted in increased BAL eotaxin-1 levels which remained elevated until 72h(3) time point at the end of the experiment (Figure 3.2G). Subsequently, eosinophil infiltration into the airways and lungs of HDM but not saline challenged mice was observed from the second time point onwards (Figure 3.2H,I). In addition to type 2 cytokines, HDM challenge was associated with increased proinflammatory TNFα (Figure 3.2J) and IL-1β (Figure 3.2K) in BAL from the second time point and until the end of the study in comparison to saline challenge. Increased TNFα were observed in saline challenged mice 2 hours after the first, second and third challenge in comparison to the saline challenge at 72(3) time point (Figure 3.2J).

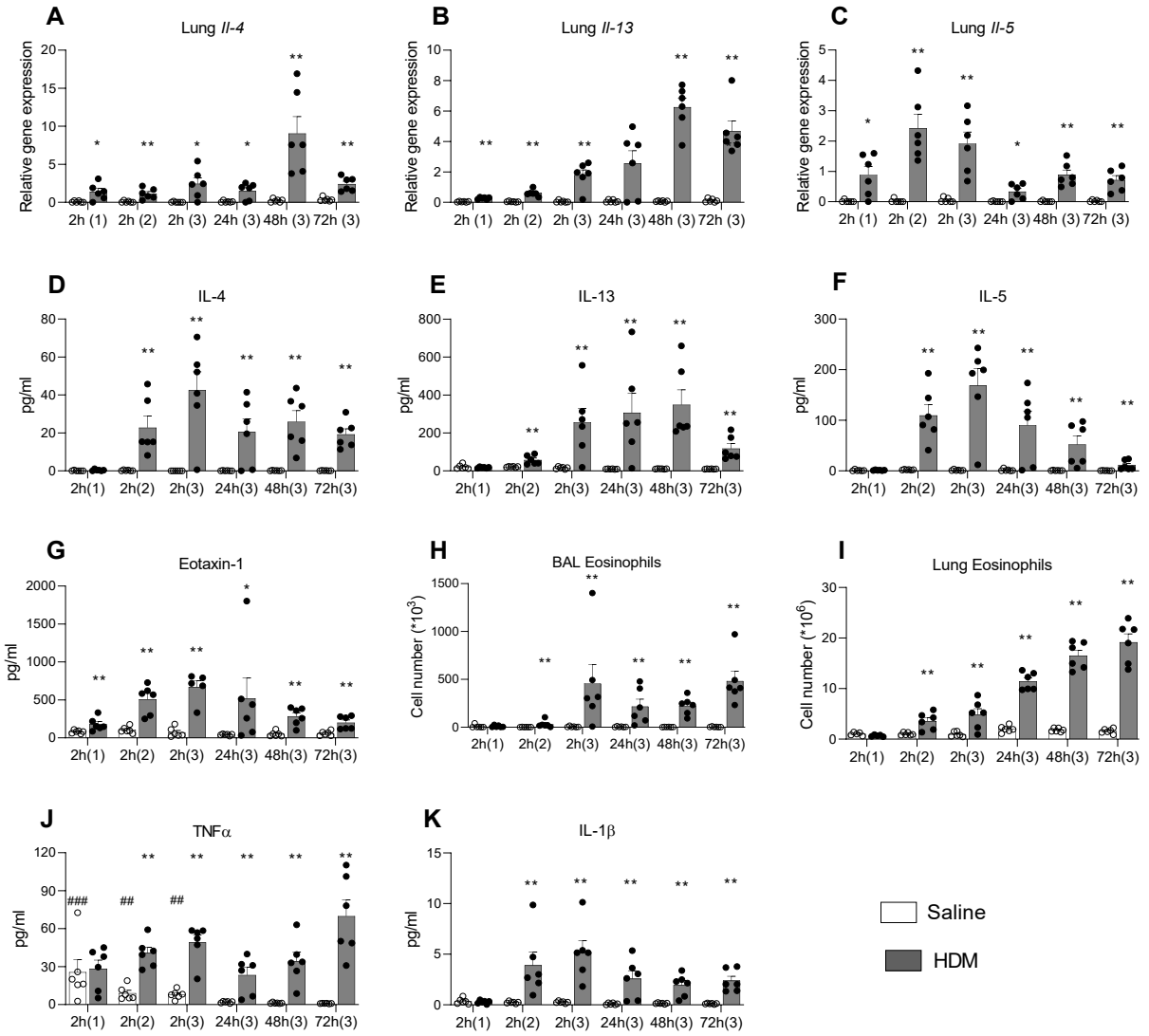


Figure 3.2: House dust mite (HDM) challenge evoked type 2 inflammation.

Female C57BL/6J mice were sensitised to HDM and then challenged with saline or HDM on one, two or three consecutive days. Mice were sacrificed 2 hours after the first (2h(1)), second (2h(2)), or third challenge (2h(3)), as well as 24, 48 and 72 hours after the third and final challenge (24h(3), 48h(3), and 72h(3), respectively). A) *Il-4,* B) *Il-13* and C) *Il-5* gene expression was determined in lung by qRT-PCR. D) IL-4, E) IL-13, F) IL-5 and G) Eotaxin-1 were determined in bronchoalveolar lavage (BAL) by MSD or ProcartaPlex assays. H) BAL and I) lung eosinophil numbers were enumerated by flow cytometry. J) TNFα, K) IL-1β in BAL determined by MSD assays. Data from a single experiment presented as mean ± S.E.M (N=6 per group). * denotes $p<0.05$ and ** $p<0.01$ comparing time matched saline and HDM challenged groups with Mann-Whitney U test. ## denotes $p<0.01$ and ### $p<0.001$ comparing saline challenged groups with saline control at 72(3) time point with Kruskal-Wallis test with post hoc Dunn's multiple comparison test.

Type 1, 17 and 22 immune responses were evaluated next to confirm whether type 2 immune responses were the preferred immune response triggered by HDM exposure. HDM challenge was associated with an increase in the type one cytokines IFNγ and CXCL10 (Figure 3.3A,B). After the initial increase 2 hours after the second and third HDM challenge their levels substantially dropped at the later time points. Compared to saline challenged animals, a small increase in IL-17A BAL levels was observed in HDM challenged mice which peaked at 2 hours after the third and final challenge (Figure 3.3C). This was associated with increased neutrophil chemokine CXCL1 two hours after each challenge and BAL neutrophilia 2 hours after the third HDM challenge, but not at other time points (Figure 3.3D,E). In the lung, neutrophil numbers remained comparable between saline and HDM challenged mice until 48 and 72 hours after the third HDM challenge when HDM exposure was associated with a reduction in lung neutrophils (Figure 3.3F). No IL-22 could be detected in BAL in any of the samples.

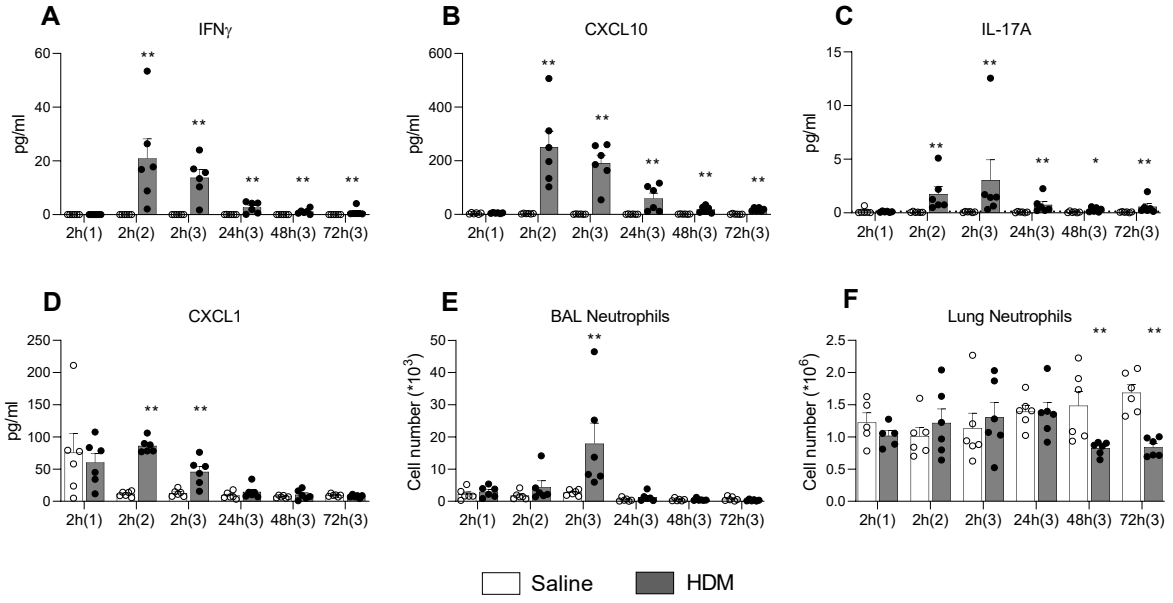


Figure 3.3: Type 1 and type 17 immune responses upon house dust mite (HDM) challenge.

Female C57BL/6J mice were sensitised to HDM and then challenged with saline or HDM on one, two or three consecutive days. Mice were sacrificed 2 hours after the first (2h(1)), second (2h(2)), or third challenge (2h(3)), as well as 24, 48 and 72 hours after the third and final challenge (24h(3), 48h(3), and 72h(3), respectively). A) IFNγ, B) CXCL10, C) IL-17A and D) CXCL1 were determined in bronchoalveolar lavage (BAL) by MSD assays. E) BAL and F) lung neutrophil populations were enumerated with the help of flow cytometry. Data from a single experiment presented as mean ± S.E.M (N=6 mice per group). Mann-Whitney U test was used to analyse differences between saline and HDM groups. * denotes $p<0.05$ and ** $p<0.01$.

3.4.1.2. CD4+ T cells and ILC2s as drivers of type two immune responses

We next investigated the dynamics of $CD4^+$ T cell responses as our laboratory has previously demonstrated the crucial role of $CD4^+$ T cells for the development of HDM-induced pathology in this model (Raemdonck et al. 2016). $CD8^+$ T cells were similarly important and were investigated alongside (Raemdonck et al. 2016). HDM challenge was associated with an increase in BAL IL-2 concentration 2 hours after each HDM challenge and falling to control levels later in the time course and was associated with increased phosphorylation of STAT5A,B in the lung (Figure 3.4A,B). Compared to saline challenged mice increased $CD4^+$ and $CD8^+$ T cell numbers were detected in BAL 2 hours after the second HDM challenge, peaked at 2 hours after the third and final HDM challenge and remained elevated for the rest of the time course (Figure 3.4C,D). In the lung, an increase in $CD4^+$ T cells was observed 72 hours after the third and final HDM challenge compared to saline challenge controls (Figure 3.4E), while $CD8^+$ T cell population remained unchanged by HDM challenge throughout the experiment (Figure 3.4F). To elucidate whether $CD4^+$ or $CD8^+$ T cells were a source of type 2 cytokines upon HDM challenge, $CD4^+$ and $CD8^+$ T cells were isolated from lung of saline and HDM challenged mice three days after three HDM challenges and expression of type 2 cytokines expressed. This time point was chosen as at this time point the effects of HDM exposure on lung T-cell numbers were the greatest. As expected, $CD4^+$ T cells expressed high levels of *Cd3* and *Cd4* and lacked the expression of *Cd8* (Figure 3.4G). Upon HDM challenge $CD4^+$ T cells upregulated *Gata-3* and *St2* as well as *Il-4, Il-5* and *Il-13* (Figure 3.4G). *Il-17a* remained unchanged with HDM challenge in $CD4^+$ T cells (Figure 3.4). $CD8^+$ T cells were characterised by high expression of *Cd3* and *Cd8* and a lack of *Cd4* expression (Figure 3.4H). No *Il-4, Il-5* or *Il-13* was detected in $CD8^+$ T cells after saline challenge, however upregulation of *Il-13*, but not *Il-4* or *Il-5* was induced by HDM challenge (Figure 3.4H).

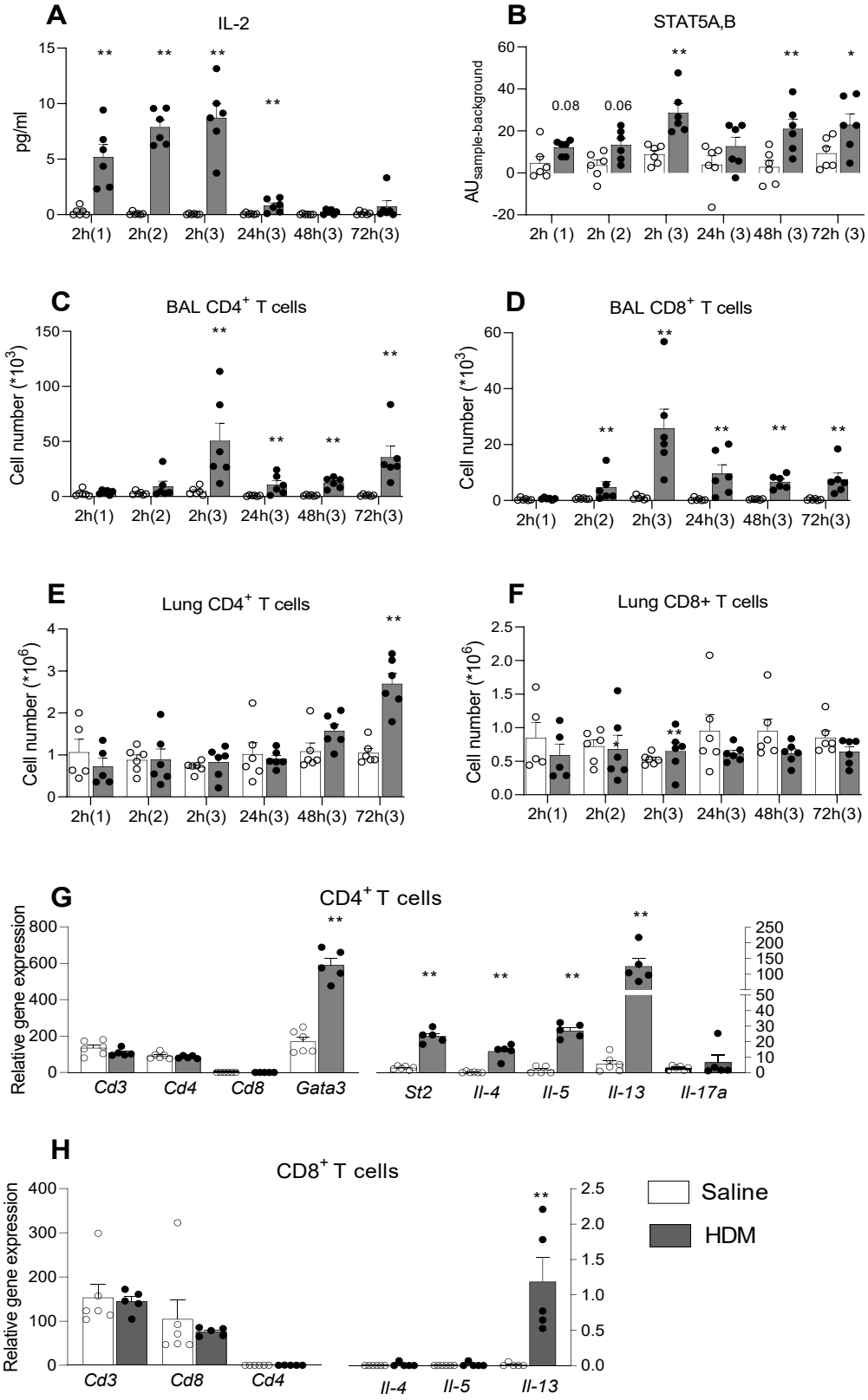


Figure 3.4: House dust mite (HDM) challenge was associated with Th2 polarisation of CD4⁺ T cells.

Female C57BL/6J mice were sensitised to HDM and then challenged with saline or HDM on one, two or three consecutive days. Mice were sacrificed 2 hours after the first (2h(1)), second (2h(2)), or third challenge (2h(3)),

as well as 24, 48 and 72 hours after the third and final challenge (24h(3), 48h(3), and 72h(3), respectively). A) IL-2 levels in BAL and B) phosphorylated STAT5A,B levels in lung whole cell protein extract. C) $CD4^+$ and D) $CD8^+$ T cell numbers in bronchoalveolar lavage (BAL), as well as E) $CD4^+$ and F) $CD8^+$ T cell numbers in lung were enumerated utilising flow cytometry. G, H) Female C57BL/6J mice sensitised to HDM were challenge with saline or HDM on three consecutive days and sacrificed 72 hours after the final challenge. G) $CD4^+$ and H) $CD8^+$ T cells were isolated from lungs using fluorescence-activated cell sorting (FACS) and mRNA extracted for determination of gene expression by qRT-PCR. Representative data from a single (A-F) or two independent experiments (G, H) presented as mean ± S.E.M (N=5-6 mice per group). Mann-Whitney U test was used to analyse differences between saline and HDM groups. * denotes $p<0.05$ and ** $p<0.01$.

Next, we characterised the dynamics of ILC2 responses as ILC2s can induce type 2 immune responses upon activation by epithelium derived cytokines such as IL-33, TSLP and IL-25 (Lloyd and Snelgrove 2018). In the time course study HDM challenge was associated with an increase in BAL IL-33 concentration 2 hours after the second and third HDM challenge, respectively, compared to saline challenged controls (Figure 3.5A). Simultaneously, HDM challenged animals had increased expression of *Il-33* in the lung from the second time point over the duration of the study (Figure 3.5B). In contrast, TSLP was detectable in BAL 2 hours after each challenge and was significantly reduced in HDM challenged mice compared to saline controls after second and third challenge (Figure 3.5C). Compared to respective saline controls, HDM challenge was associated with downregulation of lung *Tslp* expression 2 hours after the second as well as 48 and 72 hours after the third HDM challenge (Figure 3.5D). No IL-25 could be detected in BAL or *Il-25* in lung in any of the experimental groups. Nevertheless, an increase in BAL and lung ILC2 numbers was observed 24, 48 and 72 hours after the third and final HDM challenge, but not earlier in the time course (Figure 3.5E,F). To evaluate ILC2s as a source of type 2 cytokines, ILC2s were also sorted from lung of saline and HDM challenged mice three days after three HDM challenges and were characterised by a lack of *Cd3, Cd4* and *Cd8* expression and high *Gata-3* and *St2* expression (Figure 3.5G). Under control conditions, ILC2s expressed *Il-5* and *Il-13* and low levels of *Il-4,* however no change in type 2 cytokine expression was detected upon HDM challenge (Figure 3.5).

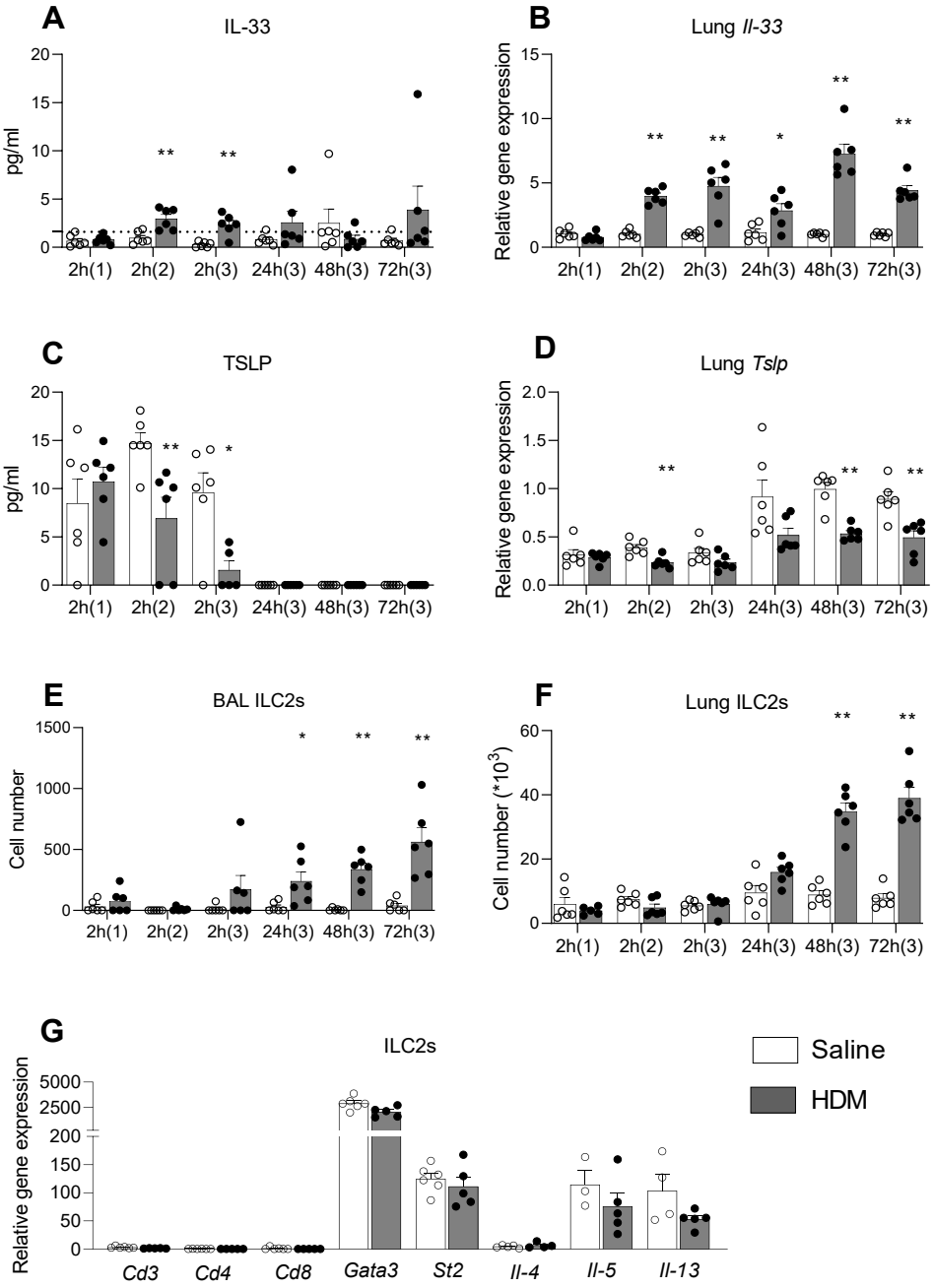


Figure 3.5: House dust mite (HDM) challenge was associated with dysregulation of alarmins, but triggered no changes in type 2 cytokine expression in ILC2s.

Female C57BL/6J mice were sensitised to HDM and then challenged with saline or HDM on one, two or three consecutive days. Mice were sacrificed 2 hours after the first (2h(1)), second (2h(2)), or third challenge (2h(3)), as well as 24, 48 and 72 hours after the third and final challenge (24h(3), 48h(3), and 72h(3), respectively). A) IL-33 concentration in bronchoalveolar lavage (BAL) determined by MSD assays. B) Lung *Il-33* gene expression determined by qRT-PCR, C) TSLP levels in BAL measured by ProcartaPlex assays. D) Lung *Tslp* gene expression assessed by qRT-PCR. Innate lymphoid cells type 2 (ILC2) numbers in E) BAL and F) lung were enumerated with a help of flow cytometry. G) Female C57BL/6J mice sensitised to HDM were challenge with saline or HDM on

three consecutive days and sacrificed 72 hours after the final challenge. $CD4^+$ T cells were isolated from lungs using flow cytometry assisted cell sorting (FACS) and mRNA extracted for determination of gene expression by qRT-PCR. Representative data from a single (A-F) or two independent experiments (G) presented as mean ± S.E.M (N=5-6 mice per group). Mann-Whitney U test was used to analyse differences between saline and HDM groups. * denotes $p<0.05$ and ** $p<0.01$.

3.4.1.3. The role of dendritic cells in HDM-induced airway inflammation

Lastly, we evaluated the role of dendritic cells in HDM-induced responses. HDM challenge resulted in a significant increase in moDCs from the second time point onwards (Figure 3.6A), compared to saline challenged controls. HDM exposure triggered an expansion of classical dendritic cell populations cDC2s and cDC1s, respectively, towards the end of the time course (from 24 and 48 hours after the third and final HDM challenge, respectively) (Figure 3.6B,C). The recruitment of moDCs was accompanied with increased concentrations of CCL2, MIP-1α and CCL17 in BAL of HDM challenged mice compared to saline controls (Figure 3.6D-F). The exposure to HDM, but not saline, triggered migration of all DC populations into the regional lymph nodes (LNs) as suggested by increased numbers of moDCs, cDC2s and cDC1s in MLNs at 2 hours after the second HDM challenge and all subsequent time points (Figure 3.6G-I).

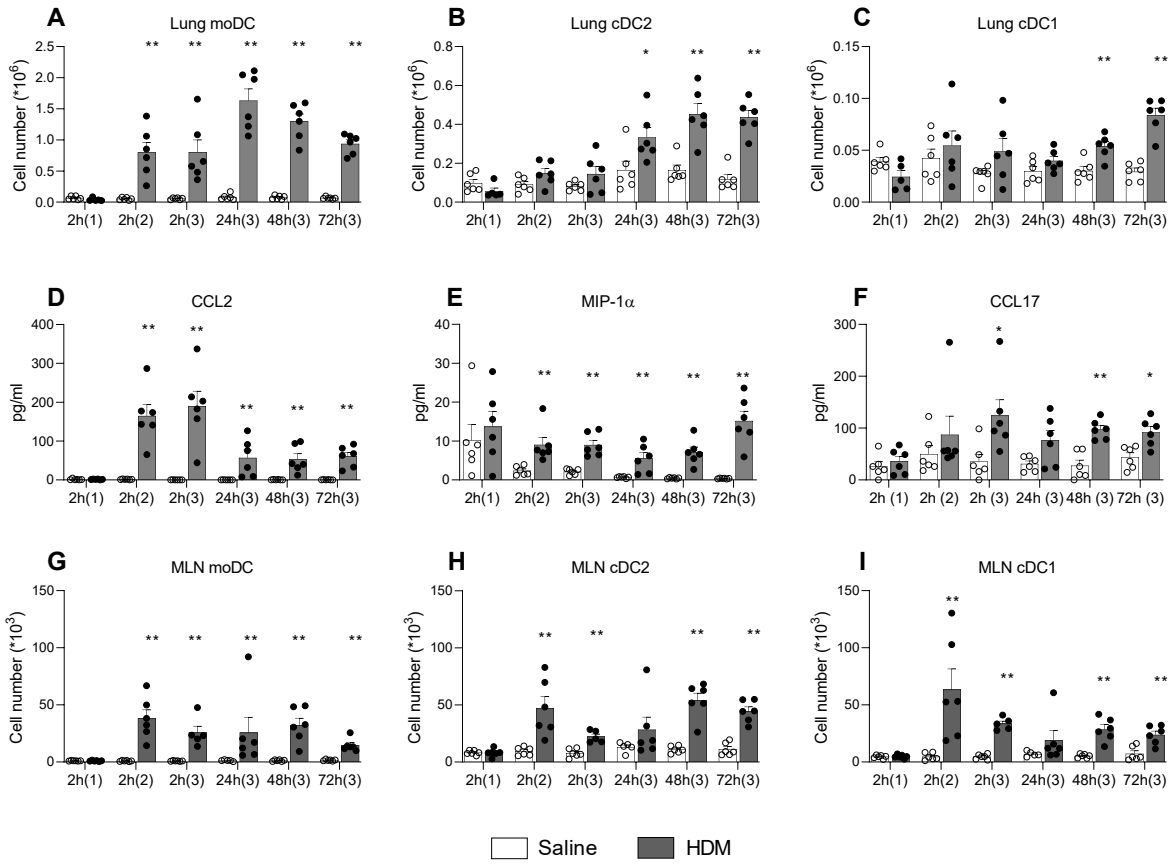


Figure 3.6: Dendritic cell (DC) dynamics upon house dust mite (HDM) challenge.

Female C57BL/6J mice were sensitised to HDM and then challenged with saline or HDM on one, two or three consecutive days. Mice were sacrificed 2 hours after the first (2h(1)), second (2h(2)), or third challenge (2h(3)), as well as 24, 48 and 72 hours after the third and final challenge (24h(3), 48h(3), and 72h(3), respectively). A) monocyte-derived moDCs, B) classical DC type 2 (cDC2s) and C) cDC1s were enumerated in lung utilising flow cytometry. D) CCL2, and E) MIP-1α were determined in bronchoalveolar lavage (BAL) by MSD assays. F) CCL17 was measured in BAL by ELISA. G) moDCs, H) cDC2s and I) cDC1s were enumerated in mediastinal lymph nodes (MLN) with a help of flow cytometry. Data from a single experiment presented as mean ± S.E.M (N=6 mice per group). Mann-Whitney U test was used to analyse differences between saline and HDM groups. * denotes $p<0.05$ and ** $p<0.01$.

3.4.2. TRPV4 signalling pathway in the key immune cells

Having identified immune cells possibly involved in HDM-induced type 2 immune responses, we next investigated whether $CD4^+$ T cells, $CD8^+$ T cells, ILC2s, moDCs, cDC2s or cDC1s could be responsible for the activation of TRPV4 signalling axis upon HDM exposure. To do so, we studied *Trpv4* and *Panx-1* gene expression in individual populations, isolated from saline and

HDM challenged mice, respectively, three days after the third and final challenge. The phenotype of $CD4^+$ T cells, $CD8^+$ T cells and ILC2s was confirmed the previous section (Figure 3.4G,H, Figure 3.5Figure 3.7G), and *Itagx* expression was verified for DCs (Figure 3.7A). *Trpv4* was expressed in $CD4^+$ T cells, ILC2s and DC subsets from saline challenged mice, and was downregulated upon HDM challenge (Figure 3.7B,D-G). *Trpv4* mRNA could not be reliably detected in $CD8^+$ T cells in this experimental setup (Figure 3.7C). *Panx-1* was expressed in all isolated populations from saline and HDM challenged mice, respectively (Figure 3.7). While no change in *Panx-1* expression upon HDM challenge was observed in $CD4^+$ and $CD8^+$ T cells (Figure 3.7B,C), HDM exposure was associated with *Panx-1* downregulation in ILC2s, cDC2s and moDCs (Figure 3.7D,F,G) and upregulation in cDC1s (Figure 3.7E). These results confirmed that $CD4^+$ T cells, ILC2s or DCs could be involved in the detrimental TRPV4 activation.

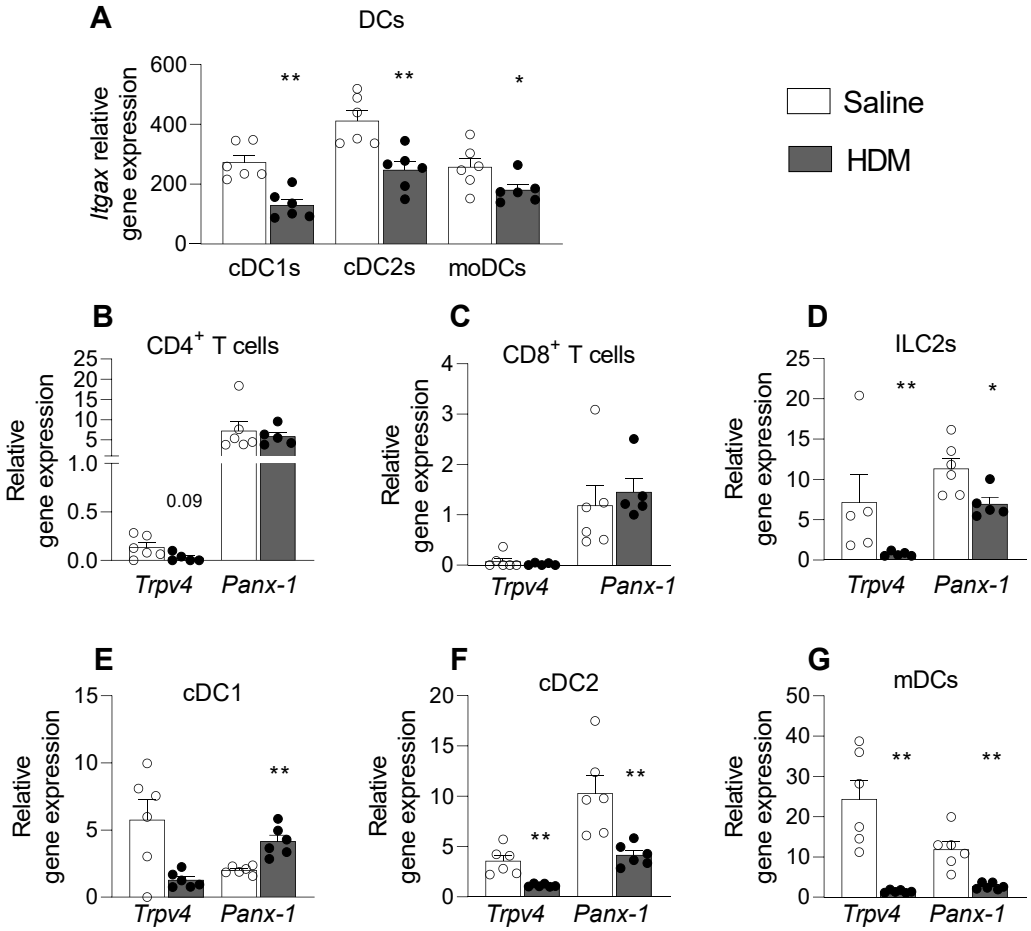


Figure 3.7: *Trpv4* and *Panx-1* expression in key immune cells.

C57BL/6 mice were sensitised to HDM and then challenged on three consecutive days with saline or HDM. Three days later immune cells were isolated from lung using fluorescence assisted cell sorting and mRNA extracted. Gene expression relative to eukaryotic *18s* internal control was determined by qRT-PCR. A) *Cd3, Cd8* and *Cd4* expression in $CD8^+$ T cells. B) *Itagx* expression in monocyte-derived dendritic cells (moDCs), classical DC type 2 (cDC2s) and cDC1s. C-H) *Trpv4* and *Panx-1* gene expression in C) $CD4^+$ T cells, D) $CD8^+$ T cells, E) group 2 innate immune cells (ILC2s), F) moDCs, G) cDC2s and H) cDC1s. Representative data from one of two (A,C-E) or from single experiment (B,D-F) presented as mean ± S.E.M (N=5-6 mice per group). Mann-Whitney U test was used to analyse differences between saline and HDM groups. * denotes $p<0.05$ and ** $p<0.01$.

We then moved on to the identification of P2X receptors that could be activated downstream of TRPV4 by studying P2X receptors expression. The analysis of gene expression in lung tissue revealed that *P2x4* receptor was the most highly expressed P2X receptor which was upregulated upon HDM challenge (1.92 ± 0.13-fold upregulation at 72h(3) time point) (Figure 3.8C,G). Among other P2X receptors *P2rx1, P2rx2, P2rx5, P2rx6* and *P2rx7* but not *P2rx3*

mRNA was also detected in the lungs of saline challenged mice (Figure 3.8). HDM challenge triggered up to 4.49 ± 0.37-fold upregulation of *P2rx1* expression at 48h(3) time point (Figure 3.8A,G), 3.32 ± 0.41-fold upregulation of *P2rx2* at 72h(3) time point (Figure 3.8B,G) and 1.82 ± 0.24-fold upregulation of *P2rx7* at 48h(3) time point (Figure 3.8F,G). *P2rx5* gene expression remained unmodulated by HDM challenge (Figure 3.8D,G), while 0.5 ± 0.06-fold downregulation was observed in *P2rx6* mRNA levels (Figure 3.8E,G).

Next, we addressed gene expression of P2X receptors in the immune cells key for the development of allergic airway inflammation. In $CD4^+$ and $CD8^+$ T cells *P2rx1, P2rx4, P2rx5* and *P2rx7* transcripts were detected (Figure 3.9A,B). HDM challenge was associated with an upregulation of *P2rx7* as well as *P2rx1,* which was otherwise hardly detectable in cells isolated from saline challenge mice. In $CD8^+$ T cells, *P2rx5* expression also could not be detected after saline challenge, but was increased after HDM exposure, while comparable levels between saline and HDM challenge were observed in $CD4^+$ T cells. No change in *P2rx4* expression was observed in neither of the T cell populations. ILC2s expressed *P2rx1, P2rx4* and *P2rx7* with no effect of HDM challenge on their expression (Figure 3.9C). In all DC subset *P2rx4, P2rx5* and *P2rx7* were highly expressed channels. HDM challenge was associated with downregulation of *P2rx7* in all populations, as well as *P2rx4* in moDCs, and *P2rx5* in cDC1s, respectively. Additionally, low expression of *P2rx1* was noted on moDCs and cDC2s which remained unchanged with HDM challenge, as well as *P2rx6,* which could be reliably detected in moDCs and cDC2s upon HDM challenge (Figure 3.9D-E).

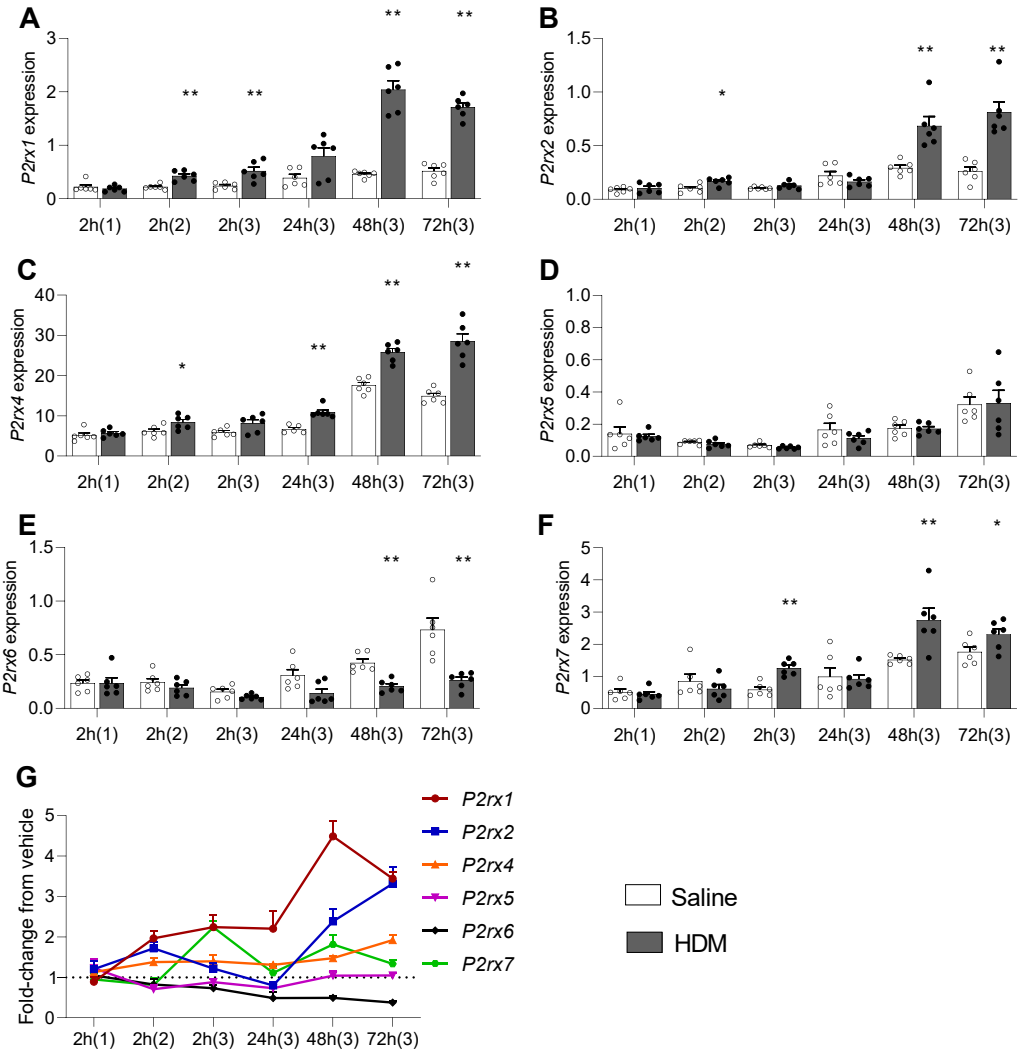


Figure 3.8: P2XR expression in the HDM time course study.

HDM-sensitised C57BL/6 mice were challenged with saline or HDM once a day on one (1) occasion, two (2) or three (3) consecutive days and lung samples collected 2 after each challenge and 24, 48 or 72h after the third and final challenges. Lung expression of A) *P2rx1*, B) *P2rx2*, C) *P2rx4*, D) *P2rx5*, E) *P2rx6* and F) *P2rx7* relative to eukaryotic *18s* expression at various time points after challenge. G) HDM-induced fold change from respective vehicle control in lung *P2rx* expression. Data from a single experiment are presented as mean ± S.E.M with N=6 mice per group. Mann-Whitney U test was used to analyse differences between saline and HDM groups for each time point. * denotes $p<0.05$ and ** $p<0.01$.

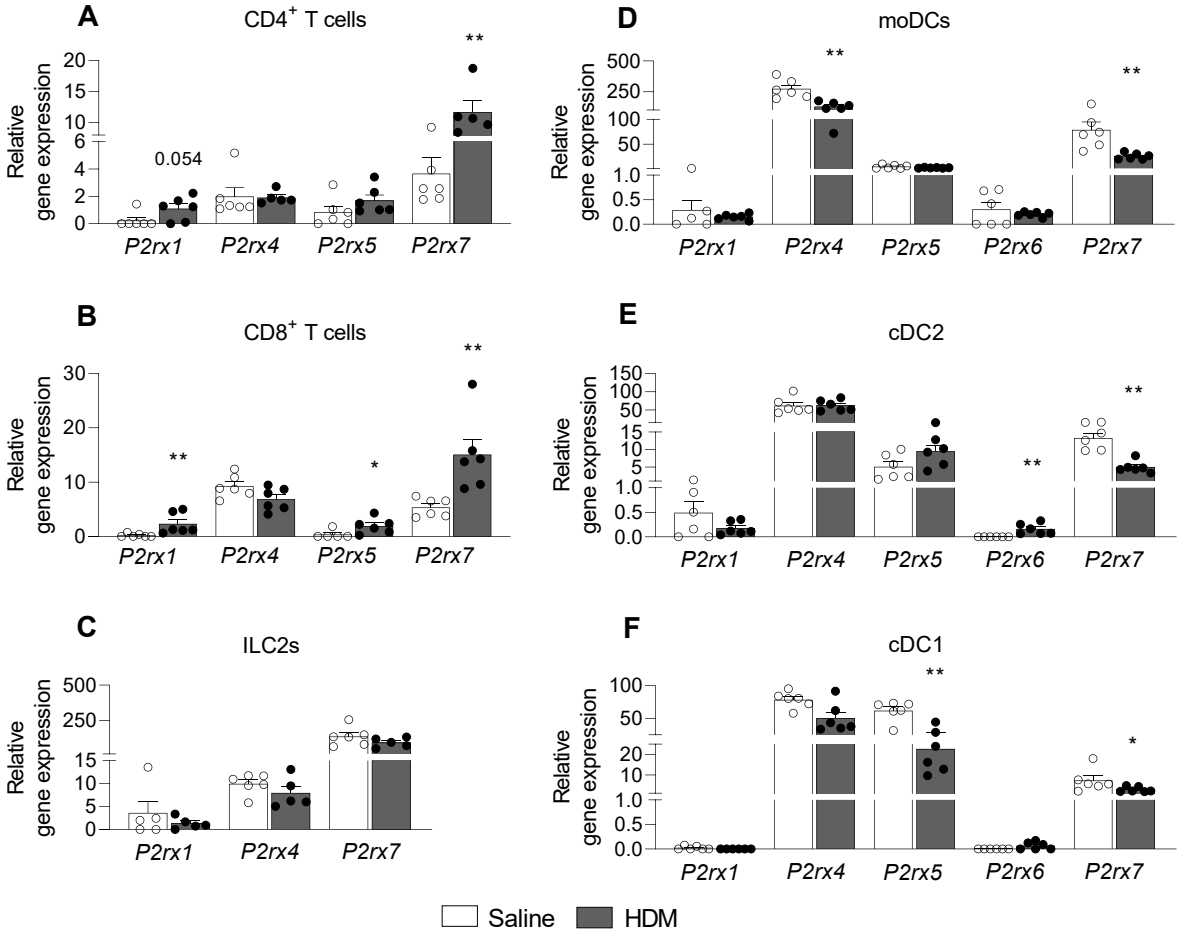


Figure 3.9: Gene expression of P2X receptors on key immune cells.

C57BL/6 mice were sensitised to HDM and then challenged on three consecutive days with saline or HDM. Three days after the last challenge immune cells were isolated from lung using fluorescence assisted cell sorting and mRNA extracted. *P2rx* gene expression relative to eukaryotic *18s* internal control was determined qRT-PCR in A) $CD4^+$ T cells, B) $CD8^+$ T cells, C) group 2 innate immune cells (ILC2s), D) monocyte-derived dendritic cells (moDCs), E) classical DC type 2 (cDC2s) and F) cDC1s. Representative data from one of two (A-C) or from single experiment (D-F) presented as mean ± S.E.M (N=5-6 mice per group). Mann-Whitney U test was used to analyse differences between saline and HDM groups. * denotes $p<0.05$ and ** $p<0.01$.

3.5. Discussion

Despite the advances in the treatment and management of asthma, current therapies are not sufficient to achieve optimal disease control in a substantial proportion of patients (González Barcala et al. 2010, Kuruvilla et al. 2019, Beasley et al. 2020). To address this unmet need and find novel therapeutic options, further understanding of mechanism driving airway

inflammation and lung function changes in asthma are needed. TRPV4, a member of transient receptor channels, has been recently implicated in the pathogenesis of asthma and has been proposed as a new therapeutic target (Cantero-Recasens et al. 2010, Birrell et al. 2016, Naumov et al. 2016, Gombedza et al. 2017, Bonvini et al. 2020, Duan et al. 2020, Wiesner et al. 2020). We have demonstrated that TRPV4 deficiency abolished hallmark features of HDM-induced AAD in a murine model, as well the protective effect of TRPV4 selective antagonist GSK2193874 on OVA-induced LAR and eosinophilic airway inflammation (Birrell et al. 2016). Panx-1 deficient mice were similarly protected against HDM-induced airway pathology, proposing TRPV4 actions were mediated by ATP release as previously suggested (Seminario-Vidal et al. 2011, Baxter et al. 2014, Dahl 2015, Bonvini et al. 2016, Rahman et al. 2018, Bonvini et al. 2020).

We therefore hypothesised that TRPV4-ATP signalling was pivotal in asthma pathogenesis and this thesis aimed to elucidate TRPV4 signalling cascade in the context of allergic asthma. The first aim of my thesis and the primary aim of this chapter was to investigate which cells could be involved in TRPV4 signalling as well as to identify receptors that could be activated downstream of TRPV4 activation. Upon TRPV4 activation ATP released into extracellular space is short-lived due to the rapid inactivation by extracellular ATPases. Thus, released ATP can only activate purinergic receptors, predominantly ionotropic P2X receptors, in the vicinity of the release (Silva-Vilches et al. 2018). We postulated that the immune cells orchestrating allergen-induced inflammation were thus the drivers of TRPV4 signalling cascade. To address this hypothesis, we turned to a previously established murine HDM model of AAD to keep in line with the initial investigations into the role of TRPV4 in allergic asthma (Birrell et al. 2016, Raemdonck et al. 2016). Our initial goal was to investigate in detail the initiation and the development of allergen-induced airway inflammation in a time course study to identify key immune cells involved in the process. We then aimed to isolate the individual populations of key immune cells and study expression of *Trpv4* and *Panx-1* to establish whether they could be responsible for TRPV4 signalling in the context of allergic airway inflammation. Lastly, our final aim was to determine gene expression profile of P2X receptors in those key immune cells to identify which P2X receptors could be implicated downstream of TRPV4 signalling.

To address the first aim, we conducted a time course assessing airway inflammation at various times after a challenge. Typically, mice would be challenged with saline or HDM once daily on

three consecutive days and airway inflammation and AHR assessed 72 hours after the last challenge (Raemdonck et al. 2016). However, to gain an insight into the initiation as well as the progression of allergic airway inflammation, the time course study was conducted in such a way that inflammation was assessed 2 hours after the first, second and third challenge, respectively, as well as 24, 48 and the typical 72 hours after the third and final HDM challenge. First, we wanted to confirm that HDM challenge triggered characteristic type 2 immune responses as previously reported (Raemdonck et al. 2016). Indeed, HDM exposure was associated with an imminent induction of type 2 cytokines. *Il-4, Il-13* and *Il-5* were upregulated in the lungs of HDM challenged mice compared to saline challenged controls from the first time point and throughout the entire study and were followed by an increase in IL-4, IL-13 and IL-5 concentrations in BAL from the second time point onwards. Upregulation of type 2 cytokines upon HDM exposure resulted in a gradual increase of BAL eotaxin-1 levels from the first challenge onwards, and was followed by a propagation of eosinophilic airway and lung inflammation from the second time point and over the duration of the study. At first, HDM challenge was also associated with upregulation of IFNγ and IL-17A, however the responses were short-lived and resulted in a transient neutrophilia only 2 hours after the second and third HDM challenge. These data confirmed the predominance of type 2 immune responses after HDM exposure and successfully recapitulated allergen-provoked responses in allergic asthma (Metzger et al. 1987, Aalbers et al. 1993, Bradding et al. 1994, Truyen et al. 2006, Kuruvilla et al. 2019). In asthmatic patients, allergen challenge has been similarly associated with eosinophilic and neutrophilic responses early after a challenge, however late responses were dominated by type 2 immune responses, which were characterised by pronounced airway eosinophilia and recruitment of T helper cells (Metzger et al. 1987, Kuruvilla et al. 2019). In our model HDM challenge was also associated with upregulated BAL TNFα and IL-1β. Upregulation of TNFα has been reported in asthmatic patients (Ying et al. 1991, Bradding et al. 1994, Baines et al. 2011) and TNFα genetic polymorphisms have been associated with increased risk of asthma in children and adults (Kang et al. 2019, Zhu et al. 2020). TNFα has been proposed to regulate various aspects of the development of allergic airway inflammation (Berry et al. 2007), including eosinophil chemotaxis and their cytotoxic effects as well as T cell activation and cytokine release (Scheurich et al. 1987, Slungaard et al. 1990, Lukacs et al. 1995a). IL-1β is also upregulated in asthmatic patients (Mattoli et al. 1991,

Borish et al. 1992, Baines et al. 2011) and is vital for the induction of Th2 immune responses (Besnard et al. 2011a, Bruchard et al. 2015).

In addition to the analysis of type 1, 2 and 17 cytokines, ATP levels were measured in BAL to confirm the proposed TRPV4-induced ATP release in this model. A standard luciferase based assay which exploits luciferin oxidation by luciferase in the presence of ATP and subsequent generation of unstable, light emitting oxyluciferin was used for this purpose (McElroy 1947, Inouye 2010). However, we were unable to reliably detect ATP in any of the experimental groups using this method, even though increased ATP levels were reported in BAL of asthmatic patients after allergen challenge as well as allergen challenged mice (Idzko et al. 2007, Vanderstocken et al. 2010, Chavez et al. 2013, Idzko et al. 2013, Zhang et al. 2017). However, ATP levels in BAL are rapidly and tightly regulated by extracellular ATPases (Pelleg et al. 2016) and indeed, whilst trying to optimise and improve ATP detection assay we have observed intrinsic ATPase activity of BAL supernatants from naïve as well as diseased laboratory animals (unpublished data). Analysis of ATP in fresh samples or addition of Ca^{2+} chelators, such as EDTA, have been utilised by some groups to minimise the effects of ATPase activity (Idzko et al. 2007, Idzko et al. 2013). In our hands EDTA did not improve the sensitivity and interfered with the luciferase assay (unpublished data). Instead, alternative approaches to ATP detection, such cell-reporting assay (Müller et al. 2017) as well as detection of ATP and its breakdown products by high performance liquid chromatography (Esther et al. 2008, Graven et al. 2014) are currently being established in our laboratory.

Nevertheless, our next aim was to clarify the initiation of type 2 immune responses. $CD4^+$ and $CD8^+$ T cell responses were characterised first as both T cell subsets have been proposed as indispensable in our HDM model as well as other AAD models (Gavett et al. 1994, Hamelmann et al. 1996, Foster et al. 2002, Isogai et al. 2004, Miyahara et al. 2004, Sawicka et al. 2004, Joetham et al. 2005, Koya et al. 2007, Raemdonck et al. 2016). Interestingly, among more than 30 inflammatory mediators evaluated in the time course study, IL-2 was the only cytokine selectively upregulated in BAL 2 hour after the initial HDM challenge and was also elevated 2 hours after each subsequent HDM challenge, but not later in the time course. As IL-2 triggers STAT5 phosphorylation (Doganci et al. 2008, Liao et al. 2008), we determined the levels of pSTAT5A,B in the lung and found that pSTAT5 was indeed upregulated simultaneously with IL-2 after each HDM challenge. HDM-evoked IL-2 signalling was suggestive of activation of

memory T cells that had been generated during the systemic allergen sensitisation phase, although it is also essential for ILC2 function and proliferation (London et al. 2000, Masopust et al. 2001, Reinhardt et al. 2001, Mojtabavi et al. 2002, Cote-Sierra et al. 2004, Masopust et al. 2004, Doganci et al. 2008, Liao et al. 2008, Wilhelm et al. 2011, Mirchandani et al. 2014, Oliphant et al. 2014, Hondowicz et al. 2016, Turner et al. 2018, Bosnjak et al. 2019). Indeed, in the time course study we observed heightened numbers of CD4+ and CD8+ T cells in BAL from the second HDM challenge onwards, although proliferative responses of T cells were slower compared to the cytokine production as previously reported (London et al. 2000). CD4+ and CD8+ T cell numbers in BAL peaked at 2 hours after the third HDM challenge and while CD8+ T cells plateaued afterwards, CD4+ T cells peaked again 72 hours after the third HDM challenge. This coincided with the expansion of lung CD4+ T cell population, a consequence of an additional CD4+ T cell recruitment from the regional lymph nodes and circulation and further amplification of type 2 immune responses (Bosnjak et al. 2019). Gene expression studies on isolated $CD4^+$ T cells confirmed that $CD4^+$ T cells acquired a Th2 phenotype upon HDM challenge as characterised by an upregulation of master Th2 transcription factor *Gata3,* IL-33 receptor *St2* as well as type 2 cytokines *Il-4, Il-5* and *Il-13* (Robinson et al. 1992, Robinson et al. 1993a, Zheng and Flavell 1997, Lohning et al. 1998, Xu et al. 1998, Kuruvilla et al. 2019). Our findings recapitulate elevated $CD4^+$ and $CD8^+$ T cell numbers in the airways of asthmatic patients and the contribution of Th2 cells to type 2 cytokine production upon allergen challenge (Metzger et al. 1987, Gerblich et al. 1991, Walker et al. 1991, Robinson et al. 1992, Robinson et al. 1993a, Lee et al. 2001, Muehling et al. 2017). Furthermore, T cells recruited into the airways of asthmatic patients appeared activated and exhibited a memory phenotype (Marathias et al. 1991, Walker et al. 1991, Robinson et al. 1993b). Simultaneously, increased levels of IL-2 in BAL or exhaled breath condensate have been measured in asthmatic patients, especially when symptomatic (Marathias et al. 1991, Robinson et al. 1992, Robinson et al. 1993b, Park et al. 1994, Boonpiyathad et al. 2013). IL-2/STAT5 signalling has been deemed critical for type 2 cytokine production, migration and proliferation of activated $CD4^+$ T cells (Ben-Sasson et al. 1990, Le Gros et al. 1990, Cote-Sierra et al. 2004, Hashimoto et al. 2006, Doganci et al. 2008, Liao et al. 2008, Hondowicz et al. 2016). Inhibition of IL-2 signalling has been associated with improved airway function and dampened eosinophilic airway inflammation in both preclinical models of AAD as well as asthmatic

patients, while treatment with IL-2 during an allergen challenge exacerbated the disease (Renzi et al. 1999, Busse et al. 2008, Doganci et al. 2008).

While the pivotal role of $CD4^+$ T in allergic airway inflammation has been extensively established (Gavett et al. 1994, Foster et al. 2002, Joetham et al. 2005, Raemdonck et al. 2016), the role of $CD8^+$ T cells is more controversial. A plethora of studies have demonstrated a protective role of $CD8^+$ T cells during sensitisation and allergen challenge and were associated with dampened of Th2 inflammation (Hansen et al. 1999, Huang et al. 1999, Stock et al. 2004, Takeda et al. 2009). Nevertheless, several research groups, including ours, have provided evidence for an indispensable role of $CD8^+$ T cells in the development of airway inflammation as well as AHR in animal models of AAD (Hamelmann et al. 1996, Isogai et al. 2004, Miyahara et al. 2004, Sawicka et al. 2004, Joetham et al. 2005, Koya et al. 2007, Koya et al. 2009, Raemdonck et al. 2016). $CD8^+$ T cells have been recognised as a source of type 2 cytokines in patients as well as animal models (Coyle et al. 1995b, Lee et al. 2001, Sawicka et al. 2004, Stock et al. 2004, Cho et al. 2005). Sawicka et al have further demonstrated a formation of $CD8^+$ Tc2 memory cells upon allergen encounter which were sufficient for induction of type 2 inflammation during subsequent allergen challenge (Sawicka et al. 2004). The contribution of $CD8^+$ T cells in human disease is not as clear, however $CD8^+$ T cell numbers in BAL have been associated with long-term lung function decline in asthmatic patients and asthma related deaths (O'Sullivan et al. 2001, van Rensen et al. 2005, den Otter et al. 2016).

An increasing body of literature has demonstrated allergens can evoke type 2 airway inflammation independently of T cells (Lloyd and Snelgrove 2018). ILC2s, a Th2 innate cell counterpart, have been recognised as an important source of type 2 cytokines and can initiate type 2 immune responses independently of adaptive immunity (Lloyd and Snelgrove 2018). To evaluate their contribution to the HDM-evoked pathology in our model, we characterised the kinetics of ILC2 responses upon HDM challenge. IL-33, IL-25 and TSLP were initially quantified in BAL and their gene expression determined in lung as they are the main cytokines responsible for ILC2 activation (Mitchell and O'Byrne 2017b). In our model we could detect no IL-25 in BAL or *Il-25* in lung. Interestingly, intranasal challenges triggered an increase in BAL TSLP concentration and from the second challenge onwards the responses were smaller in HDM challenged mice, coinciding with downregulated lung *Tslp*. Nevertheless, HDM challenge was associated with increased BAL IL-33 concentration 2 hours after the second and

third allergen challenge, respectively, and upregulated *Il-33* in lung from the second HDM challenge onwards. These data are in agreement with clinical findings demonstrating an increased expression of IL-33 in BAL, sputum as well as biopsy specimens in asthmatic patients compared to controls (Préfontaine et al. 2010, Hamzaoui et al. 2013, Saglani et al. 2013, Guo et al. 2014, Chauhan et al. 2015, Christianson et al. 2015, Kaur et al. 2015, Li et al. 2018b, Wang et al. 2018a). However, dysregulation of TSLP and IL-25 signalling was not recapitulated in our model. TSLP levels in BAL, serum and exhaled breath condensates as well as increased expression in bronchial biopsies has been found elevated in asthmatic patients (Ying et al. 2005, Gluck et al. 2016, Li et al. 2018b, Wang et al. 2018b). Allergen challenge has also evoked upregulation of IL-25 in submucosa of asthmatic patients, although no change in IL-25 levels in BAL could be measured (Cheng et al. 2014, Li et al. 2018b, Wang et al. 2018b). All three cytokines have been shown to regulate various aspects of type 2 immunity, including T cell, ILC2 and dendritic cell functions, as well as airway remodelling, and are now being evaluated as treatments of severe asthma (Mitchell and O'Byrne 2017a, Matera et al. 2020). For instance, tezepelumab, an anti-TSLP mAb, has been successful in reducing AHR and markers of systemic and airway inflammation upon allergen challenge in a proof-of-concept study, as well as exacerbation rates and blood eosinophilia in phase 2b clinical trials (Gauvreau et al. 2014, Corren et al. 2017, Matera et al. 2020). The beneficial effect of tezepelumab on exacerbation rate, asthma control and lung function in severe asthmatics has been confirmed in a phase 3 multicentre clinical trial NAVIGATOR (Menzies-Gow et al. 2021) and *Tezspire* has been approved by U.S. Food and Drug Administration as an add-on maintenance therapy in with severe asthma aged 12 years and older (2021). Results of first clinical trials testing the efficacy of anti-IL-33 or anti-ST2 therapies are as promising. Itepekimab, an anti-IL-33 mAb, was associated with improved asthma control and lung function in patients with moderate-to-severe asthma in a phase 2 trial (Wechsler et al. 2021). Astegolimab, an anti-ST2 mAb, similarly reduced exacerbation rate in patients with severe inadequately controlled asthma (Kelsen et al. 2021).

Upregulation of IL-33 as well as IL-2 upon HDM challenge demonstrated a presence of cues needed for ILC2 activation and proliferation in the presented HDM model. Indeed, HDM exposure triggered an expansion of ILC2s in BAL and lung, although with a delay, as an increase in ILC2s numbers was observed no earlier than 24 hours after the third HDM

challenge. Subsequent gene expression studies on isolated ILC2s which were characterised by a lack of T cell markers and high expression of *Gata3* as well as *St2,* confirmed expression of *Il-5, Il-13* and relatively lower levels of *Il-4* by ILC2s as previously reported (Halim et al. 2012, Li et al. 2017, Halim et al. 2018, Starkey et al. 2019). Interestingly, ILC2s expression profile remained unchanged upon HDM challenge, contradicting the proposed HDM-induced activation. ILC2s have been demonstrated to upregulate type 2 cytokines when activated, although variable effects on ST2 expression have been reported (Halim et al. 2012, Klein Wolterink et al. 2012, Li et al. 2017). Studies utilising AAD models with mucosal sensitisation to aeroallergens have established a vital role of ILC2s for the initiation of type 2 immunity, even in the absence of adaptive immunity (Halim et al. 2012, Klein Wolterink et al. 2012, Gold et al. 2014, Halim et al. 2014, Lloyd and Snelgrove 2018). Even so, ILC2-driven immune responses have been accompanied by heightened $CD4^+$ T cell numbers and ILC2s have been demonstrated to promote Th2 recruitment, differentiation and activation of Th2 cells directly or indirectly via DCs (Drake et al. 2014, Halim et al. 2014, Mirchandani et al. 2014, Oliphant et al. 2014, Bouchery et al. 2015, Halim et al. 2016, Halim et al. 2018). Although $CD4^+$ T cells might be dispensable during the initiation ILC2-driven responses, $CD4^+$ T cells have been crucial for the maintenance of type 2 pathology or robust inflammatory responses after subsequent re-exposures and T-cell derived IL-2 has been shown to regulate ILC2 function (Neill et al. 2010, Wilhelm et al. 2011, Drake et al. 2014, Halim et al. 2014, Mirchandani et al. 2014, Oliphant et al. 2014, Bouchery et al. 2015). In AAD models with systemic sensitisation phase (like Ovalbumin-induced AAD models) ILC2s have appeared dispensable for allergen-evoked airway pathology (Klein Wolterink et al. 2012, Tjota et al. 2013, Gold et al. 2014). In a Th2 driven murine Aspergillus model, Wiesner et al. have observed an early expansion of $CD4^+$ T cells followed by a delayed expansion of ILC2 (Wiesner et al. 2020). In OVA model, Tjota et al. have described an increase in ILC2 numbers upon OVA challenge, although allergen-primed $CD4^+$ T cells were sufficient for the reconstitution of OVA-induced airway pathology in $Rag^{-/-}Il2ra^{-/-}$ mice (Tjota et al. 2013). Moreover, we have data to suggest that administration of low dose HDM alone was not sufficient for ILC2 expansion in non-sensitised animals or in mice lacking mature T and B lymphocytes ($Rag^{-/-}$ mice) (unpublished data). Therefore, we postulated that ILC2s were not required for the establishment of airway inflammation upon HDM exposure, however we have not yet fully elucidated the role of ILC2s in this model. The possibility exists that with escalating lung

inflammation airway epithelial damage worsened (Oddera et al. 1996, Wilson et al. 2013) and was reflected by upregulation of lung *Il-33* (Mitchell and O'Byrne 2017b). Activation of ILC2s at this later stage could either contribute to the loss of epithelial barrier integrity, promote airway remodelling or wound healing via the secretion of EGF cytokine family member amphiregulin (Monticelli et al. 2011, Saglani et al. 2013, Monticelli et al. 2015, Lloyd and Snelgrove 2018, Sugita et al. 2018). Follow up studies using mice engineered to target ILC2s (Starkey et al. 2019), would be required to delineate the role of ILC2s in the development of allergic airway inflammation as well as airway remodelling and repair phase.

Lastly, APCs are another vital player in the induction of type 2 immunity (Vroman et al. 2017). The pivotal role of DCs during allergen sensitisation in Th2 priming and differentiation has been long known (Vroman et al. 2017). However, their function extends well beyond sensitisation as cDC2s and moDCs have been demonstrated to be indispensable for the reactivation of memory Th2 cells during allergen challenge (Lambrecht et al. 1998, Lambrecht et al. 1999, Julia et al. 2002, van Rijt et al. 2005, Medoff et al. 2009, Plantinga et al. 2013). Here, we demonstrated that HDM challenge was associated with a marked recruitment of moDCs into the lung 2 hours after the second HDM challenge and an expansion of lung classical $CD103^+$ and $CD11b^+$ DC populations toward the end of the study. A rapid recruitment of moDCs into the lung as well as expansion of cDC subsets upon allergen challenge have been described before in the context of rodent models of AAD as well as clinical observations and were shown to occur within few hours after allergen encounter (Moller et al. 1996, Jahnsen et al. 2001, Huh et al. 2003, van Rijt et al. 2005, Plantinga et al. 2013, Wiesner et al. 2020). Studies into DC airway network have demonstrated a close contact between submucosal DCs and T cells which was further strengthened by allergen exposure (Huh et al. 2003, van Rijt et al. 2005). Monocyte-derived DCs have been described as highly proinflammatory and as potent simulators of $CD4^+$ and $CD8^+$ T cells due to their high expression of co-stimulatory molecules on their surface (Masten et al. 1997, Huh et al. 2003, van Rijt et al. 2005, Kopf et al. 2015). Upon allergen challenge lung DCs have been shown to produce lymphocyte and DC attracting chemokines such as MIP-1α, MIP3α, TARC and MDC (CCL22), CCL2 and CCL17 and promote airway inflammation (Vissers et al. 2001, van Rijt et al. 2005, Plantinga et al. 2013). In line with this notion, we measured increased levels of MIP1α, TARC and CCL2 in BAL upon HDM exposure in a similar fashion to moDC dynamics. Furthermore, heightened numbers of

all three DC subsets were found in the regional LN from the second time point onwards, suggestive of their migration after encountering allergens, similar to previous reports (Plantinga et al. 2013). Interestingly, all three DC subsets were equally present in the MLN at first, although moDCs have been previously described as poorly migratory compared to cDCs (Nakano et al. 2013, Plantinga et al. 2013). However, at the end of the time course study $CD11b^+$ cDC2 population remained the predominant subset as previously suggested (Nakano et al. 2013, Plantinga et al. 2013). Antigen presentation by other APCs, such as AMs and B cells, does not appear relevant for the initiation of type 2 immune responses during allergen challenge phase. AMs have been demonstrated to uptake inhaled allergens, but were incapable of migrating to draining lymph nodes (Plantinga et al. 2013, Schneider et al. 2014). Moreover, selective depletion of AM has worsened rather than ameliorated allergic airway inflammation (Plantinga et al. 2013, Schneider et al. 2014, Mathie et al. 2015, Lambrecht et al. 2017). B cells on the other hand, are poor up-takers of inhaled allergens and are indispensable of the development of allergic airway inflammation in various AAD models, including the HDM model used in this thesis (Hamelmann et al. 1997b, Mehlhop et al. 1997, Corry et al. 1998, Plantinga et al. 2013, Raemdonck et al. 2016). However, additional studies are warranted to undoubtedly establish the importance of DCs (and particular subsets) in this model.

Taken together, we postulated that $CD4^+$ T cells, $CD8^+$ T cells and moDCs were the key immune cell populations required for the initiation of type 2 immune responses during HDM challenge phase and were hence considered as the most probable players in the TRPV4 signalling cascade in this model. As the role of ILC2s and DC subsets has not been delineated fully, the possibility exists that ILC2s as well as cDC1s and cDC2s contribute to the development and maintenance of allergic airway inflammation. Therefore, to address the second aim of this chapter, $CD4^+$ T cells, $CD8^+$ T cells, ILC2s, and all three lung DC populations were investigated for being a part of the TRPV4 axis. All those populations were isolated from lungs of saline or HDM challenged mice using FACS. *Trpv4* was found to be expressed on $CD4^+$ T cells, ILC2s, and all DC populations, and inconsistently on $CD8^+$ T cells, in line with previous reports of TRPV4 expression in human leukocytes, including monocytes, dendritic cells and lymphocytes (Inada et al. 2006, Spinsanti et al. 2008, Szollosi et al. 2013, Bertin et al. 2014, Majhi et al. 2015, Naert et al. 2019). In our model, HDM challenge triggered a suppression of *Trpv4* expression in $CD4^+$

T cells, ILC2s and DC subsets. This is in contrast to observations from murine OVA-induced, AAD models which have suggested an upregulation of lung TRPV4 after OVA exposure, although no change in TRPV4 expression was observed in murine ragweed model (Groot-Kormelink et al. 2012, Duan et al. 2020, Kim et al. 2020, Wiesner et al. 2020). The effects of allergen exposure on lymphocyte- or DC-specific TRPV4 expression have not been reported elsewhere, however the activation of T cells and maturation of DCs have been linked with increased TRPV4 expression (Szollosi et al. 2013, Majhi et al. 2015). The implications of TRPV4 signalling for lymphocyte and DC function have also not been extensively investigated. Naert et al. have demonstrated that while TRPV4 was dispensable for DC maturation and expression of costimulatory molecules upon LPS stimulation, it was crucial for FcR-dependent phagocytosis (Naert et al. 2019). They postulated that phospholipase C (PLC)-γ, activated upon FcR ligation, induced the production of inositol triphosphate (IP_3) which sensitised TRPV4 to mechanical stimuli in the vicinity of the engulfing membranes (Fernandes et al. 2008, White et al. 2016, Naert et al. 2019). FcγRIII signalling on DCs has been shown vital for the development of allergic airway inflammation in a murine OVA model (Tjota et al. 2013) and could lead to activation of TRPV4 signalling in allergic airway activation. Majhi et al. have demonstrated the presence of functional TRPV4 receptors on human and murine primary T cells which regulated T cell migration and cytokine production upon activation (Majhi et al. 2015). The mechanism of TRPV4 activation upon TCR stimulation in T cells is yet to be elucidated. TCR activation triggered activation of a structurally close TRP channel TRPV1 via phosphorylation by Src kinase (Bertin et al. 2014, White et al. 2016). Src kinases have been demonstrated to modulate the activity of TRPV4 as well (Xu et al. 2003, White et al. 2016). Additionally, TRC signalling is complex and involves activation PKC as well as PLCγ1 and generation of IP_3, which have been implicated in TRPV4 sensitisation/activation (Fernandes et al. 2008, White et al. 2016, Naert et al. 2019), however further research into the mechanism of TRPV4 activation in lymphocytes and dendritic cells are warranted.

TRPV4 activation has been linked to ATP release via Panx-1 channels space (Seminario-Vidal et al. 2011, Baxter et al. 2014, Dahl 2015, Bonvini et al. 2016, Rahman et al. 2018, Bonvini et al. 2020), thus *Panx-1* expression was studied in those populations as well. *Panx-1* was detected in all populations and was downregulated upon HDM challenge in ILC2s, cDC2s and moDCs and upregulated in cDC1s. No change in *Panx-1* expression was observed in $CD4^+$ or

$CD8^+$ T cells. $CD4^+$ and $CD8^+$ T cells have been demonstrated to express and rely on Panx-1 for ATP release into extracellular space which controls T cell effector function, migration as well as survival (Schenk et al. 2008, Woehrle et al. 2010a, Woehrle et al. 2010b, Shoji et al. 2014, Ledderose et al. 2018, Wanhainen et al. 2019). Although the importance of ATP for DC migration, priming function and survival has been previously established, the presence of functional Panx-1 channels on dendritic cells have recently demonstrated and implicated in DC migration (Saez et al. 2017, Silva-Vilches et al. 2018).

One limitation to this approach to studying TRPV4/ATP signalling in immune cells is that the function and role of TRPV4 had not been investigated. Additionally, the validation of our findings on cells isolated from human and relevance for asthma would be in place. Focusing solely on immune cells we had not addressed the potential involvement of airway epithelium in HDM-triggered TRPV4 signalling. Airway epithelium has been recognised as a primary source of IL-33, TSLP and IL-25 and actively regulates allergen-evoked type 2 immune responses (Mitchell and O'Byrne 2017a). Airway epithelial cells abundantly express TRPV4 on their apical surface and release ATP upon TRPV4 activation (Fernandez-Fernandez et al. 2008, Seminario-Vidal et al. 2011, Baxter et al. 2014). Wiesner et al. have recently demonstrated that conditional knockdown of TRPV4 in club cells was protective against the development of allergic airway inflammation in an alkaline protease 1 (AP1) model of AAD (Wiesner et al. 2020). However, AP1 model relies on mucosal sensitisation to allergens (Wiesner et al. 2020) and the contribution of epithelial TRPV4 during allergen challenge phase remains to be elucidated.

Nevertheless, having demonstrated that key immune cells could be driving TRPV4 signalling in allergic airway inflammation, the last aim of this chapter was to identify P2X receptors that could be activated by ATP downstream of TRPV4. We analysed gene expression of all seven P2X receptors in the key immune cells postulated to drive TRPV4 axis in AAD. We detected *P2rx1, P2rx4, P2rx5* and *P2rx7,* but no *P2rx2, P2rx3* and *P2rx6* mRNA in $CD4^+$ and $CD8^+$ T cells as previously reported (Schenk et al. 2008, Yip et al. 2009, Woehrle et al. 2010a, Woehrle et al. 2010b, Wang et al. 2014, Stark et al. 2018). Purinergic signalling, especially via P2X1, P2X4 and P2X7 receptors, is pivotal for T cell function, migration and survival (Mizumoto et al. 2002, Schenk et al. 2008, Yip et al. 2009, Woehrle et al. 2010a). T cells depend on ATP signalling for successful communication; they maintain ATP halo surrounding their plasma membrane to

sustain P2X1 signalling necessary for antigen recognition (Mizumoto et al. 2002, Ledderose et al. 2016). TCR stimulation triggers an additional release or ATP as well as translocation of Panx-1, P2X1 and P2X4 into the immune synapse (Schenk et al. 2008, Yip et al. 2009, Woehrle et al. 2010a, Ledderose et al. 2014, Ledderose et al. 2016). Subsequent autocrine and paracrine activation of P2X4 as well as P2X7 induces IL-2 production as well as proliferation, while P2X5 receptor has been implicated in IL-10 production (Baricordi et al. 1996, Schenk et al. 2008, Yip et al. 2009, Woehrle et al. 2010a, Abramowski et al. 2014, Ledderose et al. 2014, Wang et al. 2014, Ledderose et al. 2016). On the other hand, the absence of ATP signals during maturation or activation induces anergy of $CD4^+$ T cells (Schenk et al. 2008). P2X7 has been additionally recognised as the main receptor regulating ATP-induced cell death (Tsukimoto et al. 2006, Shoji et al. 2014, Stark et al. 2018). Detailed analysis of P2X7 expression on $CD8^+$ T cell subsets revealed a particularly high expression in resident memory population compared to low expression on naïve and central memory subsets (Stark et al. 2018). However, TCR-mediated activation triggered downregulation of P2X7 and was postulated to promote survival of tissue resident populations upon activation (Stark et al. 2018). In our studies HDM challenge was associated with upregulation of *P2rx1* and *P2rx7* in $CD4^+$ and $CD8^+$ T cells and *P2rx5* on $CD8^+$ T cells, while gene expression of other channels remained unchanged. Upregulation of P2X5 has been previously associated with T cell activation (Abramowski et al. 2014), however there is lack of information on the transcriptional regulation of P2X receptors in T cell during allergic airway inflammation. Less specifically, though, upregulation of P2X4 has been noted on BAL cells isolated from asthmatic patients compared to controls, and animals studies have reported upregulation of lung *P2rx4* and *P2rx7* upon allergen challenge (Muller et al. 2011, Chen et al. 2016, Zech et al. 2016, Ochoa-Amaya et al. 2018, Kim et al. 2020). Our P2X gene expression studies in the time course study have not only confirmed the upregulation of *P2rx4* and *P2rx7* in lung upon HDM challenge, but have also demonstrated upregulation of *P2rx1, P2rx2* and downregulation of *P2rx6,* similar to changes in liver P2X expression during sepsis (Csoka et al. 2018).

ILC2s expressed *P2rx1, P2rx4,* and *P2rx7* but no other P2X channels, with HDM challenge exerting no effect on their expression. The role of ATP signalling as well as specific function of each of the individual P2X receptors for ILC2 function and the contribution of each of the receptors is not yet clear and warrants further investigations.

Analysis of P2X receptor expression in DC subpopulations revealed an abundant expression of *P2rx4, P2rx5* and *P2rx7* and low expression of *P2rx1* and *P2rx6*, but no *P2rx2* or *P2rx3* similar to published data (Berchtold et al. 1999, Saez et al. 2017). In contrast to T cell expression data, HDM challenge was associated with reduced expression of *P2rx7* in all DC subpopulations, as well as downregulation of *P2rx4* and *P2rx5* in moDCs and cDC1s, respectively. There is a lack of information on regulation of P2X receptor expression in DCs in asthma as well the roles of P2X5 and P2X6 in DC functions (Jacob et al. 2013). Expression studies performed on moDCs from asthmatic patients found no change in *P2x7* expression compared to healthy controls (Muller et al. 2011), however the genetic profile of moDCs cultured and differentiated in vitro from blood monocytes might not reflect that of lung resident DCs or in vivo recruited moDCs. A similar study performed on mouse bone marrow derived DCs (BMDCs) demonstrated an enhanced *P2rx4* expression 24 hours ATP stimulation, but have not investigate the effect of allergen challenge on P2X receptor expression in vivo (Zech et al. 2016). The importance of ATP signalling for DC function, cytokine production, migration and survival has been well established (Silva-Vilches et al. 2018). ATP does not appear to affect maturation, but is critical for their T cell priming ability and the capacity to attract lymphocytes (Mutini et al. 1999, Idzko et al. 2007, Saez et al. 2017). Additionally, migration of naïve but not mature DCs is also regulated by ATP, however it does not appear to be mediated via P2X4 or P2X7 (la Sala et al. 2002, Li et al. 2014, Zech et al. 2016, Saez et al. 2017). P2X4 and P2X7 are the main purinergic receptors implicated in ATP-induced responses and death and their activation has been associated with NLRP3 inflammasome activation and IL-1β release (Mutini et al. 1999, Sakaki et al. 2013, Englezou et al. 2015, Zech et al. 2016, Saez et al. 2017). NLRP3 inflammasome/IL-1β signalling appears critical for the induction of Th2 immune responses in animal models of AAD (Besnard et al. 2011a, Bruchard et al. 2015), and both, P2X4 and P2X7 have both been implicated in regulation of Th cell priming and the development of type 2 immune responses (Muller et al. 2011, Zech et al. 2016). $P2X4^{-/-}$ and $P2X7^{-/-}$ DCs, respectively, have been demonstrated to be IL-1β insufficient and exhibited impaired priming capabilities after allergen exposure in vitro and in vivo (Lucattelli et al. 2011, Zech et al. 2016). In our HDM model increased IL-1β were associated with HDM challenge concurrently with type 2 inflammatory response which support the involvement of P2X4 and P2X7 in the pathogenesis of allergic airway inflammation.

These data suggested several P2X receptors could be activated downstream of TRPV4 activation. Considering published literature and the presented expression data, we postulated that P2X1, P2X4 and P2X7 were the most likely targets in TRPV4/ATP signalling axis and their role in AAD was studied in the successive chapter.

4. P2X receptors as downstream targets in TRPV4 signalling in HDM-induced model of allergic airway disease

4.1. Introduction

The aim of the thesis is to elucidate TRPV4 signalling cascade in allergic asthma. Our laboratory has previously suggested the central role of TRPV4 signalling in the development of allergic airway inflammation and allergen-induced airway responses in rodent models of AAD as inhibition of TRPV4 signalling abolished the development of allergic airway inflammation and allergen-induced changes in lung function (Birrell et al. 2016). In the murine HDM AAD model, Panx-1 deficient mice were similarly protected from the development of allergen-induced hallmark features of AAD (unpublished data), which has implicated a release of ATP into extracellular space upon TRPV4 activation as previously suggested (Seminario-Vidal et al. 2011, Baxter et al. 2014, Bonvini et al. 2020). In extracellular milieu ATP acts in an autocrine and paracrine fashion on predominantly ATP-gated P2X ion channels, although several P2Y G-protein coupled receptors have an ability to respond to ATP in addition to other purines (Illes et al. 2020).

Extracellular ATP has been increasingly implicated in the pathogenesis of chronic respiratory disease. Increased ATP levels have been measured in the airways of COPD, IPF as well as asthma patients (Lommatzsch et al. 2010, Riteau et al. 2010, Muller et al. 2011, Lazar et al. 2016). In relevance to asthma, preclinical studies have demonstrated that breakdown of ATP or inhibition of purinergic P2 receptors, P2X4 or P2X7 for example, alleviated allergic airway inflammation as well as AHR (Idzko et al. 2007, Muller et al. 2011, Ledderose et al. 2014, Amison et al. 2015, Chen et al. 2016, Zech et al. 2016, Li et al. 2018a). While a link between TRPV4 and activation of P2X3, P2X4 or P2X7 has been established in cough, bronchospasm and smoke-induced airway inflammation, respectively (Baxter et al. 2014, Bonvini et al. 2016, Bonvini et al. 2020), it remains unclear which P2X receptors mediate the effects of TRPV4 activation in asthma.

In the previous chapter, we characterised P2X gene expression profiles in the immune cells most critical for the development of allergic airway inflammation, namely $CD4^+$ and $CD8^+$ T cells, ILC2s and dendritic cells, to identify candidate P2X receptors that could be implicated in TRPV4 signalling in our murine HDM model of AAD. We hypothesised that P2X1, P2X4 and P2X7 receptors were the most likely downstream targets in TRPV4 signalling cascade due to their high expression and importance for T cell and DC functions (Chapter 3, (Schenk et al. 2008, Yip et al. 2009, Woehrle et al. 2010b, Ledderose et al. 2014, Wang et al. 2014, Ledderose

et al. 2016). Moreover, both receptors appear to be upregulated in asthmatic patients and promote the development of allergic airway inflammation and AHR in animals models of AAD (Muller et al. 2011, Chen et al. 2016, Zech et al. 2016, Li et al. 2018a, Wang et al. 2018a). Less in known about the role of P2X1 in asthma pathogenesis, however a recent study has suggested P2X1 receptors to be desensitised in asthmatic patients (Wright et al. 2016).

4.2. Hypothesis and aims

We hypothesised that P2X4 or P2X7 receptors, activated downstream of TRPV4, were critical for the development of allergic airway inflammation and AHR in our established HDM-induced model of AAD.

To investigate this hypothesis, we aimed to

- Investigate the role of P2X7 in vivo in the murine HDM model of AAD utilising P2X7 deficient mice.
- Investigate the role of P2X4 in vivo in the murine HDM model of AAD utilising P2X4 deficient mice,
- Investigate the role of P2X1 in vivo in the murine HDM model of AAD utilising P2X1 deficient mice.

4.3. Methods

This section outlines and summarises the main methods used in this chapter. All the methodology and experimental protocols are presented in detail in Chapter Methods.

4.3.1. $P2X7^{-/-}$ in the HDM model

4.3.1.1. Validation of $P2X7^{-/-}$ mice

4.3.1.1.1. Gel electrophoresis based genotyping

DNA was extracted from tail tips from WT and $P2X7^{-/-}$ mice and amplified by PCR. Products were then loaded onto agarose gels, separated by electrophoresis and visualised under UV light.

4.3.1.1.2. Functional validation – NLRP3 inflammasome activation model

The absence of functional P2X7 receptors was confirmed in vivo in NLRP3 inflammasome activation model, developed by Early Respiratory and Immunology Bioscience team,

AstraZeneca. WT and P2X7$^{-/-}$ mice were exposed to nebulised saline or LPS for 30 minutes. Five hours after the start of the study mice were intranasally administered PBS or ATP and sacrificed 90 minutes later. BAL was collected for subsequent assessment of airway inflammation. BAL total leukocyte numbers were determined by an automated cell counter (Sysmex) while leukocytes were differentiated based on a histological assessment. BAL IL-1β and TNFα levels were measured by MSD U-plex assays, and BAL IL-18 by ELISA (Invitrogen).

4.3.1.2. P2X7$^{-/-}$ HDM study

P2X7$^{-/-}$ and WT (C57BL/J6) mice were sensitised to HDM on days 0 and 14 and intranasally administered saline or HDM on days 24, 25 and 26. On day 29, AHR to increasing concentrations of 5-HT was assessed using whole body plethysmography (Buxco). Mice were then sacrificed and blood, BAL and lung samples collected for the assessment of HDM-induced inflammatory responses.

Briefly, total IgE and HDM-specific IgE were determined in plasma by ELISA. Lungs underwent enzymatic digestion to obtain single cell solution. Total leukocyte numbers in lung and BAL were quantified by an automated cell counter (Sysmex) while flow cytometry was utilised to differentiate leukocyte populations based on their expression of surface and transcription factors (analysed with Fortessa). BAL concentration of IL-1β, IL-4, IL-5, IL-10, IL-13, Eotaxin-1, CCL2 and MIP-1α were determined by ProcartaPlex assays, and CCL17 concentration was determined by ELISA (R&D).

4.3.2. P2X4$^{-/-}$ in the HDM model

4.3.2.1. Validation of P2X4$^{-/-}$ mice

4.3.2.1.1. Genotyping of P2X4$^{-/-}$ mice

To confirm the genotype of P2X4$^{-/-}$, P2X4$^{+/-}$ and P2X4$^{+/+}$ mice, DNA was extracted from tail tips and P2X4 alleles amplified by PCR. Products were loaded onto agarose gels, separated by electrophoresis and visualised under UV light.

4.3.2.1.2. *P2rx4* and *P2rx7* expression in P2X4$^{-/-}$ mice

Lungs were collected from littermate female P2X4$^{-/-}$, P2X4$^{+/-}$ and P2X4$^{+/+}$ mice and mRNA isolated. Expression of *P2rx4* and *P2rx7* was determined by RT-qPCR with eukaryotic *18s* used as an internal control.

4.3.2.2. P2X4$^{-/-}$ HDM study

Littermate male and female P2X4$^{-/-}$ (P2rx4$^{tm1b(EUCOMM)Wtsi}$), P2X4$^{+/-}$ and P2X4$^{+/+}$ mice were sensitised to HDM on days 0 and 14. On days 24, 25 and 26 mice were anaesthetised with isoflurane and intranasally administered saline or HDM. Three days after the last challenge AHR was evaluated by assessing Penh responses to increasing concentrations of 5-HT by whole body plethysmography (Buxco). Mice were then sacrificed and blood, BAL and lung samples collected for the subsequent analysis of HDM-induced immune responses.

Briefly, blood samples were used for assessment of total IgE and HDM-specific IgE by ELISA. ProcartaPlex assays were used to determine concentration of IL-1β, IL-4, IL-5, IL-13, Eotaxin-1, CCL2 and MIP-1α, and ELISA (R&D) was performed to quantify CCL17 concentration. BAL cells were isolated and an automated cell counter (Sysmex) was used to determine total leukocyte numbers. Flow cytometry was used to differentiate and enumerate BAL leukocyte populations based on their expression of surface and transcription factors (analysed with Fortessa). Upon enzymatic digestion of lung, total leukocyte numbers were quantified by an automated cell counter while flow cytometry was utilised for the differential assessment of leukocyte populations (analysed with Fortessa).

4.3.3. P2X1$^{-/-}$ in the HDM model

4.3.3.1. Genotyping of P2X1$^{-/-}$ mice

To confirm the genotype of P2X1$^{-/-}$, P2X1$^{+/-}$ and P2X1$^{+/+}$ mice, DNA was extracted from tail tips and P2X1 alleles amplified by PCR. Initially, DNA was extracted in house and products were loaded onto agarose gels, separated by electrophoresis and visualised under UV light. For routine determination of the P2X1 genetic status ear tissue or tail tips were sent and analysed by Transnetyx, Inc.

4.3.3.2. P2X1$^{-/-}$ HDM study

Littermate female P2X1$^{-/-}$, P2X1$^{+/-}$ and P2X1$^{+/+}$ mice were sensitised to HDM on days 0 and 14. On days 24, 25 and 26 mice were anaesthetised with isoflurane and intranasally administered saline or HDM. Three days after the last challenge AHR was evaluated by assessing Penh responses to increasing concentrations of serotonin (5-HT) by whole body plethysmography (Buxco). Mice were then sacrificed and blood, BAL and lung samples collected for the subsequent analysis of HDM-induced immune responses.

BAL cells were isolated and an automated cell counter (Sysmex) was used to determine total leukocyte numbers. Flow cytometry was used to differentiate and enumerate BAL leukocyte populations based on their expression of surface and transcription factors (analysed with Fortessa). Upon enzymatic digestion of lung, total leukocyte numbers were quantified by an automated cell counter while flow cytometry was utilised for the differential assessment of leukocyte populations (analysed with Fortessa).

4.4. Results

4.4.1. The role of P2X7 in allergic airway disease

To determine the role of P2X7 in the development of allergic airway disease $P2X7^{-/-}$ mice were used in our murine HDM-induced model of allergic airway disease. The lack of functional P2X7 receptors was confirmed before the effect of P2X7 deficiency was studied in the HDM model.

4.4.1.1. The validation of $P2X7^{-/-}$ mice

Genotyping by PCR followed by gel electrophoresis was performed to confirm genotype s of $P2X7^{-/-}$ and WT mice. The amplification of the normal P2X7 allele produced a 246bp long band, while 200bp long band was characteristic of the mutated P2X7 allele. WT mice were thus identified based on a presence of a single 246bp band and $P2X7^{-/-}$ mice based on a presence of a single 200bp band (Figure 4.1A).

The lack of functional P2X7 receptors in $P2X7^{-/-}$ mice was confirmed in in vivo model of NLRP3 inflammasome activation. In WT mice, LPS exposure triggered an increase in BAL IL-1β concentration in comparison to saline exposure, but had no effect on BAL IL-18 levels. ATP challenge of LPS exposed WT mice further stimulated the release of IL-1β and IL-18 compared to LPS exposure. LPS-induced responses in $P2X7^{-/-}$ mice were no different to WT controls. However, $P2X7^{-/-}$ mice were protected from ATP-induced IL-1β and IL-18 release after LPS challenge in comparison to WT controls. ATP challenge in saline exposed WT or $P2X7^{-/-}$ mice induced no IL-1β or IL-18 release as compared to PBS challenge (Figure 4.1B,C).

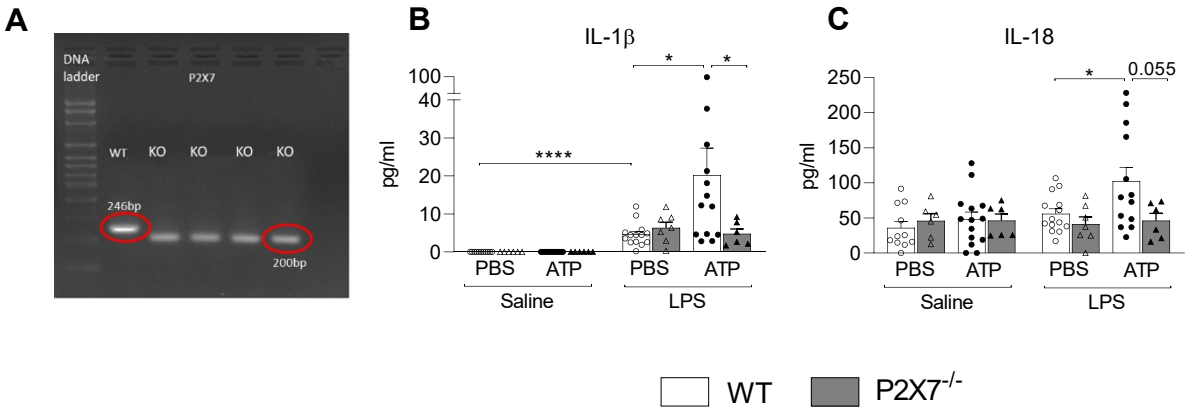


Figure 4.1: Validation of P2X7 deficient (P2X7$^{-/-}$) mice.

A) Representative genotyping results confirming the presence of P2X7 mutation in P2X7$^{-/-}$ (knockout; KO) mice. DNA extracted from mouse tail tips was amplified in PCR and products separated by gel electrophoresis. B,C) Functional validation of P2X7$^{-/-}$ in lipopolysaccharide (LPS)- adenosine-triphosphate (ATP) model. Wild type (WT) and P2X7$^{-/-}$ mice were exposed to saline or LPS and after 4.5h challenged with vehicle (PBS) or ATP. Mice were sacrificed 1.5h after the challenge and bronchoalveolar lavage (BAL) collected. B) IL-1β and C) IL-18 BAL concentration as determined by MSD assays (B) or ELISA (C). Mann-Whitney U test was used to analyse differences between experimental groups. * denotes p<0.05, ** p<0.01, *** p<0.001 and **** p<0.0001.

4.4.1.2. The role of P2X7 deficiency in the allergic airway inflammation

HDM challenge provoked an increased in total BAL leukocytes in WT mice, characterised by increased eosinophils, CD4$^+$ T cell, CD8$^+$ T cell, B cell and ILC2 numbers relative to saline challenged WT mice. NK cells and ILC1s also expanded, while neutrophil and AM populations remained unchanged upon HDM challenge. P2X7$^{-/-}$ HDM challenged mice had reduced total leukocyte numbers, eosinophil, B cell, NK and ILC1 numbers compared to their WT controls. A trend towards reduced CD4$^+$ and CD8$^+$ T cells was additionally noted in P2X7$^{-/-}$ HDM challenged mice compared to WT controls, however the differences were not statistically significant. Neutrophil, AM and ILC2 numbers were identical between P2X7$^{-/-}$ and WT HDM challenged mice (Figure 4.2).

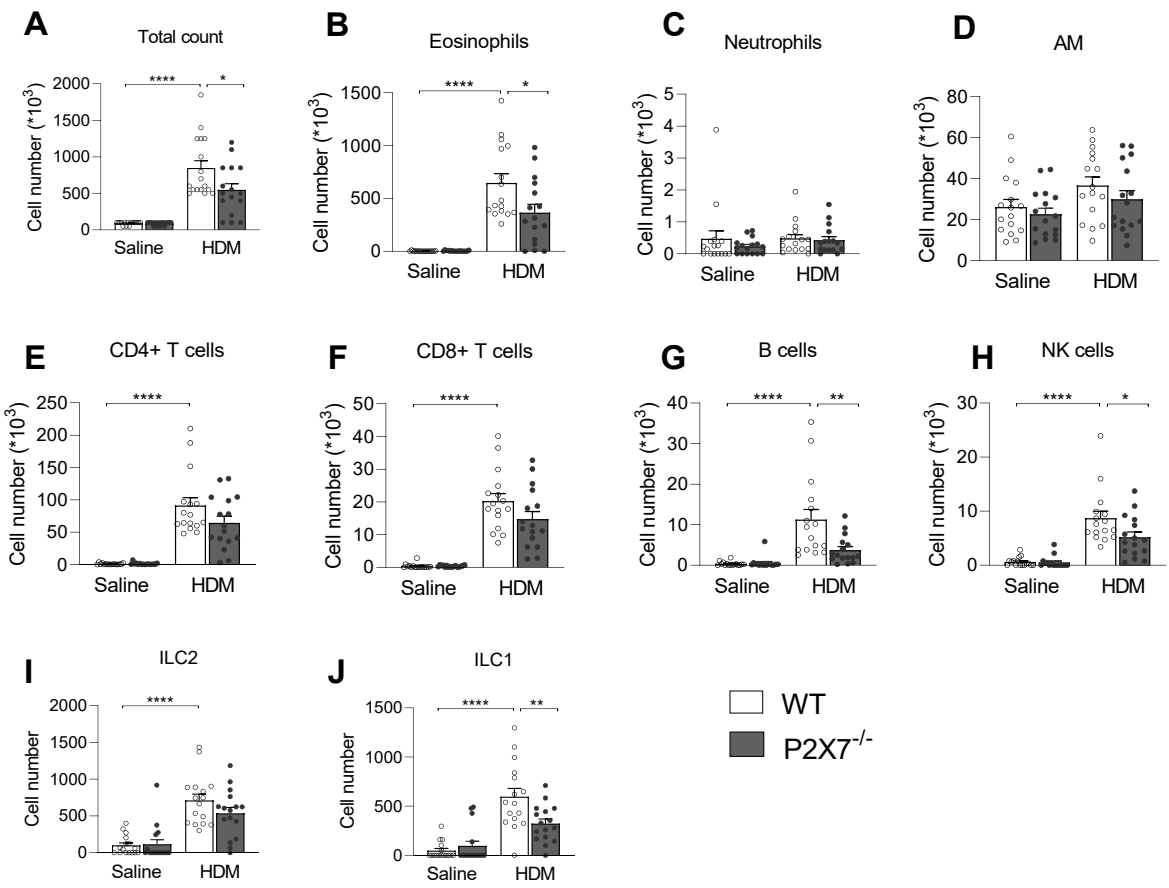


Figure 4.2: The effect of P2X7 deficiency (P2X7$^{-/-}$) on house dust mite (HDM)-induced allergic airway inflammation.

Wild type (WT) and P2X7$^{-/-}$ mice were sensitised to HDM and subjected to intranasal saline or HDM challenge on three consecutive days. Three days later mice were sacrificed and bronchoalveolar lavage (BAL) collected. A) Total leukocyte numbers as determined by an automated cell counter. B) Eosinophil, C) neutrophil, D) alveolar macrophage (AM), E) CD4$^+$ T cell, F) CD8$^+$ T cell, G) B cell, H) natural killer (NK) cells, I) group 2 innate lymphoid cells (ILC2) and J) ILC1 numbers as determined by flow cytometry. Representative data from one of two independent experiments are presented as mean ± S.E.M. with N=16-17/group. Mann-Whitney U test was used to analyse difference between respective experimental groups. * denotes p<0.05, ** p<0.01, **** p<0.0001.

4.4.1.3. The effect of P2X7 deficiency on HDM-induced lung inflammation

HDM challenge was associated with increased total leukocytes in the lungs of WT mice compared to their saline challenged controls. More specifically, HDM challenge was associated with an in increase in eosinophils, AM, CD4$^+$ T cells, CD8$^+$ T cells, B cells, natural killer (NK) cells, B cells, ILC2s as well as DCs (moDCs, cDC2s and cDC1s) in WT mice relative to their saline challenged controls. Lung neutrophil population remained unaffected upon HDM

challenge. HDM-triggered lung inflammation in P2X7$^{-/-}$ mice was comparable to that of HDM challenged WT mice. Apart from a significant reduction in lung moDCs, no differences were noted in total or differential cell counts (including eosinophils, B cells, NK cells and ILC1s) between P2X7$^{-/-}$ and WT mice upon HDM exposure (Figure 4.3).

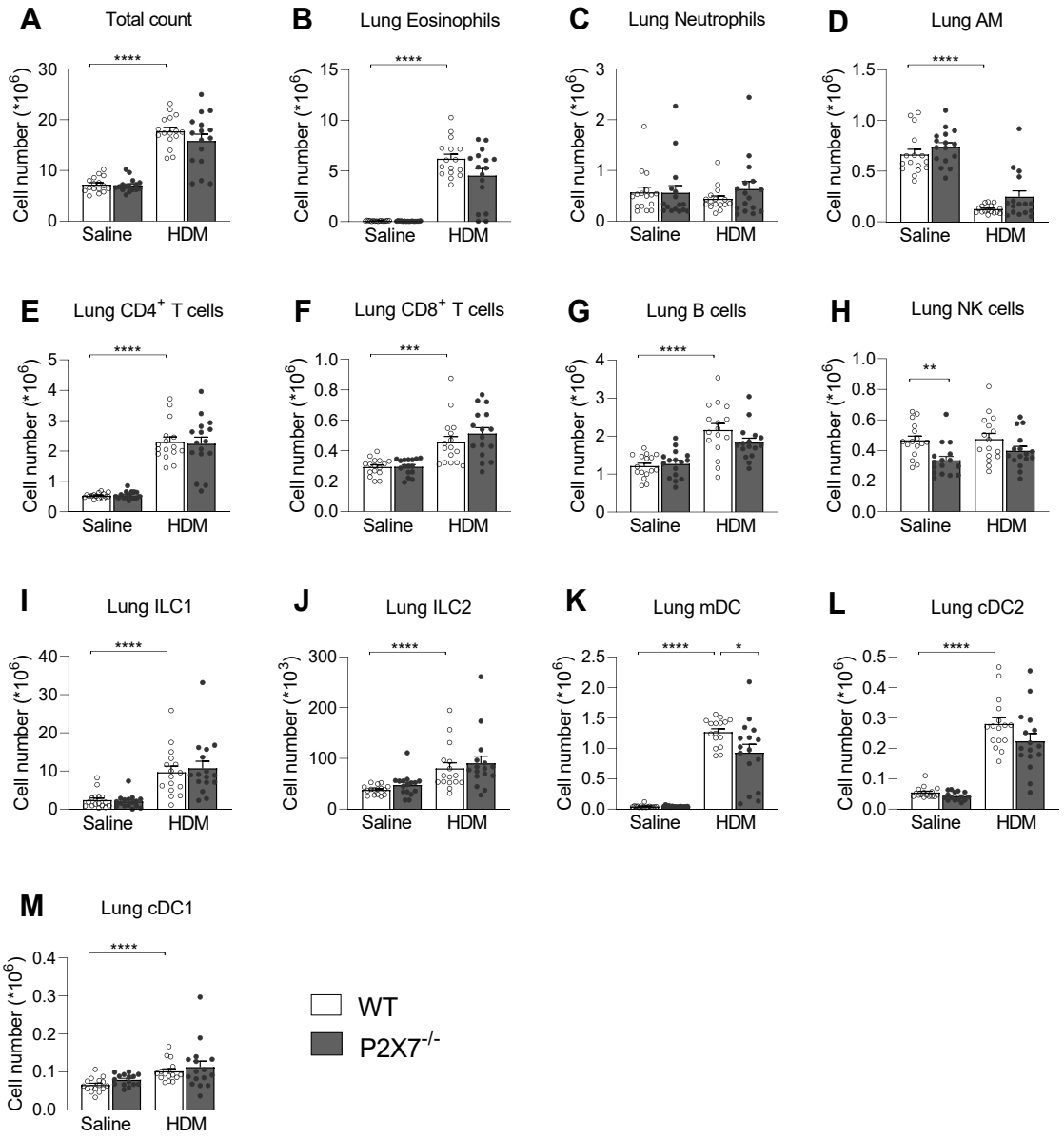


Figure 4.3: The effect of P2X7 deficiency (P2X7$^{-/-}$) on house dust mite (HDM)-induced lung inflammation.

WT and P2X7$^{-/-}$ littermate mice were sensitised to HDM and administered saline or HDM intranasally on three consecutive days. Three days later mice were sacrificed, lungs collected and enzymatically digested. A) Total leukocyte numbers as determined by an automated cell counter. B) Eosinophil, C) neutrophil, D) alveolar macrophage (AM), E) CD4$^+$ T cell, F) CD8$^+$ T cell, G) B cell, H) natural killer (NK) cells, I) group 1 innate lymphoid cells (ILC1), J) ILC2s, K) monocyte-derived dendritic cell (moDC), L) classical DC 2 (cDC2) and M) cDC1 numbers as determined by flow cytometry. Representative data from one of two independent experiments are presented as mean ± S.E.M. with N=15-16/group. Mann-Whitney U test was used to analyse difference between selected experimental groups. *** denotes p<0.001, **** p<0.0001.

4.4.1.4. The effect of P2X7 deficiency on cytokine and chemokine production

HDM challenge triggered an increase in IL-4, IL-5, IL-13, eotaxin-1, CCL2, MIP-1α, CCL17 and IL-1β concentration in BAL in WT mice compared to saline challenge. In P2X7$^{-/-}$ mice reduced concentration of BAL MIP-1α and IL-1β were measured upon HDM challenge relative to WT controls. However, IL-4, IL-5, IL-13, Eotaxin-1, CCL2 and CCL17 levels in HDM challenged P2X7$^{-/-}$ mice remained identical to those determined in WT mice (Figure 4.4).

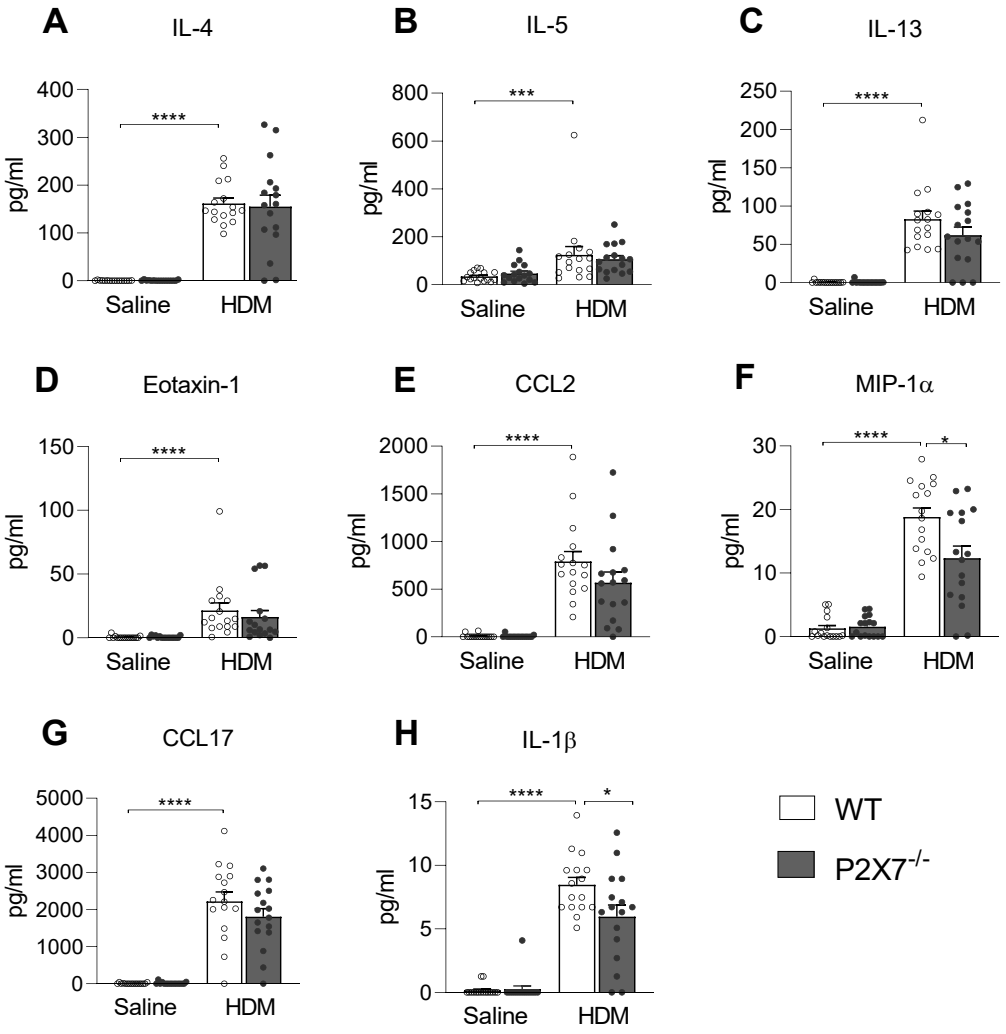


Figure 4.4: The effect of P2X7 deficiency (P2X7$^{-/-}$) on cytokine and chemokine production.

WT and P2X7$^{-/-}$ littermate mice were sensitised to house dust mite (HDM) and challenged with saline or HDM intranasally on three consecutive days. Mice were sacrificed after 3 days and bronchoalveolar lavage (BAL) collected for cytokine and chemokine assessment. BAL concentration of A) IL-4, B) IL-13, C) IL-5, D) Eotaxin-1, E) MCP-1, F) MIP-1α, G) CCL17 and H) IL-1β. Representative data from one of two independent experiments are presented as mean ± S.E.M. with N=16/group. Mann-Whitney U test was used to analyse differences between selected experimental groups. * denotes p<0.05, *** p<0.001 and **** p<0.0001.

4.4.1.5. The role of P2X7 deficiency on IgE antibody production

In WT mice HDM challenge resulted in an increase in plasma total IgE plasma levels as well as HDM-specific IgE relative to saline controls. HDM challenged P2X7$^{-/-}$ mice had identical plasma IgE and HDM-specific IgE levels as their respective WT controls (Figure 4.5).

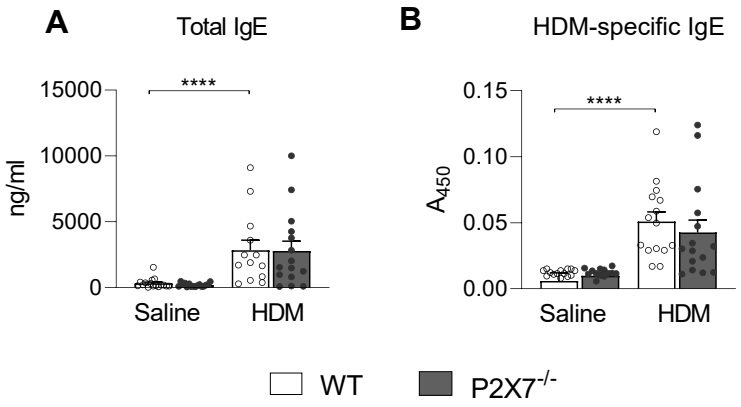


Figure 4.5: The effect of P2X7 deficiency (P2X7$^{-/-}$) on IgE antibody production.

WT and P2X7$^{-/-}$ littermate mice were sensitised to house dust mite (HDM) and challenged with saline or HDM intranasally on three consecutive days. After 3 days mice were sacrificed and blood collected. Plasma levels of A) total IgE and B) HDM-specific IgE. Representative data from one of two independent experiments are presented as mean ± S.E.M. with N=16/group. Mann-Whitney U test was used to analyse differences between experimental groups. **** denotes p<0.0001.

4.4.1.6. The role of P2X7 deficiency in allergen-induced airway hyper-responsiveness

Lastly, 5-HT challenge provoked pronounced Penh responses in HDM challenged WT and P2X7$^{-/-}$ mice in comparison to the respective saline control groups. Penh responses of P2X7$^{-/-}$ HDM challenged mice were no different to WT HDM challenged controls (Figure 4.6).

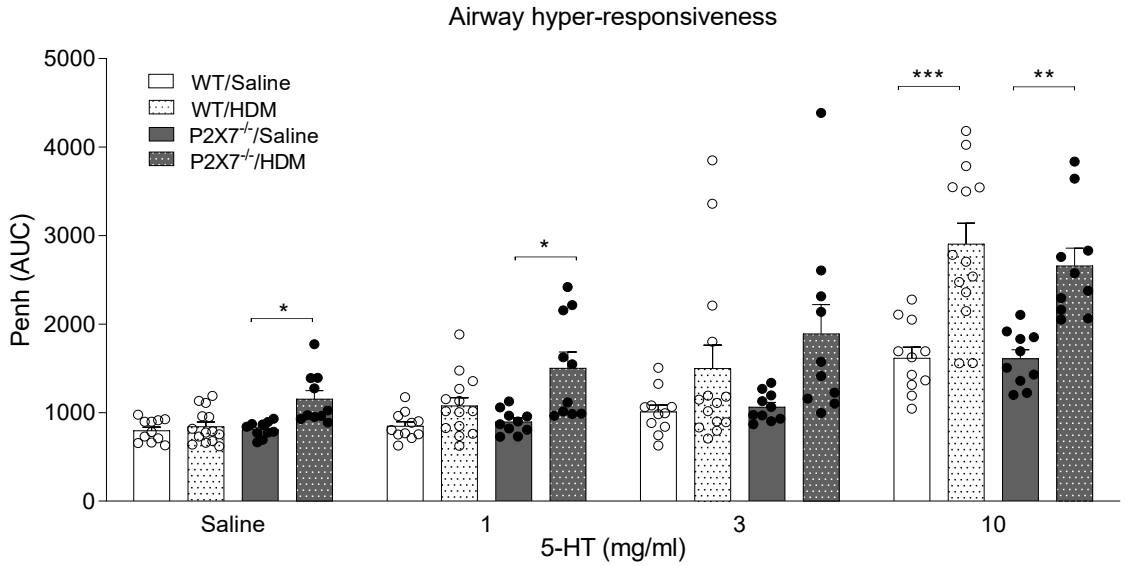


Figure 4.6: The effect of P2X7 deficiency ($P2X7^{-/-}$) on house dust mite (HDM) induced airway hyper-responsiveness.

WT and $P2X7^{-/-}$ mice were sensitised to house dust mite (HDM) and challenged with saline or HDM intranasally on three consecutive days. After 3 days whole body plethysmography was utilised to assess airway responses to nebulised saline, followed by escalating concentrations of serotonin (5-HT; 1-10mg/ml). Each exposure was monitored for 15 minutes and Penh determined (presented as area under the curve (AUC)). Representative data from one of two independent experiments are presented as mean ± S.E.M. with N=10-14/group. * denotes $p<0.05$, ** $p<0.01$ and *** $p<0.001$ in repeated measures ANOVA with Sidak's multiple comparison test.

4.4.2. The role of P2X4 in allergic airway disease

To determine the role of P2X4 in the development of AAD, $P2X4^{-/-}$ mice were used in HDM model alongside $P2X4^{+/+}$ and $P2X4^{+/-}$ littermate controls.

4.4.2.1. Validation of $P2X4^{-/-}$ mice

Genotyping by PCR with subsequent gel electrophoresis was routinely carried out to confirm genotypes of $P2X4^{-/-}$, $P2X4^{+/-}$ and $P2X4^{+/+}$ mice. The amplification of the normal P2X4 allele produced a 250bp band, while the amplification of the mutated P2X4 gene a resulted in the presence of a 120bp band. The presence of a single 250bp band was indicative of $P2X4^{+/+}$ genotype, a single 120bp band was indicative of $P2X4^{-/-}$ genotype, and both bands were present in $P2X4^{+/-}$ mice (Figure 4.7A).

Additionally, we confirmed the absence of *P2rx4* gene transcription in the lungs of P2X4$^{-/-}$ mice as drastically reduced *P2rx4* levels were noted in P2X4$^{-/-}$ mice compared to P2X4$^{+/+}$ controls. In P2X4$^{+/-}$ mice *P2rx4* expression was reduced by half (Figure 4.7Figure 4.B). Expression of *P2rx7* in P2X4$^{-/-}$ mice was identical to the expression levels in P2X4$^{+/+}$ mice, although a small reduction in *P2rx7* expression was seen in P2X4$^{+/-}$ mice in comparison to P2X4$^{+/+}$ mice (Figure 4.7Figure 4.C).

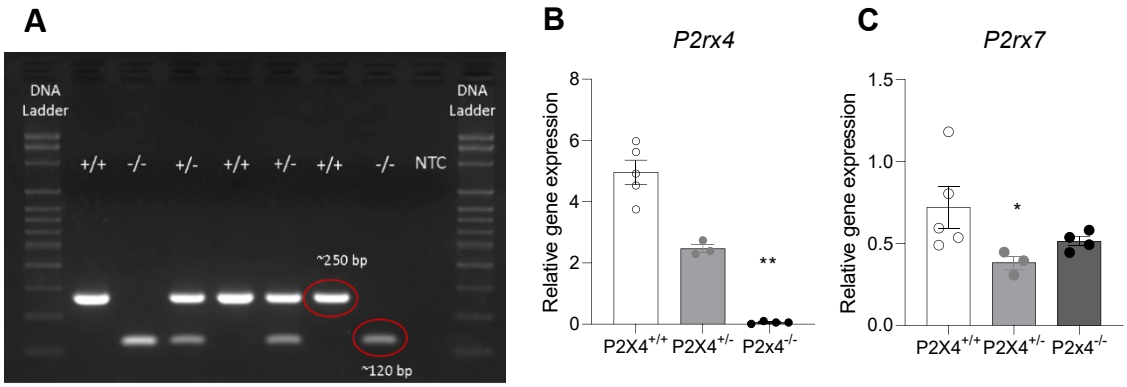


Figure 4.7: Validation of P2X4 mice.

A) A representative genotyping gel. PCR was run with DNA isolated from mouse tail tips and products were separated by agarose gel electrophoresis. B) *P2rx4* and C) *P2rx7* gene expression levels relative to eukaryotic *18s* control in lung. +/+ – P2X4$^{+/+}$, +/- – P2X4$^{+/-}$, -/- – P2X4$^{-/-}$, bp – base pairs, NTC – no DNA template control.

4.4.2.2. The effect of P2X4$^{-/-}$ on HDM-induced airway inflammation

HDM challenge triggered an increase in BAL leukocytes in P2X4$^{+/+}$ mice relative to saline challenged controls. HDM-induced airway inflammation in P2X4$^{+/+}$ was characterised by infiltration of eosinophils, neutrophils, CD4^{+} T cells, CD8^{+} T cells and ILC2s, and no change in AM as compared to saline challenged controls. In P2X4$^{-/-}$ and P2X4$^{+/-}$ mice, HDM challenge provoked airway inflammation identical to that of P2X4$^{+/+}$ mice (Figure 4.8).

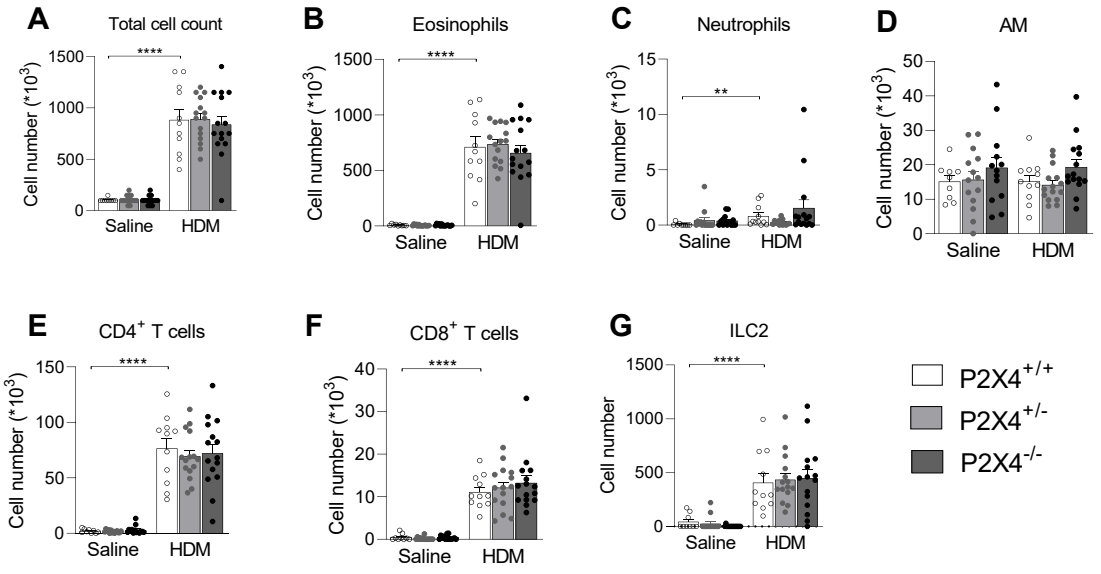


Figure 4.8: The effect of P2X4 deficiency (P2X4$^{-/-}$) on house dust mite (HDM)-induced allergic airway inflammation.

P2X4$^{+/+}$, P2X4$^{+/-}$ and P2X4$^{-/-}$ littermate mice were sensitised to HDM and subsequently challenged with HDM or saline for three consecutive days. Three days later mice were sacrificed and bronchoalveolar lavage (BAL) collected. A) Total leukocyte numbers were determined by an automated cell counter. B) Eosinophil, C) neutrophil, D) alveolar macrophage (AM), E) CD4$^+$ T cell, F) CD8$^+$ T cell and G) group 2 innate lymphoid cells (ILC2) numbers as determined by flow cytometry. Representative data from one of two independent experiments are presented as mean ± S.E.M. with N=9-15/group. Mann-Whitney U test was used to analyse difference between saline and HDM challenged P2X4$^{+/+}$ mice and Kruskal-Wallis with Dunn's multiple comparison post hoc test was used to analyse differences between P2X4$^{+/+}$, P2X4$^{+/-}$, P2X4$^{-/-}$ groups. ** denotes $p<0.01$, **** $p<0.0001$.

4.4.2.3. The effect of P2X4$^{-/-}$ on HDM-induced lung inflammation

HDM challenge was associated with increased total leukocytes, eosinophils, CD4$^+$ T cells, CD8$^+$ T cells, ILC2s as well as DCs (moDCs, cDC2s and cDC1s) in lungs of P2X4$^{+/+}$ mice in comparison to saline challenged controls. AM decreased while neutrophil numbers remained unaffected by HDM challenge in P2X4$^{+/+}$ mice. In P2X4$^{+/-}$ as well as P2X4$^{-/-}$ mice HDM challenge triggered responses identical to that of P2X4$^{+/+}$ mice (Figure 4.9).

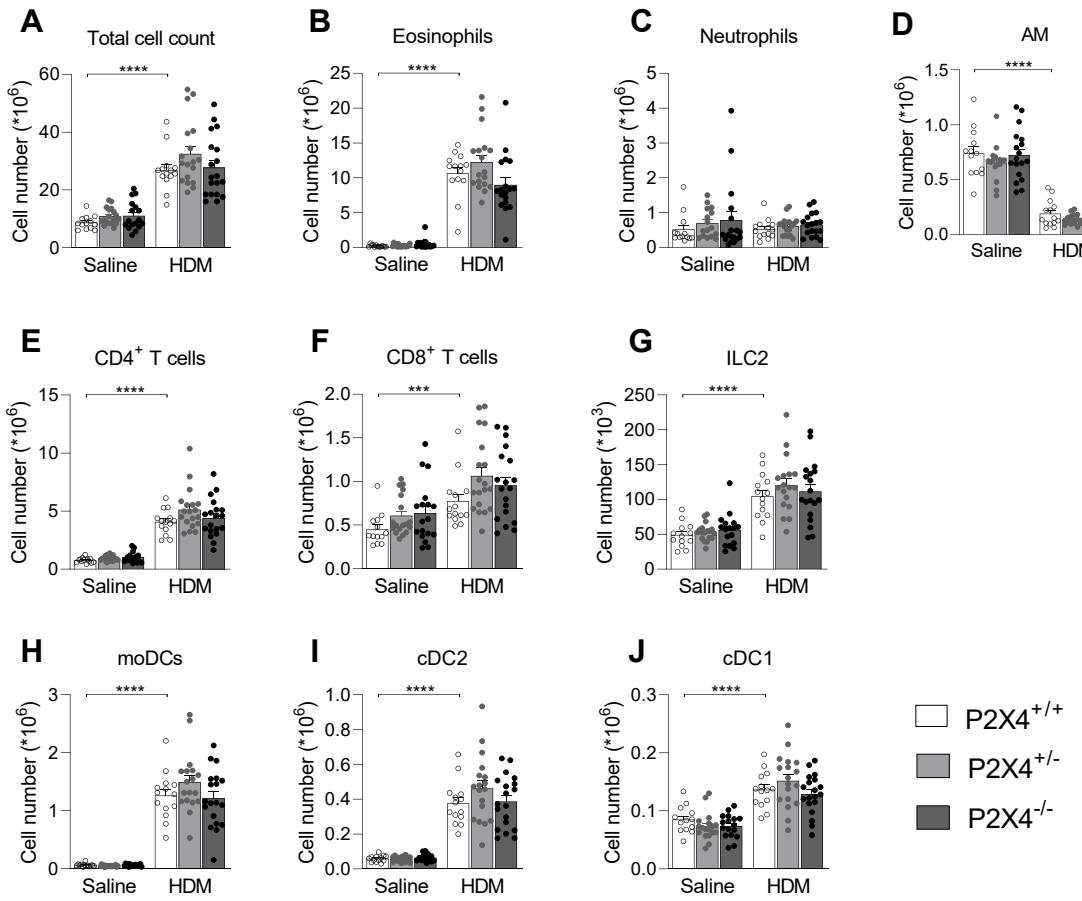


Figure 4.9: The effect of P2X4 deficiency (P2X4$^{-/-}$) on house dust mite (HDM)-induced lung inflammation.

P2X4$^{+/+}$, P2X4$^{+/-}$ and P2X4$^{-/-}$ littermate mice were sensitised to HDM and subsequently challenged with HDM or saline for three consecutive days. Three days later mice were sacrificed, lungs collected and enzymatically digested. A) Total leukocyte numbers as determined by an automated cell counter. B) Eosinophil, C) neutrophil, D) alveolar macrophage (AM), E) CD4^{+} T cell, F) CD8^{+} T cell, G) B cell, H) group 2 innate lymphoid cells (ILC2), I) monocyte-derived dendritic cell (moDC), J) classical DC 2 (cDC2) and K) cDC1 numbers as determined by flow cytometry. Representative data from one of two independent experiments are presented as mean ± S.E.M. with N=9-15/group. Mann-Whitney U test was used to analyse difference between saline and HDM challenge P2X4$^{+/+}$ mice. Kruskal-Wallis with Dunn's multiple comparison post hoc test was used to analyse differences between P2X4$^{+/+}$, P2X4$^{+/-}$, P2X4$^{-/-}$ groups. ** denotes p<0.01, **** p<0.0001.

4.4.2.4. The effect of P2X4$^{-/-}$ on type 2 cytokine and chemokine production

HDM challenge provoked an increased in BAL IL-4, IL-13, Eotaxin-1, CCL2, MIP-1α, CCL17 and IL-1β P2X4$^{+/+}$ mice in comparison to saline challenge. BAL IL-5 levels remained unchanged

upon HDM challenge. In P2X4$^{+/-}$ and P2X4$^{-/-}$ HDM challenge with cytokine and chemokine responses identical to those of P2X4$^{+/+}$ mice (Figure 4.10).

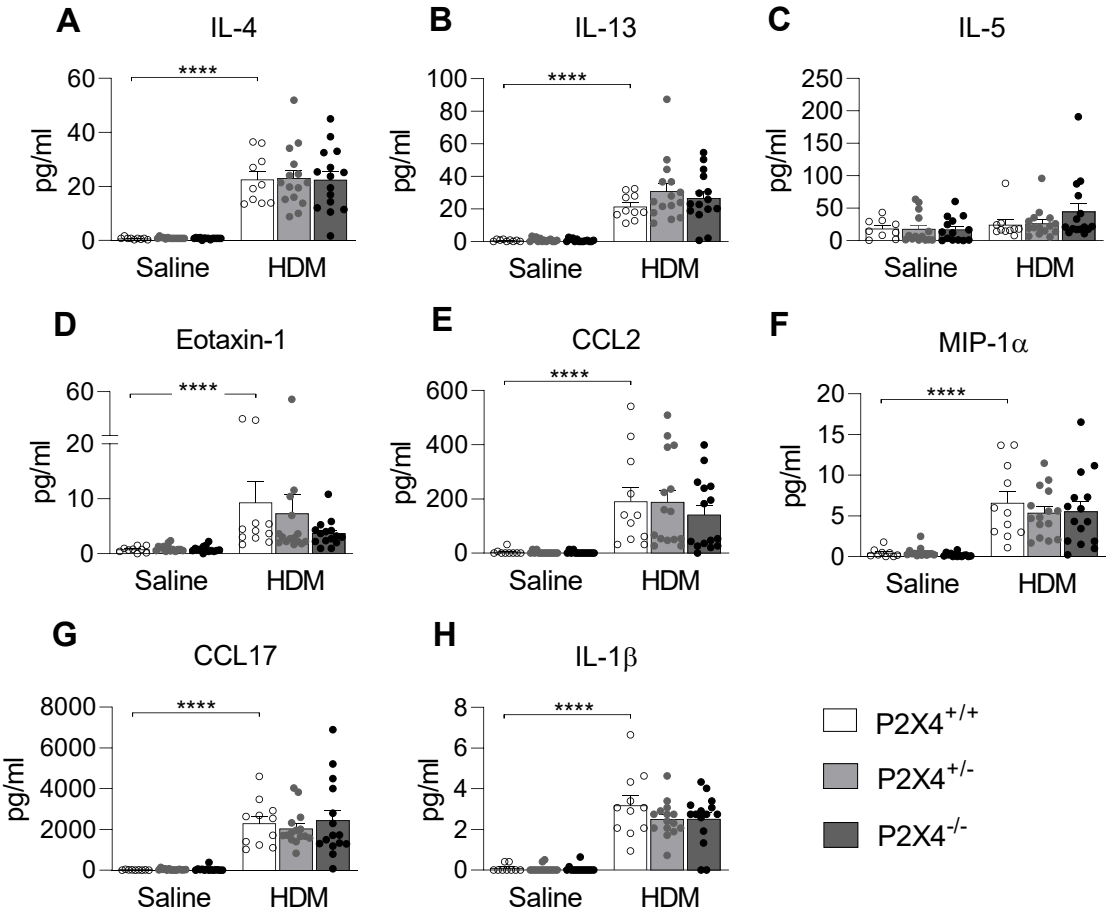


Figure 4.10: The effect of P2X4 deficiency (P2X4$^{-/-}$) on cytokine and chemokine production.

P2X4$^{+/+}$, P2X4$^{+/-}$ and P2X4$^{-/-}$ littermate mice were sensitised to house dust mite (HDM) and intranasally challenged with saline or HDM on three consecutive days. Three days later mice were sacrificed and bronchoalveolar lavage (BAL) collected for cytokine and chemokine assessment. BAL concentration of A) IL-4, B) IL-13, C) IL-5, D) Eotaxin-1, E) MCP-1, F) MIP-1α, G) CCL17 and H) IL-1β. Representative data from one of two independent experiments are presented as mean ± S.E.M. with N=9-15/group. Mann-Whitney U test was used to analyse differences between saline and HDM challenged P2X4$^{+/+}$ mice while Kruskal-Wallis with Dunn's multiple comparison post hoc test was used to analyse differences between P2X4$^{+/+}$, P2X4$^{+/-}$, P2X4$^{-/-}$ groups. ** denotes $p<0.01$, **** $p<0.0001$.

4.4.2.5. The effect of P2X4$^{-/-}$ on antibody production

HDM exposure was associated with an increase in plasma total IgE as well as HDM-specific IgE in P2X4$^{+/+}$ mice compared to their saline challenged controls. In P2X4$^{+/-}$ and P2X4$^{-/-}$ mice HDM challenge induced an increase in total IgE and HDM-specific IgE identical to that measured in P2X4$^{+/+}$ littermates (Figure 4.11).

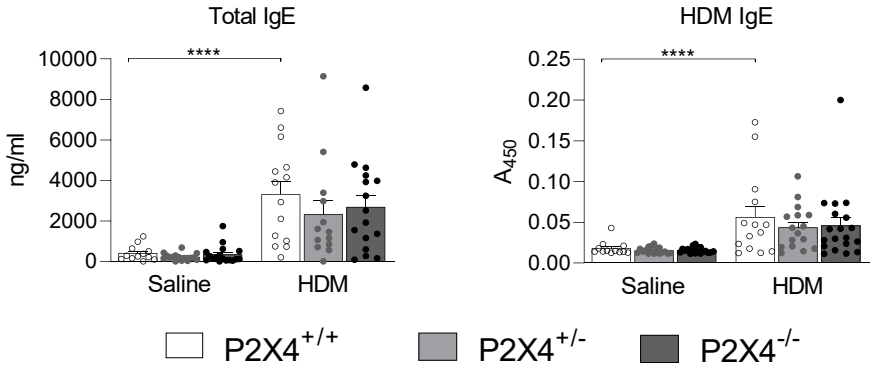


Figure 4.11: The effect of P2X4 deficiency (P2X4$^{-/-}$) on IgE antibody production.

P2X4$^{+/+}$, P2X4$^{+/-}$ and P2X4$^{-/-}$ littermate mice were sensitised to house dust mite (HDM) and subjected to intranasal saline or HDM challenge on three consecutive days. Three days later mice were sacrificed and blood collected. Plasma levels of A) total IgE and B) HDM-specific IgE. Representative data from one of two independent experiments are presented as mean ± S.E.M. with N=9-15/group. Mann-Whitney U test was used to analyse differences between saline and HDM challenge P2X4$^{+/+}$ mice while Kruskal-Wallis with Dunn's multiple comparison post hoc test was used to analyse differences between P2X4$^{+/+}$, P2X4$^{+/-}$, P2X4$^{-/-}$ groups. ** denotes $p<0.01$, **** $p<0.0001$.

4.4.2.6. The role of P2X4 in allergen-induced airway hyper-responsiveness

Lastly, in HDM challenged P2X4$^{+/+}$, P2X4$^{+/-}$ as well as P2X4$^{-/-}$ mice the administration of increasing concentrations of 5-HT led to pronounced Penh responses, most noticeable at 10 mg/ml, compared to the respective saline challenged controls. No differences in Penh responses could be observed between P2X4$^{+/+}$, P2X4$^{+/-}$ and P2X4$^{-/-}$ HDM challenged groups (Figure 4.12).

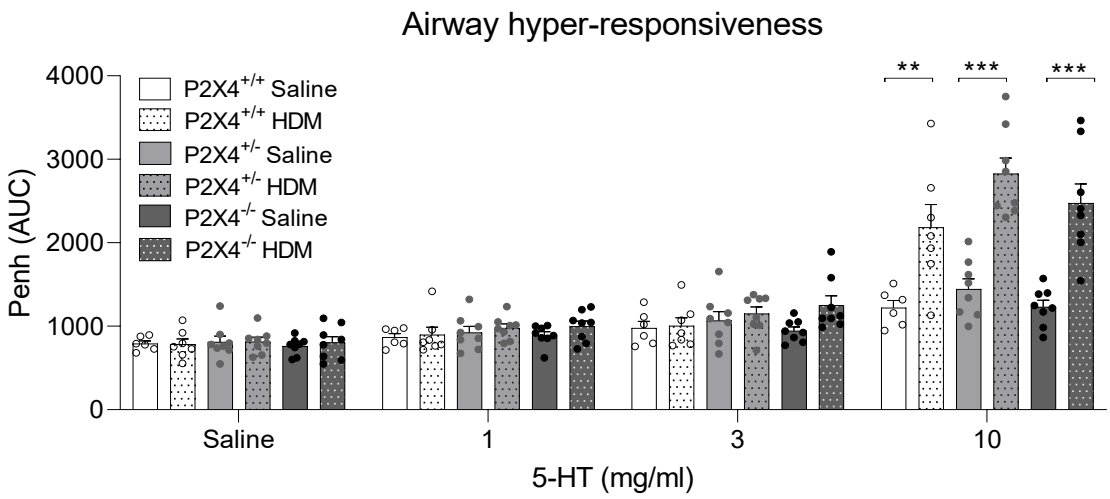


Figure 4.12: The effect of P2X4 deficiency ($P2X4^{-/-}$) on house dust mite (HDM) induced airway hyper-responsiveness.

$P2X4^{+/+}$, $P2X4^{+/-}$ and $P2X4^{-/-}$ littermate mice were sensitised to house dust mite (HDM) and subjected to intranasal saline or HDM challenge on three consecutive days. Three days later whole body plethysmography was utilised to assess airway responses to nebulised saline and increasing concentrations of serotonin (5-HT; 1-10mg/ml). Each exposure was monitored for 15 minutes and enhanced pause (Penh) determined (presented as area under the curve (AUC)). Representative data from one of two independent experiments are presented as mean ± S.E.M. with N=9-15/group. ** denotes $p<0.01$ and *** $p<0.001$ in repeated measures ANOVA with Sidak's multiple comparison test.

4.4.3. The role of P2X1 in allergic airway disease

To determine the role of P2X1 in the development of AAD, $P2X1^{-/-}$ mice were used in HDM model alongside $P2X1^{+/+}$ and $P2X1^{+/-}$ littermate controls.

4.4.3.1. Genotyping of $P2X1^{-/-}$ mice

Genotyping by PCR with subsequent gel electrophoresis was initially carried out to confirm genotypes of $P2X1^{-/-}$, $P2X1^{+/-}$ and $P2X1^{+/+}$ mice. The amplification of the normal P2X1 allele in a wild type reaction produced a 300bp long band (Figure 4.13A), while the amplification of the mutated P2X1 gene in a knockout reaction resulted in a 500bp long band (Figure 4.13B). $P2X1^{+/+}$ mice were characterised by the presence of 300bp long band in the wild type reaction, $P2X1^{-/-}$ mice by the presence of 500bp long band in the knockout reaction, and $P2X1^{+/-}$ mice by the presence of 300bp long band in the wild type reaction and 500bp long band in the knockout reaction (Figure 4.13).

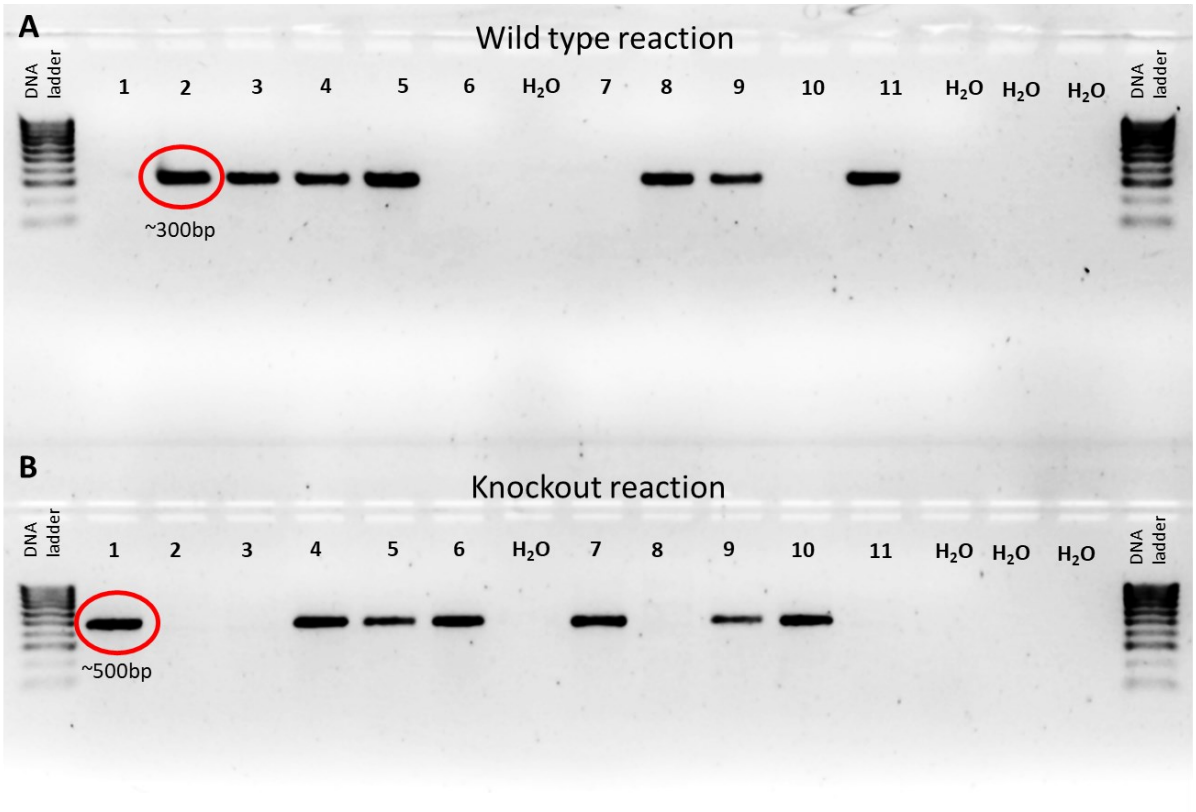


Figure 4.13: Representative genotyping gel of P2X1 mice.

PCR was run with DNA isolated from mouse ear tissue and products were separated by agarose gel electrophoresis. A) Wild type reaction amplifying normal P2X1 allele. B) Knockout reaction amplifying mutated P2X1 allele. Mice #2, #3, #8, #11 had $P2X1^{+/+}$ genotype, mice #1, #6, #7, #10 had $P2X1^{-/-}$ genotype and mice #4, #5, #9 had $P2X1^{+/-}$ genotype. H_2O – negative (water) control.

4.4.3.2. The effect of $P2X1^{-/-}$ on HDM-induced airway inflammation

In $P2X1^{+/+}$ mice HDM challenge triggered an increase in BAL total leukocyte numbers relative to saline challenged controls. More specifically, an increase in eosinophil, neutrophil, $CD4^+$ T cell, $CD8^+$ T cell and ILC2 numbers and no change in AM numbers was observed in $P2X1^{+/+}$ mice compared to saline challenged $P2X1^{+/+}$ mice. $P2X1^{+/-}$ and $P2X1^{-/-}$ mice responded to HDM challenge in a manner identical to that of $P2X1^{+/+}$ mice (Figure 4.14).

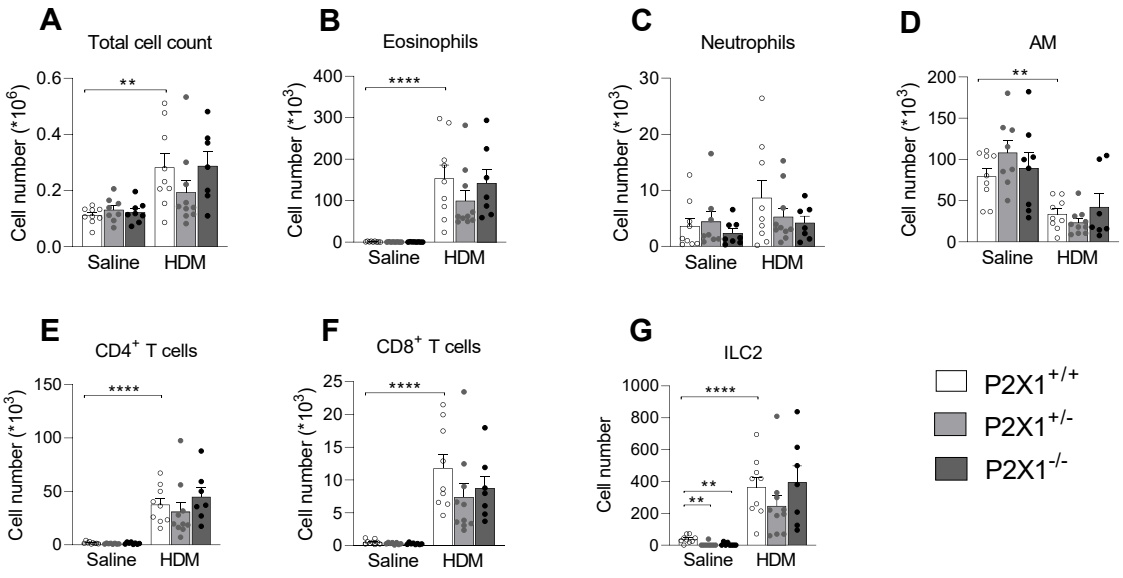


Figure 4.14: The effect of P2X1 deficiency (P2X1$^{-/-}$) on house dust mite (HDM)-induced allergic airway inflammation.

P2X1$^{+/+}$, P2X1$^{+/-}$ and P2X1$^{-/-}$ littermate mice were sensitised to HDM and subsequently challenged with HDM or saline for three consecutive days. Three days later mice were sacrificed and bronchoalveolar lavage (BAL) collected. A) Total leukocyte numbers were determined by an automated cell counter. B) Eosinophil, C) neutrophil, D) alveolar macrophage (AM), E) CD4$^+$ T cell, F) CD8$^+$ T cell and G) group 2 innate lymphoid cells (ILC2) numbers as determined by flow cytometry. Representative data from one experiment are presented as mean ± S.E.M. with N=7-10/group. Mann-Whitney U test was used to analyse difference between saline and HDM challenged P2X1$^{+/+}$ mice and Kruskal-Wallis with Dunn's multiple comparison post hoc test was used to analyse differences in HDM responses between P2X1$^{+/+}$, P2X1$^{+/-}$, P2X1$^{-/-}$ groups. ** denotes $p<0.01$, **** $p<0.0001$.

4.4.3.3. The effect of P2X1$^{-/-}$ on HDM-induced lung inflammation

In the lungs of P2X1$^{+/+}$ mice HDM challenge resulted in increased total leukocytes, eosinophils, neutrophils, CD4$^+$ T cells, CD8$^+$ T cells, ILC2s as well as DCs (moDCs, cDC2s and cDC1s) in comparison to saline challenged controls. AM numbers decreased upon HDM challenge. In P2X4$^{+/-}$ as well as P2X4$^{-/-}$ HDM challenged mice numbers of leukocyte populations were no different to that of P2X1$^{+/+}$ control group (Figure 4.15).

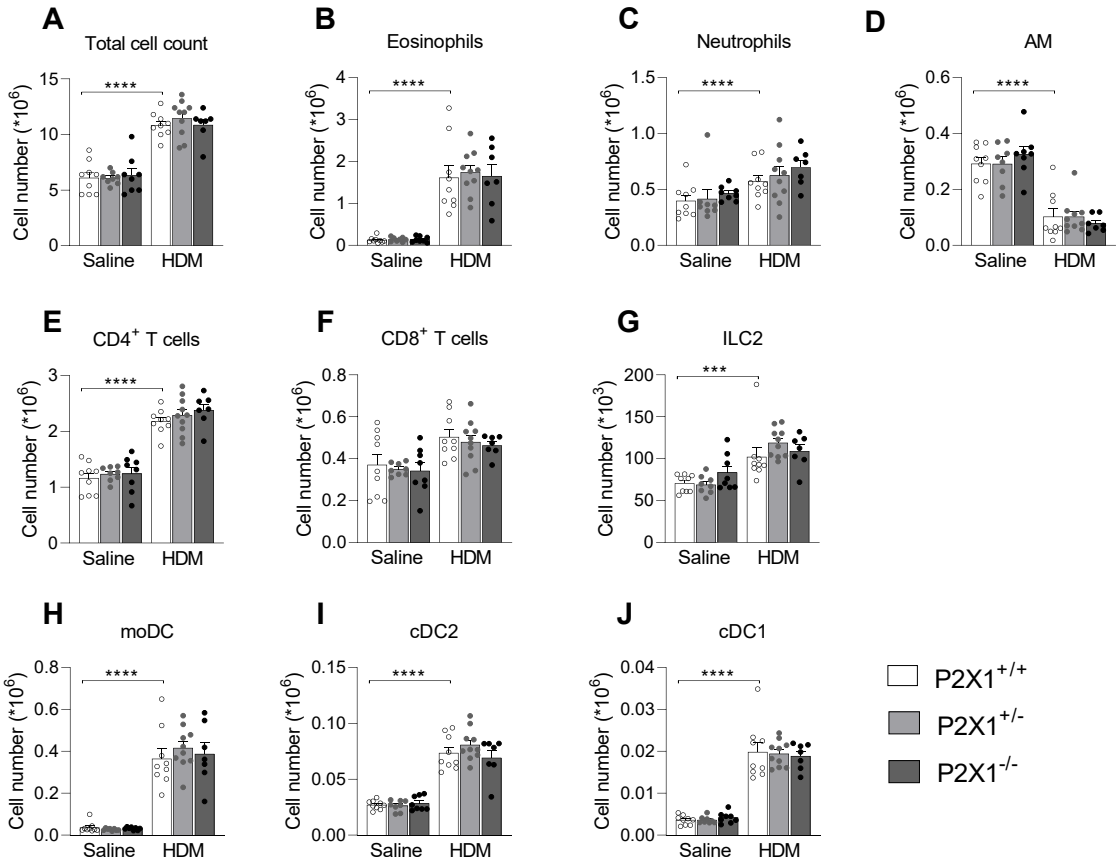


Figure 4.15: The effect of P2X1 deficiency (P2X1$^{-/-}$) on house dust mite (HDM)-induced lung inflammation. P2X1$^{+/+}$, P2X1$^{+/-}$ and P2X1$^{-/-}$ littermate mice were sensitised to HDM and subsequently challenged with HDM or saline for three consecutive days. Three days later mice were sacrificed, lungs collected and enzymatically digested. A) Total leukocyte numbers as determined by an automated cell counter. B) Eosinophil, C) neutrophil, D) alveolar macrophage (AM), E) CD4$^+$ T cell, F) CD8$^+$ T cell, G) group 2 innate lymphoid cells (ILC2), H) monocyte-derived dendritic cell (moDC), I) classical DC 2 (cDC2) and J) cDC1 numbers as determined by flow cytometry. Representative data from one of two independent experiments are presented as mean ± S.E.M. with N=7-10/group. Mann-Whitney U test was used to analyse difference between saline and HDM challenge P2X1$^{+/+}$ mice. Kruskal-Wallis with Dunn's multiple comparison post hoc test was used to analyse differences in HDM responses between P2X1$^{+/+}$, P2X1$^{+/-}$, P2X1$^{-/-}$ groups. *** denotes p<0.001, **** p<0.0001.

4.4.3.4. The role of P2X1 in allergen-induced airway hyper-responsiveness

In HDM challenged P2X1$^{+/+}$, P2X1$^{+/-}$ as well as P2X1$^{-/-}$ mice the administration of increasing concentrations of 5-HT led to pronounced Penh responses compared to the respective saline challenged controls, most noticeable at 3 and 10 mg/ml. No differences in Penh responses could be observed between P2X1$^{+/+}$, P2X1$^{+/-}$ and P2X1$^{-/-}$ HDM challenged groups (Figure 4.16).

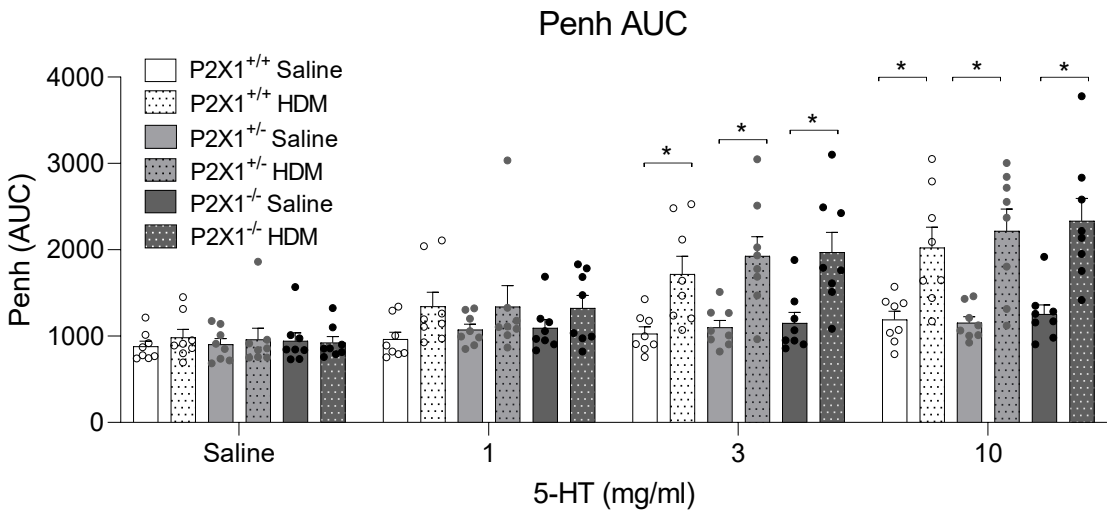


Figure 4.16: The effect of P2X1 deficiency (P2X1$^{-/-}$) on house dust mite (HDM) induced airway hyper-responsiveness.

P2X1$^{+/+}$, P2X1$^{+/-}$ and P2X1$^{-/-}$ littermate mice were sensitised to house dust mite (HDM) and subjected to intranasal saline or HDM challenge on three consecutive days. Three days later whole body plethysmography was utilised to assess airway responses to nebulised saline and increasing concentrations of serotonin (5-HT; 1-10mg/ml). Each exposure was monitored for 15 minutes and enhanced pause (Penh) determined (presented as area under the curve (AUC)). Representative data from one of two independent experiments are presented as mean ± S.E.M. with N=7-10/group. * denotes $p<0.05$ in repeated measures ANOVA with Sidak's multiple comparison test

4.5. Discussion

We have previously demonstrated the central role of TRPV4 in the development of AAD in rodent models (Birrell et al. 2016). Data from murine studies had further established the involvement of Panx-1 in the signalling cascade and suggested that TRPV4 activation in AAD models was mediated by ATP release as Panx1 deficiency ameliorated eosinophilic airway inflammation as well as AHR (unpublished data). In Chapter 3, we have demonstrated the expression of *Trpv4* and *Panx-1* on CD4$^+$ T cells, ILC2s and DC populations. As those immune cells have been deemed vital for the development of allergen induced immune responses (Raemdonck et al. 2016, Lloyd and Snelgrove 2018), we postulated that those cells were responsible for TRPV4 signalling upon allergen challenge. Furthermore, characterisation of P2X gene expression profiles revealed the presence of *P2rx1, P2rx4, P2rx5* and *P2rx7* on CD4$^+$ T cells, ILC2s and lung DC subsets. Previous reports have demonstrated the involvement of P2X4 and P2X7 in allergic airway inflammation and allergen-induced changes in lung function (Muller et al. 2011, Chen et al. 2016, Zech et al. 2016, Li et al. 2018a) and low P2X7 pore

activity has been associated with a reduced risk of developing asthma (Manthei et al. 2012). In our model HDM challenge triggered upregulation of *P2rx7* in $CD4^+$ T cells, downregulation of *P2rx7* in DCs and downregulation of *P2rx4* in moDCs (Chapter 3). Based on these observations, existing literature and availability of tools, the role of P2X1, P2X4 and P2X7 in the HDM-induced AAD was investigated further utilising genetically modified mice.

Firstly, a lack of functional P2X7 receptors in $P2X7^{-/-}$ mice was confirmed in NLRP3 inflammasome-induced model of airway inflammation. NLRP3 activation and subsequent IL-1β signalling is pivotal for the induction of Th2 immune responses in AAD models, as $NLRP3^{-/-}$ as well as $IL\text{-}1\beta^{-/-}$ abolished eosinophilic airway inflammation and type 2 cytokine production by $CD4^+$ T cells (Besnard et al. 2011a, Bruchard et al. 2015, Li et al. 2018a). Bruchard et al. have further proposed a critical role of NLRP3 inflammasome in Th2 differentiation (Bruchard et al. 2015). The link between ATP-induced P2X7 activation and activation of NLRP3 inflammasome with a subsequent release of IL-1β and IL-18 has been extensively demonstrated in vitro and in vivo (Griffiths et al. 1995, Perregaux et al. 2000, Mehta et al. 2001, Solle et al. 2001, Franchi et al. 2007, Myrtek et al. 2008, Eltom et al. 2011, Baxter et al. 2014, Englezou et al. 2015, Mishra et al. 2016, Di Virgilio et al. 2017). Thus, NLRP3 inflammasome-induced model of airway inflammation was chosen to validate the lack of P2X7 receptors in $P2X7^{-/-}$ mice. In LPS primed mice, ATP challenge provoked further IL-1β and IL-18 release in WT mice but not $P2X7^{-/-}$ mice as previously suggested (Perregaux et al. 2000, Solle et al. 2001, Eltom et al. 2011), confirming the lack of functional P2X7 receptors in $P2X7^{-/-}$ mice.

In the HDM model $P2X7^{-/-}$ mice exhibited a defect in IL-1β production as BAL IL-1β levels in $P2X7^{-/-}$ mice upon HDM challenged were lower in comparison to WT controls. However, HDM challenge still triggered IL-1β release in $P2X7^{-/-}$ mice compared to saline challenge, supporting the notion that IL-1β release can also occur independently of P2X7 (He et al. 2013). In our hands, $P2X7^{-/-}$ mice were selectively protected against the HDM-provoked infiltration of eosinophils, B cells, NK cells and ILC1s into the airways, moDCs into the lung and MIP-1α release, but had no statistically significant effect on $CD4^+$ T cells, ILC2s and type 2 cytokine production, IgE responses or AHR. This is in contrast to some other publications looking into the role of P2X7 in AAD, where $P2X7^{-/-}$ mice exhibited reduced lymphocyte numbers and impaired production of type 2 cytokines upon allergen challenge (Muller et al. 2011, Li et al.

2018a). A possible explanation for our results in the involvement of P2X7 in leukocyte migration. For instance, ATP has been demonstrated to promote eosinophil migration and adhesion, although P2Y2 has been proposed to mediate these effects (Dichmann et al. 2000, Idzko et al. 2001, Kobayashi et al. 2015). However, in asthmatic patients P2X7 is upregulated and apart from association with ATP-induced upregulation of CD11b, little is known about its function (Idzko et al. 2001, Muller et al. 2011, Ferrari et al. 2020). In addition, in our studies $P2X7^{-/-}$ mice displayed a defect in moDC recruitment into the lung upon HDM challenge, which was reflected by reduced MIP-1α concentration in BAL (Vissers et al. 2001, van Rijt et al. 2005, Plantinga et al. 2013). We and others have demonstrated expression of P2X7 on dendritic cells and P2X7 has been implicated in ATP-induced migration (Chapter 3, (Zech et al. 2015, Saez et al. 2017)) which might explain the impaired recruitment of moDCs into the lungs upon HDM exposure. Surprisingly, this did not impair T cell recruitment or type 2 cytokine production in $P2X7^{-/-}$ mice, albeit the importance of moDCs in reaction to allergens has been established before (and is discussed in more detail in Chapter 3) (Vissers et al. 2001, van Rijt et al. 2005, Plantinga et al. 2013). Surprisingly, in comparison to WT mice, $P2X7^{-/-}$ mice had reduced numbers of B cells, NK cells and ILC1s in BAL, but not lung after HDM challenge. B cells and NK cells have been previously reported to express functional P2X7 receptors (Gu et al. 2000, Sluyter et al. 2001), however the importance of these observations is unclear, especially as our group had previously demonstrated the redundancy of B cells during the development of airway inflammation and AHR in this model (Raemdonck et al. 2016). In addition, no defects in IgE production were noted in $P2X7^{-/-}$ mice, suggesting that B cell function remained intact in $P2X7^{-/-}$ mice. The role of NK and ILC1s in our model are yet to be elucidated.

Our results are in partial agreement with some of the existing literature. Clinical studies have reported upregulation of P2X7 expression on BAL AMs and blood eosinophils in asthmatic patients compared to healthy controls (Muller et al. 2011) and associated low P2X7 pore activity with reduced risk of developing asthma in 6-8 years old children or a less severe disease among 11 year olds (Manthei et al. 2012). However, the involvement of P2X7 in asthma pathogenesis is not completely clear as attenuated P2X7 pore activity has been associated with increased the risk of losing asthma control during viral infections (Denlinger

et al. 2009) as well as earlier exacerbations and more symptoms in adults (Denlinger et al. 2013).

Several preclinical studies investigating the role of P2X7 in AAD models have demonstrated the protective effect of P2X7 inhibition on airway eosinophilia, although a dispensable role for P2X7 in allergic airway inflammation and AHR has been reported as well (Kouzaki et al. 2011, Muller et al. 2011, Li et al. 2018a). Similar to our observations, Li et al. have reported that Brilliant Blue G (BBG), one of the earliest P2X7 antagonists (Jiang et al. 2000), suppressed OVA-induced eosinophilic inflammation as well as production of type 2 cytokines, but not AHR (Li et al. 2018a). However, BBG, considered a selective P2X7 antagonist, has been reported to inhibit other P2X receptors including P2X1 and P2X4, Panx-1 as well as sodium channels (Jiang et al. 2000, Seyffert et al. 2004, Qiu and Dahl 2009, Jo and Bean 2011), complicating the interpretation of these results, particularly as Panx-1 and P2X4 could be involved in the development of allergic airway inflammation (Ram et al. 2009, Chen et al. 2016, Zech et al. 2016, Khan et al. 2020). Using KN62, a selective P2X7 antagonist (Gargett and Wiley 1997), as well as $P2X7^{-/-}$ mice (Sikora et al. 1999), Müller et al. have demonstrated a reduction in type 2 airway inflammation as well as AHR in OVA model as well as HDM model with mucosal sensitisation phase (Muller et al. 2011). Utilising bone marrow chimeras, they established it was the expression of P2X7 on hematopoietic cells, and more specifically DCs, rather than structural cells that was pathogenic in their models and proposed that the impaired DC Th2 priming ability as the main mechanism of P2X7 in AAD pathogenesis (Muller et al. 2011). On contrary, Kouzaki et al. found no role of $P2X7^{-/-}$ in *Alternaria Alternata*-induced airway inflammation or AHR (Kouzaki et al. 2011), suggesting that the implication of P2X7 in the pathogenesis of AAD might be allergen dependent. Another confounding factor could be strains of $P2X7^{-/-}$ and WT mice used in those studies, including ours, due to a lack of littermate $P2X7^{+/+}$ controls (Kouzaki et al. 2011, Muller et al. 2011). Albeit we have chosen a genetic background of WT mice to match that of $P2X7^{-/-}$ mice and bred the colonies alongside one another to minimise the environmental effects, a possibility exists that the backgrounds of WT and $P2X7^{-/-}$ mice were not identical and potentially contributed to the observed differences in HDM-triggered airway inflammation (Holmdahl and Malissen 2012). In addition, C57BL/6 genetic background of mice used in all above studies might problematic due to the presence of an allelic mutation ("loss-of-function" $P2X7^{451L}$) in C57BL/6 mice which

confers a drastically reduced sensitivity to ATP-induced pore formation (Adriouch et al. 2002, Yip et al. 2009). Analysis of P2X7$^{-/-}$ mice against a background with naturally defective variant might thus underestimate the contribution of P2X7$^{-/-}$ phenotype in disease models (Adriouch et al. 2002). In order to consolidate our findings and elucidate the role of P2X7 during sensitisation and challenge phase, respectively, use of mice strains carrying P2X7^{451P} variant, like BALB/c for instance, would be more appropriate (Adriouch et al. 2002).

Another consideration in respect to P2X7$^{-/-}$ mice is that both of the two commercially available strains of P2X7$^{-/-}$ mice, one developed by Pfizer and used by us and Kouzaki et al. (Solle et al. 2001, Kouzaki et al. 2011) and the other developed by GlaxoSmithKline (GSK) and used by Muller et al. (Sikora et al. 1999, Muller et al. 2011), still express incomplete receptor transcripts or alternative splice variants, respectively, that are retained in various tissues and cells, including lung, spleen and T cells (Sanchez-Nogueiro et al. 2005, Nicke et al. 2009, Taylor et al. 2009, Masin et al. 2012). These result in an incomplete functional knockdown of P2X7 receptor, for instance GSK P2X7$^{-/-}$ mice have intact T cell responses, and complicate the interpretation of the findings (Sanchez-Nogueiro et al. 2005, Nicke et al. 2009, Taylor et al. 2009, Masin et al. 2012). Although P2X7$^{-/-}$ mice exhibited a lack of P2X7 function in our hands as validated in NLRP3 inflammasome activation model, we are unsure whether (and to what extent) the development of allergic airway inflammation in AHR in the HDM model could be affected by the presence of alternative splice variants. These limitations may be overcome by a use of pharmacological tools, particularly as number of P2X7 selective antagonists are now available (Illes et al. 2020).

Next, we investigated the role of P2X4 in the established HDM-induced AAD utilising P2X4$^{-/-}$ mice (P2rx4$^{tm1b(EUCOMM)Wtsi}$), generated under European Conditional Mouse Mutagenesis (EUCOMM) program (Skarnes et al. 2011) along with their P2X4$^{+/+}$ and P2X4$^{+/-}$ littermates. Upon HDM challenge P2X4$^{-/-}$ mice developed HDM-specific IgE, eosinophilic inflammation and AHR to the same degree as P2X4$^{+/+}$ mice. We confirmed the results in two independent experiments using male and female mice to increase the statistical power of the studies and comply with 3R principles (Aske and Waugh 2017). Albeit male and female mice were used in these experiments, data was pooled and analysed together as no statistically significant differences were observed between the sexes.

There is a limited clinical and preclinical evidence indicating the importance of P2X4 in asthma pathogenesis. So far, a single study has investigated and reported upregulation of *P2RX4* in BAL cells, blood mononuclear cells and blood eosinophils isolated from asthmatic patients compared to healthy controls (Zech et al. 2016). Bonvini et al. have recently implicated P2X4 in TRPV4-induced bronchoconstriction in human and GP ex vivo models via the release of cysteinyl leukotrienes from mast cells (Bonvini et al. 2020), implicating TRPV4-P2X4 axis could be responsible for bronchoconstriction in asthmatic patients. Interestingly, our results indicate a lack of role for P2X4 in HDM-provoked AHR, even though a selective TRPV4 agonist GSK101 induces bronchoconstriction in conscious mice (Chapter 6). This suggests that TRPV4 causes AHR in a distinct, P2X4 independent mechanism, possibly via activation of airway sensory neurons rather than direct activation of airway smooth muscle (Blake et al. 2019, Bonvini et al. 2020, Flajolet 2021). Nevertheless, a few preclinical studies have, in contrast to our data, demonstrated a pathogenic role for P2X4 in the development of allergic airway inflammation and AHR (Chen et al. 2016, Zech et al. 2016, Wang et al. 2018a). Chen et al. have reported that administration of PPADS, a non-specific P2X receptor antagonist, and 5-BDBD, a selective P2X4 antagonist, reduced eosinophil and lymphocyte infiltration into the airways in the murine OVA model of AAD, but did not evaluate the effects of P2X4 inhibitors on AHR (Chen et al. 2016). They demonstrated, though, that P2X4 inhibition reduced OVA-induced mucus production and collagen deposition in murine as well as rat AAD models (Chen et al. 2016, Wang et al. 2018b). These features of AAD have not been yet investigated and characterised in our HDM model, thus the protective effect of P2X4 on mucus production and remodelling in our HDM model remains unclear. Zech et al. have similarly reported that administration of 5-BDBD as well as $P2X4^{-/-}$ ($P2X4^{tm1Rasss}$) ameliorated eosinophilic airway inflammation and AHR in murine OVA model as well as HDM model with mucosal sensitisation phase (Zech et al. 2016). They established that P2X4 on of hematopoietic cells rather than structural cells was important in OVA-induced responses and demonstrated that specifically P2X4 deficiency on DCs was protective against Th2 priming and subsequent development of type 2 inflammation (Zech et al. 2016).

The use of pharmacological tools in P2X4 research is limited due to the lack of selective and potent P2X4 antagonists, particularly for rodent P2X4 receptors (Abdelrahman et al. 2017, Coddou et al. 2019). 5-BDBD is a moderately potent selective allosteric P2X4 antagonist with

low water solubility which is not easily handled (Abdelrahman et al. 2017, Illes et al. 2020). A recent study has demonstrated additional antagonistic activity of 5-BDBD on P2X1 and P2X3 receptors in rat, questioning its selectivity (Coddou et al. 2019). In addition, by using PPADS, a non-selective P2X receptor antagonist with limited usability, Chen et al. have suggested that other P2X receptors could be responsible for OVA-induced allergic airway inflammation (Lambrecht et al. 1992, Chen et al. 2016, Illes et al. 2020). Genetic ablation of *P2rx4* poses another challenge due to the close association between P2X4 and P2X7 channels. *P2X4* and *P2X7* genes are located in close proximity on the same chromosome (in various species, including human and mice) and have emerged from the same ancestral gene by gene duplication (Hou and Cao 2016). The insertion of neomycin cassette in the P2X4 locus in conventional $P2X4^{-/-}$ mice has thus been speculated to down-modulate the expression of *P2rx7* gene and lead to misleading conclusions as several studies have reported downregulated *P2rx7* expression in $P2X4^{-/-}$ mice (Besnard et al. 2016, Zech et al. 2016, Suurväli et al. 2017, Er-Lukowiak et al. 2020). In particular, Zech et al. have noticed drastically supressed *P2rx7* expression in $P2X4^{-/-}$ DCs along with impaired ATP-induced IL-1β production, suggesting a potential disruption of P2X7 signalling in $P2X4^{-/-}$ DCs (Zech et al. 2016). This poses a question whether disrupted P2X7 signalling was responsible for the phenotype exhibited by $P2X4^{-/-}$ mice in this study, particularly as they had previously demonstrated the crucial role of P2X7 in DC mediated Th2 priming and subsequent airway inflammation and AHR in the same AAD models (Muller et al. 2011). A recent study has confirmed downregulation of *P2rx7* gene expression as well as suppressed P2X7 function in innate immune cells, including peritoneal, spleen and bone marrow derived-(BM) macrophages, mast cells (MCs), BMMCs and BMDCs from $P2X4^{tm1Rasss}$ mice and postulated the findings to be a consequence of the strategy used to manipulate *P2rx4* locus (Er-Lukowiak et al. 2020). In addition, $CD4^+$ and $CD8^+$ T cells in $P2X4^{tm1Rasss}$ were shown to carry a passenger "gain of function" $P2X7^{451P}$ variant (compared to "loss-of-function" $P2X7^{451L}$ variant that is present in C57BL/6 mice), originating from 129 embryonic stem (ES) cells that were used in the generation of $P2X4^{tm1Rasss}$ (Er-Lukowiak et al. 2020). This mutation affects the vitality and function of T cells and might complicate the interpretation of findings in $P2X4^{tm1Rasss}$ mice (Er-Lukowiak et al. 2020). $P2X4^{tm1b(EUCOMM)Wtsi}$ mice, used in our studies, unlikely carry *P2rx7* passenger mutation as C57BL/6N ES cells (carrying $P2X7^{451L}$ allele) were used to generate them (Skarnes et al. 2011). Whether *P2rx7* was unintentionally disturbed as a side effect of *P2rx4* targeting as observed in $P2X4^{tm1Rasss}$ is

yet to be excluded. Our data showed that P2X4$^{-/-}$ mice exhibited no impairment in IL-1β production upon HDM challenge, albeit reduced in HDM challenged P2X7$^{-/-}$ mice, suggesting that P2X7 signalling in P2X4$^{-/-}$ mice was not affected. Furthermore, we saw that P2X4$^{-/-}$ mice had comparable lung *P2rx7* gene expression to P2X4$^{+/+}$ mice despite knockdown of *P2rx4* gene expression. Whether this is also the case for individual innate immune cells, such as DCs, is yet to be elucidated.

Lastly, we investigated the role of P2X1 in the HDM-induced model of AAD utilising P2X1$^{-/-}$ mice (Mulryan et al. 2000, Greve et al. 2017) that were kindly provided by Professor Praetorius from Aarhus University, Denmark. In P2X1$^{-/-}$ mice HDM exposure triggered characteristic eosinophilic airway and lung inflammation as well as AHR indistinguishable from that observed in P2X1$^{+/+}$ littermate controls. There is very limited literature investigating the role of P2X1 in asthma pathogenesis. Various cell types relevant in allergic airway inflammation, such as T cells, macrophages, mast cells, eosinophils and airway epithelial cells commonly express P2X1 (Ferrari et al. 2000, Mohanty et al. 2001, Bradding et al. 2003, Brone et al. 2007, Sim et al. 2007, Myrtek et al. 2008, Wareham et al. 2009, Woehrle et al. 2010a, Kessler et al. 2011, Wang et al. 2014, Wright et al. 2016, Chavez et al. 2019, Winkelmann et al. 2019). P2X1 is crucial for basal lymphocyte function and immune signalling upon antigen stimulation in lymphocytes (Woehrle et al. 2010a, Ledderose et al. 2016) and regulates eosinophil CD11b expression, adhesion and extravasation (Wright et al. 2016). Characterisation of P2X1 receptors on eosinophils isolated from asthmatic patients revealed constitutively reduced P2X1 responses compared to healthy subjects (Wright et al. 2016). To date there is a single preclinical publication investigating the role of P2X1 in murine OVA model (Amison et al. 2015). In line with our observations Amison et al. have reported no effect of P2X1 inhibitor NF-279 in murine OVA-induced allergic airway inflammation (Amison et al. 2015).

The investigations into the role P2X1 in our HDM model have several limitations. Due to time limitations the loss of functional P2X1 receptors in P2X1$^{-/-}$ mice has not been yet confirmed in house. Greves et al. have established reduced cytokine responses in P2X1$^{-/-}$ mice in *Escherichia coli*-induced sepsis (Greve et al. 2017) and a similar model could be used to validate P2X1$^{-/-}$ mice. Furthermore, additional independent studies are warranted to confirm the lack of role of P2X1 in HDM and OVA AAD models as well as to investigate the role of P2X1

in other AAD models. In addition to P2X1$^{-/-}$ mice, P2X1 selective antagonists could be used to disrupt P2X1 signalling, however currently available compounds (such as NF-449 and NF-279) have short half live time (Hechler et al. 2005, Illes et al. 2020) which could limit their use in AAD models.

Taken together, we have demonstrated that P2X1 and P2X4 receptors were dispensable for the development of allergic airway inflammation and AHR and thus do not appear to be part of TRPV4 signalling cascade in this model. On the other hand, P2X7 could be one of the receptors activated downstream of TRPV4, contributing to eosinophilic airway inflammation, but not other aspects of the disease, suggesting other purinergic receptors could be involved as well. Although no studies have addressed the importance of P2X5 or P2X6 functions for the development of allergic airway inflammation or AHR, both receptors have been found on leukocytes, including lymphocytes, DCs and macrophages (Berchtold et al. 1999, Myrtek et al. 2008, Woehrle et al. 2010a, Kessler et al. 2011, Abramowski et al. 2014, Wang et al. 2014). P2X5 appears to be important for T cell function upon activation, and can also present an alternative way of inflammasome activation and IL-1β release (Abramowski et al. 2014, Kim et al. 2017, Jeong et al. 2020), however little is known about P2X6 function in leukocytes. In contrast to other P2X receptors, P2X2 and P2X3 receptors do not appear to be important for immune cell function, but instead play a major role in mediating the effects of ATP in sensory neurons. The efficacy of P2X3 inhibitor AF-219 in reducing objective cough frequency in refractory chronic cough patients has been recently demonstrated (Abdulqawi et al. 2015). Cough is a burdensome symptom in many patients with asthma and P2X3 as a treatment target in asthma is yet to be addressed. However, ATP has been shown to trigger bronchoconstriction in asthmatic patients (Basoglu et al. 2005), and interestingly, ATP-induced bronchoconstriction in conscious guinea pigs was blocked by P2X3-P2X2/3 antagonist DT-0111 (Pelleg et al. 2019), suggesting that P2X3 or P2X2/3 could be implicated in allergen-provoked bronchoconstriction or AHR. Our laboratory has recently demonstrated that AF-353, a selective P2X3 antagonist, suppressed Penh responses during the late asthmatic response (LAR) and abolished the development of allergic airway inflammation in the rat OVA-induced model of AAD (Flajolet 2021). Studies looking into neuroimmune interactions in asthma have similarly linked the disruption of airway sensory neurons to reduced allergen-induced AHR, LAR as well as airway inflammation (Rogerio et al. 2011,

Raemdonck et al. 2012, Trankner et al. 2014, Talbot et al. 2015, Blake et al. 2019). The neuronal regulation of allergen induced responses in the murine HDM model used in this thesis has not been yet investigated and P2X3, P2X2/3 might regulate AHR and possibly allergic airway inflammation downstream of TRPV4.

Although we focused on P2X receptors downstream of TRPV4/ATP axis, P2Y receptors P2Y2 and P2Y11 can also be activated by ATP (Dreisig and Kornum 2016, Silva-Vilches et al. 2018). Unlike P2Y11 which is only engaged by ATP, P2Y2 can be preferentially activated by other nucleotides including UTP and UTD, (Dreisig and Kornum 2016, Silva-Vilches et al. 2018). P2Y11 has been overlooked due to a lack of murine P2Y11 orthologue and a lack of selective and potent tools (Dreisig and Kornum 2016). P2Y11 expression has been reported in various immune cells and its activation has resulted in pro-inflammatory response (Dreisig and Kornum 2016). In T cells, for instance, P2Y11 was required for T cell activation by regulating mitochondria redistribution to the immune synapse (Ledderose et al. 2021). P2Y11 is also expressed by airway epithelial cells where it regulates proliferation, migration and wound repair (Higgins et al. 2014). Yet, the contribution of P2Y11 to airway inflammation and possibly airway remodelling remains unclear. Nevertheless, much more is known about P2Y2 receptor. It is found on macrophages, eosinophils, neutrophils, dendritic cells and airway epithelial cells (Ferrari et al. 2000, Mohanty et al. 2001, Bowler et al. 2003, Kemp et al. 2004, Lommatzsch et al. 2010, Kouzaki et al. 2011, Muller et al. 2011, Shishikura et al. 2016). It regulates ATP-induced migration of DCs, eosinophils and neutrophils and cytokine production by macrophages (Bowler et al. 2003, Stokes and Surprenant 2007, Lommatzsch et al. 2010, Muller et al. 2010, Kawamura et al. 2012, Kobayashi et al. 2015). In airway epithelial cells P2Y2 was demonstrated to mediate ATP-induced mucus production as well as IL-33 release upon allergen challenge (Kemp et al. 2004, Kouzaki et al. 2011, Shishikura et al. 2016). Its expression is upregulated in asthmatic patients, and this has been mimicked by preclinical studies demonstrating upregulation of *P2ry2* in allergen exposed animals (Li et al. 2015, Zech et al. 2015). Studies utilising mice with non-functional P2Y2 receptors have further demonstrated a pathogenic role of P2Y2 in AAD, as P2Y2 deficiency ameliorated airway inflammation and AHR (Muller et al. 2010, Vanderstocken et al. 2010, Kouzaki et al. 2011). This makes P2Y2 a possible target in the TRPV4 signalling pathway in allergic asthma.

In summary, we have demonstrated that P2X7, but not P2X4 or P2X1, might have partially mediated TRPV4 signalling during allergen challenge phase and regulated airway eosinophilia, however further work is needed to consolidate the presented findings. Other P2X or P2Y receptors, individually or in combination, may be activated by ATP released upon TRPV4 activation and modulate not only allergic airway inflammation but also AHR.

5. PAR2 as a potential activator of TRPV4 signalling in HDM-induced model of allergic airway disease

5.1. Introduction

Our laboratory has demonstrated the detrimental effects of TRPV4 activation in the pathogenesis of AAD (Birrell et al. 2016), however the precise mechanism of TRPV4 activation remain unclear. The activation and opening of TRPV4 channel pores can be triggered by various environmental stimuli such as hypotonicity, mechanical stress, temperature or acidic pH, but it can also be achieved by inflammatory mediators such as arachidonic acid metabolites (Belvisi and Birrell 2017).

A membrane receptor PAR2 has been suggested as a potential activator of TRPV4 signalling. PAR2 is a GPCR playing a role in physiological processes in lung, immunity, tissue metabolism and neuronal signalling (Yau et al. 2016). It was found to be co-expressed with TRPV4 on sensory neurons as well as bronchial epithelial cells and alveolar macrophages and linked to AA metabolism (Grant et al. 2007, Poole et al. 2013, Zhao et al. 2014, Zhao et al. 2015, Rayees et al. 2019). PAR2-TRPV4 coupling has been demonstrated in LPS-mediated lung injury and mechanical hyperalgesia models (Grant et al. 2007, Poole et al. 2013, Zhao et al. 2014, Zhao et al. 2015, Rayees et al. 2019), however it has not been yet investigated in the context of asthma.

Nevertheless, PAR2 seems promising as a mechanism of TRPV4 activation in asthma due to substantial evidence implicating PAR2 in asthma pathogenesis. PAR2 is widely expressed on the airway structural cells, as well as leukocytes, including T cells, dendritic cells and alveolar macrophages, and regulates production and secretion of inflammatory cytokines (Nystedt et al. 1994, Schmidlin et al. 2001, Colognato et al. 2003, Roche et al. 2003, Ebeling et al. 2005, Johansson et al. 2005, Shichijo et al. 2006, Lewkowich et al. 2011, Lopez et al. 2014, Francis et al. 2017, Feng et al. 2018, Garcia-Gonzalez et al. 2019). In the airways of asthmatic patients, PAR2 expression as well as PAR2 activating proteases such as tryptase, tissue factor or kallikrein 14 are upregulated (Wenzel et al. 1988, Broide et al. 1991, Jarjour et al. 1991, Alvarez et al. 2000, Knight et al. 2001, Allard et al. 2014, Aubier et al. 2016). Furthermore, PAR2 has been implicated as a regulator of airway responses in healthy lung (Cocks et al. 1999, Ricciardolo et al. 2000, Cicala et al. 2001, Schmidlin et al. 2001) and pre-clinical studies have demonstrated the pathogenic role of PAR2 in the development of allergic airway inflammation and AHR in various AAD models (Schmidlin et al. 2002, Ebeling et al. 2005, Takizawa et al. 2005, Ebeling et al. 2007, Arizmendi et al. 2011, Lewkowich et al. 2011,

Davidson et al. 2013, de Boer et al. 2014, Asaduzzaman et al. 2015, Asaduzzaman et al. 2018, Yee et al. 2018, Redes et al. 2019). This led us to hypothesise that PAR2 activation is responsible for triggering TRPV4 signalling in the HDM-induced model of AAD.

5.2. Hypothesis and aims

PAR2 plays a central role in the development of allergic airway inflammation and AHR in the murine HDM model of AAD via the activation of TRPV4.

To address this hypothesis, we aimed to:

- Study the regulation of PAR2 agonists and PAR2 expression in the murine HDM model of AAD,
- Investigate the role of PAR2 in the HDM model utilising genetically modified mice and
- Investigate the role of PAR2 during the allergen challenge phase using PAR2 blocking antibody.

5.3. Methods

This section outlines and summarises main methods used in this chapter. All the methodology and experimental protocols are presented in detail in Chapter 2.

5.3.1. PAR2 signalling in the mouse HDM model

5.3.1.1. Tryptase-like activity of BAL

Tryptase-like activity in BAL was determined based on the conversion of the tryptase substrate Tosyl-Gly-Pro-Lys-pNA into pNA which absorbs light at 405 nm as described in detail in Chapter 2. BAL samples from the time course study were incubated with the substrate and absorbance was measured at 405 nm. The concentration of pNA was determined as a surrogate for tryptase-like activity by interpolation from a standard curve.

5.3.1.2. *Par2* expression

Par2 expression was determined by RT-qPCR in lung tissue in the HDM time course study as well as $CD4^+$ T cells, $CD8^+$ T cells, ILC2s, moDCs, cDC1s and cDC2s isolated from saline and HDM challenged mice using FACS. As PAR2 primers failed the multiplex validation (Table 5.1), *Par2* was assayed in a singleplex reaction beside eukaryotic *18s* internal control.

Table 5.1: Results of primer multiplex validation.

Target	Linear regression	Slope of linear regression	Reaction efficiency[1]	Suitability for multiplex	Tissue used for validation
18s	0.991	-3.628	**0.556**	NO	kidney
Par2	0.997	-3.072			
Multiplex requirements	>0.98	~-3.3	<0.1		

[1] difference in slopes of linear regressions between *18s* and *Par2* assays.

5.3.2. The role of PAR2 deficiency in the murine HDM model

5.3.2.1. Validation of PAR2$^{-/-}$ mice

5.3.2.1.1. Gel electrophoresis-based genotyping

To confirm the genotype of PAR2$^{-/-}$ and WT (C57BL/6J) mice DNA was extracted from tail tips. Mutated and normal PAR2 alleles were amplified in PCR and visualised on a gel. WT mice were identified based on the presence of 345bp long products, while 196bp long products were characteristic of PAR2$^{-/-}$ mice.

5.3.2.1.2. Functional validation

To confirm the selective loss of functional receptors in PAR2$^{-/-}$ mice, the effects of PAR2 agonists were investigated on a depolarisation of vagal nerve isolated from PAR2$^{-/-}$ mice and their littermate WT controls.

Segments of isolated vagal nerves were incubated with vehicle (0.1 % DMSO or 1 % BSA in KH solution), PAR2 agonists 2Furoyl-LIGRLO-NH_2 (100 nM), SLIGKV-NH_2 (100 nM) and AC55541 (1 µM) as well as TRPV4 agonist GSK1016790A (300 nM), TRPV1 agonist capsaicin (1 µM) and TRPA1 agonist acrolein (300 µM). The nerve was stimulated with a single concentration of each agonist for 2 minutes and was washed with KH solution until it returned back to baseline. Submaximal concentrations of PAR2 agonists were chosen based on previous extensive in-house characterisations of the compounds on isolated rat and guinea pig vagal nerves. TRPV4, TRPV1 and TRPA1 agonists were used at submaximal concentrations as previously published (Bonvini et al. 2016).

5.3.2.2. PAR2$^{-/-}$ mice in the HDM study

PAR2$^{-/-}$ and WT (C57BL/6J) mice were utilised to investigate the role of PAR2 in the development of allergic airway inflammation and AHR. PAR2$^{-/-}$ and WT mice were sensitised to HDM on days 0 and 14 and on days 24, 25 and 26 challenged with saline or HDM once daily. On day 29 lung function was assessed by monitoring responses to increasing concentrations of 5-HT (saline, 1, 3, 10 mg/ml) by whole body plethysmography. Mice were then sacrificed to obtain blood, BAL and lung samples.

Blood samples were used for subsequent assessment of IgE plasma levels by ELISA. BAL cells were isolated and total leukocyte numbers determined by an automated cell counter (Sysmex XT-300) and leukocyte populations differentiated based on the expression of surface and transcription factors by flow cytometry (analysed on Fortessa). ProcartaPlex assays were used to measure BAL concentration of IL-1β, IL-4, IL-5, IL-10, IL-13, IP-10, Eotaxin-1, MCP-1, MIP-1α and TNFα. Lungs were enzymatically digested and total cell counts determined by an automated cell counter (Sysmex XT-300). Leukocytes were differentiated based on the expression of surface and transcription factors by flow cytometry and were analysed on Fortessa.

5.3.3. Pharmacological inhibition of PAR2 during allergen challenge in the murine HDM model

Female C57BL/6J mice were sensitised to HDM on days 0 and 14 and challenged with saline or HDM on days 24, 25, and 26. Mice were lightly anaesthetised with isoflurane and administered vehicle (25mM histidine, 205 mM sucrose in PBS), Isotype antibody (Iso Ab, 10mg/kg) or PAR2 blocking antibody (PAR2 Ab, 10mg/kg) subcutaneously (5ml/kg) on days 23, 25 and 27. On day 29 mice underwent lung function assessment and were sacrificed to obtain BAL and lung samples. Lungs were enzymatically digested to obtain lung cell suspension. Total leukocyte numbers were determined n BAL and lung samples using an automated cell counter (Sysmex XT-300). Leukocytes were then discriminated based on the surface and transcription marker expression by flow cytometry (analysis performed on Fortessa) (Figure 5.1).

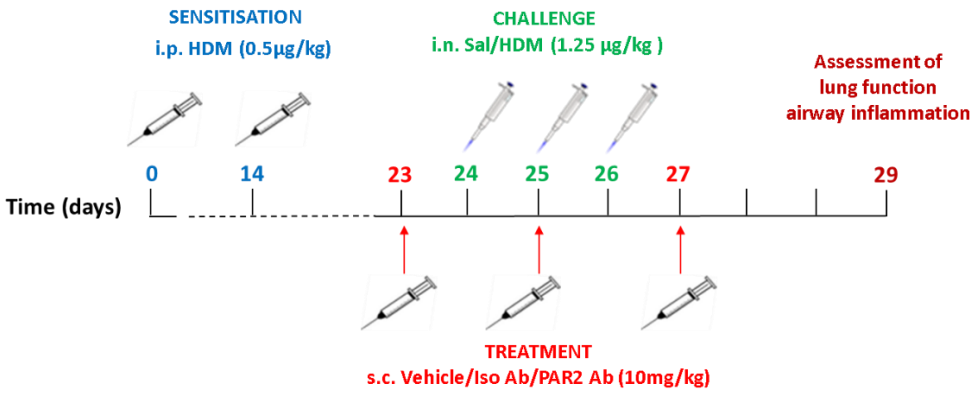


Figure 5.1: Pharmacological inhibition of PAR2 during allergen challenge in the mouse house dust mite (HDM) model – a study schematic.

Mice were administered HDM intraperitoneally (i.p.) on days 0 and 14 and daily challenged with either saline (Sal) or HDM (intranasal (i.n.) administration) on days 24-26. On days 23, 25 and 27 mice were subcutaneously (s.c.) administered vehicle, Isotype antibody (Iso Ab) or PAR2 blocking antibody (PAR2 Ab). Lung function and airway inflammation were assessed on day 29.

5.4. Results

5.4.1. PAR2 signalling in the murine HDM model of AAD

To elucidate whether PAR2 could be responsible for TRPV4 activation in the HDM-induced model of AAD, the first aim of this chapter was to study PAR2 agonist levels and PAR2 expression in the HDM model.

To determine the level of PAR2 agonists in the model, tryptase-like protease activity was initially assessed in the HDM time course study which is presented in detail in Chapter 3. Tryptase-like activity was determined in BAL by measuring the cleavage of the substrate Tosyl-Gly-Pro-Lys-pNA into pNA. Concentration of pNA was increased at 2, 24, 48 and 72 hours after the third HDM challenge compared to saline challenged controls (Figure 5.2A).

In the same time course study, lung *Par2* mRNA levels in whole lung were determined. *Par2* was increased 2 hours after the second HDM challenge, followed by a suppression of *Par2* expression 24, 48 and 72 hours after the third and final HDM challenge compared to saline challenged controls (Figure 5.2B).

Next, we determined *Par2* expression in the key immune cell populations characterised in Chapter 3. HDM challenge suppressed *Par2* in CD4+ T cells but had no impact on CD8+ T cells and ILC2 expression. *Par2* was undetectable (in 40 PCR cycles) on cDC1 and cDC2 from saline

challenged controls, but was detectable in all DC populations after the HDM challenge (Figure 5.3).

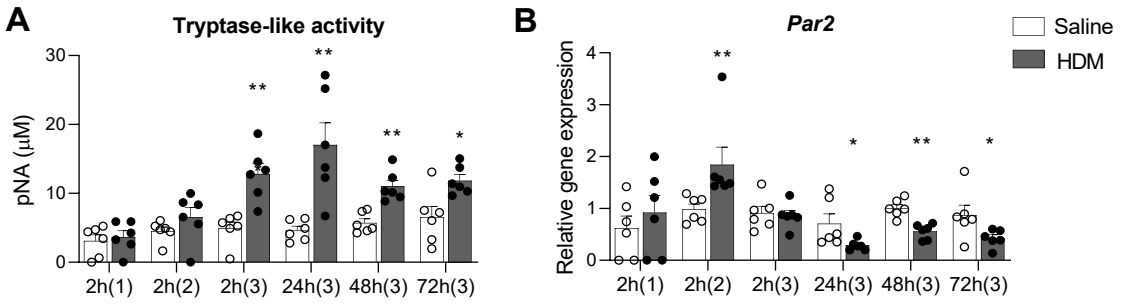


Figure 5.2: PAR2 signalling in the house dust mite (HDM) time course study.

HDM-sensitised C57BL/6 mice were challenged with saline or HDM once a day on one (1) occasion, two (2) or three (3) consecutive days and bronchoalveolar lavage (BAL) and lung samples collected 2 after each challenge and 24, 48 or 72h after the third and final challenges. A) Change in pNA concentration from baseline in BAL as a surrogate for tryptase-like activity. B) *Par2* lung expression normalised to *18s*. Data from a single experiment are presented as mean ± S.E.M with N=6 mice per group. * denotes p<0.05 and ** p<0.01 comparing saline and HDM challenged groups for each time point using Mann-Whitney U-test.

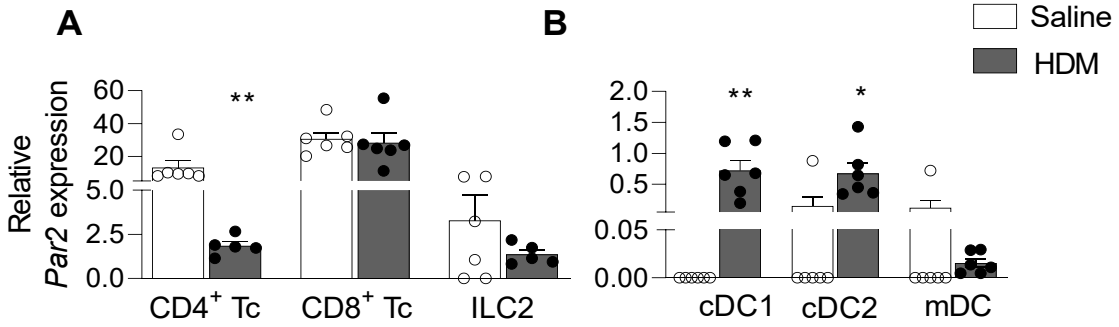


Figure 5.3: *Par2* expression in key immune cells in the house dust mite (HDM) model of allergic airway disease.

HDM-sensitised mice were challenged with saline or HDM on three consecutive days and mRNA extracted from lung immune cells isolated using fluorescence assisted cell sorting 3 days later. *Par2* relative gene expression normalised to *18s* in A) $CD4^+$T cells, $CD8^+$T cells and group 2 innate lymphoid cells (ILC2) and B) classical dendritic cells (cDC) type 1 (cDC1s), cDC2s, and monocyte derived DCs (moDCs). Representative data from two (A) or one (B) independent experiments are presented as mean ± S.E.M with N=5-6 mice per group. * denotes p<0.05 and ** p<0.01 comparing saline and HDM challenged groups using Mann-Whitney U-test.

5.4.2. The role of PAR2 deficiency in the murine HDM model

To further investigate the role of PAR2 signalling in the development of allergic airway inflammation and AHR in the HDM model, genetically modified mice with non-functional PAR2 receptors ($PAR2^{-/-}$) were utilised.

5.4.2.1. Validation of $PAR2^{-/-}$ mice

PCR and subsequent gel electrophoresis were performed on DNA extracted from tail tips of WT and $PAR2^{-/-}$ mice to confirm their genotype. DNA extracted from WT mice yielded characteristic 345bp long bands as visualised by gel electrophoresis, while $PAR2^{-/-}$ DNA was characterised by 198bp long bands (Figure 5.4A).

Next, the lack of functional PAR2 receptors in $PAR2^{-/-}$ was demonstrated in vitro on isolated mouse vagal nerves. PAR2 activating peptides AC55541, 2-Furoyl-LIGRLO-NH_2 and SLIGKV-NH_2 caused depolarisation of vagal nerves isolated from WT mice (0.143 ± 0.031 mV, 0.168 ± 0.044 mV and 0.205 ± 0.060 mV, respectively), while their vehicles had no effect (0.029 ± 0.011 mV (0.1% DMSO), 0.033 ± 0.012 mV (BSA)). The responses to AC55541, 2-Furoyl-LIGRLO-NH_2 and SLIGKV-NH_2 were absent in $PAR2^{-/-}$ mice (0.044 ± 0.007 mV, 0.025 ± 0.007 mV and 0.015 ± 0.005 mV, respectively). To confirm the viability of all the isolated nerves as well as selectivity of the mutation, TRPV1, TRPV4 and TRPA1-induced responses were additionally tested. Capsaicin (0.796 ± 0.194 mV vs 0.612 ± 0.139 mV), GSK101 (0.160 ± 0.021 mV vs 0.140 ± 0.024) and acrolein (0.400 ± 0.080 mV vs 0.355 ± 0.060 mV), respectively, induced depolarisation of isolated vagal nerves to the same degree in WT and $PAR2^{-/-}$ mice, respectively (Figure 5.4B).

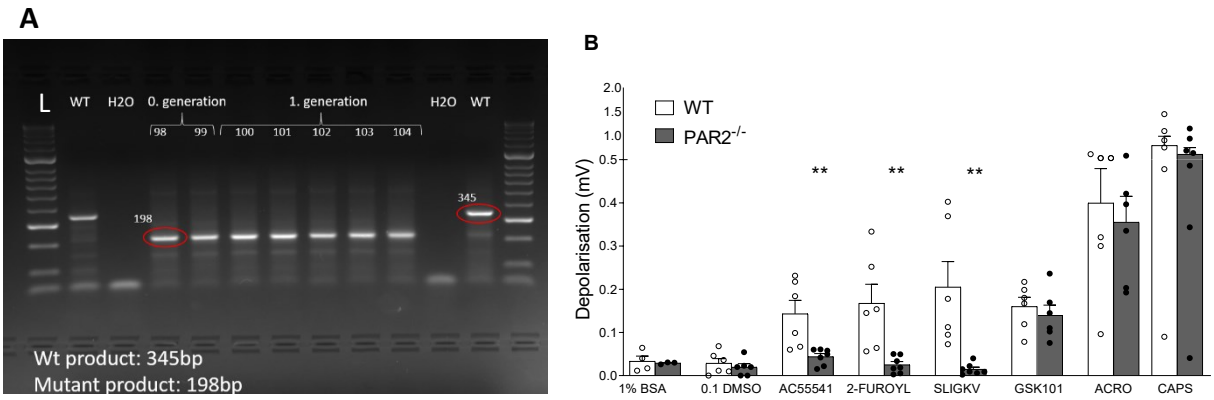


Figure 5.4: Validation of PAR2 deficient (PAR2$^{-/-}$) mice.

A) Representative genotyping results confirming the presence of PAR2 mutation in in PAR2$^{-/-}$ mice. PCR was run with DNA isolated from mouse tail tips and products were separated by agarose gel electrophoresis. L – DNA ladder, bp – base pairs, H_2O – no DNA template control, WT – wild type. B) Vagal nerves were isolated from wild type (WT) and PAR2$^{-/-}$ mice, stimulated with vehicle (1% BSA or 0.1% DMSO), PAR2 agonists AC55541 (1 µM), 2Furoyl-LIGRLO-NH_2 (2-FUROYL, 100 nM), SLIGKV-NH2 (SLIGKV, 100 nM), TRPV4 agonist GSK1016790A (GSK101, 300 nM), TRPA1 agonist acrolein (ACRO, 300 µM) and TRPV1 agonist capsaicin (CAPS, 1 µM) and depolarisation measured. Data are presented as mean ± S.E.M., N=6 mice per group. ** denotes p<0.01 using t-test comparing responses between PAR2$^{-/-}$ and WT mice.

5.4.2.2. The effect of PAR2 deficiency on HDM-induced airway inflammation

HDM challenge provoked an increase in total leukocytes in the airways of WT mice compared to saline challenge (Figure 5.5A). This was characterised by expansion of eosinophil, CD4$^+$ and CD8$^+$ T cell, B cell and ILC2 populations, while neutrophils and AM remained unaffected (Figure 5.5**Error! Reference source not found.**B-H). In comparison to WT controls, reduced t otal leukocyte numbers as well as eosinophil, CD4$^+$ and CD8$^+$ T cell numbers were observed in PAR2$^{-/-}$ mice (Figure 5.5A,B,E,F). Additionally, HDM challenge was associated with increased neutrophil and ILC2 numbers in PAR2$^{-/-}$ mice in respect to their WT controls, while AM and B cell numbers remained identical (Figure 5.5C,D,G,H).

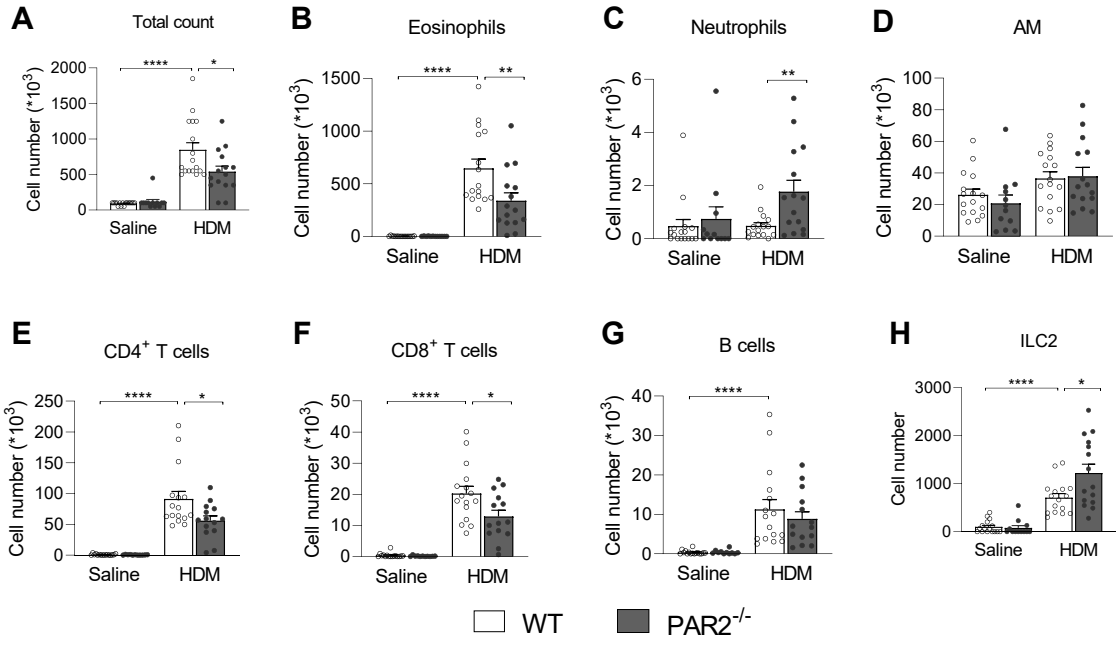


Figure 5.5: The effect of PAR2 deficiency (PAR2$^{-/-}$) on house dust mite (HDM)-induced allergic airway inflammation.

Wild type (WT) and PAR2$^{-/-}$ mice were sensitised to HDM, then challenged with saline or HDM on three consecutive days and bronchoalveolar lavage (BAL) collected 3 days after the final challenge. A) Total leukocyte number as determined by an automated cell counter. B) Eosinophil, C) neutrophil, D) alveolar macrophage (AM), E) CD4$^+$ T cell, F) CD8$^+$ T cell, G) B cell and H) group two innate lymphoid cells (ILC2) numbers in BAL as determined by flow cytometry. Representative data from one of two independent experiments are presented as mean ± S.E.M. with N=12-16/group. Mann-Whitney U test was used to analyse differences between experimental groups. * denotes $p<0.05$, ** $p<0.01$, *** $p<0.001$, **** $p<0.0001$.

5.4.2.3. The effect of PAR2 deficiency on HDM-induced lung inflammation

In WT mice, HDM challenge provoked a characteristic increase in total lung leukocytes, as well as eosinophils, CD4$^+$ and CD8$^+$ T cells, B cells, ILCs and DCs (moDCs, cDC2s, cDC1s) compared to saline controls. Additionally, AM numbers were reduced, while neutrophils population remained unaffected (Figure 5.6). In PAR2$^{-/-}$ mice, HDM challenge was associated with reduced total lung leukocyte numbers, as well as eosinophil, CD4$^+$ T cell, CD8$^+$ T cells, B cell, moDC and cDC2 numbers in comparison to HDM-challenged WT controls, while no changes were observed in neutrophil, AM, ILC2 and cDC1 populations (Figure 5.6).

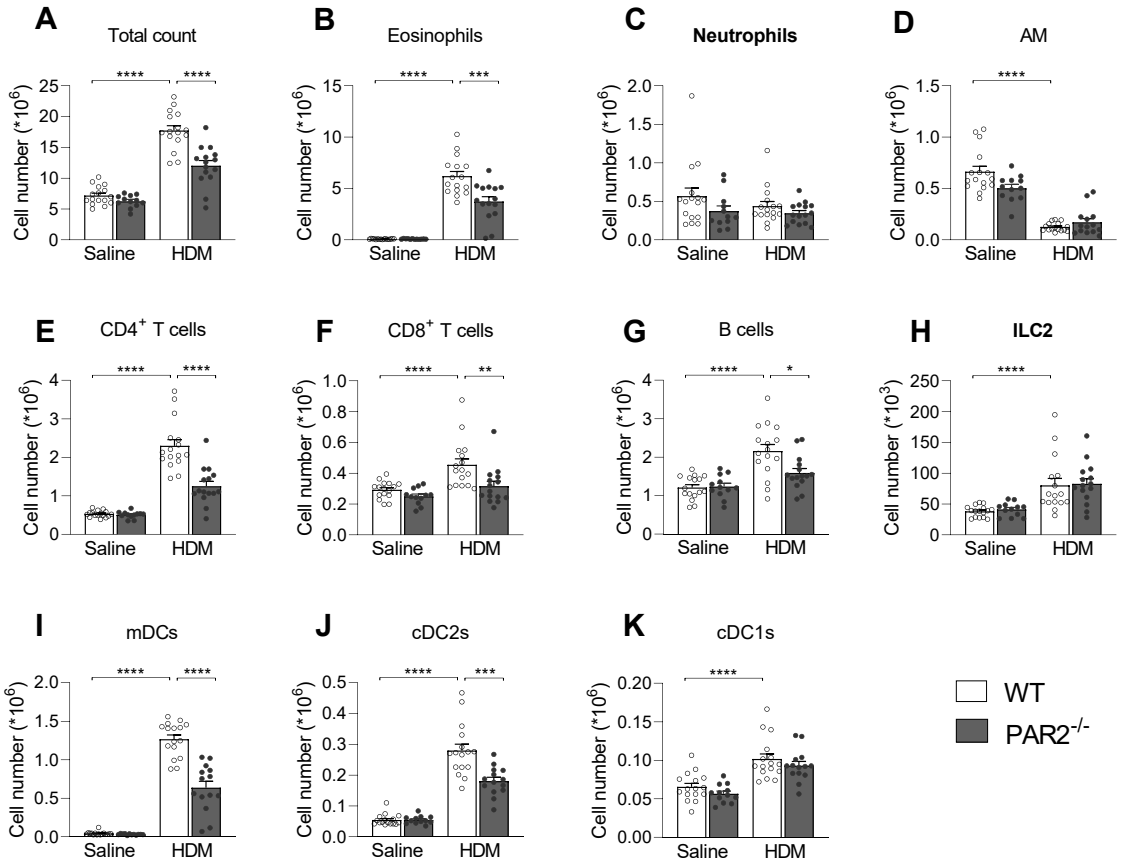


Figure 5.6: The effect of PAR2 deficiency (PAR2$^{-/-}$) on HDM-induced lung inflammation.

Wild type (WT) and PAR2$^{-/-}$ mice were sensitised to house dust mite (HDM) and challenged with saline or HDM on three consecutive days. Lungs were collected 3 days after the final challenge and enzymatically digested. A) Total leukocyte number as determined by an automated cell counter. Flow cytometry was utilised to assess numbers of B) eosinophils, C) neutrophils, D) alveolar macrophages (AM), E) CD4$^+$ T cells, F) CD8$^+$ T cells, G) B cells, H) group two innate lymphoid cells (ILC2), I) monocyte-derived dendritic cells (moDCs), J) classical DCs type 2 (cDC2s) and I) cDC1s. Representative data from one of two independent experiments are presented as mean ± S.E.M. with N=12-16/group. Mann-Whitney U test was used to analyse differences between experimental groups. * denotes p<0.05, ** p<0.01, *** p<0.001, **** p<0.0001.

5.4.2.4. The effect of PAR2 deficiency on type 2 cytokine and chemokine production

In WT mice HDM challenge was associated with an increase in BAL IL-4, IL-5, IL-13, IL-10, TNFα, IL1β, Eotaxin-1, MIP-1α, MCP-1, TARC and I-TAC relative to saline challenge (Figure 5.7). In PAR2$^{-/-}$, HDM challenge was associated with lower TNFα and MIP-1α levels and higher IL-5

concentration in comparison to WT HDM challenged controls. The concentrations of other cytokines and chemokines were identical between HDM challenged WT and PAR2$^{-/-}$ mice.

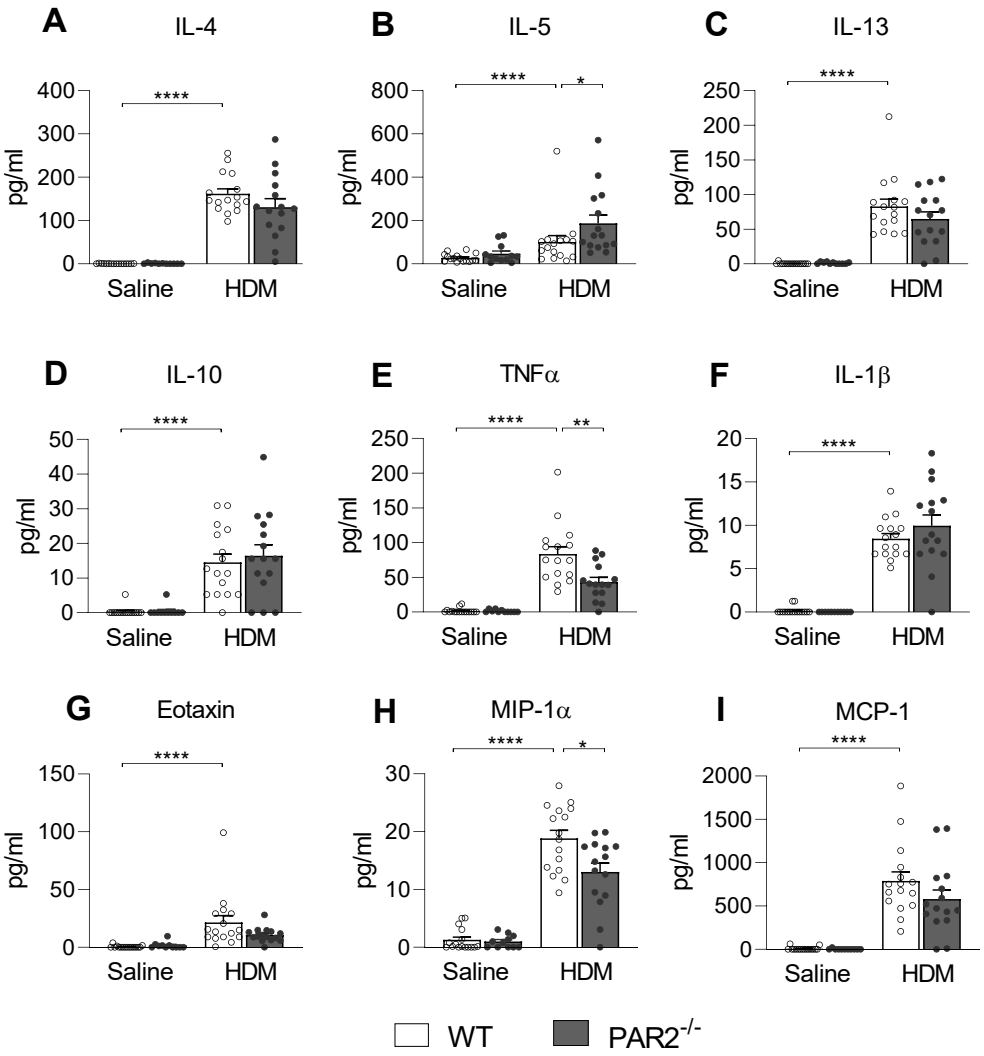


Figure 5.7: The effect of PAR2 deficiency (PAR2$^{-/-}$) on cytokine and chemokine production.

Wild type (WT) and PAR2$^{-/-}$ mice were sensitised to house dust mite (HDM) and challenged with saline or HDM on three consecutive days. Bronchoalveolar lavage (BAL) was collected 3 days after the final challenge and cytokines and chemokines assessed in the supernatant. Concentration of A) IL-4, B) IL-13, C) IL-5, D) IL-10, E) IP-10, F) TNFα, G) IL-1β, H) Eotaxin-1 (CCL11), I) MIP-1α and J) MCP-1 in BAL as determined by ProcartaPlex assays. Representative data from one of two independent experiments are presented as mean ± S.E.M., N=12-16/group. Mann-Whitney U test was used to analyse differences between experimental groups. * denotes p<0.05, ** p<0.01, *** p<0.001 and **** p<0.0001.

5.4.2.5. The effect of PAR2 deficiency on antibody secretion

In WT mice HDM challenge was associated with increased total plasma IgE and HDM-specific IgE levels as compared to saline challenge. In PAR2$^{-/-}$ mice the levels of plasma total IgE as

well as HDM-specific IgE were reduced after HDM exposure as compared to WT controls (Figure 5.8).

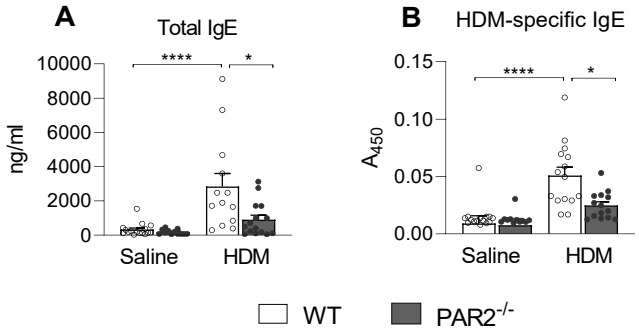


Figure 5.8: The effect of PAR2 deficiency (PAR2$^{-/-}$) on antibody production.

Wild type (WT) and PAR2$^{-/-}$ mice were sensitised to house dust mite (HDM) and challenged with saline or HDM on three consecutive days. Blood was collected 3 days after the final challenge and IgE determined in plasma. A) Total IgE concentration and B) HDM-specific IgE levels as determined by ELISA. Representative data from one of two individual experiments are presented as mean ± S.E.M., N=12-16/group. Mann-Whitney U tests were used to analyse differences between experimental groups. * $p<0.05$, **** $p<0.0001$. A_{450} – absorbance at 450 nm.

5.4.2.6. The effect of PAR2 deficiency on airway hyper-responsiveness

Administration of 5-HT led to a concentration-dependent increase in Penh in all groups. HDM challenge was associated with pronounced Penh response in WT mice as compared to saline control. The responses of HDM challenged PAR2$^{-/-}$ mice were significantly greater than responses of saline challenged PAR2$^{-/-}$ mice and were no different to the responses of WT HDM challenged mice (Figure 5.9).

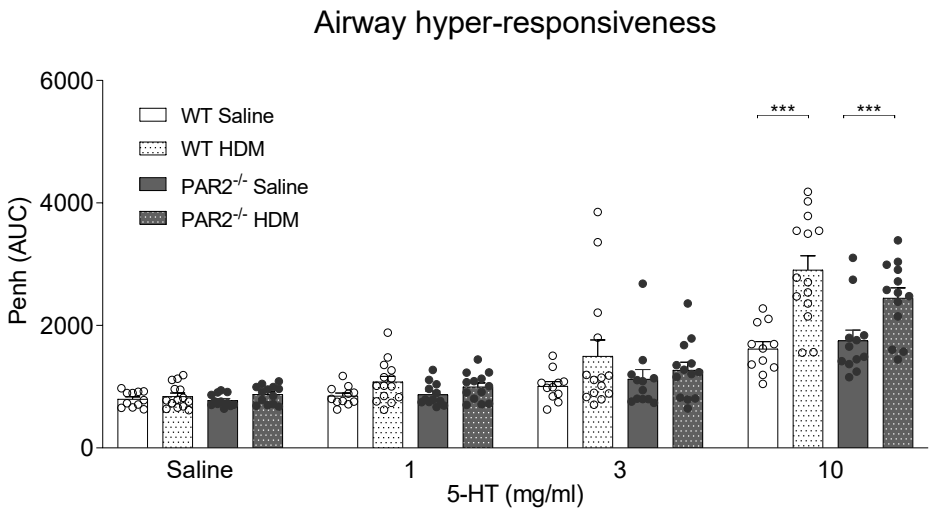


Figure 5.9: The effect of PAR2 deficiency on airway hyper-responsiveness.

Wild type (WT) and PAR2$^{-/-}$ mice were sensitised to HDM and challenged with saline or HDM on three consecutive days. Three days later mice were placed in whole body plethysmography chambers and exposed to saline, followed by increasing concentrations of 5-HT (1, 3 and 10mg/ml). Each application was monitored for 15 minutes before the subsequent solution was nebulised. Area under the curve (AUC) was determined for Penh values for each solution. Representative data from one of two independent experiments are presented as mean ± S.E.M., N=11-14/group. *** denotes $p<0.001$ in repeated measures ANOVA with Sidak's multiple comparison test.

5.4.3. Pharmacological inhibition of PAR2 during the challenge phase

By utilising PAR2$^{-/-}$ mice in the HDM model, we demonstrated a potential role of PAR2 in the development of airway inflammation, but not AHR. To further support these observations and evaluate the role of PAR2 specifically during an allergen challenge phase, pharmacological tools were utilised to disrupt PAR2 signalling during HDM challenge.

A novel monoclonal anti-PAR2 IgG blocking antibody MEDI2344 (PAR2 Ab) was validated in vitro and in vivo and was shown to prevent proteolytic cleavage of mouse PAR2 and subsequent inhibition of PAR2 signalling (data not shown). The isotype control IgG R347 and vehicle were tested alongside to account for the unspecific binding of the PAR2 Ab or vehicle effects, respectively.

5.4.3.1. The effect of PAR2 blocking antibody on HDM-induced allergic airway inflammation

HDM challenge triggered an increase in total BAL leukocyte numbers relative to saline challenge in vehicle treated mice (Figure 5.10A). More specifically, in vehicle treated mice, HDM challenge increased eosinophil, $CD4^+$ and $CD8^+$ T cell, B cell and ILC2 number compared to saline challenged controls, while neutrophil and AM numbers were unchanged (Figure 5.10B-H). Administration of PAR2 antibody was associated with greater total leukocyte, eosinophil and AM numbers upon HDM challenge relative to vehicle treated control (Figure 5.10A,B,D). A trend towards greater B cells and ILC2 numbers was also observed, while neutrophil, $CD4^+$ and $CD8^+$ T cell numbers were comparable between HDM challenge vehicle and PAR2 Ab treated mice (Figure 5.10C,E-H). The responses of isotype antibody treated animals did not differ from vehicle treated animals (Figure 5.10).

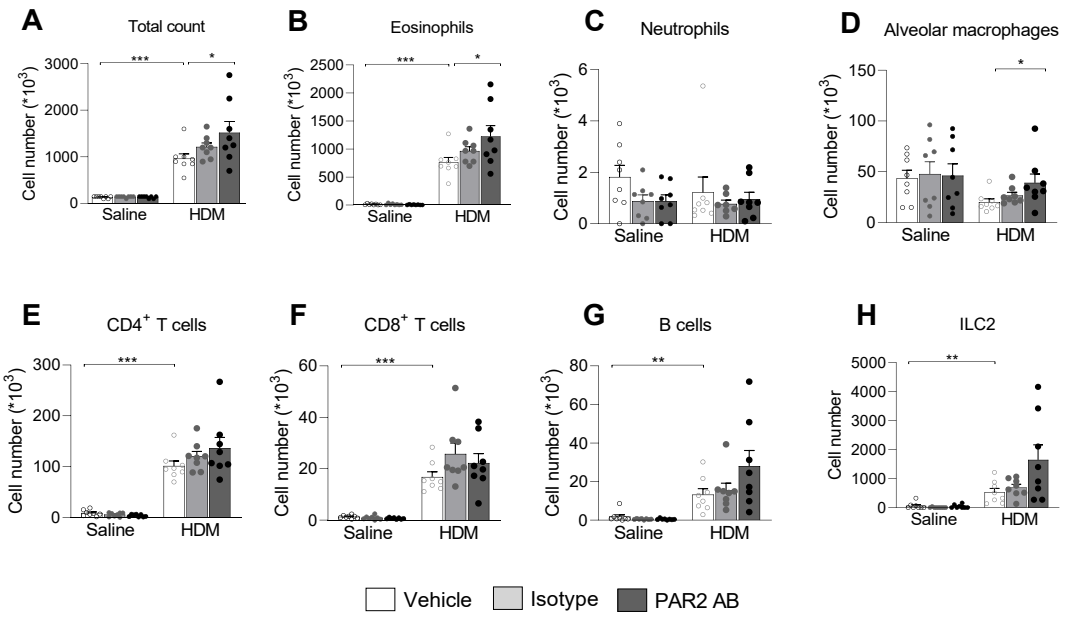


Figure 5.10: The effect of PAR2 antibody on house dust mite (HDM)-induced airway inflammation.
HDM-sensitised mice were challenged with saline or HDM on days 24, 25 and 26. On days 23, 25 and 27 mice were treated subcutaneously with vehicle (25mM histidine, 205 mM sucrose in PBS), Isotype antibody IgG R347 (10mg/kg, Iso AB) or anti-PAR2 blocking antibody (10mg/kg, PAR2 AB). Bronchoalveolar lavage (BAL) samples were collected on day 29. A) Total leukocyte numbers as determined by automated cell counter. Flow cytometry was utilised to assess numbers of B) eosinophils, C) neutrophils, D) alveolar macrophages, E) $CD4^+$ T cells, F) $CD8^+$ T cells, G) B cells, H) group two innate lymphoid cells (ILC2). Data from a single experiment are presented as mean ± S.E.M., N=8/group. Mann-Whitney U test was used to determine differences between saline and HDM challenged WT mice, while Kruskal-Wallis with Dunn's post hoc tests was used to analyse differences in HDM-induced responses between Vehicle, Iso AB and PAR2 AB treated mice. * denotes $p<0.05$, *** $p<0.001$.

5.4.3.2. The effect of PAR2 blocking antibody on HDM-induced lung inflammation

In comparison to saline challenge, HDM challenge triggered an increase in total lung leukocyte numbers in vehicle treated mice which was characterised by increased eosinophil, $CD4^+$ and $CD8^+$ T cell, B cell, ILC2, moDC, cDC2 and cDC1 numbers. Additionally, HDM challenge resulted in reduced neutrophil and AM numbers compared to saline challenge in the lungs of vehicle treated mice. Treatment with PAR2 blocking antibody did not alter HDM-induced lung inflammation as compared to vehicle control group. Similarly, responses of isotype antibody treated mice were comparable to vehicle treated mice upon HDM challenge (Figure 5.11).

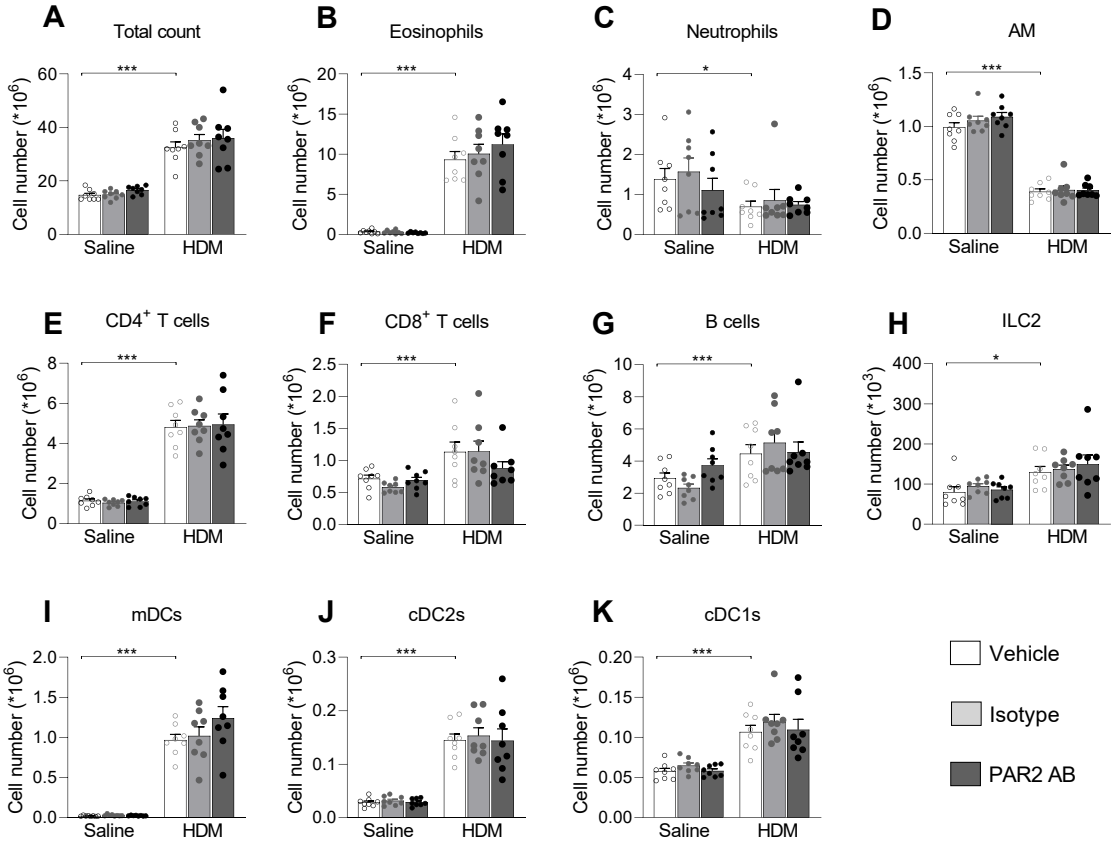


Figure 5.11: The effect of PAR2 antibody on house dust mite (HDM)-induced lung inflammation.

HDM-sensitised mice were challenged with saline or HDM on days 24, 25 and 26. On days 23, 25 and 27 mice were treated subcutaneously with vehicle (25mM histidine, 205 mM sucrose in PBS), Isotype antibody IgG R347 (10mg/kg, Iso AB) or anti-PAR2 blocking antibody (10mg/kg, PAR2 AB). Lung samples were collected and enzymatically digested on day 29. A) Total leukocyte numbers as determined by automated cell counter. Flow cytometry was utilised to assess numbers of B) eosinophils, C) neutrophils, D) alveolar macrophages, E) $CD4^+$ T cells, F) $CD8^+$ T cells, G) B cells, H) group two innate lymphoid cells (ILC2), I) monocyte-derived dendritic cells (moDCs), J) classical dendritic cells type 2 (cDC2s) and K) classical dendritic cells type 1 (cDC1s). Data from a single experiment are presented as mean ± S.E.M., N=8/group. Mann-Whitney U test was used to determine differences between saline and HDM challenged WT mice, while Kruskal-Wallis with Dunn's post hoc tests was used to analyse differences in HDM-induced responses between Vehicle, Iso AB and PAR2 AB treated mice. * denotes $p<0.05$, *** $p<0.001$.

5.4.3.3. The effect of PAR2 blocking antibody on HDM-induced AHR

Next, the effect of PAR2 Ab on development of HDM-induced AHR was investigated. 5-HT exposure led to concentration dependent increase in Penh responses in all groups. A trend towards increased 5-HT-provoked Penh responses was observed in HDM challenged groups

in comparison to the respective saline control groups, however the differences did not reach statistical significance in any of the treatment groups (Figure 5.12).

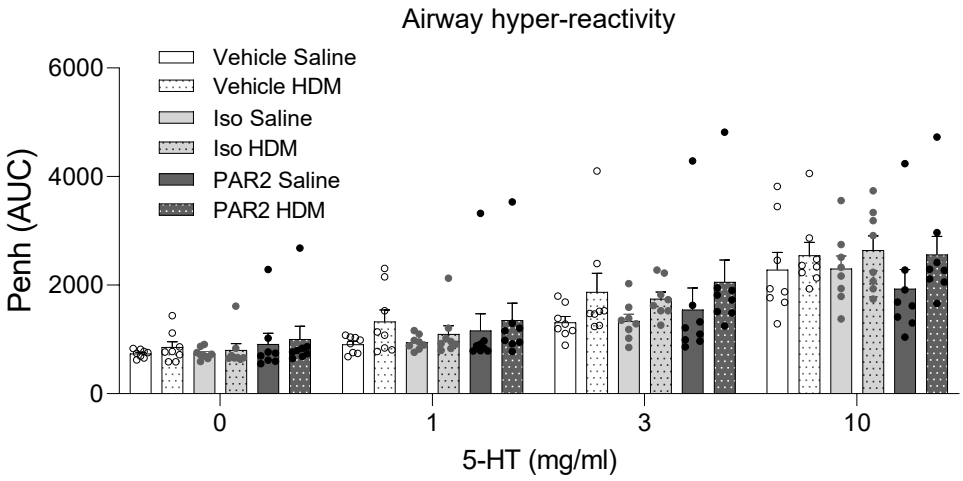


Figure 5.12: The effect of PAR2 antibody on airway hyper-reactivity.

House dust mite (HDM)-sensitised mice were challenged with saline or HDM on days 24, 25 and 26. On days 23, 25 and 27 mice were treated subcutaneously with vehicle (25mM histidine, 205 mM sucrose in PBS), Isotype antibody IgG R347 (10mg/kg, Iso AB) or anti-PAR2 blocking antibody (10mg/kg, PAR2 AB). On day 29 mice were placed in whole body plethysmography chambers and exposed to saline, followed by escalating concentrations of 5-HT (1, 3 and 10mg/ml). Each application was monitored for 15 minutes before the subsequent solution was nebulised. Area under the curve (AUC) was determined for Penh values for each solution and analysed using repeated measures ANOVA with Sidak's multiple comparison test. Data are presented as mean ± S.E.M., N=8/group.

5.5. Discussion

The aim of this thesis is to elucidate TRPV4 signalling pathway in asthma. Utilising murine HDM model of AAD we have established that immune cells, pivotal for the development of allergic airway inflammation ($CD4^+$ T cells and lung DCs) were possibly responsible for TRPV4 activation in this model (Chapter 3). P2X7 was identified as a potential downstream receptor in TRPV4 signalling axis in allergic airway inflammation, although other P2 receptors are likely involved, particularly in the development of AHR (Chapter 4). The aim of this chapter was to elucidate the mechanisms of TRPV4 activation during the development of AAD. PAR2 was studied as a potential mechanism as PAR2 has been shown to activate or modulate TRPV4 signalling in neurogenic inflammation and lung injury models (Grant et al. 2007, Poole et al. 2013, Zhao et al. 2014, Zhao et al. 2015, Rayees et al. 2019) and have been extensively implicated in asthma pathogenesis (Walker and DeFea 2014). PAR2 expression is increased in

the airways of asthmatic patients (Knight et al. 2001, Allard et al. 2014, Aubier et al. 2016) and the PAR2 chromosome region (5q13.3) has been linked to asthma onset and asthma score (Bouzigon et al. 2007). The pathogenic role of PAR2 in the development of allergic airway inflammation and AHR has been further demonstrated in preclinical studies (Schmidlin et al. 2002, Takizawa et al. 2005, Arizmendi et al. 2011, Lewkowich et al. 2011, Davidson et al. 2013, Asaduzzaman et al. 2015, Hiraishi et al. 2018, Yee et al. 2018). This led us to hypothesise that PAR2 was critical for the activation of TRPV4 signalling and subsequent airway inflammation and AHR.

Our first aim was to validate PAR2 as a target in the HDM-induced model of AAD by studying the presence of PAR2 agonists the HDM model. Although many proteases are capable of cleaving PAR2 N-terminal (Hollenberg et al. 2014, Yau et al. 2016), tryptase was considered the most relevant PAR2 agonist in our model as increased tryptase levels have been demonstrated in BAL of asthmatic patients (Wenzel et al. 1988, Broide et al. 1991, Alvarez et al. 2000, Aubier et al. 2016), particularly after an allergen challenge (Wenzel et al. 1988, Sedgwick et al. 1991). Inhibition of tryptase alleviated allergen-induced airway responses in asthmatic patients as well as preclinical models (Clark et al. 1995, Krishna et al. 2001). We found increased levels of tryptase-like activity in the time course study assessing the development of allergic airway inflammation upon HDM challenge, in line with reported clinical observations (Wenzel et al. 1988, Broide et al. 1991, Alvarez et al. 2000, Aubier et al. 2016).

To gain further insight into PAR2 signalling in the murine HDM model *Par2* expression was investigated next. HDM challenge was associated with increased *Par2* expression 2 hours after the second HDM challenge, and reduced expression 24, 48 and 72 hours after the third and last HDM challenge. *Par2* expression was then investigated further in lung $CD4^+$ T cells, $CD8^+$ T cells, ILC2 and DC populations – immune cells deemed crucial in the HDM-induced immune responses (Chapter 3). As previously reported, *Par2* could be detected in $CD4^+$ T and $CD8^+$ T cells (Lopez et al. 2014, Francis et al. 2017, Feng et al. 2018), but interestingly, HDM challenge triggered downregulation of *Par2* expression in $CD4^+$ T cells, but not $CD8^+$ T cells. Similar findings have not been yet reported, but it could be relevant for the development of allergic airway inflammation as PAR2 has been demonstrated to play a role in T cell development, T cell adhesion as well as Th2 cytokine production (Lim et al. 2006, Shichijo et

al. 2006, Francis et al. 2017, Feng et al. 2018). We have also demonstrated *Par2* expression on ILC2s, although HDM challenge had no effect on *Par2* mRNA expression. The presence of PAR2 receptors on ILC2s has not been shown before and its importance for ILC2 function is yet to be elucidated. In lung dendritic cell populations, we could only detect *Par2* after HDM challenge but not saline challenge, indicative of HDM-induced upregulation of *Par2* expression. Similarly, Lewkowich et al. failed to detect PAR2 on DCs isolated from naïve mice, but reported the upregulation of PAR2 expression on DCs upon cockroach extract (CE) challenge (Lewkowich et al. 2011). Although PAR2 cannot be easily detected in naïve DCs, PAR2 seems crucial in DC maturation, development and antigen trafficking (Fields et al. 2003, Ebeling et al. 2007, Ramelli et al. 2010).

These observations validated PAR2 as a target in the murine HDM model and warranted further investigation into the role of PAR2 in the HDM-induced model of AAD. We utilised two distinct approaches (a genetic and a pharmacological approach) to disrupt PAR2 signalling in the model.

Constitutive $PAR2^{-/-}$ mice (Schmidlin et al. 2002) were initially employed to study the role of PAR2 deficiency on the development of allergic airway inflammation and AHR. However, as inbreeding invariably leads to an accumulation of off-target mutations or to a genetic drift that could result in a loss of phenotype (Stevens et al. 2007, Purtha et al. 2012, Ji et al. 2017) the disruption of PAR2 gene was validated by genotyping, while an in vitro vagal nerve depolarisation technique was used to demonstrate the lack of functional PAR2 signalling in $PAR2^{-/-}$ mice. The later technique was chosen to study the functionality of PAR2 receptors as sensory neurons, including respiratory sensory neurones, express PAR2 and PAR2 has been shown to elicit sensory neuron activation (Sipe et al. 2008, Gu and Lee 2012, Poole et al. 2013, Bonvini et al. 2017, Flajolet 2021). Three different PAR2 agonists were probed and while all of them triggered depolarisation of vagal nerve segments in WT mice, this effect was lost in $PAR2^{-/-}$ mice. TRPV4-, TRPV1- and TRPVA1-induced responses were retained in $PAR2^{-/-}$ mice, confirming the selectivity of the genetic disruption of PAR2.

Having successfully validated $PAR2^{-/-}$ mice, the effect of PAR2 deficiency on the development of allergic airway inflammation and AHR was investigated next. $PAR2^{-/-}$ mice displayed impaired IgE responses and ameliorated airway inflammation upon HDM challenge. Limited recruitment and expansion of eosinophils, $CD4^+$ T cells, $CD8^+$ T cells, B cells, moDCs and cDC2s

was observed in BAL and lung. Surprisingly, PAR2 deficiency had no effect on BAL type 2 cytokine levels, but rather lead to an increase in BAL IL-5 levels, in spite of reduced $CD4^+$ T cell numbers. Chemokines such as Eotaxin-1 or MCP-1 were not affected by PAR2 deficiency, however, supressed levels of TNFα and MIP-1α were found in $PAR2^{-/-}$ mice upon HDM challenge. In spite of alleviated HDM-induced airway inflammation in $PAR2^{-/-}$ mice, PAR2 deficiency failed to protect against HDM-induced AHR.

There are certain limitations to the presented studies. We first conducted an initial study (N=6-8/group) however the differences in allergic airway inflammation between WT and $PAR2^{-/-}$ mice did not reach statistical significance due to small group sizes. Hence, a second experiment was conducted with increased group numbers to improve the statistical power of the study. To achieve that and at the same time comply with the 3R principles (Aske and Waugh 2017) female and male mice were used in this second study. Care was taken to age and sex match the groups as much as possible. Although no statistically significant differences in HDM-induced immune and airway responses between male and female mice could be observed, this could limit the interpretation of those results. Another limitation of this study is a lack of littermate controls. Albeit WT controls were carefully chosen to match the genetic background of $PAR2^{-/-}$ mice, it is possible that the genetic backgrounds of WT and $PAR2^{-/-}$ were not identical. The differences in the genetic background could be a confounding factor in the responses seemingly contributable to the genetic disruption of *Par2* (Holmdahl and Malissen 2012).

To confirm the observations in the knockout studies and to address whether PAR2 signalling was crucial during sensitisation or allergen challenge phase, respectively, we next employed a pharmacological approach to disrupt PAR2 signalling during allergen challenge phase in HDM sensitised mice. A PAR2 blocking antibody MEDI2344 with high affinity for murine PAR2 and demonstrated efficacy in mechanical hyperalgesia model was used for this task (unpublished data). Surprisingly, MEDI2344 offered no protection against the development of allergic airway inflammation, but rather enhanced eosinophil infiltration into the airways. No effect of MEDI2344 on AHR could be observed, however, the AHR results of this study were inconclusive, as no clear difference could be seen in responses between saline and HDM challenged vehicle dosed mice, limiting further interpretation of these results.

Whole body plethysmography used in this thesis has been heavily criticised as a measure of airway resistance (Irvin and Bates 2003, Bates et al. 2004, Lundblad et al. 2007). However, several laboratories, have reported good reproducibility as well as correlation between Penh and direct measurements of airway resistance and we have previously demonstrated the method to be a reliable assessment of lung function in lung disease (Hamelmann et al. 1997a, Lomask 2006, Verheijden et al. 2014, Raemdonck et al. 2016). Additionally, this is the only available technique that allows monitoring of airway responses in conscious animals and can therefore assess factors apart from smooth muscle hyper-reactivity that contribute to AHR, such as neuronal regulation (Lomask 2006, Meurs et al. 2008). Although we are unsure about the role of neuronal regulation in HDM-induced AHR, TRPV4 and PAR2 have both been implicated airway sensory nerve activity in lung disease (Bonvini et al. 2016, Bonvini et al. 2017, Flajolet 2021) and could potentially affect AHR via modulation of airway sensory nerve responses.

Our findings only partially agree with the existing literature on the role of PAR2 in allergic airway inflammation. Most of the studies utilising $PAR2^{-/-}$ mice to investigate the role of PAR2 in asthma, have demonstrated a pathogenic role of PAR2 in allergic airway inflammation and AHR in OVA, CE, HDM and ALT AAD models (Schmidlin et al. 2002, Takizawa et al. 2005, Page et al. 2010, Arizmendi et al. 2011, Lewkowich et al. 2011, Davidson et al. 2013, de Boer et al. 2014, Yee et al. 2018), although several reports have failed to demonstrate the protective effect of PAR2 deficiency on either airway inflammation or AHR (Schmidlin et al. 2002, Redes et al. 2019, Daines et al. 2020, Wiesner et al. 2020). The type of experimental model and particularly the mechanism of allergen sensitisation have been proposed to be crucial for the role of PAR2. For instance, in CE model PAR2 deficiency was protective when sensitisation was achieved via mucosal administration rather than systemic administration of CE (Page et al. 2010). A lack of role for PAR2 during allergen challenge phase was proposed further as inhibition of CE protease activity during challenge did not modulate immune responses (Page et al. 2010). Similar observations were made in HDM models with mucosal sensitisation (Davidson et al. 2013, de Boer et al. 2014). This hypothesis was then further strengthened by the notion that induction of immune tolerance to OVA during mucosal sensitisation was overcome by activation of PAR2 and instead triggered allergic sensitisation (Ebeling et al. 2007).

Nonetheless, findings from murine OVA-induced AAD models have additionally implicated PAR2 in systemic sensitisation as suppression of IgE and/or IgG responses in PAR2$^{-/-}$ mice is a common observation regardless of the experimental model (Schmidlin et al. 2002, Shichijo et al. 2006, Davidson et al. 2013, de Boer et al. 2014). However, those studies have also demonstrated a more complex role of PAR2 in AAD (Schmidlin et al. 2002, Takizawa et al. 2005, Shichijo et al. 2006). As such, Schmidlin et al. observed the diminished airway inflammation in PAR2$^{-/-}$ mice 24 hours after OVA challenge, but not 72 hours after the challenge despite the diminished IgE responses in PAR2$^{-/-}$ mice (Schmidlin et al. 2002). We too have observed reduced IgE responses in PAR2$^{-/-}$ mice, which might reflect a defect in sensitisation to HDM, even though B cells and IgE had been demonstrated dispensable for the development of allergic airway inflammation or AHR in our mouse HDM model (Raemdonck et al. 2016).

The mechanism behind the protective effect of PAR2 deficiency on allergic airway inflammation is not entirely clear. In our studies, type two cytokines remained unaffected by PAR2 deficiency. This is not uncommon as Redes et al. similarly observed a reduction in total BAL cell counts upon *Aspergillus fumigatus* challenge in PAR2$^{-/-}$ mice, but no changes in IL-4, IL-5 or IL-13 levels (Redes et al. 2019). However, the statistical power of those studies was limited and data on other cytokines or chemokines were not reported (Redes et al. 2019). PAR2 has been implicated in T cell development, differentiation and cytokine production (Shichijo et al. 2006, Francis et al. 2017). The involvement of PAR2 in T cell development has only been investigated in vitro and might not occur in vivo as T cell responses do not seem to be universal among different PAR2$^{-/-}$ mice strains (Schmidlin et al. 2002, Takizawa et al. 2005, Shichijo et al. 2006, Francis et al. 2017). However, we detected reduced levels of TNFα and MIP-1α in BAL of PAR2$^{-/-}$ mice. TNFα can modulate T cell activation and cytokine production (Matera et al. 2010), while MIP-1α is a potent chemotactic agent for lymphocytes, eosinophils and monocytes, including dendritic cells (Lukacs et al. 1995b, Holgate et al. 1997, Maurer and Von Stebut 2004). The lack of chemotactic cues could explain the diminished recruitment of eosinophils, lymphocytes and particularly moDCs in PAR2$^{-/-}$ mice (Lukacs et al. 1995b, Holgate et al. 1997, Pease and Williams 2001, Maurer and Von Stebut 2004, Matera et al. 2010). Another confounding factor could be impaired leukocyte rolling and migration in PAR2$^{-/-}$ mice (Lindner et al. 2000, Ebeling et al. 2007, Ramelli et al. 2010), particularly, as populations of

ILC2s, which are predominantly tissue resident and expand in situ, remained unaltered in PAR2$^{-/-}$ mice (Gasteiger et al. 2015, Moro et al. 2016, Mindt et al. 2018). A defective moDC recruitment into the lungs might be crucial for the protective effect of PAR2 deficiency as adoptive transfer of allergen-pulsed WT DCs into PAR2$^{-/-}$ recipients was alone sufficient for the initiation of allergic airway inflammation (Lewkowich et al. 2011).

The results from the PAR2 Ab study support the hypothesis that PAR2 modulates allergen sensitisation rather than immune responses during allergen challenge as administration of MEDI2344 during allergen challenge phase offered no protection against AHR or allergic airway inflammation, but rather enhanced it. We obtained similar results utilising rat OVA model of LAR, where MEDI2344 and PAR2 antagonist 18S-P2Pal failed to modulate OVA-induced LAR and airway inflammation (Flajolet 2021). In contrast to our findings, most publications have demonstrated that administration of PAR2 inhibitors during allergen challenge phase, including rabbit antiserum R5, PAR2 blocking antibody SAM-11 and PAR2 antagonists NPS-1577 and 18S-P2Pal, alleviated allergic airway inflammation and AHR in OVA and CE mouse models (Arizmendi et al. 2011, Asaduzzaman et al. 2015, Asaduzzaman et al. 2018). However, the administration of PAR2 activating peptides was reported to both enhance and reduce airway inflammation and AHR in various settings (De Campo and Henry 2005, Ebeling et al. 2005, D'Agostino et al. 2007) and the selectivity of available tools has been queried (McGuire et al. 2002, Stenton et al. 2002, Hollenberg et al. 2014, Yee et al. 2018). PAR2 activating peptides, for instance, have been shown to elicit PAR2 independent effects (McGuire et al. 2002, Stenton et al. 2002, Hollenberg et al. 2014, Yee et al. 2018) while PAR2 antibodies has been criticised for their poor sensitivity to detect PAR2 protein on cell membranes (Johansson et al. 2005, Adams et al. 2012, Lopez et al. 2014). In fact, PAR2 has been additionally proven a difficult receptor to target due to biased signalling (Hollenberg et al. 2014, Yau et al. 2016). Canonical activation of PAR2 has been linked to downstream GPCR signalling, however an alternative activation of PAR2 via β-arrestin recruitment is also possible and seems crucial for cell migration (Nichols et al. 2012, Hollenberg et al. 2014, Yee et al. 2018). Most of the available PAR2 inhibitors have been profiled against the conventional PAR2 signalling pathway and might thus fail to inhibit alternative pathways (Nichols et al. 2012, Hollenberg et al. 2014, Yau et al. 2016). Some PAR2 antagonists can even act as biased agonists, questioning their use (Nichols et al. 2012, Hollenberg et al. 2014, Yau et al. 2016).

The in vivo efficacy of PAR2 blocking antibody MEDI2344 had been previously validated in mechanical hyperalgesia model (unpublished data) and thus demonstrated a lack of role for PAR2 during allergen challenge. However, PAR2 signalling pathways in the HDM model, especially the alternative ones, and the ability of MEDI2344 to block them need to be further elucidated to confidently conclude that the lack of efficacy of MEDI2344 on allergic airway inflammation cannot be attributable to its inability to prevent PAR2 alternative signalling.

A difference in experimental design could also offer some explanation for the contrasting results between our PAR2 antibody study and the literature. Unlike our HDM model, the most commonly utilised CE and HDM models with mucosal sensitisation require high doses of allergens with intrinsic protease activity to elicit airway inflammation (Arizmendi et al. 2011, Davidson et al. 2013, Asaduzzaman et al. 2015, Asaduzzaman et al. 2018, Kim et al. 2019). The signalling pathways activated by allergen exposure in those models might thus differ substantially from our HDM model. In OVA models, on the other hand, immune responses may be modulated by LPS contamination and subsequent TLR signalling which can alter PAR2 signalling (Tsuchiya et al. 2012, Lee et al. 2017, Heuberger and Schuepbach 2019, Rayees et al. 2019). Difference in route of administration and pharmacokinetics could also affect the outcomes. A local rather than systemic administration has been advised to disrupt PAR2 signalling in the airways (Arizmendi et al. 2011, Davidson et al. 2013, Asaduzzaman et al. 2015, Asaduzzaman et al. 2018) as a systemic delivery of the antibodies was postulated insufficient to achieve PAR2 blockage (Arizmendi et al. 2011). In our study, we administered MEDI2344 subcutaneously as this was efficacious in in vivo validation studies. As instructed, 24 hours after antibody administration were given before the first HDM challenge to allow for absorption and systemic antibody distribution and additional doses were given every second day to maintain systemic antibody levels. As we were unable to evaluate the levels of MEDI2344 during the HDM study, the possibility that insufficient coverage was achieved yet remains.

Notwithstanding the amelioration of cellular inflammation in $PAR2^{-/-}$ mice, we found no evidence implicating PAR2 in the development of AHR, as Penh responses to 5-HT remained unaffected by PAR2 deficiency or MEDI2344. Additional assessment of airway resistance and lung compliance with invasive methods might be helpful in clarifying the role of PAR2 in AHR. Regardless, the role of PAR2 in airway function and AHR remains puzzling. In the healthy

airways stimulation of PAR2 was associated with bronchodilation (Cocks et al. 1999, Lan et al. 2000, Cicala et al. 2001) as well as a bronchoconstriction (Ricciardolo et al. 2000, Schmidlin et al. 2001), although we were unable to trigger bronchoconstriction with 2-Furoyl-LIGRLO-NH_2 in neither conscious rats nor mice (Flajolet 2021)(unpublished data). AAD models have generally demonstrated concomitant improvement of allergic airway inflammation and AHR by genetic or pharmacological disruption of PAR2 signalling (Arizmendi et al. 2011, Davidson et al. 2013, Asaduzzaman et al. 2015, Asaduzzaman et al. 2018). Even so, Redes et al. and Schimdlin et al. have failed to observe inhibition of AHR in $PAR2^{-/-}$ mice despite the improvement of allergic airway inflammation (Schmidlin et al. 2002, Redes et al. 2019). Over-stimulating PAR2 as an alternative approach has provided no clearer answers. Mice overexpressing PAR2 have developed worse AHR than their WT littermate controls (Schmidlin et al. 2002), however stimulation of PAR2 by PAR2 APs was associated with improved as well as worsened lung function in allergen exposed laboratory animals (De Campo and Henry 2005, Ebeling et al. 2005, D'Agostino et al. 2007). These diverse outcomes might be explained by the involvement of PAR2 in multiple downstream pathways as well as the lack of well characterised pharmacological tools (Hollenberg et al. 2014, Yau et al. 2016). They also serve as a reminder that further investigation into PAR2 and the tools to target it are needed before PAR2 can be successfully targeted in disease (Yau et al. 2016).

The results presented in this chapter demonstrated a potential role of PAR2 in the development of HDM-induced allergic airway inflammation, but not AHR, however further work is needed to establish the link between PAR2 and TRPV4. In a mechanical hyperalgesia model, TRPV4 could only be activated by a combination of inflammatory mediators (Alessandri-Haber et al. 2006). While investigations into PAR2-TRPV4 link in the nervous system have suggested that PAR2 activation can either result in opening of TRPV4 channels via receptor operation gating or sensitisation of the channel (Grant et al. 2007, Poole et al. 2013, Grace et al. 2014b, Zhao et al. 2014, Zhao et al. 2015), multiple stimuli might be needed for TRPV4 activation. A recent study has also demonstrated that TRPV4 can be activated upon allergen exposure independently of PAR2 and disruption of epithelial junctions by allergen proteases alone can be sufficient for activation of TRPV4 (Wiesner et al. 2020).

In conclusion, PAR2 might be partially responsible for the detrimental effects of TRPV4 activation during allergen sensitisation rather than allergen challenge phase. Alternative

mechanisms of TRPV4 activation, particularly during allergen challenge phase, leading to the development of allergic airway inflammation and AHR are yet to be elucidated.

6. The effect of pharmacological inhibition of TRPV4 during allergen challenge in allergic airway disease models

6.1. Introduction

There is increasing body of evidence implicating TRPV4 in asthma pathogenesis (Birrell et al. 2016, Gombedza et al. 2017, Yao et al. 2019, Duan et al. 2020, Wiesner et al. 2020). In our laboratory we have previously demonstrated that TRPV4 inhibition strikingly abolished characteristic features of AAD, including allergic airway inflammation and allergen-associated airway responses in murine and rat models of AAD (Birrell et al. 2016). Aiming to elucidate the mechanisms of TRPV4 signalling in AAD, we have demonstrated that $CD4^+$ T cells, ILC2s or DCs, the immune cells critical for HDM-induced responses in our murine AAD model, could be responsible for TRPV4 signalling in this model (Chapter 3). Investigations into downstream TRPV4 targets have uncovered P2X7 as a receptor potentially regulating allergic airway inflammation downstream of TRPV4 (Chapter 4). Alike, PAR2 was demonstrated to modulate allergic airway inflammation, preferably during sensitisation rather allergen challenge phase, and could be partially responsible for TRPV4 activation (Chapter 5).

Nevertheless, several aspects of the proposed TRPV4 role in AAD (Birrell et al. 2016) remain unanswered. For instance, we were unable to decipher the TRPV4 signalling pathway regulating AHR in the murine HDM model as P2X4, P2X7 and PAR2 were all dispensable for the development of AHR (Chapter 4, 5). In addition, whilst PAR2 deficiency alleviated allergic airway inflammation, the administration of a PAR2 blocking antibody during allergen challenge phase had no effect on allergic airway inflammation nor AHR, suggesting the importance of PAR2 during sensitisation rather than allergen challenge (Chapter 5). In the preliminary study, $TRPV4^{-/-}$ mice failed to develop HDM-induced IgE (Birrell et al. 2016), supporting the association between TRPV4 gain-of-function polymorphisms with allergen sensitisation (Wiesner et al. 2020).

The administration of the TRPV4 antagonist GSK2193874 (GSK219) during allergen challenge in the rat OVA model have additionally implicated TRPV4 in the development of allergic airway inflammation and LAR (Birrell et al. 2016). TRPV4 has been previously implicated in bronchospasm and associated with AHR in clinical gene association studies as well as pre-clinical mechanistic studies (McAlexander et al. 2014, Naumov et al. 2016, Yao et al. 2019, Bonvini et al. 2020). However, the high dose of GSK219 used in the rat OVA study has raised concerns about the potential off-target rather than TRPV4-selective effects on LAR and airway inflammation (Birrell et al. 2016). Therefore, it remains unclear whether TRPV4 activation

occurs during allergen sensitisation or allergen challenge phase, and whether this regulates the development of allergic airway inflammation, allergen-induced airway responses or both.

6.2. Hypothesis and aims

We hypothesised that selective inhibition of TRPV4 during the allergen challenge phase alleviates the development of allergic airway inflammation as well as airway responses, including AHR and LAR, in murine HDM and rat OVA models of AAD, respectively.

We aimed to:

- Characterise and validate TRPV4 antagonists in murine and rat PD and PK models,
- Investigate the efficacy of TRPV4 antagonists during the development of allergic airway inflammation and AHR in murine HDM model of AAD,
- Investigate the efficacy of TRPV4 antagonists during the development of allergic airway inflammation and LAR in rat OVA model of AAD.

6.3. Methods

This section outlines in vivo studies and main methods used in this chapter. All the experimental procedures are described in detail in Chapter 2.

6.3.1. Validation of TRPV4 antagonists

6.3.1.1. Determination of IC_{50} in human, rat, guinea pig and mouse models

GSK2193874 (GSK219) and GSK2798745 (GSK279) half-maximal inhibitory concentration (IC_{50}) was determined in human, rat, GP and mouse models. Utilising Fluorescence Imaging Plate Reader (FLIPR) assays IC_{50} was determined for TRPV4-induced intracellular Ca^{2+} mobilisation in human ASM or Chinese hamster ovary (CHO) cells expressing human, rat, GP or mouse TRPV4 receptors, respectively (performed by AstraZeneca (Research & Early Development, Respiratory & Immunology, BioPharmaceuticals R&D)). Utilising vagal nerve depolarisation technique, IC_{50} for TRPV4-induced vagal nerve depolarisation was determined in rat and GP (performed by Dr Sara Bonvini). IC_{50} values are presented as pIC_{50}.

6.3.1.2. Characterisation of GSK2798745 in murine TRPV4 PD model

6.3.1.2.1. GSK2798745 dose response

Female C57BL/6J mice were administered vehicle (2% DSPE-PEG in 5% mannitol) or GSK279 (0.3 – 30 mg/kg) by oral gavage (5 ml/kg) two hours before challenge. Mice were placed in

whole body plethysmography chambers and 20-minute baseline Penh was recorded prior to challenge. Mice were then challenged with aerosolised vehicle (1% ethanol + 1% Tween 80 in saline) or GSK1016790A (GSK101) (30 µg/ml) for 10 minutes and Penh recorded for 20 minutes. Mice were sacrificed upon the completion of the experiment and blood was collected for the PK assessment of GSK279, where free blood plasma levels were analysed by mass spectrometry (performed by Early Respiratory and Immunology, AstraZeneca).

GSK101 Penh responses were extensively characterised in our laboratory in rat and GP in vivo models as well as mouse in vitro assays (Bonvini et al. 2016, Flajolet 2021). In guinea pigs 30 µg/ml caused a submaximal response in a cough study (Bonvini et al. 2016) and was selected for murine in vivo studies. GSK279 dosing regimen was chosen based on a pilot PK study conducted by Early Respiratory and Immunology, AstraZeneca, demonstrating maximal GSK279 free plasma levels were reached 2 hours after oral administration of the compound.

6.3.1.2.2. GSK2798745 time course study

Female C57BL/6J mice were administered vehicle (2% DSPE-PEG in 5% mannitol) or GSK279 (10 mg/kg) by oral gavage (5 ml/kg) 2, 6, 12, 16, and 24 hours before challenge. Prior to challenge mice were placed in whole body plethysmography chambers and 20-minute baseline Penh was recorded. Mice were then challenged with aerosolised vehicle (1% ethanol + 1% Tween 80 in saline) or GSK101 (30 µg/ml) for 10 minutes and Penh recorded for 20 minutes. Mice were sacrificed upon the completion of the experiment and blood collected for PK analysis of GSK279 plasma concentrations by mass spectrometry (performed by Early Respiratory and Immunology, AstraZeneca).

6.3.1.3. Characterisation of GSK2193874 in rat TRPV4 PD model

Male Brown-Norway rats were administered vehicle (6% Cavitron/2-Hydroxypropyl-β-cyclodextrine in saline) or GSK219 (0.01 - 300 mg/kg) by intraperitoneal injection (10 ml/kg) one hour before challenge. Rats were placed in whole body plethysmography chambers and 20-minute baseline Penh recording was obtained. Rats were then challenged with aerosolised vehicle (1% ethanol + 1% Tween 80 in saline) or selective TRPV4 agonist GSK101 (10 µg/ml) for 10 minutes and Penh monitored for 20 minutes. Upon completion of the challenge rats were sacrificed and blood collected for PK analysis of GSK279 plasma concentrations by mass spectrometry (performed by Early Respiratory and Immunology, AstraZeneca).

GSK101 concentration response was previously characterised in BN rats in our laboratory and 10 µg/ml was chosen as submaximal concentration in subsequent studies (Flajolet 2021). GSK219 pre-dose time was previously characterised in guinea pig cough studies (Bonvini et al. 2016) and was matched with the preliminary rat OVA study investigating the effect of GSK219 dosed at 300 mg/kg on LAR and airway inflammation (Birrell et al. 2016).

6.3.1.4. Characterisation of GSK2798745 in rat TRPV4 PD model

Male Brown-Norway rats were administered vehicle (2% DSPE-PEG in 5% mannitol) or GSK279 (dose response 0.03 – 3 mg/kg) by oral gavage (2 ml/kg) two hours before challenge. Prior to challenge rats were placed in whole body plethysmography chambers and a 20-minute baseline Penh was recorded. Rats were then challenged with aerosolised vehicle (1% ethanol + 1% Tween 80 in saline) or GSK101 (10 µg/ml) for 10 minutes. Penh was monitored throughout the challenge for a total of 20 minutes. Upon completion of the challenge rats were sacrificed and blood collected for PK analysis of GSK279 plasma concentrations by mass spectrometry (performed by Early Respiratory and Immunology, AstraZeneca).

The pre-dose time of GSK279 was selected based on a pilot PK study conducted by Early Respiratory and Immunology, AstraZeneca, indicating that maximal plasma levels were achieved 2 hours after oral administration of the drug.

6.3.2. TRPV4 antagonists in murine HDM model

Female C57BL/6J mice were sensitised to HDM on days 0 and 14 and challenged with saline or HDM on days 24, 25 and 26. AHR and airway inflammation were assessed on day 29. Throughout the challenge phase and until the completion of the study mice were administered GSK279 (0.3 – 30 mg/kg) or its vehicle (2% DSPE-PEG in 5% mannitol) by oral gavage (5 ml/kg) twice daily (morning and evening dose were 10 hours apart). On the days of the challenge mice received the treatment 2 hours before the challenge. On day 29, mice received their final dose 2 hours before AHR assessment. Alongside, a separate group received budesonide (3 mg/kg, p.o.) as a positive control twice daily (10 hours apart) whilst receiving no GSK279 vehicle. Budesonide was administered 1 hour before challenge on days 24-26 as well as 1 hour prior to AHR assessment on day 29. Study is schematically summarised in Figure 6.1, while study groups are detailed in Table 6.1.

Whole body plethysmography was used to monitor the responses to increasing concentrations of 5-HT (saline, 1, 3, 10 mg/ml). Upon completion of AHR assessment, mice were sacrificed and blood, BAL and lung samples collected. Blood samples were used for the determination of GSK279 plasma levels by mass spectrometry (Early Respiratory and Immunology, AstraZeneca). BAL cells were isolated and total leukocyte numbers determined by an automated cell counter (Sysmex XT-300). Leukocyte populations were differentiated based on the expression of surface and transcription markers by flow cytometry (analysed on Fortessa). Lung were enzymatically digested to obtain lung cell suspension. Lung total leukocytes were determined by an automated cell counter (Sysmex XT-300), while leukocyte populations were discriminated based on the surface and transcription markers by flow cytometry (analysed on Fortessa).

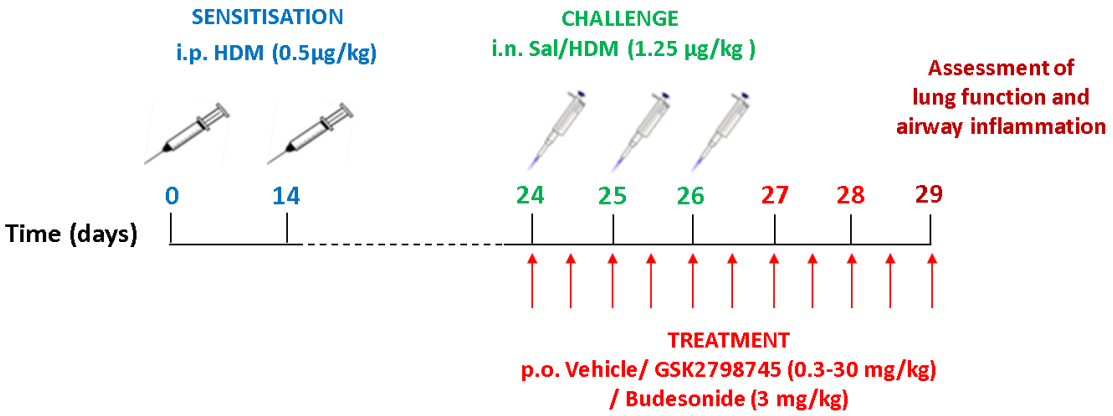


Figure 6.1: A schematic representation of the study investigating the effect of GSK2798747 on house dust mite (HDM)-induced allergic airway inflammation and airway hyper-responsiveness (AHR) in murine allergic airway disease model.

Mice were sensitised to HDM on days 0 and 14 and challenged with HDM or saline on days 24-26. From days 24-29 mice were treated with GSK2798745, GSK2798745 vehicle or budesonide twice daily. On day 29 AHR and airway inflammation were assessed.

Table 6.1: Experimental groups in a study investigating TRPV4 antagonist GSK2798745 in the murine house dust mite (HDM) model.

A group treated with budesonide received no GSK2798745 vehicle. No groups were administered budesonide vehicle. N/A – non-applicable

Group	Challenge	GSK2798745 (mg/kg)	Budesonide (mg/kg)
1	Saline	Vehicle	N/A
2	Saline	30	N/A
3	HDM	Vehicle	N/A
4	HDM	0.3	N/A
5	HDM	0.1	N/A
6	HDM	3	N/A
7	HDM	10	N/A
8	HDM	30	N/A
9	HDM	N/A	3

6.3.3. TRPV4 antagonists in rat OVA model

Male Brown-Norway rats were i.p. injected with OVA with Alum on days 0, 14 and 21 and challenged with aerosolised saline or OVA for 30 minutes on day 28. On the day of the challenge rats were briefly anaesthetised and administered the following treatments (Table 6.2):

- GSK279 (dose response 0.03 – 3 mg/kg) or its vehicle (2% DSPE-PEG in 5% mannitol) by oral gavage (2 ml/kg) 2 hours before and 30 minutes after challenge,
- GSK219 (dose response 0.03 – 3 mg/kg) or its vehicle (6% Cavitron/2-Hydroxypropyl-β-cyclodextrine in saline) by intraperitoneal injection (10 ml/kg) 1 hour before and 30 minutes after challenge.
- A positive control GSK219 at 300 mg/kg i.p. (dose shown to inhibit the LAR in previous studies (Birrell et al. 2016)) one hour before and 30 minutes after challenge.
- A positive control Budesonide (3 mg/kg) or vehicle (0.2 mg/ml polysorbate 80, 0.28 mg/ml citric acid, 0.5 mg/ml sodium citrate dihydrate, 8.5 mg/ml sodium chloride in water) was intratracheally dosed (1ml /kg) one hour before the challenge.

One hour after the challenge rats were placed in whole body plethysmography chambers and Penh was monitored for 5 hours. 24 hours after the challenge animals were sacrificed and BAL collected for subsequent analyses. An automated cell counter (Sysmex XT-300) was used to determine total leukocyte number in BAL, while leukocytes were differentiated based on their histological appearance.

Table 6.2: Experimental groups in a study investigating TRPV4 antagonists GSK2193874 and GSK2798745 in the rat Ovalbumin (OVA) model.

Budesonide treatment served as a positive control.

Group	Challenge	GSK2193874 (mg/kg)	GSK2798745 (mg/kg)	Budesonide (mg/kg)
1	Saline	Vehicle	Vehicle	Vehicle
2	Saline	3	Vehicle	Vehicle
3	Saline	Vehicle	3	Vehicle
4	Ovalbumin	Vehicle	Vehicle	Vehicle
5	Ovalbumin	0.03	Vehicle	Vehicle
6	Ovalbumin	0.1	Vehicle	Vehicle
7	Ovalbumin	0.3	Vehicle	Vehicle
8	Ovalbumin	1	Vehicle	Vehicle
9	Ovalbumin	3	Vehicle	Vehicle
10	Ovalbumin	Vehicle	0.03	Vehicle
11	Ovalbumin	Vehicle	0.01	Vehicle
12	Ovalbumin	Vehicle	0.3	Vehicle
13	Ovalbumin	Vehicle	1	Vehicle
14	Ovalbumin	Vehicle	3	Vehicle
15	Ovalbumin	300	Vehicle	Vehicle
16	Ovalbumin	Vehicle	Vehicle	3

6.4. Results

6.4.1. Determination of IC_{50} in human, rat, guinea pig and mouse models

To determine the potency of GSK219 and GSK279, respectively, IC_{50} on TRPV4-induced intracellular Ca^{2+} mobilisation was determined by a FLIPR assay on human ASM or CHO cells expressing human, rat, GP or mouse TRPV4 receptors. The vagal nerve depolarisation technique was used to determine potency of a native ion channel in a tissue environment. Only GSK279 was tested on murine TRPV4 receptors in CHO FLIPR assay. The results are presented in Table 6.3 and demonstrated a good agreement of potency across the different assays for both compounds, with the exception of the GP vagal nerve depolarisation where GSK219 appears to be a log fold less potent. Our results are in agreement with GSK279 and GSK219 potency on human and rat TRPV4 receptors (Thorneloe et al. 2012, Brooks et al. 2019, Xu et al. 2021).

Table 6.3: pIC_{50} in human, rat, guinea pig (GP) and mouse determined by airway smooth muscle cell (ASMC) or Chinese hamster ovary cell (CHO) Fluorescence Imaging Plate Reader (FLIPR) assays or vagal nerve depolarisation technique (Vagus).

	pIC_{50}						
Compound	Human ASM FLIPR	Human CHO FLIPR	Rat CHO FLIPR	Rat Vagus	GP CHO FLIPR	GP Vagus	Mouse CHO FLIPR
GSK2798745	9.4	8.4	8.83	8.9	7.97	9.3	7.96
GSK2193874	7.81	7.71	8.54	8.1	7.28	6.1	N/A

6.4.2. Characterisation of GSK2798745 in murine TRPV4 PD model

In mice, GSK101 challenge resulted in increased Penh values relative to saline challenge. GSK279 inhibited GSK101-induced responses in a dose dependent manner which was statistically significant at doses 3 mg/kg and higher (Figure 6.2A). A dose-related increase of free GSK279 levels was observed in plasma and the levels achieved were above the in vitro IC_{50} at all doses (Table 6.). In vehicle treated animals GSK279 was below the lower limit of quantification (LLOQ) of 13 nM in all but 4 animals. In these cases, GSK279 levels were just above LLOQ and considerably lower to the levels in 0.3 mg/kg dosed animals, indicating

sample contamination during the analysis (Figure 6.2B). In accordance with these results, GSK279 0.3 to 30 mg/kg were chosen for the subsequent murine HDM study.

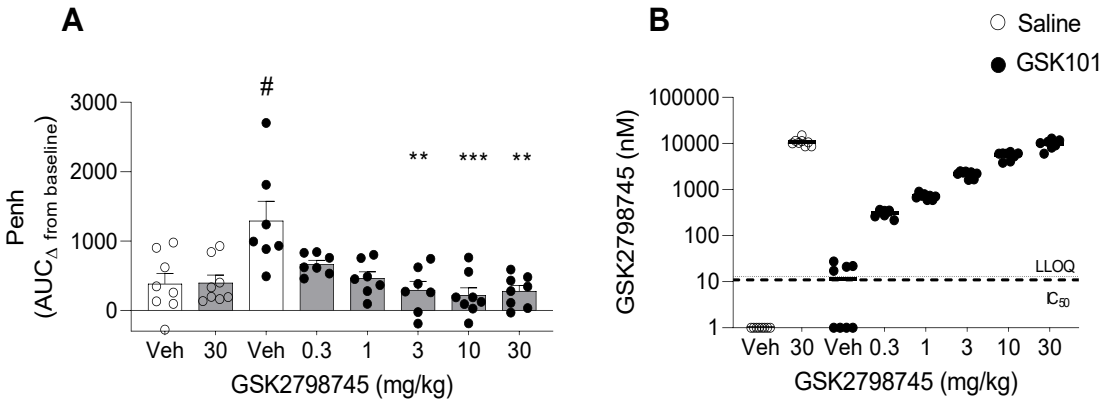


Figure 6.2: GSK2798745 dose response in murine TRPV4 pharmacodynamic (PD) model.

Mice were administered vehicle or GSK2798745 (GSK279; 0.3 – 30 mg/kg) by oral gavage (p.o.). Two hours later mice were exposed to nebulised vehicle or GSK1016790A (GSK101; 30µg/ml) for 10 minutes and enhanced pause (Penh) was monitored for 20 minutes using whole body plethysmography. 20-minute baseline recording was recorded prior to the challenge. A) Difference in Penh area under the curve (AUC) between baseline and challenge. B) GSK279 free plasma levels. Levels of GSK279845 in vehicle treated mice were below lower limit of quantification (LLOQ) and were assigned value of 1 nM for visualisation purposes. Data from a single experiment are presented as mean ± S.E.M with N=8 mice per group. # denotes $p<0.05$ comparing vehicle/vehicle with vehicle/GSK101 groups using Mann-Whitney U-test. ** denotes $p<0.01$ and *** $p<0.001$ comparing vehicle/GSK101 with GSK279/GSK101 groups using Kruskal-Wallis test with Dunn's multiple comparisons test. IC_{50} – half-maximal inhibitory concentration as determined in vitro.

Next, we evaluated the duration of GSK279 efficacy in a time course study. Mice were given a single dose of GSK279 and were challenged with saline or GSK101 2, 6, 12, 16, and 24 hours after the dosing. Compared to saline, GSK101 triggered an increase in Penh in vehicle treated mice at all time points. GSK279 inhibited GSK101-induced responses at 2, 6 and 12 hours, but no longer 16 or 24 hours after the dosing. GSK279 alone had no effect on Penh responses during saline challenge (Figure 6.3A). The analysis of free plasma GSK279 concentration confirmed a time-dependant decline in GSK279 levels which fell below 10-times IC_{50} values after 16 hours (Figure 6.3, Table 6.3). In GSK279 treated animals, levels were comparable between corresponding saline and GSK101 challenged groups. In vehicle treated animals GSK279 concentration was below LLOQ and is not shown (Figure 6.3B). These results indicated

that administration of GSK279 twice a day (ideally 12 hours apart) would be needed to achieve continuous inhibition of TRPV4.

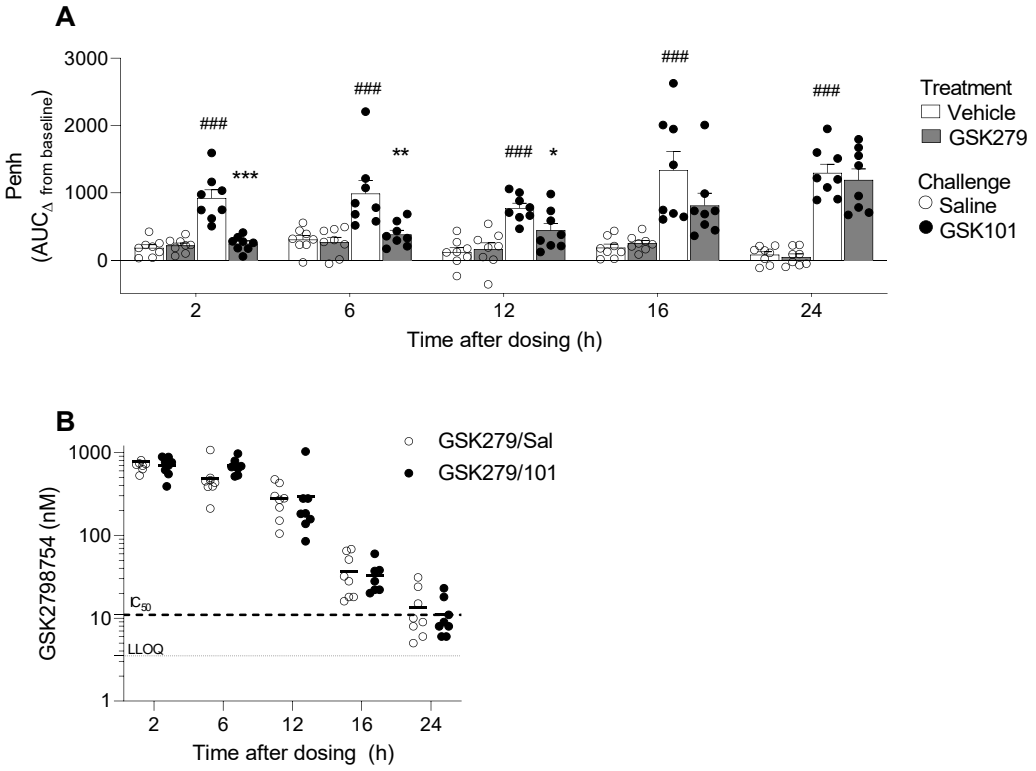


Figure 6.3: The duration of GSK2798745 efficacy in murine TRPV4 pharmacodynamic (PD) model.

Mice were administered vehicle or GSK279 10 mg/kg. Enhanced pause (Penh) responses to nebulised GSK101 (30 µg/ml) or vehicle were evaluated 2, 6, 12, 16 and 24 hours later. 20-minute baseline was recorder prior to the challenge. A) Penh presented as a change in area under the curve (AUC) between baseline and challenge. D) GSK2798745 free plasma levels. Data from a single experiment are presented as mean ± S.E.M with N=8 mice per group. ### denotes $p<0.001$ comparing vehicle/vehicle with vehicle/GSK101 groups using Mann-Whitney U-test. * denotes $p<0.05$, **$p<0.01$ and *** $p<0.001$ comparing vehicle/GSK101 with GSK279/GSK101 groups with Mann-Whitney U-test. IC_{50} – half-maximal inhibitory concentration as determined in vitro. LLOQ – half-maximal inhibitory concentration

6.4.3. The effect of TRPV4 antagonists in murine HDM model of AAD

Having demonstrated the efficacy of GSK279 in the murine TRPV4 PD model, we next investigated the efficacy of GSK279 on HDM-induced airway inflammation and AHR in the murine HDM model of AAD.

7.2.1.1. The effect of GSK279 on HDM-induced airway inflammation

In comparison to saline challenged vehicle treated mice (VEH/SAL), HDM challenge of vehicle treated mice (VEH/HDM) was associated with increased total BAL leukocyte numbers, characterised by elevated numbers of eosinophils, CD4+ T cells, CD8+ T cells and ILC2s, while AM and neutrophil numbers remained unchanged. Budesonide treatment abolished HDM-triggered airway inflammation as total leukocyte numbers as well as numbers of eosinophils, CD4+ T cells, CD8+ T cells and ILC2s were diminished to the levels observed in saline challenged animals. The responses of GSK279 treated HDM challenged animals were not statistically different to VEH/HDM group, although a dose-dependent trend towards reduced total leukocyte as well as eosinophil and CD4+ T cell numbers in BAL was observed. Additionally, there was a tendency towards increased BAL neutrophilia with GSK279 treatment, particularly at doses 1 and 30 mg/kg (Figure 6.4).

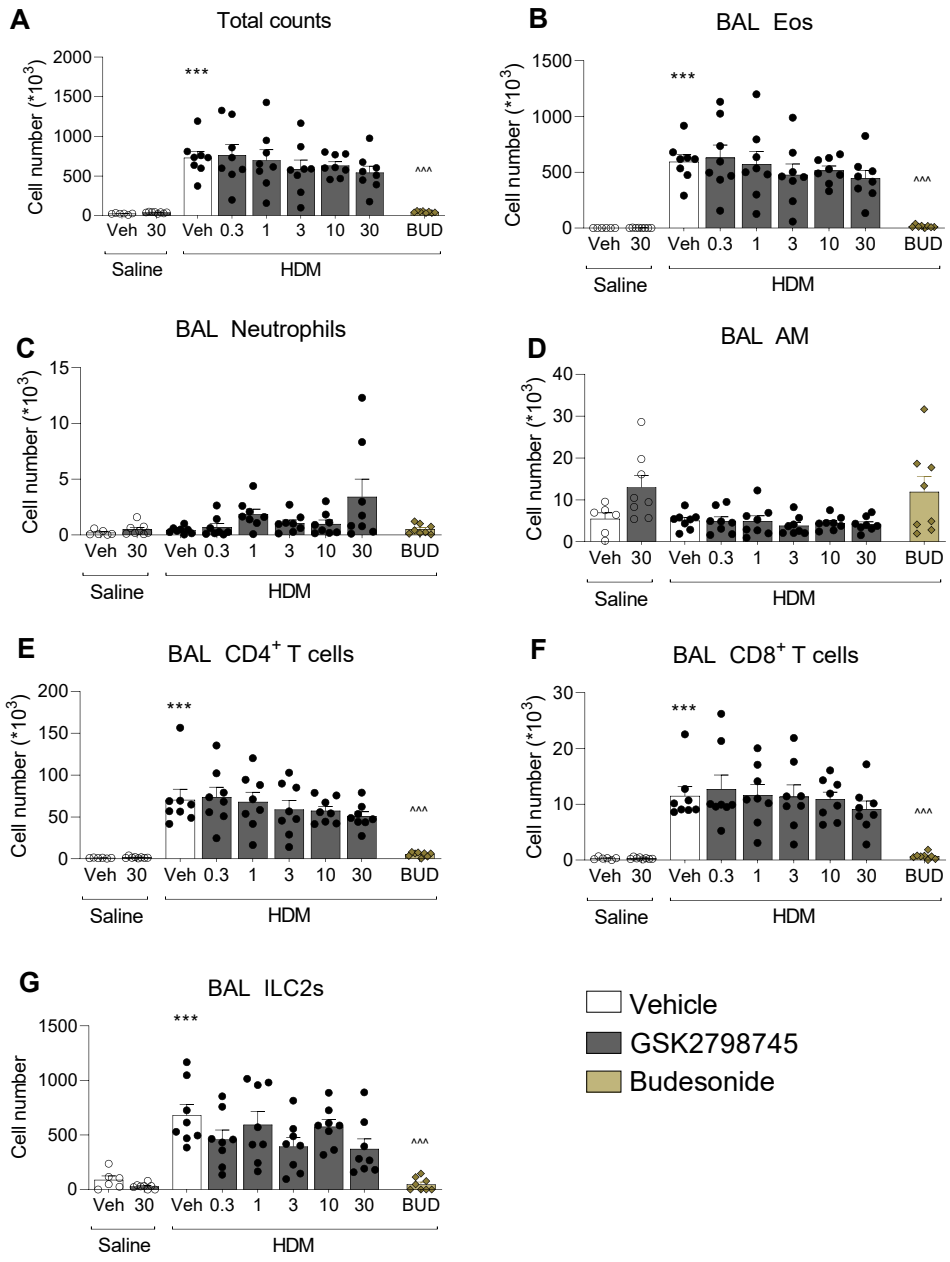


Figure 6.4: The efficacy of TRPV4 antagonist on allergic airway inflammation in the murine house dust mite (HDM) model.

Mice were sensitised to HDM on days 0 and 14 and on days 24 to 26 mice daily challenged with HDM or saline. On days 24 to 29 mice were administered GSK2798745 (GSK279; 0.3 – 30 mg/kg) or its vehicle twice daily via oral gavage (p.o.) A separate group received budesonide (3 mg/ml, p.o.) twice daily. On day 29 mice were sacrificed and bronchoalveolar lavage (BAL) obtained. A) BAL total leukocyte numbers as determined by an automated cell counter. BAL B) eosinophils, C) neutrophils, D) alveolar macrophages (AM), E) $CD4^+$ T cells, F) $CD8^+$ T cells, and G) group 2 innate lymphoid cells (ILC2s) as differentiated based on the expression of surface and transcription markers using flow cytometry. Data from a single experiment are presented as mean ± S.E.M with N=8 mice per group. *** denotes $p<0.001$ comparing vehicle/saline and vehicle/HDM groups using

Mann-Whitney U-test. ^^^ denotes p<0.001 comparing vehicle/HDM and budesonide/HDM groups using Mann-Whitney U-test. Kruskal-Wallis test with Dunn's multiple comparisons test was used to compare GSK279/HDM challenged groups with vehicle/HDM control group.

7.2.1.2. The effect of GSK279 on HDM-induced lung inflammation

In comparison to VEH/SAL mice, VEH/HDM mice exhibited increased lung total leukocyte numbers, including eosinophils, AM, $CD4^+$ T cells, ILC2s, moDCs and cDC2s. In addition, HDM challenge was associated with reduced neutrophil and unchanged $CD8^+$ T numbers. Budesonide treatment abolished HDM-induced elevation in total leukocyte numbers as well as changes in individual leukocyte populations and reduced $CD8^+$ T cell numbers as compared to VEH/HDM group. GSK279 treatment failed to modulate HDM-induced changes in total leukocyte numbers or changes in eosinophil, AM, $CD4^+$ T cell, ILC2, moDC and cDC2 populations in respect to VEH/HDM. However, at 1 and 30 mg/kg GSK279 was associated with statistically significant increase in lung neutrophil numbers. In saline challenged mice, GSK279 had no effect on lung leukocyte populations compared to VEH/SAL control group (Figure 6.5).

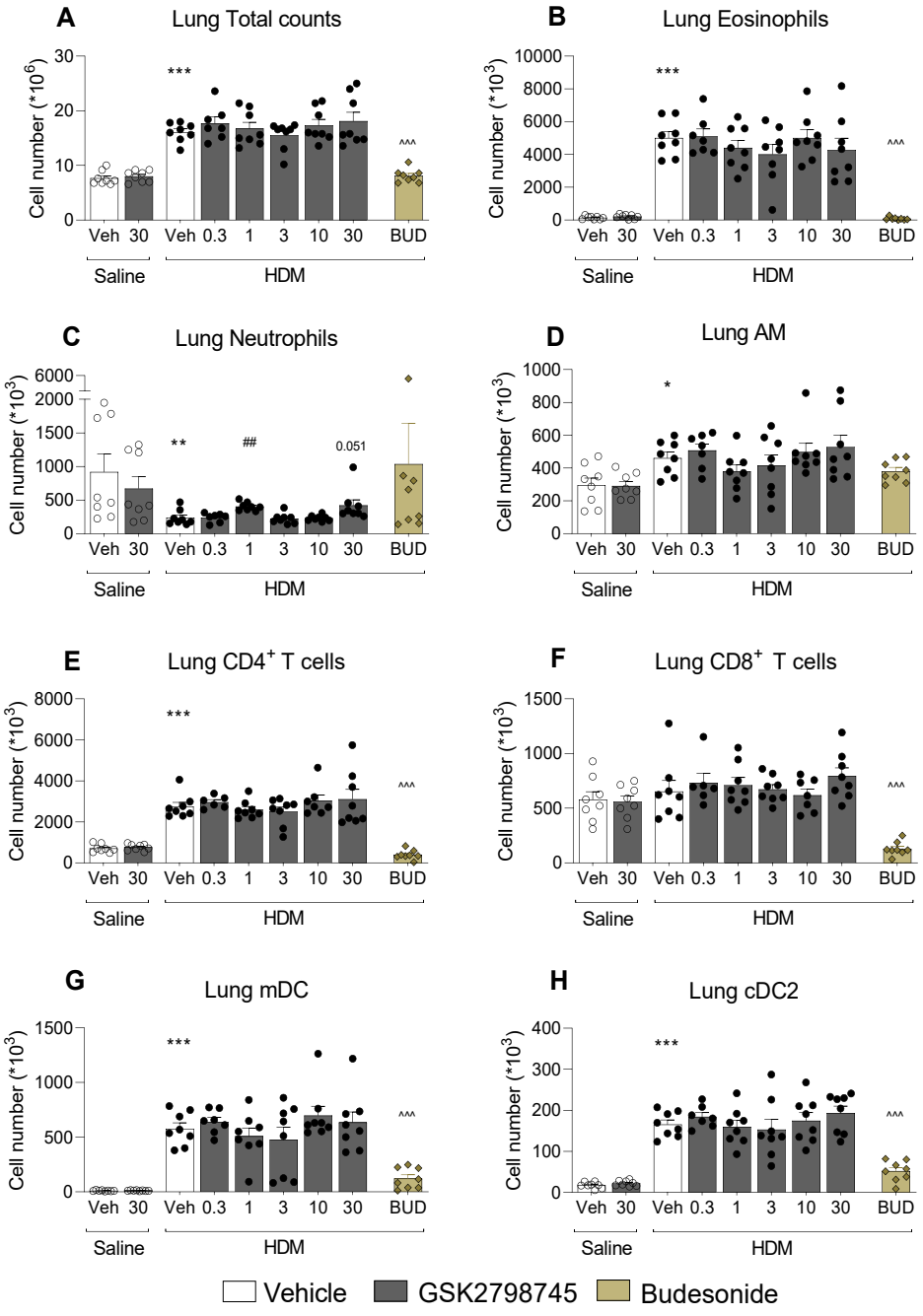


Figure 6.5: The efficacy of TRPV4 antagonist on allergic lung inflammation in the murine house dust mite (HDM) model.

Mice were sensitised to HDM on days 0 and 14 and on days 24 to 26 mice challenged with HDM or saline. On days 24 to 29 mice were administered GSK2798745 (GSK279; 0.3 – 30 mg/kg) or its vehicle twice daily via oral gavage (p.o.). A separate group was administered budesonide (3 mg/ml, p.o.) twice daily. On day 29 mice were sacrificed, lungs collected and enzymatically digested. A) Lung total leukocyte numbers as determined by an automated cell counter. B) Lung eosinophils, C) neutrophils, D) alveolar macrophages (AM), E) $CD4^+$ T cells, F) $CD8^+$ T cells, G) group 2 innate lymphoid cells (ILC2s), H) monocyte-derived dendritic cells (moDCs), I) classical dendritic cells type2 (cDC2) and J) cDC1s as differentiated based on the expression of surface and transcription

markers using flow cytometry. Data from a single experiment are presented as mean ± S.E.M with N=8 mice per group. * denotes p<0.05, ** p<0.01 and *** p<0.001 comparing vehicle/saline and vehicle/HDM groups using Mann-Whitney U-test. ^^^ denotes p<0.001 comparing vehicle/HDM and budesonide/HDM groups using Mann-Whitney U-test. Kruskal-Wallis test with Dunn's multiple comparisons test was used to compare GSK279/HDM groups with vehicle/HDM control group.

7.2.1.3. The effect of GSK279 on HDM-induced AHR

Lastly, the ability of GSK279 to modulate AHR was also evaluated. Mice were placed in whole body plethysmography chambers and exposed to increasing concentrations of 5-HT while monitoring Penh. GSK279 or its vehicle were administered 2 hours before the assessment and budesonide was administered one hour before the assessment. Escalating concentrations of 5-HT led to increased Penh responses in all groups, however the responses of VEH/HDM mice were no different to VEH/SAL mice. Comparison of saline and HDM challenged GSK279 treated mice indicated that responses of 1 and 10 mg/ml GSK279 treated HDM challenged mice were statistically significantly larger to 30 mg/kg GSK279 treated saline challenged mice. However, due to the absence of an enhanced responsiveness to 5-HT in VEH/HDM group compared to VEH/SAL group, GSK279 treated HDM challenged groups could not be compared to VEH/HDM group. (Figure 6.6A). Analysis of GSK279 free plasma levels after the AHR assessment confirmed that expected GSK279 levels were achieved and indicated that approximately 60-times IC_{50} were reached at 30 mg/kg (Figure 6.6B).

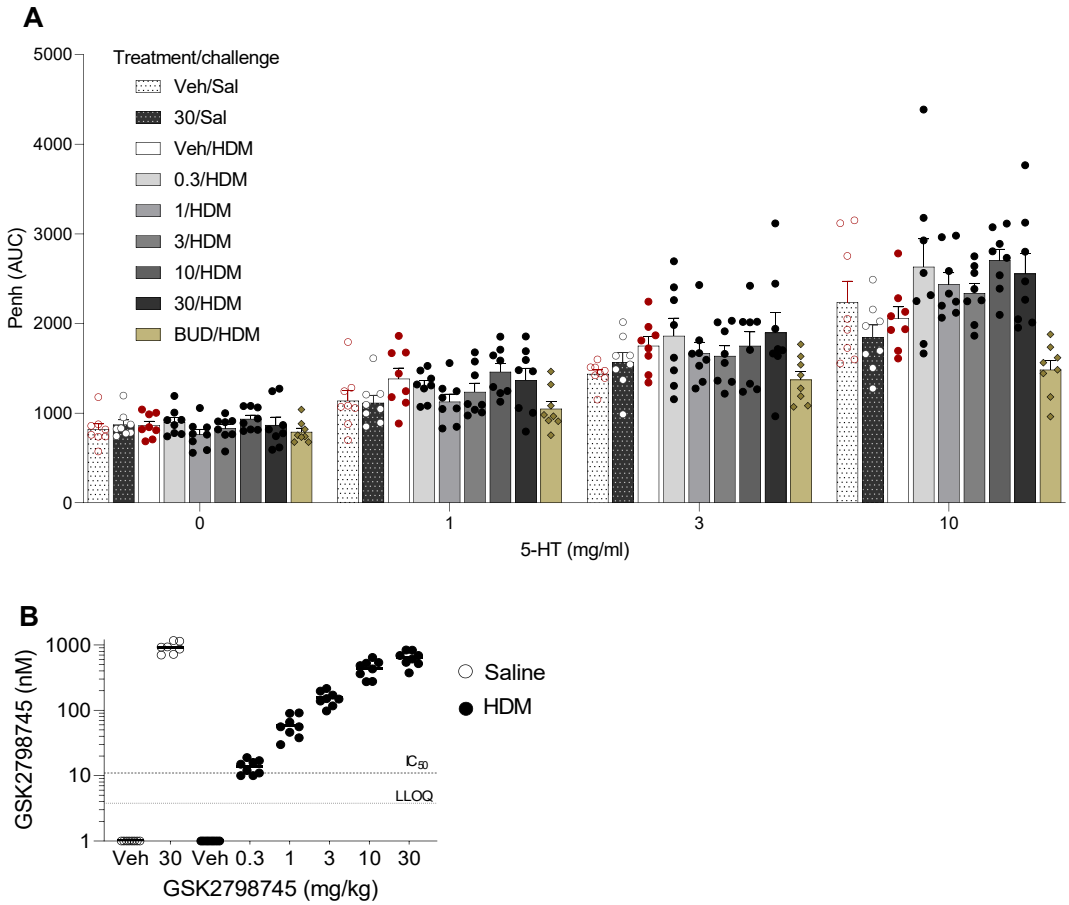


Figure 6.6: The efficacy of TRPV4 antagonist on airway hyper-responsiveness (AHR) in murine house dust mite (HDM) model.

Mice were sensitised to HDM on days 0 and 14. On days 24 to 26 mice were challenged with HDM or saline. On days 24 to 29 mice were administered GSK2798745 (GSK279; 0.3 – 30 mg/kg, p.o.) or its vehicle twice daily. A separate group was administered budesonide (BUD; 3 mg/ml, p.o.) twice daily. On day 29 mice received their last GSK279 or BUD treatment 2 or 1 hour before AHR assessment, respectively. Mice were placed in whole plethysmography chambers and exposed to saline, followed by escalating concentrations of serotonin (5-HT; 1, 3 and 10 mg/ml) whilst continuously recording enhanced pause (Penh). A) Penh presented as area under the curve (AUC). B) At the end of the experiment plasma was collected and GSK279 free plasma levels determined by mass spectrometry. In vehicle treated mice GSK279 levels were below lower limit of quantification (LLOQ) and were assigned value of 1 nM for visualisation purposes. Data from a single experiment summarised as mean ± S.E.M. (N=8 mice/group). IC_{50} – half-maximal inhibitory concentration.

6.4.4. Characterisation of GSK2193874 in rat PD model

Despite the promising preliminary data with TRPV4$^{-/-}$ mice (Birrell et al. 2016), limited efficacy of GSK279 was seen in the murine HDM model. Thus, the role of TRPV4 in AAD was further

investigated in the rat OVA model, where GSK219, albeit at a high dose, had been previously shown to supress allergic airway inflammation and LAR (Birrell et al. 2016).

To characterise the efficacy of GSK219 in the rat, GSK219 was probed in the rat TRPV4 PD model. Rats were exposed to either saline or the selective TRPV4 agonist GSK101 and airway responses monitored by whole body plethysmography. Compared to saline, GSK101 challenge triggered a statistically significant increase in Penh in vehicle treated animals. In the initial study testing GSK219 in dose range of 1 – 300 mg/kg, an inhibition of GSK101-induced responses was observed in groups receiving doses of 10 mg/kg or higher (Figure 6.7A). In order to obtain a full dose response, rats were administered GSK219 in dose range 0.1 – 30 mg/kg in the subsequent study. GSK219 suppressed GSK101-induced responses in a dose dependent manner which was statistically significant at doses 0.3 mg/kg and higher (Figure 6.7B). GSK219 at the highest dose had no effect on saline-induced responses in either of the studies. The assessment of GSK219 free plasma concentrations indicated that plasma levels achieved for all doses were above the IC_{50} determined in rat CHO FLIPR assays (2.88 nM) or vagal depolarisation technique (7.94 nM) (Table 6.3). GSK219 could not be detected in vehicle treated groups (LLOQ was 0.19 nM). GSK219 levels were above LLOQ for all other experimental groups and reached 25-times vagal IC_{50} at 3 mg/kg (Figure 6.7C). GSK219 doses ranging from 0.03 to 3 mg/kg were selected for the subsequent rat OVA study.

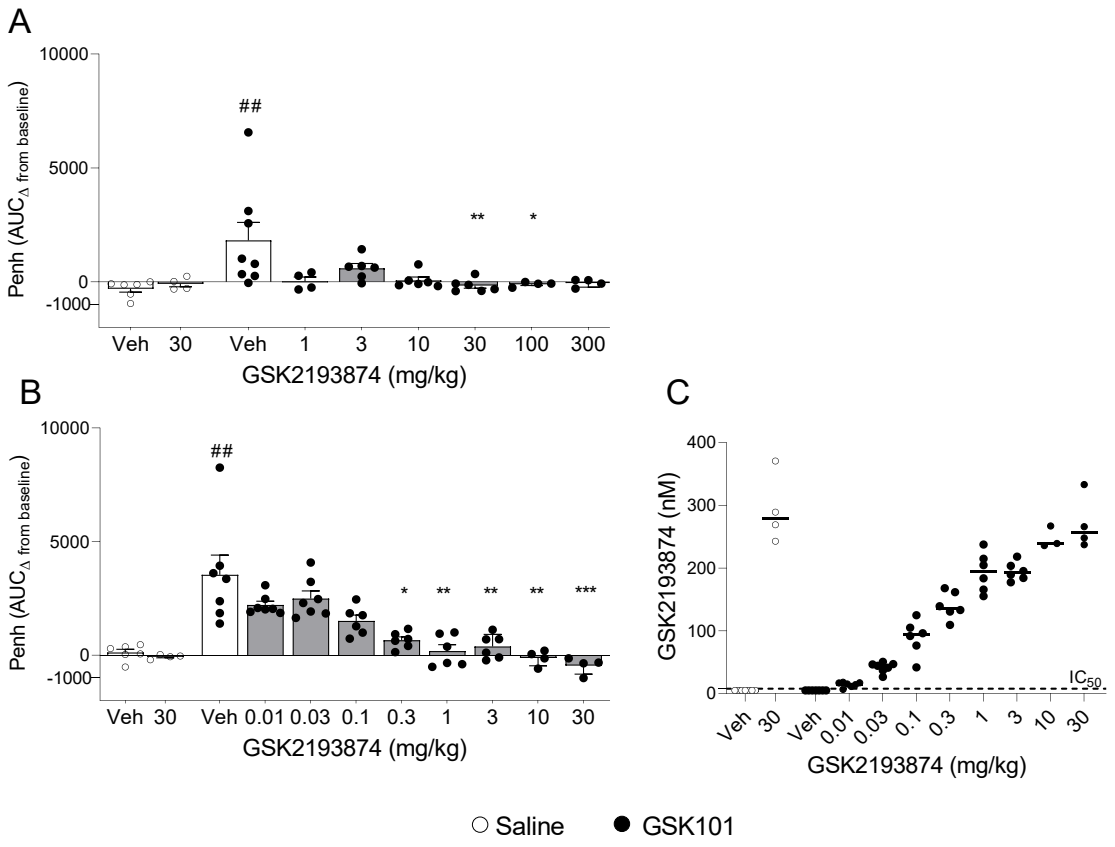


Figure 6.7: GSK2193874 dose response in the rat TRPV4 pharmacodynamic (PD) model.

Rats were administered vehicle or GSK2193874 by intraperitoneal injection and one hour later exposed to nebulised vehicle or GSK1016790A (GSK101; 10µg/ml) for 10 minutes. Enhanced pause (Penh) was monitored for 20 minutes using whole body plethysmography. 20-minute baseline was recorded prior to the challenge and was subtracted from the challenge-induced responses. Upon completion of the experiment rats were sacrificed and blood samples obtained. A) The effect of GSK2193874 in dose range from 1 to 300 mg/kg on GSK101-induced Penh responses. B) The effect of GSK2193874 in dose range from 0.01 to 30 mg/kg on GSK101-inudced responses. C) GSK219 free plasma levels for GSK2193874 dose range from 0.01 to 30 mg/kg. Data from a single experiment are presented as mean ± S.E.M with N=4-8 rats per group. ## denotes $p<0.01$ comparing vehicle/vehicle control with vehicle/GSK101 using Mann-Whitney U-test. * denotes $p<0.05$, **$p<0.01$ and $p<0.001$ comparing vehicle/GSK101 with GSK2193874/GSK101 groups using Kruskal-Wallis test with Dunn's multiple comparisons test. IC_{50} – half-maximal inhibitory concentration.

6.4.5. Characterisation of GSK2798745 in rat PD model

Using the same model, GSK279 was also characterised in vivo. Exposure of vehicle treated animals to GSK101 triggered an increase in Penh responses compared to vehicle challenged animals, although the difference did not reach statistical significance (p=0.054). Nonetheless, GSK279 inhibited GSK101-inudced responses in a dose dependent manner. The inhibition was

statistically significant at doses 0.3 mg/kg and higher. GSK279 at the highest concentration of 3 mg/kg had no effect on saline-induced Penh responses (Figure 6.8A). The analysis of plasma samples confirmed the dose-dependent increase in GSK279 free plasma levels and indicated that concentrations achieved were above the rat IC_{50} (1.48 nM and 1.26 nM in CHO FLIPR and vagal nerve depolarisation assays, respectively; Table 6.3) for all doses, reaching 1200-times IC_{50} at 3 mg/kg. GSK279 levels were below the LLOQ of 3 nM in vehicle treated animals, but were assigned value of 1 nM for visualisation purposes. In all other experimental groups GSK279 were above the LLOQ (Figure 6.8B). GSK279 dose range of 0.03 to 3 mg/kg was selected for the subsequent rat OVA study.

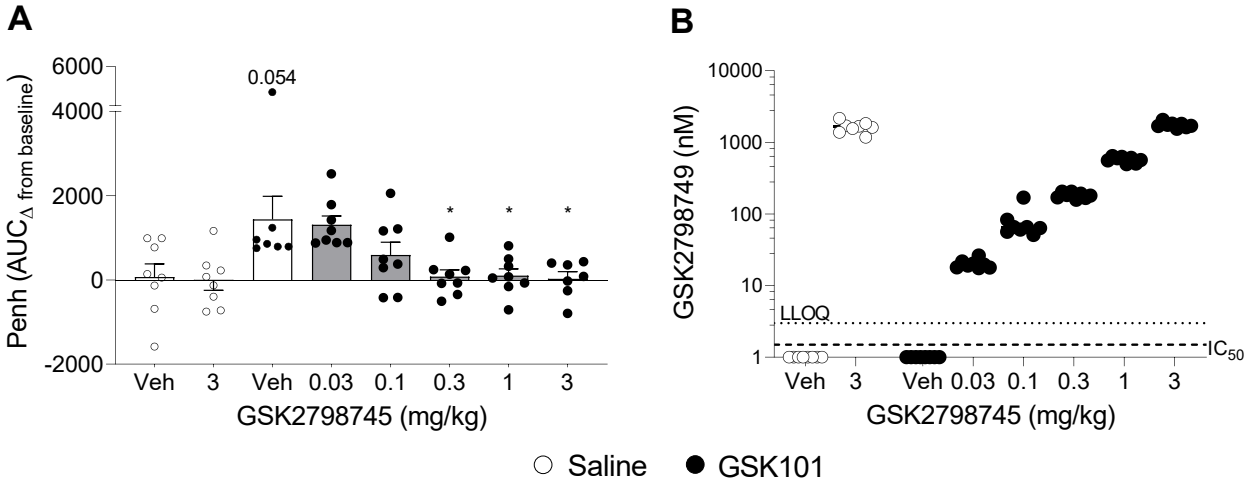


Figure 6.8: GSK2798745 dose response in rat TRPV4 pharmacodynamic (PD) model.

Rats were administered vehicle or GSK2798745 by oral gavage and two hours later were exposed to nebulised vehicle or GSK1016790A (GSK101; 10µg/ml) for 10 minutes. Enhanced pause (Penh) was monitored for 20 minutes using whole body plethysmography. A 20-minute baseline was determined before the challenge and was subtracted from Penh responses during challenge. Upon completion of the experiment rats were sacrificed and blood samples obtained. A) The effect of GSK2798745 in dose range 0.03 to 3 mg/kg on GSK101-induced Penh responses. C) GSK2798745 free plasma levels. In vehicle treated rats GSK279 levels were below lower limit of quantification (LLOQ) and were assigned value of 1 nM for visualisation purposes. Data from a single experiment are presented as mean ± S.E.M with N=6-8 rats per group. Mann-Whitney U-test was used to compare vehicle/vehicle with vehicle/GSK101 groups. * denotes $p<0.05$ comparing vehicle/GSK101 with GSK2193874/GSK101 groups using Kruskal-Wallis test with Dunn's multiple comparisons test. IC_{50} – half-maximal inhibitory concentration.

6.4.6. The effect of TRPV4 antagonists in rat OVA LAR model

6.4.6.1. The effect of GSK219 and GSK279 on OVA-induced LAR

Having characterised and determined the doses for the two TRPV4 antagonists, GSK219 and GSK279, respectively, we next tested the efficacy of both compounds on OVA-induced LAR and airway inflammation in the rat OVA model of AAD. Budesonide and GSK219 300 mg/kg were included in the study as positive controls.

In vehicle treated animals (VEH/OVA), OVA challenge resulted in increased Penh levels 1 to 6 hours after the challenge relative to saline challenged animals (VEH/SAL). GSK219 at 300 mg/kg reduced OVA-induced Penh changes compared to VEH/OVA group. There was a trend towards reduced LAR in budesonide treated animals, however the effect was not statistically significant. No statistically significant effects on OVA-triggered increases in Penh were observed for neither GSK219 nor GSK279 in doses ranging from 0.03 to 3 mg/kg relative to VEH/OVA responses, although a trend towards reduced Penh was noted in rats given 0.3 mg/kg GSK219. Penh responses of GSK219 or GSK279 saline challenged rats did not differ from the responses of VEH/SAL rats. For the clarity purposes GSK219 and GSK279 results are presented on separate graphs (Figure 6.9).

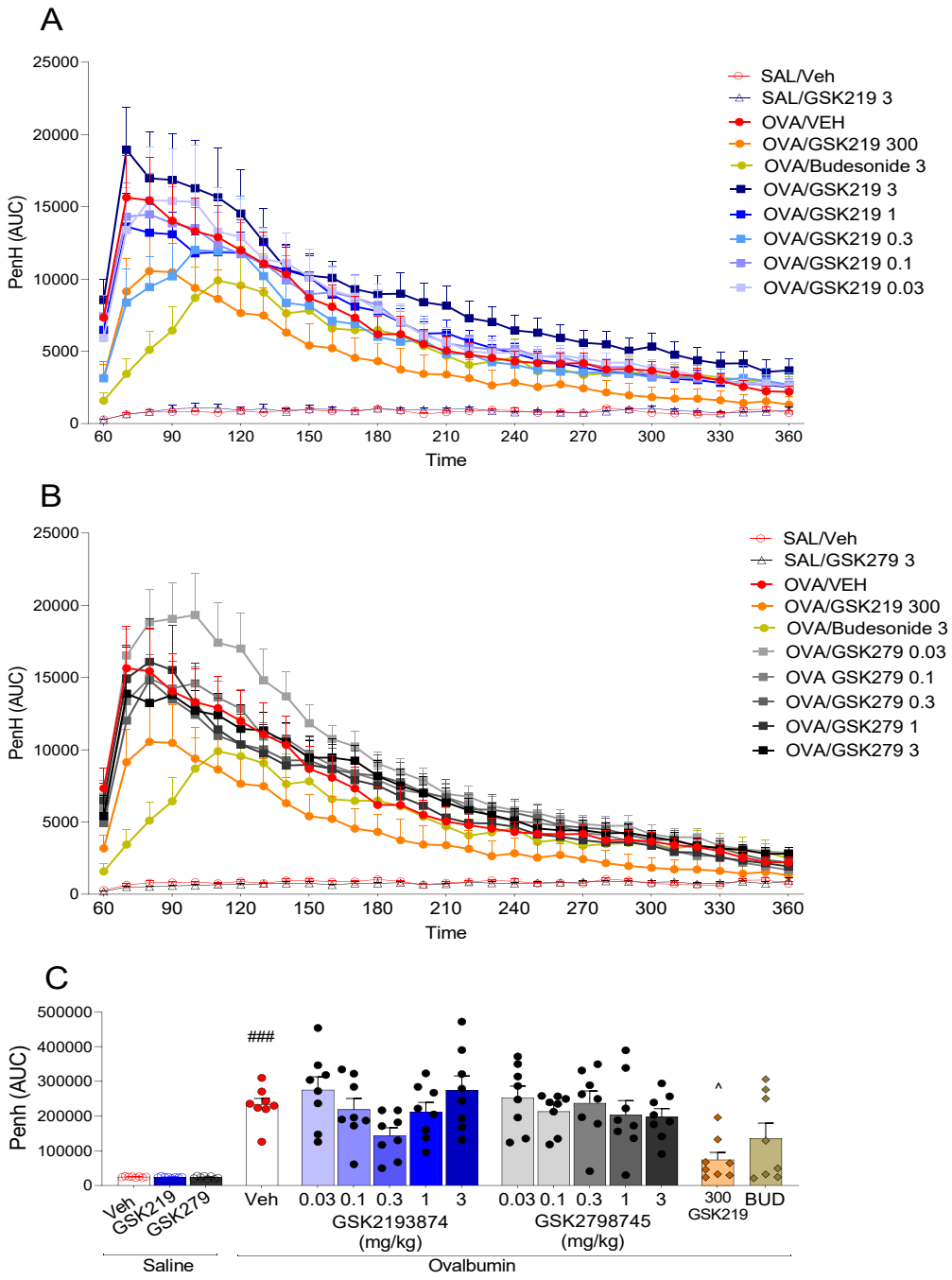


Figure 6.9: The efficacy of TRPV4 antagonists on late asthmatic response (LAR) in rat Ovalbumin (OVA) model. Rats were sensitised to OVA with Alum on days 0, 7 and 14. On day 21 rats were challenged with OVA or saline and were administered GSK2193874 (GSK219; 0.03 – 3 mg/kg and 300 mg/kg) or its vehicle 1 hour before challenge and 30 min after challenge, GSK2798745 (GSK279; 0.03 – 3 mg/kg) or its vehicle 2 hours before challenge and 30 min after challenge as well as budesonide (BUD; 3 mg/kg) or its vehicle 1 hour before challenge. One hour after the challenge rats were placed into whole body plethysmography chambers and enhanced pause (Penh) recorded for 5 hours. Penh recordings of A) GSK219 and B) GSK279 dosed rats, both graphs showing vehicle and positive controls. C) Summarised Penh values as area under the curve (AUC). Data from a single

experiment are presented as mean ± S.E.M with N=7-8 rats per group. ### denotes p<0.001 comparing vehicle/OVA and vehicle/saline groups with Mann-Whitney U-test. ^ denotes p<0.05 comparing vehicle/OVA with GSK219 300/OVA and budesonide/OVA groups using Kruskal-Wallis test with Dunn's multiple comparisons test. Kruskal-Wallis test with Dunn's multiple comparisons test was used to compare responses of vehicle/OVA with GSK219/OVA and GSK279/OVA groups, respectively.

6.4.6.2. The effect of GSK219 and GSK279 on OVA-induced airway inflammation

OVA challenge provoked leukocyte recruitment to the BAL of VEH/OVA rats and resulted in increased BAL eosinophil and neutrophil numbers in comparison to VEH/SAL control. A trend, although not statistically significant, towards increased lymphocyte and AM numbers was also associated with OVA challenge. OVA-challenged rats treated with GSK219 300 mg/kg had reduced total leukocyte numbers as well as lower eosinophil, neutrophil, AM and lymphocyte numbers compared to VEH/OVA control. Although not statistically significant change on OVA-induced increase in total leukocytes was associated with budesonide treatment, these animals displayed lower numbers of eosinophils, AM and lymphocytes in BAL relative to VEH/OVA group. In comparison to VEH/OVA, GSK219 in dose range 0.03 to 3 mg/kg caused a trend towards U-shaped reduction of OVA-induced increase in BAL total leukocyte numbers, and particularly eosinophils and neutrophils, peaking at 0.3 mg/kg, however none of changes were statistically significant. GSK279 in dose range 0.03 to 3 mg/kg resulted in a dose-dependent trend towards reduced OVA-induced increase in total leukocyte numbers, eosinophils and neutrophils compared to VEH/OVA control, however the changes were not statistically significant (Figure 6.10).

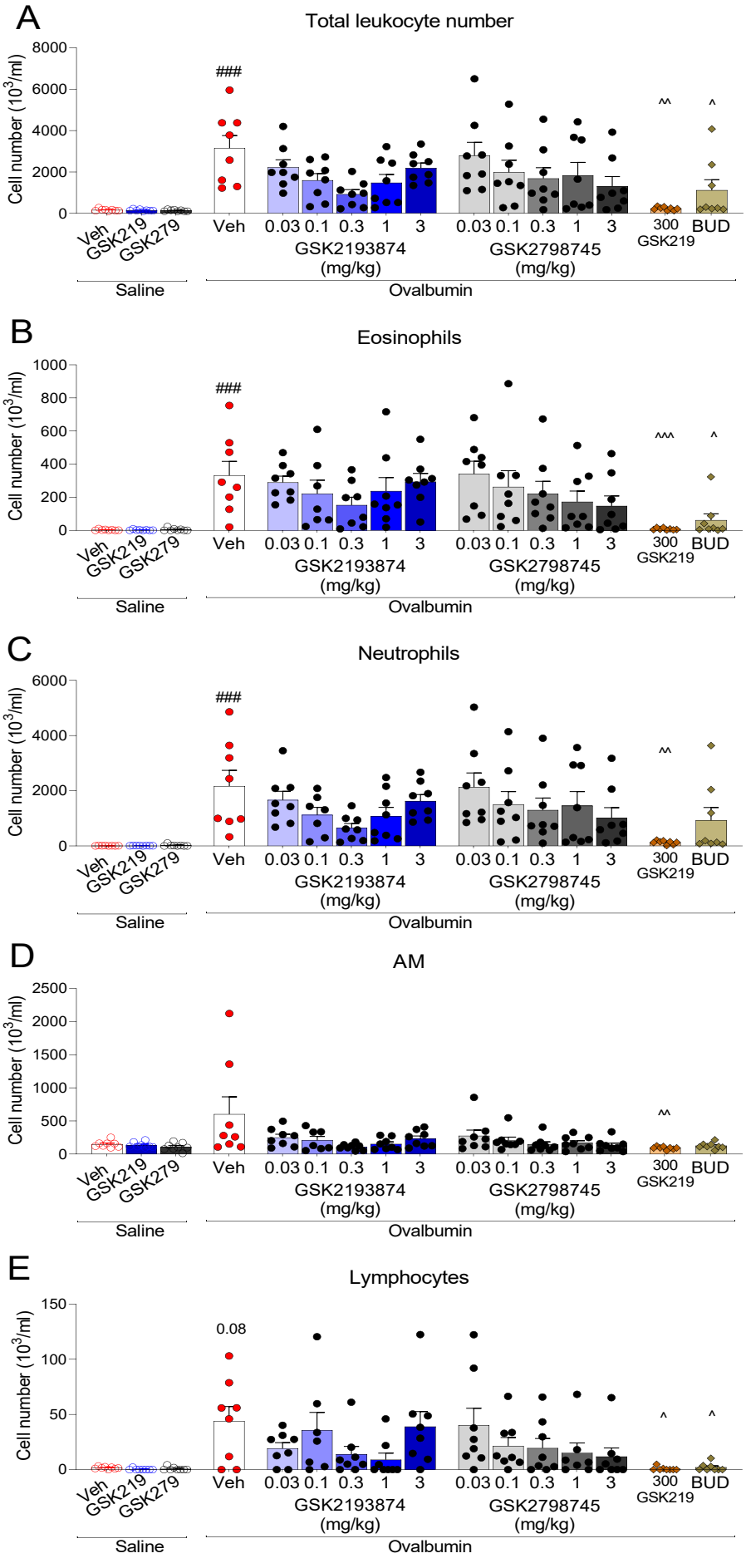

A
Total leukocyte number
Cell number (10^3/ml)
8000
6000
4000
2000
0
###
^^
^
Veh
GSK219
GSK279
Veh
0.03 0.1 0.3 1 3
GSK2193874 (mg/kg)
0.03 0.1 0.3 1 3
GSK2798745 (mg/kg)
300 GSK219
BUD
Saline
Ovalbumin
B
Eosinophils
1000
800
600
400
200
0
###
^^^
^
C
Neutrophils
6000
4000
2000
0
###
^^
D
AM
2500
2000
1500
1000
500
0
^^
E
Lymphocytes
150
100
50
0
0.08
^
^

Figure 6.10: The efficacy of TRPV4 antagonists on allergic airway inflammation in rat Ovalbumin (OVA) model. Rats were sensitised to OVA with Alum on days 0, 7 and 14. On day 21 rats were challenged with OVA or saline and were administered GSK2193874 (GSK219; 0.03 – 3 mg/kg and 300 mg/kg, i.p.) or its vehicle 1 hour before challenge and 30 min after challenge, GSK2798745 (GSK279; 0.03 – 3 mg/kg, p.o.) or its vehicle 2 hours before challenge and 30 min after challenge as well as budesonide (BUD, 3 mg/kg, i.t.) or its vehicle 1 hour before challenge. Rats were sacrificed 24 hours after the challenge and bronchoalveolar lavage (BAL) obtained. A) Total leukocyte numbers in BAL as determined by an automated cell counter. B) BAL eosinophil, C) neutrophil, D) alveolar macrophage (AM), and E) lymphocyte numbers as determined based on histological appearance. Data from a single experiment are presented as mean ± S.E.M with N=7-8 rats per group. ### denotes $p<0.001$ comparing vehicle/saline and vehicle/OVA groups using Mann-Whitney U-test. ^ denotes $p<0.05$, ^^ $p<0.01$ and ^^^ $p<0.001$ comparing vehicle/OVA with GSK219 300/OVA and BUD/OVA groups using Kruskal-Wallis test with Dunn's multiple comparisons test. Kruskal-Wallis test with Dunn's multiple comparisons test was used to compare vehicle/OVA with GSK219/OVA and GSK279/OVA groups, respectively.

6.5. Discussion

The role of TRPV4 in asthma pathogenesis has been initially proposed by our laboratory (Birrell et al. 2016). Several other laboratories have shown the involvement of TRPV4 in the pathogenesis of allergic airway disease in murine AAD models (Gombedza et al. 2017, Yao et al. 2019, Duan et al. 2020, Wiesner et al. 2020), although a dispensable role for TRPV4 in AAD has also been reported (Palaniyandi et al. 2020). More specifically, our group has demonstrated that disruption of TRPV4 signalling abolished all the cardinal features of asthma in murine and rat AAD models, including airway inflammation, AHR and LAR (Birrell et al. 2016). The aim of this chapter was to consolidate the preliminary findings utilising pharmacologically relevant doses of compounds as well as to further our understanding of the role of TRPV4 in asthma pathogenesis using selective TRPV4 pharmacological tools in the rat and mouse AAD models, originally used to study the role of TRPV4 in allergic asthma.

Our laboratory has previously observed that TRPV4$^{-/-}$ mice failed to develop HDM-induced allergic airway inflammation and AHR in a murine HDM model of AAD (Birrell et al. 2016). Interestingly, TRPV4$^{-/-}$ mice failed to respond with increased total or HDM-specific IgE upon HDM challenge despite being sensitised to HDM (Birrell et al. 2016). Albeit IgE was shown to be indispensable for the development of allergic airway inflammation in this model (Raemdonck et al. 2016), the production of HDM-specific IgE could still be an indicator of sensitisation to HDM, meaning that genetic ablation of TRPV4 signalling impeded sensitisation

to allergens rather than the immune response during an allergen challenge phase. To decipher the role of TRPV4 during challenge and sensitisation phase, respectively, we conducted a study inhibiting TRPV4 signalling during allergen challenge phase. To achieve this, we used a novel, highly potent, selective and orally bioavailable clinical TRPV4 antagonist GSK279 (Brooks et al. 2019).

The potency of GSK279 on murine TRPV4 receptors was initially determined in vitro and compared to the potency on human, rat and GP TRPV4 receptors. The potency of GSK279 on human, rat and GP TRPV4 receptors was around 1.5 nM and was in good agreement with published literature (Brooks et al. 2019, Xu et al. 2021), but it appeared to be approximately 10-fold lower on murine TRPV4 receptors. Next, a preliminary PK study was conducted by AstraZeneca (Research & Early Development, Respiratory & Immunology, BioPharmaceuticals R&D), which confirmed the oral bioavailability of GSK279 in mice and demonstrated that GSK279 free plasma concentration peaked 2 hours after oral GSK279 administration. We than validated GSK279 efficacy in in vivo PD model. In this model, GSK101, a selective TRPV4 agonist (Willette et al. 2008), was used to provoke TRPV4-induced bronchoconstriction in mice. GSK101 had been previously shown to trigger TRPV4 selective constriction of human, GP and rat airways in ex vivo models as well as bronchoconstriction in in vivo GP and rat models (McAlexander et al. 2014, Gu et al. 2016, Bonvini et al. 2020, Flajolet 2021). Due to extensive in house characterisation of GSK101 responses in mouse, rat and GP in vitro models as well as rat and GP in vivo models (Bonvini et al. 2016, Flajolet 2021) and in accordance with 3R principles (Aske and Waugh 2017), further in vivo characterisation of GSK101 was deemed unnecessary. Hence, GSK101 30 µg/ml which triggered a submaximal cough response in the GP (Bonvini et al. 2016) was chosen and used in the murine TRPV4 PD model. As expected, GSK101 challenge evoked an increase in Penh in mice, which was inhibited by GSK279 in a dose dependent manner, validating GSK279 as an in vivo TRPV4 tool in mice. The analysis of free plasma GSK279 concentration indicated that approximately 10 to 800-times in vitro IC_{50} were achieved with doses ranging from 0.3 to 30 mg/kg, which were deemed sufficient for the complete inhibition of TRPV4 receptors in vivo at the highest doses.

Moving on, we evaluated the duration of GSK279 efficacy after a single exposure to determine the dosing regimen required to achieve complete and continuous inhibition of TRPV4 during the 6-day allergen challenge phase in the HDM model. In the TRPV4 PD model, a single 10

mg/kg dose of GSK279 inhibited GSK101-evoked Penh increase at 2, 6 and 12 hours, but no longer 16 and 24 hours after dosing. This was accompanied with a drop in free plasma GSK279 concentration 10-times below the IC_{50} at 16 and 24 hours after dosing, indicating an administration of GSK279 twice daily was needed to achieve continuous TRPV4 inhibition in mice. Unexpectedly, free GSK279 levels were approximately 10-times lower in the time course PD study compared to the initial PD study. The reason for these discrepancies remains unclear. We did, however, assure the use of the same batch and preparation of GSK279 in both studies (as well as the subsequent HDM study), and employed the same person to administer the treatments. Thus, the inconsistencies most likely arose during plasma sample analysis rather than compound preparation and administration.

Having validated GSK279 as an in vivo tool and determined the dosing regimen, GSK279 was finally probed in the mouse HDM model. As expected, HDM challenge triggered eosinophilic inflammation in BAL and lung in vehicle treated mice. Unfortunately, AHR could not be reliably evaluated in this study due to the lack of differences in Penh responses between VEH/SAL and VEH/HDM groups. A positive control, budesonide, abolished HDM-induced inflammation in BAL in lung as previously reported (Raemdonck et al. 2016). As budesonide treatment had been previously well characterised in this model (Raemdonck et al. 2016), budesonide vehicle control groups were omitted in this study in order to reduce the number of animals required to evaluate the effect of GSK279 as per 3R principles (Aske and Waugh 2017). As repeated dosing was required for GSK279 during the challenge phase, administration of budesonide vehicle was omitted in GSK279 or vehicle treated animals to improve their well-being and avoid oral gavage four times daily in line with 3R principles (Aske and Waugh 2017). GSK279 treatment during the challenge phase (days 24 – 29) was associated with a trend towards reduced eosinophilic BAL inflammation and increased BAL neutrophil numbers in a dose-related manner. Even so, GSK279 treatment failed to modulate HDM-induced eosinophil, DC, T cell and ILC2 expansion in the lung. GSK279 also appeared to be ineffective at modulating the HDM-induced AHR, however the effect of GSK279 on AHR could not be reliably assessed and would need to be repeated. The analysis of GSK279 free plasma concentration after the AHR assessment indicated that GSK279 levels were at least 60-times above IC_{50} at 30 mg/kg during AHR assessment. Regardless, a concern that such levels might be sufficient for complete inhibition of TRPV4 in vivo has been raised and higher doses of

GSK279 proposed to be tested in HDM model. Another limitation of this study was a lack of increased Penh responses in VEH/HDM mice relative to VEH/SAL. It is unclear why Penh responses to 5-HT were variable in this study, particularly in the VEH/SAL group. Alternative, direct assessments of lung resistance and lung compliance by invasive lung function techniques could reduce the intragroup variability and more reliably evaluated lung resistance and compliance, however as these techniques are performed on anaesthetised animals, they are not suitable for assessing potential neuronal components of AHR (Bates and Irvin 2003, Bates et al. 2004, Lomask 2006, Blake et al. 2019). AHR has not been comprehensively characterised in our HDM model and the neuronal regulation of AHR is yet to be elucidated. However, TRPV4 has been implicated in airway sensory nerve reflexes, such as cough (Bonvini et al. 2016), and might contribute to AHR in such a manner.

The results from the murine HDM model suggested only a minor role of TRPV4 in the development of HDM-induced allergic airway inflammation in sensitised mice and together with the previous TRPV4$^{-/-}$ study suggest a more important and critical role of TRPV4 during sensitisation to HDM (Birrell et al. 2016). These results were in contrast to the results obtained in the rat OVA model where a single high dose of GSK219 (300 mg/kg), a selective pre-clinical TRPV4 antagonist (Thorneloe et al. 2012), administered prior to OVA challenge completely abolished LAR as well as eosinophilic airway inflammation (Birrell et al. 2016). In contrast to the murine studies, these findings supported a pivotal role of TRPV4 in allergen-induced responses during an allergen challenge. However, the administration of a such high dose raised a concern that off-target rather than TRPV4 selective effects were observed with GSK219. Therefore, to clarify the role of TRPV4 during allergen challenge and consolidate the preliminary data from the rat OVA model, two selective TRPV4 antagonists, GSK279 and GSK219, were tested in the rat OVA model. The in vitro characterisation of GSK279 and GSK219 confirmed the expected potency of both small molecules as previously published for rat and human TRPV4 receptors (Thorneloe et al. 2012, Cheung et al. 2017, Brooks et al. 2019, Xu et al. 2021) and demonstrated an approximately 20-fold loss of potency of GSK219 on GP receptors.

Both compounds were initially validated in the in vivo rat TRPV4 PD model that had been characterised previously in our laboratory (Flajolet 2021) to validate their efficacy in vivo as well as to select a dose range that would allow us to observe TRPV4-selective effects. Both, GSK219 and GSK279, inhibited GSK101-induced airway responses in a dose dependent manner with first inhibitory effects noted at 0.3 mg/kg for both compounds. In the case of GSK219, complete inhibition of GSK101-induced responses was achieved at 1 mg/kg, a dose 300-times less than the dose used in the preliminary OVA study (Birrell et al. 2016). The comparison of free plasma concentrations to respective in vitro determined IC_{50} indicated that levels approximately 30- and 1200-times above IC_{50} were achieved at 3 mg/kg for GSK219 and GSK279, respectively. This was deemed sufficient for the complete selective inhibition of TRPV4 in vivo and hence a dose range from 0.03 to 3 mg/kg was selected to study the effects of both small molecules on LAR and airway inflammation in the rat OVA model. The dosing regimen for GSK219 was chosen based on previous in vivo studies (Birrell et al. 2016, Bonvini et al. 2016). Oral dosing with a 2 hour pre-dose time was chosen for GSK279 based on a preliminary PK study conducted by Early Respiratory and Immunology, AstraZeneca (data not shown), however an additional dose of GSK279 half an hour after the challenge was added to match the GSK219 dosing regimen (Birrell et al. 2016).

In the rat OVA model, OVA exposure triggered a delayed bronchoconstrictor response, resembling LAR in allergen sensitised individuals, one to six hours after the challenge as well as eosinophilic airway inflammation 24 hours later as previously established (Underwood et al. 2002, Raemdonck et al. 2012). As previously reported, positive controls budesonide and GSK219 300 mg/kg ameliorated OVA-induced airway inflammation and LAR (Underwood et al. 2002, Raemdonck et al. 2012, Birrell et al. 2016). At a dose range 0.03 to 3 mg/kg GSK219 displayed a trend towards U-shaped inhibition of OVA-induced LAR and airway inflammation, peaking at 0.3 mg/kg, which did not reach statistical significance. GSK279 exhibited a trend towards dose-dependent reduction in OVA-induced airway inflammation, but not LAR. The U-shaped efficacy of GSK219 was unusual and had not been reported before despite frequent in vivo use (Thorneloe et al. 2012, Bonvini et al. 2016, Yin et al. 2016, Cheung et al. 2017, Li et al. 2019b, Yao et al. 2019), allowing for the possibility that the U-shaped trend was observed by chance. Nevertheless, at 300 mg/kg GSK219 still ameliorated airway inflammation as well as LAR. Although GSK219 doses administered in this study were carefully selected based on

the demonstrated efficacy and PK profile in the PD study, the possibility exists they might not have been sufficiently high for the complete inhibition of TRPV4 in the disease settings. However, the more potent clinical TRPV4 antagonist GSK279 (Brooks et al. 2019) exerted only modest efficacy on eosinophilic airway inflammation and failed to alleviate OVA-induced LAR. These results resembled the outcomes from the mouse HDM model and suggested that 300 mg/kg GSK219 likely exerted off-target rather than TRPV4-selective effects in the rat OVA model. The dose of GSK219 in this study was based on the efficacy in the GP cough model (Bonvini et al. 2016), although GSK219 potency drop in GP in comparison to rat has been demonstrated in vitro (Table 6.3), supporting the notion of overdosing GSK219 in the rat.

In addition to TRPV4, other TRP channels have been implicated in asthma pathogenesis and could be blocked by high doses of GSK219. TRPA1 and TRPV1 are abundantly expressed in the lung and have both been implicated in asthma pathogenesis (Grace et al. 2014a). TRPA1 SNPs are associated with childhood asthma (Gallo et al. 2017) and preclinical studies have implicated TRPA1 in the development of allergic airway inflammation, AHR and/or LAR (Caceres et al. 2009, Raemdonck et al. 2012, Hox et al. 2013, Devos et al. 2016, Yao et al. 2019, Reese et al. 2020). TRPV1 genetic polymorphisms have been also associated with asthma susceptibility (Wang et al. 2009). In addition, a loss of function genetic TRPV1 variant has been associated with reduced wheezing or cough in asthmatic patients (Cantero-Recasens et al. 2010) and increased TRPV1 bronchial expression, especially in steroid resistant asthma, has been reported (McGarvey et al. 2014). TRPV1 regulates activation and proinflammatory properties of $CD4^+$ T cells (Bertin et al. 2014, Balestrini et al. 2021) and activation of $TRPV1^+$ airway sensory neurons appear essential for Th2 differentiation in response to allergens (Perner et al. 2020). In AAD models, inhibition of TRPV1 signalling has alleviated allergic airway inflammation, AHR and/or airway remodelling (Mabalirajan et al. 2013, Rehman et al. 2013, Devos et al. 2016, Choi et al. 2018, Duan et al. 2020). However, there are several contradictions in the published literature in respect to the involvement of TRPV1 and TRPA1 in asthma pathogenesis and appear to depend on genetic background of laboratory animals as well as AAD models (Veronesi et al. 2000, Caceres et al. 2009, Hox et al. 2013, Rehman et al. 2013, Devos et al. 2016). In our laboratory, for example, TRPA1 has been shown to regulate LAR in the rat OVA model (Raemdonck et al. 2012), demonstrating a potential off-target mechanism for a high GSK219 dose in this model .

Taken together, this chapter has demonstrated that TRPV4 inhibition during allergen challenge diminished eosinophilic airway inflammation in both murine and rat AAD model, but was not efficacious in modulating bronchoconstrictor responses. Together with preliminary observations in TRPV4$^{-/-}$ mice, our investigations have uncovered a potential, more critical, role of TRPV4 during allergen sensitisation (Birrell et al. 2016). Although more in depth investigations are warranted to address the hypothetical role of TRPV4 during allergen sensitisation, our findings support a recent association of a gain-of-function TRPV4 SNP rs6606743 (Li et al. 2011) with increased incidence of asthma and sensitisation to fungal allergens (Wiesner et al. 2020). There are several preclinical studies that support the proposed role of TRPV4 in sensitisation to allergens. Utilising constitutive TRPV4$^{-/-}$ mice, Gombedza et al. have also demonstrated an inability of TRPV4$^{-/-}$ mice to mount type 2 immune responses upon HDM exposure in a chronic HDM model with mucosal sensitisation phase (Gombedza et al. 2017). These mice were additionally protected from HDM-associated airway remodelling, proposing a profibrotic role of TRPV4 (Gombedza et al. 2017). We have not investigated the role of TRPV4 in fibrosis or airway remodelling, but TRPV4 has been implicated in myofibroblast differentiation and development of fibrosis in other chronic disease setting, such as IPF (Rahaman et al. 2014, Gombedza et al. 2017, Grove et al. 2019). Duan et al. have similarly reported that administration of TRPV4 antagonist HC067047 throughout the sensitisation and challenge phase inhibited OVA-induced IL-4 and IL-1β increased in BAL as well mucus production (Duan et al. 2020), mimicking the studies utilising global TRPV4$^{-/-}$ mice (Birrell et al. 2016, Gombedza et al. 2017). Wiesner et al. have also suggested the involvement of TRPV4 in allergen sensitisation (Wiesner et al. 2020). In mice with conditional selective club cell TRPV4 deficiency reduced generation of Th2 CD4^{+} T cells, recruitment of moDCs and ameliorated eosinophilic airway inflammation were seen in response to alkaline protease 1 (Alp1), the most abundant protein secreted by *Aspergillus* (Sriranganadane et al. 2010, Wartenberg et al. 2011, Wiesner et al. 2020). Overexpression of TRPV4 in those cells had the opposite effects and aggravated these responses (Wiesner et al. 2020). The authors proposed that Alp1 protease activity damaged and disrupted epithelial cell junctions which triggered TRPV4 activation independently of PAR2, MyD88 or NFκB signalling, leading to calcineurin signalling and Th2 sensitisation (Wiesner et al. 2020). Although we have demonstrated a role for PAR2 in our murine AAD model in Chapter 5, it remains unclear to what extent PAR2 activation is responsible for TRPV4 activation. Other

mechanisms of TRPV4 activation, including the role of immune cells or airway epithelium in the process, remain unclear and warrant further investigations. On the other hand, Palaniyandi et al. have recently reported a lack of role for TRPV4 in AHR and allergic airway inflammation in murine OVA, demonstrating OVA-induced changes in TRPV4$^{-/-}$ mice to be identical to that of WT mice (Palaniyandi et al. 2020), contradicting all other studies investigating the role of TRPV4 in AAD (Birrell et al. 2016, Gombedza et al. 2017, Duan et al. 2020, Wiesner et al. 2020). Whilst the lack of a role of TRPV4 could be model specific, the authors provided no functional validation of their TRPV4$^{-/-}$ mice to confirm a lack of TRPV4-induced responses (Palaniyandi et al. 2020). In-breeding is known to introduce a genetic shift which can result in phenotypical change, including gain of function mutations (Stevens et al. 2007, Purtha et al. 2012, Ji et al. 2017). We ourselves have experienced several genetically modified mice, particularly those with targeted TRP genes, to re-acquire a function of the disrupted gene, and thus suggest functional validation of genetically modified mice in such experiments.

The above mentioned studies demonstrated that the absence of TRPV4 signalling during allergen sensitisation and allergen challenge phase resulted in alleviation of allergic airway disease, but did not address the relevance of TRPV4 signalling during each phase separately or evaluate the role of TRPV4 in airway responses, such as AHR or LAR (Gombedza et al. 2017, Duan et al. 2020, Wiesner et al. 2020). If TRPV4 is to be considered a novel therapeutic target in asthma, it is of vital importance to understand whether targeting TRPV4 can modulate the development of allergic airway inflammation or airway responses during allergen challenge phase. Clinical expression studies have suggested that TRPV4 expression is increased in airway epithelium of asthmatic patients, but does not seem to be changed acutely after allergen challenge (Wiesner et al. 2020). This has been recapitulated in several animal models of AAD (Yu et al. 2017, Duan et al. 2020, Kim et al. 2020), yet in our model HDM challenge was associated with downregulation of *Trpv4* in CD4^{+} T cells and DCs (Chapter 3). More interestingly, GWAS meta-analysis has associated genetic variations in *TRPV4* locus with lung function measures (Obeidat et al. 2011) and TRPV4 SPN rs7971845 and SNP rs6606743, more specifically, have been associated with hypoosmolar-induced AHR in asthmatic patients (Naumov et al. 2016). Our results have demonstrated that pharmacological inhibition of TRPV4 during allergen challenge phase had a small effect on airway eosinophilia, but no effect

on AHR in our murine or LAR in our rat AAD models. In contrast to our findings, Yao et al. have reported that in a chemical-induced AAD model administration of GSK219 during challenge phase alleviated toluene diisocyanate (TDI)-induced eosinophilic airway inflammation as well as AHR (Yao et al. 2019). In TDI model the mechanisms behind AHR and airway inflammation could be substantially different to HDM-induced disease triggering alternative TRPV4 signalling pathways. To elucidate those, more preclinical studies utilising different AAD models and selective pharmacological tools are warranted.

Nevertheless, to ultimately evaluate the importance of TRPV4 for human disease, additional human expression and in vitro functional studies as well clinical proof of concept studies are required. GSK279, a clinical TRPV4 antagonist, has been recently reported safe and well tolerated in healthy volunteers and patients with stable heart failure (HF) and improved lung diffusion parameters in HF (Goyal et al. 2019, Mole et al. 2020, Stewart et al. 2020). A potential concern in respect to administering TRPV4 antagonist in asthmatic patients is inhibition of TRPV4-regulated mechanisms protecting against bacterial infections, such as mucocilliary clearance or AM bacterial phagocytosis (Alenmyr et al. 2014, Scheraga et al. 2016, Alpizar et al. 2017, Scheraga et al. 2020), although such TRPV4 properties have been disputed (Dalsgaard et al. 2016, Li et al. 2019b). The outcomes of a recent clinical trial suggest this might not be an issue as GSK279 failed to modulate LPS-induced increases in BAL protein or neutrophil numbers after a segmental LPS challenge (Mole et al. 2020).

In conclusion, this chapter demonstrated a modest role of TRPV4 in allergen-induced airway inflammation and a lack of role in airway responses such as AHR or LAR in Th2 driven models of AAD. Further work is needed to elucidate the importance of TRPV4 during allergen sensitisation or allergen-induced innate immune responses.

7. Summary and future directions

7.1. Thesis summary

Asthma is one of the most common chronic respiratory diseases, affecting nearly 10 % of the population (Asthma UK 2021). Despite the advances in the treatment and management of asthma, some patients remain poorly controlled on top of standard care (González Barcala et al. 2010, Chung et al. 2014, Price et al. 2014, Beasley et al. 2020). These patients in particular have reduced quality of life and present a big social and health care burden (Nunes et al. 2017). Therefore, better understanding of asthma pathogenesis and identification of novel therapeutic targets are warranted to fulfil the unmet need.

Asthma is a heterogenous disease and Th2 high atopic asthma is the most common phenotype (Kuruvilla et al. 2019). The hallmark of atopic asthma is type 2 airway inflammation that was traditionally viewed as Th2 cell driven immune response (Lloyd and Snelgrove 2018). During the last decade with the discovery of ILC2s it has become clear that these responses are a consequence of complex interactions between airway epithelium, Th2 cells, ILC2s and DCs (Lloyd and Snelgrove 2018). In addition, immune mediators such as ATP have been implicated in asthma pathology (Pelleg 2020). Allergen challenge provokes an increase in BAL ATP levels in asthmatic patients (Idzko et al. 2007) and has been shown to trigger an inflammatory response, AHR and LAR though the activation of P2 receptors, namely P2X3, P2X4 and P2X7 (Muller et al. 2011, Chen et al. 2016, Zech et al. 2016, Li et al. 2018a, Flajolet 2021).

The mechanism behind increased ATP release in asthma is not yet fully understood. TRPV4, a TRP family member is commonly expressed receptor on airway structural cells as well as immune cells such as AM, T cells and DCs and its activation has been linked with ATP release (White et al. 2016). In the airways TRPV4 regulates mucocilliary clearance and may contribute to protection against bacterial respiratory infections (Lorenzo et al. 2008, Alenmyr et al. 2014, Scheraga et al. 2016, Alpizar et al. 2017, Scheraga et al. 2020). However, aberrant TRPV4 activation has been associated with respiratory diseases and symptoms (Belvisi and Birrell 2017). For example, TRPV4 has been shown to trigger cough, bronchospasm as well neutrophilic airway inflammation (Baxter et al. 2014, McAlexander et al. 2014, Bonvini et al. 2016, Henry et al. 2016, Bonvini et al. 2020). Our preliminary observations have also suggested a crucial role of TRPV4 in asthma, as $TRPV4^{-/-}$ as well as a TRPV4 antagonist abolished cardinal features of asthma in our rodent AAD models – airway inflammation, AHR

and LAR (Birrell et al. 2016, Flajolet 2021). In addition, similar results were obtained with Panx1$^{-/-}$ mice in the murine model as well as P2X3 inhibitor in the rat AAD model, respectively, implicating ATP as a mediator downstream of TRPV4 activation (Flajolet 2021)(Figure 1.5).

We therefore hypothesised that activation of the TRPV4-ATP axis was detrimental in asthma pathogenesis. We utilised animal models of AAD to elucidate the TRPV4 signalling pathway. Firstly, we investigated which cells could be responsible for TRPV4 signalling and identified P2X receptors possibly activated downstream of TRPV4 (Chapter 3). Next, we investigated the role of candidate P2X receptors in the development of AAD (Chapter 4). PAR2 was then evaluated as a possible mechanism of TRPV4 activation (Chapter 5). Lastly, we aimed to consolidate the preliminary TRPV4 observations and further investigate the role of TRPV4 specifically during allergen challenge phase (Chapter 6).

Recent publications have demonstrated the expression of TRPV4 on T cells, one of the main orchestrators of type 2 immune responses in asthma (Bertin et al. 2014, Majhi et al. 2015, Lloyd and Snelgrove 2018). Thus, we postulated that immune cells driving the allergen-induced immune responses could be responsible for the activation of TRPV4 axis. To elucidate the main players in immune responses, we turned to the murine HDM model that had been used during the preliminary investigations into the role of TRPV4 and characterised the development of allergic airway inflammation in a time course study. We demonstrated that HDM challenge triggered an increase in BAL IL-2 levels as well as an upregulation of type 2 cytokines in lung and BAL as early as 2 hours after the initial challenge, suggesting the activation of memory Th2 cells immediately after the HDM challenge (Hondowicz et al. 2016, Bosnjak et al. 2019). Indeed, CD4$^+$ and CD8$^+$ T cells were upregulated in BAL 2 hours after the second HDM challenge. Gene expression analysis of isolated populations revealed that CD4$^+$ T cells acquired Th2 phenotype and upregulated *Il-4, Il-5* and *Il-13,* while CD8$^+$ T cells upregulated *Il-13,* but not other type 2 cytokines. Both populations were previously characterised as pivotal for the development of allergic airway inflammation and AHR in this model (Raemdonck et al. 2016). Simultaneously, moDCs were recruited into the lung of HDM challenged mice and all lung DC populations were found in increased numbers in MLN after the HDM challenge, implicating DCs in the early responses during allergen encounter (Vroman et al. 2017). ILC2s had not previously investigated in this model and their contribution to the allergic airway inflammation in this model was uncertain. We found that HDM challenge

triggered a delayed recruitment of ILC2s into BAL and expansion of lung ILC2s, but did not further stimulate their production of *Il-4, Il-5* or *Il-13.* Although this suggested a dispensable role in the initiation of HDM-induced airway inflammation, their contribution to the development of type 2 immune responses could not be fully elucidated, hence ILC2s were investigated along with $CD4^+$ T cells, $CD8^+$ T cells and DCs as potential activators of TRPV4 axis in the murine HDM model of AAD. Gene expression studies confirmed the presence of *Trpv4* as well as *Panx-1* on all immune cell populations, however downregulation of *Trpv4* was associated with HDM challenge in lung $CD4^+$ T cells, ILC2s and DC populations. This suggested that those populations could drive TRPV4-ATP axis in AAD, especially as TRPV4 has been implicated in T cell effector function and FcR mediated activation in DCs (Majhi et al. 2015, Naert et al. 2019). Among P2X receptors, high expression of *P2rx4* and *P2rx7* was found on all cells and upon HDM challenge *P2rx7* was upregulated in $CD4^+$ and $CD8^+$ T cells and downregulated in DC populations. A crucial role in T cell and DC has been demonstrated for both P2X4 and P2X7, and both receptors have been implicated in allergen sensitisation as well as the development of allergic airway inflammation and AHR (Muller et al. 2011, Burnstock and Boeynaems 2014, Chen et al. 2016, Zech et al. 2016, Li et al. 2018a, Silva-Vilches et al. 2018). In addition, *P2rx1* was the most highly upregulated P2X receptors in the lungs of HDM challenged mice and increased *P2rx1* levels were detected on $CD4^+$ and $CD8^+$ T cells isolated from HDM challenged mice. There is limited knowledge on the role of P2X1 in asthma pathogenesis, however P2X1 receptor is crucial for lymphocyte function and immune signalling upon antigen stimulation (Woehrle et al. 2010a, Ledderose et al. 2016).

This led us to investigate a role of P2X1, P2X4 and P2X7, respectively, in our AAD model. Utilising $P2X1^{-/-}$ and $P2X4^{-/-}$ mice, respectively, we demonstrated that both P2X1 and P2X4 were dispensable for the development of allergic airway inflammation and AHR. In contrast, $P2X7^{-/-}$ mice were partially protected from the development of BAL eosinophilia, but not from AHR or the development of HDM-induced IgE responses. This implicated P2X7 as a potential partial mediator of TRPV4-driven allergic airway inflammation, however the involvement of other P2X receptors in AAD pathogenesis is highly likely.

Next, we addressed PAR2 as a possible mechanism of TRPV4 activation using the murine HDM-induced model of AAD. TRPV4 can be activated by numerous environmental stimuli, but also inflammatory mediators (Belvisi and Birrell 2017). PAR2 has been implicated in AA

metabolism and has been linked to TRPV4 activation in various pain models as well as acute lung injury models (Grant et al. 2007, Poole et al. 2013, Zhao et al. 2014, Zhao et al. 2015, Rayees et al. 2019). PAR2 activating ligands, such as tryptase, and *Par2* expression are increased in asthmatic patients and substantial pre-clinical literature has implicated PAR2 in allergic sensitisation as well as the development of allergic airway inflammation and AHR (Wenzel et al. 1988, Broide et al. 1991, Jarjour et al. 1991, Alvarez et al. 2000, Knight et al. 2001, Schmidlin et al. 2002, Ebeling et al. 2005, Takizawa et al. 2005, Allard et al. 2014, Aubier et al. 2016). In our murine model, HDM challenge resulted in increased BAL tryptase levels as well as upregulation of lung *Par2* expression during the first time points and downregulation later in the time course study. *Par2* was also expressed on the immune cells deemed key for the development of allergic airway inflammation in the HDM model, and was downregulated in T cell subsets and upregulated in DCs upon HDM challenge. This validated PAR2 as a target in the HDM AAD model. Utilising $PAR2^{-/-}$ mice and the PAR2 blocking antibody MEDI2344, we then investigated the role of PAR2 in the development of allergic airway inflammation and AHR in this model. $PAR2^{-/-}$ ameliorated HDM-induced eosinophilic inflammation in BAL and lung and was associated with reduced $CD4^+$ T cell, $CD8^+$ T cell and moDC numbers as well as HDM-induced increase in plasma IgE. PAR2 blocking antibody did not ameliorate HDM-induced allergic airway inflammation, but rather promoted airway eosinophilia, and interestingly, neither $PAR2^{-/-}$ not PAR2 blocking antibody modulated HDM-induced AHR. This implicated PAR2 in allergen sensitisation rather than immune responses associated with allergen challenge, and suggested that PAR2 could be partially responsible for TRPV4 signalling during allergen sensitisation.

Nevertheless, the investigations into downstream and upstream TRPV4 targets failed to elucidate TRPV4 signalling pathways in AAD. The preliminary observations strongly implicated TRPV4 in AHR (Birrell et al. 2016), however none of the investigated downstream or upstream targets modulated AHR. It was possible that $TRPV4^{-/-}$ mice were protected against HDM sensitisation and that the protective effect of $TRPV4^{-/-}$ was merely a consequence of "failed" allergen sensitisation that rather than a direct effect on airway responses, as suggested by PAR2 studies in Chapter 5. Nevertheless, the observations in the OVA LAR model demonstrated that TRPV4 inhibition prevented both allergic airway inflammation as well as LAR in OVA-sensitised rats, suggesting that TRPV4 could also be directly implicated in

responses during an allergen challenge (Birrell et al. 2016, Flajolet 2021). A single high dose of a single TRPV4 antagonist had been tested, though (Birrell et al. 2016, Flajolet 2021), and a concern for an off-target rather than TRPV4 selective effect was raised. Therefore, the last chapter aimed to consolidate the preliminary findings and decipher the importance of TRPV4 signalling during allergen challenge phase in the murine and the rat AAD models using the selective TRPV4 antagonists. GSK279 and GSK219 were profiled in in vivo TRPV4 PD models and were shown to block GSK101-induced responses in a dose-related manner. In the murine HDM-induced AAD model a trend towards dose-related reduction in eosinophilic airway inflammation was observed with GSK279, however GSK279 was inefficacious in alleviating inflammation in the lungs or AHR to 5-HT. In the rat OVA model, a trend towards bell-shaped inhibition of airway eosinophilia and LAR was observed with GSK219, while a trend towards dose-dependent inhibition of airway inflammation but not LAR was seen with the more potent and highly selective TRPV4 antagonist GSK279, suggesting only a modest contribution of TRPV4 to eosinophilic inflammation but not LAR during allergen challenge. PK analysis of plasma samples taken in those studies indicated free plasma levels of the compounds were at sufficient to block the TRPV4 channel.

In summary, this thesis identified PAR2-TRPV4-P2X7 axis in the development of allergic airway inflammation. TRPV4 appeared to have predominantly promoted sensitisation to allergens, with PAR2 potentially contributing to this process. P2X7 was found to be involved in the development of eosinophilic airway inflammation with patterns similar to that seen in TRPV4 antagonist studies, proposing a role for P2X7 as a mediator of TRPV4-induced eosinophilic airway inflammation in allergen challenge phase. Even so, the involvement of TRPV4 in immune responses during allergen challenge phase or AHR remains uncertain and further investigations are warranted to confirm the proposed PAR2-TRPV4 and TRPV4-P2X7 links and identify potential alternative TRPV4 signalling pathways. Lastly, and most importantly, translational studies are in place to evaluate TRPV4 and associated targets in asthma.

7.2. Thesis limitations

There are a number of limitations to the methods used and the findings presented in this thesis and have mostly been discussed in individual result chapters.

The animal models of AAD used in this thesis were chosen to study the TRPV4 signalling pathway as those were the models that had initially implicated TRPV4 in the development of allergic airway inflammation, AHR and LAR (Birrell et al. 2016, Flajolet 2021). Albeit both models have been characterised and demonstrated to respond to gold asthma therapies (Underwood et al. 2002, Raemdonck et al. 2016), they do not fully recapitulate asthma pathogenesis. For example, OVA-driven models have been heavily criticised as OVA is not a clinically relevant allergen and systemic sensitisation with an adjuvant is required to induce antigen sensitisation rather than tolerance (Aun et al. 2017). No other models have been developed yet that would recapitulate LAR using clinically relevant allergens or without the need for systemic sensitisation. On the other hand, HDM is a clinically relevant allergen, but systemic sensitisation phase required to prime type 2 immune responses does not reflect the course of sensitisation to aeroallergens and subsequent establishment of allergen specific lung resident memory leukocyte populations (Aun et al. 2017, Lloyd and Snelgrove 2018). Models with mucosal sensitisation to allergens have been developed with various clinically relevant allergens, including HDM, and mimic ILC2-driven aspect of airway inflammation particularly in severe asthma (Aun et al. 2017). However, the benefit of our HDM model are distinct allergen sensitisation and allergen challenge phases as well as well characterised Th2-driven type 2 immune response which can be helpful for profiling of novel therapeutic targets.

Another important limitation of this work is the use of whole body plethysmography to evaluate lung function changes and airway responses in AAD models. The most important consideration is that Penh is not a direct measure of airway resistance and was criticised for being influenced by changes in breathing patterns, animal movement or obstruction of upper airways (Bates and Irvin 2003, Bates et al. 2004, Lundblad et al. 2007). These factors could contribute to the unconclusive AHR results in a couple of presented studies. Additionally, although a correlation between Penh and direct measurement of airway resistance has been demonstrated (Hamelmann et al. 1997a, Bergren 2001, Glaab et al. 2005, Verheijden et al. 2014), FWBP is less sensitive than the invasive lung function assessment techniques (Verheijden et al. 2014) and might not be sufficient to detect the potential impact of $P2X4^{-/-}$, $P2X7^{-/-}$, $PAR2^{-/-}$ or TRPV4 antagonists on AHR. Alternative techniques could be used to assess changes in lung function parameters in the murine AAD model, but the neuronal regulation

of airway responses would be lost due to general anaesthesia (Bates and Irvin 2003, Verheijden et al. 2014). The loss of nervous reflexes is also the main reason why WBP is the only suitable method for the evaluation of LAR. In the rat OVA model, LAR has been proposed to be driven by airway sensory reflexes and was abolished with anaesthesia (Raemdonck et al. 2012), which is required for the invasive assessment of lung function. In addition, WBP is the only approach ethically acceptable to monitor lung function for the duration of 5 hours.

Another limitation of this work is combining female and male mice in some of the studies presented in Chapters 4 and 5. Albeit the HDM-induced responses were identical between female and male mice and groups were sex and aged matched, this could introduce additional variability to the responses. However, as the genetically modified mice were bred in house and could not be used for other purposes, we considered it unethical and against the 3R principles (Aske and Waugh 2017) to increase the group sizes whilst restraining to only one sex. In addition, the preliminary study with TRPV4$^{-/-}$ mice was conducted with male mice only (Birrell et al. 2016) and this approach enabled us to confirm that sex was not a confounding factor in TRPV4 signalling axis.

The lack of proper littermate controls for P2X7$^{-/-}$ and PAR2$^{-/-}$ mice is another limitation interpretation of the presented results. The genetic background of WT mice was chosen to match those of P2X7$^{-/-}$ and PAR2$^{-/-}$ mice as recommended by the supplier, however differences in the genetic background between WT and PAR2$^{-/-}$ or P2X7$^{-/-}$ mice, respectively, might still exist and could potentially contribute to the observed outcomes (Holmdahl and Malissen 2012).

7.3. Future directions

7.3.1. Clarification of the role of TRPV4 in asthma pathogenesis

Chapter 6 has demonstrated that GSK279, a highly selective TRPV4 antagonist (Brooks et al. 2019), was associated with a modest trend towards reduction of allergen induced airway eosinophilia in our murine and rat AAD models. However, the preliminary study with TRPV4$^{-/-}$ mice suggested a central role for TRPV4 in the development of HDM-induced AAD (Birrell et al. 2016). We thus postulated that TRPV4 signalling was fundamental in sensitisation to allergens rather than allergen-induced responses. To address this hypothesis, the study with TRPV4$^{-/-}$ mice would need to be repeated initially to confirm the preliminary observations

as a recently published study reported no effect of TRPV4$^{-/-}$ on the development of AAD in murine asthma model, using the same TRPV4$^{-/-}$ mice that had been used in our preliminary work (Palaniyandi et al. 2020). Alternatively, TRPV4 signalling could be blocked during sensitisation phase with TRPV4 antagonists such as GSK279. To understand TRPV4 mechanisms in allergen sensitisation further, the contribution of individual cells could be studied next. For example, using bone marrow adoptive transfer in WT and TRPV4$^{-/-}$ mice would allow us to understand the contribution of structural cell- versus haematopoietic cell- expressed TRPV4. The adoptive transfer of TRPV4$^{-/-}$ individual immune cells, such as CD4^{+} T cells, DCs or ILC2s into WT mice would allow us to directly assess the role of TRPV4 on specific immune population in allergen sensitisation.

However, as discussed in Chapter 3, the immune cells might not be the drivers of TRPV4 signalling in this model. We have only demonstrated gene expression on immune cell, but have not confirmed the expression of proteins or functionality of those channels. Little is known about the role of TRPV4 for function of DCs, CD4^{+} T cells and ILC2s and in vitro studies on isolated human cells are warranted to establish whether TRPV4 signalling is required for proliferation, differentiation, cytokine production, antigen presentation, Th2 priming to name a few. In vitro studies would also allow us to confirm the postulated TRPV4-P2X7 and PAR2-TRPV4 links, respectively. In addition, TRPV4 is highly expressed on airway epithelial cells (Fernández-Fernández et al. 2002, Andrade et al. 2005) and airway epithelium is an active player in allergen sensitisation (Lloyd and Snelgrove 2018) which is not recapitulated in the HDM-induced model of AAD. This means that TRPV4, particularly epithelial TRPV4 could be fundamental in mucosal sensitisation to aeroallergens. Indeed, Wiesner et al. have recently demonstrated club cell TRPV4 to be responsible for mucosal sensitisation to Alp1 (Wiesner et al. 2020). It would be therefore interesting to investigate this further using AAD models relying on mucosal sensitisation to allergens such as HDM, ALT or CE. Wiesner et al. have also developed methodology to induce conditional TRPV4 knockout or overexpression of TRPV4 selectively in club cells, which could be extremely useful when studying the role of airway epithelial TRPV4 in the development of AAD (Wiesner et al. 2020).

In addition to allergen sensitisation, TRPV4 could be also involved in respiratory symptoms commonly experienced by asthmatic patients. TRPV4 is highly expressed on airway smooth muscle cells (Jia et al. 2004) and it has been recently implicated in bronchoconstriction in a

mast cell dependent way (McAlexander et al. 2014, Bonvini et al. 2020). Although the results of this thesis show a lack of role for TRPV4 in AHR, there are considerable mouse and human interspecies differences and limitations of this model to comprehensively address the involvement of TRPV4 in bronchoconstriction in asthmatic patients. For example, mouse airway anatomy differs greatly to human and there is limited airway smooth muscle in mice in comparison to human (Zosky and Sly 2007). Although GSK101 induced bronchoconstriction in naïve mice, it does not appear to be mediated by P2X4 receptors (unpublished observations), suggestive of a different mechanism behind GSK101-induced bronchoconstriction as in man. Moreover, we have been unable to establish TRPV4-induced contraction in isolated murine trachea even though this has been done on isolated GP and human trachea (Bonvini et al. 2020)(unpublished observations). Mice and rats are less responsive to cysteinyl leukotrienes which are responsible for TRPV4-induced contraction in GP and human (Martin et al. 1988, Held et al. 1999, McAlexander et al. 2014, Bonvini et al. 2020). The murine HDM model used in this thesis is not dependent on mast cells (unpublished data), which could perhaps explain some of the discrepancies. Therefore, interrogating TRPV4 in AHR in GP AAD models may be more appropriate due to greater similarity in airway anatomy and airway responses (Zosky and Sly 2007). For the same reasons GP AAD models could also be used to confirm the lack of role for TRPV4 in LAR as demonstrated in the rat OVA model.

Cough is another symptom that is commonly experienced by asthmatic patients, however the mechanisms leading to enhanced cough reflex in asthmatic patients are not yet fully understood (Satia et al. 2020). Our laboratory has demonstrated that TRPV4 can trigger cough via the activation of P2X2/3 receptors on airway sensory nerves (Bonvini et al. 2016) and it could potentially contribute to cough in asthma. To investigate this, a GP AAD model with spontaneous cough could be established as GPs are the only rodents with a cough reflex similar to humans (Zosky and Sly 2007, Ramos-Ramírez et al. 2020).

7.3.2. Elucidate the role of ATP and P2X receptors in asthma

The importance of ATP signalling for the development of HDM-induced model of AAD is based on the preliminary work demonstrating that Panx-1 deficiency alleviated allergic airway inflammation and AHR upon HDM challenge (Figure 1.5) and has not yet been confirmed. We aimed to measure ATP release to demonstrate that allergen challenge was indeed associated

with increased ATP levels in the airways. So far, only a couple of laboratories have demonstrated increased ATP levels in the airways of asthmatic patients or in AAD models (Idzko et al. 2007, Vanderstocken et al. 2010). Unfortunately, ATP could not be measured with commercially available ATP assays based on luciferin-luciferase reaction, although the two publications used such methods to detect ATP (Idzko et al. 2007, Vanderstocken et al. 2010). Establishing a reliable technique to measure ATP in BAL samples from our AAD models as well as asthmatic patients would greatly contribute to the understanding of TRPV4 signalling pathways in respiratory disease. Measuring ATP has been proven to be quite challenging and in our laboratory we have been optimising sample collection and handling protocol to minimise ATP breakdown prior to the analysis as well as ATP detection methods. One possibility is mass spectrometry as it would allow not only for the detection of ATP but also ATP breakdown products, increasing the sensitivity of the method and adding additional information. In addition to directly measuring ATP levels, other approaches could be used to demonstrate the importance of ATP for the development of AAD upon HDM challenge. One possibility is enhancing ATP breakdown in the airways by administering enzymes such as apyrase (CD39) prior to an allergen challenge and this has been used in several AAD models to show the importance of purinergic signalling (Idzko et al. 2007, Li et al. 2014, Zhang et al. 2017). Alternatively, CD39 deficient mice or CD39 inhibitors could be used to inhibit ATP breakdown and then study whether this intervention exacerbates allergen-related pathology (Idzko et al. 2013, Li et al. 2015).

Whilst these studies would confirm the role of ATP in the model, they would not be particularly informative about which P2 receptors are responsible for the detrimental effects of ATP. In this thesis we thus tried to use a more selective approach by identifying P2X receptors dysregulated upon HDM challenge and investigated their role in vivo by using genetically modified mice without an individual functional P2X receptor. We have investigated P2X1, P2X4 and P2X7 as they were the most abundantly expressed receptors in the lungs and on isolated immune cells and were dysregulated upon HDM challenge. Our results suggest that P2X1 and P2X4 are dispensable for the HDM-induced AAD model and P2X7 might partially contribute to eosinophilic airway inflammation but not AHR. However, we have only used genetically modified mice to study those and due to the limitation of these mice, particularly $P2X7^{-/-}$ mice, these results would need to be verified using alternative

approaches (Adriouch et al. 2002, Masin et al. 2012). Several P2X7 selective antagonists are available and have been used in various in vivo experimental models (Bartlett et al. 2014, Illes et al. 2020).

Nevertheless, the investigations into the individual P2 receptors in asthma pathology need to extend beyond P2X1, P2X4 and P2X7 as other P2 receptors alone or in combination could be involved in the mechanisms leading to allergic airway inflammation and/or AHR as discussed in Chapter 4.

7.3.3. Validating the role of PAR2 as an asthma target

This thesis has demonstrated that PAR2$^{-/-}$ but not inhibition of PAR2 with anti-PAR2 antibody alleviated allergic airway inflammation, suggesting the role of PAR2 in sensitisation to HDM. Unfortunately, we could not obtain PK or other functional data confirming the inhibition of PAR2 signalling by MEDI2344 in the HDM AAD model. Thus, alternative PAR2 inhibitors could be characterised and then used to confirm the MEDI2344 outcomes which would also aid PAR2 related research in general. PAR2 tools are poorly characterised and can exert agonist and antagonist reactions simultaneously due to biased signalling (Hollenberg et al. 2014, Yau et al. 2016). Depending on the PAR2 signalling pathways activated PAR2 activation can have either protective or deleterious effects (Hollenberg et al. 2014, Yau et al. 2016). In addition, the use of PAR2 inhibitors during sensitisation phase would allow us to verify the outcomes of PAR2 knockout studies and confirm the involvement of PAR2 in allergen sensitisation. The effect of PAR2$^{-/-}$ was relatively modest in our studies and increased group sizes were needed to observe statistically significant differences.

7.3.4. Further characterisation of murine HDM-induced model of AAD

We have extensively, but not completely characterised allergic airway inflammation in the murine HDM model of AAD. It is becoming increasingly evident that mechanisms beyond Th2 cells are important in asthma and are responsible for the diversity of asthma phenotypes (Lloyd and Snelgrove 2018, Kuruvilla et al. 2019). The models of AAD are incomplete and only mimic certain aspect of the human disease (Zosky and Sly 2007, Aun et al. 2017). Therefore, it is of paramount importance to understand the limitations of the models we use in order to advance our understanding of disease, finding and testing novel therapeutic targets.

The importance of airway epithelium and ILC2s for asthma pathogenesis has been established in the last decade (Lloyd and Snelgrove 2018). However, we do not have a complete understanding to what extent airway epithelium or ILC2s contribute to the development of airway inflammation and AHR in our models. We have established that $CD4^+$ T cells are required for the initiation of immune responses as non-sensitised mice or mice lacking mature lymphocytes or specifically $CD4^{+/+}$ T cells do not develop any inflammation upon HDM challenge (Raemdonck et al. 2016)(unpublished data). However, it remains unclear if ILC2s are needed for the maintenance of airway inflammation and whether they contribute to AHR. To address these ILC2 deficient models could be used, with the conditional KOs giving the potential to evaluate the role of ILC2s selectively during allergen challenge phase (Cording et al. 2018). The role of airway epithelium could be addressed by investigating the role of individual epithelial derived cytokines. Based on gene expression data IL-33 appears to be the most important epithelial derived cytokine in the HDM-induced model and its contribution to the pathology could be investigated using genetically modified mice and/or monoclonal antibodies targeting IL-33/ST2 interaction (Hong et al. 2020).

Lastly, AHR is a hallmark feature of the HDM-induced AAD model, however, the mechanisms behind AHR remain poorly understood (Raemdonck et al. 2016). Particularly, it is unclear to what extent (if at all) the exaggerated responses induced by 5-HT are modulated by nervous system (Pincus et al. 2021). Airway nervous system plays an important role in AHR and ATP has been shown to activate P2X2/3 on airway sensory neurons triggering nerve reflexes (Bonvini et al. 2016, Pelleg 2020, Pincus et al. 2021). It would be interesting to see if a P2X2/3 antagonist can alleviate AHR and potentially airway inflammation as AHR often remains unmodulated with anti-inflammatory therapies in asthmatic patients (Leckie et al. 2000).

7.4. Concluding remarks

The aim of this thesis was to elucidate TRPV4 signalling pathways that lead to airway inflammation and AHR in asthma following up the preliminary observations demonstrating that disruption of TRPV4 signalling abolished cardinal features of asthma in our rodent models. We have demonstrated that $P2X7^{-/-}$ ameliorated eosinophilic airway inflammation in the murine HDM model, suggesting P2X7 could be part of TRPV4 signalling pathways leading to airway inflammation. PAR2 was found to potentially contribute to TRPV4 activation during allergen sensitisation, as $PAR2^{-/-}$ but not PAR2 blocking antibody ameliorated eosinophilic

airway inflammation in the HDM model. Lastly, we investigated the role of TRPV4 during allergen challenge phase in order to consolidate the preliminary findings and to address the role of TRPV4 during allergen challenge phase specifically. We have demonstrated that TRPV4 inhibition during allergen challenge phase modestly reduced airway eosinophilia in our mouse and rat AAD models, but had no effect on AHR or LAR. Overall, this thesis demonstrated that targeting TRPV4 in patients with atopic asthma may not be very efficacious in supressing airway inflammation nor controlling airway response as demonstrated in the rodent models used. However, a role for the TRPV4-ATP-P2 receptor pathway is yet to be fully elucidated in other asthma phenotypes and associated symptoms such as cough.

8. References

Aalbers, R., Kauffman, H. F., Vrugt, B., Koeter, G. H. and de Monchy, J. G. Allergen-induced recruitment of inflammatory cells in lavage 3 and 24 h after challenge in allergic asthmatic lungs. *Chest.* 1993; 103(4): 1178-1184. DOI: 10.1378/chest.103.4.1178.

Aarafi, H., Yadegari, A., Dastgheib, S. A., Bahrami, R., Shajari, A., Nafei, Z., et al. Association of +1923C > T, -1112C > T and +2044A > G Polymorphisms in IL-13 Gene with Susceptibility to Pediatric Asthma: A Systematic Review and Meta-Analysis. *Fetal Pediatr Pathol.* 2020: 1-19. DOI: 10.1080/15513815.2020.1783406.

Abdelrahman, A., Namasivayam, V., Hinz, S., Schiedel, A. C., Kose, M., Burton, M., et al. Characterization of P2X4 receptor agonists and antagonists by calcium influx and radioligand binding studies. *Biochem Pharmacol.* 2017; 125: 41-54. DOI: 10.1016/j.bcp.2016.11.016.

Abdulqawi, R., Dockry, R., Holt, K., Layton, G., McCarthy, B. G., Ford, A. P., et al. P2X3 receptor antagonist (AF-219) in refractory chronic cough: a randomised, double-blind, placebo-controlled phase 2 study. *Lancet.* 2015; 385(9974): 1198-1205. DOI: 10.1016/s0140-6736(14)61255-1.

Abramowski, P., Ogrodowczyk, C., Martin, R. and Pongs, O. A truncation variant of the cation channel P2RX5 is upregulated during T cell activation. *PLoS One.* 2014; 9(9): e104692. DOI: 10.1371/journal.pone.0104692.

Adams, M. N., Pagel, C. N., Mackie, E. J. and Hooper, J. D. Evaluation of antibodies directed against human protease-activated receptor-2. *Naunyn Schmiedebergs Arch Pharmacol.* 2012; 385(9): 861-873. DOI: 10.1007/s00210-012-0783-6.

Adriouch, S., Dox, C., Welge, V., Seman, M., Koch-Nolte, F. and Haag, F. Cutting edge: a natural P451L mutation in the cytoplasmic domain impairs the function of the mouse P2X7 receptor. *J Immunol.* 2002; 169(8): 4108-4112. DOI: 10.4049/jimmunol.169.8.4108.

Akers, I. A., Parsons, M., Hill, M. R., Hollenberg, M. D., Sanjar, S., Laurent, G. J., et al. Mast cell tryptase stimulates human lung fibroblast proliferation via protease-activated receptor-2. *Am J Physiol Lung Cell Mol Physiol.* 2000; 278(1): L193-L201. DOI: 10.1152/ajplung.2000.278.1.L193.

Akuthota, P., Wang, H. and Weller, P. F. Eosinophils as antigen-presenting cells in allergic upper airway disease. *Curr Opin Allergy Clin Immunol.* 2010; 10(1): 14-19. DOI: 10.1097/ACI.0b013e328334f693.

Al-Ramli, W., Préfontaine, D., Chouiali, F., Martin, J. G., Olivenstein, R., Lemière, C., et al. TH17-associated cytokines (IL-17A and IL-17F) in severe asthma. *Journal of Allergy and Clinical Immunology.* 2009; 123(5): 1185-1187. DOI: https://doi.org/10.1016/j.jaci.2009.02.024.

Al-Shami, A., Spolski, R., Kelly, J., Keane-Myers, A. and Leonard, W. J. A role for TSLP in the development of inflammation in an asthma model. *J Exp Med.* 2005; 202(6): 829-839. DOI: 10.1084/jem.20050199.

Alam, R., York, J., Boyars, M., Stafford, S., Grant, J. A., Lee, J., et al. Increased MCP-1, RANTES, and MIP-1alpha in bronchoalveolar lavage fluid of allergic asthmatic patients. *Am J Respir Crit Care Med.* 1996; 153(4 Pt 1): 1398-1404. DOI: 10.1164/ajrccm.153.4.8616572.

Alenmyr, L., Uller, L., Greiff, L., Hogestatt, E. D. and Zygmunt, P. M. TRPV4-mediated calcium influx and ciliary activity in human native airway epithelial cells. *Basic & clinical pharmacology & toxicology.* 2014; 114(2): 210-216. DOI: 10.1111/bcpt.12135.

Alessandri-Haber, N., Dina, O. A., Joseph, E. K., Reichling, D. and Levine, J. D. A transient receptor potential vanilloid 4-dependent mechanism of hyperalgesia is engaged by concerted action of inflammatory mediators. *J Neurosci.* 2006; 26(14): 3864-3874. DOI: 10.1523/jneurosci.5385-05.2006.

Alessandrini, F., Musiol, S., Schneider, E., Blanco-Pérez, F. and Albrecht, M. Mimicking Antigen-Driven Asthma in Rodent Models—How Close Can We Get? *Front Immunol.* 2020; 11(2394). DOI: 10.3389/fimmu.2020.575936.

Allard, B., Bara, I., Gilbert, G., Carvalho, G., Trian, T., Ozier, A., et al. Protease activated receptor-2 expression and function in asthmatic bronchial smooth muscle. *PLoS One.* 2014; 9(2): e86945. DOI: 10.1371/journal.pone.0086945.

Alpizar, Y. A., Boonen, B., Sanchez, A., Jung, C., Lopez-Requena, A., Naert, R., et al. TRPV4 activation triggers protective responses to bacterial lipopolysaccharides in airway epithelial cells. *Nat Commun.* 2017; 8(1): 1059. DOI: 10.1038/s41467-017-01201-3.

Alvarez, M. J., Olaguibel, J. M., Garcia, B. E., Rodriquez, A., Tabar, A. I. and Urbiola, E. Airway inflammation in asthma and perennial allergic rhinitis. Relationship with nonspecific bronchial responsiveness and maximal airway narrowing. *Allergy.* 2000; 55(4): 355-362. DOI: 10.1034/j.1398-9995.2000.00312.x.

Amadesi, S., Nie, J., Vergnolle, N., Cottrell, G. S., Grady, E. F., Trevisani, M., et al. Protease-activated receptor 2 sensitizes the capsaicin receptor transient receptor potential vanilloid receptor 1 to induce hyperalgesia. *J Neurosci.* 2004; 24(18): 4300-4312. DOI: 10.1523/jneurosci.5679-03.2004.

Amison, R. T., Momi, S., Morris, A., Manni, G., Keir, S., Gresele, P., et al. RhoA signaling through platelet P2Y(1) receptor controls leukocyte recruitment in allergic mice. *J Allergy Clin Immunol.* 2015; 135(2): 528-538. DOI: 10.1016/j.jaci.2014.09.032.

Andrade, Y. N., Fernandes, J., Vazquez, E., Fernandez-Fernandez, J. M., Arniges, M., Sanchez, T. M., et al. TRPV4 channel is involved in the coupling of fluid viscosity changes to epithelial ciliary activity. *J Cell Biol.* 2005; 168(6): 869-874. DOI: 10.1083/jcb.200409070.

Arizmendi, N. G., Abel, M., Mihara, K., Davidson, C., Polley, D., Nadeem, A., et al. Mucosal allergic sensitization to cockroach allergens is dependent on proteinase activity and proteinase-activated receptor-2 activation. *J Immunol.* 2011; 186(5): 3164-3172. DOI: 10.4049/jimmunol.0903812.

Asaduzzaman, M., Davidson, C., Nahirney, D., Fiteih, Y., Puttagunta, L. and Vliagoftis, H. Proteinase-activated receptor-2 blockade inhibits changes seen in a chronic murine asthma model. *Allergy.* 2018; 73(2): 416-420. DOI: 10.1111/all.13313.

Asaduzzaman, M., Nadeem, A., Arizmendi, N., Davidson, C., Nichols, H. L., Abel, M., et al. Functional inhibition of PAR2 alleviates allergen-induced airway hyperresponsiveness and inflammation. *Clin Exp Allergy.* 2015; 45(12): 1844-1855. DOI: 10.1111/cea.12628.

Aske, K. C. and Waugh, C. A. Expanding the 3R principles: More rigour and transparency in research using animals. *EMBO Rep.* 2017; 18(9): 1490-1492. DOI: 10.15252/embr.201744428.

Asthma UK. (2021). "Asthma facts and statistics." Retrieved 19/03/2021, from https://www.asthma.org.uk/.

Aubier, M., Thabut, G., Hamidi, F., Guillou, N., Brard, J., Dombret, M. C., et al. Airway smooth muscle enlargement is associated with protease-activated receptor 2/ligand overexpression in patients with difficult-to-control severe asthma. *J Allergy Clin Immunol.* 2016; 138(3): 729-739 e711. DOI: 10.1016/j.jaci.2015.12.1332.

Aun, M. V., Bonamichi-Santos, R., Arantes-Costa, F. M., Kalil, J. and Giavina-Bianchi, P. Animal models of asthma: utility and limitations. *J Asthma Allergy.* 2017; 10: 293-301. DOI: 10.2147/jaa.S121092.

Ayars, G. H., Altman, L. C., Gleich, G. J., Loegering, D. A. and Baker, C. B. Eosinophil- and eosinophil granule-mediated pneumocyte injury. *Journal of Allergy and Clinical Immunology.* 1985; 76(4): 595-604. DOI: https://doi.org/10.1016/0091-6749(85)90781-X.

Baines, K. J., Simpson, J. L., Wood, L. G., Scott, R. J. and Gibson, P. G. Transcriptional phenotypes of asthma defined by gene expression profiling of induced sputum samples. *Journal of Allergy and Clinical Immunology.* 2011; 127(1). DOI: 10.1016/j.jaci.2010.10.024.

Baker, K., Raemdonck, K., Dekkak, B., Snelgrove, R. J., Ford, J., Shala, F., et al. Role of the ion channel, transient receptor potential cation channel subfamily V member 1 (TRPV1), in allergic asthma. *Respiratory Research.* 2016; 17(1): 67. DOI: 10.1186/s12931-016-0384-x.

Baker, K., Raemdonck, K., Snelgrove, R. J., Belvisi, M. G. and Birrell, M. A. Characterisation of a murine model of the late asthmatic response. *Respiratory Research.* 2017; 18(1): 55. DOI: 10.1186/s12931-017-0541-x.

Balestrini, A., Joseph, V., Dourado, M., Reese, R. M., Shields, S. D., Rouge, L., et al. A TRPA1 inhibitor suppresses neurogenic inflammation and airway contraction for asthma treatment. *J Exp Med.* 2021; 218(4). DOI: 10.1084/jem.20201637.

Baricordi, O. R., Ferrari, D., Melchiorri, L., Chiozzi, P., Hanau, S., Chiari, E., et al. An ATP-activated channel is involved in mitogenic stimulation of human T lymphocytes. *Blood.* 1996; 87(2): 682-690. DOI: DOI 10.1182/blood.V87.2.682.bloodjournal872682.

Barlow, J. L., Bellosi, A., Hardman, C. S., Drynan, L. F., Wong, S. H., Cruickshank, J. P., et al. Innate IL-13–producing nuocytes arise during allergic lung inflammation and contribute to airways hyperreactivity. *Journal of Allergy and Clinical Immunology.* 2012; 129(1): 191-198.e194. DOI: https://doi.org/10.1016/j.jaci.2011.09.041.

Barlow, J. L., Peel, S., Fox, J., Panova, V., Hardman, C. S., Camelo, A., et al. IL-33 is more potent than IL-25 in provoking IL-13–producing nuocytes (type 2 innate lymphoid cells) and airway contraction. *Journal of Allergy and Clinical Immunology.* 2013; 132(4): 933-941. DOI: https://doi.org/10.1016/j.jaci.2013.05.012.

Barnes, P. J. Targeting cytokines to treat asthma and chronic obstructive pulmonary disease. *Nature reviews. Immunology.* 2018. DOI: 10.1038/s41577-018-0006-6.

Bartemes, K. R., Iijima, K., Kobayashi, T., Kephart, G. M., McKenzie, A. N. and Kita, H. IL-33-responsive lineage- CD25+ CD44(hi) lymphoid cells mediate innate type 2 immunity and allergic inflammation in the lungs. *J Immunol.* 2012; 188(3): 1503-1513. DOI: 10.4049/jimmunol.1102832.

Bartlett, R., Stokes, L. and Sluyter, R. The P2X7 receptor channel: recent developments and the use of P2X7 antagonists in models of disease. *Pharmacol Rev.* 2014; 66(3): 638-675. DOI: 10.1124/pr.113.008003.

Basoglu, O. K., Barnes, P. J., Kharitonov, S. A. and Pelleg, A. Effects of Aerosolized Adenosine 5'-Triphosphate in Smokers and Patients With COPD. *Chest.* 2015; 148(2): 430-435. DOI: 10.1378/chest.14-2285.

Basoglu, O. K., Pelleg, A., Essilfie-Quaye, S., Brindicci, C., Barnes, P. J. and Kharitonov, S. A. Effects of aerosolized adenosine 5'-triphosphate vs adenosine 5'-monophosphate on dyspnea and airway caliber in healthy nonsmokers and patients with asthma. *Chest.* 2005; 128(4): 1905-1909. DOI: 10.1378/chest.128.4.1905.

Basoglu, O. K., Pelleg, A., Kharitonov, S. A. and Barnes, P. J. Contrasting effects of ATP and adenosine on capsaicin challenge in asthmatic patients. *Pulm Pharmacol Ther.* 2017; 45: 13-18. DOI: 10.1016/j.pupt.2017.04.004.

Bates, J., Irvin, C., Brusasco, V., Drazen, J., Fredberg, J., Loring, S., et al. The use and misuse of Penh in animal models of lung disease. *American Journal of Respiratory Cell and Molecular Biology.* 2004; 31: 373-374. DOI: 10.1165/ajrcmb.31.3.1.

Bates, J. H. T. and Irvin, C. G. Measuring lung function in mice: The phenotyping uncertainty principle. *Journal of Applied Physiology.* 2003; 94: 1297-1306. DOI: 10.1152/japplphysiol.00706.2002.

Baxter, M., Eltom, S., Dekkak, B., Yew-Booth, L., Dubuis, E. D., Maher, S. A., et al. Role of transient receptor potential and pannexin channels in cigarette smoke-triggered ATP release in the lung. *Thorax.* 2014; 69(12): 1080-1089. DOI: 10.1136/thoraxjnl-2014-205467.

Beasley, R., Braithwaite, I., Semprini, A., Kearns, C., Weatherall, M. and Pavord, I. D. Optimal Asthma Control: Time for a New Target. *Am J Respir Crit Care Med.* 2020; 201(12): 1480-1487. DOI: 10.1164/rccm.201910-1934CI.

Bel, E. H., Wenzel, S. E., Thompson, P. J., Prazma, C. M., Keene, O. N., Yancey, S. W., et al. Oral Glucocorticoid-Sparing Effect of Mepolizumab in Eosinophilic Asthma. *New England Journal of Medicine.* 2014; 371(13): 1189-1197. DOI: 10.1056/NEJMoa1403291.

Belvisi, M. G. and Birrell, M. A. The emerging role of transient receptor potential channels in chronic lung disease. *European Respiratory Journal.* 2017; 50(2): 1601357. DOI: 10.1183/13993003.01357-2016.

Ben-Sasson, S. Z., Le Gros, G., Conrad, D. H., Finkelman, F. D. and Paul, W. E. IL-4 production by T cells from naive donors. IL-2 is required for IL-4 production. *Journal of immunology.* 1990; 145(4): 1127-1136.

Ben-Zimra, M., Bachelet, I., Seaf, M., Gleich, G. J. and Levi-Schaffer, F. Eosinophil major basic protein activates human cord blood mast cells primed with fibroblast membranes by integrin-β1. *Allergy.* 2013; 68(10): 1259-1268. DOI: https://doi.org/10.1111/all.12232.

Benítez-Angeles, M., Morales-Lázaro, S. L., Juárez-González, E. and Rosenbaum, T. TRPV1: Structure, Endogenous Agonists, and Mechanisms. *International Journal of Molecular Sciences.* 2020; 21(10): 3421.

Bentley, A. M., Meng, Q., Robinson, D. S., Hamid, Q., Kay, A. B. and Durham, S. R. Increases in activated T lymphocytes, eosinophils, and cytokine mRNA expression for interleukin-5 and granulocyte/macrophage colony-stimulating factor in bronchial biopsies after allergen inhalation challenge in atopic asthmatics. *Am J Respir Cell Mol Biol.* 1993; 8(1): 35-42. DOI: 10.1165/ajrcmb/8.1.35.

Berchtold, S., Ogilvie, A. L. J., Bogdan, C., Muhl-Zurbes, P., Ogilvie, A., Schuler, G., et al. Human monocyte derived dendritic cells express functional P2X and P2Y receptors as well as ecto-nucleotidases. *Febs Letters.* 1999; 458(3): 424-428. DOI: Doi 10.1016/S0014-5793(99)01197-7.

Bergren, D. R. Chronic tobacco smoke exposure increases airway sensitivity to capsaicin in awake guinea pigs. *J Appl Physiol.* 2001; 90(2): 695-704. DOI: 10.1152/jappl.2001.90.2.695.

Berry, M., Brightling, C., Pavord, I. and Wardlaw, A. J. TNF-α in asthma. *Curr Opin Pharmacol.* 2007; 7(3): 279-282. DOI: 10.1016/j.coph.2007.03.001.

Berry, M. A., Parker, D., Neale, N., Woodman, L., Morgan, A., Monk, P., et al. Sputum and bronchial submucosal IL-13 expression in asthma and eosinophilic bronchitis. *Journal of Allergy and Clinical Immunology.* 2004; 114(5): 1106-1109. DOI: https://doi.org/10.1016/j.jaci.2004.08.032.

Bertin, S., Aoki-Nonaka, Y., de Jong, P. R., Nohara, L. L., Xu, H., Stanwood, S. R., et al. The ion channel TRPV1 regulates the activation and proinflammatory properties of CD4(+) T cells. *Nat Immunol.* 2014; 15(11): 1055-1063. DOI: 10.1038/ni.3009.

Bertin, S., Aoki-Nonaka, Y., Lee, J., de Jong, P. R., Kim, P., Han, T., et al. The TRPA1 ion channel is expressed in CD4+ T cells and restrains T-cell-mediated colitis through inhibition of TRPV1. *Gut.* 2017; 66(9): 1584-1596. DOI: 10.1136/gutjnl-2015-310710.

Besnard, A., Gautherot, J., Julien, B., Tebbi, A., Garcin, I., Doignon, I., et al. The P2X4 purinergic receptor impacts liver regeneration after partial hepatectomy in mice through the regulation of biliary homeostasis. *Hepatology.* 2016; 64(3): 941-953. DOI: 10.1002/hep.28675.

Besnard, A. G., Guillou, N., Tschopp, J., Erard, F., Couillin, I., Iwakura, Y., et al. NLRP3 inflammasome is required in murine asthma in the absence of aluminum adjuvant. *Allergy.* 2011a; 66(8): 1047-1057. DOI: 10.1111/j.1398-9995.2011.02586.x.

Besnard, A. G., Togbe, D., Guillou, N., Erard, F., Quesniaux, V. and Ryffel, B. IL-33-activated dendritic cells are critical for allergic airway inflammation. *Eur J Immunol.* 2011b; 41(6): 1675-1686. DOI: 10.1002/eji.201041033.

Bhavsar, I., Miller, C. S. and Al-Sabbagh, M. Macrophage Inflammatory Protein-1 Alpha (MIP-1 alpha)/CCL3: As a Biomarker. *General Methods in Biomarker Research and their Applications. Biomarkers in Disease: Methods, Discoveries and Applications.* 2015; 1-2: 223-249. DOI: 10.1007/978-94-007-7696-8_27.

Bi, J., Cui, L., Yu, G., Yang, X., Chen, Y. and Wan, X. NK Cells Alleviate Lung Inflammation by Negatively Regulating Group 2 Innate Lymphoid Cells. *J Immunol.* 2017; 198(8): 3336-3344. DOI: 10.4049/jimmunol.1601830.

Bianconi, V., Sahebkar, A., Atkin, S. L. and Pirro, M. The regulation and importance of monocyte chemoattractant protein-1. *Curr Opin Hematol.* 2018; 25(1): 44-51. DOI: 10.1097/moh.0000000000000389.

Birrell, M., Bonvini, S. J., Baker, K. E., Dekkak, B., Miralpeix, M., Tarrason, G., et al. The TRPV4 ion channel plays a key role in allergic asthma. Conference Abstract. *Eur Respir J.* 2016; 48: OA1792. DOI: 10.1183/13993003.congress-2016.OA1792.

Birrell, M. A., Crispino, N., Hele, D. J., Patel, H. J., Yacoub, M. H., Barnes, P. J., et al. Effect of dopamine receptor agonists on sensory nerve activity: possible therapeutic targets for the treatment of asthma and COPD. *British Journal of Pharmacology.* 2002; 136(4): 620-628. DOI: https://doi.org/10.1038/sj.bjp.0704758.

Birrell, M. A., Van Oosterhout, A. J. and Belvisi, M. G. Do the current house dust mite-driven models really mimic allergic asthma? *Eur Respir J.* 2010; 36(5): 1220-1221. DOI: 10.1183/09031936.00069110.

Blake, K. J., Jiang, X. R. and Chiu, I. M. Neuronal Regulation of Immunity in the Skin and Lungs. *Trends Neurosci.* 2019; 42(8): 537-551. DOI: 10.1016/j.tins.2019.05.005.

Bleecker, E. R., FitzGerald, J. M., Chanez, P., Papi, A., Weinstein, S. F., Barker, P., et al. Efficacy and safety of benralizumab for patients with severe asthma uncontrolled with high-dosage inhaled corticosteroids and long-acting β2-agonists (SIROCCO): a randomised, multicentre, placebo-controlled phase 3 trial. *The Lancet.* 2016; 388(10056): 2115-2127. DOI: https://doi.org/10.1016/S0140-6736(16)31324-1.

Bolton, S. J., McNulty, C. A., Thomas, R. J., Hewitt, C. R. and Wardlaw, A. J. Expression of and functional responses to protease-activated receptors on human eosinophils. *J Leukoc Biol.* 2003; 74(1): 60-68. DOI: 10.1189/jlb.0702351.

Bønnelykke, K., Sleiman, P., Nielsen, K., Kreiner-Møller, E., Mercader, J. M., Belgrave, D., et al. A genome-wide association study identifies CDHR3 as a susceptibility locus for early childhood asthma with severe exacerbations. *Nat Genet.* 2014; 46(1): 51-55. DOI: 10.1038/ng.2830.

Bonvini, S. J., Birrell, M. A., Dubuis, E., Adcock, J. J., Wortley, M. A., Flajolet, P., et al. Novel airway smooth muscle-mast cell interactions and a role for the TRPV4-ATP axis in non-atopic asthma. *Eur Respir J.* 2020; 56(1). DOI: 10.1183/13993003.01458-2019.

Bonvini, S. J., Birrell, M. A., Grace, M. S., Maher, S. A., Adcock, J. J., Wortley, M. A., et al. Transient receptor potential cation channel, subfamily V, member 4 and airway sensory afferent activation: Role of adenosine triphosphate. *J Allergy Clin Immunol.* 2016; 138(1): 249-261 e212. DOI: 10.1016/j.jaci.2015.10.044.

Bonvini, S. J., Wortley, M., Birrell, M. A. and Belvisi, M. Identification Of Endogenous, Disease Relevant Activators Of Trpv4 In The Airways. *Am J Respir Crit Care Med.* 2017: 195:A3146.

Boonpiyathad, S., Pornsuriyasak, P., Buranapraditkun, S. and Klaewsongkram, J. Interleukin-2 levels in exhaled breath condensates, asthma severity, and asthma control in nonallergic asthma. *Allergy Asthma Proc.* 2013; 34(5): e35-41. DOI: 10.2500/aap.2013.34.3680.

Borish, L., Mascali, J. J., Dishuck, J., Beam, W. R., Martin, R. J. and Rosenwasser, L. J. Detection of alveolar macrophage-derived IL-1 beta in asthma. Inhibition with corticosteroids. *J Immunol.* 1992; 149(9): 3078-3082.

Bosnjak, B., Kazemi, S., Altenburger, L. M., Mokrovic, G. and Epstein, M. M. Th2-TRMs Maintain Life-Long Allergic Memory in Experimental Asthma in Mice. *Front Immunol.* 2019; 10(APR): 840. DOI: 10.3389/fimmu.2019.00840.

Bouchery, T., Kyle, R., Camberis, M., Shepherd, A., Filbey, K., Smith, A., et al. ILC2s and T cells cooperate to ensure maintenance of M2 macrophages for lung immunity against hookworms. *Nat Commun.* 2015; 6: 6970. DOI: 10.1038/ncomms7970.

Bouzigon, E., Ulgen, A., Dizier, M. H., Siroux, V., Lathrop, M., Kauffmann, F., et al. Evidence for a pleiotropic QTL on chromosome 5q13 influencing both time to asthma onset and asthma score in French EGEA families. *Hum Genet.* 2007; 121(6): 711-719. DOI: 10.1007/s00439-007-0363-x.

Bowler, J. W., Bailey, R. J., North, R. A. and Surprenant, A. P2X4, P2Y1 and P2Y2 receptors on rat alveolar macrophages. *Br J Pharmacol.* 2003; 140(3): 567-575. DOI: 10.1038/sj.bjp.0705459.

Bradding, P. and Arthur, G. Mast cells in asthma – state of the art. *Clinical & Experimental Allergy.* 2016; 46(2): 194-263. DOI: https://doi.org/10.1111/cea.12675.

Bradding, P., Okayama, Y., Howarth, P. H., Church, M. K. and Holgate, S. T. Heterogeneity of human mast cells based on cytokine content. *J Immunol.* 1995; 155(1): 297-307.

Bradding, P., Okayama, Y., Kambe, N. and Saito, H. Ion channel gene expression in human lung, skin, and cord blood-derived mast cells. *J Leukoc Biol.* 2003; 73(5): 614-620. DOI: 10.1189/jlb.1202602.

Bradding, P., Roberts, J. A., Britten, K. M., Montefort, S., Djukanovic, R., Mueller, R., et al. Interleukin-4, -5, and -6 and tumor necrosis factor-alpha in normal and asthmatic airways: evidence for the human mast cell as a source of these cytokines. *Am J Respir Cell Mol Biol.* 1994; 10(5): 471-480. DOI: 10.1165/ajrcmb.10.5.8179909.

Brandt, C., Thronicke, A., Roehmel, J. F., Krannich, A., Staab, D. and Schwarz, C. Impact of Long-Term Tiotropium Bromide Therapy on Annual Lung Function Decline in Adult Patients with Cystic Fibrosis. *PLoS One.* 2016; 11(6): e0158193. DOI: 10.1371/journal.pone.0158193.

Brightling, C. E., Bradding, P., Symon, F. A., Holgate, S. T., Wardlaw, A. J. and Pavord, I. D. Mast-cell infiltration of airway smooth muscle in asthma. *N Engl J Med.* 2002; 346(22): 1699-1705. DOI: 10.1056/NEJMoa012705.

Broide, D. H., Gleich, G. J., Cuomo, A. J., Coburn, D. A., Federman, E. C., Schwartz, L. B., et al. Evidence of ongoing mast cell and eosinophil degranulation in symptomatic asthma airway. *J Allergy Clin Immunol.* 1991; 88(4): 637-648. DOI: 10.1016/0091-6749(91)90158-k.

Brone, B., Moechars, D., Marrannes, R., Mercken, M. and Meert, T. P2X currents in peritoneal macrophages of wild type and P2X4 -/- mice. *Immunol Lett.* 2007; 113(2): 83-89. DOI: 10.1016/j.imlet.2007.07.015.

Brooks, C. A., Barton, L. S., Behm, D. J., Eidam, H. S., Fox, R. M., Hammond, M., et al. Discovery of GSK2798745: A Clinical Candidate for Inhibition of Transient Receptor Potential Vanilloid 4 (TRPV4). *ACS Med Chem Lett.* 2019; 10(8): 1228-1233. DOI: 10.1021/acsmedchemlett.9b00274.

Bruchard, M., Rebe, C., Derangere, V., Togbe, D., Ryffel, B., Boidot, R., et al. The receptor NLRP3 is a transcriptional regulator of TH2 differentiation. *Nat Immunol.* 2015; 16(8): 859-870. DOI: 10.1038/ni.3202.

Brusselle, G. G., Kips, J. C., Tavernier, J. H., van der Heyden, J. G., Cuvelier, C. A., Pauwels, R. A., et al. Attenuation of allergic airway inflammation in IL-4 deficient mice. *Clin Exp Allergy.* 1994; 24(1): 73-80. DOI: 10.1111/j.1365-2222.1994.tb00920.x.

Burnstock, G. and Boeynaems, J.-M. Purinergic signalling and immune cells. *Purinergic Signal.* 2014; 10(4): 529-564. DOI: 10.1007/s11302-014-9427-2.

Busse, W., Chupp, G., Nagase, H., Albers, F. C., Doyle, S., Shen, Q., et al. Anti–IL-5 treatments in patients with severe asthma by blood eosinophil thresholds: Indirect treatment comparison. *Journal of Allergy and Clinical Immunology.* 2019; 143(1): 190-200.e120. DOI: https://doi.org/10.1016/j.jaci.2018.08.031.

Busse, W. W., Holgate, S., Kerwin, E., Chon, Y., Feng, J., Lin, J., et al. Randomized, double-blind, placebo-controlled study of brodalumab, a human anti-IL-17 receptor monoclonal antibody, in moderate to severe asthma. *Am J Respir Crit Care Med.* 2013; 188(11): 1294-1302. DOI: 10.1164/rccm.201212-2318OC.

Busse, W. W., Israel, E., Nelson, H. S., Baker, J. W., Charous, B. L., Young, D. Y., et al. Daclizumab improves asthma control in patients with moderate to severe persistent asthma: a randomized, controlled trial. *Am J Respir Crit Care Med.* 2008; 178(10): 1002-1008. DOI: 10.1164/rccm.200708-1200OC.

Button, B., Okada, S. F., Frederick, C. B., Thelin, W. R. and Boucher, R. C. Mechanosensitive ATP release maintains proper mucus hydration of airways. *Sci Signal.* 2013; 6(279): ra46. DOI: 10.1126/scisignal.2003755.

Caceres, A. I., Brackmann, M., Elia, M. D., Bessac, B. F., Del Camino, D., D'Amours, M., et al. A sensory neuronal ion channel essential for airway inflammation and hyperreactivity in asthma. *Proceedings of the National Academy of Sciences of the United States of America.* 2009; 106(22): 9099-9104. DOI: 10.1073/pnas.0900591106.

Calvén, J., Ax, E. and Rådinger, M. The Airway Epithelium—A Central Player in Asthma Pathogenesis. *International Journal of Molecular Sciences.* 2020; 21(23): 8907.

Cantero-Recasens, G., Gonzalez, J. R., Fandos, C., Duran-Tauleria, E., Smit, L. A., Kauffmann, F., et al. Loss of function of transient receptor potential vanilloid 1 (TRPV1) genetic variant is associated with lower risk of active childhood asthma. *J Biol Chem.* 2010; 285(36): 27532-27535. DOI: 10.1074/jbc.C110.159491.

Cardoso, V., Chesné, J., Ribeiro, H., García-Cassani, B., Carvalho, T., Bouchery, T., et al. Neuronal regulation of type 2 innate lymphoid cells via neuromedin U. *Nature.* 2017; 549(7671): 277-281. DOI: 10.1038/nature23469.

Castan, L., Magnan, A. and Bouchaud, G. Chemokine receptors in allergic diseases. *Allergy.* 2017; 72(5): 682-690. DOI: https://doi.org/10.1111/all.13089.

Castro, M., Corren, J., Pavord, I. D., Maspero, J., Wenzel, S., Rabe, K. F., et al. Dupilumab Efficacy and Safety in Moderate-to-Severe Uncontrolled Asthma. *N Engl J Med.* 2018; 378(26): 2486-2496. DOI: 10.1056/NEJMoa1804092.

Cenac, N., Altier, C., Motta, J.-P., d'Aldebert, E., Galeano, S., Zamponi, G. W., et al. Potentiation of TRPV4 signalling by histamine and serotonin: an important mechanism for visceral hypersensitivity. *Gut.* 2010; 59(4): 481-488. DOI: 10.1136/gut.2009.192567.

Chapman, D. G. and Irvin, C. G. Mechanisms of airway hyper-responsiveness in asthma: the past, present and yet to come. *Clin Exp Allergy.* 2015; 45(4): 706-719. DOI: 10.1111/cea.12506.

Chauhan, A., Singh, M., Agarwal, A. and Paul, N. Correlation of TSLP, IL-33, and CD4 + CD25 + FOXP3 + T regulatory (Treg) in pediatric asthma. *J Asthma.* 2015; 52(9): 868-872. DOI: 10.3109/02770903.2015.1026441.

Chavez, J., Vargas, M. H., Martinez-Zuniga, J., Falfan-Valencia, R., Ambrocio-Ortiz, E., Carbajal, V., et al. Allergic sensitization increases the amount of extracellular ATP hydrolyzed by guinea pig leukocytes. *Purinergic Signal.* 2019; 15(1): 69-76. DOI: 10.1007/s11302-019-09644-7.

Chavez, J., Vargas, M. H., Rebollar-Ayala, D. C., Diaz-Hernandez, V., Cruz-Valderrama, J. E., Flores-Soto, E., et al. Inhibition of extracellular nucleotides hydrolysis intensifies the allergic bronchospasm. A novel protective role of ectonucleotidases. *Allergy.* 2013; 68(4): 462-471. DOI: 10.1111/all.12113.

Chen, H., Xia, Q., Feng, X., Cao, F., Yu, H., Song, Y., et al. Effect of P2X4R on airway inflammation and airway remodeling in allergic airway challenge in mice. *Mol Med Rep.* 2016; 13(1): 697-704. DOI: 10.3892/mmr.2015.4622.

Chen, L., Grabowski, K. A., Xin, J. P., Coleman, J., Huang, Z., Espiritu, B., et al. IL-4 induces differentiation and expansion of Th2 cytokine-producing eosinophils. *J Immunol.* 2004; 172(4): 2059-2066. DOI: 10.4049/jimmunol.172.4.2059.

Chen, Z. G., Zhang, T. T., Li, H. T., Chen, F. H., Zou, X. L., Ji, J. Z., et al. Neutralization of TSLP inhibits airway remodeling in a murine model of allergic asthma induced by chronic exposure to house dust mite. *PLoS One.* 2013; 8(1): e51268. DOI: 10.1371/journal.pone.0051268.

Cheng, D., Xue, Z., Yi, L., Shi, H., Zhang, K., Huo, X., et al. Epithelial interleukin-25 is a key mediator in Th2-high, corticosteroid-responsive asthma. *Am J Respir Crit Care Med.* 2014; 190(6): 639-648. DOI: 10.1164/rccm.201403-0505OC.

Cheung, M., Bao, W., Behm, D. J., Brooks, C. A., Bury, M. J., Dowdell, S. E., et al. Discovery of GSK2193874: An Orally Active, Potent, and Selective Blocker of Transient Receptor Potential Vanilloid 4. *ACS Med Chem Lett.* 2017; 8(5): 549-554. DOI: 10.1021/acsmedchemlett.7b00094.

Cho, S. H., Stanciu, L. A., Holgate, S. T. and Johnston, S. L. Increased interleukin-4, interleukin-5, and interferon-gamma in airway CD4+ and CD8+ T cells in atopic asthma. *Am J Respir Crit Care Med.* 2005; 171(3): 224-230. DOI: 10.1164/rccm.200310-1416OC.

Choi, J. Y., Lee, H. Y., Hur, J., Kim, K. H., Kang, J. Y., Rhee, C. K., et al. TRPV1 blocking alleviates airway inflammation and remodeling in a chronic asthma murine model. *Allergy, Asthma and Immunology Research.* 2018; 10(3): 216-224. DOI: 10.4168/aair.2018.10.3.216.

Christianson, C. A., Goplen, N. P., Zafar, I., Irvin, C., Good, J. T., Jr., Rollins, D. R., et al. Persistence of asthma requires multiple feedback circuits involving type 2 innate lymphoid cells and IL-33. *J Allergy Clin Immunol.* 2015; 136(1): 59-68 e14. DOI: 10.1016/j.jaci.2014.11.037.

Chung, K. F., Wenzel, S. E., Brozek, J. L., Bush, A., Castro, M., Sterk, P. J., et al. International ERS/ATS guidelines on definition, evaluation and treatment of severe asthma. *European Respiratory Journal.* 2014; 43(2): 343-373. DOI: 10.1183/09031936.00202013.

Cicala, C., Spina, D., Keir, S. D., Severino, B., Meli, R., Page, C. P., et al. Protective effect of a PAR2-activating peptide on histamine-induced bronchoconstriction in guinea-pig. *Br J Pharmacol.* 2001; 132(6): 1229-1234. DOI: 10.1038/sj.bjp.0703934.

Clark, J. M., Abraham, W. M., Fishman, C. E., Forteza, R., Ahmed, A., Cortes, A., et al. Tryptase inhibitors block allergen-induced airway and inflammatory responses in allergic sheep. *Am J Respir Crit Care Med.* 1995; 152(6 Pt 1): 2076-2083. DOI: 10.1164/ajrccm.152.6.8520778.

Cocks, T. M., Fong, B., Chow, J. M., Anderson, G. P., Frauman, A. G., Goldie, R. G., et al. A protective role for protease-activated receptors in the airways. *Nature.* 1999; 398(6723): 156-160. DOI: 10.1038/18223.

Coddou, C., Sandoval, R., Hevia, M. J. and Stojilkovic, S. S. Characterization of the antagonist actions of 5-BDBD at the rat P2X4 receptor. *Neurosci Lett.* 2019; 690: 219-224. DOI: 10.1016/j.neulet.2018.10.047.

Cohen, E. S., Scott, I. C., Majithiya, J. B., Rapley, L., Kemp, B. P., England, E., et al. Oxidation of the alarmin IL-33 regulates ST2-dependent inflammation. *Nat Commun.* 2015; 6: 8327. DOI: 10.1038/ncomms9327.

Coleman, J. M., Naik, C., Holguin, F., Ray, A., Ray, P., Trudeau, J. B., et al. Epithelial eotaxin-2 and eotaxin-3 expression: relation to asthma severity, luminal eosinophilia and age at onset. *Thorax.* 2012; 67(12): 1061-1066. DOI: 10.1136/thoraxjnl-2012-201634.

Colognato, R., Slupsky, J. R., Jendrach, M., Burysek, L., Syrovets, T. and Simmet, T. Differential expression and regulation of protease-activated receptors in human peripheral monocytes and monocyte-derived antigen-presenting cells. *Blood.* 2003; 102(7): 2645-2652. DOI: 10.1182/blood-2002-08-2497.

Cording, S., Medvedovic, J., Lécuyer, E., Aychek, T., Déjardin, F. and Eberl, G. Mouse models for the study of fate and function of innate lymphoid cells. *Eur J Immunol.* 2018; 48(8): 1271-1280. DOI: 10.1002/eji.201747388.

Corren, J., Castro, M., O'Riordan, T., Hanania, N. A., Pavord, I. D., Quirce, S., et al. Dupilumab Efficacy in Patients with Uncontrolled, Moderate-to-Severe Allergic Asthma. *J Allergy Clin Immunol Pract.* 2020; 8(2): 516-526. DOI: 10.1016/j.jaip.2019.08.050.

Corren, J., Parnes, J. R., Wang, L., Mo, M., Roseti, S. L., Griffiths, J. M., et al. Tezepelumab in Adults with Uncontrolled Asthma. *N Engl J Med.* 2017; 377(10): 936-946. DOI: 10.1056/NEJMoa1704064.

Corry, D. B., Grunig, G., Hadeiba, H., Kurup, V. P., Warnock, M. L., Sheppard, D., et al. Requirements for allergen-induced airway hyperreactivity in T and B cell-deficient mice. *Mol Med.* 1998; 4(5): 344-355. DOI: 10.1007/bf03401741.

Costello, R. W., Evans, C. M., Yost, B. L., Belmonte, K. E., Gleich, G. J., Jacoby, D. B., et al. Antigen-induced hyperreactivity to histamine: role of the vagus nerves and eosinophils. *Am J Physiol Lung Cell Mol Physiol.* 1999; 276(5): L709-L714. DOI: 10.1152/ajplung.1999.276.5.L709.

Cote-Sierra, J., Foucras, G., Guo, L., Chiodetti, L., Young, H. A., Hu-Li, J., et al. Interleukin 2 plays a central role in Th2 differentiation. *Proc Natl Acad Sci U S A.* 2004; 101(11): 3880-3885. DOI: 10.1073/pnas.0400339101.

Coyle, A. J., Ackerman, S. J., Burch, R., Proud, D. and Irvin, C. G. Human eosinophil-granule major basic protein and synthetic polycations induce airway hyperresponsiveness in vivo dependent on bradykinin generation. *J Clin Invest.* 1995a; 95(4): 1735-1740. DOI: 10.1172/JCI117850.

Coyle, A. J., Erard, F., Bertrand, C., Walti, S., Pitcher, H. and Le Gros, G. Virus-specific CD8+ cells can switch to interleukin 5 production and induce airway eosinophilia. *J Exp Med.* 1995b; 181(3): 1229-1233. DOI: 10.1084/jem.181.3.1229.

Csoka, B., Nemeth, Z. H., Szabo, I., Davies, D. L., Varga, Z. V., Paloczi, J., et al. Macrophage P2X4 receptors augment bacterial killing and protect against sepsis. *JCI Insight.* 2018; 3(11). DOI: 10.1172/jci.insight.99431.

Cui, L., Jia, J., Ma, C. F., Li, S. Y., Wang, Y. P., Guo, X. M., et al. IL-13 polymorphisms contribute to the risk of asthma: a meta-analysis. *Clin Biochem.* 2012; 45(4-5): 285-288. DOI: 10.1016/j.clinbiochem.2011.12.012.

D'Agostino, B., Roviezzo, F., De Palma, R., Terracciano, S., De Nardo, M., Gallelli, L., et al. Activation of protease-activated receptor-2 reduces airways inflammation in experimental allergic asthma. *Clin Exp Allergy.* 2007; 37(10): 1436-1443. DOI: 10.1111/j.1365-2222.2007.02793.x.

D'Andrea, M. R., Derian, C. K., Leturcq, D., Baker, S. M., Brunmark, A., Ling, P., et al. Characterization of protease-activated receptor-2 immunoreactivity in normal human tissues. *J Histochem Cytochem.* 1998; 46(2): 157-164. DOI: 10.1177/002215549804600204.

Dahl, G. ATP release through pannexon channels. *Philos Trans R Soc Lond B Biol Sci.* 2015; 370(1672): 1-11. DOI: 10.1098/rstb.2014.0191.

Dai, Y., Wang, S., Tominaga, M., Yamamoto, S., Fukuoka, T., Higashi, T., et al. Sensitization of TRPA1 by PAR2 contributes to the sensation of inflammatory pain. *J Clin Invest.* 2007; 117(7): 1979-1987. DOI: 10.1172/jci30951.

Daines, M., Zhu, L., Pereira, R., Zhou, X., Bondy, C., Pryor, B. M., et al. Alternaria induces airway epithelial cytokine expression independent of protease-activated receptor. *Respirology.* 2020; 25(5): 502-510. DOI: 10.1111/resp.13675.

Dalsgaard, T., Sonkusare, S. K., Teuscher, C., Poynter, M. E. and Nelson, M. T. Pharmacological inhibitors of TRPV4 channels reduce cytokine production, restore endothelial function and increase survival in septic mice. *Sci Rep.* 2016; 6: 33841. DOI: 10.1038/srep33841.

Davidson, C. E., Asaduzzaman, M., Arizmendi, N. G., Polley, D., Wu, Y., Gordon, J. R., et al. Proteinase-activated receptor-2 activation participates in allergic sensitization to house dust mite allergens in a murine model. *Clin Exp Allergy.* 2013; 43(11): 1274-1285. DOI: 10.1111/cea.12185.

de Boer, J. D., Van't Veer, C., Stroo, I., van der Meer, A. J., de Vos, A. F., van der Zee, J. S., et al. Protease-activated receptor-2 deficient mice have reduced house dust mite-evoked allergic lung inflammation. *Innate Immun.* 2014; 20(6): 618-625. DOI: 10.1177/1753425913503387.

De Campo, B. A. and Henry, P. J. Stimulation of protease-activated receptor-2 inhibits airway eosinophilia, hyperresponsiveness and bronchoconstriction in a murine model of allergic inflammation. *Br J Pharmacol.* 2005; 144(8): 1100-1108. DOI: 10.1038/sj.bjp.0706150.

de Heer, H. J., Hammad, H., Soullié, T., Hijdra, D., Vos, N., Willart, M. A., et al. Essential role of lung plasmacytoid dendritic cells in preventing asthmatic reactions to harmless inhaled antigen. *J Exp Med.* 2004; 200(1): 89-98. DOI: 10.1084/jem.20040035.

De Logu, F., Patacchini, R., Fontana, G. and Geppetti, P. TRP functions in the broncho-pulmonary system. *Seminars in Immunopathology.* 2016; 38(3): 321-329. DOI: 10.1007/s00281-016-0557-1.

De Yang, Qian., C., Rosenberg, H. F., Rybak, S. M., Newton, D. L., Wang, Z. Y., et al. Human Ribonuclease A Superfamily Members, Eosinophil-Derived Neurotoxin and Pancreatic Ribonuclease, Induce

Dendritic Cell Maturation and Activation. *J Immunol.* 2004; 173(10): 6134-6142. DOI: 10.4049/jimmunol.173.10.6134.

del Rio, M.-L., Rodriguez-Barbosa, J.-I., Kremmer, E. and Förster, R. CD103[−] and CD103⁺ Bronchial Lymph Node Dendritic Cells Are Specialized in Presenting and Cross-Presenting Innocuous Antigen to CD4⁺ and CD8⁺ T Cells. *The Journal of Immunology.* 2007; 178(11): 6861-6866. DOI: 10.4049/jimmunol.178.11.6861.

Delescluse, I., Mace, H. and Adcock, J. J. Inhibition of airway hyper-responsiveness by TRPV1 antagonists (SB-705498 and PF-04065463) in the unanaesthetized, ovalbumin-sensitized guinea pig. *Br J Pharmacol.* 2012; 166(6): 1822-1832. DOI: 10.1111/j.1476-5381.2012.01891.x.

Demenais, F., Margaritte-Jeannin, P., Barnes, K. C., Cookson, W. O. C., Altmüller, J., Ang, W., et al. Multiancestry association study identifies new asthma risk loci that colocalize with immune-cell enhancer marks. *Nat Genet.* 2018; 50(1): 42-53. DOI: 10.1038/s41588-017-0014-7.

den Otter, I., Willems, L. N., van Schadewijk, A., van Wijngaarden, S., Janssen, K., de Jeu, R. C., et al. Lung function decline in asthma patients with elevated bronchial CD8, CD4 and CD3 cells. *Eur Respir J.* 2016; 48(2): 393-402. DOI: 10.1183/13993003.01525-2015.

Denlinger, L. C., Manthei, D. M., Seibold, M. A., Ahn, K., Bleecker, E., Boushey, H. A., et al. P2X7-regulated protection from exacerbations and loss of control is independent of asthma maintenance therapy. *Am J Respir Crit Care Med.* 2013; 187(1): 28-33. DOI: 10.1164/rccm.201204-0750OC.

Denlinger, L. C., Shi, L., Guadarrama, A., Schell, K., Green, D., Morrin, A., et al. Attenuated P2X7 pore function as a risk factor for virus-induced loss of asthma control. *Am J Respir Crit Care Med.* 2009; 179(4): 265-270. DOI: 10.1164/rccm.200802-293OC.

Devos, F. C., Boonen, B., Alpizar, Y. A., Maes, T., Hox, V., Seys, S., et al. Neuro-immune interactions in chemical-induced airway hyperreactivity. *Eur Respir J.* 2016; 48(2): 380-392. DOI: 10.1183/13993003.01778-2015.

Di Virgilio, F., Dal Ben, D., Sarti, A. C., Giuliani, A. L. and Falzoni, S. The P2X7 Receptor in Infection and Inflammation. *Immunity.* 2017; 47(1): 15-31. DOI: 10.1016/j.immuni.2017.06.020.

Diamant, Z., Gauvreau, G. M., Cockcroft, D. W., Boulet, L. P., Sterk, P. J., de Jongh, F. H., et al. Inhaled allergen bronchoprovocation tests. *J Allergy Clin Immunol.* 2013; 132(5): 1045-1055 e1046. DOI: 10.1016/j.jaci.2013.08.023.

Dichmann, S., Idzko, M., Zimpfer, U., Hofmann, C., Ferrari, D., Luttmann, W., et al. Adenosine triphosphate-induced oxygen radical production and CD11b up-regulation: Ca(++) mobilization and actin reorganization in human eosinophils. *Blood.* 2000; 95(3): 973-978. DOI: 10.1182/blood.v95.3.973.003k47_973_978.

Doganci, A., Karwot, R., Maxeiner, J. H., Scholtes, P., Schmitt, E., Neurath, M. F., et al. IL-2 receptor beta-chain signaling controls immunosuppressive CD4+ T cells in the draining lymph nodes and lung during allergic airway inflammation in vivo. *J Immunol.* 2008; 181(3): 1917-1926. DOI: 10.4049/jimmunol.181.3.1917.

Dou, L., Chen, Y.-F., Cowan, P. J. and Chen, X.-P. Extracellular ATP signaling and clinical relevance. *Clinical Immunology.* 2018; 188: 67-73. DOI: https://doi.org/10.1016/j.clim.2017.12.006.

Dragunas, G., Woest, M. E., Nijboer, S., Bos, S. T., van Asselt, J., de Groot, A. P., et al. Cholinergic neuroplasticity in asthma driven by TrkB signaling. *The FASEB Journal.* 2020; 34(6): 7703-7717. DOI: https://doi.org/10.1096/fj.202000170R.

Drake, L. Y., Iijima, K. and Kita, H. Group 2 innate lymphoid cells and CD4+ T cells cooperate to mediate type 2 immune response in mice. *Allergy.* 2014; 69(10): 1300-1307. DOI: 10.1111/all.12446.

Drake, M. G., Scott, G. D., Blum, E. D., Lebold, K. M., Nie, Z., Lee, J. J., et al. Eosinophils increase airway sensory nerve density in mice and in human asthma. *Science Translational Medicine.* 2018; 10(457): eaar8477. DOI: 10.1126/scitranslmed.aar8477.

Dreisig, K. and Kornum, B. R. A critical look at the function of the P2Y11 receptor. *Purinergic Signal.* 2016; 12(3): 427-437. DOI: 10.1007/s11302-016-9514-7.

Droguett, K., Rios, M., Carreno, D. V., Navarrete, C., Fuentes, C., Villalon, M., et al. An autocrine ATP release mechanism regulates basal ciliary activity in airway epithelium. *J Physiol.* 2017; 595(14): 4755-4767. DOI: 10.1113/jp273996.

Dua, B., Tang, W., Watson, R., Gauvreau, G. and O'Byrne, P. M. Myeloid dendritic cells type 2 after allergen inhalation in asthmatic subjects. *Clinical & Experimental Allergy.* 2014; 44(7): 921-929. DOI: https://doi.org/10.1111/cea.12297.

Dua, B., Watson, R. M., Gauvreau, G. M. and O'Byrne, P. M. Myeloid and plasmacytoid dendritic cells in induced sputum after allergen inhalation in subjects with asthma. *Journal of Allergy and Clinical Immunology.* 2010; 126(1): 133-139. DOI: https://doi.org/10.1016/j.jaci.2010.04.006.

Duan, J., Xie, J., Deng, T., Xie, X., Liu, H., Li, B., et al. Exposure to both formaldehyde and high relative humidity exacerbates allergic asthma by activating the TRPV4-p38 MAPK pathway in Balb/c mice. *Environ Pollut.* 2020; 256: 113375. DOI: 10.1016/j.envpol.2019.113375.

Dutton, E. E., Camelo, A., Sleeman, M., Herbst, R., Carlesso, G., Belz, G. T., et al. Characterisation of innate lymphoid cell populations at different sites in mice with defective T cell immunity. *Wellcome Open Res.* 2017; 2: 117. DOI: 10.12688/wellcomeopenres.13199.3.

Ebeling, C., Forsythe, P., Ng, J., Gordon, J. R., Hollenberg, M. and Vliagoftis, H. Proteinase-activated receptor 2 activation in the airways enhances antigen-mediated airway inflammation and airway hyperresponsiveness through different pathways. *J Allergy Clin Immunol.* 2005; 115(3): 623-630. DOI: 10.1016/j.jaci.2004.11.042.

Ebeling, C., Lam, T., Gordon, J. R., Hollenberg, M. D. and Vliagoftis, H. Proteinase-activated receptor-2 promotes allergic sensitization to an inhaled antigen through a TNF-mediated pathway. *J Immunol.* 2007; 179(5): 2910-2917. DOI: 10.4049/jimmunol.179.5.2910.

Elbon, C. L., Jacoby, D. B. and Fryer, A. D. Pretreatment with an antibody to interleukin-5 prevents loss of pulmonary M2 muscarinic receptor function in antigen-challenged guinea pigs. *Am J Respir Cell Mol Biol.* 1995; 12(3): 320-328. DOI: 10.1165/ajrcmb.12.3.7873198.

Eltom, S., Stevenson, C. S., Rastrick, J., Dale, N., Raemdonck, K., Wong, S., et al. P2X7 receptor and caspase 1 activation are central to airway inflammation observed after exposure to tobacco smoke. *PLoS One.* 2011; 6(9): e24097. DOI: 10.1371/journal.pone.0024097.

Endo, Y., Hirahara, K., Iinuma, T., Shinoda, K., Tumes, D. J., Asou, H. K., et al. The interleukin-33-p38 kinase axis confers memory T helper 2 cell pathogenicity in the airway. *Immunity.* 2015; 42(2): 294-308. DOI: 10.1016/j.immuni.2015.01.016.

Englezou, P. C., Rothwell, S. W., Ainscough, J. S., Brough, D., Landsiedel, R., Verkhratsky, A., et al. P2X7R activation drives distinct IL-1 responses in dendritic cells compared to macrophages. *Cytokine.* 2015; 74(2): 293-304. DOI: 10.1016/j.cyto.2015.05.013.

Enomoto, Y., Orihara, K., Takamasu, T., Matsuda, A., Gon, Y., Saito, H., et al. Tissue remodeling induced by hypersecreted epidermal growth factor and amphiregulin in the airway after an acute asthma attack. *J Allergy Clin Immunol.* 2009; 124(5): 913-920.e911-917. DOI: 10.1016/j.jaci.2009.08.044.

Er-Lukowiak, M., Duan, Y., Rassendren, F., Ulmann, L., Nicke, A., Ufer, F., et al. A P2rx7 passenger mutation affects the vitality and function of immune cells in P2X4ko and other transgenic mice. *bioRxiv.* 2020: 06.10.139410. DOI: 10.1101/2020.06.10.139410.

Esther, C. R., Alexis, N. E., Clas, M. L., Lazarowski, E. R., Donaldson, S. H., Pedrosa Ribeiro, C. M., et al. Extracellular purines are biomarkers of neutrophilic airway inflammation. *European Respiratory Journal.* 2008; 31(5): 949. DOI: 10.1183/09031936.00089807.

Evans, C. M., Fryer, A. D., Jacoby, D. B., Gleich, G. J. and Costello, R. W. Pretreatment with antibody to eosinophil major basic protein prevents hyperresponsiveness by protecting neuronal M2 muscarinic receptors in antigen-challenged guinea pigs. *The Journal of Clinical Investigation.* 1997; 100(9): 2254-2262. DOI: 10.1172/jci119763.

Farhadi, N., Lambert, L., Triulzi, C., Openshaw, P. J., Guerra, N. and Culley, F. J. Natural killer cell NKG2D and granzyme B are critical for allergic pulmonary inflammation. *J Allergy Clin Immunol.* 2014; 133(3): 827-835.e823. DOI: 10.1016/j.jaci.2013.09.048.

Fattouh, R., Al-Garawi, A., Fattouh, M., Arias, K., Walker, T. D., Goncharova, S., et al. Eosinophils Are Dispensable for Allergic Remodeling and Immunity in a Model of House Dust Mite–induced Airway Disease. *Am J Respir Cell Mol Biol.* 2011; 183(2): 179-188. DOI: 10.1164/rccm.200905-0736OC.

Fear, V. S., Lai, S. P., Zosky, G. R., Perks, K. L., Gorman, S., Blank, F., et al. A pathogenic role for the integrin CD103 in experimental allergic airways disease. *Physiological Reports.* 2016; 4(21): e13021. DOI: https://doi.org/10.14814/phy2.13021.

Feng, B. S., Wu, Y. J., Zeng, X. H., Yu, D., Liu, Z. Q., Zhou, C. J., et al. Bcl2L12 mediates effects of protease-activated receptor-2 on the pathogenesis of Th2-dominated responses of patients with ulcerative colitis. *Arch Biochem Biophys.* 2018; 657: 8-14. DOI: 10.1016/j.abb.2018.09.003.

Fernandes, J., Lorenzo, I. M., Andrade, Y. N., Garcia-Elias, A., Serra, S. A., Fernandez-Fernandez, J. M., et al. IP3 sensitizes TRPV4 channel to the mechano- and osmotransducing messenger 5'-6'-epoxyeicosatrienoic acid. *J Cell Biol.* 2008; 181(1): 143-155. DOI: 10.1083/jcb.200712058.

Fernandez-Fernandez, J. M., Andrade, Y. N., Arniges, M., Fernandes, J., Plata, C., Rubio-Moscardo, F., et al. Functional coupling of TRPV4 cationic channel and large conductance, calcium-dependent potassium channel in human bronchial epithelial cell lines. *Pflugers Arch.* 2008; 457(1): 149-159. DOI: 10.1007/s00424-008-0516-3.

Fernández-Fernández, J. M., Nobles, M., Currid, A., Vázquez, E. and Valverde, M. A. Maxi K+ channel mediates regulatory volume decrease response in a human bronchial epithelial cell line. *Am J Physiol Cell Physiol.* 2002; 283(6): C1705-1714. DOI: 10.1152/ajpcell.00245.2002.

Ferrari, D., Idzko, M., Dichmann, S., Purlis, D., Virchow, C., Norgauer, J., et al. P2 purinergic receptors of human eosinophils: characterization and coupling to oxygen radical production. *FEBS Lett.* 2000; 486(3): 217-224. DOI: 10.1016/s0014-5793(00)02306-1.

Ferrari, D., Vuerich, M., Casciano, F., Longhi, M. S., Melloni, E., Secchiero, P., et al. Eosinophils and Purinergic Signaling in Health and Disease. *Front Immunol.* 2020; 11: 1339. DOI: 10.3389/fimmu.2020.01339.

Ferrini, M. E., Hong, S., Stierle, A., Stierle, D., Stella, N., Roberts, K., et al. CB2 receptors regulate natural killer cells that limit allergic airway inflammation in a murine model of asthma. *Allergy.* 2017; 72(6): 937-947. DOI: 10.1111/all.13107.

Fields, R. C., Schoenecker, J. G., Hart, J. P., Hoffman, M. R., Pizzo, S. V. and Lawson, J. H. Protease-activated receptor-2 signaling triggers dendritic cell development. *Am J Pathol.* 2003; 162(6): 1817-1822. DOI: 10.1016/s0002-9440(10)64316-7.

FitzGerald, J. M., Bleecker, E. R., Nair, P., Korn, S., Ohta, K., Lommatzsch, M., et al. Benralizumab, an anti-interleukin-5 receptor α monoclonal antibody, as add-on treatment for patients with severe, uncontrolled, eosinophilic asthma (CALIMA): a randomised, double-blind, placebo-controlled phase 3 trial. *The Lancet.* 2016; 388(10056): 2128-2141. DOI: https://doi.org/10.1016/S0140-6736(16)31322-8.

Flajolet, P. M. The role of the ion channel TRPV4 in the Late Asthmatic Response. Doctor of Philosophy Thesis, Imperial College London 2021.

Foster, P. S., Maltby, S., Rosenberg, H. F., Tay, H. L., Hogan, S. P., Collison, A. M., et al. Modeling TH2 responses and airway inflammation to understand fundamental mechanisms regulating the pathogenesis of asthma. *Immunol Rev.* 2017; 278(1): 20-40. DOI: 10.1111/imr.12549.

Foster, P. S., Yang, M., Herbert, C. and Kumar, R. K. CD4(+) T-lymphocytes regulate airway remodeling and hyper-reactivity in a mouse model of chronic asthma. *Lab Invest.* 2002; 82(4): 455-462. DOI: 10.1038/labinvest.3780438.

Franchi, L., Kanneganti, T. D., Dubyak, G. R. and Nunez, G. Differential requirement of P2X7 receptor and intracellular K+ for caspase-1 activation induced by intracellular and extracellular bacteria. *J Biol Chem.* 2007; 282(26): 18810-18818. DOI: 10.1074/jbc.M610762200.

Francis, N., Every, A. L., Ayodele, B. A., Pike, R. N., Mackie, E. J. and Pagel, C. N. A T cell-specific knockout reveals an important role for protease-activated receptor 2 in lymphocyte development. *Int J Biochem Cell Biol.* 2017; 92: 95-103. DOI: 10.1016/j.biocel.2017.09.015.

Frigas, E. and Gleich, G. J. The eosinophil and the pathophysiology of asthma. *Journal of Allergy and Clinical Immunology.* 1986; 77(4): 527-537. DOI: https://doi.org/10.1016/0091-6749(86)90341-6.

Fryer, A. D., Stein, L. H., Nie, Z., Curtis, D. E., Evans, C. M., Hodgson, S. T., et al. Neuronal eotaxin and the effects of ccr3 antagonist on airway hyperreactivity and M2 receptor dysfunction. *The Journal of Clinical Investigation.* 2006; 116(1): 228-236. DOI: 10.1172/jci25423.

Furuhashi, K., Suda, T., Hasegawa, H., Suzuki, Y., Hashimoto, D., Enomoto, N., et al. Mouse lung CD103+ and CD11bhigh dendritic cells preferentially induce distinct CD4+ T-cell responses. *Am J Respir Cell Mol Biol.* 2012; 46(2): 165-172. DOI: 10.1165/rcmb.2011-0070OC.

Gallo, V., Dijk, F. N., Holloway, J. W., Ring, S. M., Koppelman, G. H., Postma, D. S., et al. TRPA1 gene polymorphisms and childhood asthma. *Pediatr Allergy Immunol.* 2017; 28(2): 191-198. DOI: 10.1111/pai.12673.

Garcia-Gonzalez, G., Sanchez-Gonzalez, A., Hernandez-Bello, R., Gonzalez, G. M., Franco-Molina, M. A., Coronado-Cerda, E. E., et al. Triggering of protease-activated receptors (PARs) induces alternative M2 macrophage polarization with impaired plasticity. *Mol Immunol.* 2019; 114: 278-288. DOI: 10.1016/j.molimm.2019.08.004.

Gargett, C. E. and Wiley, J. S. The isoquinoline derivative KN-62 a potent antagonist of the P2Z-receptor of human lymphocytes. *Br J Pharmacol.* 1997; 120(8): 1483-1490. DOI: 10.1038/sj.bjp.0701081.

Gasteiger, G., Fan, X., Dikiy, S., Lee, S. Y. and Rudensky, A. Y. Tissue residency of innate lymphoid cells in lymphoid and nonlymphoid organs. *Science.* 2015; 350(6263): 981-985. DOI: 10.1126/science.aac9593.

Gauvreau, G. M., El-Gammal, A. I. and O'Byrne, P. M. Allergen-induced airway responses. *European Respiratory Journal.* 2015; 46(3): 819-831. DOI: 10.1183/13993003.00536-2015.

Gauvreau, G. M., O'Byrne, P. M., Boulet, L. P., Wang, Y., Cockcroft, D., Bigler, J., et al. Effects of an anti-TSLP antibody on allergen-induced asthmatic responses. *N Engl J Med.* 2014; 370(22): 2102-2110. DOI: 10.1056/NEJMoa1402895.

Gavett, S. H., Chen, X., Finkelman, F. and Wills-Karp, M. Depletion of murine CD4+ T lymphocytes prevents antigen-induced airway hyperreactivity and pulmonary eosinophilia. *Am J Respir Cell Mol Biol.* 1994; 10(6): 587-593. DOI: 10.1165/ajrcmb.10.6.8003337.

Gerblich, A. A., Salik, H. and Schuyler, M. R. Dynamic T-cell changes in peripheral blood and bronchoalveolar lavage after antigen bronchoprovocation in asthmatics. *Am Rev Respir Dis.* 1991; 143(3): 533-537. DOI: 10.1164/ajrccm/143.3.533.

Glaab, T., Ziegert, M., Baelder, R., Korolewitz, R., Braun, A., Hohlfeld, J. M., et al. Invasive versus noninvasive measurement of allergic and cholinergic airway responsiveness in mice. *Respiratory Research.* 2005; 6(1): 139. DOI: 10.1186/1465-9921-6-139.

Global Initiative for Asthma. (2021). "Global strategy for asthma management and prevention." from www.ginasthma.org.

Gluck, J., Rymarczyk, B., Kasprzak, M. and Rogala, B. Increased Levels of Interleukin-33 and Thymic Stromal Lymphopoietin in Exhaled Breath Condensate in Chronic Bronchial Asthma. *Int Arch Allergy Immunol.* 2016; 169(1): 51-56. DOI: 10.1159/000444017.

Gold, M. J., Antignano, F., Halim, T. Y., Hirota, J. A., Blanchet, M. R., Zaph, C., et al. Group 2 innate lymphoid cells facilitate sensitization to local, but not systemic, TH2-inducing allergen exposures. *J Allergy Clin Immunol.* 2014; 133(4): 1142-1148. DOI: 10.1016/j.jaci.2014.02.033.

Gombedza, F., Kondeti, V., Al-Azzam, N., Koppes, S., Duah, E., Patil, P., et al. Mechanosensitive transient receptor potential vanilloid 4 regulates Dermatophagoides farinae-induced airway remodeling via 2 distinct pathways modulating matrix synthesis and degradation. *FASEB J.* 2017; 31(4): 1556-1570. DOI: 10.1096/fj.201601045R.

González Barcala, F. J., de la Fuente-Cid, R., Alvarez-Gil, R., Tafalla, M., Nuevo, J. and Caamaño-Isorna, F. [Factors associated with asthma control in primary care patients: the CHAS study]. *Archivos de bronconeumologia.* 2010; 46(7): 358-363. DOI: 10.1016/j.arbres.2010.01.007.

Gonzalo, J. A., Lloyd, C. M., Wen, D., Albar, J. P., Wells, T. N., Proudfoot, A., et al. The coordinated action of CC chemokines in the lung orchestrates allergic inflammation and airway hyperresponsiveness. *J Exp Med.* 1998; 188(1): 157-167. DOI: 10.1084/jem.188.1.157.

Goyal, N., Skrdla, P., Schroyer, R., Kumar, S., Fernando, D., Oughton, A., et al. Clinical Pharmacokinetics, Safety, and Tolerability of a Novel, First-in-Class TRPV4 Ion Channel Inhibitor, GSK2798745, in Healthy and Heart Failure Subjects. *American Journal of Cardiovascular Drugs.* 2019; 19(3): 335-342. DOI: 10.1007/s40256-018-00320-6.

Grace, M., Birrell, M. A., Dubuis, E., Maher, S. A. and Belvisi, M. G. Transient receptor potential channels mediate the tussive response to prostaglandin E2 and bradykinin. *Thorax.* 2012; 67(10): 891-900. DOI: 10.1136/thoraxjnl-2011-201443.

Grace, M. S., Baxter, M., Dubuis, E., Birrell, M. A. and Belvisi, M. G. Transient receptor potential (TRP) channels in the airway: role in airway disease. *Br J Pharmacol.* 2014a; 171(10): 2593-2607. DOI: 10.1111/bph.12538.

Grace, M. S., Bonvini, S. J., Belvisi, M. G. and McIntyre, P. Modulation of the TRPV4 ion channel as a therapeutic target for disease. *Pharmacol Ther.* 2017; 177: 9-22. DOI: 10.1016/j.pharmthera.2017.02.019.

Grace, M. S., Lieu, T., Darby, B., Abogadie, F. C., Veldhuis, N., Bunnett, N. W., et al. The tyrosine kinase inhibitor bafetinib inhibits PAR2-induced activation of TRPV4 channels in vitro and pain in vivo. *Br J Pharmacol.* 2014b; 171(16): 3881-3894. DOI: 10.1111/bph.12750.

Grant, A. D., Cottrell, G. S., Amadesi, S., Trevisani, M., Nicoletti, P., Materazzi, S., et al. Protease-activated receptor 2 sensitizes the transient receptor potential vanilloid 4 ion channel to cause mechanical hyperalgesia in mice. *J Physiol.* 2007; 578(Pt 3): 715-733. DOI: 10.1113/jphysiol.2006.121111.

Graven, P., Tambalo, M., Scapozza, L. and Perozzo, R. Purine metabolite and energy charge analysis of Trypanosoma brucei cells in different growth phases using an optimized ion-pair RP-HPLC/UV for the quantification of adenine and guanine pools. *Experimental Parasitology.* 2014; 141: 28-38. DOI: https://doi.org/10.1016/j.exppara.2014.03.006.

Greve, A. S., Skals, M., Fagerberg, S. K., Tonnus, W., Ellermann-Eriksen, S., Evans, R. J., et al. P2X1, P2X4, and P2X7 Receptor Knock Out Mice Expose Differential Outcome of Sepsis Induced by alpha-Haemolysin Producing Escherichia coli. *Front Cell Infect Microbiol.* 2017; 7(APR): 113. DOI: 10.3389/fcimb.2017.00113.

Griffiths, R. J., Stam, E. J., Downs, J. T. and Otterness, I. G. ATP induces the release of IL-1 from LPS-primed cells in vivo. *J Immunol.* 1995; 154(6): 2821-2828.

Groot-Kormelink, P. J., Fawcett, L., Wright, P. D., Gosling, M. and Kent, T. C. Quantitative GPCR and ion channel transcriptomics in primary alveolar macrophages and macrophage surrogates. *BMC Immunol.* 2012; 13: 57. DOI: 10.1186/1471-2172-13-57.

Grove, L. M., Mohan, M. L., Abraham, S., Scheraga, R. G., Southern, B. D., Crish, J. F., et al. Translocation of TRPV4-PI3Kgamma complexes to the plasma membrane drives myofibroblast transdifferentiation. *Sci Signal.* 2019; 12(607). DOI: 10.1126/scisignal.aau1533.

Grunig, G., Warnock, M., Wakil, A. E., Venkayya, R., Brombacher, F., Rennick, D. M., et al. Requirement for IL-13 independently of IL-4 in experimental asthma. *Science.* 1998; 282(5397): 2261-2263. DOI: 10.1126/science.282.5397.2261.

Gu, B. J., Zhang, W. Y., Bendall, L. J., Chessell, I. P., Buell, G. N. and Wiley, J. S. Expression of P2X(7) purinoceptors on human lymphocytes and monocytes: evidence for nonfunctional P2X(7) receptors. *Am J Physiol Cell Physiol.* 2000; 279(4): C1189-1197. DOI: 10.1152/ajpcell.2000.279.4.C1189.

Gu, Q. and Lee, L. Y. House dust mite potentiates capsaicin-evoked Ca2+ transients in mouse pulmonary sensory neurons via activation of protease-activated receptor-2. *Exp Physiol.* 2012; 97(4): 534-543. DOI: 10.1113/expphysiol.2011.060764.

Gu, Q. H., Moss, C. R., Kettelhut, K. L., Gilbert, C. A. and Hu, H. Z. Activation of TRPV4 Regulates Respiration through Indirect Activation of Bronchopulmonary Sensory Neurons. *Front Physiol.* 2016; 7(FEB). DOI: 10.3389/fphys.2016.00065.

Güler, A. D., Lee, H., Iida, T., Shimizu, I., Tominaga, M. and Caterina, M. Heat-evoked activation of the ion channel, TRPV4. *J Neurosci.* 2002; 22(15): 6408-6414. DOI: 10.1523/jneurosci.22-15-06408.2002.

Gundel, R. H., Letts, L. G. and Gleich, G. J. Human eosinophil major basic protein induces airway constriction and airway hyperresponsiveness in primates. *The Journal of Clinical Investigation.* 1991; 87(4): 1470-1473. DOI: 10.1172/jci115155.

Guo, H., Callaway, J. B. and Ting, J. P. Y. Inflammasomes: mechanism of action, role in disease, and therapeutics. *Nature Medicine.* 2015; 21(7): 677-687. DOI: 10.1038/nm.3893.

Guo, Z., Wu, J., Zhao, J., Liu, F., Chen, Y., Bi, L., et al. IL-33 promotes airway remodeling and is a marker of asthma disease severity. *J Asthma.* 2014; 51(8): 863-869. DOI: 10.3109/02770903.2014.921196.

Halim, T. Y., Hwang, Y. Y., Scanlon, S. T., Zaghouani, H., Garbi, N., Fallon, P. G., et al. Group 2 innate lymphoid cells license dendritic cells to potentiate memory TH2 cell responses. *Nat Immunol.* 2016; 17(1): 57-64. DOI: 10.1038/ni.3294.

Halim, T. Y., Krauss, R. H., Sun, A. C. and Takei, F. Lung natural helper cells are a critical source of Th2 cell-type cytokines in protease allergen-induced airway inflammation. *Immunity.* 2012; 36(3): 451-463. DOI: 10.1016/j.immuni.2011.12.020.

Halim, T. Y., Steer, C. A., Matha, L., Gold, M. J., Martinez-Gonzalez, I., McNagny, K. M., et al. Group 2 innate lymphoid cells are critical for the initiation of adaptive T helper 2 cell-mediated allergic lung inflammation. *Immunity.* 2014; 40(3): 425-435. DOI: 10.1016/j.immuni.2014.01.011.

Halim, T. Y. F., Rana, B. M. J., Walker, J. A., Kerscher, B., Knolle, M. D., Jolin, H. E., et al. Tissue-Restricted Adaptive Type 2 Immunity Is Orchestrated by Expression of the Costimulatory Molecule OX40L on Group 2 Innate Lymphoid Cells. *Immunity.* 2018; 48(6): 1195-1207 e1196. DOI: 10.1016/j.immuni.2018.05.003.

Hamanaka, K., Jian, M. Y., Townsley, M. I., King, J. A., Liedtke, W., Weber, D. S., et al. TRPV4 channels augment macrophage activation and ventilator-induced lung injury. *Am J Physiol Lung Cell Mol Physiol.* 2010; 299(3): L353-362. DOI: 10.1152/ajplung.00315.2009.

Hamelmann, E., Oshiba, A., Paluh, J., Bradley, K., Loader, J., Potter, T. A., et al. Requirement for CD8+ T cells in the development of airway hyperresponsiveness in a marine model of airway sensitization. *J Exp Med.* 1996; 183(4): 1719-1729. DOI: 10.1084/jem.183.4.1719.

Hamelmann, E., Schwarze, J., Takeda, K., Oshiba, A., Larsen, G. L., Irvin, C. G., et al. Noninvasive measurement of airway responsiveness in allergic mice using barometric plethysmography. *Am J Respir Crit Care Med.* 1997a; 156(3 Pt 1): 766-775. DOI: 10.1164/ajrccm.156.3.9606031.

Hamelmann, E., Vella, A. T., Oshiba, A., Kappler, J. W., Marrack, P. and Gelfand, E. W. Allergic airway sensitization induces T cell activation but not airway hyperresponsiveness in B cell-deficient mice. *Proc Natl Acad Sci U S A.* 1997b; 94(4): 1350-1355. DOI: 10.1073/pnas.94.4.1350.

Hamid, Q., Azzawi, M., Ying, S., Moqbel, R., Wardlaw, A. J., Corrigan, C. J., et al. Expression of mRNA for interleukin-5 in mucosal bronchial biopsies from asthma. *J Clin Invest.* 1991; 87(5): 1541-1546. DOI: 10.1172/jci115166.

Hammad, H., Charbonnier, A.-S., Duez, C., Jacquet, A., Stewart, G. A., Tonnel, A.-B., et al. Th2 polarization by Der p 1–pulsed monocyte-derived dendritic cells is due to the allergic status of the donors. *Blood.* 2001; 98(4): 1135-1141. DOI: 10.1182/blood.V98.4.1135.

Hamzaoui, A., Berraies, A., Kaabachi, W., Haifa, M., Ammar, J. and Kamel, H. Induced sputum levels of IL-33 and soluble ST2 in young asthmatic children. *J Asthma.* 2013; 50(8): 803-809. DOI: 10.3109/02770903.2013.816317.

Hansen, G., Berry, G., DeKruyff, R. H. and Umetsu, D. T. Allergen-specific Th1 cells fail to counterbalance Th2 cell-induced airway hyperreactivity but cause severe airway inflammation. *J Clin Invest.* 1999; 103(2): 175-183. DOI: 10.1172/jci5155.

Harada, M., Obara, K., Hirota, T., Yoshimoto, T., Hitomi, Y., Sakashita, M., et al. A Functional Polymorphism in IL-18 Is Associated with Severity of Bronchial Asthma. *Am J Respir Cell Mol Biol.* 2009; 180(11): 1048-1055. DOI: 10.1164/rccm.200905-0652OC.

Hardman, C. S., Panova, V. and McKenzie, A. N. IL-33 citrine reporter mice reveal the temporal and spatial expression of IL-33 during allergic lung inflammation. *Eur J Immunol.* 2013; 43(2): 488-498. DOI: 10.1002/eji.201242863.

Harrison, T., Canonica, G. W., Chupp, G., Lee, J., Schleich, F., Welte, T., et al. Real-world mepolizumab in the prospective severe asthma REALITI-A study: initial analysis. *Eur Respir J.* 2020; 56(4). DOI: 10.1183/13993003.00151-2020.

Hart, T. K., Blackburn, M. N., Brigham-Burke, M., Dede, K., Al-Mahdi, N., Zia-Amirhosseini, P., et al. Preclinical efficacy and safety of pascolizumab (SB 240683): a humanized anti-interleukin-4 antibody with therapeutic potential in asthma. *Clin Exp Immunol.* 2002; 130(1): 93-100. DOI: 10.1046/j.1365-2249.2002.01973.x.

Hartl, D., Koller, B., Mehlhorn, A. T., Reinhardt, D., Nicolai, T., Schendel, D. J., et al. Quantitative and functional impairment of pulmonary CD4+CD25hi regulatory T cells in pediatric asthma. *Journal of Allergy and Clinical Immunology.* 2007; 119(5): 1258-1266. DOI: https://doi.org/10.1016/j.jaci.2007.02.023.

Hashimoto, T., Kobayashi, N., Kajiyama, Y., Kaminuma, O., Suko, M. and Mori, A. IL-2-induced IL-13 production by allergen-specific human helper T cell clones. *Int Arch Allergy Immunol.* 2006; 140(1): 51-54. DOI: 10.1159/000092711.

Haspeslagh, E., van Helden, M. J., Deswarte, K., De Prijck, S., van Moorleghem, J., Boon, L., et al. Role of NKp46+ natural killer cells in house dust mite-driven asthma. *EMBO Molecular Medicine.* 2018; 10(4): e8657. DOI: https://doi.org/10.15252/emmm.201708657.

Hayakawa, H., Hayakawa, M., Kume, A. and Tominaga, S. Soluble ST2 blocks interleukin-33 signaling in allergic airway inflammation. *J Biol Chem.* 2007; 282(36): 26369-26380. DOI: 10.1074/jbc.M704916200.

He, Y., Franchi, L. and Nunez, G. TLR agonists stimulate Nlrp3-dependent IL-1beta production independently of the purinergic P2X7 receptor in dendritic cells and in vivo. *J Immunol.* 2013; 190(1): 334-339. DOI: 10.4049/jimmunol.1202737.

Hechler, B., Magnenat, S., Zighetti, M. L., Kassack, M. U., Ullmann, H., Cazenave, J.-P., et al. Inhibition of Platelet Functions and Thrombosis through Selective or Nonselective Inhibition of the Platelet P2 Receptors with Increasing Doses of NF449 [4,4′,4″,4‴-(Carbonylbis(imino-5,1,3-benzenetriylbis-(carbonylimino)))tetrakis-benzene-1,3-disulfonic Acid Octasodium Salt]. *Journal of Pharmacology and Experimental Therapeutics.* 2005; 314(1): 232-243. DOI: 10.1124/jpet.105.084673.

Held, H.-D., Martin, C. and Uhlig, S. Characterization of airway and vascular responses in murine lungs. *British Journal of Pharmacology.* 1999; 126(5): 1191-1199. DOI: https://doi.org/10.1038/sj.bjp.0702394.

Henry, C. O., Dalloneau, E., Perez-Berezo, M. T., Plata, C., Wu, Y., Guillon, A., et al. In vitro and in vivo evidence for an inflammatory role of the calcium channel TRPV4 in lung epithelium: Potential involvement in cystic fibrosis. *Am J Physiol Lung Cell Mol Physiol.* 2016; 311(3): L664-675. DOI: 10.1152/ajplung.00442.2015.

Heuberger, D. M. and Schuepbach, R. A. Protease-activated receptors (PARs): Mechanisms of action and potential therapeutic modulators in PAR-driven inflammatory diseases. *Thromb J.* 2019; 17: 4-4. DOI: 10.1186/s12959-019-0194-8.

Higgins, G., Buchanan, P., Perriere, M., Al-Alawi, M., Costello, R. W., Verriere, V., et al. Activation of P2RY11 and ATP release by lipoxin A4 restores the airway surface liquid layer and epithelial repair in cystic fibrosis. *Am J Respir Cell Mol Biol.* 2014; 51(2): 178-190. DOI: 10.1165/rcmb.2012-0424OC.

Hinks, T. S. C., Hoyle, R. D. and Gelfand, E. W. CD8+ Tc2 cells: Underappreciated contributors to severe asthma. *Eur Respir Rev.* 2019; 28(154). DOI: 10.1183/16000617.0092-2019.

Hiraishi, Y., Yamaguchi, S., Yoshizaki, T., Nambu, A., Shimura, E., Takamori, A., et al. IL-33, IL-25 and TSLP contribute to development of fungal-associated protease-induced innate-type airway inflammation. *Sci Rep.* 2018; 8(1): 18052. DOI: 10.1038/s41598-018-36440-x.

Hirota, N., Risse, P. A., Novali, M., McGovern, T., Al-Alwan, L., McCuaig, S., et al. Histamine may induce airway remodeling through release of epidermal growth factor receptor ligands from bronchial epithelial cells. *Faseb j.* 2012; 26(4): 1704-1716. DOI: 10.1096/fj.11-197061.

Ho, J. E., Chen, W.-Y., Chen, M.-H., Larson, M. G., McCabe, E. L., Cheng, S., et al. Common genetic variation at the IL1RL1 locus regulates IL-33/ST2 signaling. *The Journal of Clinical Investigation.* 2013; 123(10): 4208-4218. DOI: 10.1172/jci67119.

Ho, L. H., Ohno, T., Oboki, K., Kajiwara, N., Suto, H., Iikura, M., et al. IL-33 induces IL-13 production by mouse mast cells independently of IgE-FcepsilonRI signals. *J Leukoc Biol.* 2007; 82(6): 1481-1490. DOI: 10.1189/jlb.0407200.

Holgate, S. T., Bodey, K. S., Janezic, A., Frew, A. J., Kaplan, A. P. and Teran, L. M. Release of RANTES, MIP-1 alpha, and MCP-1 into asthmatic airways following endobronchial allergen challenge. *Am J Respir Crit Care Med.* 1997; 156(5): 1377-1383. DOI: 10.1164/ajrccm.156.5.9610064.

Holgate, S. T., Noonan, M., Chanez, P., Busse, W., Dupont, L., Pavord, I., et al. Efficacy and safety of etanercept in moderate-to-severe asthma: a randomised, controlled trial. *Eur Respir J.* 2011; 37(6): 1352-1359. DOI: 10.1183/09031936.00063510.

Holgate, S. T., Wenzel, S., Postma, D. S., Weiss, S. T., Renz, H. and Sly, P. D. Asthma. *Nat Rev Dis Primers.* 2015; 1(1): 15025. DOI: 10.1038/nrdp.2015.25.

Hollenberg, M. D., Mihara, K., Polley, D., Suen, J. Y., Han, A., Fairlie, D. P., et al. Biased signalling and proteinase-activated receptors (PARs): targeting inflammatory disease. *Br J Pharmacol.* 2014; 171(5): 1180-1194. DOI: 10.1111/bph.12544.

Holmdahl, R. and Malissen, B. The need for littermate controls. *Eur J Immunol.* 2012; 42(1): 45-47. DOI: 10.1002/eji.201142048.

Hondowicz, B. D., An, D., Schenkel, J. M., Kim, K. S., Steach, H. R., Krishnamurty, A. T., et al. Interleukin-2-Dependent Allergen-Specific Tissue-Resident Memory Cells Drive Asthma. *Immunity.* 2016; 44(1): 155-166. DOI: 10.1016/j.immuni.2015.11.004.

Hong, H., Liao, S., Chen, F., Yang, Q. and Wang, D.-Y. Role of IL-25, IL-33, and TSLP in triggering united airway diseases toward type 2 inflammation. *Allergy.* 2020; 75(11): 2794-2804. DOI: https://doi.org/10.1111/all.14526.

Hossny, E. M., El-Sayed, S. S., El-Hadidi, E. S. and Moussa, S. R. Serum interleukin-18 expression in children with bronchial asthma. *World Allergy Organ J.* 2009; 2(5): 63-68. DOI: 10.1097/WOX.0b013e3181a33649.

Hou, Z. and Cao, J. Comparative study of the P2X gene family in animals and plants. *Purinergic Signal.* 2016; 12(2): 269-281. DOI: 10.1007/s11302-016-9501-z.

Howells, G. L., Macey, M. G., Chinni, C., Hou, L., Fox, M. T., Harriott, P., et al. Proteinase-activated receptor-2: expression by human neutrophils. *J Cell Sci.* 1997; 110(7): 881-887.

Hox, V., Vanoirbeek, J. A., Alpizar, Y. A., Voedisch, S., Callebaut, I., Bobic, S., et al. Crucial role of transient receptor potential ankyrin 1 and mast cells in induction of nonallergic airway hyperreactivity in mice. *Am J Respir Crit Care Med.* 2013; 187(5): 486-493. DOI: 10.1164/rccm.201208-1358OC.

Huang, C., Li, F., Wang, J. and Tian, Z. Innate-like Lymphocytes and Innate Lymphoid Cells in Asthma. *Clin Rev Allergy Immunol.* 2020; 59(3): 359-370. DOI: 10.1007/s12016-019-08773-6.

Huang, S. K., Xiao, H. Q., Kleine-Tebbe, J., Paciotti, G., Marsh, D. G., Lichtenstein, L. M., et al. IL-13 expression at the sites of allergen challenge in patients with asthma. *J Immunol.* 1995; 155(5): 2688-2694.

Huang, T. J., MacAry, P. A., Kemeny, D. M. and Chung, K. F. Effect of CD8+ T-cell depletion on bronchial hyper-responsiveness and inflammation in sensitized and allergen-exposed Brown-Norway rats. *Immunology.* 1999; 96(3): 416-423. DOI: 10.1046/j.1365-2567.1999.00699.x.

Hughes, J. M., Stringer, R. S., Black, J. L. and Armour, C. L. The effects of tumour necrosis factor alpha on mediator release from human lung. *Pulm Pharmacol.* 1995; 8(1): 31-36. DOI: 10.1006/pulp.1995.1004.

Huh, J. C., Strickland, D. H., Jahnsen, F. L., Turner, D. J., Thomas, J. A., Napoli, S., et al. Bidirectional interactions between antigen-bearing respiratory tract dendritic cells (DCs) and T cells precede the late phase reaction in experimental asthma: DC activation occurs in the airway mucosa but not in the lung parenchyma. *J Exp Med.* 2003; 198(1): 19-30. DOI: 10.1084/jem.20021328.

Humbles, A. A., Lloyd, C. M., McMillan, S. J., Friend, D. S., Xanthou, G., McKenna, E. E., et al. A Critical Role for Eosinophils in Allergic Airways Remodeling. *Science.* 2004; 305(5691): 1776-1779. DOI: 10.1126/science.1100283.

Idzko, M., C, K. A., Muller, T., Durk, T., Grimm, M., Baudiss, K., et al. Attenuated allergic airway inflammation in Cd39 null mice. *Allergy.* 2013; 68(4): 472-480. DOI: 10.1111/all.12119.

Idzko, M., Dichmann, S., Panther, E., Ferrari, D., Herouy, Y., Virchow, C., Jr., et al. Functional characterization of P2Y and P2X receptors in human eosinophils. *J Cell Physiol.* 2001; 188(3): 329-336. DOI: 10.1002/jcp.1129.

Idzko, M., Hammad, H., van Nimwegen, M., Kool, M., Willart, M. A., Muskens, F., et al. Extracellular ATP triggers and maintains asthmatic airway inflammation by activating dendritic cells. *Nat Med.* 2007; 13(8): 913-919. DOI: 10.1038/nm1617.

Iikura, M., Suto, H., Kajiwara, N., Oboki, K., Ohno, T., Okayama, Y., et al. IL-33 can promote survival, adhesion and cytokine production in human mast cells. *Lab Invest.* 2007; 87(10): 971-978. DOI: 10.1038/labinvest.3700663.

Illes, P., Müller, C. E., Jacobson, K. A., Grutter, T., Nicke, A., Fountain, S. J., et al. Update of P2X receptor properties and their pharmacology: IUPHAR Review 30. *Br J Pharmacol.* 2020; 178(3): 489-514. DOI: 10.1111/bph.15299.

Imaoka, H., Gauvreau, G. M., Watson, R. M., Smith, S. G., Dua, B., Baatjes, A. J., et al. Interleukin-18 and interleukin-18 receptor-α expression in allergic asthma. *European Respiratory Journal.* 2011; 38(4): 981-983. DOI: 10.1183/09031936.00033811.

Inada, H., Iida, T. and Tominaga, M. Different expression patterns of TRP genes in murine B and T lymphocytes. *Biochem Biophys Res Commun.* 2006; 350(3): 762-767. DOI: 10.1016/j.bbrc.2006.09.111.

Inouye, S. Firefly luciferase: an adenylate-forming enzyme for multicatalytic functions. *Cell Mol Life Sci.* 2010; 67(3): 387-404. DOI: 10.1007/s00018-009-0170-8.

Irvin, C. G. and Bates, J. H. Measuring the lung function in the mouse: the challenge of size. *Respir Res.* 2003; 4(1): 4. DOI: doi:10.1186/rr199.

Isogai, S., Taha, R., Tamaoka, M., Yoshizawa, Y., Hamid, Q. and Martin, J. G. CD8+ alphabeta T cells can mediate late airway responses and airway eosinophilia in rats. *J Allergy Clin Immunol.* 2004; 114(6): 1345-1352. DOI: 10.1016/j.jaci.2004.09.021.

Ito, T., Wang, Y. H., Duramad, O., Hori, T., Delespesse, G. J., Watanabe, N., et al. TSLP-activated dendritic cells induce an inflammatory T helper type 2 cell response through OX40 ligand. *J Exp Med.* 2005; 202(9): 1213-1223. DOI: 10.1084/jem.20051135.

Jacob, F., Novo, C. P., Bachert, C. and Van Crombruggen, K. Purinergic signaling in inflammatory cells: P2 receptor expression, functional effects, and modulation of inflammatory responses. *Purinergic Signal.* 2013; 9(3): 285-306. DOI: 10.1007/s11302-013-9357-4.

Jacobsen, E. A., Doyle, A. D., Colbert, D. C., Zellner, K. R., Protheroe, C. A., LeSuer, W. E., et al. Differential activation of airway eosinophils induces IL-13-mediated allergic Th2 pulmonary responses in mice. *Allergy.* 2015; 70(9): 1148-1159. DOI: https://doi.org/10.1111/all.12655.

Jacquet, A. Interactions of airway epithelium with protease allergens in the allergic response. *Clinical & Experimental Allergy.* 2011; 41(3): 305-311. DOI: https://doi.org/10.1111/j.1365-2222.2010.03661.x.

Jahnsen, F. L., Moloney, E. D., Hogan, T., Upham, J. W., Burke, C. M. and Holt, P. G. Rapid dendritic cell recruitment to the bronchial mucosa of patients with atopic asthma in response to local allergen challenge. *Thorax.* 2001; 56(11): 823-826. DOI: 10.1136/thorax.56.11.823.

Jairaman, A., Maguire, C. H., Schleimer, R. P. and Prakriya, M. Allergens stimulate store-operated calcium entry and cytokine production in airway epithelial cells. *Sci Rep.* 2016; 6. DOI: 10.1038/srep32311.

James, S. L., Abate, D., Hassen, A. K., Abay, S. M., Abbafati, C., Abbasi, N., et al. Global, regional, and national incidence, prevalence, and years lived with disability for 354 diseases and injuries for 195 countries and territories, 1990-2017: a systematic analysis for the Global Burden of Disease Study 2017. *Lancet.* 2018; 392(10159): 1789-1858. DOI: 10.1016/s0140-6736(18)32279-7.

Jarjour, N. N., Calhoun, W. J., Schwartz, L. B. and Busse, W. W. Elevated bronchoalveolar lavage fluid histamine levels in allergic asthmatics are associated with increased airway obstruction. *Am Rev Respir Dis.* 1991; 144(1): 83-87. DOI: 10.1164/ajrccm/144.1.83.

Jeong, Y. H., Walsh, M. C., Yu, J., Shen, H., Wherry, E. J. and Choi, Y. Mice Lacking the Purinergic Receptor P2X5 Exhibit Defective Inflammasome Activation and Early Susceptibility to Listeria monocytogenes. *J Immunol.* 2020; 205(3): 760-766. DOI: 10.4049/jimmunol.1901423.

Ji, H., Pai, A. V., West, C. A., Wu, X., Speth, R. C. and Sandberg, K. Loss of Resistance to Angiotensin II-Induced Hypertension in the Jackson Laboratory Recombination-Activating Gene Null Mouse on the C57BL/6J Background. *Hypertension.* 2017; 69(6): 1121-1127. DOI: 10.1161/hypertensionaha.117.09063.

Jia, X., Zhang, H., Cao, X., Yin, Y. and Zhang, B. Activation of TRPV1 mediates thymic stromal lymphopoietin release via the Ca2+/NFAT pathway in airway epithelial cells. *FEBS Letters.* 2014; 588(17): 3047-3054. DOI: https://doi.org/10.1016/j.febslet.2014.06.018.

Jia, Y., Wang, X., Varty, L., Rizzo, C. A., Yang, R., Correll, C. C., et al. Functional TRPV4 channels are expressed in human airway smooth muscle cells. *Am J Physiol Lung Cell Mol Physiol.* 2004; 287(2): L272-278. DOI: 10.1152/ajplung.00393.2003.

Jiang, L. H., Mackenzie, A. B., North, R. A. and Surprenant, A. Brilliant blue G selectively blocks ATP-gated rat P2X(7) receptors. *Mol Pharmacol.* 2000; 58(1): 82-88.

Jo, S. and Bean, B. P. Inhibition of neuronal voltage-gated sodium channels by brilliant blue G. *Mol Pharmacol.* 2011; 80(2): 247-257. DOI: 10.1124/mol.110.070276.

Joetham, A., Takeda, K., Taube, C., Miyahara, N., Kanehiro, A., Dakhama, A., et al. Airway hyperresponsiveness in the absence of CD4+ T cells after primary but not secondary challenge. *Am J Respir Cell Mol Biol.* 2005; 33(1): 89-96. DOI: 10.1165/rcmb.2004-0414OC.

Johansson, U., Lawson, C., Dabare, M., Syndercombe-Court, D., Newland, A. C., Howells, G. L., et al. Human peripheral blood monocytes express protease receptor-2 and respond to receptor activation by production of IL-6, IL-8, and IL-1{beta}. *J Leukoc Biol.* 2005; 78(4): 967-975. DOI: 10.1189/jlb.0704422.

Julia, V., Hessel, E. M., Malherbe, L., Glaichenhaus, N., O'Garra, A. and Coffman, R. L. A restricted subset of dendritic cells captures airborne antigens and remains able to activate specific T cells long after antigen exposure. *Immunity.* 2002; 16(2): 271-283. DOI: 10.1016/s1074-7613(02)00276-5.

Kamada, F., Suzuki, Y., Shao, C., Tamari, M., Hasegawa, K., Hirota, T., et al. Association of the hCLCA1 gene with childhood and adult asthma. *Genes & Immunity.* 2004; 5(7): 540-547. DOI: 10.1038/sj.gene.6364124.

Kang, S. W., Kim, S. K., Han, Y. R., Hong, D., Chon, J., Chung, J. H., et al. Promoter Polymorphism (-308G/A) of Tumor Necrosis Factor-Alpha (TNF-α) Gene and Asthma Risk: An Updated Meta-Analysis. *Genetic testing and molecular biomarkers.* 2019; 23(6). DOI: 10.1089/gtmb.2018.0238.

Kaur, D., Gomez, E., Doe, C., Berair, R., Woodman, L., Saunders, R., et al. IL-33 drives airway hyper-responsiveness through IL-13-mediated mast cell: airway smooth muscle crosstalk. *Allergy.* 2015; 70(5): 556-567. DOI: 10.1111/all.12593.

Kavanagh, J. E., Hearn, A. P., Dhariwal, J., d'Ancona, G., Douiri, A., Roxas, C., et al. Real-World Effectiveness of Benralizumab in Severe Eosinophilic Asthma. *Chest.* 2021; 159(2): 496-506. DOI: 10.1016/j.chest.2020.08.2083.

Kawamura, H., Kawamura, T., Kanda, Y., Kobayashi, T. and Abo, T. Extracellular ATP-stimulated macrophages produce macrophage inflammatory protein-2 which is important for neutrophil migration. *Immunology.* 2012; 136(4): 448-458. DOI: 10.1111/j.1365-2567.2012.03601.x.

Kawashima, Y., Sugimura, M., Hwang, Y.-C. and Kudo, N. The lymph system in mice. *Japanese Journal of Veterinary Research.* 1964; 12(4): 9. DOI: 10.14943/jjvr.12.4.69.

Kelsen, S. G., Agache, I. O., Soong, W., Israel, E., Chupp, G. L., Cheung, D. S., et al. Astegolimab (anti-ST2) efficacy and safety in adults with severe asthma: A randomized clinical trial. *J Allergy Clin Immunol.* 2021; 148(3): 790-798. DOI: 10.1016/j.jaci.2021.03.044.

Kemp, P. A., Sugar, R. A. and Jackson, A. D. Nucleotide-mediated mucin secretion from differentiated human bronchial epithelial cells. *Am J Respir Cell Mol Biol.* 2004; 31(4): 446-455. DOI: 10.1165/rcmb.2003-0211OC.

Kerstjens, H. A., Casale, T. B., Bleecker, E. R., Meltzer, E. O., Pizzichini, E., Schmidt, O., et al. Tiotropium or salmeterol as add-on therapy to inhaled corticosteroids for patients with moderate symptomatic asthma: two replicate, double-blind, placebo-controlled, parallel-group, active-comparator, randomised trials. *Lancet Respir Med.* 2015; 3(5): 367-376. DOI: 10.1016/s2213-2600(15)00031-4.

Kerstjens, H. A., Engel, M., Dahl, R., Paggiaro, P., Beck, E., Vandewalker, M., et al. Tiotropium in asthma poorly controlled with standard combination therapy. *N Engl J Med.* 2012; 367(13): 1198-1207. DOI: 10.1056/NEJMoa1208606.

Kessler, S., Clauss, W. G., Gunther, A., Kummer, W. and Fronius, M. Expression and functional characterization of P2X receptors in mouse alveolar macrophages. *Pflugers Arch.* 2011; 462(3): 419-430. DOI: 10.1007/s00424-011-0980-z.

Khan, M., Huang, Y. A., Kuo, C. Y., Lin, T., Lu, C. H., Chen, L. C., et al. Blocking pannexin1 reduces airway inflammation in a murine model of asthma. *Am J Transl Res.* 2020; 12(7): 4074-4083.

Kim, B. G., Park, M. K., Lee, P. H., Lee, S. H., Hong, J., Aung, M. M. M., et al. Effects of nanoparticles on neuroinflammation in a mouse model of asthma. *Respir Physiol Neurobiol.* 2020; 271: 103292. DOI: 10.1016/j.resp.2019.103292.

Kim, H., Walsh, M. C., Takegahara, N., Middleton, S. A., Shin, H. I., Kim, J., et al. The purinergic receptor P2X5 regulates inflammasome activity and hyper-multinucleation of murine osteoclasts. *Sci Rep.* 2017; 7(1): 196. DOI: 10.1038/s41598-017-00139-2.

Kim, H. J., Lee, S. H., Jeong, S. and Hong, S. J. Protease-Activated Receptors 2-Antagonist Suppresses Asthma by Inhibiting Reactive Oxygen Species-Thymic Stromal Lymphopoietin Inflammation and Epithelial Tight Junction Degradation. *Allergy Asthma Immunol Res.* 2019; 11(4): 560-571. DOI: 10.4168/aair.2019.11.4.560.

Kim, H. Y., Lee, H. J., Chang, Y. J., Pichavant, M., Shore, S. A., Fitzgerald, K. A., et al. Interleukin-17-producing innate lymphoid cells and the NLRP3 inflammasome facilitate obesity-associated airway hyperreactivity. *Nat Med.* 2014; 20(1): 54-61. DOI: 10.1038/nm.3423.

Kim, K. W., Jee, H. M., Park, Y. H., Choi, B. S., Sohn, M. H. and Kim, K. E. Relationship between amphiregulin and airway inflammation in children with asthma and eosinophilic bronchitis. *Chest.* 2009; 136(3): 805-810. DOI: 10.1378/chest.08-2972.

Kistemaker, L. E. M. and Prakash, Y. S. Airway Innervation and Plasticity in Asthma. *Physiology.* 2019; 34(4): 283-298. DOI: 10.1152/physiol.00050.2018.

Klausen, T. K., Pagani, A., Minassi, A., Ech-Chahad, A., Prenen, J., Owsianik, G., et al. Modulation of the transient receptor potential vanilloid channel TRPV4 by 4alpha-phorbol esters: a structure-activity study. *J Med Chem.* 2009; 52(9): 2933-2939. DOI: 10.1021/jm9001007.

Klein Wolterink, R. G., Kleinjan, A., van Nimwegen, M., Bergen, I., de Bruijn, M., Levani, Y., et al. Pulmonary innate lymphoid cells are major producers of IL-5 and IL-13 in murine models of allergic asthma. *Eur J Immunol.* 2012; 42(5): 1106-1116. DOI: 10.1002/eji.201142018.

Knight, D. A., Lim, S., Scaffidi, A. K., Roche, N., Chung, K. F., Stewart, G. A., et al. Protease-activated receptors in human airways: upregulation of PAR-2 in respiratory epithelium from patients with asthma. *J Allergy Clin Immunol.* 2001; 108(5): 797-803. DOI: 10.1067/mai.2001.119025.

Kobayashi, T., Soma, T., Noguchi, T., Nakagome, K., Nakamoto, H., Kita, H., et al. ATP drives eosinophil effector responses through P2 purinergic receptors. *Allergol Int.* 2015; 64 Suppl: S30-36. DOI: 10.1016/j.alit.2015.04.009.

Köhler, R., Heyken, W. T., Heinau, P., Schubert, R., Si, H., Kacik, M., et al. Evidence for a functional role of endothelial transient receptor potential V4 in shear stress-induced vasodilatation. *Arterioscler Thromb Vasc Biol.* 2006; 26(7): 1495-1502. DOI: 10.1161/01.ATV.0000225698.36212.6a.

Kool, M., van Nimwegen, M., Willart, M. A. M., Muskens, F., Boon, L., Smit, J. J., et al. An Anti-Inflammatory Role for Plasmacytoid Dendritic Cells in Allergic Airway Inflammation. *The Journal of Immunology.* 2009; 183(2): 1074. DOI: 10.4049/jimmunol.0900471.

Kopf, M., Schneider, C. and Nobs, S. P. The development and function of lung-resident macrophages and dendritic cells. *Nat Immunol.* 2015; 16(1): 36-44. DOI: 10.1038/ni.3052.

Koppelman, G. H., Meyers, D. A., Howard, T. D., Zheng, S. L., Hawkins, G. A., Ampleford, E. J., et al. Identification of PCDH1 as a novel susceptibility gene for bronchial hyperresponsiveness. *Am J Respir Crit Care Med.* 2009; 180(10): 929-935. DOI: 10.1164/rccm.200810-1621OC.

Korsgren, M., Persson, C. G., Sundler, F., Bjerke, T., Hansson, T., Chambers, B. J., et al. Natural killer cells determine development of allergen-induced eosinophilic airway inflammation in mice. *J Exp Med.* 1999; 189(3): 553-562. DOI: 10.1084/jem.189.3.553.

Kouzaki, H., Iijima, K., Kobayashi, T., O'Grady, S. M. and Kita, H. The danger signal, extracellular ATP, is a sensor for an airborne allergen and triggers IL-33 release and innate Th2-type responses. *J Immunol.* 2011; 186(7): 4375-4387. DOI: 10.4049/jimmunol.1003020.

Kouzaki, H., Tojima, I., Kita, H. and Shimizu, T. Transcription of Interleukin-25 and Extracellular Release of the Protein Is Regulated by Allergen Proteases in Airway Epithelial Cells. *American Journal of Respiratory Cell and Molecular Biology.* 2013; 49(5): 741-750. DOI: 10.1165/rcmb.2012-0304OC.

Koya, T., Matsuda, H., Matsubara, S., Miyahara, N., Dakhama, A., Takeda, K., et al. Differential effects of dendritic cell transfer on airway hyperresponsiveness and inflammation. *Am J Respir Cell Mol Biol.* 2009; 41(3): 271-280. DOI: 10.1165/rcmb.2008-0256OC.

Koya, T., Miyahara, N., Takeda, K., Matsubara, S., Matsuda, H., Swasey, C., et al. CD8+ T cell-mediated airway hyperresponsiveness and inflammation is dependent on CD4+IL-4+ T cells. *J Immunol.* 2007; 179(5): 2787-2796. DOI: 10.4049/jimmunol.179.5.2787.

Krishna, M. T., Chauhan, A., Little, L., Sampson, K., Hawksworth, R., Mant, T., et al. Inhibition of mast cell tryptase by inhaled APC 366 attenuates allergen-induced late-phase airway obstruction in asthma. *J Allergy Clin Immunol.* 2001; 107(6): 1039-1045. DOI: 10.1067/mai.2001.115631.

Krug, N., Madden, J., Redington, A. E., Lackie, P., Djukanovic, R., Schauer, U., et al. T-cell cytokine profile evaluated at the single cell level in BAL and blood in allergic asthma. *Am J Respir Cell Mol Biol.* 1996; 14(4): 319-326. DOI: 10.1165/ajrcmb.14.4.8600935.

Kurokawa, M., Matsukura, S., Kawaguchi, M., Ieki, K., Suzuki, S., Odaka, M., et al. Expression and effects of IL-33 and ST2 in allergic bronchial asthma: IL-33 induces eotaxin production in lung fibroblasts. *Int Arch Allergy Immunol.* 2011; 155 Suppl 1: 12-20. DOI: 10.1159/000327259.

Kuruvilla, M. E., Lee, F. E. and Lee, G. B. Understanding Asthma Phenotypes, Endotypes, and Mechanisms of Disease. *Clin Rev Allergy Immunol.* 2019; 56(2): 219-233. DOI: 10.1007/s12016-018-8712-1.

la Sala, A., Sebastiani, S., Ferrari, D., Di Virgilio, F., Idzko, M., Norgauer, J., et al. Dendritic cells exposed to extracellular adenosine triphosphate acquire the migratory properties of mature cells and

show a reduced capacity to attract type 1 T lymphocytes. *Blood.* 2002; 99(5): 1715-1722. DOI: 10.1182/blood.v99.5.1715.

Lambrecht, B. N., Carro-Muino, I., Vermaelen, K. and Pauwels, R. A. Allergen-induced changes in bone-marrow progenitor and airway dendritic cells in sensitized rats. *Am J Respir Cell Mol Biol.* 1999; 20(6): 1165-1174. DOI: 10.1165/ajrcmb.20.6.3484.

Lambrecht, B. N., Hammad, H. and Fahy, J. V. (2019). The Cytokines of Asthma, Cell Press. **50:** 975-991.

Lambrecht, B. N., Persson, E. K. and Hammad, H. Myeloid Cells in Asthma. *Microbiol Spectr.* 2017; 5(1): 739-757. DOI: 10.1128/microbiolspec.mchd-0053-2016.

Lambrecht, B. N., Salomon, B., Klatzmann, D. and Pauwels, R. A. Dendritic cells are required for the development of chronic eosinophilic airway inflammation in response to inhaled antigen in sensitized mice. *J Immunol.* 1998; 160(8): 4090-4097.

Lambrecht, G., Friebe, T., Grimm, U., Windscheif, U., Bungardt, E., Hildebrandt, C., et al. PPADS, a novel functionally selective antagonist of P2 purinoceptor-mediated responses. *Eur J Pharmacol.* 1992; 217(2-3): 217-219. DOI: 10.1016/0014-2999(92)90877-7.

Lan, R. S., Stewart, G. A. and Henry, P. J. Modulation of airway smooth muscle tone by protease activated receptor-1,-2,-3 and -4 in trachea isolated from influenza A virus-infected mice. *Br J Pharmacol.* 2000; 129(1): 63-70. DOI: 10.1038/sj.bjp.0703007.

Lazar, Z., Mullner, N., Lucattelli, M., Ayata, C. K., Cicko, S., Yegutkin, G. G., et al. NTPDase1/CD39 and aberrant purinergic signalling in the pathogenesis of COPD. *Eur Respir J.* 2016; 47(1): 254-263. DOI: 10.1183/13993003.02144-2014.

Le Gros, G., Ben-Sasson, S. Z., Seder, R., Finkelman, F. D. and Paul, W. E. Generation of interleukin 4 (IL-4)-producing cells in vivo and in vitro: IL-2 and IL-4 are required for in vitro generation of IL-4-producing cells. *J Exp Med.* 1990; 172(3): 921-929. DOI: 10.1084/jem.172.3.921.

Lebold, K. M., Drake, M. G., Hales-Beck, L. B., Fryer, A. D. and Jacoby, D. B. IL-5 Exposure In Utero Increases Lung Nerve Density and Airway Reactivity in Adult Offspring. *Am J Respir Cell Mol Biol.* 2020; 62(4): 493-502. DOI: 10.1165/rcmb.2019-0214OC.

Leckie, M. J., ten Brinke, A., Khan, J., Diamant, Z., O'Connor, B. J., Walls, C. M., et al. Effects of an interleukin-5 blocking monoclonal antibody on eosinophils, airway hyper-responsiveness, and the late asthmatic response. *Lancet.* 2000; 356(9248): 2144-2148. DOI: 10.1016/s0140-6736(00)03496-6.

Ledderose, C., Bao, Y., Ledderose, S., Woehrle, T., Heinisch, M., Yip, L., et al. Mitochondrial Dysfunction, Depleted Purinergic Signaling, and Defective T Cell Vigilance and Immune Defense. *J Infect Dis.* 2016; 213(3): 456-464. DOI: 10.1093/infdis/jiv373.

Ledderose, C., Bao, Y., Lidicky, M., Zipperle, J., Li, L., Strasser, K., et al. Mitochondria are gate-keepers of T cell function by producing the ATP that drives purinergic signaling. *J Biol Chem.* 2014; 289(37): 25936-25945. DOI: 10.1074/jbc.M114.575308.

Ledderose, C., Bromberger, S., Slubowski, C. J., Sueyoshi, K. and Junger, W. G. Frontline Science: P2Y11 receptors support T cell activation by directing mitochondrial trafficking to the immune synapse. *J Leukoc Biol.* 2021; 109(3): 497-508. DOI: 10.1002/jlb.2hi0520-191r.

Ledderose, C., Liu, K., Kondo, Y., Slubowski, C. J., Dertnig, T., Denicolo, S., et al. Purinergic P2X4 receptors and mitochondrial ATP production regulate T cell migration. *J Clin Invest.* 2018; 128(8): 3583-3594. DOI: 10.1172/jci120972.

Lee, H. Y., Hur, J., Kim, I. K., Kang, J. Y., Yoon, H. K., Lee, S. Y., et al. Effect of nintedanib on airway inflammation and remodeling in a murine chronic asthma model. *Exp Lung Res.* 2017; 43(4-5): 187-196. DOI: 10.1080/01902148.2017.1339141.

Lee, J. J., Dimina, D., Macias, M. P., Ochkur, S. I., McGarry, M. P., O'Neill, K. R., et al. Defining a Link with Asthma in Mice Congenitally Deficient in Eosinophils. *Science.* 2004; 305(5691): 1773-1776. DOI: 10.1126/science.1099472.

Lee, S. Y., Kim, S. J., Kwon, S. S., Kim, Y. K., Kim, K. H., Moon, H. S., et al. Distribution and cytokine production of CD4 and CD8 T-lymphocyte subsets in patients with acute asthma attacks. *Ann Allergy Asthma Immunol.* 2001; 86(6): 659-664. DOI: 10.1016/s1081-1206(10)62295-8.

Lefebvre, P., Duh, M. S., Lafeuille, M. H., Gozalo, L., Desai, U., Robitaille, M. N., et al. Acute and chronic systemic corticosteroid-related complications in patients with severe asthma. *J Allergy Clin Immunol.* 2015; 136(6): 1488-1495. DOI: 10.1016/j.jaci.2015.07.046.

Lefrançais, E., Roga, S., Gautier, V., Gonzalez-de-Peredo, A., Monsarrat, B., Girard, J. P., et al. IL-33 is processed into mature bioactive forms by neutrophil elastase and cathepsin G. *Proc Natl Acad Sci U S A.* 2012; 109(5): 1673-1678. DOI: 10.1073/pnas.1115884109.

Lewkowich, I. P., Day, S. B., Ledford, J. R., Zhou, P., Dienger, K., Wills-Karp, M., et al. Protease-activated receptor 2 activation of myeloid dendritic cells regulates allergic airway inflammation. *Respir Res.* 2011; 12(1): 122. DOI: 10.1186/1465-9921-12-122.

Lewkowich, I. P., Lajoie, S., Clark, J. R., Herman, N. S., Sproles, A. A. and Wills-Karp, M. Allergen uptake, activation, and IL-23 production by pulmonary myeloid DCs drives airway hyperresponsiveness in asthma-susceptible mice. *PLoS One.* 2008; 3(12): e3879. DOI: 10.1371/journal.pone.0003879.

Li, B. W. S., Stadhouders, R., de Bruijn, M. J. W., Lukkes, M., Beerens, D., Brem, M. D., et al. Group 2 Innate Lymphoid Cells Exhibit a Dynamic Phenotype in Allergic Airway Inflammation. *Front Immunol.* 2017; 8(DEC): 1684. DOI: 10.3389/fimmu.2017.01684.

Li, H., Wang, K., Huang, H., Cheng, W. and Liu, X. A meta-analysis of anti-interleukin-13 monoclonal antibodies for uncontrolled asthma. *PloS one.* 2019a; 14(1): e0211790-e0211790. DOI: 10.1371/journal.pone.0211790.

Li, J., Kanju, P., Patterson, M., Chew, W. L., Cho, S. H., Gilmour, I., et al. TRPV4-mediated calcium influx into human bronchial epithelia upon exposure to diesel exhaust particles. *Environ Health Perspect.* 2011; 119(6): 784-793. DOI: 10.1289/ehp.1002807.

Li, M., Fang, X. Z., Zheng, Y. F., Xie, Y. B., Ma, X. D., Liu, X. T., et al. Transient receptor potential vanilloid 4 is a critical mediator in LPS mediated inflammation by mediating calcineurin/NFATc3 signaling. *Biochem Biophys Res Commun.* 2019b; 513(4): 1005-1012. DOI: 10.1016/j.bbrc.2019.04.020.

Li, P., Cao, J., Chen, Y., Wang, W. and Yang, J. Apyrase protects against allergic airway inflammation by decreasing the chemotactic migration of dendritic cells in mice. *Int J Mol Med.* 2014; 34(1): 269-275. DOI: 10.3892/ijmm.2014.1771.

Li, P., Gao, Y., Cao, J., Wang, W., Chen, Y., Zhang, G., et al. CD39+ regulatory T cells attenuate allergic airway inflammation. *Clin Exp Allergy.* 2015; 45(6): 1126-1137. DOI: 10.1111/cea.12521.

Li, R., Shang, Y., Hu, X., Yu, Y., Zhou, T., Xiong, W., et al. ATP/P2X7r axis mediates the pathological process of allergic asthma by inducing M2 polarization of alveolar macrophages. *Exp Cell Res.* 2020; 386(1): 111708. DOI: 10.1016/j.yexcr.2019.111708.

Li, R., Wang, J., Li, R., Zhu, F., Xu, W., Zha, G., et al. ATP/P2X7-NLRP3 axis of dendritic cells participates in the regulation of airway inflammation and hyper-responsiveness in asthma by mediating HMGB1 expression and secretion. *Exp Cell Res.* 2018a; 366(1): 1-15. DOI: 10.1016/j.yexcr.2018.03.002.

Li, Y., Wang, W., Lv, Z., Li, Y., Chen, Y., Huang, K., et al. Elevated Expression of IL-33 and TSLP in the Airways of Human Asthmatics In Vivo: A Potential Biomarker of Severe Refractory Disease. *J Immunol.* 2018b; 200(7): 2253-2262. DOI: 10.4049/jimmunol.1701455.

Liao, W., Schones, D. E., Oh, J., Cui, Y., Cui, K., Roh, T. Y., et al. Priming for T helper type 2 differentiation by interleukin 2-mediated induction of interleukin 4 receptor alpha-chain expression. *Nat Immunol.* 2008; 9(11): 1288-1296. DOI: 10.1038/ni.1656.

Liedtke, W., Choe, Y., Marti-Renom, M. A., Bell, A. M., Denis, C. S., Sali, A., et al. Vanilloid receptor-related osmotically activated channel (VR-OAC), a candidate vertebrate osmoreceptor. *Cell.* 2000; 103(3): 525-535. DOI: 10.1016/s0092-8674(00)00143-4.

Lieu, T. M., Myers, A. C., Meeker, S. and Undem, B. J. TRPV1 induction in airway vagal low-threshold mechanosensory neurons by allergen challenge and neurotrophic factors. *Am J Physiol Lung Cell Mol Physiol.* 2012; 302(9): L941-L948. DOI: 10.1152/ajplung.00366.2011.

Lim, S. Y., Tennant, G. M., Kennedy, S., Wainwright, C. L. and Kane, K. A. Activation of mouse protease-activated receptor-2 induces lymphocyte adhesion and generation of reactive oxygen species. *Br J Pharmacol.* 2006; 149(5): 591-599. DOI: 10.1038/sj.bjp.0706905.

Lin, R. L., Gu, Q., Khosravi, M. and Lee, L. Y. Sustained sensitizing effects of tumor necrosis factor alpha on sensory nerves in lung and airways. *Pulm Pharmacol Ther.* 2017; 47: 29-37. DOI: 10.1016/j.pupt.2017.06.001.

Lin, Y. L., Shieh, C. C. and Wang, J. Y. The functional insufficiency of human CD4+CD25 high T-regulatory cells in allergic asthma is subjected to TNF-alpha modulation. *Allergy.* 2008; 63(1): 67-74. DOI: 10.1111/j.1398-9995.2007.01526.x.

Lindner, J. R., Kahn, M. L., Coughlin, S. R., Sambrano, G. R., Schauble, E., Bernstein, D., et al. Delayed onset of inflammation in protease-activated receptor-2-deficient mice. *J Immunol.* 2000; 165(11): 6504-6510. DOI: 10.4049/jimmunol.165.11.6504.

Liu, L. Y., Bates, M. E., Jarjour, N. N., Busse, W. W., Bertics, P. J. and Kelly, E. A. B. Generation of Th1 and Th2 Chemokines by Human Eosinophils: Evidence for a Critical Role of TNF-α. *The Journal of Immunology.* 2007; 179(7): 4840-4848. DOI: 10.4049/jimmunol.179.7.4840.

Lloyd, C. M., Delaney, T., Nguyen, T., Tian, J., Martinez, A. C., Coyle, A. J., et al. CC chemokine receptor (CCR)3/eotaxin is followed by CCR4/monocyte-derived chemokine in mediating pulmonary T helper lymphocyte type 2 recruitment after serial antigen challenge in vivo. *J Exp Med.* 2000; 191(2): 265-274. DOI: 10.1084/jem.191.2.265.

Lloyd, C. M. and Snelgrove, R. J. Type 2 immunity: Expanding our view. *Sci Immunol.* 2018; 3(25): 1604-1604. DOI: 10.1126/sciimmunol.aat1604.

Lohning, M., Stroehmann, A., Coyle, A. J., Grogan, J. L., Lin, S., Gutierrez-Ramos, J. C., et al. T1/ST2 is preferentially expressed on murine Th2 cells, independent of interleukin 4, interleukin 5, and interleukin 10, and important for Th2 effector function. *Proc Natl Acad Sci U S A.* 1998; 95(12): 6930-6935. DOI: 10.1073/pnas.95.12.6930.

Lomask, M. Further exploration of the Penh parameter. *Exp Toxicol Pathol.* 2006; 57 Suppl 2: 13-20. DOI: 10.1016/j.etp.2006.02.014.

Lombardi, V., Speak, A. O., Kerzerho, J., Szely, N. and Akbari, O. CD8α+β− and CD8α+β+ plasmacytoid dendritic cells induce Foxp3+ regulatory T cells and prevent the induction of airway hyper-reactivity. *Mucosal Immunology.* 2012; 5(4): 432-443. DOI: 10.1038/mi.2012.20.

Lommatzsch, M., Cicko, S., Muller, T., Lucattelli, M., Bratke, K., Stoll, P., et al. Extracellular adenosine triphosphate and chronic obstructive pulmonary disease. *Am J Respir Crit Care Med.* 2010; 181(9): 928-934. DOI: 10.1164/rccm.200910-1506OC.

London, C. A., Lodge, M. P. and Abbas, A. K. Functional responses and costimulator dependence of memory CD4+ T cells. *J Immunol.* 2000; 164(1): 265-272. DOI: 10.4049/jimmunol.164.1.265.

Lopez, M. L., Soriano-Sarabia, N., Bruges, G., Marquez, M. E., Preissner, K. T., Schmitz, M. L., et al. Expression pattern of protease activated receptors in lymphoid cells. *Cell Immunol.* 2014; 288(1-2): 47-52. DOI: 10.1016/j.cellimm.2014.02.004.

Lorenzo, I. M., Liedtke, W., Sanderson, M. J. and Valverde, M. A. TRPV4 channel participates in receptor-operated calcium entry and ciliary beat frequency regulation in mouse airway epithelial cells. *Proc Natl Acad Sci U S A.* 2008; 105(34): 12611-12616. DOI: 10.1073/pnas.0803970105.

Loukin, S., Zhou, X., Su, Z., Saimi, Y. and Kung, C. Wild-type and brachyolmia-causing mutant TRPV4 channels respond directly to stretch force. *J Biol Chem.* 2010; 285(35): 27176-27181. DOI: 10.1074/jbc.M110.143370.

Lucattelli, M., Cicko, S., Muller, T., Lommatzsch, M., De Cunto, G., Cardini, S., et al. P2X7 receptor signaling in the pathogenesis of smoke-induced lung inflammation and emphysema. *Am J Respir Cell Mol Biol.* 2011; 44(3): 423-429. DOI: 10.1165/rcmb.2010-0038OC.

Lukacs, N. W., Strieter, R. M., Chensue, S. W., Widmer, M. and Kunkel, S. L. TNF-alpha mediates recruitment of neutrophils and eosinophils during airway inflammation. *The Journal of Immunology.* 1995a; 154(10).

Lukacs, N. W., Strieter, R. M., Shaklee, C. L., Chensue, S. W. and Kunkel, S. L. Macrophage inflammatory protein-1 alpha influences eosinophil recruitment in antigen-specific airway inflammation. *Eur J Immunol.* 1995b; 25(1): 245-251. DOI: 10.1002/eji.1830250140.

Lundblad, L. K., Irvin, C. G., Hantos, Z., Sly, P., Mitzner, W. and Bates, J. H. Penh is not a measure of airway resistance! *Eur Respir J.* 2007; 30(4): 805. DOI: 10.1183/09031936.00091307.

Mabalirajan, U., Rehman, R., Ahmad, T., Kumar, S., Singh, S., Leishangthem, G. D., et al. Linoleic acid metabolite drives severe asthma by causing airway epithelial injury. *Scientific Reports.* 2013; 3(1): 1-12. DOI: 10.1038/srep01349.

Majhi, R. K., Sahoo, S. S., Yadav, M., Pratheek, B. M., Chattopadhyay, S. and Goswami, C. Functional expression of TRPV channels in T cells and their implications in immune regulation. *FEBS J.* 2015; 282(14): 2661-2681. DOI: 10.1111/febs.13306.

Makwana, R., Gozzard, N., Spina, D. and Page, C. TNF-α-induces airway hyperresponsiveness to cholinergic stimulation in guinea pig airways. *Br J Pharmacol.* 2012; 165(6): 1978-1991. DOI: 10.1111/j.1476-5381.2011.01675.x.

Maltby, S., Tay, H. L., Yang, M. and Foster, P. S. Mouse models of severe asthma: Understanding the mechanisms of steroid resistance, tissue remodelling and disease exacerbation. *Respirology.* 2017; 22(5): 874-885. DOI: 10.1111/resp.13052.

Mangan, N. E., Dasvarma, A., McKenzie, A. N. and Fallon, P. G. T1/ST2 expression on Th2 cells negatively regulates allergic pulmonary inflammation. *Eur J Immunol.* 2007; 37(5): 1302-1312. DOI: 10.1002/eji.200636520.

Manthei, D. M., Jackson, D. J., Evans, M. D., Gangnon, R. E., Tisler, C. J., Gern, J. E., et al. Protection from asthma in a high-risk birth cohort by attenuated P2X(7) function. *J Allergy Clin Immunol.* 2012; 130(2): 496-502. DOI: 10.1016/j.jaci.2012.05.040.

Marathias, K. P., Preffer, F. I., Pinto, C. and Kradin, R. L. Most human pulmonary infiltrating lymphocytes display the surface immune phenotype and functional responses of sensitized T cells. *Am J Respir Cell Mol Biol.* 1991; 5(5): 470-476. DOI: 10.1165/ajrcmb/5.5.470.

Marone, G., Granata, F., Pucino, V., Pecoraro, A., Heffler, E., Loffredo, S., et al. The Intriguing Role of Interleukin 13 in the Pathophysiology of Asthma. *Front Pharmacol.* 2019; 10: 1387. DOI: 10.3389/fphar.2019.01387.

Martín-Orozco, E., Norte-Muñoz, M. and Martínez-García, J. Regulatory T Cells in Allergy and Asthma. *Frontiers in Pediatrics.* 2017; 5: 117.

Martin, T. R., Gerard, N. P., Galli, S. J. and Drazen, J. M. Pulmonary responses to bronchoconstrictor agonists in the mouse. *J Appl Physiol.* 1988; 64(6): 2318-2323. DOI: 10.1152/jappl.1988.64.6.2318.

Masin, M., Young, C., Lim, K., Barnes, S. J., Xu, X. J., Marschall, V., et al. Expression, assembly and function of novel C-terminal truncated variants of the mouse P2X7 receptor: re-evaluation of P2X7 knockouts. *Br J Pharmacol.* 2012; 165(4): 978-993. DOI: 10.1111/j.1476-5381.2011.01624.x.

Masopust, D., Vezys, V., Marzo, A. L. and Lefrancois, L. Preferential localization of effector memory cells in nonlymphoid tissue. *Science.* 2001; 291(5512): 2413-2417. DOI: 10.1126/science.1058867.

Masopust, D., Vezys, V., Usherwood, E. J., Cauley, L. S., Olson, S., Marzo, A. L., et al. Activated primary and memory CD8 T cells migrate to nonlymphoid tissues regardless of site of activation or tissue of origin. *J Immunol.* 2004; 172(8): 4875-4882. DOI: 10.4049/jimmunol.172.8.4875.

Masten, B. J., Yates, J. L., Pollard Koga, A. M. and Lipscomb, M. F. Characterization of accessory molecules in murine lung dendritic cell function: roles for CD80, CD86, CD54, and CD40L. *Am J Respir Cell Mol Biol.* 1997; 16(3): 335-342. DOI: 10.1165/ajrcmb.16.3.9070619.

Matera, M. G., Calzetta, L. and Cazzola, M. TNF-alpha inhibitors in asthma and COPD: we must not throw the baby out with the bath water. *Pulm Pharmacol Ther.* 2010; 23(2): 121-128. DOI: 10.1016/j.pupt.2009.10.007.

Matera, M. G., Rogliani, P., Calzetta, L. and Cazzola, M. TSLP Inhibitors for Asthma: Current Status and Future Prospects. *Drugs.* 2020; 80(5): 449-458. DOI: 10.1007/s40265-020-01273-4.

Mathie, S. A., Dixon, K. L., Walker, S. A., Tyrrell, V., Mondhe, M., O'Donnell, V. B., et al. Alveolar macrophages are sentinels of murine pulmonary homeostasis following inhaled antigen challenge. *Allergy.* 2015; 70(1): 80-89. DOI: 10.1111/all.12536.

Mattes, J., Yang, M., Siqueira, A., Clark, K., MacKenzie, J., McKenzie, A. N., et al. IL-13 induces airways hyperreactivity independently of the IL-4R alpha chain in the allergic lung. *J Immunol.* 2001; 167(3): 1683-1692. DOI: 10.4049/jimmunol.167.3.1683.

Mattoli, S., Mattoso, V. L., Soloperto, M., Allegra, L. and Fasoli, A. Cellular and biochemical characteristics of bronchoalveolar lavage fluid in symptomatic nonallergic asthma. *J Allergy Clin Immunol.* 1991; 87(4): 794-802. DOI: 10.1016/0091-6749(91)90125-8.

Matucci, A., Maggi, E. and Vultaggio, A. Eosinophils, the IL-5/IL-5Rα axis, and the biologic effects of benralizumab in severe asthma. *Respir Med.* 2019; 160: 105819. DOI: 10.1016/j.rmed.2019.105819.

Maurer, M. and Von Stebut, E. Macrophage inflammatory protein-1. *Int J Biochem Cell Biol.* 2004; 36(10): 1882-1886. DOI: 10.1016/j.biocel.2003.10.019.

Mazzone, S. B. and Undem, B. J. Vagal Afferent Innervation of the Airways in Health and Disease. *Physiol Rev.* 2016; 96(3): 975-1024. DOI: 10.1152/physrev.00039.2015.

McAlexander, M. A., Luttmann, M. A., Hunsberger, G. E. and Undem, B. J. Transient receptor potential vanilloid 4 activation constricts the human bronchus via the release of cysteinyl leukotrienes. *J Pharmacol Exp Ther.* 2014; 349(1): 118-125. DOI: 10.1124/jpet.113.210203.

McBrien, C. N. and Menzies-Gow, A. The Biology of Eosinophils and Their Role in Asthma. *Front Med.* 2017; 4(93). DOI: 10.3389/fmed.2017.00093.

McCreanor, J., Cullinan, P., Nieuwenhuijsen, M. J., Stewart-Evans, J., Malliarou, E., Jarup, L., et al. Respiratory effects of exposure to diesel traffic in persons with asthma. *N Engl J Med.* 2007; 357(23): 2348-2358. DOI: 10.1056/NEJMoa071535.

McElroy, W. D. The Energy Source for Bioluminescence in an Isolated System. *Proc Natl Acad Sci U S A.* 1947; 33(11): 342-345. DOI: 10.1073/pnas.33.11.342.

McGarvey, L. P., Butler, C. A., Stokesberry, S., Polley, L., McQuaid, S., Abdullah, H. A., et al. Increased expression of bronchial epithelial transient receptor potential vanilloid 1 channels in patients with severe asthma. *Journal of Allergy and Clinical Immunology.* 2014; 133(3): 704-704. DOI: 10.1016/j.jaci.2013.09.016.

McGuire, J. J., Dai, J., Andrade-Gordon, P., Triggle, C. R. and Hollenberg, M. D. Proteinase-activated receptor-2 (PAR2): vascular effects of a PAR2-derived activating peptide via a receptor different than PAR2. *J Pharmacol Exp Ther.* 2002; 303(3): 985-992. DOI: 10.1124/jpet.102.040352.

Medoff, B. D., Seung, E., Hong, S., Thomas, S. Y., Sandall, B. P., Duffield, J. S., et al. CD11b+ myeloid cells are the key mediators of Th2 cell homing into the airway in allergic inflammation. *J Immunol.* 2009; 182(1): 623-635. DOI: 10.4049/jimmunol.182.1.623.

Mehlhop, P. D., van de Rijn, M., Goldberg, A. B., Brewer, J. P., Kurup, V. P., Martin, T. R., et al. Allergen-induced bronchial hyperreactivity and eosinophilic inflammation occur in the absence of IgE in a mouse model of asthma. *Proc Natl Acad Sci U S A.* 1997; 94(4): 1344-1349. DOI: 10.1073/pnas.94.4.1344.

Mehta, V. B., Hart, J. and Wewers, M. D. ATP-stimulated release of interleukin (IL)-1beta and IL-18 requires priming by lipopolysaccharide and is independent of caspase-1 cleavage. *J Biol Chem.* 2001; 276(6): 3820-3826. DOI: 10.1074/jbc.M006814200.

Menzies-Gow, A., Corren, J., Bourdin, A., Chupp, G., Israel, E., Wechsler, M. E., et al. Tezepelumab in Adults and Adolescents with Severe, Uncontrolled Asthma. 2021; 384(19): 1800-1809. DOI: 10.1056/NEJMoa2034975.

Metzger, W. J., Zavala, D., Richerson, H. B., Moseley, P., Iwamota, P., Monick, M., et al. Local allergen challenge and bronchoalveolar lavage of allergic asthmatic lungs. Description of the model

and local airway inflammation. *Am Rev Respir Dis.* 1987; 135(2): 433-440. DOI: 10.1164/arrd.1987.135.2.433.

Meurs, H., Gosens, R. and Zaagsma, J. Airway hyperresponsiveness in asthma: Lessons from in vitro model systems and animal models. *Eur Respir J.* 2008; 32(2): 487-502. DOI: 10.1183/09031936.00023608.

Miike, S., McWilliam, A. S. and Kita, H. Trypsin induces activation and inflammatory mediator release from human eosinophils through protease-activated receptor-2. *J Immunol.* 2001; 167(11): 6615-6622. DOI: 10.4049/jimmunol.167.11.6615.

Mindt, B. C., Fritz, J. H. and Duerr, C. U. Group 2 innate lymphoid cells in pulmonary immunity and tissue homeostasis. *Front Immunol.* 2018; 9: 1-1. DOI: 10.3389/fimmu.2018.00840.

Mirchandani, A. S., Besnard, A. G., Yip, E., Scott, C., Bain, C. C., Cerovic, V., et al. Type 2 innate lymphoid cells drive CD4+ Th2 cell responses. *J Immunol.* 2014; 192(5): 2442-2448. DOI: 10.4049/jimmunol.1300974.

Mishra, A., Brown, A. L., Yao, X., Yang, S., Park, S.-J., Liu, C., et al. Dendritic cells induce Th2-mediated airway inflammatory responses to house dust mite via DNA-dependent protein kinase. *Nature Communications.* 2015; 6(1): 6224. DOI: 10.1038/ncomms7224.

Mishra, A., Guo, Y., Zhang, L., More, S., Weng, T., Chintagari, N. R., et al. A Critical Role for P2X7 Receptor-Induced VCAM-1 Shedding and Neutrophil Infiltration during Acute Lung Injury. *J Immunol.* 2016; 197(7): 2828-2837. DOI: 10.4049/jimmunol.1501041.

Mitchell, P. D. and O'Byrne, P. M. Biologics and the lung: TSLP and other epithelial cell-derived cytokines in asthma. *Pharmacol Ther.* 2017a; 169: 104-112. DOI: 10.1016/j.pharmthera.2016.06.009.

Mitchell, P. D. and O'Byrne, P. M. Epithelial-Derived Cytokines in Asthma. *Chest.* 2017b; 151(6): 1338-1344. DOI: 10.1016/j.chest.2016.10.042.

Miyahara, N., Takeda, K., Kodama, T., Joetham, A., Taube, C., Park, J. W., et al. Contribution of antigen-primed CD8+ T cells to the development of airway hyperresponsiveness and inflammation is associated with IL-13. *J Immunol.* 2004; 172(4): 2549-2558. DOI: 10.4049/jimmunol.172.4.2549.

Mizumoto, N., Kumamoto, T., Robson, S. C., Sevigny, J., Matsue, H., Enjyoji, K., et al. CD39 is the dominant Langerhans cell-associated ecto-NTPDase: modulatory roles in inflammation and immune responsiveness. *Nat Med.* 2002; 8(4): 358-365. DOI: 10.1038/nm0402-358.

Moffatt, M. F., Kabesch, M., Liang, L., Dixon, A. L., Strachan, D., Heath, S., et al. Genetic variants regulating ORMDL3 expression contribute to the risk of childhood asthma. *Nature.* 2007; 448(7152): 470-473. DOI: 10.1038/nature06014.

Mohanty, J. G., Raible, D. G., McDermott, L. J., Pelleg, A. and Schulman, E. S. Effects of purine and pyrimidine nucleotides on intracellular Ca2+ in human eosinophils: activation of purinergic P2Y receptors. *J Allergy Clin Immunol.* 2001; 107(5): 849-855. DOI: 10.1067/mai.2001.114658.

Mojtabavi, N., Dekan, G., Stingl, G. and Epstein, M. M. Long-lived Th2 memory in experimental allergic asthma. *J Immunol.* 2002; 169(9): 4788-4796. DOI: 10.4049/jimmunol.169.9.4788.

Mole, S., Harry, A., Fowler, A., Hotee, S., Warburton, J., Waite, S., et al. Investigating the effect of TRPV4 inhibition on pulmonary-vascular barrier permeability following segmental endotoxin challenge. *Pulmonary Pharmacology and Therapeutics.* 2020; 64: 101977-101977. DOI: 10.1016/j.pupt.2020.101977.

Molfino, N. A., Slutsky, A. S., Julià-Serdà, G., Hoffstein, V., Szalai, J. P., Chapman, K. R., et al. Assessment of airway tone in asthma. Comparison between double lung transplant patients and healthy subjects. *Am Rev Respir Dis.* 1993; 148(5): 1238-1243. DOI: 10.1164/ajrccm/148.5.1238.

Moller, G. M., Overbeek, S. E., Van Helden-Meeuwsen, C. G., Van Haarst, J. M., Prens, E. P., Mulder, P. G., et al. Increased numbers of dendritic cells in the bronchial mucosa of atopic asthmatic patients: downregulation by inhaled corticosteroids. *Clin Exp Allergy.* 1996; 26(5): 517-524. DOI: 10.1111/j.1365-2222.1996.tb00571.x.

Montell, C. and Rubin, G. M. Molecular characterization of the Drosophila trp locus: a putative integral membrane protein required for phototransduction. 1989;(0896-6273 (Print)).

Monticelli, L. A., Osborne, L. C., Noti, M., Tran, S. V., Zaiss, D. M. and Artis, D. IL-33 promotes an innate immune pathway of intestinal tissue protection dependent on amphiregulin-EGFR interactions. *Proc Natl Acad Sci U S A.* 2015; 112(34): 10762-10767. DOI: 10.1073/pnas.1509070112.

Monticelli, L. A., Sonnenberg, G. F., Abt, M. C., Alenghat, T., Ziegler, C. G., Doering, T. A., et al. Innate lymphoid cells promote lung-tissue homeostasis after infection with influenza virus. *Nat Immunol.* 2011; 12(11): 1045-1054. DOI: 10.1031/ni.2131.

Moran, A. and Pavord, I. D. Anti-IL-4/IL-13 for the treatment of asthma: the story so far. *Expert Opin Biol Ther.* 2020; 20(3): 283-294. DOI: 10.1080/14712598.2020.1714027.

Mori, T., Saito, K., Ohki, Y., Arakawa, H., Tominaga, M. and Tokuyama, K. Lack of Transient Receptor Potential Vanilloid-1 Enhances Th2-Biased Immune Response of the Airways in Mice Receiving Intranasal, but Not Intraperitoneal, Sensitization. *International Archives of Allergy and Immunology.* 2011; 156(3): 305-312. DOI: 10.1159/000323889.

Morianos, I. and Semitekolou, M. Dendritic Cells: Critical Regulators of Allergic Asthma. *Int J Mol Sci.* 2020; 21(21). DOI: 10.3390/ijms21217930.

Morjaria, J. B., Chauhan, A. J., Babu, K. S., Polosa, R., Davies, D. E. and Holgate, S. T. The role of a soluble TNFalpha receptor fusion protein (etanercept) in corticosteroid refractory asthma: a double blind, randomised, placebo controlled trial. *Thorax.* 2008; 63(7): 584-591. DOI: 10.1136/thx.2007.086314.

Moro, K., Kabata, H., Tanabe, M., Koga, S., Takeno, N., Mochizuki, M., et al. Interferon and IL-27 antagonize the function of group 2 innate lymphoid cells and type 2 innate immune responses. *Nat Immunol.* 2016; 17(1): 76-86. DOI: 10.1038/ni.3309.

Mortaz, E., Folkerts, G., Nijkamp, F. P. and Henricks, P. A. ATP and the pathogenesis of COPD. *Eur J Pharmacol.* 2010; 638(1-3): 1-4. DOI: 10.1016/j.ejphar.2010.04.019.

Muehling, L. M., Lawrence, M. G. and Woodfolk, J. A. Pathogenic CD4(+) T cells in patients with asthma. *J Allergy Clin Immunol.* 2017; 140(6): 1523-1540. DOI: 10.1016/j.jaci.2017.02.025.

Mukhopadhyay, I., Gomes, P., Aranake, S., Shetty, M., Karnik, P., Damle, M., et al. Expression of functional TRPA1 receptor on human lung fibroblast and epithelial cells. *J Recept Signal Transduct Res.* 2011; 31(5): 350-358. DOI: 10.3109/10799893.2011.602413.

Müller, T., Fay, S., Vieira, R. P., Karmouty-Quintana, H., Cicko, S., Ayata, K., et al. The purinergic receptor subtype P2Y2 mediates chemotaxis of neutrophils and fibroblasts in fibrotic lung disease. *Oncotarget.* 2017; 8(22): 35962-35972. DOI: 10.18632/oncotarget.16414.

Muller, T., Robaye, B., Vieira, R. P., Ferrari, D., Grimm, M., Jakob, T., et al. The purinergic receptor P2Y2 receptor mediates chemotaxis of dendritic cells and eosinophils in allergic lung inflammation. *Allergy.* 2010; 65(12): 1545-1553. DOI: 10.1111/j.1398-9995.2010.02426.x.

Muller, T., Vieira, R. P., Grimm, M., Durk, T., Cicko, S., Zeiser, R., et al. A potential role for P2X7R in allergic airway inflammation in mice and humans. *Am J Respir Cell Mol Biol.* 2011; 44(4): 456-464. DOI: 10.1165/rcmb.2010-0129OC.

Mulryan, K., Gitterman, D. P., Lewis, C. J., Vial, C., Leckie, B. J., Cobb, A. L., et al. Reduced vas deferens contraction and male infertility in mice lacking P2X1 receptors. *Nature.* 2000; 403(6765): 86-89. DOI: 10.1038/47495.

Mutini, C., Falzoni, S., Ferrari, D., Chiozzi, P., Morelli, A., Baricordi, O. R., et al. Mouse dendritic cells express the P2X7 purinergic receptor: characterization and possible participation in antigen presentation. *J Immunol.* 1999; 163(4): 1958-1965.

Myrtek, D., Muller, T., Geyer, V., Derr, N., Ferrari, D., Zissel, G., et al. Activation of human alveolar macrophages via P2 receptors: coupling to intracellular Ca2+ increases and cytokine secretion. *J Immunol.* 2008; 181(3): 2181-2188. DOI: 10.4049/jimmunol.181.3.2181.

Naert, R., Lopez-Requena, A., Voets, T., Talavera, K. and Alpizar, Y. A. Expression and Functional Role of TRPV4 in Bone Marrow-Derived CD11c(+) Cells. *Int J Mol Sci.* 2019; 20(14). DOI: 10.3390/ijms20143378.

Nagakumar, P., Denney, L., Fleming, L., Bush, A., Lloyd, C. M. and Saglani, S. Type 2 innate lymphoid cells in induced sputum from children with severe asthma. *J Allergy Clin Immunol.* 2016; 137(2): 624-626.e626. DOI: 10.1016/j.jaci.2015.06.038.

Nagakumar, P., Puttur, F., Gregory, L. G., Denney, L., Fleming, L., Bush, A., et al. Pulmonary type-2 innate lymphoid cells in paediatric severe asthma: phenotype and response to steroids. *European Respiratory Journal.* 2019; 54(2): 1801809. DOI: 10.1183/13993003.01809-2018.

Nair, P., Wenzel, S., Rabe, K. F., Bourdin, A., Lugogo, N. L., Kuna, P., et al. Oral Glucocorticoid–Sparing Effect of Benralizumab in Severe Asthma. *New England Journal of Medicine.* 2017; 376(25): 2448-2458. DOI: 10.1056/NEJMoa1703501.

Nakae, S., Komiyama, Y., Yokoyama, H., Nambu, A., Umeda, M., Iwase, M., et al. IL-1 is required for allergen-specific Th2 cell activation and the development of airway hypersensitivity response. *International Immunology.* 2003; 15(4): 483-490. DOI: 10.1093/intimm/dxg054.

Nakano, H., Burgents, J. E., Nakano, K., Whitehead, G. S., Cheong, C., Bortner, C. D., et al. Migratory properties of pulmonary dendritic cells are determined by their developmental lineage. *Mucosal Immunol.* 2013; 6(4): 678-691. DOI: 10.1038/mi.2012.106.

Nakano, H., Free, M. E., Whitehead, G. S., Maruoka, S., Wilson, R. H., Nakano, K., et al. Pulmonary CD103+ dendritic cells prime Th2 responses to inhaled allergens. *Mucosal Immunology.* 2012; 5(1): 53-65. DOI: 10.1038/mi.2011.47.

Nassenstein, C., Kwong, K., Taylor-Clark, T., Kollarik, M., Macglashan, D. M., Braun, A., et al. Expression and function of the ion channel TRPA1 in vagal afferent nerves innervating mouse lungs. *J Physiol.* 2008; 586(6): 1595-1604. DOI: 10.1113/jphysiol.2007.148379.

Nassini, R., Pedretti, P., Moretto, N., Fusi, C., Carnini, C., Facchinetti, F., et al. Transient receptor potential ankyrin 1 channel localized to non-neuronal airway cells promotes non-neurogenic inflammation. *PLoS One.* 2012; 7(8): e42454. DOI: 10.1371/journal.pone.0042454.

Nathan, A. T., Peterson, E. A., Chakir, J. and Wills-Karp, M. Innate immune responses of airway epithelium to house dust mite are mediated through beta-glucan-dependent pathways. *J Allergy Clin Immunol.* 2009; 123(3): 612-618. DOI: 10.1016/j.jaci.2008.12.006.

Naumov, D. E., Kolosov, V. P., Perelman, J. M. and Prikhodko, A. G. Influence of TRPV4 gene polymorphisms on the development of osmotic airway hyperresponsiveness in patients with bronchial asthma. *Doklady. Biochemistry and biophysics.* 2016; 469(1): 260-263. DOI: 10.1134/s1607672916040074.

Neill, D. R., Wong, S. H., Bellosi, A., Flynn, R. J., Daly, M., Langford, T. K., et al. Nuocytes represent a new innate effector leukocyte that mediates type-2 immunity. *Nature.* 2010; 464(7293): 1367-1370. DOI: 10.1038/nature08900.

Nichols, H. L., Saffeddine, M., Theriot, B. S., Hegde, A., Polley, D., El-Mays, T., et al. beta-Arrestin-2 mediates the proinflammatory effects of proteinase-activated receptor-2 in the airway. *Proc Natl Acad Sci U S A.* 2012; 109(41): 16660-16665. DOI: 10.1073/pnas.1208881109.

Nicke, A., Kuan, Y. H., Masin, M., Rettinger, J., Marquez-Klaka, B., Bender, O., et al. A functional P2X7 splice variant with an alternative transmembrane domain 1 escapes gene inactivation in P2X7 knock-out mice. *J Biol Chem.* 2009; 284(38): 25813-25822. DOI: 10.1074/jbc.M109.033134.

Nie, Z., Maung, J. N., Jacoby, D. B. and Fryer, A. D. Lung eosinophils increase vagus nerve-mediated airway reflex bronchoconstriction in mice. *Am J Physiol Lung Cell Mol Physiol.* 2020; 318(2): L242-l251. DOI: 10.1152/ajplung.00040.2019.

Nunes, C., Pereira, A. M. and Morais-Almeida, M. Asthma costs and social impact. *Asthma Res Pract.* 2017; 3: 1-1. DOI: 10.1186/s40733-016-0029-3.

Nystedt, S., Emilsson, K., Wahlestedt, C. and Sundelin, J. Molecular cloning of a potential proteinase activated receptor. *Proc Natl Acad Sci U S A.* 1994; 91(20): 9208-9212. DOI: 10.1073/pnas.91.20.9208.

Nystedt, S., Ramakrishnan, V. and Sundelin, J. The proteinase-activated receptor 2 is induced by inflammatory mediators in human endothelial cells. Comparison with the thrombin receptor. *J Biol Chem.* 1996; 271(25): 14910-14915. DOI: 10.1074/jbc.271.25.14910.

O'Sullivan, S., Cormican, L., Faul, J. L., Ichinohe, S., Johnston, S. L., Burke, C. M., et al. Activated, cytotoxic CD8(+) T lymphocytes contribute to the pathology of asthma death. *Am J Respir Crit Care Med.* 2001; 164(4): 560-564. DOI: 10.1164/ajrccm.164.4.2102018.

Obeidat, M., Wain, L. V., Shrine, N., Kalsheker, N., Soler Artigas, M., Repapi, E., et al. A comprehensive evaluation of potential lung function associated genes in the SpiroMeta general population sample. *PLoS One.* 2011; 6(5): e19382. DOI: 10.1371/journal.pone.0019382.

Ochoa-Amaya, J. E., Queiroz-Hazarbassanov, N., Namazu, L. B., Calefi, A. S., Tobaruela, C. N., Margatho, R., et al. Short-Term Hyperprolactinemia Reduces the Expression of Purinergic P2X7 Receptors during Allergic Inflammatory Response of the Lungs. *Neuroimmunomodulation.* 2018; 25(1): 34-41. DOI: 10.1159/000489312.

Oddera, S., Silvestri, M., Balbo, A., Jovovich, B. O., Penna, R., Crimi, E., et al. Airway eosinophilic inflammation, epithelial damage, and bronchial hyperresponsiveness in patients with mild-moderate, stable asthma. *Allergy.* 1996; 51(2): 100-107. DOI: 10.1111/j.1398-9995.1996.tb04565.x.

Oguma, T., Ito, S., Kondo, M., Makino, Y., Shimokata, K., Honjo, H., et al. Roles of P2X receptors and Ca2+ sensitization in extracellular adenosine triphosphate-induced hyperresponsiveness in airway smooth muscle. *Clin Exp Allergy.* 2007; 37(6): 893-900. DOI: 10.1111/j.1365-2222.2007.02719.x.

Ohno, I., Nitta, Y., Yamauchi, K., Hoshi, H., Honma, M., Woolley, K., et al. Transforming growth factor beta 1 (TGF beta 1) gene expression by eosinophils in asthmatic airway inflammation. *Am J Respir Cell Mol Biol.* 1996; 15(3): 404-409. DOI: 10.1165/ajrcmb.15.3.8810646.

Oliphant, C. J., Hwang, Y. Y., Walker, J. A., Salimi, M., Wong, S. H., Brewer, J. M., et al. MHCII-mediated dialog between group 2 innate lymphoid cells and CD4(+) T cells potentiates type 2 immunity and promotes parasitic helminth expulsion. *Immunity.* 2014; 41(2): 283-295. DOI: 10.1016/j.immuni.2014.06.016.

Ortega, H. G., Liu, M. C., Pavord, I. D., Brusselle, G. G., FitzGerald, J. M., Chetta, A., et al. Mepolizumab treatment in patients with severe eosinophilic asthma. *N Engl J Med.* 2014; 371(13): 1198-1207. DOI: 10.1056/NEJMoa1403290.

Oskeritzian, C. A., Zhao, W., Min, H. K., Xia, H. Z., Pozez, A., Kiev, J., et al. Surface CD88 functionally distinguishes the MCTC from the MCT type of human lung mast cell. *J Allergy Clin Immunol.* 2005; 115(6): 1162-1168. DOI: 10.1016/j.jaci.2005.02.022.

Osterlund, C., Grönlund, H., Polovic, N., Sundström, S., Gafvelin, G. and Bucht, A. The non-proteolytic house dust mite allergen Der p 2 induce NF-kappaB and MAPK dependent activation of bronchial epithelial cells. *Clin Exp Allergy.* 2009; 39(8): 1199-1208. DOI: 10.1111/j.1365-2222.2009.03284.x.

Page, K., Ledford, J. R., Zhou, P., Dienger, K. and Wills-Karp, M. Mucosal sensitization to German cockroach involves protease-activated receptor-2. *Respir Res.* 2010; 11(1): 62. DOI: 10.1186/1465-9921-11-62.

Paggiaro, P., Halpin, D. M., Buhl, R., Engel, M., Zubek, V. B., Blahova, Z., et al. The Effect of Tiotropium in Symptomatic Asthma Despite Low- to Medium-Dose Inhaled Corticosteroids: A Randomized Controlled Trial. *J Allergy Clin Immunol Pract.* 2016; 4(1): 104-113.e102. DOI: 10.1016/j.jaip.2015.08.017.

Palaniyandi, S., Rajendrakumar, A. M., Periasamy, S., Goswami, R., Tuo, W., Zhu, X., et al. TRPV4 is dispensable for the development of airway allergic asthma. *Lab Invest.* 2020; 100(2): 265-273. DOI: 10.1038/s41374-019-0305-y.

Panettieri, R. A., Jr., Sjöbring, U., Péterffy, A., Wessman, P., Bowen, K., Piper, E., et al. Tralokinumab for severe, uncontrolled asthma (STRATOS 1 and STRATOS 2): two randomised, double-blind,

placebo-controlled, phase 3 clinical trials. *Lancet Respir Med.* 2018; 6(7): 511-525. DOI: 10.1016/s2213-2600(18)30184-x.

Panina-Bordignon, P., Papi, A., Mariani, M., Di Lucia, P., Casoni, G., Bellettato, C., et al. The C-C chemokine receptors CCR4 and CCR8 identify airway T cells of allergen-challenged atopic asthmatics. *J Clin Invest.* 2001; 107(11): 1357-1364. DOI: 10.1172/jci12655.

Park, C. S., Lee, S. M., Chung, S. W., Uh, S., Kim, H. T. and Kim, Y. H. Interleukin-2 and soluble interleukin-2 receptor in bronchoalveolar lavage fluid from patients with bronchial asthma. *Chest.* 1994; 106(2): 400-406. DOI: 10.1378/chest.106.2.400.

Patel, D. F., Peiro, T., Bruno, N., Vuononvirta, J., Akthar, S., Puttur, F., et al. Neutrophils restrain allergic airway inflammation by limiting ILC2 function and monocyte-dendritic cell antigen presentation. *Sci Immunol.* 2019; 4(41). DOI: 10.1126/sciimmunol.aax7006.

Patel, H. J., Barnes, P. J., Takahashi, T., Tadjkarimi, S., Yacoub, M. H. and Belvisi, M. G. Evidence for prejunctional muscarinic autoreceptors in human and guinea pig trachea. *Am J Respir Crit Care Med.* 1995; 152(3): 872-878. DOI: 10.1164/ajrccm.152.3.7663798.

Pavord, I. D., Korn, S., Howarth, P., Bleecker, E. R., Buhl, R., Keene, O. N., et al. Mepolizumab for severe eosinophilic asthma (DREAM): a multicentre, double-blind, placebo-controlled trial. *Lancet.* 2012; 380(9842): 651-659. DOI: 10.1016/s0140-6736(12)60988-x.

Pease, J. E. and Williams, T. J. Eotaxin and asthma. *Current Opinion in Pharmacology.* 2001; 1(3): 248-253. DOI: https://doi.org/10.1016/S1471-4892(01)00044-3.

Pégorier, S., Wagner, L. A., Gleich, G. J. and Pretolani, M. Eosinophil-Derived Cationic Proteins Activate the Synthesis of Remodeling Factors by Airway Epithelial Cells. *The Journal of Immunology.* 2006; 177(7): 4861. DOI: 10.4049/jimmunol.177.7.4861.

Pelleg, A. Extracellular adenosine 5'-triphosphate in pulmonary disorders. *Biochem Pharmacol.* 2020; 187: 114319-114319. DOI: 10.1016/j.bcp.2020.114319.

Pelleg, A., Schulman, E. S. and Barnes, P. J. Extracellular Adenosine 5'-Triphosphate in Obstructive Airway Diseases. *Chest.* 2016; 150(4): 908-915. DOI: 10.1016/j.chest.2016.06.045.

Pelleg, A., Xu, F., Zhuang, J., Undem, B. and Burnstock, G. DT-0111: a novel drug-candidate for the treatment of COPD and chronic cough. *Ther Adv Respir Dis.* 2019; 13: 1753466619877960. DOI: 10.1177/1753466619877960.

Pellegrino, R., Wilson, O., Jenouri, G. and Rodarte, J. R. Lung mechanics during induced bronchoconstriction. *J Appl Physiol.* 1996a; 81(2): 964-975. DOI: 10.1152/jappl.1996.81.2.964.

Pellegrino, R., Wilson, O., Jenouri, G. and Rodarte, J. R. Lung mechanics during induced bronchoconstriction. *J Appl Physiol (1985).* 1996b; 81(2): 964-975. DOI: 10.1152/jappl.1996.81.2.964.

Perner, C., Flayer, C. H., Zhu, X., Aderhold, P. A., Dewan, Z. N. A., Voisin, T., et al. Substance P Release by Sensory Neurons Triggers Dendritic Cell Migration and Initiates the Type-2 Immune Response to Allergens. *Immunity.* 2020; 53(5): 1063-1077 e1067. DOI: 10.1016/j.immuni.2020.10.001.

Perregaux, D. G., McNiff, P., Laliberte, R., Conklyn, M. and Gabel, C. A. ATP acts as an agonist to promote stimulus-induced secretion of IL-1 beta and IL-18 in human blood. *J Immunol.* 2000; 165(8): 4615-4623. DOI: 10.4049/jimmunol.165.8.4615.

Piliponsky, A. M., Gleich, G. J., Nagler, A., Bar, I. and Levi-Schaffer, F. Non-IgE–dependent activation of human lung– and cord blood–derived mast cells is induced by eosinophil major basic protein and modulated by the membrane form of stem cell factor. *Blood.* 2003; 101(5): 1898-1904. DOI: 10.1182/blood-2002-05-1488.

Pincus, A. B., Fryer, A. D. and Jacoby, D. B. Mini review: Neural mechanisms underlying airway hyperresponsiveness. *Neurosci Lett.* 2021; 751: 135795. DOI: 10.1016/j.neulet.2021.135795.

Pinkerton, J. W., Kim, R. Y., Robertson, A. A. B., Hirota, J. A., Wood, L. G., Knight, D. A., et al. Inflammasomes in the lung. *Molecular Immunology.* 2017; 86: 44-55. DOI: https://doi.org/10.1016/j.molimm.2017.01.014.

Plantinga, M., Guilliams, M., Vanheerswynghels, M., Deswarte, K., Branco-Madeira, F., Toussaint, W., et al. Conventional and monocyte-derived CD11b(+) dendritic cells initiate and maintain T helper 2 cell-mediated immunity to house dust mite allergen. *Immunity.* 2013; 38(2): 322-335. DOI: 10.1016/j.immuni.2012.10.016.

Poole, D. P., Amadesi, S., Veldhuis, N. A., Abogadie, F. C., Lieu, T., Darby, W., et al. Protease-activated receptor 2 (PAR2) protein and transient receptor potential vanilloid 4 (TRPV4) protein coupling is required for sustained inflammatory signaling. *J Biol Chem.* 2013; 288(8): 5790-5802. DOI: 10.1074/jbc.M112.438184.

Préfontaine, D., Nadigel, J., Chouiali, F., Audusseau, S., Semlali, A., Chakir, J., et al. Increased IL-33 expression by epithelial cells in bronchial asthma. *J Allergy Clin Immunol.* 2010; 125(3): 752-754. DOI: 10.1016/j.jaci.2009.12.935.

Price, D., Fletcher, M. and van der Molen, T. Asthma control and management in 8,000 European patients: the REcognise Asthma and LInk to Symptoms and Experience (REALISE) survey. *NPJ Prim Care Respir Med.* 2014; 24: 14009. DOI: 10.1038/npjpcrm.2014.9.

Purtha, W. E., Swiecki, M., Colonna, M., Diamond, M. S. and Bhattacharya, D. Spontaneous mutation of the Dock2 gene in Irf5-/- mice complicates interpretation of type I interferon production and antibody responses. *Proc Natl Acad Sci U S A.* 2012; 109(15): E898-904. DOI: 10.1073/pnas.1118155109.

Qiu, F. and Dahl, G. A permeant regulating its permeation pore: inhibition of pannexin 1 channels by ATP. *Am J Physiol Cell Physiol.* 2009; 296(2): C250-255. DOI: 10.1152/ajpcell.00433.2008.

Quindry, J. C., Ballmann, C. G., Epstein, E. E. and Selsby, J. T. Plethysmography measurements of respiratory function in conscious unrestrained mice. *J Physiol Sci.* 2016; 66(2): 157-164. DOI: 10.1007/s12576-015-0408-1.

Rabe, K. F., Celli, B. R., Wechsler, M. E., Abdulai, R. M., Luo, X., Boomsma, M. M., et al. Safety and efficacy of itepekimab in patients with moderate-to-severe COPD: a genetic association study and randomised, double-blind, phase 2a trial. *Lancet Respir Med.* 2021; 9(11): 1288-1298. DOI: 10.1016/s2213-2600(21)00167-3.

Rabe, K. F., Nair, P., Brusselle, G., Maspero, J. F., Castro, M., Sher, L., et al. Efficacy and Safety of Dupilumab in Glucocorticoid-Dependent Severe Asthma. *N Engl J Med.* 2018; 378(26): 2475-2485. DOI: 10.1056/NEJMoa1804093.

Raemdonck, K., Baker, K., Dale, N., Dubuis, E., Shala, F., Belvisi, M. G., et al. CD4(+) and CD8(+) T cells play a central role in a HDM driven model of allergic asthma. *Respir Res.* 2016; 17(1): 45. DOI: 10.1186/s12931-016-0359-y.

Raemdonck, K., de Alba, J., Birrell, M. A., Grace, M., Maher, S. A., Irvin, C. G., et al. A role for sensory nerves in the late asthmatic response. *Thorax.* 2012; 67(1): 19-25. DOI: 10.1136/thoraxjnl-2011-200365.

Rahaman, S. O., Grove, L. M., Paruchuri, S., Southern, B. D., Abraham, S., Niese, K. A., et al. TRPV4 mediates myofibroblast differentiation and pulmonary fibrosis in mice. *J Clin Invest.* 2014; 124(12): 5225-5238. DOI: 10.1172/jci75331.

Rahman, M., Sun, R., Mukherjee, S., Nilius, B. and Janssen, L. J. TRPV4 Stimulation Releases ATP via Pannexin Channels in Human Pulmonary Fibroblasts. *Am J Respir Cell Mol Biol.* 2018; 59(1): 87-95. DOI: 10.1165/rcmb.2017-0413OC.

Ram, A., Singh, S. K., Singh, V. P., Kumar, S. and Ghosh, B. Inhaled carbenoxolone prevents allergic airway inflammation and airway hyperreactivity in a mouse model of asthma. *Int Arch Allergy Immunol.* 2009; 149(1): 38-46. DOI: 10.1159/000176305.

Ramelli, G., Fuertes, S., Narayan, S., Busso, N., Acha-Orbea, H. and So, A. Protease-activated receptor 2 signalling promotes dendritic cell antigen transport and T-cell activation in vivo. *Immunology.* 2010; 129(1): 20-27. DOI: 10.1111/j.1365-2567.2009.03144.x.

Ramos-Ramírez, P., Noreby, M., Liu, J., Ji, J., Abdillahi, S. M., Olsson, H., et al. A new house dust mite–driven and mast cell–activated model of asthma in the guinea pig. *Clinical & Experimental Allergy.* 2020; 50(10): 1184-1195. DOI: https://doi.org/10.1111/cea.13713.

Rayees, S., Joshi, J. C., Tauseef, M., Anwar, M., Baweja, S., Rochford, I., et al. PAR2-Mediated cAMP Generation Suppresses TRPV4-Dependent Ca(2+) Signaling in Alveolar Macrophages to Resolve TLR4-Induced Inflammation. *Cell Rep.* 2019; 27(3): 793-805 e794. DOI: 10.1016/j.celrep.2019.03.053.

Raymond, M., Rubio, M., Fortin, G., Shalaby, K. H., Hammad, H., Lambrecht, B. N., et al. Selective control of SIRP-α–positive airway dendritic cell trafficking through CD47 is critical for the development of TH2-mediated allergic inflammation. *Journal of Allergy and Clinical Immunology.* 2009; 124(6): 1333-1342.e1331. DOI: https://doi.org/10.1016/j.jaci.2009.07.021.

Redes, J. L., Basu, T., Ram-Mohan, S., Ghosh, C. C., Chan, E. C., Sek, A. C., et al. Aspergillus fumigatus-Secreted Alkaline Protease 1 Mediates Airways Hyperresponsiveness in Severe Asthma. *Immunohorizons.* 2019; 3(8): 368-377. DOI: 10.4049/immunohorizons.1900046.

Reese, R. M., Dourado, M., Anderson, K., Warming, S., Stark, K. L., Balestrini, A., et al. Behavioral characterization of a CRISPR-generated TRPA1 knockout rat in models of pain, itch, and asthma. *Sci Rep.* 2020; 10(1): 979. DOI: 10.1038/s41598-020-57936-5.

Regateiro, F. S., Botelho Alves, P., Moura, A. L., Azevedo, J. P. and Regateiro, D. T. The diverse roles of T cell subsets in asthma. *Eur Ann Allergy Clin Immunol.* 2020;(online first). DOI: 10.23822/EurAnnACI.1764-1489.177.

Rehman, R., Bhat, Y. A., Panda, L. and Mabalirajan, U. TRPV1 inhibition attenuates IL-13 mediated asthma features in mice by reducing airway epithelial injury. *International Immunopharmacology.* 2013; 15(3): 597-605. DOI: 10.1016/j.intimp.2013.02.010.

Reinhardt, R. L., Khoruts, A., Merica, R., Zell, T. and Jenkins, M. K. Visualizing the generation of memory CD4 T cells in the whole body. *Nature.* 2001; 410(6824): 101-105. DOI: 10.1038/35065111.

Renzi, P. M., Xu, L., Yang, X. X., Powell, W. S. and Martin, J. G. IL-2 enhances allergic airway responses in rats by increased inflammation but not through increased synthesis of cysteinyl leukotrienes. *J Allergy Clin Immunol.* 1999; 104(1): 145-152. DOI: 10.1016/s0091-6749(99)70126-0.

Ricciardolo, F. L., Steinhoff, M., Amadesi, S., Guerrini, R., Tognetto, M., Trevisani, M., et al. Presence and bronchomotor activity of protease-activated receptor-2 in guinea pig airways. *Am J Respir Crit Care Med.* 2000; 161(5): 1672-1680. DOI: 10.1164/ajrccm.161.5.9907133.

Riteau, N., Gasse, P., Fauconnier, L., Gombault, A., Couegnat, M., Fick, L., et al. Extracellular ATP is a danger signal activating P2X7 receptor in lung inflammation and fibrosis. *Am J Respir Crit Care Med.* 2010; 182(6): 774-783. DOI: 10.1164/rccm.201003-0359OC.

Robinson, D., Hamid, Q., Bentley, A., Ying, S., Kay, A. B. and Durham, S. R. Activation of CD4+ T cells, increased TH2-type cytokine mRNA expression, and eosinophil recruitment in bronchoalveolar lavage after allergen inhalation challenge in patients with atopic asthma. *J Allergy Clin Immunol.* 1993a; 92(2): 313-324. DOI: 10.1016/0091-6749(93)90175-f.

Robinson, D. S., Bentley, A. M., Hartnell, A., Kay, A. B. and Durham, S. R. Activated memory T helper cells in bronchoalveolar lavage fluid from patients with atopic asthma: relation to asthma symptoms, lung function, and bronchial responsiveness. *Thorax.* 1993b; 48(1): 26-32. DOI: 10.1136/thx.48.1.26.

Robinson, D. S., Hamid, Q., Ying, S., Tsicopoulos, A., Barkans, J., Bentley, A. M., et al. Predominant TH2-like bronchoalveolar T-lymphocyte population in atopic asthma. *N Engl J Med.* 1992; 326(5): 298-304. DOI: 10.1056/nejm199201303260504.

Robinson, R. K., Birrell, M. A., Adcock, J. J., Wortley, M. A., Dubuis, E. D., Chen, S., et al. Mechanistic link between diesel exhaust particles and respiratory reflexes. *J Allergy Clin Immunol.* 2018; 141(3): 1074-1084.e1079. DOI: 10.1016/j.jaci.2017.04.038.

Roche, N., Stirling, R. G., Lim, S., Oliver, B. G., Oates, T., Jazrawi, E., et al. Effect of acute and chronic inflammatory stimuli on expression of protease-activated receptors 1 and 2 in alveolar macrophages. *J Allergy Clin Immunol.* 2003; 111(2): 367-373. DOI: 10.1067/mai.2003.6.

Rogerio, A. P., Andrade, E. L. and Calixto, J. B. C-fibers, but not the transient potential receptor vanilloid 1 (TRPV1), play a role in experimental allergic airway inflammation. *Eur J Pharmacol.* 2011; 662(1-3): 55-62. DOI: 10.1016/j.ejphar.2011.04.027.

Rovina, N., Dima, E., Bakakos, P., Tseliou, E., Kontogianni, K., Papiris, S., et al. Low interleukin (IL)-18 levels in sputum supernatants of patients with severe refractory asthma. *Respir Med.* 2015; 109(5): 580-587. DOI: 10.1016/j.rmed.2015.03.002.

Saez, P. J., Vargas, P., Shoji, K. F., Harcha, P. A., Lennon-Dumenil, A. M. and Saez, J. C. ATP promotes the fast migration of dendritic cells through the activity of pannexin 1 channels and P2X7 receptors. *Sci Signal.* 2017; 10(506). DOI: 10.1126/scisignal.aah7107.

Sagar, S., Akbarshahi, H. and Uller, L. Translational value of animal models of asthma: Challenges and promises. *European Journal of Pharmacology.* 2015; 759: 272-277. DOI: https://doi.org/10.1016/j.ejphar.2015.03.037.

Saglani, S. and Lloyd, C. M. Novel concepts in airway inflammation and remodelling in asthma. *Eur Respir J.* 2015; 46(6): 1796-1804. DOI: 10.1183/13993003.01196-2014.

Saglani, S., Lui, S., Ullmann, N., Campbell, G. A., Sherburn, R. T., Mathie, S. A., et al. IL-33 promotes airway remodeling in pediatric patients with severe steroid-resistant asthma. *J Allergy Clin Immunol.* 2013; 132(3): 676-685 e613. DOI: 10.1016/j.jaci.2013.04.012.

Sahoo, S. S., Majhi, R. K., Tiwari, A., Acharya, T., Kumar, P. S., Saha, S., et al. Transient Receptor Potential Ankyrin1 channel is endogenously expressed in T cells and regulates immune functions. *bioRxiv.* 2019: 621854. DOI: 10.1101/621854.

Sakaki, H., Fujiwaki, T., Tsukimoto, M., Kawano, A., Harada, H. and Kojima, S. P2X4 receptor regulates P2X7 receptor-dependent IL-1beta and IL-18 release in mouse bone marrow-derived dendritic cells. *Biochem Biophys Res Commun.* 2013; 432(3): 406-411. DOI: 10.1016/j.bbrc.2013.01.135.

Sanchez-Nogueiro, J., Marin-Garcia, P. and Miras-Portugal, M. T. Characterization of a functional P2X(7)-like receptor in cerebellar granule neurons from P2X(7) knockout mice. *FEBS Lett.* 2005; 579(17): 3783-3788. DOI: 10.1016/j.febslet.2005.05.073.

Satia, I., Nagashima, A. and Usmani, O. S. Exploring the role of nerves in asthma; insights from the study of cough. *Biochemical Pharmacology.* 2020; 179: 113901. DOI: https://doi.org/10.1016/j.bcp.2020.113901.

Satia, I., Tsamandouras, N., Holt, K., Badri, H., Woodhead, M., Ogungbenro, K., et al. Capsaicin-evoked cough responses in asthmatic patients: Evidence for airway neuronal dysfunction. *Journal of Allergy and Clinical Immunology.* 2017; 139(3): 771-779.e710. DOI: https://doi.org/10.1016/j.jaci.2016.04.045.

Satia, I., Watson, R., Scime, T., Dockry, R. J., Sen, S., Ford, J. W., et al. Allergen challenge increases capsaicin-evoked cough responses in patients with allergic asthma. *J Allergy Clin Immunol.* 2019; 144(3): 788-795.e781. DOI: 10.1016/j.jaci.2018.11.050.

Savenije, O. E., Mahachie John, J. M., Granell, R., Kerkhof, M., Dijk, F. N., de Jongste, J. C., et al. Association of IL33–IL-1 receptor–like 1 (IL1RL1) pathway polymorphisms with wheezing phenotypes and asthma in childhood. *Journal of Allergy and Clinical Immunology.* 2014; 134(1): 170-177. DOI: https://doi.org/10.1016/j.jaci.2013.12.1080.

Sawada, M., Kawayama, T., Imaoka, H., Sakazaki, Y., Oda, H., Takenaka, S.-i., et al. IL-18 Induces Airway Hyperresponsiveness and Pulmonary Inflammation via CD4+ T Cell and IL-13. *PLOS ONE.* 2013; 8(1): e54623. DOI: 10.1371/journal.pone.0054623.

Sawicka, E., Noble, A., Walker, C. and Kemeny, D. M. Tc2 cells respond to soluble antigen in the respiratory tract and induce lung eosinophilia and bronchial hyperresponsiveness. *Eur J Immunol.* 2004; 34(9): 2599-2608. DOI: 10.1002/eji.200425018.

Schenk, U., Westendorf, A. M., Radaelli, E., Casati, A., Ferro, M., Fumagalli, M., et al. Purinergic control of T cell activation by ATP released through pannexin-1 hemichannels. *Sci Signal.* 2008; 1(39): ra6. DOI: 10.1126/scisignal.1160583.

Scheraga, R. G., Abraham, S., Grove, L. M., Southern, B. D., Crish, J. F., Perelas, A., et al. TRPV4 Protects the Lung from Bacterial Pneumonia via MAPK Molecular Pathway Switching. *J Immunol.* 2020; 204(5): 1310-1321. DOI: 10.4049/jimmunol.1901033.

Scheraga, R. G., Abraham, S., Niese, K. A., Southern, B. D., Grove, L. M., Hite, R. D., et al. TRPV4 Mechanosensitive Ion Channel Regulates Lipopolysaccharide-Stimulated Macrophage Phagocytosis. *J Immunol.* 2016; 196(1): 428-436. DOI: 10.4049/jimmunol.1501688.

Scheurich, P., Thoma, B., Ucer, U. and Pfizenmaier, K. Immunoregulatory activity of recombinant human tumor necrosis factor (TNF)-alpha: induction of TNF receptors on human T cells and TNF-alpha-mediated enhancement of T cell responses. *The Journal of Immunology.* 1987; 138(6).

Schmid-Grendelmeier, P., Altznauer, F., Fischer, B., Bizer, C., Straumann, A., Menz, G., et al. Eosinophils Express Functional IL-13 in Eosinophilic Inflammatory Diseases. *The Journal of Immunology.* 2002; 169(2): 1021-1027. DOI: 10.4049/jimmunol.169.2.1021.

Schmidlin, F., Amadesi, S., Dabbagh, K., Lewis, D. E., Knott, P., Bunnett, N. W., et al. Protease-activated receptor 2 mediates eosinophil infiltration and hyperreactivity in allergic inflammation of the airway. *J Immunol.* 2002; 169(9): 5315-5321. DOI: 10.4049/jimmunol.169.9.5315.

Schmidlin, F., Amadesi, S., Vidil, R., Trevisani, M., Martinet, N., Caughey, G., et al. Expression and function of proteinase-activated receptor 2 in human bronchial smooth muscle. *Am J Respir Crit Care Med.* 2001; 164(7): 1276-1281. DOI: 10.1164/ajrccm.164.7.2101157.

Schmitz, J., Owyang, A., Oldham, E., Song, Y., Murphy, E., McClanahan, T. K., et al. IL-33, an interleukin-1-like cytokine that signals via the IL-1 receptor-related protein ST2 and induces T helper type 2-associated cytokines. *Immunity.* 2005; 23(5): 479-490. DOI: 10.1016/j.immuni.2005.09.015.

Schneider, C., Nobs, S. P., Heer, A. K., Kurrer, M., Klinke, G., van Rooijen, N., et al. Alveolar macrophages are essential for protection from respiratory failure and associated morbidity following influenza virus infection. *PLoS Pathog.* 2014; 10(4): e1004053. DOI: 10.1371/journal.ppat.1004053.

Schwartz, L. B., Irani, A. M., Roller, K., Castells, M. C. and Schechter, N. M. Quantitation of histamine, tryptase, and chymase in dispersed human T and TC mast cells. *J Immunol.* 1987; 138(8): 2611-2615.

Sedgwick, J. B., Calhoun, W. J., Gleich, G. J., Kita, H., Abrams, J. S., Schwartz, L. B., et al. Immediate and late airway response of allergic rhinitis patients to segmental antigen challenge. Characterization of eosinophil and mast cell mediators. *Am Rev Respir Dis.* 1991; 144(6): 1274-1281. DOI: 10.1164/ajrccm/144.6.1274.

Seminario-Vidal, L., Okada, S. F., Sesma, J. I., Kreda, S. M., van Heusden, C. A., Zhu, Y., et al. Rho signaling regulates pannexin 1-mediated ATP release from airway epithelia. *J Biol Chem.* 2011; 286(30): 26277-26286. DOI: 10.1074/jbc.M111.260562.

Seyffert, C., Schmalzing, G. and Markwardt, F. Dissecting individual current components of co-expressed human P2X1 and P2X7 receptors. *Curr Top Med Chem.* 2004; 4(16): 1719-1730. DOI: 10.2174/1568026043387160.

Shaw, D. E., Sousa, A. R., Fowler, S. J., Fleming, L. J., Roberts, G., Corfield, J., et al. Clinical and inflammatory characteristics of the European U-BIOPRED adult severe asthma cohort. *Eur Respir J.* 2015; 46(5): 1308-1321. DOI: 10.1183/13993003.00779-2015.

Shi, H.-Z., Humbles, A., Gerard, C., Jin, Z. and Weller, P. F. Lymph node trafficking and antigen presentation by endobronchial eosinophils. *The Journal of Clinical Investigation.* 2000; 105(7): 945-953. DOI: 10.1172/jci8945.

Shi, J. P., Wang, S. Y., Chen, L. L., Zhang, X. Y., Zhao, Y. H., Du, B., et al. P2Y6 contributes to ovalbumin-induced allergic asthma by enhancing mast cell function in mice. *Oncotarget.* 2016; 7(38): 60906-60918. DOI: 10.18632/oncotarget.11758.

Shi, L., Leu, S. W., Xu, F., Zhou, X., Yin, H., Cai, L., et al. Local blockade of TSLP receptor alleviated allergic disease by regulating airway dendritic cells. *Clin Immunol.* 2008; 129(2): 202-210. DOI: 10.1016/j.clim.2008.07.015.

Shichijo, M., Kondo, S., Ishimori, M., Watanabe, S., Helin, H., Yamasaki, T., et al. PAR-2 deficient CD4+ T cells exhibit downregulation of IL-4 and upregulation of IFN-gamma after antigen challenge in mice. *Allergol Int.* 2006; 55(3): 271-278. DOI: 10.2332/allergolint.55.271.

Shimbara, A., Christodoulopoulos, P., Soussi-Gounni, A., Olivenstein, R., Nakamura, Y., Levitt, R. C., et al. IL-9 and its receptor in allergic and nonallergic lung disease: increased expression in asthma. *J Allergy Clin Immunol.* 2000; 105(1 Pt 1): 108-115. DOI: 10.1016/s0091-6749(00)90185-4.

Shishikura, Y., Koarai, A., Aizawa, H., Yamaya, M., Sugiura, H., Watanabe, M., et al. Extracellular ATP is involved in dsRNA-induced MUC5AC production via P2Y2R in human airway epithelium. *Respir Res.* 2016; 17(1): 121. DOI: 10.1186/s12931-016-0438-0.

Shoji, K. F., Saez, P. J., Harcha, P. A., Aguila, H. L. and Saez, J. C. Pannexin1 channels act downstream of P2X 7 receptors in ATP-induced murine T-cell death. *Channels (Austin).* 2014; 8(2): 142-156. DOI: 10.4161/chan.28122.

Shrine, N., Portelli, M. A., John, C., Soler Artigas, M., Bennett, N., Hall, R., et al. Moderate-to-severe asthma in individuals of European ancestry: a genome-wide association study. *The Lancet Respiratory Medicine.* 2019; 7(1): 20-34. DOI: https://doi.org/10.1016/S2213-2600(18)30389-8.

Sikora, A., Liu, J., Brosnan, C., Buell, G., Chessel, I. and Bloom, B. R. Cutting edge: purinergic signaling regulates radical-mediated bacterial killing mechanisms in macrophages through a P2X7-independent mechanism. *J Immunol.* 1999; 163(2): 558-561.

Silva-Vilches, C., Ring, S. and Mahnke, K. ATP and its metabolite adenosine as regulators of dendritic cell activity. *Front Immunol.* 2018; 9: 2581-2581. DOI: 10.3389/fimmu.2018.02581.

Sim, J. A., Park, C. K., Oh, S. B., Evans, R. J. and North, R. A. P2X1 and P2X4 receptor currents in mouse macrophages. *Br J Pharmacol.* 2007; 152(8): 1283-1290. DOI: 10.1038/sj.bjp.0707504.

Simons, B., Ferrini, M. E., Carvalho, S., Bassett, D. J., Jaffar, Z. and Roberts, K. PGI2 Controls Pulmonary NK Cells That Prevent Airway Sensitization to House Dust Mite Allergen. *J Immunol.* 2017; 198(1): 461-471. DOI: 10.4049/jimmunol.1600275.

Sipe, W. E., Brierley, S. M., Martin, C. M., Phillis, B. D., Cruz, F. B., Grady, E. F., et al. Transient receptor potential vanilloid 4 mediates protease activated receptor 2-induced sensitization of colonic afferent nerves and visceral hyperalgesia. *Am J Physiol Gastrointest Liver Physiol.* 2008; 294(5): G1288-1298. DOI: 10.1152/ajpgi.00002.2008.

Skarnes, W. C., Rosen, B., West, A. P., Koutsourakis, M., Bushell, W., Iyer, V., et al. A conditional knockout resource for the genome-wide study of mouse gene function. *Nature.* 2011; 474(7351): 337-342. DOI: 10.1038/nature10163.

Slungaard, A., Vercellotti, G. M., Walker, G., Nelson, R. D. and Jacob, H. S. Tumor necrosis factor α/cachectin stimulates eosinophil oxidant production and toxicity towards human endothelium. *Journal of Experimental Medicine.* 1990; 171(6): 2025-2041. DOI: 10.1084/jem.171.6.2025.

Sluyter, R., Barden, J. A. and Wiley, J. S. Detection of P2X purinergic receptors on human B lymphocytes. *Cell Tissue Res.* 2001; 304(2): 231-236. DOI: 10.1007/s004410100372.

Smit, M., Zuidhof, A. B., Bos, S. I., Maarsingh, H., Gosens, R., Zaagsma, J., et al. Bronchoprotection by olodaterol is synergistically enhanced by tiotropium in a guinea pig model of allergic asthma. *J Pharmacol Exp Ther.* 2014; 348(2): 303-310. DOI: 10.1124/jpet.113.208439.

Smith, S. G., Chen, R., Kjarsgaard, M., Huang, C., Oliveria, J. P., O'Byrne, P. M., et al. Increased numbers of activated group 2 innate lymphoid cells in the airways of patients with severe asthma and persistent airway eosinophilia. *J Allergy Clin Immunol.* 2016; 137(1): 75-86 e78. DOI: 10.1016/j.jaci.2015.05.037.

Snelgrove, R. J., Gregory, L. G., Peiró, T., Akthar, S., Campbell, G. A., Walker, S. A., et al. Alternaria-derived serine protease activity drives IL-33–mediated asthma exacerbations. *Journal of Allergy and Clinical Immunology.* 2014; 134(3): 583-592.e586. DOI: https://doi.org/10.1016/j.jaci.2014.02.002.

Solle, M., Labasi, J., Perregaux, D. G., Stam, E., Petrushova, N., Koller, B. H., et al. Altered cytokine production in mice lacking P2X(7) receptors. *J Biol Chem.* 2001; 276(1): 125-132. DOI: 10.1074/jbc.M006781200.

Spinsanti, G., Zannolli, R., Panti, C., Ceccarelli, I., Marsili, L., Bachiocco, V., et al. Quantitative Real-Time PCR Detection of TRPV1–4 Gene Expression in Human Leukocytes from Healthy and Hyposensitive Subjects. *Mol Pain.* 2008. DOI: 10.1186_1744-8069-4-51.

Sriranganadane, D., Waridel, P., Salamin, K., Reichard, U., Grouzmann, E., Neuhaus, J. M., et al. Aspergillus protein degradation pathways with different secreted protease sets at neutral and acidic pH. *Journal of Proteome Research.* 2010; 9(7): 3511-3519. DOI: 10.1021/pr901202z.

Stark, R., Wesselink, T. H., Behr, F. M., Kragten, N. A. M., Arens, R., Koch-Nolte, F., et al. T RM maintenance is regulated by tissue damage via P2RX7. *Sci Immunol.* 2018; 3(30). DOI: 10.1126/sciimmunol.aau1022.

Starkey, M. R., McKenzie, A. N., Belz, G. T. and Hansbro, P. M. Pulmonary group 2 innate lymphoid cells: surprises and challenges. *Mucosal Immunol.* 2019; 12(2): 299-311. DOI: 10.1038/s41385-018-0130-4.

Stenton, G. R., Nohara, O., Dery, R. E., Vliagoftis, H., Gilchrist, M., Johri, A., et al. Proteinase-activated receptor (PAR)-1 and -2 agonists induce mediator release from mast cells by pathways distinct from PAR-1 and PAR-2. *J Pharmacol Exp Ther.* 2002; 302(2): 466-474. DOI: 10.1124/jpet.302.2.466.

Stevens, J. C., Banks, G. T., Festing, M. F. W. and Fisher, E. M. C. Quiet mutations in inbred strains of mice. *Trends Mol Med.* 2007; 13(12): 512-519. DOI: 10.1016/j.molmed.2007.10.001.

Stewart, G. M., Johnson, B. D., Sprecher, D. L., Reddy, Y. N. V., Obokata, M., Goldsmith, S., et al. Targeting pulmonary capillary permeability to reduce lung congestion in heart failure: a randomized, controlled pilot trial. *European Journal of Heart Failure.* 2020; 22(9): 1641-1645. DOI: 10.1002/ejhf.1809.

Stock, P., Kallinich, T., Akbari, O., Quarcoo, D., Gerhold, K., Wahn, U., et al. CD8(+) T cells regulate immune responses in a murine model of allergen-induced sensitization and airway inflammation. *Eur J Immunol.* 2004; 34(7): 1817-1827. DOI: 10.1002/eji.200324623.

Stokes, L. and Surprenant, A. Purinergic P2Y2 receptors induce increased MCP-1/CCL2 synthesis and release from rat alveolar and peritoneal macrophages. *J Immunol.* 2007; 179(9): 6016-6023. DOI: 10.4049/jimmunol.179.9.6016.

Stolarski, B., Kurowska-Stolarska, M., Kewin, P., Xu, D. and Liew, F. Y. IL-33 exacerbates eosinophil-mediated airway inflammation. *J Immunol.* 2010; 185(6): 3472-3480. DOI: 10.4049/jimmunol.1000730.

Strotmann, R., Harteneck, C., Nunnenmacher, K., Schultz, G. and Plant, T. D. OTRPC4, a nonselective cation channel that confers sensitivity to extracellular osmolarity. *Nat Cell Biol.* 2000; 2(10): 695-702. DOI: 10.1038/35036318.

Sugita, K., Steer, C. A., Martinez-Gonzalez, I., Altunbulakli, C., Morita, H., Castro-Giner, F., et al. Type 2 innate lymphoid cells disrupt bronchial epithelial barrier integrity by targeting tight junctions through IL-13 in asthmatic patients. *J Allergy Clin Immunol.* 2018; 141(1): 300-310 e311. DOI: 10.1016/j.jaci.2017.02.038.

Sung, S. S., Fu, S. M., Rose, C. E., Jr., Gaskin, F., Ju, S. T. and Beaty, S. R. A major lung CD103 (alphaE)-beta7 integrin-positive epithelial dendritic cell population expressing Langerin and tight junction proteins. *J Immunol.* 2006; 176(4): 2161-2172. DOI: 10.4049/jimmunol.176.4.2161.

Suurväli, J., Boudinot, P., Kanellopoulos, J. and Rüütel Boudinot, S. P2X4: A fast and sensitive purinergic receptor. *Biomed J.* 2017; 40(5): 245-256. DOI: 10.1016/j.bj.2017.06.010.

Suzuki, M., Mizuno, A., Kodaira, K. and Imai, M. Impaired pressure sensation in mice lacking TRPV4. *J Biol Chem.* 2003; 278(25): 22664-22668. DOI: 10.1074/jbc.M302561200.

Szollosi, A. G., Olah, A., Toth, I. B., Papp, F., Czifra, G., Panyi, G., et al. Transient receptor potential vanilloid-2 mediates the effects of transient heat shock on endocytosis of human monocyte-

derived dendritic cells. *FEBS Lett.* 2013; 587(9): 1440-1445. DOI: 10.1016/j.febslet.2013.03.027.

Takeda, K., Dow, S. W., Miyahara, N., Kodama, T., Koya, T., Taube, C., et al. Vaccine-induced CD8+ T cell-dependent suppression of airway hyperresponsiveness and inflammation. *J Immunol.* 2009; 183(1): 181-190. DOI: 10.4049/jimmunol.0803967.

Takizawa, T., Tamiya, M., Hara, T., Matsumoto, J., Saito, N., Kanke, T., et al. Abrogation of bronchial eosinophilic inflammation and attenuated eotaxin content in protease-activated receptor 2-deficient mice. *J Pharmacol Sci.* 2005; 98(1): 99-102. DOI: 10.1254/jphs.scz050138.

Talbot, S., Abdulnour, R. E., Burkett, P. R., Lee, S., Cronin, S. J., Pascal, M. A., et al. Silencing Nociceptor Neurons Reduces Allergic Airway Inflammation. *Neuron.* 2015; 87(2): 341-354. DOI: 10.1016/j.neuron.2015.06.007.

Tanaka, H., Kawada, N., Yamada, T., Kawada, K., Takatsu, K. and Nagai, H. Allergen-induced airway inflammation and bronchial responsiveness in interleukin-5 receptor alpha chain-deficient mice. *Clin Exp Allergy.* 2000; 30(6): 874-881. DOI: 10.1046/j.1365-2222.2000.00828.x.

Taube, C., Duez, C., Cui, Z.-H., Takeda, K., Rha, Y.-H., Park, J.-W., et al. The Role of IL-13 in Established Allergic Airway Disease. *The Journal of Immunology*. 2002; 169(11): 6482-6489. DOI: 10.4049/jimmunol.169.11.6482.

Taylor, S. R., Gonzalez-Begne, M., Sojka, D. K., Richardson, J. C., Sheardown, S. A., Harrison, S. M., et al. Lymphocytes from P2X7-deficient mice exhibit enhanced P2X7 responses. *J Leukoc Biol.* 2009; 85(6): 978-986. DOI: 10.1189/jlb.0408251.

Thorneloe, K. S., Cheung, M., Bao, W., Alsaid, H., Lenhard, S., Jian, M. Y., et al. An orally active TRPV4 channel blocker prevents and resolves pulmonary edema induced by heart failure. *Sci Transl Med.* 2012; 4(159): 159ra148. DOI: 10.1126/scitranslmed.3004276.

Thorneloe, K. S., Sulpizio, A. C., Lin, Z., Figueroa, D. J., Clouse, A. K., McCafferty, G. P., et al. N-((1S)-1-{[4-((2S)-2-{[(2,4-dichlorophenyl)sulfonyl]amino}-3-hydroxypropanoyl)-1-piperazinyl]carbonyl}-3-methylbutyl)-1-benzothiophene-2-carboxamide (GSK1016790A), a novel and potent transient receptor potential vanilloid 4 channel agonist induces urinary bladder contraction and hyperactivity: Part I. *J Pharmacol Exp Ther.* 2008; 326(2): 432-442. DOI: 10.1124/jpet.108.139295.

Tjota, M. Y., Williams, J. W., Lu, T., Clay, B. S., Byrd, T., Hrusch, C. L., et al. IL-33-dependent induction of allergic lung inflammation by FcgammaRIII signaling. *J Clin Invest.* 2013; 123(5): 2287-2297. DOI: 10.1172/jci63802.

Tominaga, M., Caterina, M. J., Malmberg, A. B., Rosen, T. A., Gilbert, H., Skinner, K., et al. The Cloned Capsaicin Receptor Integrates Multiple Pain-Producing Stimuli. *Neuron.* 1998; 21(3): 531-543. DOI: https://doi.org/10.1016/S0896-6273(00)80564-4.

Trankner, D., Hahne, N., Sugino, K., Hoon, M. A. and Zuker, C. Population of sensory neurons essential for asthmatic hyperreactivity of inflamed airways. *Proc Natl Acad Sci U S A.* 2014; 111(31): 11515-11520. DOI: 10.1073/pnas.1411032111.

Truyen, E., Coteur, L., Dilissen, E., Overbergh, L., Dupont, L. J., Ceuppens, J. L., et al. Evaluation of airway inflammation by quantitative Th1/Th2 cytokine mRNA measurement in sputum of asthma patients. *Thorax.* 2006; 61(3): 202-208. DOI: 10.1136/thx.2005.052399.

Tsuchiya, K., Siddiqui, S., Risse, P. A., Hirota, N. and Martin, J. G. The presence of LPS in OVA inhalations affects airway inflammation and AHR but not remodeling in a rodent model of asthma. *Am J Physiol Lung Cell Mol Physiol.* 2012; 303(1): L54-63. DOI: 10.1152/ajplung.00208.2011.

Tsukimoto, M., Maehata, M., Harada, H., Ikari, A., Takagi, K. and Degawa, M. P2X7 receptor-dependent cell death is modulated during murine T cell maturation and mediated by dual signaling pathways. *J Immunol.* 2006; 177(5): 2842-2850. DOI: 10.4049/jimmunol.177.5.2842.

Turner, D. L., Goldklang, M., Cvetkovski, F., Paik, D., Trischler, J., Barahona, J., et al. Biased Generation and In Situ Activation of Lung Tissue-Resident Memory CD4 T Cells in the Pathogenesis of Allergic Asthma. *J Immunol.* 2018; 200(5): 1561-1569. DOI: 10.4049/jimmunol.1700257.

Underwood, S. L., Haddad el, B., Birrell, M. A., McCluskie, K., Pecoraro, M., Dabrowski, D., et al. Functional characterization and biomarker identification in the Brown Norway model of allergic airway inflammation. *Br J Pharmacol.* 2002; 137(2): 263-275. DOI: 10.1038/sj.bjp.0704865.

US Food and Drug Administration. (2021). "*Tezspire* (tezepelumab) US prescribing information." Retrieved 09/01/2022, from www.accessdata.fda.gov/drugsatfda_docs/label/2021/761224s000lbl.pdf.

Van den Broeck, W., Derore, A. and Simoens, P. Anatomy and nomenclature of murine lymph nodes: Descriptive study and nomenclatory standardization in BALB/cAnNCrl mice. *J Immunol Methods.* 2006; 312(1-2): 12-19. DOI: 10.1016/j.jim.2006.01.022.

van Rensen, E. L., Sont, J. K., Evertse, C. E., Willems, L. N., Mauad, T., Hiemstra, P. S., et al. Bronchial CD8 cell infiltrate and lung function decline in asthma. *Am J Respir Crit Care Med.* 2005; 172(7): 837-841. DOI: 10.1164/rccm.200504-619OC.

van Rijt, L. S., Jung, S., Kleinjan, A., Vos, N., Willart, M., Duez, C., et al. In vivo depletion of lung CD11c+ dendritic cells during allergen challenge abrogates the characteristic features of asthma. *J Exp Med.* 2005; 201(6): 981-991. DOI: 10.1084/jem.20042311.

Vanderstocken, G., Bondue, B., Horckmans, M., Di Pietrantonio, L., Robaye, B., Boeynaems, J. M., et al. P2Y2 receptor regulates VCAM-1 membrane and soluble forms and eosinophil accumulation during lung inflammation. *J Immunol.* 2010; 185(6): 3702-3707. DOI: 10.4049/jimmunol.0903908.

Verheijden, K. A., Henricks, P. A., Redegeld, F. A., Garssen, J. and Folkerts, G. Measurement of airway function using invasive and non-invasive methods in mild and severe models for allergic airway inflammation in mice. *Front Pharmacol.* 2014; 5: 190. DOI: 10.3389/fphar.2014.00190.

Veronesi, B., Oortgiesen, M., Roy, J., Carter, J. D., Simon, S. A. and Gavett, S. H. Vanilloid(Capsaicin) receptors influence inflammatory sensitivity in response to particulate matter. *Toxicology and Applied Pharmacology.* 2000; 169(1): 66-76. DOI: 10.1006/taap.2000.9040.

Vijayanand, P., Durkin, K., Hartmann, G., Morjaria, J., Seumois, G., Staples, K. J., et al. Chemokine receptor 4 plays a key role in T cell recruitment into the airways of asthmatic patients. *J Immunol.* 2010; 184(8): 4568-4574. DOI: 10.4049/jimmunol.0901342.

Virchow, J. C., Kuna, P., Paggiaro, P., Papi, A., Singh, D., Corre, S., et al. Single inhaler extrafine triple therapy in uncontrolled asthma (TRIMARAN and TRIGGER): two double-blind, parallel-group, randomised, controlled phase 3 trials. *Lancet.* 2019; 394(10210): 1737-1749. DOI: 10.1016/s0140-6736(19)32215-9.

Vissers, J. L., Hartgers, F. C., Lindhout, E., Teunissen, M. B., Figdor, C. G. and Adema, G. J. Quantitative analysis of chemokine expression by dendritic cell subsets in vitro and in vivo. *J Leukoc Biol.* 2001; 69(5): 785-793. DOI: 10.1189/jlb.69.5.785.

Vivier, E., Artis, D., Colonna, M., Diefenbach, A., Di Santo, J. P., Eberl, G., et al. Innate Lymphoid Cells: 10 Years On. *Cell.* 2018; 174(5): 1054-1066. DOI: 10.1016/j.cell.2018.07.017.

Vroman, H., Hendriks, R. W. and Kool, M. Dendritic Cell Subsets in Asthma: Impaired Tolerance or Exaggerated Inflammation? *Front Immunol.* 2017; 8: 941. DOI: 10.3389/fimmu.2017.00941.

Walker, C., Bode, E., Boer, L., Hansel, T. T., Blaser, K. and Virchow, J. C., Jr. Allergic and nonallergic asthmatics have distinct patterns of T-cell activation and cytokine production in peripheral blood and bronchoalveolar lavage. *Am Rev Respir Dis.* 1992; 146(1): 109-115. DOI: 10.1164/ajrccm/146.1.109.

Walker, C., Kaegi, M. K., Braun, P. and Blaser, K. Activated T cells and eosinophilia in bronchoalveolar lavages from subjects with asthma correlated with disease severity. *J Allergy Clin Immunol.* 1991; 88(6): 935-942. DOI: 10.1016/0091-6749(91)90251-i.

Walker, J. K. and DeFea, K. A. Role for β-arrestin in mediating paradoxical β2AR and PAR2 signaling in asthma. *Current opinion in pharmacology.* 2014; 16: 142-147. DOI: 10.1016/j.coph.2014.03.007.

Wallrapp, A., Riesenfeld, S. J., Burkett, P. R., Abdulnour, R.-E. E., Nyman, J., Dionne, D., et al. The neuropeptide NMU amplifies ILC2-driven allergic lung inflammation. *Nature.* 2017; 549(7672): 351-356. DOI: 10.1038/nature24029.

Wan, H., Winton, H. L., Soeller, C., Gruenert, D. C., Thompson, P. J., Cannell, M. B., et al. Quantitative structural and biochemical analyses of tight junction dynamics following exposure of epithelial cells to house dust mite allergen Der p 1. *Clin Exp Allergy.* 2000; 30(5): 685-698. DOI: 10.1046/j.1365-2222.2000.00820.x.

Wan, H., Winton, H. L., Soeller, C., Tovey, E. R., Gruenert, D. C., Thompson, P. J., et al. Der p 1 facilitates transepithelial allergen delivery by disruption of tight junctions. *The Journal of Clinical Investigation.* 1999; 104(1): 123-133. DOI: 10.1172/jci5844.

Wang, C. M., Ploia, C., Anselmi, F., Sarukhan, A. and Viola, A. Adenosine triphosphate acts as a paracrine signaling molecule to reduce the motility of T cells. *EMBO J.* 2014; 33(12): 1354-1364. DOI: 10.15252/embj.201386666.

Wang, L., Feng, X., Hu, B., Xia, Q., Ni, X. and Song, Y. P2X4R promotes airway remodeling by acting on the phenotype switching of bronchial smooth muscle cells in rats. *Purinergic Signal.* 2018a; 14(4): 433-442. DOI: 10.1007/s11302-018-9625-4.

Wang, Q., Bai, X., Xu, D., Xu, D., Li, H., Fang, J., et al. [TRPV1 UTR-3 polymorphism and susceptibility of childhood asthma of the Han Nationality in Beijing]. *Wei sheng yan jiu = Journal of hygiene research.* 2009; 38(5): 516-521.

Wang, W., Li, Y., Lv, Z., Chen, Y., Li, Y., Huang, K., et al. Bronchial Allergen Challenge of Patients with Atopic Asthma Triggers an Alarmin (IL-33, TSLP, and IL-25) Response in the Airways Epithelium and Submucosa. *J Immunol.* 2018b; 201(8): 2221-2231. DOI: 10.4049/jimmunol.1800709.

Wanhainen, K. M., Jameson, S. C. and da Silva, H. B. Self-Regulation of Memory CD8 T Cell Metabolism through Extracellular ATP Signaling. *Immunometabolism.* 2019; 1(1). DOI: 10.20900/immunometab20190009.

Wareham, K., Vial, C., Wykes, R. C., Bradding, P. and Seward, E. P. Functional evidence for the expression of P2X1, P2X4 and P2X7 receptors in human lung mast cells. *Br J Pharmacol.* 2009; 157(7): 1215-1224. DOI: 10.1111/j.1476-5381.2009.00287.x.

Wartenberg, D., Lapp, K., Jacobsen, I. D., Dahse, H. M., Kniemeyer, O., Heinekamp, T., et al. Secretome analysis of Aspergillus fumigatus reveals Asp-hemolysin as a major secreted protein. *International Journal of Medical Microbiology.* 2011; 301(7): 602-611. DOI: 10.1016/j.ijmm.2011.04.016.

Watanabe, H., Davis, J. B., Smart, D., Jerman, J. C., Smith, G. D., Hayes, P., et al. Activation of TRPV4 channels (hVRL-2/mTRP12) by phorbol derivatives. *J Biol Chem.* 2002a; 277(16): 13569-13577. DOI: 10.1074/jbc.M200062200.

Watanabe, H., Vriens, J., Prenen, J., Droogmans, G., Voets, T. and Nilius, B. Anandamide and arachidonic acid use epoxyeicosatrienoic acids to activate TRPV4 channels. *Nature.* 2003; 424(6947): 434-438. DOI: 10.1038/nature01807.

Watanabe, H., Vriens, J., Suh, S. H., Benham, C. D., Droogmans, G. and Nilius, B. Heat-evoked activation of TRPV4 channels in a HEK293 cell expression system and in native mouse aorta endothelial cells. *J Biol Chem.* 2002b; 277(49): 47044-47051. DOI: 10.1074/jbc.M208277200.

Wechsler, M. E., Ruddy, M. K., Pavord, I. D., Israel, E., Rabe, K. F., Ford, L. B., et al. Efficacy and Safety of Itepekimab in Patients with Moderate-to-Severe Asthma. *N Engl J Med.* 2021; 385(18): 1656-1668. DOI: 10.1056/NEJMoa2024257.

Wenzel, S., Castro, M., Corren, J., Maspero, J., Wang, L., Zhang, B., et al. Dupilumab efficacy and safety in adults with uncontrolled persistent asthma despite use of medium-to-high-dose inhaled corticosteroids plus a long-acting β2 agonist: a randomised double-blind placebo-controlled pivotal phase 2b dose-ranging trial. *Lancet.* 2016; 388(10039): 31-44. DOI: 10.1016/s0140-6736(16)30307-5.

Wenzel, S. E., Barnes, P. J., Bleecker, E. R., Bousquet, J., Busse, W., Dahlén, S. E., et al. A randomized, double-blind, placebo-controlled study of tumor necrosis factor-alpha blockade in severe

persistent asthma. *Am J Respir Crit Care Med.* 2009; 179(7): 549-558. DOI: 10.1164/rccm.200809-1512OC.

Wenzel, S. E., Fowler, A. A., 3rd and Schwartz, L. B. Activation of pulmonary mast cells by bronchoalveolar allergen challenge. In vivo release of histamine and tryptase in atopic subjects with and without asthma. *Am Rev Respir Dis.* 1988; 137(5): 1002-1008. DOI: 10.1164/ajrccm/137.5.1002.

White, J. P., Cibelli, M., Urban, L., Nilius, B., McGeown, J. G. and Nagy, I. TRPV4: Molecular Conductor of a Diverse Orchestra. *Physiol Rev.* 2016; 96(3): 911-973. DOI: 10.1152/physrev.00016.2015.

Wiesner, D. L., Merkhofer, R. M., Ober, C., Kujoth, G. C., Niu, M., Keller, N. P., et al. Club Cell TRPV4 Serves as a Damage Sensor Driving Lung Allergic Inflammation. *Cell Host Microbe.* 2020; 27(4): 614-628 e616. DOI: 10.1016/j.chom.2020.02.006.

Wild, J. S., Sigounas, A., Sur, N., Siddiqui, M. S., Alam, R., Kurimoto, M., et al. IFN-γ-Inducing Factor (IL-18) Increases Allergic Sensitization, Serum IgE, Th2 Cytokines, and Airway Eosinophilia in a Mouse Model of Allergic Asthma. *The Journal of Immunology.* 2000; 164(5): 2701-2710. DOI: 10.4049/jimmunol.164.5.2701.

Wilhelm, C., Hirota, K., Stieglitz, B., Van Snick, J., Tolaini, M., Lahl, K., et al. An IL-9 fate reporter demonstrates the induction of an innate IL-9 response in lung inflammation. *Nat Immunol.* 2011; 12(11): 1071-1077. DOI: 10.1038/ni.2133.

Willette, R. N., Bao, W., Nerurkar, S., Yue, T. L., Doe, C. P., Stankus, G., et al. Systemic activation of the transient receptor potential vanilloid subtype 4 channel causes endothelial failure and circulatory collapse: Part 2. *J Pharmacol Exp Ther.* 2008; 326(2): 443-452. DOI: 10.1124/jpet.107.134551.

Williams, D. M. and Rubin, B. K. Clinical Pharmacology of Bronchodilator Medications. *Respiratory Care.* 2018; 63(6): 641-654. DOI: 10.4187/respcare.06051.

Willis, C. R., Siegel, L., Leith, A., Mohn, D., Escobar, S., Wannberg, S., et al. IL-17RA Signaling in Airway Inflammation and Bronchial Hyperreactivity in Allergic Asthma. *Am J Respir Cell Mol Biol.* 2015; 53(6): 810-821. DOI: 10.1165/rcmb.2015-0038OC.

Wilson, S. J., Rigden, H. M., Ward, J. A., Laviolette, M., Jarjour, N. N. and Djukanovic, R. The relationship between eosinophilia and airway remodelling in mild asthma. *Clin Exp Allergy.* 2013; 43(12): 1342-1350. DOI: 10.1111/cea.12156.

Winkelmann, V. E., Thompson, K. E., Neuland, K., Jaramillo, A. M., Fois, G., Schmidt, H., et al. Inflammation-induced upregulation of P2X4 expression augments mucin secretion in airway epithelia. *Am J Physiol Lung Cell Mol Physiol.* 2019; 316(1): L58-L70. DOI: 10.1152/ajplung.00157.2018.

Wisniewski, J. A., Muehling, L. M., Eccles, J. D., Capaldo, B. J., Agrawal, R., Shirley, D. A., et al. T(H)1 signatures are present in the lower airways of children with severe asthma, regardless of allergic status. *J Allergy Clin Immunol.* 2018; 141(6): 2048-2060.e2013. DOI: 10.1016/j.jaci.2017.08.020.

Woehrle, T., Yip, L., Elkhal, A., Sumi, Y., Chen, Y., Yao, Y., et al. Pannexin-1 hemichannel-mediated ATP release together with P2X1 and P2X4 receptors regulate T-cell activation at the immune synapse. *Blood.* 2010a; 116(18): 3475-3484. DOI: 10.1182/blood-2010-04-277707.

Woehrle, T., Yip, L., Manohar, M., Sumi, Y., Yao, Y., Chen, Y., et al. Hypertonic stress regulates T cell function via pannexin-1 hemichannels and P2X receptors. *J Leukoc Biol.* 2010b; 88(6): 1181-1189. DOI: 10.1189/jlb.0410211.

Wortley, M. A., Dubuis, E., Bonvini, S. J., Wong, S., Shala, F., Maher, S. A., et al. Making Sense of Sensory Nerves: An In Vitro Characterisation of Gene Expression Profiles of Airway-Innervating Guinea-Pig Airway Neurons Using Single-Cell Analysis. C78. NOT STRANGERS IN THE NIGHT: SLEEP AND THORACIC DISEASES. Conference Abstract. *Am J Respir Crit Care Med.* 2016;(193): A6002. DOI: 10.1164/ajrccm-conference.2016.193.1_MeetingAbstracts.A6002.

Wright, A., Mahaut-Smith, M., Symon, F., Sylvius, N., Ran, S., Bafadhel, M., et al. Impaired P2X1 Receptor-Mediated Adhesion in Eosinophils from Asthmatic Patients. *J Immunol.* 2016; 196(12): 4877-4884. DOI: 10.4049/jimmunol.1501585.

Xiao, C., Puddicombe, S. M., Field, S., Haywood, J., Broughton-Head, V., Puxeddu, I., et al. Defective epithelial barrier function in asthma. *Journal of Allergy and Clinical Immunology.* 2011; 128(3): 549-556.e512. DOI: https://doi.org/10.1016/j.jaci.2011.05.038.

Xiong, X. F., Zhu, M., Wu, H. X., Fan, L. L. and Cheng, D. Y. Efficacy and safety of dupilumab for the treatment of uncontrolled asthma: a meta-analysis of randomized clinical trials. *Respir Res.* 2019; 20(1): 108. DOI: 10.1186/s12931-019-1065-3.

Xu, D., Chan, W. L., Leung, B. P., Huang, F., Wheeler, R., Piedrafita, D., et al. Selective expression of a stable cell surface molecule on type 2 but not type 1 helper T cells. *J Exp Med.* 1998; 187(5): 787-794. DOI: 10.1084/jem.187.5.787.

Xu, H., Zhao, H., Tian, W., Yoshida, K., Roullet, J. B. and Cohen, D. M. Regulation of a transient receptor potential (TRP) channel by tyrosine phosphorylation. SRC family kinase-dependent tyrosine phosphorylation of TRPV4 on TYR-253 mediates its response to hypotonic stress. *J Biol Chem.* 2003; 278(13): 11520-11527. DOI: 10.1074/jbc.M211061200.

Xu, X., Goyal, N., Costell, M. H., Roethke, T., James, C. H., Thorneloe, K. S., et al. Identification of a Human Whole Blood–Based Endothelial Cell Impedance Assay for Assessing Clinical Transient Receptor Potential Vanilloid 4 Target Engagement Ex Vivo. 2021; 376(3): 436-443. DOI: 10.1124/jpet.120.000307 %J Journal of Pharmacology and Experimental Therapeutics.

Yao, L., Chen, S., Tang, H., Huang, P., Wei, S., Liang, Z., et al. Transient Receptor Potential Ion Channels Mediate Adherens Junctions Dysfunction in a Toluene Diisocyanate-Induced Murine Asthma Model. *Toxicol Sci.* 2019; 168(1): 160-170. DOI: 10.1093/toxsci/kfy285.

Yau, M. K., Lim, J., Liu, L. and Fairlie, D. P. Protease activated receptor 2 (PAR2) modulators: a patent review (2010-2015). *Expert Opin Ther Pat.* 2016; 26(4): 471-483. DOI: 10.1517/13543776.2016.1154540.

Yee, M. C., Nichols, H. L., Polley, D., Saifeddine, M., Pal, K., Lee, K., et al. Protease-activated receptor-2 signaling through beta-arrestin-2 mediates Alternaria alkaline serine protease-induced airway inflammation. *Am J Physiol Lung Cell Mol Physiol.* 2018; 315(6): L1042-L1057. DOI: 10.1152/ajplung.00196.2018.

Yin, J., Michalick, L., Tang, C., Tabuchi, A., Goldenberg, N., Dan, Q., et al. Role of Transient Receptor Potential Vanilloid 4 in Neutrophil Activation and Acute Lung Injury. *Am J Respir Cell Mol Biol.* 2016; 54(3): 370-383. DOI: 10.1165/rcmb.2014-0225OC.

Yin, J., You, S., Liu, H., Chen, L., Zhang, C., Hu, H., et al. Role of P2X7R in the development and progression of pulmonary hypertension. *Respir Res.* 2017; 18(1): 127. DOI: 10.1186/s12931-017-0603-0.

Ying, S., Meng, Q., Zeibecoglou, K., Robinson, D. S., Macfarlane, A., Humbert, M., et al. Eosinophil Chemotactic Chemokines (Eotaxin, Eotaxin-2, RANTES, Monocyte Chemoattractant Protein-3 (MCP-3), and MCP-4), and C-C Chemokine Receptor 3 Expression in Bronchial Biopsies from Atopic and Nonatopic (Intrinsic) Asthmatics. *The Journal of Immunology.* 1999; 163(11): 6321-6329.

Ying, S., O'Connor, B., Ratoff, J., Meng, Q., Mallett, K., Cousins, D., et al. Thymic stromal lymphopoietin expression is increased in asthmatic airways and correlates with expression of Th2-attracting chemokines and disease severity. *J Immunol.* 2005; 174(12): 8183-8190. DOI: 10.4049/jimmunol.174.12.8183.

Ying, S., Robinson, D. S., Meng, Q., Rottman, J., Kennedy, R., Ringler, D. J., et al. Enhanced expression of eotaxin and CCR3 mRNA and protein in atopic asthma. Association with airway hyperresponsiveness and predominant co-localization of eotaxin mRNA to bronchial epithelial and endothelial cells. *European Journal of Immunology.* 1997; 27(12): 3507-3516. DOI: https://doi.org/10.1002/eji.1830271252.

Ying, S., Robinson, D. S., Varney, V., Meng, Q., Tsicopoulos, A., Moqbel, R., et al. TNFα mRNA expression in allergic inflammation. *Clin Exp Allergy.* 1991; 21(6): 745-750. DOI: 10.1111/j.1365-2222.1991.tb03205.x.

Yip, L., Woehrle, T., Corriden, R., Hirsh, M., Chen, Y., Inoue, Y., et al. Autocrine regulation of T-cell activation by ATP release and P2X7 receptors. *FASEB J.* 2009; 23(6): 1685-1693. DOI: 10.1096/fj.08-126458.

Yu, Z., Wang, Y., Qin, L. and Chen, H. Functional Cooperation between KCa3.1 and TRPV4 Channels in Bronchial Smooth Muscle Cell Proliferation Associated with Chronic Asthma. *Front Pharmacol.* 2017; 8: 559. DOI: 10.3389/fphar.2017.00559.

Zech, A., Ayata, C. K., Pankratz, F., Meyer, A., Baudiss, K., Cicko, S., et al. MicroRNA-155 modulates P2R signaling and Th2 priming of dendritic cells during allergic airway inflammation in mice. *Allergy.* 2015; 70(9): 1121-1129. DOI: 10.1111/all.12643.

Zech, A., Wiesler, B., Ayata, C. K., Schlaich, T., Durk, T., Hossfeld, M., et al. P2rx4 deficiency in mice alleviates allergen-induced airway inflammation. *Oncotarget.* 2016; 7(49): 80288-80297. DOI: 10.18632/oncotarget.13375.

Zhang, F., Su, X., Huang, G., Xin, X. F., Cao, E. H., Shi, Y., et al. Adenosine Triphosphate Promotes Allergen-Induced Airway Inflammation and Th17 Cell Polarization in Neutrophilic Asthma. *Journal of immunology research.* 2017; 2017: 5358647. DOI: 10.1155/2017/5358647.

Zhang, G., Lin, R.-L., Wiggers, M., Snow, D. M. and Lee, L.-Y. Altered expression of TRPV1 and sensitivity to capsaicin in pulmonary myelinated afferents following chronic airway inflammation in the rat. *The Journal of Physiology.* 2008; 586(23): 5771-5786. DOI: https://doi.org/10.1113/jphysiol.2008.161042.

Zhao, P., Lieu, T., Barlow, N., Metcalf, M., Veldhuis, N. A., Jensen, D. D., et al. Cathepsin S causes inflammatory pain via biased agonism of PAR2 and TRPV4. *J Biol Chem.* 2014; 289(39): 27215-27234. DOI: 10.1074/jbc.M114.599712.

Zhao, P., Lieu, T., Barlow, N., Sostegni, S., Haerteis, S., Korbmacher, C., et al. Neutrophil Elastase Activates Protease-activated Receptor-2 (PAR2) and Transient Receptor Potential Vanilloid 4 (TRPV4) to Cause Inflammation and Pain. *J Biol Chem.* 2015; 290(22): 13875-13887. DOI: 10.1074/jbc.M115.642736.

Zheng, W. P. and Flavell, R. A. The transcription factor GATA-3 is necessary and sufficient for Th2 cytokine gene expression in CD4 T cells. *Cell.* 1997; 89(4): 587-596. DOI: Doi 10.1016/S0092-8674(00)80240-8.

Zhu, G., Investigators, I., Gulsvik, A., Bakke, P., Ghatta, S., Anderson, W., et al. Association of TRPV4 gene polymorphisms with chronic obstructive pulmonary disease. *Human molecular genetics.* 2009; 18(11): 2053-2062. DOI: 10.1093/hmg/ddp111.

Zhu, Q., Zhang, H., Wang, J., Wu, Y. and Chen, X. Associations of TNF-α -238G/A, TNF-α -308G/A, and IL-6 -174G/C polymorphisms with the risk of asthma: Evidence from a meta-analysis. *Pediatric Pulmonology.* 2020; 55(11): 2893-2900. DOI: 10.1002/ppul.25043.

Zhu, Z., Homer, R. J., Wang, Z., Chen, Q., Geba, G. P., Wang, J., et al. Pulmonary expression of interleukin-13 causes inflammation, mucus hypersecretion, subepithelial fibrosis, physiologic abnormalities, and eotaxin production. *The Journal of clinical investigation.* 1999; 103(6): 779-788. DOI: 10.1172/jci5909.

Zosky, G. R. and Sly, P. D. Animal models of asthma. *Clinical & Experimental Allergy.* 2007; 37(7): 973-988. DOI: https://doi.org/10.1111/j.1365-2222.2007.02740.x.